



School of Civil and Building Engineering

PhD Thesis

Academic Year 2011-2015

Eftychia Spentzou

**Refurbishment of Apartment Buildings in the
Mediterranean Region for Natural Ventilation:
Implications for Building Design**

Supervisors

Professor M.J. Cook

Professor S. Emmitt

This thesis is submitted in partial fulfilment of the requirements
for the degree of Doctor of Philosophy

© Loughborough University, 2015. All rights reserved.
No part of this publication may be reproduced without the permission of the copyright holder.

Abstract

With the emergence of climate change, the increasing figure of energy consumption for cooling in buildings expresses an urgent need for energy conscious design of new and existing buildings, and there is a significant opportunity for implementation of natural ventilation strategies. The high-energy consumption of the Greek domestic sector, the number of existing multi-storey apartment buildings, the small rate of building retrofitting in Greece and the warm, dry climate of Greece, indicate the potential to achieve significant energy reductions for cooling via natural ventilation. The aim of this research was to evaluate the energy saving potential of natural ventilation solutions for domestic buildings in the Mediterranean climate to deliver summer comfort, and to propose a low-energy refurbishment design guide.

The natural ventilation efficiency of an urban multi-storey apartment building in Athens and the potential implementation of advanced natural ventilation strategies, were evaluated using modelling tools. This would provide the knowledge for future energy refurbishments. The building was a representative example of over 4 million buildings in Greece. Several ventilation strategies were implemented in a single apartment (51.4m²) and evaluated in order to enhance the existing single-sided ventilation strategy of the building, including: daytime and nighttime ventilation; cross ventilation strategies; use of a wind-catcher; lightweight dynamic façade with shading system; new internal openings; and passive downdraught evaporative cooling strategies.

The ventilation performance of the strategies was investigated over the full cooling period using DTM simulations. Controlled natural ventilation strategies, in response to internal and external air properties, delivered: occupants' comfort; ventilation rates increase; and reductions in air temperatures and in CO₂ levels. Natural day and night ventilation contributed to significant temperature reductions (up to 7°C) relative to the base-case ventilation strategy. The proposed strategies marginally reduced the hours during the cooling period for which the CO₂ levels exceeded the upper acceptable limit for comfort. The strategies also achieved air change rates above the minimum acceptable values for comfort were provided; and therefore occupants' comfort was achieved.

De-coupled internal-external steady state CFD airflow simulations were performed to predict wind pressures across the building openings, and to predict detailed ventilation rates for a number of climate scenarios. Using CFD it was possible to overcome the limitation of DTM and predict average pressures at the location of the openings, considering the location of the building within its surroundings (both external and internal flow simulations were performed), leading to accurate results. It was predicted that the ventilation performance of the wind catcher was significant relative to the simple single or cross-ventilation strategies. The downdraft evaporative cooling performed best at low ventilation rates providing up to 4°C further temperature reductions. Indoor comfort was provided during windless hours for specific strategies (buoyancy driven); this is significant considering that low wind speeds (below 1m/s) were predicted for 14% of the cooling period. The performance of the strategies varies considerably with regard to both wind speed and direction; these should be considered when retrofitting natural ventilation strategies in existing buildings.

The proposed strategies delivered natural cooling and adequate ventilation rates, relative the base-case strategy. The combined wind catcher and dynamic façade strategy performed the best; this combined strategy would be recommended for the Mediterranean sub-climate, and for buildings comparable to the type studied. This should be combined with evaporative cooling strategies particularly during windless hours, and mechanical cooling only when these strategies do not provide sufficient performance.

For both the CFD and DTM results, empirical relationships were established with statistical methods between indoor air properties and climate characteristics, which can be used to predict behaviours under conditions that have not been examined using simulations. This assists extrapolation of patterns in ventilation performance, to facilitate design guidance of the natural ventilation strategies for implementation in similar buildings. The established performance of the natural ventilation strategies in the case study building assisted the development of a prototype scenario for similar building designs with comparable climatic context. A low-energy refurbishment design guide for natural ventilation was proposed that provides guidelines and design recommendations. Retrofitting such natural ventilation strategies in existing apartment buildings in similar climates presents a significant opportunity to achieve significant energy consumption reductions.

Acknowledgements

First and foremost, I would like to express my sincere gratitude to my supervisors Professor Malcolm Cook and Professor Stephen Emmitt for being tremendous mentors for me, whose support, encouragement and guidance throughout both my research and my career has been priceless. I am excited to work again in the future with you.

I would like to express my thanks to the examiners, Dr Neveen Hamza and Dr Steven Firth, for their valuable feedback and interesting discussions.

The assistance of the software developer during the computational part of this work, Dr. David Glynn (Cham), the HPC services research computing team manager Dr. Julian Highfield (Loughborough University), and the IT technicians of the Civil and Building Labs, is gratefully acknowledged. Special thanks to Dr. Steven Firth who helped me gain valuable teaching experience from the beginning of my PhD. I would like to thank the interviewees of the project; I am grateful for the time they took to share their knowledge and experiences. This research was supported with funding from the School of Civil and Building Engineering, Loughborough University and my two supervisors for further training and support.

I have been extremely lucky to have truly good friends that bring balance in my life, and who were there for me even when I was too busy working. I would like to thank my family in Greece for loving me even though I rarely visit.

My parents have been a rock for me through the years; their love, encouragement, support and sincere belief in me has been invaluable. I would like to thank my sister Dr Georgia Spentzou MD, for being my role model and for teaching me early in my life to be passionate and always work hard.

Finally, I would like to thank my partner Alister who has been a constant source of support, energy and motivation, experiencing all of the ups and downs of my research with patience, and helping me to be strong, positive and content.

Table of Contents

Abstract	i
Acknowledgements	iii
Table of Contents	v
List of Figures	x
List of Tables.....	xxvi
Nomenclature	xxix
List of Abbreviations.....	xxix
Chapter 1 : Introduction	1
1.1. Background of Research.....	1
1.2. Justification of Research.....	4
1.3. Aim and Objectives	6
1.4. Overview of Research Methods	7
1.5. Defining the Research Focus: Exploratory interviews, details and findings... 8	
1.6. Structure and content of thesis	12
Chapter 2 : Literature review	15
2.1. Introduction	15
2.2. Geographic and Climatic Properties of the Mediterranean Region Studied . 15	
2.2.1. The Heat Island Phenomenon.....	18
2.3. Buildings Energy Consumption	20
2.4. Architectural Characteristics of Domestic Buildings in Greece.....	23
2.4.1. Characteristics of vernacular settlements	23
2.4.2. Building classifications in Greek cities since 1900.....	26
2.5. Thermal Comfort and Indoor Air Quality in Free-Running Buildings	33
2.5.1. Energy benchmarks	34
2.5.2. Adaptive thermal comfort model	37
2.5.3. Occupants' adaptation and control	39
2.6. Natural Ventilation and Cooling Strategies.....	41
2.6.1. Natural day and night ventilation strategies	43
2.6.1.1. Façade relief elements	44
2.6.1.2. Wind-catchers.....	47

2.6.2.	Description of evaporative cooling techniques	49
2.6.3.	Natural ventilation modelling methods	52
2.7.	Discussion	55
Chapter 3 :	Research methodology, justification and methods	57
3.1.	Introduction	57
3.2.	Methodological debate	59
3.3.	Methods and Structure of the Research.....	60
3.3.1.	Brief description of the case study building	62
3.3.2.	Natural ventilation strategies.....	63
3.3.3.	Computer-based modelling	66
3.3.3.1.	Thermal building energy modelling	68
3.3.3.2.	Application and use of CFD: software package	69
3.3.4.	Ventilation Performance Investigation and Evaluation Analysis.....	72
Chapter 4 :	Case study building and ventilation strategies	75
4.1.	Introduction	75
4.2.	Description of the Case study Building.....	75
4.2.1.	Description of the apartment studied.....	79
4.3.	Study of the Surrounding Buildings	80
4.4.	Climate Study	84
4.5.	Natural Ventilation Strategies: Design.....	90
4.5.1.	Designing a wind-catcher for the case study building	91
4.5.2.	Design characteristics of a dynamic façade (DF).....	93
4.5.3.	Supplementary natural ventilation strategies	98
4.5.3.1.	Façade wind-catchers	98
4.5.3.2.	Internal openings	99
4.6.	Summary.....	100
Chapter 5 :	Indoor environmental performance evaluation.....	101
5.1.	Introduction	101
5.2.	Parametric Study, Building Operation and Properties: Model Setup.....	102
5.2.1.	Developing an occupancy profile.....	109
5.3.	Dynamic Thermal Simulations: Analysis and Results	114
5.3.1.	Performance evaluation of the base-case ventilation strategy (I).....	114

5.3.2.	Performance evaluation of the new natural daytime ventilation strategy (II)	117
5.3.3.	Performance evaluation of natural nighttime ventilation (II).....	119
5.3.4.	Performance evaluation of natural ‘day & night’ ventilation, (II)	122
5.3.4.1.	Overall performance evaluation of the base-case (I) and the new natural ventilation strategies (II)	123
5.3.5.	Implementation of a wind-catcher (III)	126
5.3.6.	Implementation of a dynamic façade (III).....	130
5.3.7.	Evaluation of new internal openings (III)	133
5.3.8.	Combined ventilation performance of a wind-catcher and a dynamic façade (IV).....	136
5.4.	DTM Results: IAQ Assessment and Performance Evaluation of the Different Ventilation Strategies.....	139
5.4.1.	Evaluation of occupants’ thermal comfort	143
5.4.2.	Quantification of the potential energy savings.....	148
5.4.3.	Ventilation performance evaluation of the apartment studied and the adjacent spaces	151
5.4.4.	Modelling wind-driven flows: Limitations	154
5.5.	Discussion	155
Chapter 6 : Airflow modelling analysis and ventilation performance results.....		157
6.1.	Introduction	157
6.2.	Description of the Individual Natural Ventilation Strategies and CFD Models	158
6.3.	Study of the External Flow: Model Setup	163
6.3.1.	Mesh independency study	166
6.3.2.	Study of the contribution of the surrounding buildings in the modelling process	169
6.3.3.	Prediction of pressure values at the building’s openings	171
6.4.	Study of the Internal Flow: Model Setup	172
6.4.1.	Single-Sided natural ventilation	175
6.4.2.	Cross ventilation.....	175
6.4.3.	Natural ventilation with a wind-catcher	176
6.4.4.	Dynamic louvered façade.....	180
6.4.5.	Passive draught evaporative cooling (PDEC)	183
6.5.	Ventilation Performance Simulation Results: External Flow	185

6.6.	Ventilation Performance Simulation Results for a Climate Scenario: Internal Flow Field	192
6.6.1.	Evaluation of buoyancy-driven flows: North winds	192
6.6.2.	Evaluation of wind-driven flows: North winds.....	196
6.6.2.1.	Assessment of individual wind-driven ventilation strategies .	196
6.6.2.2.	Overall performance evaluation of the simulation results: North wind direction	202
6.7.	Discussion: Ventilation Performance Evaluation of the Apartment During all Climate Scenarios	205
6.7.1.	Description of the most efficient strategy	211
6.8.	Characteristics of Individual Ventilation Strategies.....	212
6.8.1.	Passive downdraught evaporative cooling system	212
6.8.2.	Lightweight dynamic façade	213
6.9.	Ventilation Performance Study of Additional Designs and Justification of the CFD Modelling Methods Used.....	217
6.9.1.	Ventilation performance study of the total building	217
6.9.2.	Additional ventilation strategies: Façade wind-catchers.....	225
6.9.3.	Additional ventilation strategies: Internal openings configuration ...	227
6.9.4.	Performing steady state CFD simulations: Justification	230
6.10.	Discussion	231
Chapter 7 : Further analysis and design implications.....		233
7.1.	Introduction	233
7.2.	Establishing Relationships between Driving Pressure, Wind Speed and Ventilation Rates	233
7.3.	Defining Relationships between Ventilation Rates and Wind Speeds for the Climate Studied	237
7.4.	Defining Relationships between Indoor Air Temperatures and Wind Speeds	240
7.4.1.	Projecting the relationship between wind speed and temperature difference.....	243
7.5.	Comparative analysis: DTM-CFD simulation results	246
7.5.1.	Evaluation of natural ventilation strategies: Base-case strategy	247
7.5.2.	Evaluation of natural ventilation strategies: Day and night ventilation strategy	249
7.5.3.	Evaluation of natural ventilation strategies: Wind-catcher strategy .	251

7.5.4.	Evaluation of natural ventilation strategies: Dynamic façade and wind-catcher strategy.....	254
7.6.	Overview of the comparative analysis between the DTM-CFD simulation results.....	256
7.7.	Low-Energy refurbishment design guide: Strategy.....	258
7.8.	Low-Energy Refurbishment Design Guide for apartments in the Mediterranean: Natural Ventilation.....	260
7.9.	Discussion	272
Chapter 8 :	Conclusions and future work	273
8.1.	Summary of the Research Carried Out.....	273
8.1.1.	Methods of performance evaluation.....	274
8.2.	Principal Findings.....	275
8.2.1.	Predicted performance: natural ventilation and cooling strategies ...	278
8.2.2.	Research output	281
8.3.	Contribution to knowledge	283
8.4.	Limitations of this Research.....	284
8.4.1.	Occupancy and Building Design.....	284
8.4.2.	CFD modelling	285
8.5.	Recommendations for Further Work.....	286
References	289	
Appendices	1	
Appendix A.	Airflow modelling using CFD simulations.....	2
A.1.	Study of the external flow field.....	2
A.1.1.	Additional codes and driving pressures.....	5
A.1.2.	Study of the flow along urban passages	7
A.2.	Study of the internal flow field.....	9
A.2.1.	Prediction of airflow at internal passages.....	9
A.2.2.	Study of the internal flow for DBT 35°C.....	16
A.3.	Predicted average pressure values on openings.....	19
A.4.	Simulations performed	20
A.4.1.	Limitations and advantages of CFD computer simulations in serial and parallel operations.....	22
Appendix B.	Extrapolation of patterns in ventilation performance: CFD simulation results	24

List of Figures

Figure 2.1 Köppen-Geiger climate types map of the Mediterranean region. Combined maps of Africa and Europe after Peel et al. (2007).....	16
Figure 2.2 Spatial distribution of CWD trends over Greece. Proportional in size trends and rings for statistically significant trends at 95% confidence level (Nastos and Zerefos, 2009)	17
Figure 2.3 Total greenhouse gas emissions (in CO ₂ equivalent) indexed to Kyoto base year (index base year = 100 – Target). (Eurostat, 2011b)	20
Figure 2.4 Energy-related CO ₂ emissions per GDP in Greece and in selected IEA countries, 1973 to 2003 (tonnes of CO ₂ emissions per thousand USD GDP using 2000 prices).Cited in IEA (2006).....	20
Figure 2.5 Final energy consumption of the EU-27 in 2009 (Eurostat, 2011a).....	21
Figure 2.6 Electricity consumption shares of Greece in 2009 (IEA, 2011)	21
Figure 2.7 Final energy consumption of Greek households in Mtoe, after Eurostat (2008).....	21
Figure 2.8 Purchase of air conditioning equipment in Greece per capita (after Butera, 1994)	22
Figure 2.9 Qualitative assessment of natural ventilation in a traditional house in Florina (cited in Oikonomou and Bougiatioti, 2011, p. 683).....	24
Figure 2.10 Bioclimatic elements of the vernacular architecture (Kalogirou and Sagia, 2010)	24
Figure 2.11 Traditional dwelling in in Pelion (Sakarellou-Tousi and Lau, 2009).....	25
Figure 2.12 Summertime internal migration in section (Sakarellou-Tousi and Lau, 2009).	25
Figure 2.13 The medieval fortified buildings’ layout of the villages in 4 Greek Islands, from left to right: Antiparos, Kimolos, Santorini, Siphnos (Sinou, 2006)	26
Figure 2.14 Refugee apartment building at Alexandras Avenue, Athens, 1933-1935 (Drymiotis, 2014).....	27
Figure 2.15 Neoclassical 2-storey, Tripodon Street, Athens (Roubien, 2014)	27
Figure 2.16 Apartment building of 1950-90s. Saronida, Greece (photograph by author, 2012)	27
Figure 2.17 Two-storey apartment building in Saronida, Greece (photograph by author, 2012)	27
Figure 2.18 Modern apartment building with pilotis used for parking area in Saronida, Greece (photograph by author, 2012)	28

Figure 2.19 Contemporary single families dwelling, built in 2011. Saronida, Greece (photograph by author, 2012).....	29
Figure 2.20 Measured air change rates in a naturally ventilated building in central Athens, under night ventilation (Geros et al., 1999).....	35
Figure 2.21 Minimum indoor air velocities required corresponding to 80% and 90% air movement acceptability (Cândido et al., 2011)	36
Figure 2.22 Air speed required to offset increased temperature after BS EN15251 CEN (2007)	38
Figure 2.23 A vertical cross-section of a house with wind scoop (Peppes et al., 2002)	48
Figure 2.24 A vertical cross-section showing the air ducts in a Malkaf (Peppes et al., 2002)	48
Figure 2.25 European map showing areas of low and high potential for evaporative cooling implementation according to the need for cooling (Salmeron et al., 2012)	50
Figure 2.26 Test building with an evaporative cooling chimney (left) and a tower (Givoni, 1998).....	51
Figure 2.27 Traditional wind-catcher design, cross section and plan view by Bahadori (1985).....	51
Figure 2.28 Proposed wind-catcher design by Bahadori (1985).....	51
Figure 3.1 Research design and layout of the thesis	58
Figure 3.2 Research project: objectives, means and methods.....	61
Figure 3.3 Street view of the building and the apartment studied (Photograph by author, 2012)	63
Figure 3.4 Psychrometric chart with the climate dataset of the building site during the cooling period (produced in Climate consultant 5.5 (ClimateConsultant, 2014))	64
Figure 3.5 A schematic diagram of the simulations performed for the ventilation strategies evaluated, presented in steps starting with the existing ventilation strategy up to the final proposed strategy	69
Figure 3.6 Flow diagram of the airflow simulation sequence conducted for each natural ventilation strategy examined in CFD	70
Figure 4.1 First floor, plan view CAD drawing of the building studied, showing the case study apartment (dimensions in metres, nts).....	76
Figure 4.2 Penthouse plan view CAD drawing of the building studied, by author (dimensions in metres, nts) showing the position of the light wells	77

Figure 4.3 East Elevation, CAD drawing of the building studied by author (metres, nts).....	77
Figure 4.4 Picture of the top part of the existing light well, at the rooftop level (Photograph by author, 2012)	78
Figure 4.5 Floor plan of the case study apartment, internal openings and area of spaces (m)	80
Figure 4.6 Views of the case study building (Photographs by author, 2012)	81
Figure 4.7 Views of the neighbourhood and different urban blocks (Photographs by author, 2012)	81
Figure 4.8 Plan view of the site showing building heights in metres, with different colours the 1-metre contours, and a front elevation.....	83
Figure 4.9 Hourly values of DBT and wind speed presented as a scatter plot. Superimposed are zones of the maximum, minimum and average values of wind speed and temperature; their points of intersection define 6 ‘climate scenarios’ during the cooling period for the CFD simulations	86
Figure 4.10 Hourly values of wind speed frequency during the cooling period.....	86
Figure 4.11 Wind-rose, showing the percentage of incident of each wind direction and the shares of the wind speeds (discretised every 2m/s).....	87
Figure 4.12 Mean wind speeds for the site, per day group during the examined period (m/s)	88
Figure 4.13 Frequency of DBT for the cooling period	89
Figure 4.14 Number of daily average and maximum of DBTs.....	89
Figure 4.15 Average DBTs values per daily group for the cooling period.....	89
Figure 4.16 Model of the apartment under investigation, showing the zones of interest, connecting points, and the implementation zones of the various natural ventilation systems and strategies	90
Figure 4.17 Wind-catcher 3-D representations (left) and plan view (right) showing the frequency of wind directions (%), CAD drawing by author.....	91
Figure 4.18 Cross-section (left) and elevation (right) of the wind-catcher (CAD drawing by author, nts, after Bahadori, 1985)	92
Figure 4.19 Southeast elevation of the building under investigation, showing the three wind-catchers in the core spaces (dimensions in metres, nts).....	93
Figure 4.20 Sketch representation of the main façade showing the proposed dynamic façade (left) and the partition walls on the balcony zones (right).....	94
Figure 4.21 Plan view of the apartment’s balcony, showing the louvres and partition walls	95

Figure 4.22 Detailed cross-section of the louvres, after: Colt (2006).....	95
Figure 4.23 Detail 3-dimensional view of the louvres and the carrier system, after: Colt (2006)	95
Figure 4.24 Cross-sections of the balcony and the dynamic façade, showing the current (F) operation of the louvres, the proposed (A, B, C) and potential future operations (D, E)	96
Figure 4.25 A southeast elevation showing the operation of the shading system at each balcony in relation to solar shade.	97
Figure 4.26 Potential areas for wind-catcher inclusion, in the core spaces (light wells) and the balconies	98
Figure 4.27 Plan view of the apartment’s balcony, showing the façade wind-catcher, the closed louvres and the partition walls, nts	99
Figure 4.28 Southeast elevation of the building under investigation, showing the operation of the shading system on each balcony and the façade wind-catchers, nts	99
Figure 4.29 Three-dimensional detail representation of the apartment showing the new hallway openings for the ‘internal openings’ ventilation strategy	100
Figure 5.1 (left) A 3D view of the IESVE model of the existing building design, showing as shaded yellow the apartment openings and the horizontal top opening of the light well shaded red	105
Figure 5.2 (right) Three-dimensional model of the apartment studied in IESVE, showing the location of the internal doors (in green), the internal opening (in yellow), the external openings (in purple), and the openings at the top of the light well (light blue) with the light well cover	105
Figure 5.3 Plan layout of the building studied (shaded) and its surroundings in IESVE, indicating the heights of the buildings in metres and the location of the apartment under investigation in the building (shaded red).....	106
Figure 5.4 Shadows generated at different times during the 21 st of June, showing the hours of the day that the main building façade has access to direct sunlight....	107
Figure 5.5 Hourly distribution and shares of the different groups of occupants during the typical day, repeated throughout the cooling period, after Papakostas and Sotiropoulos (1997).....	110
Figure 5.6 Overall and individual percentages of occupants’ presence during the day, in the apartment under investigation (groups in relation to age, gender and occupation), after Papakostas and Sotiropoulos (1997).....	110
Figure 5.7 Ratio of occupants per property size in the county of Attica, Greece (number of rooms per dwelling) (EL.STAT., 2014).....	111
Figure 5.8 Daily profiles of occupancy profile, lighting and equipment operation .	112

Figure 5.9 Flow diagram of the openings' operation profile for the [base-case] ventilation strategy, DTM simulations.....	115
Figure 5.10 Flow diagram of the openings' operational profile used in the [DV] strategy DTM simulations.....	118
Figure 5.11 Flow diagram of the openings' operational profile used in the [NV] strategy DTM simulations.....	120
Figure 5.12 Flow diagram of the openings' operational profile used in the [DV & NV] strategy DTM simulations.....	122
Figure 5.13 Average daily operative temperatures predicted for the four natural ventilation strategies, in the apartment under investigation.....	124
Figure 5.14 Average values of CO ₂ concentration during the first six-hour group of the day (midnight-6am) and the four ventilation strategies	125
Figure 5.15 Average values of CO ₂ concentration during the second six-hour group of the day (6am-12pm) and the four ventilation strategies	125
Figure 5.16 Average values of CO ₂ concentration during the third six-hour group of the day (12pm-6pm) and the four ventilation strategies	125
Figure 5.17 Average values of CO ₂ concentration during the last six-hour group of the day (6pm-midnight) and the four ventilation strategies.....	126
Figure 5.18 A 3D view of the DTS model of the wind-catcher and the apartment studied (left)	127
Figure 5.19 Wind diagram showing the wind directions (angles) for each of the four wind-catcher openings, nts.....	127
Figure 5.20 Flow diagram of the openings' operational profile used in the [WC] strategy DTM simulations.....	128
Figure 5.21 Comparison of the average daily indoor air temperatures predicted at the [DV & NV] and the [WC] strategies	129
Figure 5.22 A 3D-model of the apartment, the dynamic façade and the air shaft, in IEVE.....	130
Figure 5.23 Flow diagram of the openings' operational profile used in the [DF] strategy DTM simulations.....	131
Figure 5.24 Flow diagram of the openings' operational profile used in the [InOp] ventilation strategy DTM simulations.....	134
Figure 5.25 The DTM three-dimensional model of the apartment and wind-catcher, showing the operation of the [InOp]	134
Figure 5.26 Three-dimensional model of the apartment, showing the operating dynamic façade and the wind-catcher in IESVE	136

Figure 5.27 Flow diagram of the openings' operational profile used in the [DF & WC] ventilation strategy DTM simulations.....	137
Figure 5.28 Daily average operative temperatures for five natural ventilation strategies during an example 7-day period.....	139
Figure 5.29 Average per 6-hour group predicted operative temperatures of three natural ventilation strategies and DBTs during an example 7-day period.....	140
Figure 5.30 Predicted average values of hourly operative temperatures (°C) for the cooling period, and their standard deviation, for six natural ventilation strategies	140
Figure 5.31 Predicted average, air change rate (ach ⁻¹) during each of the four daily groups, during an example 7-day period.....	142
Figure 5.32 Predicted average hourly air change rate (ach ⁻¹) of the apartment under investigation for the cooling period, and their standard deviation, for six ventilation strategies	142
Figure 5.33 Predicted air change rate distribution (5) at five ranges (in ach ⁻¹) during the cooling period, for seven natural ventilation strategies.....	142
Figure 5.34 Comfort temperature ranges defined by EN15251 and the ACA by the SCATs project.....	144
Figure 5.35 Relationship between outdoor running mean and operative temperatures for the four openings operation strategies.....	145
Figure 5.36 Relationship between outdoor running mean and average operative temperatures for the [DV & NV] ventilation strategy, showing the maximum and minimum acceptable levels according to BSEN15251	146
Figure 5.37 Relationship between outdoor running mean and average operative temperatures for four natural ventilation strategies, showing the maximum and minimum acceptable levels according to BSEN15251	147
Figure 5.38 Predicted daily operative temperatures for mechanical and natural ventilation strategies during the cooling period.....	149
Figure 5.39 Three-dimensional model of the building connected to the central wind-catcher, in IESVE, showing the apartment under investigation and the five apartments attached to the air shaft.....	151
Figure 5.40 Average daily values of operative temperatures (°C) and volume flow rates (l/s) predicted in the apartment studied, with (building) or without the surrounding apartments, for the period of a month.....	152
Figure 5.41 Predicted operative temperatures for the apartment studied, the three apartments above, and the average of the eight apartments connected to the wind-catcher for a period of a month.....	153

Figure 6.1 Graphical representation of the de-coupled internal/external airflow modelling flow diagram showing inputs and outputs, repeated for all natural ventilation strategies examined.....	162
Figure 6.2 Plan view of the building (centred in grey) and its surroundings' at the neighbourhood scale, with blue and red arrows pointing at north and the wind direction, respectively. Invisible objects that do not affect the airflow calculations assist the refinement of the computational mesh and divide the domain into 9 zones	164
Figure 6.3 Plan view of the three-dimensional model of the building in PHOENICS, showing the air shaft highlighted in red, the position of the apartment with dash line, the position of the balconies (in light blue) and the penthouse (in dark blue)	165
Figure 6.4 Convergence monitoring plot showing the reduction in error and the variable values at a user-specified monitor location in the grid ([DF & WC], northeast, Mesh 5).....	167
Figure 6.5 Driving pressures (Pa) predicted by simulations with different number of cells, study of the external flow field.....	167
Figure 6.6 Representation of the building studied, surroundings, computational mesh and domain size in plan xy view for the study of the external flow.	168
Figure 6.7 Representation of the buildings, computational mesh and domain in x,z view.....	168
Figure 6.8 Plan view of the flow field around the wind-catcher and the penthouse, showing contour lines of the pressure distribution and vectors of the wind direction at 20m above the ground (north wind of 7m/s) (stand-alone building).	170
Figure 6.9 Plan view of the flow field, showing contour lines of the pressure distribution and vectors of the wind speed around the wind-catcher and the penthouse at 20m height level above the ground (north wind of 7m/s), study of the building with its' surroundings.	170
Figure 6.10 View of the three-dimensional model of the building in PHOENICS, the air shaft highlighted in red, the penthouse in blue and the apartment examined with dashed line	171
Figure 6.11 Three-dimensional models of the apartment in CFD for the four ventilation strategies, study of the internal flow field.....	172
Figure 6.12 Plan view of the apartment's layout, the five measuring points (red arrow) and their coordinates from x,y,z zero point.....	174
Figure 6.13 Three-dimensional building model of the 'cross ventilation' strategy, showing the areas of flow calculations (internal openings 'D') and the external openings ('W')	176

Figure 6.14 Proposed design of the four-directional wind-catcher in PHOENICS .	176
Figure 6.15 Detailed plan view of the final partitions arrangement and mesh properties.....	176
Figure 6.16 Plan view of the apartment studied and [WC] ventilation strategy, showing the computational mesh (coarse and fine zones) for the evaluation of buoyancy-driven flow	177
Figure 6.17 Plan view of the apartment studied and [WC] ventilation strategy, showing the computational mesh (coarse and fine zones) for the evaluation of wind-driven flow.....	178
Figure 6.18 Convergence monitoring plot showing the residual for each solved variable and the variable values at a user-specified monitor location in the grid ([WC], north wind, Mesh 2).....	178
Figure 6.19 Indoor air temperatures at horizontal plane across all spaces (1.5m above the apartment floor) and number of cells for the study of the [WC] ventilation strategy	179
Figure 6.20 Predicted indoor air velocities (m/s) at 100 points along a line (from (3.65, 0, 1.5) to (3.65, 9.3, 1.5)) for 7 different computational meshes.....	180
Figure 6.21 Three-dimensional building model of the [DF & WC] strategy, showing the areas of flow predictions (internal openings ‘D’), the DF openings and external openings (D11-12)	180
Figure 6.22 Convergence monitoring plot showing the residual for each solved variable and the variable values at a user-specified monitor location in the grid ([DF&WC], north, Mesh 4)	181
Figure 6.23 Convergence monitoring plot showing the residual for each solved variable and the variable values at a monitor location in the grid ([DF&WC], northwest, Mesh 4).....	182
Figure 6.24 Indoor air temperatures (°C) at horizontal plane across all spaces (1.5m above the apartment floor) and number of cells, for the study of the [DF & WC] strategy	182
Figure 6.25 Predicted air velocities (m/s) at 100 points along a line at 1.5m height (from (3.65, 0, 1.5) to (3.65, 9.3, 1.5) for 5 different meshes of the [DF & WC]	183
Figure 6.26 Driving pressures for 3.6m/s wind speed, 5 wind directions and 3 models	185
Figure 6.27 Driving pressure for 7m/s wind speed, 5 wind directions and 3 models	186
Figure 6.28 Driving pressure increase (%) with regard to the addition of the wind-catcher [WC] to the base-case strategy (existing building design).....	186

Figure 6.29 Pressure contours on xy plane at 7.50m height above the ground, showing the 9 urban blocks, areas of low (leeward buildings) and high pressure (windward buildings). The blue arrow points at north and the red indicates the wind direction for 3.6m/s wind speed.	187
Figure 6.30 Velocity vectors (xy plane) at the neighbourhood scale. The blue dot at the centre of the buildings arrangement shows the location of the lowest wind speed value, and the red, the maximum of the domain, at 7.5m height above the ground level.....	188
Figure 6.31 Velocity vectors on xy plane at 18m height (North wind direction and 3.6m/s wind speed) predicting wind speeds of up to 2m/s in the apartments' façade windows.....	189
Figure 6.32 As previous at 19m height, showing wind distribution around the wind-catchers shaft and the attached penthouse, as well as recirculation areas at the leeward sides.....	189
Figure 6.33 As previous, at 23m height showing wind speeds of up to 4m/s at the wind-catchers windward surfaces.....	189
Figure 6.34 Pressure distribution across all openings (low to high) for 3.6m/s north wind direction, at the wind-catcher model.....	190
Figure 6.35 Pressure distribution at the building openings (low to high) for 3.6m/s north wind direction, base-case ventilation.....	190
Figure 6.36 Temperature (left figure) and velocity contours and vectors (right figure) on xy plane, during buoyancy-driven ventilation of the [SS] strategy (for 26°C DBT).....	192
Figure 6.37 Temperature (left figure) and velocity contours (right figure) on xy plane, during buoyancy-driven ventilation of the [CV] strategy (for 26°C DBT).....	193
Figure 6.38 Temperature (left figure) and velocity contours and vectors (right figure) on plan view, during buoyancy-driven ventilation of the [WC] strategy (for 26°C DBT) (at 1.50m height above the apartment floor level).....	193
Figure 6.39 Streamlines of the airflow movement in the spaces, showing the starting (blue) and ending point (red) of the flow ([WC], buoyancy-driven flow, 26°C).....	194
Figure 6.40 Temperature (left figure) and velocity contours and vectors (right figure) on plan view, during buoyancy-driven ventilation of the [DF & WC] strategy (for 26°C DBT).....	194
Figure 6.41 Indoor air temperatures (°C) for each of the four strategies during buoyancy-driven flow, calculated at set points of each room, at 1.50m height above the apartment floor.....	195

Figure 6.42 Indoor air velocity (m/s) for each of the four strategies during buoyancy-driven flow, calculated at set points of each room, at 1.50m height above the apartment floor.....	195
Figure 6.43 Temperature (left) and velocity (right) contours and vectors on xy plane during the wind-driven ventilation of the [SS] strategy (north, 7 m/s at 26°C)	196
Figure 6.44 Streamlines of the airflow movement in the spaces, showing the starting and final point of the flow ([SS] ventilation, 7m/s north wind, 26°C).....	197
Figure 6.45 Temperature (left) and velocity (right) contours and vectors on xy plane during the wind-driven ventilation of the [CV] strategy (north, 7 m/s at 26°C)	197
Figure 6.46 Streamlines of the airflow movement in the spaces, showing the initial and final points of the flow ([CV], 7m/s north wind, 26°C).	198
Figure 6.47 Temperature (left) and velocity (right) contours and vectors on xy plane during the wind-driven ventilation of the [WC] model (north, 7m/s at 26°C)..	198
Figure 6.48 Streamlines of the airflow movement in the spaces, showing the starting and final points of the flow ([WC], 7m/s north wind, 26°C).	199
Figure 6.49 Temperature (left) and velocity (right) contours and vectors on xy plane during wind-driven ventilation of the [PDEC-WC] of 8L/h (North, 7m/s at 26°C)	199
Figure 6.50 Temperature (left) and velocity (right) contours and vectors on xy plane during the wind-driven ventilation of the [DF & WC] (north, 7m/s at 26°C) ..	200
Figure 6.51 Streamlines of the airflow movement in the spaces, showing the initial and final points of the flow ([DF & WC], 7m/s north wind, 26°C).....	200
Figure 6.52 Temperature (left) and velocity (right) contours and vectors on xy plane during the wind-driven ventilation of the [PDEC-DF] (north, 7m/s at 26°C) ..	201
Figure 6.53 Indoor air temperatures predicted at 5 points in the spaces (at xy points, 1.50m on z) and the average of the six strategies (north wind direction, 3.6m/s and 26°C DBT).....	202
Figure 6.54 Indoor air velocity predicted at 5 points in the spaces (at xy points, 1.50m on z) and the average of the six ventilation strategies (north wind direction, 3.6m/s and 26°C DBT).....	203
Figure 6.55 Indoor air temperatures (°C) of the six natural ventilation strategies (north wind of 7m/s at 26°C DBT) at 5 points in the spaces and the average of the apartment.....	203
Figure 6.56 Indoor air velocity (m/s) at five spaces and the apartment's average (north wind direction, 7 m/s and 26°C DBT).....	204
Figure 6.57 Average air velocities (m/s) predicted at the internal openings during the wind-driven ventilation of 5 strategies (North wind, 3.6m/s and 26°C DBT) ..	204

Figure 6.58 Predicted ventilation rates of each natural ventilation scenario for different wind speeds and directions (m ³ /hr)	206
Figure 6.59 Average values of indoor air temperature (°C) at a horizontal plane at 1.5m height for 3.6m/s (left) and 7m/s (right) wind incidents (26°C DBT)	207
Figure 6.60 Average indoor air velocities (m/s) predicted in the two internal bedroom doors.....	208
Figure 6.61 Average indoor air speeds (m/s) across all spaces calculated at a horizontal plane at 1.5m height above the apartment floor, across all apartment spaces (26°C).....	209
Figure 6.62 Predicted air change rates (ach-1) at the building under investigation for all natural ventilation strategies (26°C DBT).....	210
Figure 6.63 Predicted indoor values of air velocity, temperature and relative humidity predicted at a horizontal plane for different water consumptions for [PDEC-DF] (26°C and 7m/s north)	212
Figure 6.64 Temperature and relative humidity change for the [PDEC-WC] and [PDEC-DF], normalised as a percentage of the values predicted for the [WC] and [DF & WC] strategies respectively (averaged temperature and velocity values, at 1.50m level above the floor level, 7m/s north wind, 26°C DBT)	213
Figure 6.65 Velocity contours and vectors at y,z cross section of the second bedroom, balcony and DF. All louvres fully open (3.6 m/s east wind at 26°C)	214
Figure 6.66 Velocity contours and vectors at y,z cross section of the second bedroom, balcony and dynamic façade. Only the top louvres open (3.6 m/s east wind at 26°C)	215
Figure 6.67 Velocity contours and vectors at y,z cross section of the second bedroom, balcony and dynamic façade. The top and bottom louvres open (3.6 m/s east wind, 26°C)	215
Figure 6.68 Predicted temperatures (°C) at 100 points along two lines at 1.5m height (from (1.2,0,1.5) to (1.2,9.3,1.5) and from (3.6,0,1.5) to (3.6,9.3,1.5) respectively) from the façade to the rear spaces, for 3 louvres positions	216
Figure 6.69 Predicted velocity (m/s) at 100 points along a line at 1.5m height (from (1.2,0,1.5) to (1.2,9.3,1.5) and from (3.6,0,1.5) to (3.6,9.3,1.5) respectively), for 3 louvres positions	216
Figure 6.70 Predicted air change rates (ach ⁻¹) of the apartment spaces for the natural ventilation strategies (26°C DBT) during the part operation of the air shaft (1/8 th)	218
Figure 6.71 Average values of indoor air velocity in the two bedrooms (average of the two internal doors), during the part operation of the air shaft (1/8 th).....	219

Figure 6.72 Temperature difference ($^{\circ}\text{C}$) during the 1/8 th shaft operation relative to the previous full operation of the shaft	220
Figure 6.73 Air temperature contours and vectors on xyz view (left) and of velocity on xz plane (right) during wind-driven ventilation of the [WC] strategy (north, 7m/s at 26°C) showing the flow field in the four building floors and apartments	221
Figure 6.74 Temperature (left) and velocity (right) contours and vectors on xy plane, during wind-driven [WC] strategy (north, 7m/s at 26°C) of the apartment modelled with the top 3 floors	222
Figure 6.75 Temperature (left) and velocity (right) contours and vectors on xy plane, of the buoyancy-driven wind-catcher strategy (26°C) of the apartment modelled with the top 3 floors	223
Figure 6.76 Volume flow rates (m^3/h) predicted in the bedroom openings of each apartment studied, at the four floors, for six ventilation strategies	223
Figure 6.77 Temperature (left) and velocity (right) contours and vectors on xy plane of the selected apartment for the [fWC] strategy (wind-driven flow, north, 7 m/s at 26°C)	225
Figure 6.78 Streamlines of the airflow movement in the spaces, showing the inflow and the outflow from the spaces ([fWC], 7m/s north wind, 26°C)	226
Figure 6.79 Temperature (left) and velocity (right) contours and vectors on xy plane of the selected apartment. New openings configuration for the wind-driven [WC] (north, 7 m/s at 26°C)	227
Figure 6.80 Temperature (left) and velocity (right) contours and vectors on xy plane (at 1.5m height) of the apartment studied during wind-driven ventilation of the ‘internal openings’ strategy (north, 7 m/s , 26°C)	229
Figure 6.81 Velocity contours and vectors on xy plane (at 2.5m height) of the apartment at the ‘internal openings’ configuration (north, 7 m/s, 26°C)	229
Figure 7.1 Relation of wind speed and pressure difference across the openings for the [CV] strategy	234
Figure 7.2 Relation of wind speed and pressure difference across the openings for the [WC] strategy	234
Figure 7.3 Relation of wind speed and pressure difference across the openings for the [DF & WC] strategy	235
Figure 7.4 Relation of driving pressure at the openings and ventilation rates, [CV] strategy	236
Figure 7.5 Relation of driving pressure in the openings and ventilation rates, [WC] strategy	236

Figure 7.6 Relation of driving pressure at the openings and ventilation rates, [DF & WC] strategy	236
Figure 7.7 Relation of driving pressure at the openings and ventilation rates, [PDEC-WC] strategy	236
Figure 7.8 Relation of driving pressure at the openings and ventilation rates, [PDEC-DF] strategy.....	237
Figure 7.9 Ventilation rates as a function of wind speeds of the [CV] strategy	238
Figure 7.10 Ventilation rates as a function of wind speeds of the [WC] strategy for various wind directions	239
Figure 7.11 Ventilation rates as a function of wind speeds of the [DF & WC] strategy	239
Figure 7.12 Ventilation rates as a function of wind speeds of the [PDEC-WC] strategy	239
Figure 7.13 Ventilation rates as a function of wind speeds of the [PDEC-DF] strategy	240
Figure 7.14 Indoor air temperature and ventilation rates relationship for the [CV] strategy for DBT 26°C (left) and 35°C (right)	241
Figure 7.15 Indoor air temperature and ventilation rates relationship for the [WC] strategy for DBT 26°C (left) and 35°C (right)	241
Figure 7.16 Indoor air temperature and ventilation rates relationship for the [DF & WC] strategy for DBT 26°C (left) and 35°C (right).....	241
Figure 7.17 Indoor air temperature and ventilation rates relationship, [PDEC-WC] strategy for DBT 26°C (left) and 35°C (right)	242
Figure 7.18 Indoor air temperature and ventilation rates relationship, [PDEC-DF] strategy for DBT 26°C (left) and 35°C (right)	242
Figure 7.19 Relationship between temperature difference (internal-external, ΔT) and ventilation rates for three natural ventilation strategies (for 26°C and 35°C external temperatures).....	243
Figure 7.20 Predicted indoor air temperature with regard to the wind speed and each ventilation strategy examined, for 26°C and 35°C DBTs and wind speeds below 4m/s.....	244
Figure 7.21 Predicted indoor air temperature with regard to the wind speed and each ventilation strategy examined, averaged values for 26°C and 35°C DBTs.....	245
Figure 7.22 Wind speed and ventilation rates relationship, for the cooling period, DTM results from the [base-case] ventilation strategy	247
Figure 7.23 Daily distribution of ventilation rates for the cooling period, [base-case] strategy	247

Figure 7.24 Relationship between wind speed and ventilation rates, with elimination of the zero flow rates due to closed openings, DTM results from the [base-case] strategy	248
Figure 7.25 Wind speed and ventilation rates relationships through the apartment's openings, for the cooling period, DTM results from the [DV & NV] strategy.	249
Figure 7.26 Daily distributions of ventilation rates, for the cooling period, [DV & NV] strategy	249
Figure 7.27 Wind speed distribution during the day (corrected weather file values)	250
Figure 7.28 Internal heat gains due to occupants, lighting and equipment thought the day presented with red dots and DBTs of the climate file for the cooling period	250
Figure 7.29 Relationships established between wind speed and ventilation rates for the cooling period, with elimination of the zero flow rates due to closed openings, for [DV & NV] strategy.....	251
Figure 7.30 Wind speed and total ventilation rate relationship during the cooling period. DTM results from the [WC] strategy investigated	252
Figure 7.31 Daily distributions of ventilation rates for the cooling period, [WC] strategy	252
Figure 7.32 First population group above 3m/s wind speeds and 1,000m ³ /h ventilation rates, showing correlation only between wind speed and ventilation rates	253
Figure 7.33 Second population group, below 3m/s wind speed and above 500m ³ /h ventilation rates, showing correlation only between temperature difference (Tin-Text) and ventilation rates.....	253
Figure 7.34 Third population group of ventilation rates below 1,000m ³ /h.....	254
Figure 7.35 Wind speed and ventilation rates relationship, for the cooling period [DF & WC].....	254
Figure 7.36 Relationship defined between wind speed and ventilation rates for the cooling period, DTM results from the [DF & WC] strategy.	255
Figure 7.37 Ventilation rates and temperature difference (Tin – Text) relationships, during the cooling period and for the [DF & WC] strategy.....	255
Figure 7.38 Thermal designs for thermal comfort (after [2]).....	260
Figure 7.39 Wind-catcher elevations. CAD drawings by author after [18]	261
Figure 7.40 Street view of the apartment building studied	262
Figure 7.41 Plan view of the building floor, showing with different colours the 8 apartments and the apartment under study.....	263

Figure 7.42 Plan view of the urban building blocks with their heights in metres and front view of the building studied	263
Figure 7.43 Frequency of DBTs for the cooling period.....	263
Figure 7.44 Daily profiles of occupants, lighting and equipment operation.....	263
Figure 7.45 Schematic 3D presentation of the spaces, connecting openings and points of interest.....	264
Figure 7.46 Location on of potential areas for wind-catcher inclusion, within the core spaces (light wells) and the balconies	265
Figure 7.47 South-east elevation of the building under investigation, showing the three wind-catchers at the core spaces	265
Figure 7.48 Frequency of wind directions (%) on the wind-catcher openings	265
Figure 7.49 Relation of ventilation rates and wind speeds of the wind-catcher strategy for various wind directions.....	266
Figure 7.50 Detail three-dimensional view of the louvres, and carrier system (after: [30]).....	266
Figure 7.51 South-east elevation of the building studied, showing the operation of the shading system in response to solar shade.....	266
Figure 7.52 Cross-sections of the balcony and the dynamic façade showing the current different operation of the louvres.....	267
Figure 7.53 Relation of ventilation rates and wind speeds of the DF strategy	267
Figure 7.54 South-east elevation of the building studied, showing the operation of the shading system in response to solar radiation, and the wind-catchers.....	267
Figure 7.55 Plan view (left) and updated plan view (right) of the apartment studied showing the wind-catcher, the façade wind-catcher and optimization the dynamic façade	268
Figure 7.56 Predicted indoor air temperature with regard to the wind speed and each ventilation strategy examined, averaged values for 26°C and 35°C DBTs.....	269
Figure A. 1 Defining the plan layout of the surrounding, after Google Maps (2013), showing the layout of each building, the building height, location of the building under investigation and a measuring point of the terrain heights	2
Figure A. 2 Map showing ground elevation measurements on every crossroad, modified with zero level the ‘red’ point on the map (Viklund, 2010).....	3
Figure A. 3 Refinement stage of the urban building blocks, showing with dashed line the layout of the existing buildings and with solid the new layout, CAD drawing by author, nts.....	3

Figure A. 4 Three dimensional representation of the site in CAD software.....	4
Figure A. 5 Additional coding for the prediction of average pressures at the openings in PHOENICS	5
Figure A. 6 Site view of the building under investigation, the surroundings and the measuring line.....	7
Figure A. 7 Prediction of wind velocities, at measured points every 20m at 1.5m height above the ground plane, along a line throughout the domain, 3 wind directions, 3.6m/s wind speed.	8
Figure A. 8 Prediction of pressure distribution, at measured points every 20m at 1.5m height above the ground plane, along a line throughout the domain, 3 directions, 3.6m/s wind speed.	8
Figure A. 9 Additional coding for the prediction of airflow through measuring 2D-objects at the computational domain.....	9
Figure A. 10 Indoor air temperatures (at xy points at 1.50m height above the apartment floor level) of the six natural ventilation strategies, north wind direction of 3.6m/s and 35°C DBT.	16
Figure A. 11 Indoor air velocity (at xy points at 1.50m height above the apartment floor level) of the six natural ventilation strategies at five spaces, north wind direction, 3.6m/s and 35°C DBT.....	17
Figure A. 12 Indoor air temperatures (at xy points at 1.50m height above the apartment floor level) of the six natural ventilation strategies, north wind direction of 7m/s and 35°C DBT.	17
Figure A. 13 Indoor air velocity (at xy points at 1.50m height above the apartment floor level) of the six natural ventilation strategies at five spaces, north wind direction of 7m/s and 35°C DBT.....	17
Figure A. 14 Average measured values of indoor temperature and velocity at horizontal plane (at 1.5m above the floor) for 35°C and 3.6m/s wind speed	18
Figure A. 15 Average measured values of indoor temperature and velocity at horizontal plane for 35°C and 7m/s wind speed.....	18
Figure A. 16 Indoor temperature and wind speed relationships for the [CV] strategy, for DBT 26°C and different wind directions	24
Figure A. 17 Indoor temperature and wind speed relationships for the [WC] strategy, for DBT 26°C and various wind directions.	24
Figure A. 18 Indoor temperature and wind speed relationships for the [DF & WC] strategy, for DBT 26°C and various wind directions.....	25
Figure A. 19 Indoor temperature and wind speed relationships for the [PDEC-WC] strategy, for DBT 26°C and various wind directions.....	25
Figure A. 20 Indoor temperature and wind speed relationships for the [PDEC-DF] strategy, for DBT 26°C and various wind directions.....	25

List of Tables

Table 2.1 Applicability of natural cooling techniques. After Givoni (1994) and Santamouris and Asimakopoulos (1996)	42
Table 3.1 List of natural ventilation strategies evaluated with DTM and CFD simulations	67
Table 3.2 Environmental conditions used for evaluating the DTM and CFD results respectively	73
Table 4.1 Building elements, properties and characteristic, by Androutsopoulos et al. (2012)	78
Table 4.2 Average monthly maximum DBT of the different climate datasets (°C) ..	85
Table 4.3 Average monthly maximum wind speed of the three different datasets (m/s)	85
Table 4.4 Incidents of frequency of wind speeds (hourly rounded data for the examined period) for each orientation (m/s)	87
Table 5.1 Average, maximum and minimum air properties during the cooling period	102
Table 5.2 List of the natural ventilation strategies and abbreviations	104
Table 5.3 Building element properties	108
Table 5.4 Sensible heat output of the internal heat gains, after Androutsopoulos et al. (2012)	112
Table 5.5 Default thermal zones and additional zones for each natural ventilation strategy	113
Table 5.6 Temperature difference (operative-DBT), for the [base-case] ventilation strategy, and the four groups of the day during the cooling period	116
Table 5.7 Average values of indoor air properties during the cooling period, per daily group, for the [base-case] ventilation strategy	117
Table 5.8 Temperature difference (operative-DBT), for the [DV] strategy and the six-hour groups of the day during the cooling period	119
Table 5.9 Average values of indoor air properties of the cooling period per daily group, for the [DV] strategy	119
Table 5.10 Temperature difference (operative-DBT), for the [NV] strategy and the six-hour groups of the day during the cooling period	121
Table 5.11 Average values of indoor air properties of the cooling period per daily group, for the [NV] strategy	121

Table 5.12 Temperature difference (operative-DBT), for the [DV & NV] strategy and the six-hour groups of the day during the cooling period.....	123
Table 5.13 Average values of indoor air properties of the cooling period per daily group, [DV & NV] strategy	123
Table 5.14 Temperature difference (operative-DBT), for the [WC] strategy and the six-hour groups of the day during the cooling period.....	129
Table 5.15 Average values of indoor air properties of the cooling period per day group, for the [WC] ventilation strategy	130
Table 5.16 Temperature difference (operative-DBT), for the [DF] strategy and the six-hour groups of the day during the cooling period.....	132
Table 5.17 Average values of indoor air properties of the cooling period per daily group, for the [DF] ventilation strategy	133
Table 5.18 Temperature difference (operative-DBT), for the [InOp] strategy and the six-hour groups of the day during the cooling period.....	135
Table 5.19 Average values of indoor air properties of the cooling period per daily group, [InOp] strategy.....	135
Table 5.20 Temperature difference (operative-DBT), for the [DF & WC] strategy and the six-hour groups of the day during the cooling period.....	138
Table 5.21 Average values of indoor air properties of the cooling period per daily group, for the [DF & WC] strategy.....	138
Table 5.22 Percentage of hours during the cooling period that the operative temperatures were lower than the DBT, and of CO ₂ concentration in the spaces within three ranges	141
Table 5.23 Percentage of hours above the temperature thresholds for overheating, during all natural ventilation strategies evaluated, per daily group	143
Table 6.1 List of the natural ventilation strategies and their abbreviations	160
Table 6.2 Computational meshes evaluated for the study of the external flow showing the number of cells at the wind catcher zone, the number of cells of each domain axis and the total number of cells	166
Table 6.3 Average pressure values (Pa) at the openings, and driving pressures for north wind direction of 7m/s, predicted by the external flow simulation of the building under investigation with and without the surrounding buildings	169
Table 6.4 Computational domains and mesh for the internal flow investigation	172
Table 6.5 Heat gains of each of the four occupied building spaces, explained	173
Table 6.6 Computational meshes and their properties, for the study of the internal flow of the [WC] ventilation strategy and the evaluation of wind-driven flow	179

Table 6.7 Computational meshes and their properties, for the internal flow investigation of the [DF & WC] ventilation strategy, for the evaluation of wind-driven flow.	181
Table 6.8 Average temperatures (°C) of the water supply network in Athens, Argiriou et al.(2010)	183
Table 6.9 Heat reduction of incoming air due to water evaporation for water at 22.78°C.....	184
Table 6.10 Predicted average pressure values at the openings of each natural ventilation strategy and CFD model (for WC openings see Figure 6.14).....	191
Table 6.11 Mass flow rates (kg/s) on the inlets of each ventilation strategy and percentage of increase due to the contribution of wind than the buoyancy-driven ventilation for each strategy respectively.....	205
Table 6.12 Description of the strategies evaluated and climate scenarios and results from the performance evaluation of the case study apartment when modelled with the adjacent apartments (percentage difference relative to stand-alone) ..	221
Table 6.13 Predicted indoor average air temperatures and velocities at a horizontal plane (1.5m height above each apartment floor) for the natural ventilation strategies studied at the four apartments	224
Table 7.1 Interpolation within different ranges of volumetric flow rates for each strategy	238
Table 7.2 Terrain coefficients for wind speed corrections.....	246
Table A. 1 Average pressure values (Pa) at the openings and driving pressure for four ventilation strategies.	6
Table A. 2 Calculated values of average velocity, volume flow rate and mass flow rate in the internal openings of each ventilation strategy and climate scenario evaluated.....	10
Table A. 3 Calculated values of average velocity, volume flow and mass flow rates in the internal openings of each ventilation strategy for 26°C DBT and 7m/s wind speed.....	12
Table A. 4 Pressure difference at the openings for every wind speed and direction, predicted by the external flow CFD simulations	19
Table A. 5 Study of the External Flow field; simulations performed for each ventilation strategy for different wind direction and wind speeds (m/s).....	20
Table A. 6 Simulations of the ventilation performance of the natural ventilation strategies investigated for different climate scenarios; Internal Flow. With ‘×’ are marked the simulations included in the analysis of Chapter 6 and with ‘■’ the simulations performed for the additional studied.....	20

Nomenclature

C_p	Wind pressure coefficient (-)
f	Loss coefficient (-)
Q	Ventilation flow rates (m^3/hr)
T_c	Comfort temperature ($^{\circ}C$)
T_{ext}	External air temperature ($^{\circ}C$)
T_i	Indoor air temperature ($^{\circ}C$)
T_{om}	Monthly mean outdoor temperature ($^{\circ}C$)
T_{rm}	Running mean outdoor temperature ($^{\circ}C$)
T_{RM80}	Running mean outdoor temperature for index 0.80 ($^{\circ}C$)
U_n	Velocity (m/s)
Uvalue	Thermal transmittance (W/m^2K)
v_m	Wind speed measured at 10m height (m/s)
v_z	Wind speed at the building height (m/s)
ΔP	Pressure difference (Pa)
ΔT	Temperature difference ($^{\circ}C$)
Θ_{ed}	Daily mean temperature ($^{\circ}C$)
Θ_{ed-1}	Daily mean external temperature for the previous day ($^{\circ}C$)
ρ	Air density (kg/m^3)

List of Abbreviations

ACA	Adaptive control algorithm
ACH	Air change rate (ach^{-1})
CAD	Computer-aided design
CH₄	Methane
CDD	Consecutive dry days
CFD	Computational Fluid Dynamics
CO₂	Carbon dioxide
COP	Coefficient of performance
CWD	Consecutive wet days
DBT	Dry-bulb temperature
DTM	Dynamic thermal modelling
EER	Effective Exchange Rate

ECU	European Currency Unit
GDP	Gross Domestic Product
GHG	Greenhouse gas
HPC	High-performance computing
IAQ	Indoor air quality
KE	Kinetic energy
KENAK	Energy performance buildings regulation, abbreviated from Greek letters
LES	Large-eddy simulations
L/s	Litres per second
L/h	Litres per hour
Mtoe	Million tonnes of oil equivalent
NO	Nitrous Oxide
PDEC	Passive Draught Evaporative Cooling
PMV	predicted mean vote
PPD	predicted percentage dissatisfied
RANS	Reynolds Averaged Navier-Stokes
RH	Relative Humidity
UHI	Urban heat island
USD	US Dollar
WBT	Wet-bulb temperature

***Chapter 1* : INTRODUCTION**

1.1. Background of Research

Climate change is defined as the alteration of the general state of the climate for a prolonged period of time (Met Office, 2012), typically induced by the increase in concentration of greenhouse gases (GHG) within the atmosphere due to man-made activities, and is thus acknowledged as the most significant environmental threat facing the world (DECC, n.d.). The global average air and ocean temperature rise, the changes in rainfall patterns, the sea-level rise and the melting glaciers, are some of the prevailing results of climate change (IPCC, 2007; Met Office, 2012).

GHG emissions increased by up to 80% between 1970 and 2004 (IPCC, 2007). It is acknowledged that even if the GHG concentrations remained at the 2000 levels a further global warming of about 0.1°C per decade would be expected. The European Union (EU) countries have committed to a GHG reduction of 30% on average relative to the 1990 levels, until the year 2020 (UNFCCC, 2013). Industrialisation and urbanisation influence the human settlements, microclimates and life. It is projected that by 2025 the urban inhabitants will reach five billion (Kolokotsa et al., 2009). The so called heat island phenomenon results further in higher air temperatures relative to the rural suburbs; cities today face inadvertent climate modifications (Oke, 1978; Mihalakakou et al., 2004).

With the emergence of climate change, energy shortage, population increase, indoor air quality (IAQ) health related problems, global recession and fuel poverty, authorities have now recognised an urgent need to reduce energy consumption within sustainable development. It is now main concern of governments to improve the environmental building performance with appropriate legislation (Emmitt and Ruikar, 2013).

The domestic sector in the Mediterranean country of Greece corresponds to the 80% of the existing Greek building stock (I. Theodoridou et al., 2011) and has the highest

energy consumption in Europe (Asimakopoulos et al., 2012). The 2011 census documented up to 4 million multi-storey apartment buildings in Greece (EL.STAT., 2012) of which 50% were constructed before 1979, the year of the Greek energy regulations were introduced (I. Theodoridou et al., 2011). According to the Hellenic Statistical Authority in 2010, Greek construction activity is currently in a deep depression due to the economic situation of the country, facing up to 62.4% drop from 2008 levels (Theodoridou et al., 2012). The new building permits have been significantly reduced, reaching in 2011 the one fifth of the 2005 levels, while up to 98% of the Greek citizens do not intend to construct or buy a new residence within at least a year (SATE, 2012). The construction and refurbishment rate of buildings has fallen drastically (Papamanolis, 2015a).

The EU building sector accounts for approximately 40% of the total energy consumption required for provision of heating, cooling, lighting and appliances. The energy required for cooling in hot climates has been predicted to be more than double the energy required for heating (Santamouris and Asimakopoulos, 1996). Residential buildings consume more electricity than other sectors, such as industry, and a little less than commercial buildings (IEA, 2011). There is a continuous increase in air-conditioning (A/C) installations (Yun and Steemers, 2011) especially in the southern EU countries (Geros et al., 1999). Research in Greek dwellings has shown that up to 70% of occupants operate A/C systems during summertime and up to 45% use fans (Drakou et al, 2011). All these highlight the significant potential for energy savings if natural ventilation strategies were implemented. The strong link between occupants and householder needs (73% of occupants being the homeowners (ELSTAT, 2012)) further demonstrates the substantial potential for energy savings.

The discouraging facts of the Greek Governments' Gazette for the period 1990 and 2000 show up to 23% increase in three basic greenhouse gas emissions (CO₂, CH₄, NO) (F.E.K., 2003) and demonstrate the country's inability to meet the target set in Kyoto to reduce the Greek emissions by 25% relative to the 1990 levels by 2012 (Theodoridou et al., 2012). There is an increased need to promote energy conscious design, energy responsive behaviours and low carbon technologies in the Greek context. Cultural sustainability, economic initiatives, and environmental and social aspects of sustainability, should be considered along with minimising waste and energy consumption and avoiding low indoor air quality, as well as maximising occupants' quality of life and ethical practice (Emmitt, 2012).

Building designers often turn to traditional architecture and techniques for lessons in making climate and environment work to their advantage (Kimura, 1994; Canas, 2004; Stasinopoulos, 2006; Serghides, 2010; Foruzanmehr and Vellinga, 2011). Vernacular knowledge should be treated as a great source of know-how, integrating locality and sustainability into modern buildings (Asquith and Vellinga, 2006).

Heat waves in hot climates contribute to increase in mechanical cooling peak load demand, threatening to disrupt supply (Kolokotroni et al., 2007). Fuel poverty in relation to both cooling and heating demand has been reported at more than 20% of Greek households (M Santamouris, Kapsis, et al., 2007). Atmospheric pollution in Greek cities remains a significant factor affecting comfort in open urban spaces, despite a number of measurements to achieve EU targets for greener cities (Ministry for the Environment, 2009). However, the concentrations of common air pollutants have been recently reduced as reported by (Papamanolis, 2015b). Air-tight buildings and reductions in ventilation rates have led to reported concerns over IAQ (M Santamouris, Argiroudis, et al., 2007; Lai et al., 2009).

Given the warm, dry climate of Greece (Psomas et al., 2014) with the lowest levels of relative humidity and the highest wind speeds in the Mediterranean, it is possible to deliver occupants' thermal comfort utilising natural ventilation strategies (Santamouris and Asimakopoulos, 1996). Increase in ventilation rates could significantly improve the indoor environmental quality of the dwellings (M Santamouris, Argiroudis, et al., 2007). Natural ventilation should be considered at the early stages of design as well as during refurbishment studies of existing buildings to ensure resilience to future climates.

Ventilation is necessary for IAQ (removal of stale air, odours and harmful chemicals), for provision of natural cooling (excess heat reduction), and for removal of heat and pollution at localised sources (Cook, 1998; CIBSE, 2005). Natural ventilation provides direct human comfort and/or decreases internal daytime temperatures by cooling the thermal mass during nighttime (Givoni, 1994). Natural day and night ventilation is utilised in different ways, via envelope opening configurations, with inclusion of wind-catchers, solar chimneys, dynamic façades, and wing-walls. Direct or indirect evaporative cooling strategies could be exploited to provide further passive cooling by water evaporation.

1.2. Justification of Research

In view of climate change, aging domestic building stock, and increasing domestic building energy consumption and demand, it is vital to promote refurbishment of residential buildings and modernisation, with the aim of improving the residential environmental quality and reducing energy consumption, and overheating risks (Yun and Steemers, 2011). The large existing building stock of the typical multi-family buildings of the Mediterranean countries represents a substantial opportunity for energy refurbishment plans. The 2011 census reported up to 4 million multi-storey buildings in Greece, which is considered to be the most common domestic building type in Greece (EL.STAT., 2012).

There are various refurbishment programs in Mediterranean countries involving energy improvement of public buildings, educational buildings, hotels (Nearly Zero Energy Hotels-NEZEH), and domestic buildings. The EU-funded project ELIH-MED (Energy Efficiency in Low Income Housing in the Mediterranean) aims to assist the low income society of the Northern Mediterranean sea coast (30 to 40% of the Mediterranean households) meeting the EU 2020 targets (Refalo, 2014). However, the rate of building retrofitting in Greece is very low. As reported by the Hellenic National Statistics Service every year only 250 domestic buildings of the existing Greek building stock (4 million) proceed to refurbishments. These refurbishments mainly concern the implementation of wall and roof insulation, or double-glazing openings (Santamouris et al., 2007; Dascalaki et al., 2010).

In Greece, energy refurbishments of domestic buildings could promote economic growth, support environmental benefits with compliance in EU energy targets, provide higher living standards with regard to occupants' indoor air quality, and redefine and promote the most typical urban building, the multi-storey apartment building (Theodoridou et al., 2012). Refurbishments assist reduction in maintenance costs as they improve the condition of buildings and extend their service to accommodate the needs of future climates. There is thus a clear need for energy improvements in the existing building stock in order to minimise the energy consumption, improve occupants' thermal comfort, particularly in low-income houses, and proceed to GHG emissions reduction.

The undoubtable benefits and potential of natural ventilation strategies implemented in the existing building stock have been widely evaluated by others. Although research has been undertaken on the energy behaviour of Greek urban dwellings, their possible renovation (Theodoridou et al., 2011; Papamanolis, 2006) and their natural ventilation evaluation (Niachou et al., 2008), little research has been carried out on the implementation of passive cooling solutions in existing apartment buildings and their potential performance (Santamouris et al., 2010; Yik and Lun, 2010). In times of low construction activity, due to Greece's financial crisis, and the energy consuming domestic buildings (the highest energy consumption in Europe), the need for energy improvement of the existing buildings is emerging and the primary solution to a financial recovery of the construction sector (Asimakopoulos et al., 2012).

Furthermore, despite studies regarding the efficiency of passive ventilation strategies in buildings, little research has been carried out in domestic buildings and specifically in the Mediterranean Region. A significant gap in knowledge remains for a natural ventilation refurbishment study of multi-storey, free-running, urban, domestic buildings in the Mediterranean that could provide guidance for future refurbishment projects.

Low-energy refurbishment design guides (LERDG) for natural ventilation and cooling can be valuable tools that could extend the life of buildings, reinvent the indoor spaces, enhance their architectural identity, while providing sustainable development and having an impact on the wellbeing of people. In the case of the Greek building stock, the potential benefits of an LERDG are beyond energy reduction. Appropriate refurbishments guides in Greece could offer a potential economic recovery of the construction sector, while preserving the most dominant urban domestic building. It would further attempt to transfer knowledge to practitioners and counteract the information and skills gap in construction, as there is extensive understanding of the need, but a lack of widespread know-how.

If natural ventilation strategies deliver occupants' thermal comfort expectations within multi-storey apartment buildings, there is a potential to implement this on a large scale (e.g. 4 million multi-storey buildings exist in Greece alone (ELSTAT, 2012)), in order to proceed to significant energy consumption reduction.

1.3. Aim and Objectives

The aim of this research project was to evaluate the energy saving potential of natural ventilation solutions for domestic buildings in the Mediterranean climate.

The main questions that this research attempted to address are:

- ❖ Which traditional natural ventilation strategies with application in different building types and climates could be suitable in the Mediterranean sub-climate of Greece?
- ❖ How could these strategies be introduced in the vast majority of the existing domestic building stock in Greece and what is the most typical domestic building design? Which building design modifications would be required and how would they affect the building operation and occupants?
- ❖ Which control strategies for comfort ventilation and natural ventilation should be employed, in order to meet occupants' thermal comfort expectations?
- ❖ Can we predict the performance of natural ventilation and cooling in existing domestic buildings in hot climates? Can natural ventilation and cooling be an efficient alternative to air-conditioning for enhancing indoor air quality?
- ❖ Would the inclusion of passive systems in a country in recession be viable, and could they satisfy occupants' needs? Could these natural ventilation designs be integrated into similar buildings, and could this research disseminated and become available to practitioners?

The above research aim and research questions were addressed by the following objectives:

1. Identify natural ventilation strategies in hot climates and define their applicability criteria. Carry out a literature review on architectural building typologies in Greece, on energy consumption in domestic buildings, and on modelling techniques. In a typical Mediterranean climate, identify a representative building type and applicable ventilation strategies.

2. Use dynamic thermal modelling tools to predict indoor air quality during the cooling period and for the different ventilation strategies evaluated. Evaluate occupants' thermal comfort using different criteria.
3. Use computational fluid dynamics techniques to predict ventilation performance, detailed internal airflow patterns, and indoor air temperature distributions at the scale of a single apartment for a number of natural ventilation strategies. Identify and quantify where possible the benefits and limitations of each natural ventilation strategy.
4. Evaluate the potential implementation of various natural ventilation strategies on existing domestic buildings, using analytical methods and propose the most efficient solution for the Mediterranean sub-climate and building typology studied.
5. Propose a low-energy refurbishment design guide, including detailed information about the design and performance of the natural ventilation strategies evaluated, presented in a concise and user-friendly way for building designers, with the aim to reduce the domestic buildings' cooling load in hot climates.

1.4. Overview of Research Methods

An in-depth review of literature was conducted to identify the gaps in knowledge and justify the scope of the research, covering subjects of: climate; building design; energy performance; simulation tools; natural ventilation; and passive cooling strategies. The literature review was accompanied with some public engagement with elite exploratory interviews to identify the need for energy refurbishment for natural ventilation of the existing Greek domestic building stock (presented in this section). A multi-storey apartment building was selected that is statistically representative for the average Greek dwelling for its design, year and type of construction. Several natural ventilation strategies were included in the building design. The ventilation performance of the strategies (at the scale of a single apartment) was evaluated using dynamic thermal modelling (DTM) and computational fluid dynamics (CFD) techniques. Quantitative data were obtained and evaluated with regard to the

buildings' indoor air quality improvement and enhancement of occupants' thermal comfort. Validation was provided with regard to expected performance of the strategies as presented in literature. The most appropriate natural ventilation strategies for the specific building type and climate were identified and evaluated. The design implications were reported and conclusions were drawn providing recommendations for future, energy, refurbishment projects in the form of a design guide.

1.5. Defining the Research Focus: Exploratory interviews, details and findings

Prior to determining the focus of this project, it was decided to solicit the opinion and advice of individuals working in the field and living in the country. This provided insights regarding the suitability, applicability of this research at the specific context, location, current and/or future climates, offering a real world perspective of the research. A number of elite exploratory semi-structured interviews were performed in the form of standard questions focusing on the research topic, with no use of closed questionnaires. The purpose of the interviews was to gain a qualitative knowledge conveyed in informal language without seeking quantification. The style of interviews was open-ended, directed by the participant's views and enhanced with information considered important to them. Elite interviewing is a common method to collect primary data (Berry, 2002). Elites are considered those with particular expertise (Morris, 2009). The type of the questions concerned the personal experience, opinion, knowledge and sensory aspects of the interviewee (Greenfield, 1996; Leedy and Ormrod, 2001; King and Horrocks, 2010).

The interviews seek information regarding the Greek designer's views and knowledge on: passive ventilation in buildings and the current context of implementation in the Greek construction sector; occupants' environmental or economic concerns on passive ventilation techniques; the future trend of the Greek domestic building sector after a potential recession recovery; the Greek energy regulations.

Five participants with different background and experience in the field were interviewed, through the phone, via email (by providing discussion points and receiving thoroughly developed answers) and in person. The questions were modified according to the discipline of each interviewee. On the beginning of each session, the subject of this research was explained followed by a series of open questions. The interviews were conducted in Greek within a five-day visit in the country, in May 2012. The interviewees were individuals with a variety of professions, working and living in different regions of Greece and within a thirty years age band (30-60), these were:

Interviewee ‘A’: Professor of Physics at a Greek University, part time Lecturer in international Universities and editor of international journals. Interview conducted in person.

Interviewee ‘B’: Architect working in a private architectural and construction firm in Athens focusing in architecture, sustainable design, urban planning and construction. Interview questions by email.

Interviewee ‘C’: Architect and owner of construction firm in a high-end location in terms of real state. Interview conducted in person.

Interviewee ‘D’: Civil engineer, manager in a construction company based on the southwest suburbs of Athens, a residential and holiday-resort area. Interview conducted in person.

Interviewee ‘E’: Lecturer of sustainable architectural design at the department of Architecture, National Technical University of Athens, and architect at a private firm. Interview conducted over Skype.

The output of the open questions of the interviews were categorised in three main themes as presented in the following list:

I. An up-to-date perspective of the Greek construction section

The decline of the annual construction activity has reached 30% of the annual reduction levels of 2008, which would potentially require up to 10 years for recovery (interviewee D). The construction of new multi-storey buildings has stopped indefinitely (interviewee E). There is a large stock of unoccupied new-build apartment buildings unable to be distributed in the market (interviewee C, D, and E).

In the next few years and after a potential recovery, refurbishments will significantly influence the construction activity (interviewee A, D and E).

The financial security provided by the ownership of more than one properties, part of the Greek culture, as well as the remaining current demand of housing 1.5 million citizens (interviewee D) are expected to re-establish the amplified construction activity of the past, after an economic growth (interviewee C). People will turn their investment interest to bioclimatic domestic design (interviewee B) due to the available funds in the private sector (interviewee C).

II. Natural cooling and ventilation techniques

The interviewees had limited knowledge of natural cooling and ventilation strategies, concerning mainly the building form, windows materials, and creation of vertical air paths in the buildings (interviewee C). Lack of interest was observed, regarding the currently enforced first energy performance buildings regulation (KENAK) published in 2010 (interviewee D), supported by the governments' indifference to building energy refurbishments (interviewee C). The newly introduced energy performance and construction regulation (KENAK) and the accompanying energy certificate software, were characterised by the interviewees as inefficient in promoting sustainable design. They explained that the software concerns mostly the adequate application of thermal insulation in buildings (interviewee B).

The potential of energy cost reduction and not the potential energy savings, or the CO₂ emissions reduction, would drive occupants' interest to sustainable design and natural ventilation systems (interviewee C and D). With regard to the salary reductions and the increasing fossil fuel prices, an important number of low-income households suffer from fuel poverty, spending up to 40% of their annual income on energy for domestic heating and cooling (interviewee D). Despite the noticeable increase of the heating degree hours between 2001 and 2002, the energy consumption decreased by 45% (interviewee A). This expresses occupants' inability to obtain thermal comfort due to the energy cost.

III. Scenarios of future trends in the building sector

Refurbishments of Greek multi-storey buildings are usually restrained by the complicated proprietary scheme and the lack of common agreement between the

different owners, making the energy improvement of existing buildings difficult and impractical (interviewee B). Refurbishments of non-domestic buildings could be a more viable idea (interviewee C). The idea of designing new single-family houses with passive systems is considered more viable for the near future (interviewee B). Practicing and implementing passive strategies is an easy process in new buildings (interviewee C), especially if the future occupants contribute to the design process (buildings designed for 'someone' and not 'anyone') (interviewee B). However, interviewee A suggests that designing energy efficient new-builds would have an insignificant contribution to building energy reductions, because new-builds correspond to 0.1% of the building stock. Although zero energy buildings could be designed by 'almost anyone', it is challenging to proceed to low energy improvements of the existing buildings whilst satisfying occupants' expectations and at the lowest cost. There is a need to re-design existing buildings to be zero energy buildings (especially for cooling), and comply with international energy standards. Further, the large stock of multi-storey apartment building in the Greek cities built in 50s, 60s or 70s was described to be in urgent need for energy refurbishments. The aesthetic contribution of passive strategies to the existing building design should be considered (interviewee A).

1.6. Structure and content of thesis

The thesis is subdivided into eight chapters: starting with an introductory chapter; a literature review; a chapter on methodology; the building description; two performance evaluation chapters; a discussion chapter of the overall output of the research conducted; and the concluding chapter. The contents of the thesis chapters are summarised below:

Chapter 1 Introduction

The background and justification of the research, along with an outline of the aim and objectives of the project are presented in this chapter. Findings of a number of elite exploratory interviews performed are presented.

Chapter 2 Literature Review

This chapter includes an overview of the building typologies and climate characteristics of the area studied, an analysis of the energy consumption in domestic buildings, and a description of the occupants' thermal comfort expectations. Natural ventilation strategies and modelling techniques available for the evaluation of natural ventilation are reviewed.

Chapter 3 Research Methodology

This chapter presents the nature and structure of this research, the methods adopted and the modelling techniques used. The research gap and the research problem to be addressed are identified and the research design is presented. Evaluation methods are reviewed.

Chapter 4 Case Study Building and Ventilation Strategies

This chapter describes the selected building under investigation by presenting detailed CAD drawings and photographs. It includes a brief description of the climate studied, and illustrates the design of the individual natural ventilation strategies evaluated.

Chapter 5 Indoor Environmental Performance Evaluation

This chapter presents the DTM analysis and results of the performance investigation of the natural ventilation strategies implemented in the case study building. It provides information regarding the indoor air quality (IAQ), occupants' thermal comfort, and the overall performance of the natural ventilation strategies during the cooling period in hourly intervals.

Chapter 6 Airflow Modelling Analysis and Ventilation Performance Results

Here, the internal and external airflow of the building and apartment studied are evaluated using CFD, in order to explore the natural ventilation potential of the building under consideration and passive strategies implemented. The chapter includes a detailed description of the model setup, presentation of the simulation results and the results analysis.

Chapter 7 Further analysis and design implications

A comparison study between steady state and time-dependent results is reported here, with the aim of extrapolating broad patterns of the ventilation performance and operation of the natural ventilation strategies evaluated. A discussion of the key findings of the research conducted, with recommendation for potential refurbishment studies in existing apartment buildings in hot climates is presented. A low-energy refurbishment design guide is proposed, a sample of which is also presented.

Chapter 8 Conclusions and recommendations

This chapter presents an overview of the research findings. It draws together the conclusions, describes the contribution to knowledge, limitations of the research and provides recommendations for future research.

Chapter 2 : LITERATURE REVIEW

2.1. Introduction

The aim of this chapter was to review what has been reported by others in order to identify the research gaps, and underpin and justify the subject of this research. A review of the climatic properties and climate classifications of the region studied is presented. The chapter further provides a description of the Greek vernacular settlements and their traditional passive cooling strategies, as well as a building classification of the domestic building stock during the last two centuries. It addresses the energy consumption of the European dwellings with a focus on the energy use in the Greek context. The importance of occupants' thermal comfort and indoor air quality, the available regulations regarding thermal comfort in domestic environments, as well as the significant role of occupants' adaptation in free-running buildings are reviewed. Natural ventilation strategies are identified, with a focus on systems originating in vernacular architecture, such as wind-catchers, and evaporative cooling towers. The chapter concludes with descriptions of modelling techniques for evaluation of airflow distribution and thermal comfort during natural ventilation in buildings.

2.2. Geographic and Climatic Properties of the Mediterranean Region Studied

Mediterranean countries are typified by unique climatic conditions (Köppen-Geiger map of Figure 2.1) with regard to the terrain morphology, influence of the sea, and patterns of vegetation and soils (Santamouris and Asimakopoulos, 1996; FAO, 1999). The Mediterranean climate also occurs in other parts of the world, for example in California, central parts of Chile, Western Cape in South Africa and south-western

Australia (Gildemeister, 2004). Simply, the Mediterranean is divided with respect to the climate and topography into: the eastern (e.g. Greece), the central, and the western zones (Santamouris and Asimakopoulos, 1996).

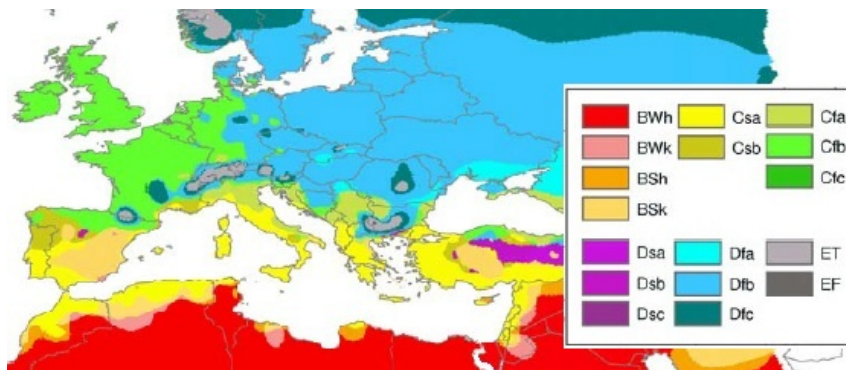


Figure 2.1 Köppen-Geiger climate types map of the Mediterranean region. Combined maps of Africa and Europe after Peel et al. (2007)

Mediterranean climate is characterised by “mild and wet winters and relatively calm, hot and dry summers” (Santamouris and Asimakopoulos, 1996). With average temperatures above 0°C (Butera, 1994; Lionello et al., 2006), the calendar year consists of primarily two seasons, the hot (June to September) and cool season (October to May), and the transitional months of May and October. The maximum yearly temperature varies between 27°C and 34°C during the hot season (Butera, 1994).

At this transitional zone between Africa and Europe the annual average wind speed exceeds the 4m/s; the highest values have been measured at Greek Islands (Butera, 1994). The Mediterranean is characterised by: uniform air moisture content distribution; annual relative humidity (RH) between 55% to 74%; and light to medium cloudiness with maximum values measured at the central and western areas during the warm period (Santamouris and Asimakopoulos, 1996). Accordingly, eastern Mediterranean regions are characterised by: the lowest levels of RH; the highest levels of wind speed recorded in a Greek islands; and the lowest values of cloudiness (i.e. over 3,000 hours of sunshine through the year).

The Greek region (the mainland, the Aegean and Ionian islands) consists of a variety of climatic Mediterranean subtypes (HNMS, n.d.). Greece is considered a mountainous country with 2,000 islands occupying more than one-fifth of the Greek land (average altitude approximately 585 metres) (IEA, 2006; Gialamas, 2011). The

air temperature drops by 6°C per 1,000 metre of elevation (Gialamas, 2011), and by 0.7°C per latitude during summer (Papamanolis, 2005).

The typical Greek weather is defined by relatively warm, dry summers and mild, rainy winters (Psomas et al., 2014) while the annual cycle can be divided into two main weather seasons: the cold and rainy (mid-October till March) and the warm and dry season (April until September) (Papamanolis, 2015b). High air temperatures, up to 45°C, have been reported during heat waves in the mainland and low as -25°C in the mountainous north regions (Papamanolis, 2005). The average relative humidity is considered to be between 65% and 75%. During the warm season, there is a period of 10 days with air temperatures between 29-35°C. In this season, the air temperature is governed by the sea breezes in the coastal zones and by north winds mostly in the Aegean sea (HNMS, n.d.).

The dominant Greek climate according to Köppen Climate Classification System is marine (between 0°C and 18°C average temperatures of the coldest months), and is specifically classified into the Mediterranean climate types of Csa (56%), Cfa (13%), Cfb (10%), Csb (9%) and Dfb (6%) as shown in Figure 2.1 (Gialamas, 2011). During the warm months, the weather is characterised by stability with clear skies, brightness and non-rainy days. Rainfall varies considerably across the country (Mpalafoutis, 2004). Research by Nastos and Zerefos (2009) shows that the wet days are proportional to latitude. For the period examined (1958 to 2007), the shortest consecutive wet days (CWD) were measured in eastern continental Greece (i.e. in Athens), as shown in Figure 2.2.

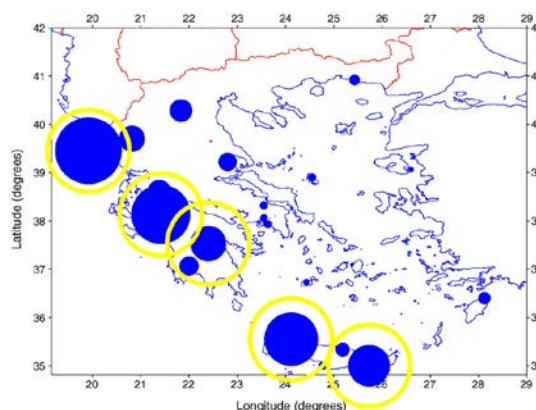


Figure 2.2 Spatial distribution of CWD trends over Greece. Proportional in size trends and rings for statistically significant trends at 95% confidence level (Nastos and Zerefos, 2009)

There is a climatic non-uniformity across Greece from north to south and from west to east. The country is divided into three zones (west, east and islands) with respect to the mountain chain of Pindus, which runs from north to south parallel to the coast and divides the peninsula and the climate into zones (Matzarakis and Katsoulis, 2005). Tassiopoulou et al. (1996) described five distinct zones in relation to the local climate, topography, latitude, wind and the proximity to sea. A more recent study conducted for the Energy Efficiency Regulation in Buildings (2010) divided the Greek climate into four zones with respect to the heating degree days.

Athens is located within the east side of the Greek mainland and has the shortest consecutive wet days (CWD) of the eastern continental Greece. The mean ambient temperature during summer is 27°C (Tsinonis et al., 1993). Wind speeds in Greek cities have been reported to be 20-30% lower than the open countryside, while the street layout and the surrounding structures influence the wind directions. However, Greece is characterised by the highest winds in the Mediterranean (Butera, 1994). However, the low ratio of the urban streets' width to the buildings' height (about 0.6) results in reduced airflows at the street level, in higher wind flows above the rooftops, and thus in low wind pressures at the buildings' façades and potential of natural ventilation via openings (Papamanolis, 2000).

2.2.1. The Heat Island Phenomenon

Industrialisation and urbanisation have a significant impact on earth's climate. People migrate from rural to urban areas, expanding the city boundaries and introducing new microclimates (Santamouris et al., 2001). It is predicted that by the end of this century more than half of the world's population will be urban inhabitants (Santamouris et al., 2001), reaching up to five billion by the year 2025 (Kolokotsa et al., 2009). The new urban microclimates are characterised by higher air temperatures to the rural suburbs, which contributes to rise of energy demand for cooling and to thermal comfort deterioration (Mihalakakou et al., 2004).

Givoni (1998) defines the urban heat island phenomenon (UHI) as the elevation of the air temperature above the temperature of the rural areas during nighttime, the intensity of which is the highest temperature difference between urban and rural areas (Oke, 1978). Typical UHI intensities vary between 3°C and 5°C, although incidents of up to 10°C have been recorded around the world (Givoni, 1998). Akbari

et al. (1992) explains that every 1°F UHI increase contributes to 1-2% increase in the peak hour demand. Mechanical cooling consumption of 260kWh/year, costs \$20 billion per year of which about \$1 billion is the cost of the UHI (Akbari et al., 1992).

The morphology and pattern of the urban heat island is unique for every region with respect to a number of variables such as the meteorological characteristics (Oke, 1978), topography (Akbari et al., 1992) and industrialisation (Mihalakakou et al., 2004). According to Akbari et al. (1992), heat island is caused by “*denuded landscapes, impermeable surfaces, massive buildings, heat-generating cars and machines, and pollutants*”. The development of an UHI is attributed to a number of factors and particularly to the thermal balance of the urban areas. Some of these are: the impermeable, non-reflective materials; the high levels of air-pollution; the heat stored in buildings’ fabric and released at night; meteorological parameters; the size, density and urban geometry of the area (Akbari et al., 1992; Givoni, 1998; Mihalakakou et al., 2004).

In Athens, a strong heat island phenomenon has been observed that has increased the ecological footprint of the city up to twice the city’s political area (M. Santamouris et al., 2007). Research conducted by Santamouris et al. (2001) using 30 weather stations installed Athens, predicted during the daytime UHI intensity of 10°C in the centre and 2-6°C in the suburbs. During nighttime, the intensity was less and about 2-5°C. It was observed that when the UHI intensity exceeded the 10°C, the cooling load of the buildings doubled and the peak electricity load tripled (Kolokotroni et al., 2007). Research conducted in a small but densely populated coastal city of Greece, Hania in Crete, predicted UHI intensity up to 8°C between 3 and 5pm (Kolokotsa et al., 2009).

In warm year-round regions and areas with summer seasons the UHI intensifies the cooling loads (Akbari et al., 1992; Kolokotroni et al., 2007). On the contrary, urban heat islands could be beneficial for cold climates and even winter seasons in warm climates, as the elevation of the urban air temperature reduces the need for heating, i.e. warmth island (Givoni, 1998). Research has shown that in cities such as London and Munich the annual heating degree days have been reduced of almost 10% and 14% respectively, relative to the rural areas (Kolokotroni et al., 2007). During the winter season the UHI intensity in Athens remains almost the same, resulting in a heating degree hours decrease of up to 40% relative to the suburbs (Santamouris et al., 2001).

2.3. Buildings Energy Consumption

The Mediterranean countries account for the highest CO₂ emission indexed to the Kyoto base year. Greece lies in the group of countries with the highest greenhouse gas emissions in Europe, as seen in Figure 2.3 (IEA, 2006; Eurostat/map, 2011; The World Bank, 2012). The CO₂ emissions in Greece have experienced a continuous increase since the 1980s (Figure 2.4) (IEA, 2006).

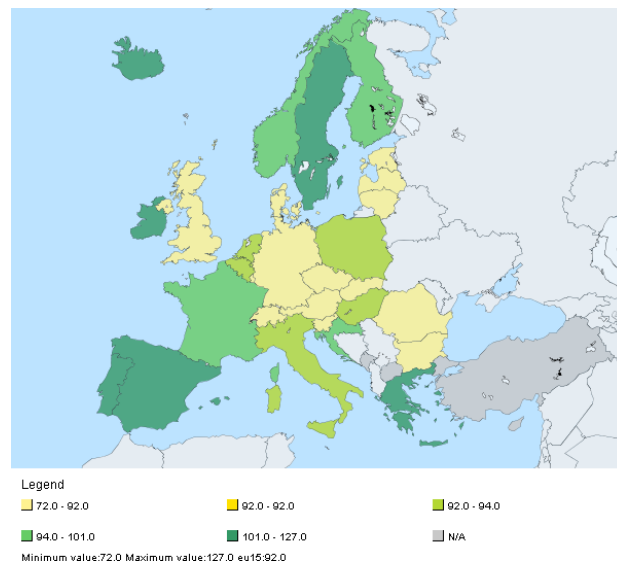


Figure 2.3 Total greenhouse gas emissions (in CO₂ equivalent) indexed to Kyoto base year (index base year = 100 – Target). (Eurostat, 2011b)

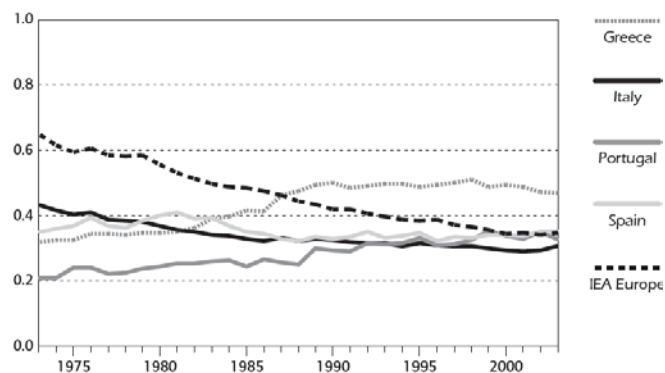


Figure 2.4 Energy-related CO₂ emissions per GDP in Greece and in selected IEA countries, 1973 to 2003 (tonnes of CO₂ emissions per thousand USD GDP using 2000 prices). Cited in IEA (2006)

The European building sector is accountable for 40% of the total energy consumption required for provision of heating, cooling, lighting and appliances (Santamouris and Asimakopoulos, 1996). Energy required for cooling and heating

accounts for 6.7% of the worlds' energy consumption that with appropriate sustainable design could be reduced by about 2.35% (Santamouris and Asimakopoulos, 1996). Energy for cooling in hot regions is two to three times more than the energy for heating (Goulding et al. 1993, cited in Santamouris and Asimakopoulos, 1996, p.35). During 2009 the European households were responsible for the 26.5% of the total energy consumption (Eurostat, 2011a), (Figure 2.5).

Greek residential buildings consume more electricity than other sectors and a little less than commercial buildings (Figure 2.6) (IEA, 2011). The annual average energy consumption of Greek buildings accounts for one third of the country's total energy consumption and up to 45% of the total carbon dioxide emissions (Balaras, 2001).

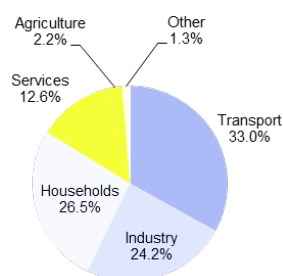


Figure 2.5 Final energy consumption of the EU-27 in 2009 (Eurostat, 2011a)

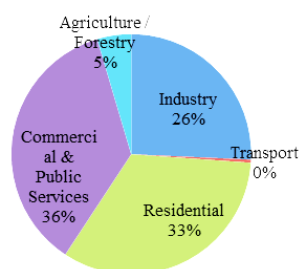


Figure 2.6 Electricity consumption shares of Greece in 2009 (IEA, 2011)

The final energy consumption of Greek households (Figure 2.7) doubled between 1990 to 2006 (from around 3Mtoe to 5.49Mtoe) (Eurostat, 2008). Domestic sector in Greece accounts for the highest energy consumption in Europe (almost 30% more than that of Spain and 50% of Portugal), considerably higher to the EU countries with colder climates (Asimakopoulos et al., 2012) and up to 24.5% of the county's total energy consumption (M Santamouris, Kapsis, et al., 2007).

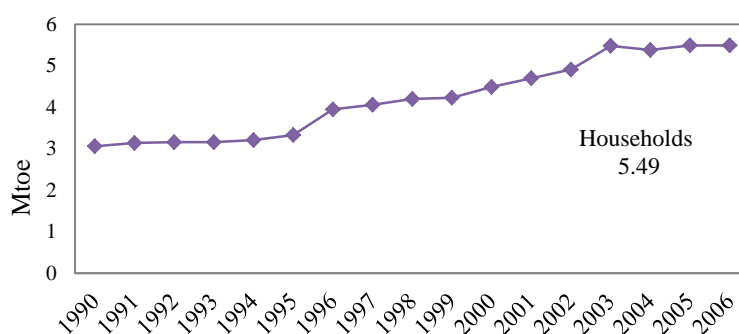


Figure 2.7 Final energy consumption of Greek households in Mtoe, after Eurostat (2008)

Mechanical cooling provides appropriate yearly control of IAQ in buildings (Santamouris and Asimakopoulos, 1996). The air-conditioning (A/C) penetration has significantly increased in Greek households during the latest years. This is due to: inadequate building design; increased internal heat gains; higher comfort expectations; improvement of living standards; urbanisation; increase of window to wall ratio (in offices large glazed façades) (Butera, 1994); and the reduction of the A/C units cost (Santamouris and Asimakopoulos, 1996). Geros et al. (1999) reported a significant increase in A/C installations in the southern European countries. In Greece, A/C installations increased more than ten times between 1987-90 (Figure 2.8), becoming dominant elements of the buildings' façades (Butera, 1994). Mechanical cooling systems were installed in more than half of the residential buildings in Greece in the 1990s (Hassid et al., 2000).

Energy consumption, summer peak electricity demand (intensive A/C use) and the cost of electricity have increased, resulting in energy shortage and frequent power cuts (Givoni, 1994; Santamouris and Asimakopoulos, 1996). High air temperatures reduce the A/C efficiency resulting in over-sizing of the mechanical cooling equipment and hence increase in the peak electricity demand (Santamouris et al., 2001; Kolokotroni et al., 2007).

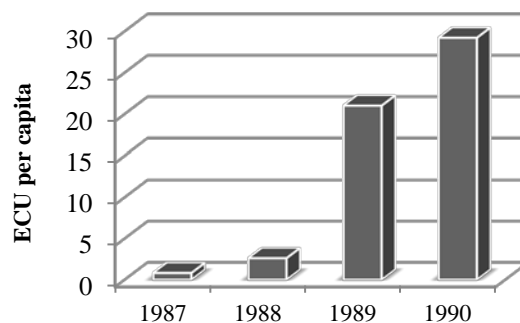


Figure 2.8 Purchase of air conditioning equipment in Greece per capita (after Butera, 1994)

Despite the widespread use of mechanical means for summer comfort, natural ventilation techniques can contribute to an appreciable reduction in indoor air temperatures and demand for cooling. O'Sullivan and Kolokotroni (2014) reported that the energy consumption of free running buildings corresponds to up to 50% less of that of air-conditioned buildings. Natural ventilation assists largely in the provision of passive cooling, thus being an important tool in the battle against climate change and the resilience of buildings for future climates.

2.4. Architectural Characteristics of Domestic Buildings in Greece

This section provides a discussion on the Greek building stock and covers two areas. Overview of the sustainable and architectural properties of the traditional settlements in rural and urban regions of Greece is provided. The development of the urban Greek buildings during the 20th century and the design characteristics of the typical Greek buildings, with an architectural and energy perspective are then presented.

Vernacular architecture exhibits traditional techniques that enhance thermal comfort and offer protection from environmental conditions (Serghides, 2010). The variety of vernacular settlements around Greece demonstrates the design expertise and construction techniques of each sub-climate of the country (Canas, 2004). Such knowledge could find application in designing sustainable buildings, as precondition for the implementation of further passive or mechanical cooling/heating/ventilation techniques. The transition from the few-storey vernacular building designs to the highly energy consuming 20th century multi-storey buildings was guided by urbanisation, industrialisation, globalisation and profit (Koch-Nielsen, 2002). It is important to restore this transition and proceed to building designs for the climate.

2.4.1. Characteristics of vernacular settlements

Building designers should turn to traditional architecture for lessons in making climate and environment to work to their advantage. Using nature in design should not be regarded as a lack of desire for modernity and progress (Koch-Nielsen, 2002). Climate change amplifies the need to achieve energy reductions through buildings while preserving the sociocultural identity of each place (Tassiopoulou et al., 1996). Vernacular architecture is defined as: the buildings of a specific place and time; product of only local materials, components and methods; built at a local dialect; and the distinct architectural identity of that specific area (Carter and Cromley, 2005; Asquith and Vellinga, 2006; Oikonomou, 2008). Vernacular knowledge should be treated as a great warehouse of know-how, important for integrating locality and sustainability to modern building practices (Asquith and Vellinga, 2006).

In the coldest Greek climates, various building typologies with similar thermal control strategies are identified. Typically they consist of a semi-open, buffer space providing further insulation and assisting the shading and ventilation of the spaces (Figure 2.9). Openings on south and east walls assist the passive heating and lighting of the buildings, and projections provide shading (Oikonomou and Bougiatioti, 2011). Thick ground floor walls support the light-weight upper floors and assist a reduction in high summer internal temperatures (Oikonomou and Bougiatioti, 2011). Natural ventilation is enhanced by the stack-effect via openings above stairwells.

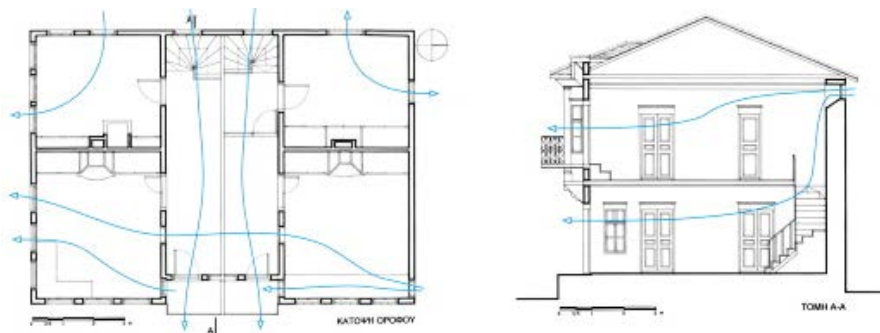


Figure 2.9 Qualitative assessment of natural ventilation in a traditional house in Florina (cited in Oikonomou and Bougiatioti, 2011, p. 683)

Towards warmer areas in Greece, buildings of rural settlements are densely built at the slope with their long axis oriented on south (Kalogirou and Sagia, 2010). Yards and open spaces ensure thermal comfort during summer. The streets layout utilise the prevailing winds. Running waters and fountains provide passive evaporative cooling. The position and layout of the openings enhance the natural ventilation (Figure 2.10). Shutters provide movable insulation in winter and shading in summer.

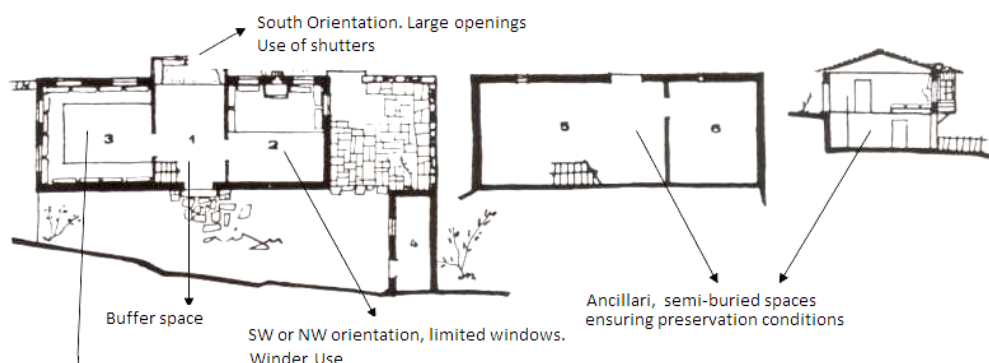


Figure 2.10 Bioclimatic elements of the vernacular architecture (Kalogirou and Sagia, 2010)

Typically, in Greek vernacular architecture, spaces with different orientation and size of openings are occupied according to the season (Kalogirou and Sagia, 2010). As an example, the three-storey dwelling build in 1791 utilises the first floor for winter accommodation and the second for summer. It is further divided horizontally into the south-communal space of the lightweight walls with large windows, and the north-private zone of the heavyweight construction (Figure 2.11).

The key environmental approach of this defensive domestic architecture is the idea of dividing the house horizontally and vertically developing a two-dimensional flow of internal migration (Figure 2.12). The second floor, the ground floor and the sheltered outdoor areas find use in summer, expressing the typical extroverted character of Greek buildings (Vissilia, 2009). Ventilation was achieved by the half closed shutters when windows were fully open and the horizontal trapdoors controlling the airflow through the floors.



Figure 2.11 Traditional dwelling in in Pelion (Sakarellou-Tousi and Lau, 2009).

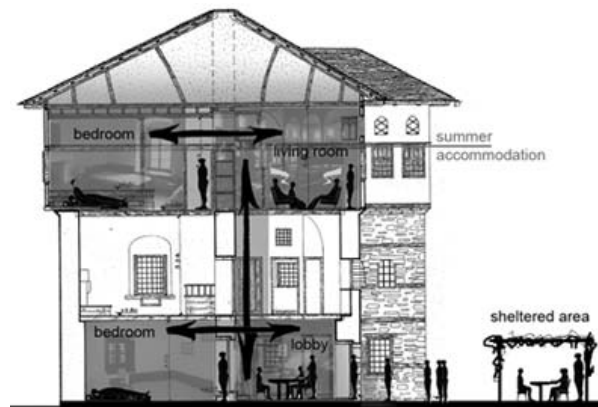


Figure 2.12 Summertime internal migration in section (Sakarellou-Tousi and Lau, 2009).

In warmer parts of Greece, such as the Islands, the urban planning involved settlements designed according to the landscapes topography, developed in linked buildings (semi-detached houses) with their exterior walls forming the outer line of fortification and the rest of the walls defining internal common spaces (Sinou, 2006). Despite their primary use for safety, these settlements were also designed for protection against climatic conditions i.e. the strong winds and sunlight (Figure 2.13) utilising small building width, whitewashed roofs and the wall thickness.

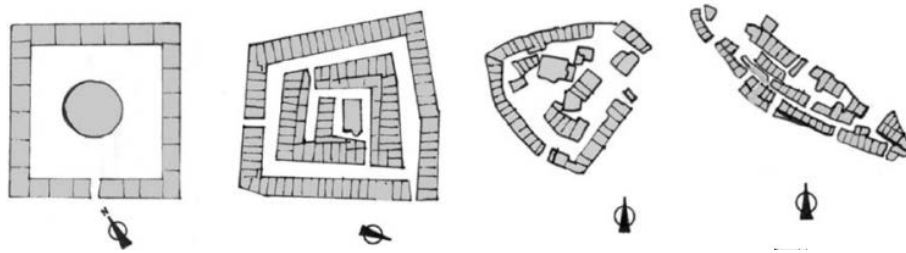


Figure 2.13 The medieval fortified buildings' layout of the villages in 4 Greek Islands, from left to right: Antiparos, Kimolos, Santorini, Siphnos (Sinou, 2006)

2.4.2. Building classifications in Greek cities since 1900

During the 20th century the political, social and economic instability, along with architectural styles and influences from abroad, shaped various architectural typologies of Greek buildings creating an aesthetic anarchy. Until today, it is difficult to define a dominant architectural type of Greek domestic buildings. The European Directive 2006/32/EC aims to achieve overall national energy savings of 9% by 2020s. This expresses the need to gain knowledge regarding the characteristics of the existing building stock, within organised collection, categorisation and analysis of the characteristics and information of the building sector (Dascalaki et al., 2010). An investigation and classification of the existing buildings stock was conducted in relation to the year of construction, the energy performance and design, in order to determine the characteristics of the typical Greek residential building.

Since the beginning of the 19th century, the morphology of Athens constitutes by small, two storeys neoclassical (Figure 2.15) and usually illegally constructed buildings. With the first tall buildings, the urban blocks were formed by a continuous line of apartment buildings at the perimeter and a non-constructed surface at the centre (Papamanolis, 2000). The construction of tall buildings was encouraged by the introduction of concrete, the increase in allowed buildings' height, and the division into smaller plots of land (I. Theodoridou et al., 2011).

According to IEA (2006), in 2001 the population of Greece was approximately 11 million, experiencing an increase of 7% from 1991. Citizens account for the 66% of the population, while 35.5% is concentrated in Attica peninsula (up to 3 million inhabitants of Athens). A type of multi-storey apartment building, known as 'polykatoikia' responded to the housing demand imposed by the population increase

and the ever-growing urbanization, and dominated the cityscape (Figure 2.14) (Papamanolis, 2006).



Figure 2.14 Refugee apartment building at Alexandras Avenue, Athens, 1933-1935 (Drymiotis, 2014)



Figure 2.15 Neoclassical 2-storey, Tripodon Street, Athens (Roubien, 2014)

In 1929, the first general construction regulation established the horizontal ownership and the use of elevators (I. Theodoridou et al., 2011). The density of the buildings increased against common spaces. All these formed a period of lack of innovative architectural design that continues today (Figure 2.16 and Figure 2.17).



Figure 2.16 Apartment building of 1950-90s. Saronida, Greece (photograph by author, 2012)



Figure 2.17 Two-storey apartment building in Saronida, Greece (photograph by author, 2012)

Following the general construction regulation of 1955, a continuous building system of blocks is formed in densely built centres of cities (I. Theodoridou et al., 2011). Greece is one of the most seismogenic places in the world lying at the meeting point of the lithospheric plates of Europe and Africa (Papamanolis, 2005). The Greek

Seismic Code of 1999 proposed the use of strong supporting structures, leading to a new construction and architectural element, the Pilotis (empty space at the ground level), as shown in Figure 2.18 (I. Theodoridou et al., 2011).



Figure 2.18 Modern apartment building with pilotis used for parking area in Saronida, Greece (photograph by author, 2012)

Apartment buildings usually consist of a ground floor and a series of floors (maximum seven) with repeated floor layout (Papamanolis, 2006). The ground level is usually not occupied (ancillary spaces, heating equipment) and the ground apartments are at a raised level (around 1.50m). They have accessible terraced roofs, accommodating the penthouses, reinforced concrete supporting structure and walls of perforated double brick rows with internal insulation.

Balconies are dominant façade features of Greek residencies, formed in different shapes and styles of parapets (railing, solid or translucent). Balconies act as shadings, reduce external noise by creating barriers, control wind forces and thus the natural ventilation distribution of the spaces (Papamanolis, 2005). Balconies create strong wind pressure gradients on the windward façades, enhancing the positive pressures (Papamanolis, 2000). However, as balconies are non-insulated they result in thermal bridges. Typically Greek balconies and openings are shaded by operable awnings of canvas blinds suspended from each balcony, controlled by hand-operated systems (Papamanolis, 2006).

The majority of the Greek dwellings are naturally ventilated (Papamanolis, 2000). In domestic buildings, wet spaces mainly facilitate extractor fans when access to fresh air is not somehow else provided. Despite the high buildings' density and the small sizes of indoor spaces, Papamanolis (2006) argues that natural ventilation in apartment buildings could be potentially benefited by utilising the pressure

difference across openings and the occasional use of light wells. Further, Stavrakakis et al. (2010) suggest that in hot humid climates such as in Greece, nighttime ventilation could be an efficient alternative to air-conditioning use.

A thermal comfort field study by Sakka et al. (2010) in ten residential buildings in Athens during the summer months of 2009 predicted that for typical summer outdoor conditions of 39.7°C maximum DBT, indoor air temperatures varied between 23 and 38.9°C. Highest temperatures were recorded for east facing, without shading dwellings. Relative humidity was measured to be approximately 40.5%. Mean air temperatures of 30°C were predicted for 70% of the period and up to 35°C for 40%.

In response to climate change, energy dependency in foreign countries and the need for energy improvement of the existing building stock, Greece committed to EU and Directive 2002/91/EC (Energy Performance Building Directive, EPBD) of the European Parliament to proceed into relevant national regulations (Argiriou et al., 2010). In our days, in response to the economic situation of the country, construction activity continues but in a slower pace to the previous period. The construction of the multi-family buildings has shown a decline, relative to the single-family contemporary style houses (Figure 2.19). According to published data of the Hellenic Statistical Authority in 2010, the construction sector is under a deep depression with a drop of more than 62.4% since 2008 (Theodoridou et al., 2012).



Figure 2.19 Contemporary single families dwelling, built in 2011. Saronida, Greece (photograph by author, 2012)

The first thermal insulation regulation of buildings in Greece introduced in 1979, was used until September 2010 as a generic tool with the aim to improve the energy behaviour of buildings (I. Theodoridou et al., 2011). In 2010 the new energy performance building regulation (abbreviated from the Greek letters as KENAK), was published. This energy certification regulation is compulsory for existing, newly build and new buildings. It includes measures for systematically energy consumption

reduction with regard to the building properties and operation (Gaglia, 2010). The accompanying software (TOTEE) provides energy rating categories expressed on primary energy consumption values (kWh/m²) (Gaglia, 2010). The buildings are classified on a percentage relative to a reference building: a building automatically designed by the software always rated Energy Class B. Newly builds or refurbished buildings must be rated higher than Class B.

The Greek energy regulation was introduced to set tighter energy standards for the newly constructed buildings and achieve up to 20% energy savings (Iatridis and Karamani, 2009). However, for the existing building stock would be required *“drastic energy renovation interventions to off-set the poor quality of construction practiced until the 1990s”*(Theodoridou et al., 2011). As most construction activity in Greece occurred before the introduction and implementation of the first thermal insulation regulation, it is estimated that the majority of the existing building stock (around 71%) is non-insulated (I. Theodoridou et al., 2011). According to the Greek Ministry of Development (n/a) the ratio of energy consumption and of heating/cooling cost in buildings, with and without insulation is 1 to 3 respectively. Balaras (2001) describes that although insulation today is mandatory in Greece, only 5.1% of the domestic sector has wall insulation, 30.4% roof insulation, 12.7% pilotis insulation, 1.5% floor insulation and 2.1% double glazed. However, the enforcement of the energy performance building regulation has coincided with a deep economic depression (Papamanolis, 2015a). Within the first three years of the legislation enforcement, energy inspections have been performed in just 509,000 buildings.

Energy consumption in Greek dwellings experienced an increase of 72% between 1990 and 2007 (Iatridis and Karamani, 2009). Papamanolis (2006) argues that the limited construction of low energy designs is related to the limited knowledge of designers in the field, and occupants’ indifference to energy savings. The thermal energy consumption in Greek domestic buildings varies on average between 70 to 155kWh/m²/year (Dascalaki et al., 2010), although in multi-storey apartment buildings in the climatic region of Athens it has been predicted up to 220kWh/m²/year (Papamanolis, 2015a).

A survey in domestic Greek buildings shown that, 70% of occupants operate air-conditioning systems (A/C) during summertime, and 45% fans (Drakou et al. 2011). The A/C units would simultaneously operate with natural night-ventilation to provide

reductions in indoor temperatures during nighttime and reductions in air pollutants. Yun and Steemers (2011) argue that A/C ownership in dwellings is strongly linked to climate and household income. The most dominant factors defining the A/C operation are physical parameters (e.g. climate), the occupants' behaviour (frequency and spaces), socioeconomic factors (e.g. income, age, size of property), and outdoor conditions.

The relation between income and energy consumption (official figures of the 1991 national survey and sample of Athenian households), showing that 52% of the buildings examined were fully or partly insulated (without considering its condition) and 45% had double-glazing (M Santamouris, Kapsis, et al., 2007). The percentage of households with at least one A/C unit varied between 48% and 69% for the lower and higher income occupants respectively. The lower the income the higher: the percentage of occupants in apartments; the age of the building (around 30 years); the percentage of non-insulated walls and single-glazing windows; and the density of installed A/C units (M Santamouris, Kapsis, et al., 2007). Considering that more than 20% of Greek households suffer from fuel poverty (i.e. they spend more than 10% of their income for energy (Guy Palmer, 2002)), the relative cost for comfort for the lower income occupants in cold and warm months is higher.

Greek cities have similar town-planning characteristics. Atmospheric pollution remains a significant factor affecting comfort in open urban spaces, despite a number of measurements to achieve EU targets for greener cities (Ministry for the Environment, 2009). The concentrations of common air pollutants have been recently reduced as reported by (Papamanolis, 2015b). However, indoor air quality measurements in 50 households in Athens predicted high levels of indoor pollution (up to 1800ppm); this was correlated to the low measured ventilation rates. Increase in ventilation rates could significantly improve the indoor environmental quality of the dwellings (M Santamouris, Argiroudis, et al., 2007). The most typical air-conditioning system used in dwellings is the individual split unit installed per building space. These operate by re-circulating and cooling the existing indoor air; no ventilation is provided. All these indicate that the potential of natural ventilation, in an urban environment with even higher levels of air pollution with regard to the time of the year and the day (Papamanolis, 2015b), would provide occupants' comfort and adequate indoor environmental quality.

Despite the limited enforcement of the “energy performance building regulation” (KENAK) and the significant reduction of the construction and refurbishment rate of buildings due to the economic depression, an upward trend in renewables in buildings was observed during this period. It is possible that under the economic recession and the new legislation, occupants are more sensitive to energy efficiency in buildings and to the related measures (Papamanolis, 2015a).

These findings suggest that improvement of the existing building stock and use of alternatives to conventional mechanical cooling techniques could improve comfort especially in low-income households and decrease the environmental pollution from buildings. Introduction of bioclimatic strategies in modern building designs could temper extreme weather conditions by utilising natural resources of energy.

2.5. Thermal Comfort and Indoor Air Quality in Free-Running Buildings

Occupants spend more than 80% of their time indoors (at home, the workplace or either at places of leisure). Indoor air quality has become an important public health concern (Assimakopoulos et al., 2008). The relation between poor health and inadequate buildings design has been recognised and is a major concern of the authorities. Enhancements of IAQ (caused by pollutants within the spaces or from external sources) should be treated as equally important as the significance of the outdoor air quality improvement (Emmitt, 2012).

Thermal comfort is described by ASHRAE 55-2004 as the “*state of mind which expresses satisfaction with the thermal environment*” (ASHRAE, 2009). Several studies have predicted that the thermal comfort ranges defined by comfort indices such as the PMV (predicted main vote) and PPD (predicted percentage dissatisfied), are more suitable in static, controlled environments (Nicol, 2004; Moujalled et al., 2008; Peeters et al., 2009; Wang et al., 2010). The Fanger model itself, was created in steady state laboratory experiments and thus ignores the psychological aspect of adaptation, which is the changing perception of the thermal environment (de Dear and Brager, 2002; Peeters et al., 2009). Occupants proceed to adaptive adjustments either consciously or unconsciously (ASHRAE, 2009). This adaptation may refer to psychological, physiological, and acclimatization parameters (Brager and Dear, 2000; Peeters et al., 2009; Wang et al., 2010).

Peeters et al. (2009) argued that as the majority of domestic buildings are free running, they are highly unlikely to be steady state and that there is lack of available data on domestic thermal comfort. Research conducted in naturally ventilated Greek residential buildings during summer period predicted that the PMV often overestimated the subjective warm (Sakka et al., 2010). The thermal environment in naturally ventilated buildings changes in response to the outdoor environment. It is thus important to acknowledge and predict the indoor comfort temperature (the temperature were most occupants feel comfortable at) and to engage the results of adaptation (Nicol and Humphreys, 2002).

2.5.1. Energy benchmarks

International, national regulations and energy guides provide set point values for the higher and lower comfort conditions at which occupants feel comfortable. These are usually used for the sizing of systems and for the evaluation of thermal comfort. The BSEN15251 standard defines minimum comfort indoor temperature in existing buildings of 22°C during summer, and 18°C during winter (BS EN15251 CEN, 2007). Further, CIBSE Guide A defines summer temperature thresholds for comfort (operative temperature) for non-air conditioned buildings in the UK of 25°C in living spaces and 23°C in bedrooms. It is specified that sleep could be impaired above 24°C (CIBSE, 2006). In order to avert overheating, no more than 1% of the occupied hours should exceed the 28°C in the living spaces and the 26°C in the bedrooms (CIBSE, 2006).

The Greek technical directive TOTEE 20701-1/2010 was developed according to international standards (e.g. ISO 15251:2007 and ASHRAE 62.1-2010), with aim to set national standards for the calculation of the building energy performance of new and existing buildings. Internal air temperatures for dwellings of 20°C in winter and 26°C during summer, and relative humidity of 40% and 45% respectively are suggested (Androutsopoulos et al., 2012). CIBSE Guide B, suggests relative humidity in domestic buildings no more than 70% for prolonged periods (CIBSE, 2005). For adequate ventilation, CO₂ concentrations between 800 and 1000ppm are considered acceptable in the UK and between 600 and 800ppm in Sweden. Also, CO₂ levels between 600 and 1000ppm can contribute to stiffness (CIBSE, 2005). Further, ASHRAE defines acceptable CO₂ levels of 1000ppm (ASHRAE, 2013).

Recommended values of ventilation rates in dwellings for IAQ are the 15m³/hour per person (4.17 l/s/person) and 0,75m³/h/m², as in 100m² correspond five people (Androutsopoulos et al., 2012). CIBSE Guide A recommends minimum values of air changes per hour (ACH) in dwellings of 0.4-1 in living spaces and 60l/s/person in kitchens (CIBSE, 2006). Accordingly, in Greek apartments with estimated number of seven person per 100m², the minimum ventilation rates should be 8.5m³/h/person in living spaces and bedrooms, and the recommended between 12 and 17m³/h/person (Dimitroulopoulou, 2012). In addition, for bathrooms and kitchens the suggested minimum ventilation rates are 34m³/h/person, and the recommended between 50 and 85 m³/h/person. ISO 7730 recommends mean air velocity less than 0.25m/s for

moderate environments during cooling. However, assessment of predicted percentage dissatisfaction suggests that air velocities up to 1m/s can offset high indoor temperatures (CIBSE, 2005). With regard to mechanical ventilation, in order to provide adequate background fresh air ventilation between 1 to 2ach⁻¹ would be acceptable and in order to achieve adequate cooling by ventilation between 5 and 10ach⁻¹ (CIBSE, 2005).

Despite the recommended values ventilation rates by standards, research has shown that high values of air change rates when delivered in unoccupied spaces during the night, contributes in significant reductions in air temperatures at the next day (Geros et al., 1999). Air change rates of 10, 20 and 30ach⁻¹, provide peak temperature reduction of up to 0.6°C, as well as reduction of the daily mean by 1.6°C. Measured values of air change rates in an existing free running building in Greece, were predicted with large standard deviation (Figure 2.20). Further, and experimental work in Greek apartment buildings in Athens by Niachou et al. (2005) reported high values of ACH in cross ventilated apartments, reaching up to 20ach⁻¹. Up to 5ach⁻¹ have been measured in residential buildings during winter (M Santamouris, Argiroudis, et al., 2007).

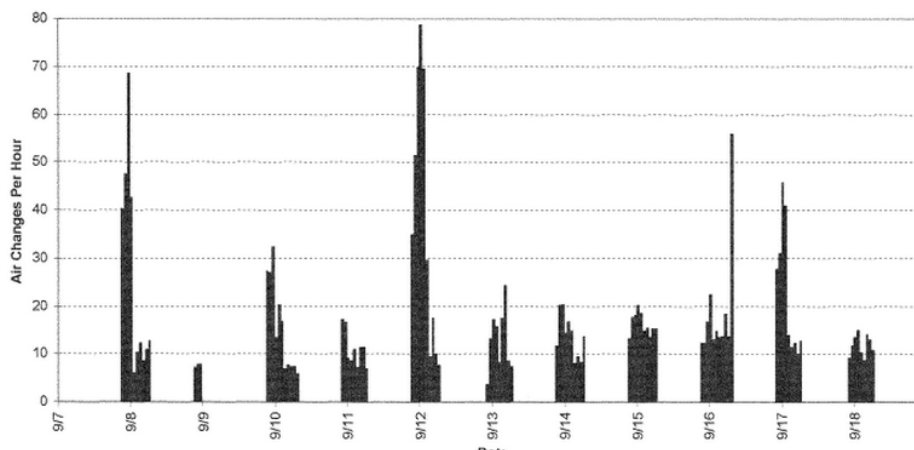


Figure 2.20 Measured air change rates in a naturally ventilated building in central Athens, under night ventilation (Geros et al., 1999)

Literature reviewed by Sundell et al. (2011) reported the association between ventilation rates and indoor air pollutants. It was concluded that lower ventilation rates result in health related problems, i.e. sick building syndromes. Occupants prefer indoor air movement within a range defined with regard to both ambient and local parameters (Gong et al., 2006). Cândido et al. (2011) concluded that the benefits of increased air velocities highly involve occupants' thermal comfort in warm climates.

Higher air speeds extend the comfort limits and deliver direct physiological cooling (Givoni, 2011). Further research on thermal comfort by Cândido et al., (2008) considered acceptable indoor air speeds between 0.2-1.5 m/s. However, 0.2m/s is regarded as the upper acceptable limit of draft perception by ASHRAE Standard 55 (Cândido et al., 2008). Higher limits are usually established to avoid drafts. Although drafts are a relevant concern in cold climates, they are not in warm climates (Cândido et al., 2011). Further, Gong et al. (2006) reported occupants' preference in higher velocity ranges relative to the values of ASHRAE Standard 55, and described an urgent need for further research in hot and humid climates.

Research by Cândido et al. (2008) (232 participants) identified the relationship between indoor air speed, operative temperature and comfort perception for the climate of Brazil. It was predicted that, occupants require higher indoor air speeds of the values suggested in the literature, in order to improve their thermal comfort condition. The participants were comfortable in operative temperatures between 26.5°C and 27.5, and air speeds between 0.25-0.5m/s. For air speeds exceeding 1.5m/s and operative temperature up to 25.5°C, approximately 80% of the participants expressed no interest for additional or less air movement.

Field survey by Khedari et al. (2000) in Thailand classrooms reported that 80% of the occupants perceived as comfortable indoor temperature up to 34°C, for corresponding indoor air velocities of 3m/s. Gong et al. (2006) reported that occupants in Tropical climates prefer air velocities between 0.3-0.45m/s and 0.3-0.9m/s for ambient temperatures of 23°C and 26°C respectively. Cândido et al. (2011) defined a relationship between the lowest values of indoor air speed and the operative temperatures, which provide information regarding the 80% and 90% occupants' acceptability for thermal comfort (Figure 2.21).

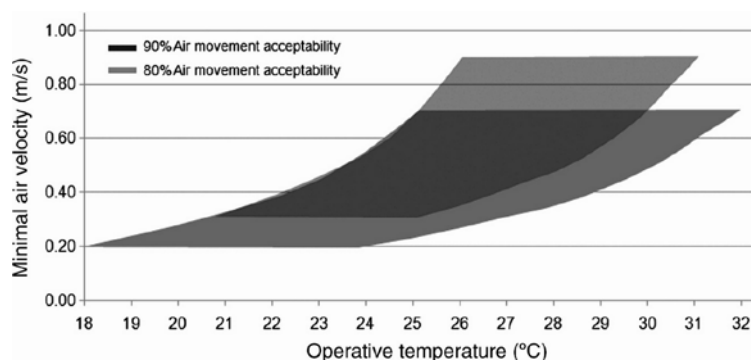


Figure 2.21 Minimum indoor air velocities required corresponding to 80% and 90% air movement acceptability (Cândido et al., 2011)

2.5.2. Adaptive thermal comfort model

As previously described, occupants' thermal comfort expectations differ between conditioned and free-running buildings. Although CIBSE Guide A suggests summer comfort temperatures between 23-25°C, research by Sakka et al. (2010) exhibited that occupants consider as neutral temperatures between 27-28°C. Adaptive thermal comfort standards should be considered in free-running buildings as they allow designers to consider occupants' natural ability to adapt. They have been developed with data from measurements in real buildings, and they offer methods to assess the acceptability of indoor comfort relative to external temperatures and conditions.

Adaptive control algorithms (ACAs) have been developed as alternatives to static thresholds of temperatures, providing a range of indoor comfort temperatures in response to other climatic parameters which occupants feel comfortable at. ASHRAE standard 55-2004 provided an adaptive equation (Nicol and Humphreys, 2010) defining comfort temperature as:

$$T_c = 0.31T_{om} + 17.8 \quad (2-1)$$

where T_{om} is the monthly mean outdoor temperature (°C)

The British standard, EN15251 suggests a different ACA that derived by the SCATs (Smart Controls and Thermal Comfort) measurements, specifically for Europe (BS EN15251 CEN, 2007), and is considered an improvement to the ASHRAE standard 55-2004 (Nicol and Humphreys, 2010):

$$\Theta_o = 0.33\Theta_{rm} + 18.8 \quad (2-2)$$

where Θ_{rm} is the running mean outdoor temperature (°C). This equation defines the operative temperature (Θ_o) for comfort, which can be treated as the comfort temperature, T_o . These limits apply for Θ_{rm} below 30°C, whereas indoor operative temperatures above 25°C could be balanced with increased ventilation rates, as shown in Figure 2.22 (BS EN15251 CEN, 2007). Acceptable ranges of upper and lower limits are provided to accommodate three categories of buildings with regard to their thermal performance. The European union project, SCATs involved measurements in 26 European free-running offices (Nicol and Humphreys, 2010).

The standard was developed for non-industrial buildings and is applicable for single domestic buildings, apartment buildings and offices (BS EN15251 CEN, 2007).

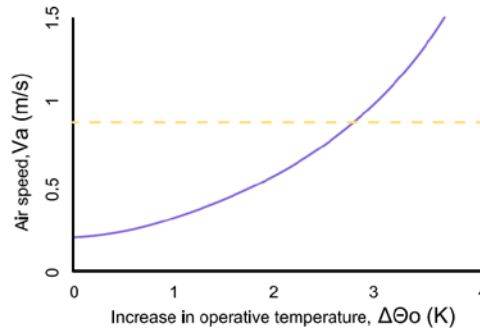


Figure 2.22 Air speed required to offset increased temperature after BS EN15251 CEN (2007)

Although the equations given by ASHRAE 55-2004 and EN15251 standards (Equations 2-1 and 2-2) appear similar, they are not identical. The outdoor temperature is defined with different methods using monthly mean and running mean temperatures respectively. This allows Equation 2-2 to utilise varying weather conditions. Also, different databases were used for the prediction of the equations, and due to that, Equation 2-2 is considered directly applicable in European buildings (Nicol and Humphreys, 2010). Although equation 2-1 is only applicable in naturally ventilated buildings, Equation 2-2 is widely applicable in buildings during free-running modes (Nicol and Humphreys, 2010). Observations by Roetzel et al. (2011) regarding the two equations suggest that, the former allows for lower temperatures while the latter for higher temperatures.

In response to this, a variety of Adaptive Control Algorithms (ACAs) has been developed to assist the individual requirements of different climates as described in the literature (McCartney and Nicol, 2002; Luo et al., 2007; Wang et al., 2010). An individual ACA was generated through the SCATs' project measurements exclusively for Greece (McCartney and Nicol, 2002) expressed by the equation:

$$T_c = 0.205T_{RM80} + 21.69 \quad (2-3)$$

where T_c is the comfort temperature ($^{\circ}\text{C}$) and T_{RM80} the running mean outdoor temperature for index 0.80 ($^{\circ}\text{C}$). Santamouris and Sfakianaki (2009) argue that very high dry-bulb temperatures during summer in the hot Mediterranean climates, allow occupants to find acceptable and feel comfortable at indoor temperatures exceeding the 26°C .

Two further equations are used, provided by EN15251, for the prediction of the exponentially weighted running mean of the daily mean external temperature Θ_{ed} :

$$\Theta_{rm} = (1-\alpha) \Theta_{ed-1} + \alpha \Theta_{rm-1} \quad (2-4)$$

$$\Theta_{rm} = (\Theta_{ed-1} + 0,8 \Theta_{ed-2} + 0,6 \Theta_{ed-3} + 0,5 \Theta_{ed-4} + 0,4 \Theta_{ed-5} + 0,3 \Theta_{ed-6} + 0,2 \Theta_{ed-7}) / 3,8 \quad (2-5)$$

Where Θ_{rm-1} is the running mean temperature for the previous day and Θ_{ed-1} is the daily mean external temperature for the previous day, using for α , the recommended constant of 0.8.

2.5.3. Occupants' adaptation and control

There is a strong link between occupants' behaviour and energy use in buildings. In free running buildings, controls are consciously utilised by occupants in response to discomfort (Raja et al., 2001; Yun and Steemers, 2008; Zhang and Barrett, 2012). Roetzel et al. (2010) concluded that energy performance modelling which neglects occupants' behaviour could be a source of error. The lack of guidelines for occupants' behaviour creates a gap in the world of building energy simulations. Most studies have been conducted in offices (Herkel et al., 2008; Yun and Steemers, 2008; Roetzel et al., 2010) rather than in residences (Papakostas and Sotiropoulos, 1997; Becker and Paciuk, 2009; Encinas Pino and de Herde, 2011), despite the amplified energy consumption of the domestic sector. This expresses a need to quantify and define such a set of standard behaviours (Andersen et al., 2009; Fabi et al., 2012).

Adaptation is defined by BS EN15251 (2007) as the “*physiological, psychological or behavioural adjustment of building occupants to the interior thermal environment in order to avoid discomfort*”. In non-mechanically ventilated buildings these behavioural adjustments often respond to the effect of the external environment to the internal (BS EN15251 CEN, 2007). Physical, physiological, psychological and social factors, affect occupants' behaviour and interaction with the available controls (Mavrogianni et al., 2014). According to literature, operation of blinds, curtains and primarily of windows, significantly influence the indoor climate (Raja et al., 2001).

Blinds are operated according to thermal, visual comfort, privacy etc. and less frequently to windows (Raja et al., 2001; Van Den Wymelenberg, 2012).

There is a substantial correlation between occupants' interaction with windows and indoor (Yun and Steemers, 2008) and outdoor temperatures (Herkel et al., 2008; Andersen et al., 2009), although it remains unclear which is the most appropriate indicator of the occupants interaction with windows (Fabi et al., 2012). The percentage of open windows in office spaces increases with the rise of the outdoor temperature up to a certain value (20°C) (Herkel et al., 2008). Raja et al. (2001) reported that for temperatures above 25°C the majority of windows in naturally ventilated offices were open, and reaches the maximum at temperatures exceeding 27°C. On the contrary, field study in Greek residential buildings showed that occupants consider temperatures of 27-28°C neutral (Sakka et al., 2010).

In dwellings, the number of open windows is higher during the morning and early afternoon (cooking activity), it increases during the housecleaning, and then gradually reduces during the afternoon until the return of the working occupants (around 5pm) (Papakostas and Sotiropoulos, 1997; Fabi et al., 2012; Mavrogianni et al., 2014). Furthermore, the percentage of open windows reaches the peak during summer (Herkel et al., 2008; Roetzel et al., 2010); the season with the most difficult to predict window opening patterns (Papakostas and Sotiropoulos, 1997).

Season, gender, floor level, and personal preference, are all influencing factors of the end-of-day position of windows in mixed mode office building (Wei et al., 2013). Research in office spaces by Roetzel et al. (2010) shown that occupants would willingly sacrifice fresh air in order to eliminate possible drafts, in response to wind speed and direction. However, research conducted in dwellings by Andersen et al. (2009) reported that wind speed is not a relevant factor. Drakou et al (2011) predicted that occupants in naturally ventilated Greek dwellings interact with windows and balcony doors to achieve comfort with regard to IAQ (by 67%) and the indoor temperature (by 32%). External openings remain closed in order to avoid overheating. Occupants are considered to proceed in control of the openings and the shading systems between two to three times daily (Drakou et al, 2011).

2.6. Natural Ventilation and Cooling Strategies

Cooling applications (i.e. the process of attaining lower indoor temperatures and humidity levels relative to the outdoor conditions) have advanced through the years, from traditional passive techniques such as wind towers, shadings and water features, to some more or entirely mechanical systems, e.g. air conditioners (Santamouris and Asimakopoulos, 1996). Ventilation is necessary for: IAQ (removal of stale air, odours and harmful chemicals); provision of natural cooling (excess heat reductions) during or not the occupied periods; removal of heat and pollution at localised sources; and prevention of condensation of the building fabric (CIBSE, 2005). Essential ventilation rates vary according to the building zone (Cook, 1998) and occupants' needs.

Air-tight buildings and reductions in ventilation rates have led to reported concerns over IAQ (Lai et al., 2009). The sick-building syndrome is a significant problem of modern buildings (Raw et al, 1992) during which, occupants' may experience discomfort, headaches, fatigue, significant health effects (e.g. asthma, allergies, infections) and loss of productivity in spaces without adequate forced ventilation (Emmitt, 2012; Dimitroulopoulou, 2012). Study in bedrooms in Singapore predicted high CO₂ values (>1000ppm) when A/C was in operation during bed-time, relative to free running modes (Wong and Huang, 2004). Occupants would experience more sick-building syndromes during the mechanical cooling of the bedrooms. On the contrary, use of outdoor air for natural ventilation should be also treated with concern as epidemiological studies associate outdoor air pollutants to severe illnesses (Sundell et al., 2011).

Natural cooling and ventilation systems describe “*all naturally occurring processes and techniques of heat dissipation and modulation, as well as overheat protection and related building design techniques*” without any energy input from mechanical systems (Santamouris and Asimakopoulos, 1996). Passive and natural cooling is achieved by: thermal and solar protection techniques (e.g. solar control, form and layout); heat gain modulation (e.g. thermal storage capacity of the building); and heat dissipation (Santamouris M., 2006). The term passive cooling refers to the two first techniques. Natural cooling involves disposal of excess heat to environmental sinks

(ambient air, sky, ground and water) from spaces with higher air temperatures (M Santamouris, Pavlou, et al., 2007). The performance is dependent to the availability of sinks, the thermal coupling and temperature (Santamouris M., 2006).

Givoni (1994) reports that appropriate application of bioclimatic architecture (building layout, orientation, details of windows etc.) could provide indoor conditions similar to the external. To achieve lower indoor air temperatures, natural cooling would be required. The key practices of heat dissipation techniques are classified by Givoni (1994) and Santamouris and Asimakopoulos (1996) as the radiant cooling (sky), soil cooling (ground), natural ventilation (air), and direct/indirect evaporative cooling (water). Their application and applicability are described in Table 2.1.

Table 2.1 Applicability of natural cooling techniques. After Givoni (1994) and Santamouris and Asimakopoulos (1996)

Strategies	Applicability	Applications
Comfort ventilation	Warm, humid regions Small diurnal range (<10°C) At indoor air speed of 1.5-2m/s external air temperature should not exceed 28-32°C (Givoni, 1994)	Ventilation via openings Wind-catchers
Night ventilative cooling	Regions with large diurnal range Higher than the comfort zone upper limit (air speed around 1.5m/s) Daytime temperature 30-36°C Nighttime temperatures < 20°C Security concerns (Givoni, 1994)	Atrium Solar chimneys Dynamic façades
Radiant cooling	Any area with low cloudiness at night Non-dependent on relative humidity (Givoni, 1994)	High-mass concrete roofs Roof ponds Roof externally insulated during daytime (Batty et al., 1991) Whitewashed vaulted roofs (Stasinopoulos, 2006)
Evaporative cooling	Indirect: in areas with around 25°C WBT and maximum DBT 46°C Direct: areas with 22-24°C WBT and max DBT 42-46°C (Santamouris and Asimakopoulos, 1996)	PDEC tower Water elements and features
Soil cooling	Indirect: Hot summers, cold winters Direct: Hot, dry areas with mild winters (Givoni, 1994)	Earth-integrated buildings System of underground pipes circulating air from the building

2.6.1. Natural day and night ventilation strategies

Natural or forced ventilation provides direct human comfort (i.e. comfort ventilation) and by cooling the thermal mass during nighttime reduces the internal daytime temperatures (i.e. diurnal ventilative cooling) (Givoni, 1994). Natural ventilation is the air exchange between indoor spaces and the environment within openings (Papakonstantinou et al., 2000). The efficiency of natural ventilation systems depends on the building design and properties (such as orientation, openings size, location, building shape, form), the site characteristics (surrounding buildings, microclimate) and occupants' behaviour (interaction with the building envelope and openings) (Koch-Nielsen, 2002; Jiru and Bitsuamlak, 2010).

Natural ventilation is one of the most common applications of natural cooling that employs two distinct mechanisms: the natural forces of pressure difference induced by wind (wind-driven ventilation); and the temperature gradients between interior and exterior (buoyancy-driven ventilation) (Santamouris and Asimakopoulos, 1996; Cook, 1998; Jiru and Bitsuamlak, 2010; Prajongsan and Sharples, 2012; Dehghan et al., 2013).

Single-sided ventilation occurs when all external openings are located only in one wall, commonly found in urban buildings with one exposed façade (Dascalaki et al., 1999; Visagavel and Srinivasan, 2009). Cross ventilation is dependent on the wind properties and the pressure difference across all openings (Dascalaki et al., 1995). Comfort ventilation, occurs when the external air penetrating at higher speeds the occupied spaces, delivers direct physiological cooling, during air temperatures up to 30°C (Givoni, 1994). Natural ventilation in apartment buildings in Greece is usually provided via single-sided or cross ventilation (Niachou et al., 2005).

The efficiency of night ventilation depends on: the airflow rates; the thermal mass properties; the internal-external temperature difference; and the daytime ventilation (Santamouris et al., 2010). Night ventilative cooling is suitable in regions with lower night temperatures below 22°C as the efficiency of the strategy increases with the reduction in night DBTs (Graça et al., 2002). In areas with daytime temperatures above 36°C, passive cooling strategies should be considered in addition to night ventilation (Givoni, 1994).

Natural ventilation strategies have been widely evaluated in buildings, such as the traditional Italian semidetached dwelling (Cardinale et al., 2003), the application of traditional Korean openings in a contemporary house to satisfy thermal comfort (Kim and Park, 2010), and the vernacular settlements of Zevareh (Iravani et al., 2009). Graça et al. (2002) evaluated the ventilation efficiency of wind-driven day and night ventilation for an apartment building in Beijing. Although day ventilation delivered comfort, the performance of night ventilation was significant and able to counterbalance up to 90% of the need for mechanical cooling.

In hot humid climates such as in Greece, night ventilation can be an efficient alternative to air-conditioning (Geros et al., 1999; Stavrakakis et al., 2010). Santamouris et al. (2010) evaluated the efficiency of night ventilation in 214 single family air-conditioned dwellings of suburban and rural zones in Greece. It was reported that nocturnal ventilation reduced the cooling load by up to 40 kWh/m²/year (12kWh/m²/year on average), while the ventilation efficiency increased in response to higher initial cooling needs. Further, the benefits of ventilation within a stairwell (13m height) of a three-storey naturally ventilated dwelling outside Athens were explored using computational fluid dynamics (CFD) simulations. These were validated using measurements from real scale (Peppes et al., 2002). The geometry of the stairs provided a relatively steady velocity distribution, and the temperature difference between the floors, resulted in dual upwards and downwards flow.

2.6.1.1. Façade relief elements

Natural ventilation in urban environments is subject to the urban geometry that modifies the prevailing winds, with regard to both speed and direction, due to the densely high-rise buildings (Cheung and Liu, 2011). Single-sided ventilation of apartment buildings, commonly found in urban areas, could be improved by exploitation of façade relief elements or green features, such as the wing walls, balconies, overhangs, shadings (Mohamed et al., 2009; Mohamed et al., 2011). Façade reliefs are building features regulating noise and air-borne pollutants. They control heat, air and daylight transfer between the external and internal environments (Mak et al., 2007).

Balconies are façade relief elements reducing the vertical wind flow movement against the façades. Mohamed et al. (2009) used CFD to investigate the influence of

balconies to the airflow properties at different heights of an apartment building. The balconies contributed to higher wind pressures at the façade, provided cross ventilation of indoor spaces, which reduced the effectiveness of wind driven single-sided ventilation. Likewise, wind-walls are vertical fins that channel air to the interior of spaces (Mak et al., 2005). Using CFD models Mak et al. (2007), predicted that wing walls could sufficiently increase the ventilation rates in spaces. Yik and Lun (2010) reported that inclusion of wing-walls provided up to 25% reduction of the A/C operation. Koinakis (2005) reported that the combined use of wing-walls and overhangs could appropriately reduce the solar radiation in the spaces.

Solar chimneys provide natural ventilation by buoyancy-driven flows (Batty et al., 1991). Their performance is dependent on their properties (e.g. wall thickness, the insulation properties) and the type of glazing used (Pavlou et al., 2007). Double-skin façades (DSF) consists of multiple layer skins (Zhou and Chen, 2010), usually a pair of glass skins forming a cavity (Koinakis and Sakellaris, 2007; Pappas and Zhai, 2008). Sun-shading systems, commonly venetian blinds (Hanby et al., 2008), are located in the cavity (buffer space) in order to protect the interior spaces from excess solar radiation (Zhou and Chen, 2010). The exterior skin layer provides protection against weather conditions and noise. Openings positioned along the height provide ventilation of the intermediate space (Oesterle, 2001). Widely designed in commercial buildings, they assist the buoyancy-driven natural ventilation during summer and contribute to an increase in heat gains during cold months (Hanby et al., 2008). Implemented in the building design externally, DSFs provide design and implementation flexibility in buildings during refurbishments projects without disrupting the building operation (Koinakis and Sakellaris, 2007).

In DSFs, the air circulates by either passive, mechanical, or hybrid means (additional use of fans) (Koinakis and Sakellaris, 2007) and with different ventilation modes (Loncour et al., 2004; Zhou and Chen, 2010). During passive modes, inlets and/or outlets are situated at the lower and higher parts of the façades (Koinakis and Sakellaris, 2007). The flow in the buffer space is either buoyancy or wind-driven through the external openings (Oesterle, 2001).

Except for the aesthetic contribution at the building's façades, DSFs provide buffer spaces and contribute to reductions in the heating and cooling energy loads, peak demands and energy for artificial light (Koinakis and Sakellaris, 2007; Zhou and

Chen, 2010; Hamza et al., 2011). DSFs provide a semi-outdoor environment that improves comfort on the balconies (Montazeri et al., 2013). Main concerns include the construction cost, the façade maintenance (cost and access) and the compliance to fire regulations (Koinakis and Sakellaris, 2007; Torres et al., 2007).

Five main types of DSFs have been described in literature: the box window; the shaft-box façade; the corridor façade; the multi-storey façade; and the multi-storey louvre type (Oesterle, 2001; Loncour et al., 2004). The box window is the oldest type of DSFs and is designed with horizontal partitions and vertical partitions between floors or windows (Oesterle, 2001). The multi-storey louvre type is designed similarly to the continuous type but with a second layer of pivoting louvres (not airtight design) (Loncour et al., 2004).

Studies on the performance of DSFs should not be generalised; every design is specific to the building type, scale, location, climate requirements, and energy targets set (Pappas and Zhai, 2008). DSFs have been recently designed for buildings in warm climates, such as in China (Zhou and Chen, 2010), in the Mediterranean and in other hot arid climates (Koinakis and Sakellaris, 2007). Yet, limited research on the performance of DSFs and dynamic façades has been conducted in hot climates (Hammad and Abu-Hijleh, 2010; Zhou and Chen, 2010).

Implementation of DSFs in hot climates could deliver thermal comfort with appropriate natural ventilation (Baharvand et al., 2014). Baldinelli (2009) recommends the continuous operation of the DSF openings and shading devices during summer, with high tilt angle to prevent overheating and direct solar radiation. Hashemi et al. (2010) predicted up to 5°C temperatures in the cavity above the ambient, which with appropriate shading would be reduced by up to 7°C. Night ventilation could assist the heat reduction of the thermal mass. East and west oriented glazed DSFs were mostly in favour of overheating (Gratia and De Herde, 2004). Palmero-Marrero and Oliveira (2010) suggest the application of adjustable vertical mechanisms in order to prevent direct sunlight. Montazeri et al. (2013) using CFD investigated how a DSF design could reduce discomfort due to wind forces, at the balconies of a high-rise building.

Study conducted by Koinakis and Sakellaris (2007) in Greece, shown that DSF could deliver energy consumption reduction and satisfy thermal comfort in office buildings, especially when combined with appropriate night ventilation and solar shading.

Baldinelli, (2009) developed a DSF design to overcome the cavity overheating problems, integrating an operable glass-shading device. During hot periods, the shading devices remained open with a fixed angle configuration to prevent direct solar gains. Ji et al. (2008) evaluated natural ventilation using CFD in a natural ventilated DSF with angled blinds. The cavity between glazing and external louvres should be naturally ventilated to sufficiently remove the heat absorbed (Palmero-Marrero and Oliveira, 2010).

Tsangrassoulis et al. (1997) and Safer et al. (2005) investigated using computational tools how the size, position, and tilt angle of venetian blinds operating inside the DSF cavity influence the cavity airflow. Louvres can be controlled to prevent glare and solar gains, enhance views and provide architectural aesthetics (Hammad and Abu-Hijleh, 2010). Oh et al. (2013) reported the importance of automatic control of blinds with regard to occupants' incoherent interaction with the blinds. Hamza (2008) measured the impact of multi-layered façade configurations using DTM tools at a non-domestic air-condition building. It was predicted that a DSF of reflective glass delivered substantial energy reductions (30%).

A dynamic façade responds to increase in solar gains with control of shading devices, which is important considering that climate and occupant's comfort are dynamic variables (Hammad and Abu-Hijleh, 2010). Dynamic façades respond to environmental parameters (i.e. temperature, humidity) by automatically controlling their operation, offering potential for low energy buildings. Automatic shadings result in reductions of energy consumption for cooling, heating and artificial lighting (GhaffarianHoseini et al., 2012).

2.6.1.2. Wind-catchers

Traditional architecture of Iran, Egypt and other Gulf States offers vernacular strategies such as the wind scoop, wind towers (Figure 2.23) and malkaafs (Figure 2.24), which utilise the relatively cool breezes and prevailing winds (Batty et al., 1991). Wind towers utilise the pressure differences between the inlets and outlets on the building surfaces, they capture wind at high levels and channel it down in the occupied spaces (Hughes et al., 2012; Dehghan et al., 2013). With regard to their design, they could operate as both wind-catcher and exhaust, under both wind and buoyancy-driving pressures (Calautit et al., 2012).

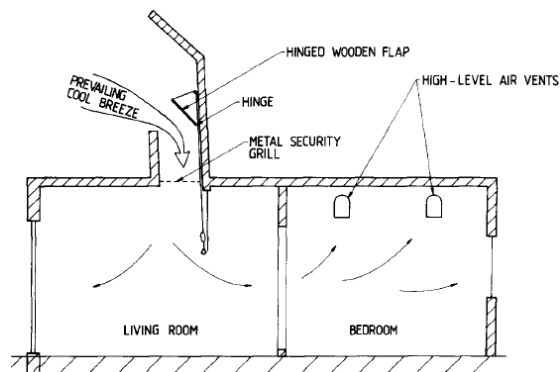


Figure 2.23 A vertical cross-section of a house with wind scoop (Peppes et al., 2002)

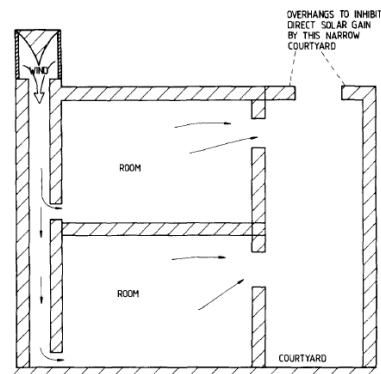


Figure 2.24 A vertical cross-section showing the air ducts in a Malkaf (Peppes et al., 2002)

Research by Dehghan et al. (2013) showed that the internal flow patterns, rates and pressure field are sensitive to the geometry of the wind-catcher, the wind speed and direction. The airflow rate entering the occupied space is dependent on the wind direction (Li & Mak, 2007). For zero degree incidents, the maximum airflow speed was predicted almost equal to the external wind speed. Wind catchers are designed with multiple sides and openings. Multi-directional wind-catchers are favoured in areas of no prevailing wind direction, and four-directional are commonly found in the Middle East (Hughes et al., 2012). In areas with predictable wind directions, they are designed unidirectional (Koch-Nielsen, 2002). In traditional Iranian architecture, wind-catchers are designed with various forms and cross-sections of internal blades (Ghadiri et al., 2013).

The natural ventilation performance and design optimization of the traditional wind-catcher has been widely discussed in the literature (Hughes et al., 2012; Moghaddam et al., 2011; Suleiman and Himmo, 2012). Calautit et al. (2012) investigated the feasibility of retrofitting traditional wind-catchers and proposed a new wind-catcher design as a sustainable alternative to the vernacular design. Mavrogianni and Mumovic (2010) evaluated the performance of wind-catchers in typical classrooms for thermal comfort in future climates. Ghadiri et al. (2013) categorised and evaluated the performance of various types of square plan wind-catchers using CFD.

2.6.2. Description of evaporative cooling techniques

Evaporative cooling utilises the energy required to convert water from liquid to vapour, the latent heat of vaporization (Fathy, 1986). It is achieved when air contacts water in evaporation (direct) or a wet surface that an evaporation process occurs (indirect) (Erell, 2007). This process could be adiabatic when no energy is added or extracted from the system. During direct evaporative cooling, air passes over a wet surface and while it is cooled, sensible heat converts to latent at constant wet bulb temperatures (WBT) increasing simultaneously the moisture content of the air (Santamouris and Asimakopoulos, 1996; Erell, 2007). The efficiency of this strategy depends on various parameters including the temperature, moisture content, velocity of ventilated air, the temperature of the water or of the wet surface (Santamouris and Asimakopoulos, 1996), and the design characteristics of the system.

Evaporative cooling is applicable to both internal and external spaces, although there are limited applications in conventional buildings (Erell, 2007). Some of the vernacular cooling techniques are the wetting of flat roofs and pavements (Erell, 2007), the use of water features; and the use of vegetation for evapotranspiration (Santamouris and Asimakopoulos, 1996).

The performance of three evaporative cooling systems was evaluated in a non-occupied apartment of a 5-storey building in Osaka City (Narumi et al., 2009): rooftop spraying; spraying of the exterior unit of A/C system; and direct spraying of fine mist of water to the veranda able to pre-cool the air entering the spaces. The combined operation of these reduced the energy consumption for cooling by 80%. The rooftop spraying strategy alone, provided reductions in air temperatures by 1.2°C, the veranda spraying 0.9°C, and the A/C spraying 36% energy consumption reduction (Narumi et al., 2009).

Passive downdraught evaporative cooling towers (PDECT or PDEct) are developed wind-catcher designs widely used in vernacular architecture of middle-east countries. Fathy (1986) describes wind towers as shafts rising above the buildings with openings on the direction of prevailing winds, trapping air from the top, which by utilising different means (i.e. water mist, spray, wet pads) provide further cooling by water evaporation. Wind-catchers with wetted surfaces can sufficiently improve the

cooling performance of the conventional wind-catchers (Hughes et al., 2012). The performance of these strategies has been evaluated by many (Givoni, 1997; Belarbi et al., 2006; Hughes et al., 2012; Ibraheem and Ford, 2012). PDEct could be a viable alternative to traditional mechanical cooling systems in domestic buildings in hot and dry climates (Ford et al., 2012).

Salmeron et al. (2012) predicted zones of PDEct applicability in Europe (for DBT above 25°C), the levels of intervention priority, and the areas with energy needs during summer suitable for PDEct. The climate of Athens was considered suitable for evaporative cooling solutions when provided using control devices to avoid hours of high humidity levels, as shown in Figure 2.25 (Salmeron et al., 2012). Further study in the southern-European countries predicted up to 70% PDEct applicability to the existing building stock, which if implemented in domestic buildings could provide energy and carbon savings (Ford et al., 2012).

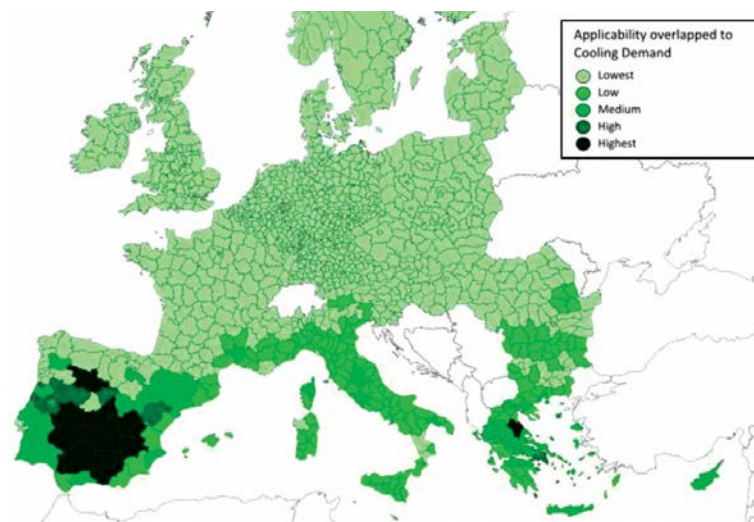


Figure 2.25 European map showing areas of low and high potential for evaporative cooling implementation according to the need for cooling (Salmeron et al., 2012)

Cunningham and Thomson's tower designed at a test building in Arizona (Figure 2.26), utilised wet porous mats at the vertical top openings in order to cool the incoming air by evaporation (Erell, 2007). The cooling performance of the strategy was significant. For air temperature of 40.6°C and WBT 21.6°C the temperature of the air entering the spaces was measured to be 23.9°C with 0.75m/sec velocity (Givoni, 1994). In '92 EXPO, Givoni (2011) applied the same principles to a cooling tower for thermal comfort in outdoor spaces. Fine drops were sprayed vertically from the top of a tower their momentum was transmitted to the air resulting in inertial air

movement downwards and reductions in air temperatures by up to 72% of the WBT. Both sea and fresh water were tested providing comparable results. Excess water can be collected at the bottom of the shaft and recycled again in the system (Givoni, 1994).



Figure 2.26 Test building with an evaporative cooling chimney (left) and a tower (Givoni, 1998)

Bahadori (1985) proposed an improved design of the traditional wind-catchers and evaporative cooling towers, Baud-Geers (in Persian) that captured air at higher flow rates from all directions. The new design maximised its cooling potential with water evaporation and eliminated losses through other openings (see Figure 2.27 and Figure 2.28).

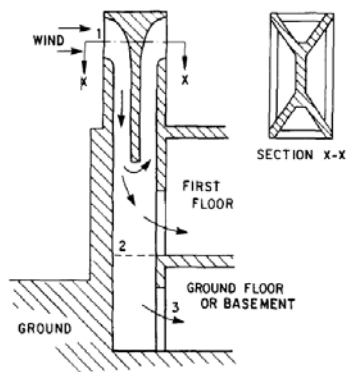


Figure 2.27 Traditional wind-catcher design, cross section and plan view by Bahadori (1985)

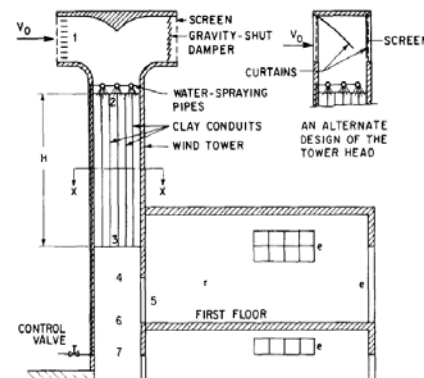


Figure 2.28 Proposed wind-catcher design by Bahadori (1985)

Ford et al. (2012) evaluated the performance of the first PDEC application in a Mediterranean dwelling. The PDEC was equipped with a system of a novel design with eight nozzles (peak water consumption of 8L/h) with a pump and air compressors with peak power requirements of approximately 700W. The system operating with high performance building envelope and nocturnal ventilation,

delivered comfortable conditions of up to 16°C indoor temperatures below the dry-bulb temperature (DBT).

2.6.3. Natural ventilation modelling methods

The complex flows of natural ventilation can be explored using three techniques: analytical methods; full-scale or wind-tunnel experiments; and numerical modelling such as computation fluid dynamics (CFD) (Allocca et al., 2003; Jiru and Bitsuamlak, 2010). CFD requires a significant knowledge of fluid mechanics, it has a high level of detailed input information regarding the model and modelling specifications, and is computationally intensive and time-consuming to set up and run. On the contrary, dynamic thermal modelling (DTM) performs simulation at an insignificant time relative to CFD, using less input parameters, and performs whole-building simulations for entire calendar years. DTM can predict: IAQ, thermal comfort and energy consumption of systems. One of the limitations of DTM is that it assumes that the air of each zone or the contaminant distribution is well-mixed; prediction of the flow distribution in the spaces is neglected. There are many available DTM tools, e.g. EnergyPlus, DesignBuilder, IES, ESP-r and ECOTEC. Concerns over locality with regard to the materials used within the thermal modelling simulations in relation to the country that the software was developed, have been reported. Research has been conducted on the development of 'local' materials databases, e.g. database of Greek construction materials (Papadopoulos et al., 2008).

CFD numerically solves the conservation equations of mass, momentum and energy (Chen and Srebric, 2002). CFD can be less expensive, both in time and resources, relative to traditional wind tunnel testing (Douglas et al., 2005) and real scale experiments, as the computer costs continuously decrease, unlike the cost of materials (Papakonstantinou et al., 2000). CFD provides greater design flexibility (Niu et al., 2005) and whole field data collection compared to data measurements in selected positions, at noticeably less time to the *in situ* real scale experiments (Montazeri et al., 2013) and with ease of testing alternative ideas and designs (Stavarakakis et al., 2010) in controlled, easy to manipulate and optimise environments.

CFD is a well-established detailed modelling technique widely used for the prediction of airflow patterns, distribution of air temperature, velocity, pressure, moisture content, and contaminants concentrations. It has proven to be an efficient tool in this area of research by having good correlation with experimental (Montazeri et al., 2010; Dehghan et al., 2013) and wind tunnel results (Mak et al., 2007; Ghadiri et al., 2013). Further, Allocca et al. (2003) and K. Papakonstantinou et al. (2000) predicted good correlation with semi-analytical results using the CFD software package PHOENICS to evaluate buoyancy and wind-driven natural ventilation flows.

CFD calculations can be either steady state or transient, for the evaluation of static conditions or time-varying processes respectively, of buoyancy and wind driven forces. Most common CFD mode is the RANS approach (Reynolds Averaged Navier-Stokes equations) preferably used for steady state application. An alternative mode that predicts with high accuracy natural ventilation is the very promising time-dependent large eddy simulation (LES) (Allocca et al., 2003). LES adequately evaluates unsteady turbulent flows of buoyancy-driven ventilation and overcomes the limitations of RANS (Durrani et al., 2012). LES filters the time-dependent equations, resolves the large-scale eddies and models the small scale eddies (Durrani et al., 2013).

Despite the variety of turbulence models for RANS modelling, the $k-\epsilon$ turbulence model of Launder and Spalding (1974) is the most commonly practiced eddy viscosity model for natural ventilation applications (Mak et al., 2005; Visagavel and Srinivasan, 2009; Yik and Lun, 2010; Calautit et al., 2012; Montazeri et al., 2013). The modified k -epsilon model of Chen and Kim that reduces the dissipative nature of the standard k -epsilon model (CHAM Ltd., 2008), is also widely used for the prediction of natural ventilation. The Boussinesq approximation, considers the density variations in the momentum equations (Cook, 1998; CHAM Ltd., 2008), has been suggested in the literature for steady state modelling of buoyancy-driven flows (Dascalaki et al., 1999; Visagavel and Srinivasan, 2009). Apart from selecting appropriate modelling techniques, one of the most important considerations when modelling numerically ventilation is the selection of boundary conditions, such as geometry settings, inlet/outlet properties, and wall properties.

CFD techniques have been widely employed for the performance evaluation natural ventilation strategies (Visagavel and Srinivasan, 2009; Mohamed et al., 2010; Jiru

and Bitsuamlak, 2010), wind-catcher models (Tominaga and Stathopoulos, 2007; Montazeri et al., 2010), evaporative cooling towers (Kang and Strand, 2013) and dynamic façades designs (Hanby et al., 2008). Allocca et al. (2003) using CFD evaluated single-sided natural ventilation strategies for buoyancy-driven flows (computational domain equal to the size of the simulated spaces), for wind-driven flows using the domain coupling approach (domain larger than the size of the building) and during combined buoyancy and wind-driven flows.

The study of the wind driven ventilation requires investigation of the external flow field of the building studied together with investigation of the internal flow field. Jiru and Bitsuamlak (2010) describe two validated modelling techniques providing simulation results in good agreement: the whole domain and the domain-decoupling approach. At the whole domain approach, the internal and external environments are simultaneously modelled, allowing prediction of the airflow around the building, through the ventilation openings, and at the interior of spaces. The domain decoupling approach involves investigation and prediction of the external flow field and boundary conditions at the building openings prior to the prediction of the internal flow field. The latter is less time consuming (Graça et al., 2002), offers optimum mesh refinement (Norton et al., 2007), and allows changes to the interior without affecting the exterior providing design flexibility (Jiru and Bitsuamlak, 2010).

When studying the wind-driven ventilation of buildings the computational domain needs to be sufficiently large to realistically reproduce the external flow field (Graça et al., 2002). The flow field around buildings in urban environments has been evaluated, modelled either as stand-alone, isolated cases (Graça et al., 2002; Mak et al., 2005; Visagavel and Srinivasan, 2009; Mohamed et al., 2011; Calautit et al., 2012) or within their surrounding buildings and environment (Baskaran and Kashef, 1996; Rizk and Henze, 2010; Montazeri et al., 2013). In literature, the location of the building in the domain varies between centred or positioned closer to the domain faces which act as wind inlets (Mak et al., 2005; Wang and Wong, 2008; Mohamed et al., 2009; Visagavel and Srinivasan, 2009). The computational domain dimensions are usually proportional to those of one or more building surfaces. Ayad (1999) and Mohamed et al. (2009) suggest domain height five times the building height, Visagavel and Srinivasan (2009) and Yik and Lun (2010) three times, and Dagnew et al. (2009) twice.

2.7. Discussion

The study of the literature review suggests that with the emergence of climate change, the increasing figure of energy consumption for cooling in buildings and the large number of the existing apartment building stock, there is an urgent need for energy conscious design of new and existing buildings. Architectural typologies of the existing building stock in Greece were reviewed in this chapter. It was concluded that the most typical domestic building in Greece is the multi-storey apartment building: the case study building selected for the purpose of this research was considered representative of over 4 million buildings in Greece (Chapters 3 & 4).

The potential and the availability of natural ventilation techniques suitable for the Mediterranean sub-climate of Greece presented in this chapter, provide a significant opportunity for energy consumption reduction for cooling and improvement of the indoor air quality. It was possible through the literature presented in this chapter to identify the most suitable natural ventilation strategies for the climate and building type studied (Chapters 3 and 4). The ventilation and cooling performance of these strategies was evaluated using computational techniques presented in this chapter (Section 2.6.3); their ventilation potential and limitations are included in Chapters 5, 6 and 7. For the performance evaluation of these strategies, it is important to consider the strong link between occupants' behaviour and energy use in buildings, as well as occupants' adaptation (highlighted in Chapter 5). The following chapters address these issues and present the research to fill the gaps in knowledge reported.

***Chapter 3* : RESEARCH METHODOLOGY, JUSTIFICATION AND METHODS**

3.1. Introduction

Methodology is the critical study on how estimated relationships among variables (Creswell, 2009) will be answered by discussing different conceptual approaches, sources, and the limitations or potential of different methods (Grix, 2004). In the literature three categories of research methods are available, the qualitative, the quantitative, and the mixed methods (Fellows and Liu, 2008), with regard to the intersection of philosophical worldviews, strategies of inquiry and methods (Creswell, 2009).

For the purpose of this research, quantitative methods were employed for testing objective theories, the framework and research aim of the project (Creswell, 2009) and for giving answers by examining the interaction among measured variables (Leedy and Ormrod, 2001) using scientific techniques (numerical techniques via computer simulations) (Fellows and Liu, 2008). The research process consists of four steps as described by Greenfield (1996) that were also identified in this research: literature review (Chapters 1, 2 and 3); theory building by induction (specific to general) (Chapters 4, 5, and 6); theory testing (Chapters 5, 6 and 7); reflection and integration (Chapters 7 and 8). A schematic figure of the research design of the project is shown in Figure 3.1.

This chapter addresses the approach, scope of this research, the methods considered, and tools used, as well as the justification of this research. The review of literature was supported by elite exploratory interviews that identified the contribution of this project, explored the objectives, and justified the research scope, presented in Chapters 2 and 1 respectively. This chapter details the development of a methodology to address the research questions, presented in Chapter 1, and: outlines the gaps in literature; describes the case study building and natural ventilation strategies selected for the purpose of this work; the evaluation tools and

computational methods employed; and concludes with the performance evaluation strategies.

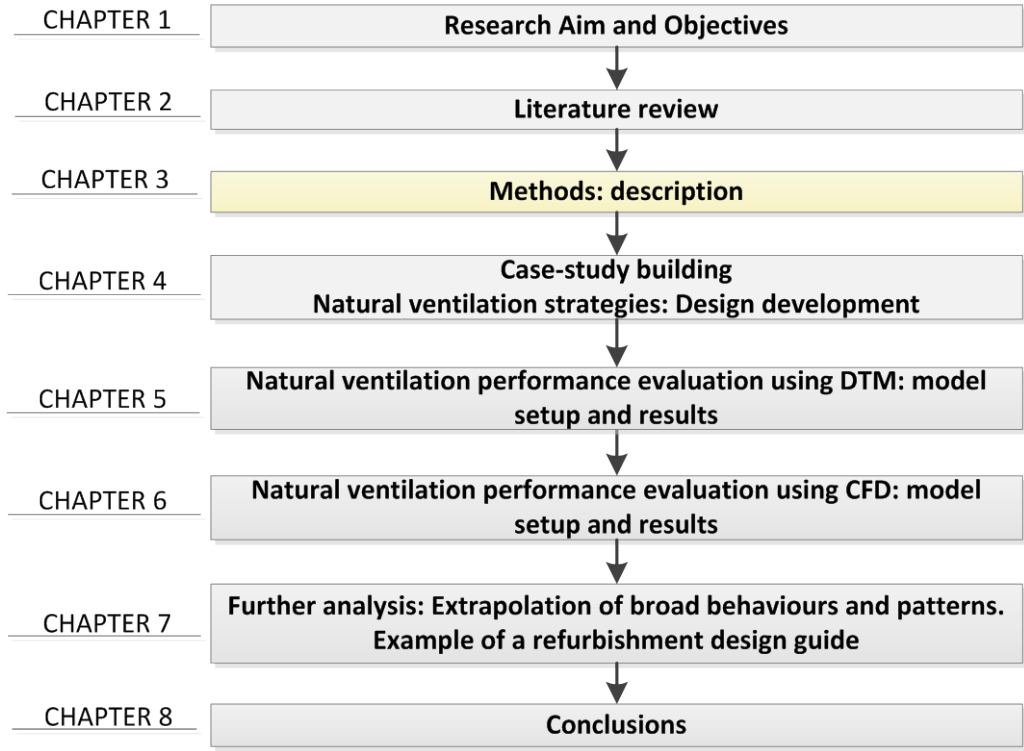


Figure 3.1 Research design and layout of the thesis

3.2. Methodological debate

The findings from the elite interviews (Chapter 1.5) suggest that there is a continuous decline of the construction activity in Greece due to the current economic situation of the country. Building refurbishments are expected to be the primary drive of the market with regard to the energy consuming existing building stock and the current economic constraints on buying or building new properties. Fuel poverty for both heating and cooling energy demand is a relatively new phenomenon in Greek dwellings and addresses the inability of low-income households and occupants to obtain thermal comfort. Despite the widespread need for knowledge transfer of energy saving measures and passive strategies, designers have limited understanding of natural ventilation techniques. However, suitable strategies for the climate, urban environment and type of buildings within Greece were identified in the literature (Chapter 2). The energy required for cooling in hot climates indicates a substantial opportunity for energy savings (Chapter 2). The domestic sector corresponds to the 79% of the existing building stock in Greece and accounts for up to 24.5% of the country's energy consumption, the highest in Europe. The multi-family buildings and apartment buildings define the majority of the urban Greek domestic stock (up to four million buildings).

All these express an urgent need for energy refurbishments to extend the life of buildings and enhance architectural identity. Given the warm, dry climate of Greece, with the highest hours of sunshine and the strongest winds in the Mediterranean region, occupants' thermal comfort expectations could be achieved by employing natural ventilation throughout the year. Research has shown that the climate of Athens could be suitable for implementation of natural ventilation and evaporative cooling techniques. Despite the increasing air-conditioning installations, literature suggests that vernacular passive techniques and natural ventilation systems could sufficiently reduce energy consumption, if appropriately selected, designed and implemented in the urban multi-storey apartments.

3.3. Methods and Structure of the Research

The study of the literature and the findings of the elite interviews defined the knowledge gaps and developed the research design, methodological focus and layout of this research by mapping the objectives. This research explores the concept of natural ventilation strategies and evaluates their performance using computational modelling techniques, with aim to deliver occupants' summer comfort to an existing domestic building that could provide the know-how for future building refurbishments. The research methodology was developed with regard to the aim and objectives (Chapter 1) of this project. A schematic relation of the objectives and detailed methods of this research project, are presented in Figure 3.2.

Chapters 4, 5, 6, and 7 of this research present the methods used to explore if natural ventilation strategies (and which) could deliver summer comfort and be a sustainable refurbishment measure in existing domestic buildings in hot climates. At first, a typical case study building was selected with regard to the location, climate, type of building, construction year, use, and operation. Natural ventilation systems reviewed in the literature (Chapter 2.6.1.) were developed for the specific building type and design (Chapter 4). The thermal performance of the base-case ventilation strategy and the proposed ventilation strategies implemented in the case study building were evaluated with DTM (Chapter 5) for the cooling period; occupants' thermal comfort was reviewed. This provided information of the performance of the strategies over the cooling period. Detailed airflow modelling study was performed using CFD (Chapter 6) including investigation of the internal and external flow fields. This predicted the detailed natural ventilation potential and limitations of each strategy with regard to climate, the case study building design and the surroundings. Using statistical methods behaviours were extrapolated from the simulation results. The most appreciable natural ventilation strategy for the specific type of building and climate was identified and evaluated with simulation techniques. Conclusions were drawn providing recommendations for future low-energy refurbishment projects, in the form of a low-energy refurbishment design guide (Chapter 7 and 8).

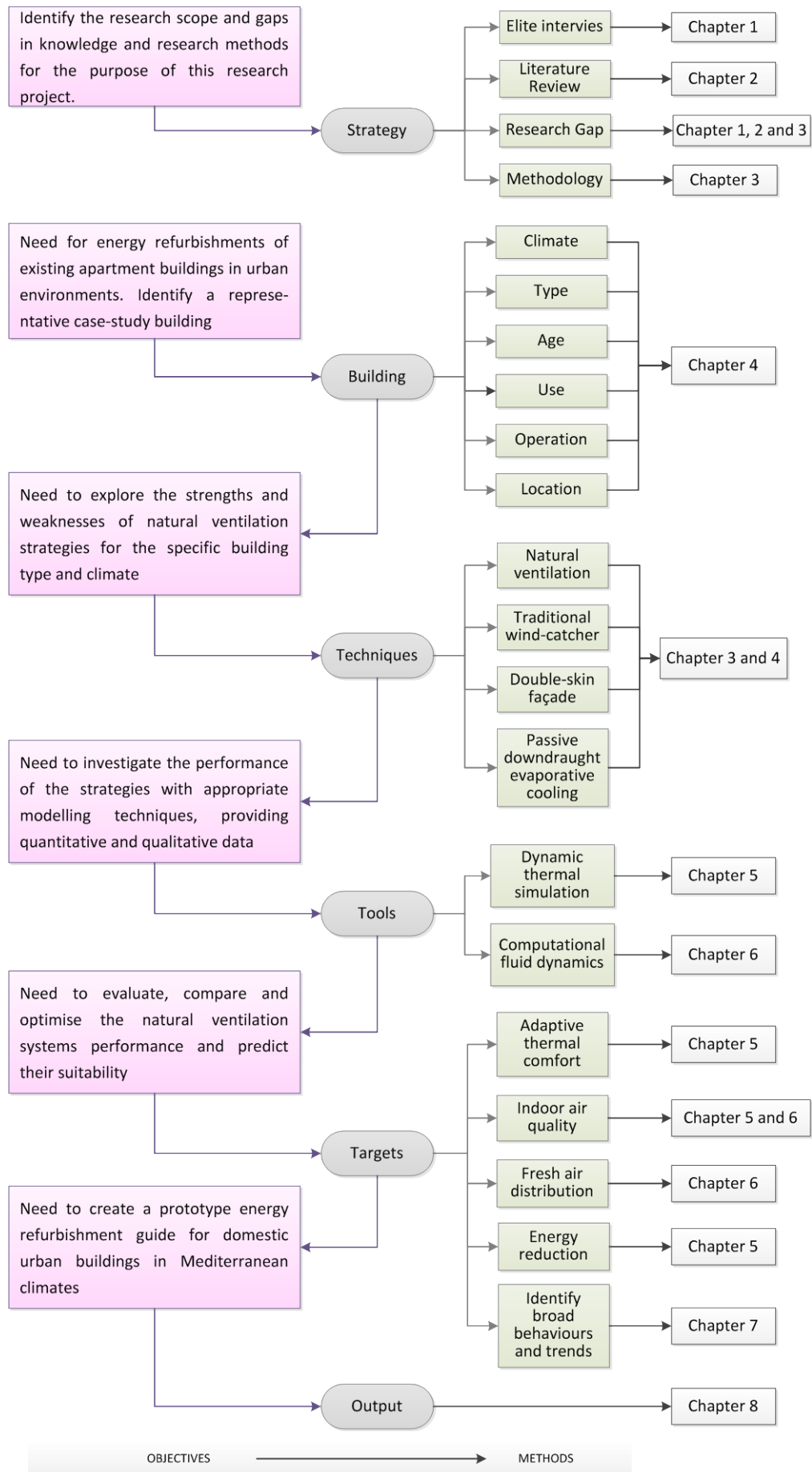


Figure 3.2 Research project: objectives, means and methods

3.3.1. Brief description of the case study building

Researchers decide whether to know “*more about less*” or know “*less about more*” (Gerring, 2007). Often, working with specific examples provides better understanding of the whole, including an in-depth, holistic analysis in terms of detail and completeness. An existing building was selected for this research to explore the properties of a single phenomenon or instance under specific conditions, with the aim of gaining insights and generalisations of a larger set of cases. The building was selected for utilising certain type of evidence, having a real-life context and for being a representative sample on average (criteria for case study research according to Gerring, 2007).

The case study building is an existing five-storey building of eight apartments per floor, with a basement and a penthouse, constructed in the early 1970s for domestic use (Figure 3.3). During the 70s, up to 850,000 multi-storey domestic buildings were constructed, which were more than twice the number of the dwellings constructed during this decade (EL.STAT., 2014). The building selected is located in an urban zone of the centre-north Athens with a typical Mediterranean climate and is considered one of the most characteristic urban Greek domestic buildings with regard to the design, year of construction, materials used, operation (24 hours occupied and free-running) and its location (within a densely populated area), as described in Chapter 2.4.2. A two bedroom apartment was selected (51.3m²) as it was considered a typical example of the Greek building stock (38% of dwellings have 3 living spaces (EL.STAT., 2014)). Direct access to daylight and outdoor air is restricted to the two bedroom openings. A light well on the rear spaces assists the extraction of stale air from the core spaces with no access to daylight. An extended description of the building design and the apartment studied is included in Chapter 4.

A survey of the building site was conducted to provide information regarding the surrounding buildings and site, which were important for the thermal and airflow performance investigation of the building under investigation, described in Chapter 4.3. The densely populated urban area consists of a continuous line of urban blocks with non-constructed spaces in the centre. The buildings vary from single-storey detached houses to ten-storey apartment buildings.



Figure 3.3 Street view of the building and the apartment studied (Photograph by author, 2012)

3.3.2. Natural ventilation strategies

Natural ventilation and cooling strategies presented in Chapter 2.6, were considered suitable refurbishment options for the purpose of this research project. The natural ventilation strategies were selected with regard to: the climate applicability; design flexibility; potential energy efficiency; ease of implementation in existing buildings; maintenance; disruption to the occupants; ease of use; first and life-cycle cost; and indoor environmental quality. The number of thermal comfort hours that could be achieved for the building site during the cooling period was predicted by a preliminary climate analysis (Figure 3.4), using the adaptive comfort model in ASHRAE standard 55-2010 (ClimateConsultant, 2014). For the purpose of this a climate file was used (*climate file 2*) presented in detail in Chapter 4.4. It was predicted that natural ventilation could potentially deliver up to 59% comfort hours during the cooling season. The least comfort hours were predicted in May (45% with 80% acceptability) with regard to the low ambient temperatures in the site.

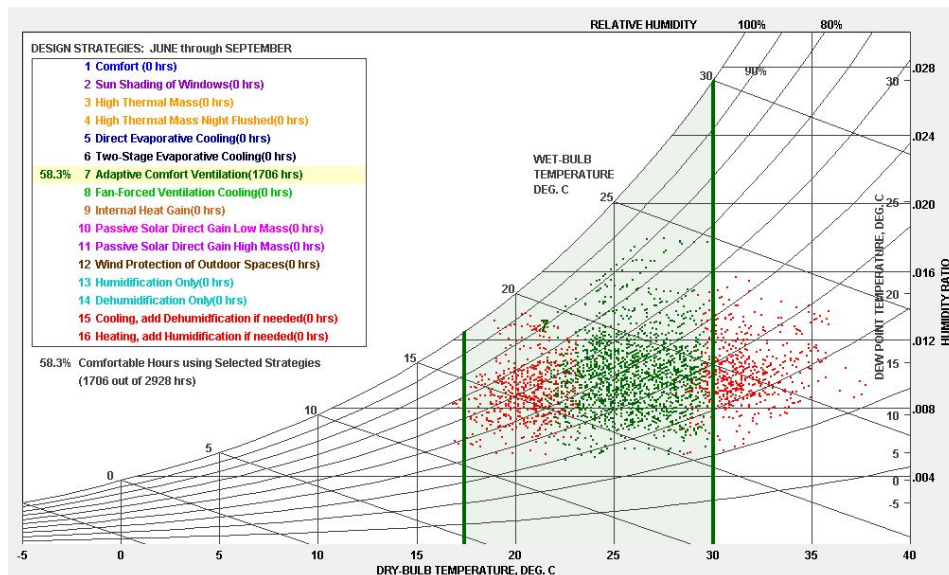


Figure 3.4 Psychrometric chart with the climate dataset of the building site during the cooling period (produced in Climate consultant 5.5 (ClimateConsultant, 2014))

A number of natural ventilation and cooling strategies have been identified suitable (i.e. to improve ventilation performance) for the purpose of this project. These strategies were implemented in the case study building in response to the building form, layout and operation, presented in detail in Chapter 4.5. The expected environmental performance of each system is dependent on the local climate, building properties configuration, operation, gains, etc. These strategies were evaluated individually and in groups. Complementary operation was expected to provide the most efficient design strategy with regard to their natural ventilation potential. The strategies evaluated, existing or proposed are the following:

- I. **Natural ventilation strategies:** Evaluation of the performance of simple natural ventilation strategies during the cooling period via existing and new building openings
 - *Base-case ventilation strategy:* the ventilation performance of the apartment under investigation was evaluated. The building openings operated with regard to the estimated interaction of occupants with the openings, developed according to published work (Chapter 5.2.). Measurements in Greek dwellings during wintertime with closed openings predicted CO₂ concentrations exceeding the maximum acceptable threshold for comfort (M Santamouris, Argiroudis, et al., 2007); this was expected to be also predicted for the case study building during the hours of the day that the openings remain closed.

- *Daytime ventilation* in relation to indoor/outdoor air properties: Day ventilation was considered suitable for the studied climate according to applicability criteria in Chapter 2.6, because the external temperatures were predicted below 30°C for the 72.4% of the cooling season. This was predicted using Excel and the climate data of the site under study.
 - *Nighttime ventilation* in response to indoor/outdoor air properties: Night ventilation was considered suitable with regard to the substantial diurnal temperature difference (average of 7-8°C) as predicted with Excel and the climate data of the site under study (applicability criteria Chapter 2.6.). Efficient night ventilation provides decrease of the peak indoor temperature during the next day by up to 3°C (Geros et al., 1999).
 - *Combined day and night ventilation* strategies were also evaluated as the controlled openings' operation during both day and night was expected to have optimum ventilation performance relative to the two individual strategies.
- II. **Single-sided ventilation - dual openings:** Literature on single-sided natural ventilation has shown better performance when two openings located on the same external wall are utilised for natural ventilation, providing up to two times higher ventilation rates (6ach⁻¹ predicted in domestic buildings) (Niachou et al., 2005). The ventilation performance of this strategy was evaluated.
 - III. **Cross ventilation:** An existing light well connected to the rear spaces was used to assist the cross ventilation via the façade openings. Cross ventilation could provide up to three times higher ventilation rates than single-sided ventilation in domestic buildings in Greece (up to 12ach⁻¹ for less than 0.5m/s wind speeds) (Niachou et al., 2005).
 - IV. **Indoor airflow paths:** Unoccupied spaces could be used to create new flow paths in order to avoid spaces of higher internal gains, i.e. kitchen. This strategy was explored during specific hours of the day for the apartment under investigation and it was expected to deliver comfort when the internal doors remain closed.
 - V. **Four-directional wind-catcher:** Ventilation performance of this vernacular ventilation strategy was evaluated. The strategy was selected as strong winds were recorded in the area (above 10m/s); wind speeds above 2m/s for more than 75% of the cooling period and above 4m/s for more than 42% (Chapter 4.4). As reported

by others, the potential of natural ventilation in reducing indoor air temperatures is dependent on the conditions inside urban canyons (Geros et al., 2005). This strategy was thus selected as it could provide indoor comfort in densely populated areas (Chapter 2.6.1.2). A wind-catcher could operate as inlet and exhaust of stale air. However, experimental and CFD results have shown that wind-driven forces provide 76% higher ventilation rates than buoyancy-driven forces (Calautit et al., 2012). Further, wind-catchers can increase the average indoor velocity by 63% relative to simple natural ventilation strategies.

- VI. **Lightweight dynamic façade (DF):** The performance of façade relief techniques, including wing walls and an external layer of horizontal shading systems, was evaluated. Experimental calculations shown that utilisation of sun shading could provide up to 52% comfortable hours during the daylight hours for the cooling season (predicted according to the ASHRAE handbook of Fundamentals Comfort Model, 2005 using ClimateConsultant, (2014)). Different DF designs have been evaluated by others, showing significant contributions to the natural ventilation of occupied spaces in hot climates (Chapter 2.6.1.1).
- VII. **Passive draught evaporative cooling (PDEC):** The PDEC strategy ventilation strategy could be implemented in the tower of the wind-catcher. For the building site, selected, passive cooling via water evaporation systems could provide up to 30% comfortable hours during the day (predicted using the ASHRAE handbook of Fundamentals Comfort Model, 2005 within the ClimateConsultant, (2014)). PDEC can provide a viable alternative to mechanical systems implemented in domestic buildings in hot and dry regions in the world. This could provide significant temperature reduction of up to 14°C and maintain the relative humidity of the spaces levels below 65% (Ford et al., 2012).

3.3.3. Computer-based modelling

Numerical techniques within simulation tools offer flexibility and modelling-ease in evaluating different strategies, building configurations, and providing detailed information about the buildings' operation and thermal performance. Dynamic thermal modelling (DTM) and computational fluid dynamics (CFD) software have a complementary practice on the buildings performance information they provide.

DTM software delivers building thermal modelling analysis of sub-hourly basis for a period of up to a calendar year, and provides spaced-averaged values of indoor air properties, loads and gains in response to a number of set variables and time-steps. By assuming that the air in spaces is well mixed, DTM software does not predict the detailed airflow distribution of spaces especially under conditions of natural ventilation.

On the contrary, CFD simulation tools predict detailed internal and external flow fields of buildings and deliver information regarding the air properties, airflow distribution, and IAQ of spaces. CFD calculates ventilation rates of both density and temperature driven flows. Input information can be exchanged from the DTM to the CFD software in relation to internal gains, surface temperatures and solar gains. For this research, selection criteria of the specific DTM and CFD software were the user-friendliness, validation, training available and user support. For the purpose of this work, the two modelling techniques were used to evaluate the performance of different natural ventilation strategies with regard to the benefits and limitations of each technique (addressed in the Chapters 5 and 6), a list of which is presented in Table 3.1.

Table 3.1 List of natural ventilation strategies evaluated with DTM and CFD simulations

DTM simulations	CFD simulations
Existing natural ventilation strategy of the case study building (combined single-sided and cross ventilations)	Single-sided ventilation
Controlled daytime ventilation	
Controlled nighttime ventilation	
Controlled day and night ventilation	Cross ventilation
Four-directional wind-catcher	
Dynamic façade	Façade wind-catchers
Wind-catcher and dynamic façade	
	Passive downdraught evaporative cooling with a wind-catcher
	Passive downdraught evaporative cooling with a wind-catcher and dynamic façade
New internal openings	

3.3.3.1. Thermal building energy modelling

DTM simulations were performed to assess bulk values of indoor air properties in the context of seasonal variations, in response to building operation and occupancy during the cooling period. This would address Objective 2, as presented in Chapter 1.3. The DTM simulations assessed the potential of the new ventilation strategies to improve the ventilation rates upon the base-case strategy and extend the comfort hours during the cooling period. It was therefore beyond the scope of this research to evaluate the building's envelope performance with regard to building materials.

The software Integrated Environmental Solutions - Virtual Environment (IESVE, 2012) was selected for its user-friendliness, performance and number of options for results visualisation. IESVE has been highly rated by users for its usability and graphical visualization of its interface, and template driven approach (Attia et al., 2009). Simulation results using IESVE have been shown to be in good agreement with experimental results (Hamza, 2008). For the evaluation of natural ventilation, the software incorporates models of wind pressure coefficients (empirical data), buoyancy, flow characteristics of large openings and cracks, two-way flows and Rayleigh instability (IESVE, 2012).

For the DTM simulations, a three-dimensional model of the building studied was created (alternatively, geometries are imported from CAD software) and detailed information was introduced regarding: the building orientation; geographic location; climate; construction properties; building operation; and usage (internal gains).

The flow diagram of Figure 3.5 describes the thermal modelling simulations performed. After evaluating the thermal performance of case study apartment during the existing ventilation strategy, different operations of the openings are investigated to enhance the natural ventilation of the building studied (controlled day and/or night ventilation). Changes to the building design were evaluated including: inclusion of a four-directional wind-catcher with internal partitions; a lightweight dynamic façade of external shadings; and the creation of alternative airflow paths in the interior spaces. With regard to the ventilation performance of each strategy, the most efficient design was predicted. The DTM simulations provided hourly information regarding indoor temperature, relative humidity, airflow rates, CO₂ concentrations and solar gains, for the cooling period and the apartment studied.

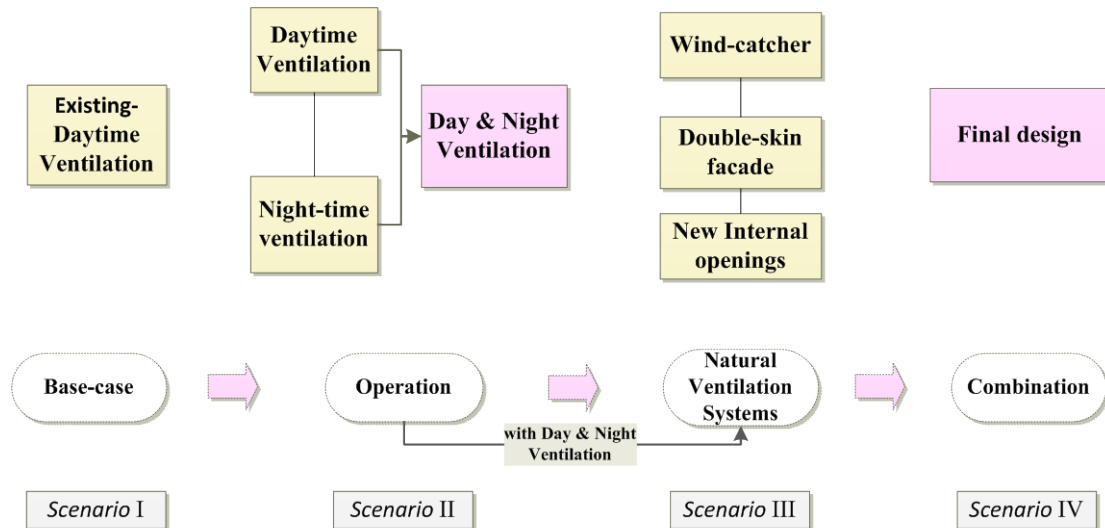


Figure 3.5 A schematic diagram of the simulations performed for the ventilation strategies evaluated, presented in steps starting with the existing ventilation strategy up to the final proposed strategy

3.3.3.2. Application and use of CFD: software package

Computational fluid dynamics (CFD) simulations are a detailed modelling technique widely used for the prediction of airflow patterns in and around spaces that by calculating velocities, temperatures and pressures at numerous locations throughout spaces recreate the whole flow field. CFD can be less expensive, both in time and resources, relative to traditional wind tunnel testing (Douglas et al., 2005) and the *in situ* real scale experiments (Montazeri and Blocken, 2013). It provides great design flexibility (Niu et al., 2005) and has good correlation with experimental results (Cook et al., 2003; Montazeri et al., 2010). The most frequently used CFD commercial codes are the CFX, FLUENT, PHOENICS (Norton et al., 2007). For the buoyancy and wind-driven ventilation strategies evaluation using CFD for this research study, the commercial CFD software package PHOENICS (CHAM Ltd., 2013) was used to solve the three-dimensional Reynolds Averaged Navier-Stokes equations using a steady state three-dimensional structured Cartesian mesh.

Steady state airflow simulations were performed to predict indoor temperature distribution, ventilation rates and airflow patterns of the apartment studied and the natural ventilation strategies investigated. This work was conducted to address Objective 3, as presented in Chapter 1.3. A climate analysis was conducted using the climate data for the cooling period, to obtain the most typical and/or extreme climate

conditions in terms of frequency and intensity of the DBT, wind speed and direction (Figure 4.9 of Chapter 4). The simulations were performed for a combination of the average (mean) and highest DBTs, the minimum, average (mean) and highest (75 percentile) wind speeds, and for three predominant wind directions.

The different ventilation strategies were evaluated with reference to both reductions in indoor temperatures and enhancement in ventilation rates. Each natural ventilation strategy was designed and the apartment studied was tested under both buoyancy and wind-driven forces subject to the different climate scenarios but with the same building design and internal heat gains. The domain de-coupling approach (Jiru and Bitsuamlak, 2010) was employed for the study of the airflow patterns due to wind induced ventilation and not due to buoyancy-driven flows, in order to reduce the computational power required to simultaneously model both internal and external thermal environments. Hence, the building and its surroundings were first simulated to obtain the external airflow distribution and pressure values at the location of the openings, which were subsequently included as input values on the building's openings for the study of the internal flow.

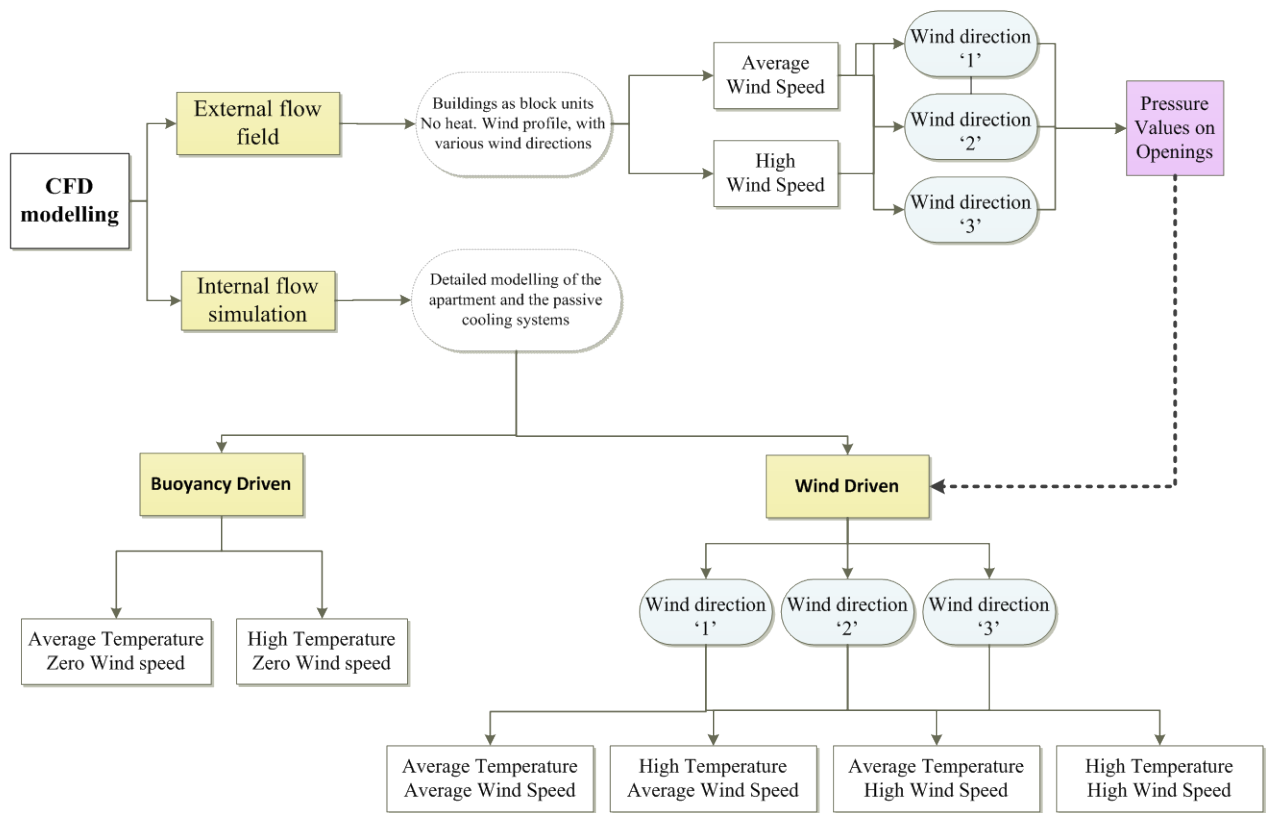


Figure 3.6 Flow diagram of the airflow simulation sequence conducted for each natural ventilation strategy examined in CFD

Results were obtained in the form of: indoor air temperatures; relative humidity; air velocity; ventilation rates; volume flow rates through openings; and pressure distribution in the spaces. The schematic diagram of Figure 3.6 illustrates the simulation process with reference to the climate scenarios, which was performed and repeated for each individual natural ventilation strategy.

There are three components in all CFD codes (Douglas et al., 2005): the pre-processor (input) for problem definition by the user; the solver (data-processor) for the major computation of the mathematical models employed by iterative methods (Norton et al., 2007); and the post-processor (output) for the visualisation of the computed results (CHAM Ltd., 2008). At the pre-processor the user makes statements about the geometry, computational mesh, processes, materials, boundary conditions, and numerical parameters affecting the accuracy of the simulation (CHAM Ltd., 2008). PHOENICS solves equations expressing the “*balances of mass, momentum, energy, material and other conserved entities, over discrete elements of space and time, i.e. 'finite volumes' known as 'cells'*” (CHAM Ltd., 2008). The quality of the CFD modelling is determined at the pre-processor, with regard to the accuracy of results within acceptable computational time. At this stage the fluid flow phenomena to be modelled are defined as well as the numerical parameters and boundary conditions (Douglas et al., 2005). An appropriately detailed mesh is important to minimise errors in the results and thus investigations of mesh independent solutions were considered necessary prior to the simulation analysis of this study. A mesh investigation aims to establish the number of cells on all three dimensions that further mesh refinement will yield no significant changes at an acceptable amount of computing time (Cook, 1998).

Simulations were performed in serial runs using the windows version of PHOENICS (Windows 7 desktop computer with 2 Intel Xeon E5520 processors of 2.27GHz and 64Gb RAM) and in parallel with the Linux version of the software, with respect to the requirements of each model. For the parallel computing, Loughborough university IT services provided access to the high performance computing (HPC) service which comprises of the hydra cluster, running the Red Hat Linux operating system (Bull Linux AS5), of 1956 64-bit Intel Xeon processors. The operation of parallel PHOENICS provided noticeable reductions in the overall computational hours required for the total number of mostly the external flow field simulations, expected on average to require up to 200 days of continuous computational time if

run in windows serial version. Details regarding the limitation and benefits of the two modelling techniques (i.e. parallel and serial) are included in Appendix A.4.1.

3.3.4. Ventilation Performance Investigation and Evaluation

Analysis

In naturally ventilated buildings, the internal environment is strongly dependent on external environmental conditions, the influence of which was quantified using the modelling techniques. Both DTM and CFD simulation strategies provided details of time-dependent and steady state indoor air properties respectively, with regard to the indoor air temperatures, ventilation rates, carbon dioxide concentration, relative humidity and air speeds.

The aim of conducting DTM simulations was to evaluate the improved openings operation in response to both occupants' interaction and environmental parameters, and to evaluate the thermal performance of the new natural ventilation strategies with regard to IAQ and occupants' comfort (Chapter 5). The airflow modelling analysis evaluated the detailed characteristics of natural flows due to wind and/or temperature difference (Chapter 6). For a number of climate scenarios and by maintaining a fixed number of parameters (internal gains, adiabatic walls and percentage of openings operation) it was possible to ensure performance evaluation of the different natural ventilation strategies with regard to base-case ventilation strategy. CFD results delivered detailed airflow rates through the building openings, indoor temperatures in all spaces, and predicted IAQ with in response to the building geometry and climate (Chapter 6).

Using DTM and CFD simulations it is possible to evaluate the performance of the ventilation strategies, relative to the base-case ventilation strategy of the apartment studied. Results were evaluated according to the acceptable values of IAQ defined by literature, presented in Chapter 2.5. The hours during which thermal conditions fall within the thermal comfort range, as defined by standards would be predicted. Using CFD simulations it was expected to predict whether the new ventilation strategies would deliver reductions in indoor air temperatures and increase in ventilation rates, relative to the single-sided ventilation strategy of the apartment studied. The natural ventilation performance of the strategies was also evaluated relative to the expected

performance as reported by others (Geros et al., 1999; Niachou et al., 2005; M Santamouris, Argiroudis, et al., 2007; Calautit et al., 2012; Ford et al., 2012; Papamanolis, 2015b).

A set of environmental conditions that are acceptable were defined according to literature (Chapter 2.5.1 and Chapter 2.5.2) and used for the evaluation of all ventilation strategies examined and with regard to the modelling technique used, included in Table 3.2.

Table 3.2 Environmental conditions used for evaluating the DTM and CFD results respectively

Air variable	DTM	CFD
Indoor air temperature and operative temperature (°C)	Approximate thresholds of 28°C in living spaces and 26°C in bedrooms (CIBSE, 2006)	
	26°C: optimum internal temperatures in dwellings (Androutsopoulos et al., 2012)	
	22°C: minimum comfort temperature during summer (BS EN15251 CEN, 2007)	
	18°C: minimum outdoor temperature for ventilation (recommended as the minimum comfort temperature during winter) (BS EN15251 CEN, 2007)	
	Overheating criteria: indoor air temperatures that exceed the 26°C (bedrooms) and 28°C (other rooms) for minimum 1% of the occupied hours (CIBSE, 2006)	
	Adaptive control algorithms (BS EN15251 CEN, 2007) (McCartney and Fergus Nicol, 2002)	
	Reductions in indoor air temperatures below the DBT	
Air change rates (ach ⁻¹)	Above 1ach ⁻¹ for adequate ventilation (CIBSE, 2006)	
	Between 5-10 ach ⁻¹ (CIBSE, 2005) and up to 30ach ⁻¹ for provision of cooling	
Indoor air velocity (m/s)	Mean air velocity of 0.25m/s and above 1m/s to offset increased indoor temperatures (CIBSE, 2005)	
Relative Humidity (%)	About 45% for 26°C indoor air temperature (Androutsopoulos et al., 2012)	
	No more than 70% for prolonged periods (CIBSE, 2005)	
CO ₂ concentration (ppm)	Acceptable all values below 1000ppm and preferably below 800ppm (CIBSE, 2005)	

Statistical methods established relationships between indoor air properties and climate characteristics. Ventilation behaviours under conditions that have not been examined using simulations (extrapolate broad behaviours) were predicted (Chapter 7). These provided confidence in the modelling techniques, the CFD models, and the results predicted. The sensitivity of the indoor air characteristics to the building design, operation, the external environment and efficiency of the ventilation strategies was identified. These findings would be used as valuable feedback to improve the individual operation scenarios of the ventilation systems (i.e. openings) in order to provide optimum control and occupants' comfort. The statistical methods employed provided further visual representation of the results. This work was conducted to address Objective 4, presented in Chapter 1.3.

This information could assist future refurbishment projects of similar buildings and microclimates. This will answer the last objective of this research work, Objective 5. The overall output of the research conducted would be summarised in an example of a low-energy refurbishment design guide for natural ventilation in apartments in the Mediterranean, including guidance and instructions extracted from the ventilation performance of the case study building. The design guide includes the most efficient natural ventilation strategy as identified within the computational simulations. Recommendation for potential refurbishment studies in existing apartment buildings in hot climates is provided.

Chapter 4 : CASE STUDY BUILDING AND VENTILATION STRATEGIES

4.1. Introduction

The chapter provides a brief description of the building under study, its context and the design only characteristics of the natural ventilation strategies proposed. It is divided into three parts: firstly, the building selected for this research is introduced and presented with detailed drawings, pictures, information about materials and use; secondly, detailed information about the climate and the building site are presented; and thirdly, a detailed description of the design and properties of the individual natural ventilation strategies is presented. These will feed into Chapters 5, 6 and 7.

4.2. Description of the Case study Building

An existing apartment building in a centre-North area of Athens, Galatsi, was selected for this project. The main selection criteria were: the location (urban); the microclimate (typical Mediterranean climate, Chapter 2.2); the architectural design (70% of the total domestic building stock in Greece, Chapter 2.4.2); use of the building (80% of the buildings in the wider region, Attica); and ease of access of the researcher to one of the apartments.

Constructed in 1970, it was exclusively built for domestic use and comprises of an underground floor for ancillary use, a ground floor, four floors with the same floor layout (Figure 4.1) and a single-bedroom flat penthouse (Figure 4.2). It is semidetached and adjacent to surrounding apartment buildings from both the northeast and the southwest sides. The main entrance is oriented southeast (Figure 4.3). The building drawings were created in AutoCad 2011 (student edition) according to the original hand drawings provided by the local Planning Office during a site visit in May 2012 by the author.

The building is positioned on a 642m² site area and has 67% utilisation factor. It occupies the total length of the site (from northeast and southwest) and has a 4m setback from both the main road (southeast) and the rear (northwest). It comprises of 40 single and double bedroom apartments, defined according to the number of occupants. The apartments have repeated space layout. The sleeping spaces are located closer to the façades and the living spaces at the building's core. Balconies along the width of the building (1.6m width) located in the front view, are the most dominant architectural element of the façade. The floors are connected vertically via an elevator (shaft of approximately 1.62m²) and a staircase (6.5m²), and horizontally by a 15.2m long central corridor (18.4m²).

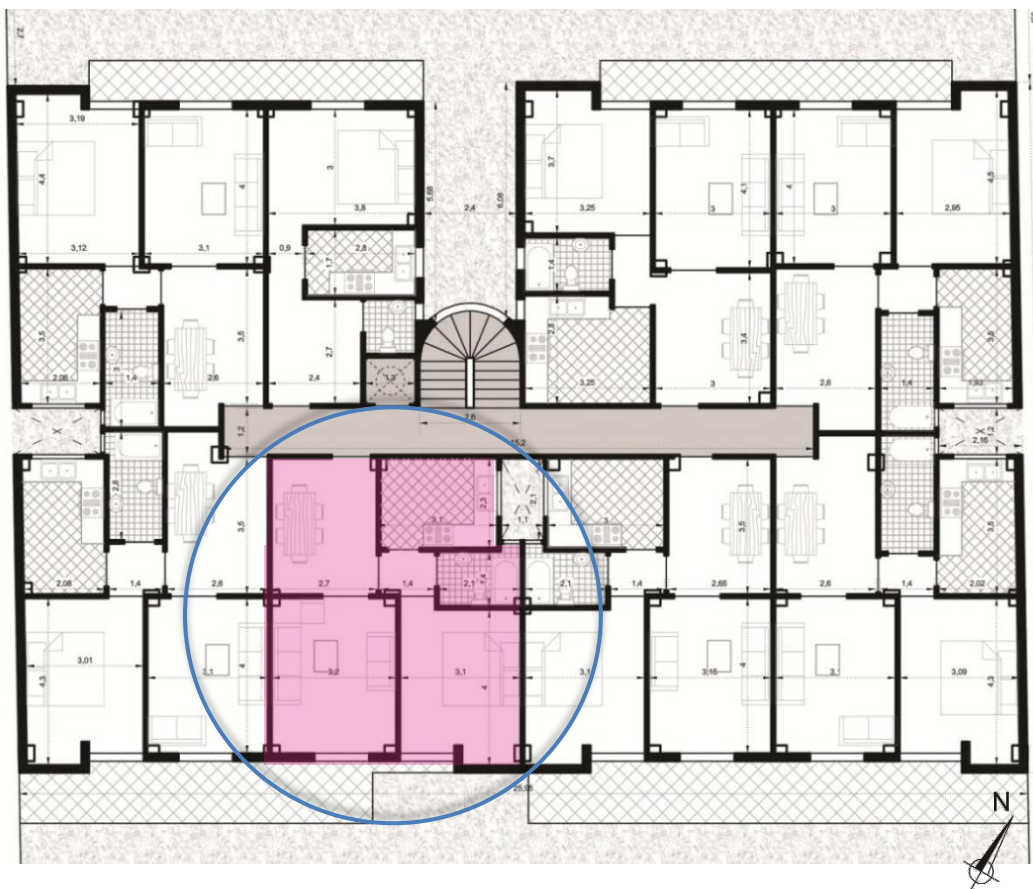


Figure 4.1 First floor, plan view CAD drawing of the building studied, showing the case study apartment (dimensions in metres, nts)

The apartments have limited access to daylight through the windows at southeast and northwest façades. Three light wells (area of 2.5m²) assist the extraction of stale air from the core spaces (Figure 4.2). The light/air wells are connected via openings to both the bathroom and kitchens of all apartments (excluding the penthouse). The height of the light wells is equal to the total height of the building. On the top part of the light wells a horizontal opening levelled to the floor of the penthouse shaded by a

suspended roof at 1m height, operates as a ventilation inlet and outlet, as shown in the photograph of Figure 4.4, preventing the daylighting of the spaces.

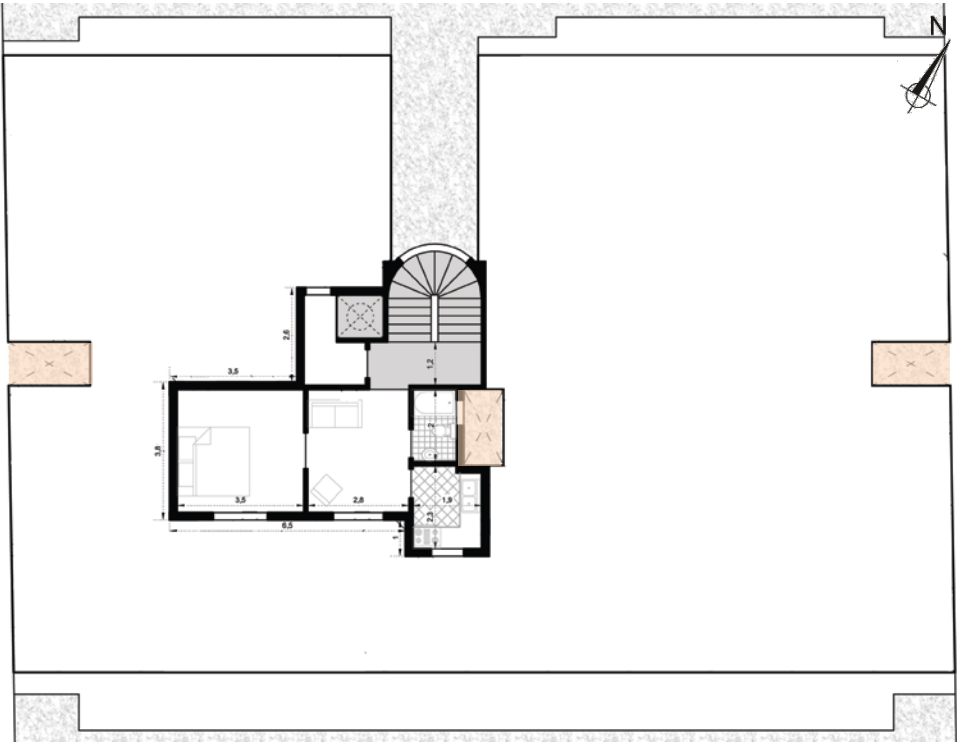


Figure 4.2 Penthouse plan view CAD drawing of the building studied, by author (dimensions in metres, nts) showing the position of the light wells



Figure 4.3 East Elevation, CAD drawing of the building studied by author (metres, nts)



Figure 4.4 Picture of the top part of the existing light well, at the rooftop level (Photograph by author, 2012)

Limited information regarding the building properties and thermal characteristics was available due to lack of respective legislation and construction information regarding buildings constructed before the implementation of the thermal insulation law in Greece (in 1980). Information regarding the materials of the building's envelope and the techniques employed were identified in literature. A brief description of the building properties was provided by the civil engineers of the project. They were contacted by phone for the purpose of this research in 2012. This information was validated and supplemented when no data were available, with the National Regulations and the energy directive TOTE (Androutsopoulos et al., 2012) which include details of the construction properties of buildings constructed prior to 1979 (Table 4.1). Briefly, the exterior walls are non-insulated double brick walls and the internal partitions are single brick walls. The supporting building structure, the roof and the floors are made with *in situ* reinforced concrete. All operating windows and patio windows are single-glazed, wooden framed, with external shutters.

Table 4.1 Building elements, properties and characteristic, by Androutsopoulos et al. (2012)

Component	U-value, W/m ² K	Thickness, mm	Layer Description
External Wall	2.20	220	Double row of bricks, plastered from both wall faces
Internal Partition	2.40	100	Single row of bricks, plastered from both wall faces
Floors/ceilings	2.06	200	Asphalt Mastic Roofing, cast concrete and plastering
Balcony projection	2.75	200	Asphalt Mastic Roofing, cast concrete and plastering
Ground Floor	3.10	650	Unknown construction
Roof	0.95	300	Considered to have been insulated after the 1979 thermal insulation regulation took action, according to the civil engineers of the project.
External Glazing	4.70	--	Single Glazing, Wooden 30% Frame, Net curtain (shading coefficient: 0.2)
Internal Glazing	4.13	60	Single Glazing, Wooden 30% Frame
Internal Doors	3.50	50	Oak

Furthermore, heating was provided in the building spaces by a central oil fired boiler operating strictly within set timetable during the day, during the heating season. For the provision of cooling, individual split air-conditioning units are installed per building space according to occupants' needs and preferences. The exact types of heating and cooling systems have not been identified.

4.2.1. Description of the apartment studied

The residential unit selected for this research is located on the first floor. The apartment has a total floor area of 53m², and floor to ceiling height of 2.7m (Figure 4.5). The two bedrooms are oriented southeast, having one patio window each. The apartment is naturally ventilated via façade opening operated manually by the occupants. The living room, kitchen and bathroom are located at the rear spaces (northwest), they have no external openings and are connected to one of the three light wells (Figure 4.2). The two 'internal' windows of the kitchen and bathroom provide indirect access to daylight, via the one of the three light wells in the building (Figure 4.4). However, due to the suspended ceiling at the top of the light well (rain protection), the primary use of the light well is for extraction of stale air from the connected spaces. Fresh air is provided at the apartment spaces from the two façade openings (bedrooms) and stale air escapes either from the two façade openings (single-sided ventilation dual openings) or from the two light well openings (kitchen and bathroom) and finally from the top horizontal opening of the light well (cross ventilation).

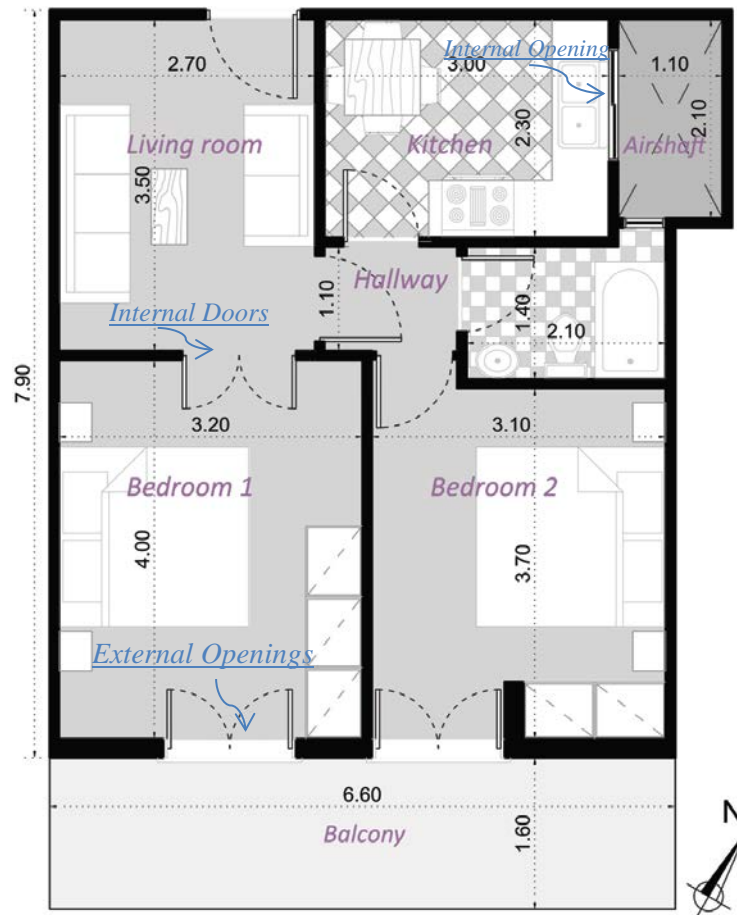


Figure 4.5 Floor plan of the case study apartment, internal openings and area of spaces (m)

4.3. Study of the Surrounding Buildings

The climate of every site is modified by specific conditions and the microclimate (i.e. wind, sunlight and air quality) is defined by urban forms, spaces, and the urban density (THERMIE, 1999). During a site visit in June 2012 a survey was conducted of the case study building and its surroundings. This provided information regarding the site topography and surrounding buildings. The information was recorded in the form of a ‘map’ including the main building, the form of the surrounding buildings, and the street layout. The data collected included the number, use, location and dimensions of the surrounding buildings, as well as the terrain heights.

Nine urban blocks were surveyed. Despite the significant differences between the layout, size and dimensions of the urban blocks and their buildings, a common pattern of the buildings location on each urban block was observed (see Figures 4.6 and 4.7). Most of the buildings were detached from two sides creating an open

rectangular space (not clearly defined), formed by the various building layouts, at the rear of the buildings and middle of the block. This is typically of the urban Greek architecture (Papamanolis, 2000).



Figure 4.6 Views of the case study building (Photographs by author, 2012)



Figure 4.7 Views of the neighbourhood and different urban blocks (Photographs by author, 2012)

The area is predominantly residential, with only a small number of mixed-use buildings (23 out of 103 properties) with commercial use at the ground floor and residential use at the floors above. The majority of the buildings are multi-storey apartment buildings of up to eight storeys. The building heights were predicted with reference to: the number of floors; the existence of a ground floor; the pilotis (when the ground floor is used as a parking area); the semi-basements floors; and the elevated ground floors for either residential or commercial use. A set value of the average floor to floor height was considered for each different type of floors. The typical residential floor height was considered equal to 3.2m, the ground floor commercial space equal to 3.8m, the pilotis equal to 2.8m, and the elevated ground floor equal to 3.8m. As access was not possible to the different properties, the number and location of the penthouses, balconies and external shading devices were excluded for the purpose of this survey.

The data collected during the survey were implemented in the site map from Google maps (Google Maps, 2013). With a use of an online tool generating elevation maps the altitude of the site was defined. As the information regarding the surrounding buildings and terrain morphology is valuable for the DTM and CFD simulations, simplification of the building forms was required to potentially reduce computational time, as explained in detail in Chapters 5 and 6. Geometrical ‘corrections’ were applied to the buildings’ layout to achieve dimensions rounded to metre integers (e.g. façade length of 3.79 m would become 4 m). Similarly, the distance between the buildings and the blocks was rounded to metre integers (e.g. road width of 10.23m would become 10m). A contour map of the terrain was created for every one metre height. It was noticed that the elevation had a non-symmetrical increase towards more than one point of the site, thus simplifications were required of the contour lines. The terrain heights were simplified in metre integers, gradually increasing on a single axis (southwest, northeast). Further details are included in Appendix A.1. Figure 4.8 presents a plan view of the area showing the shape and height in metres of all the surrounding buildings, the terrain heights (simplified on one axis), and an elevation of the building studied and adjacent buildings.



Figure 4.8 Plan view of the site showing building heights in metres, with different colours the 1-metre contours, and a front elevation

4.4. Climate Study

In order to perform building thermal performance modelling on an hourly basis of a period up to a calendar year, hourly climate information is required. For the existing building site in Athens (the area of Galatsi located at 38.02 Latitude, 23.76 Longitude and 160m altitude) the most suitable climate file was identified. Due to the lack of weather stations in close proximity to the building site, climate data were not available from the local authorities.

The climate file provided by the dynamic thermal modelling (DTM) software selected for the purpose of this work (IESVE), included climate data recorded in meteorological stations within a substantial distance to the site. The closest area, the Ellinikon (37.90 Latitude, 23.73 Longitude and in 15m Altitude), is a suburban area with considerable altitude difference with the site under investigation. It was thus considered unsuitable for this research (*climate file 1*). Instead, a climate file of hourly measurements was generated in Meteonorm software (Meteonorm 7, 2012) for the period of 1961-1990. Meteonorm is a well-established tool that interpolates monthly mean values from surrounding meteorological stations and creates climate databases for modelling applications in areas without weather stations (*climate file 2*). Climate data were also collected at a local and private weather station (Koukousianos, 2011) with close proximity to the site (*climate file 3*). The short data-measuring period (2011 to 2013) was considered insufficient to generate a climate file of a representative, typical year. In addition, some of the required information for DTM simulations had not been recorded e.g. cloud cover. A comparison study was performed between the three aforementioned climate files to define the most suitable climate file.

A comparison study was performed between the three climate data to identify the most suitable data set for the purpose of this work, using Excel (Microsoft, 2010). Table 4.2 and Table 4.3 summarise the average (mean) monthly maximum DBTs and wind speeds of the three available climate data for the site. The climate data from the IESVE (for the area of Ellinikon) varied significantly to those of the local weather station, while those of Meteonorm were predicted between these two. The climate data of the local station are significantly high to the other two, because they have not

been normalised (i.e. monitored data of only two calendar years). Although *climate file 2* suggest lower DBTs by approximately 9% and higher wind speeds by 25% than *climate file 3*, *climate file 2* was selected. This climate file (*climate file 2*) was used for the ventilation and cooling performance investigation of the proposed natural ventilation strategies throughout the cooling period, using DTM simulations (Chapter 5) and for specific climate conditions using steady state CFD (Chapter 6).

Table 4.2 Average monthly maximum DBT of the different climate datasets (°C)

Month	Climate file 1 IES	Climate file 2 Meteonorm	Climate file 3 Local station
May	24.1	25	26.3
June	28.7	29.2	32.2
July	31.6	32.1	35.7
August	31.7	31.8	34.3
September	27.7	27.8	31.3

Table 4.3 Average monthly maximum wind speed of the three different datasets (m/s)

Month	IES	Meteonorm	Local station
May	6.9	6.1	4.5
June	6.8	6.3	5
July	7.3	6.8	5.4
August	7.7	6.9	6.2
September	6.3	6.9	5.2

For the climate data selected (*climate file 2*,) the average, best and extreme scenarios of wind speed, directions and DBTs for the cooling period were identified, as presented in Figure 4.9. These were predicted using the *climate file 2* and Excel calculations (Microsoft, 2010). The cooling season is defined by Greek regulations for buildings' energy efficiency, between 15th of May and 15th of September and the heating season between 1st of November and 15th of April (Androutsopoulos et al., 2012).

Evaluation of the ventilation and cooling potential of the ventilation strategies during the average climate conditions of the cooling period could provide information during the potentially most frequent operation of the strategies. Conversely, during the extreme climate scenarios, information could be provided for the least frequent operation of the strategies, although with significant impact on the peak energy loads (i.e. mechanical cooling), as described in Chapter 2.3. Designing for extreme weather today, provides resilience of the existing domestic building stock to the future climate and acknowledges the implications of climate change.

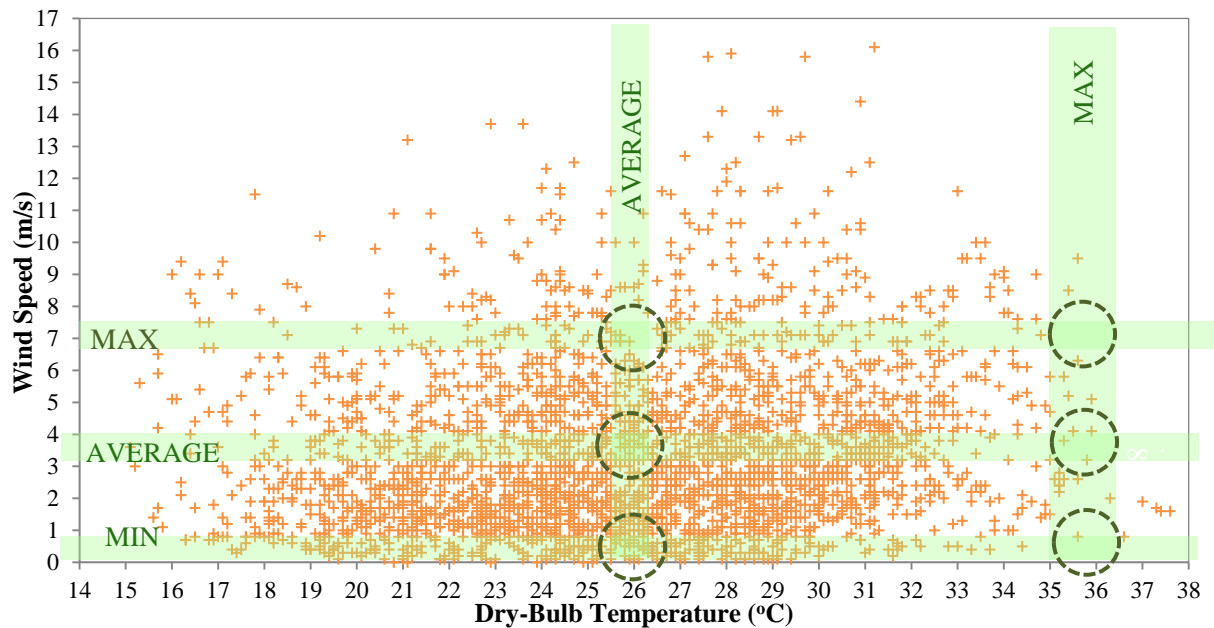


Figure 4.9 Hourly values of DBT and wind speed presented as a scatter plot. Superimposed are zones of the maximum, minimum and average values of wind speed and temperature; their points of intersection define 6 'climate scenarios' during the cooling period for the CFD simulations

Wind speeds incidents between 0.5-5.5m/s occur for up to 75% of the cooling period (see Figure 4.10). It was predicted that north wind directions have the highest frequency; followed by northeast and northwest (Figure 4.11). Average wind speed (mean) was predicted to be 3.6m/s, as shown in Table 4.4, by calculating the average wind speed of each direction in Excel. This value is also recommended by the national Greek energy regulations TOTEE KENAK 20701-3 for energy calculations, for the area of Athens and the cooling period. Highest values of wind speed were considered all values above 7m/s, with 15% frequency. Therefore, the 85 percentile of the wind speeds, the 7m/s, will be regarded as the 'maximum' wind speed (Figure 4.9). If adequate ventilation rates are provided for 7m/s wind speeds, it will be provided for higher wind speeds too.

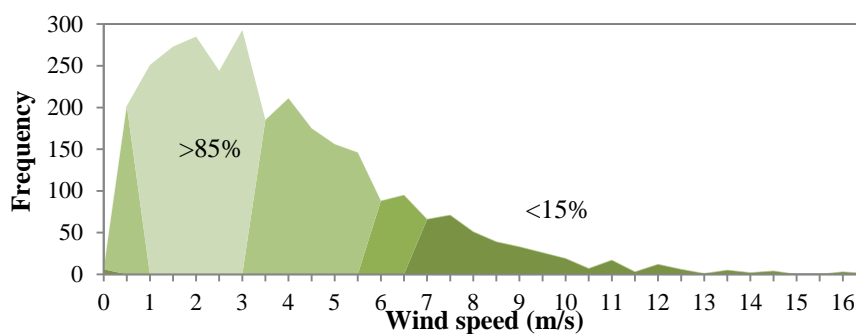


Figure 4.10 Hourly values of wind speed frequency during the cooling period

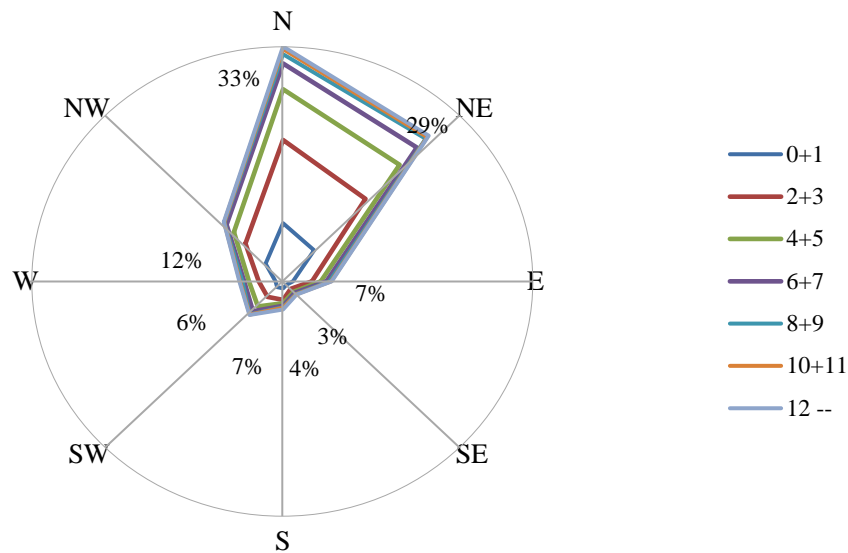


Figure 4.11 Wind-rose, showing the percentage of incident of each wind direction and the shares of the wind speeds (discretised every 2m/s)

Table 4.4 Incidents of frequency of wind speeds (hourly rounded data for the examined period) for each orientation (m/s)

Wind Speed	N	NE	E	SE	S	SW	W	NW	All Directions	Frequency (%)
0 m/s	62	42	6	5	6	14	4	23	162	5%
1 m/s	181	141	35	15	24	21	28	81	526	18%
2 m/s	197	158	40	12	23	26	33	71	560	19%
3 m/s	151	146	40	13	25	31	37	48	491	16%
4 m/s	119	123	22	12	8	34	17	39	374	13%
5 m/s	93	79	15	5	6	23	24	29	274	9%
6 m/s	68	59	13	3	7	18	12	24	204	7%
7 m/s	40	43	10	4	4	11	8	20	140	5%
8 m/s	26	32	5	2	5	9	5	8	92	3%
9 m/s	13	20	8	4	1	9	2	4	61	2%
10 m/s	15	5	6	2	1	1	6	2	38	1%
11 m/s	6	5	1		1		4		17	1%
12 m/s	7	3	1	1	2		3	1	18	1%
13 m/s	2	2		1	3			1	9	0%
14 m/s	1	3			1	1			6	0%
15 m/s									0	0%
16 m/s	1		1		1	1			4	0%
Average	3.36	3.54	3.68	3.67	3.71	3.96	3.89	3.09	3.61	

Due to the large variation of air temperatures and wind properties throughout the day (i.e. diurnal temperature difference), average daily values are not representative of the indoor conditions in the spaces during the occupied periods. As reported by others (Prajongsan and Sharples, 2012), each calendar day could be divided into four groups of six hours (1am-6am, 6pm-12am, 12pm-6pm, 6pm-midnight) with regard to climatic characteristics as well as occupants' presence (see further in Chapter 5). For the climate studied, similar wind patterns were observed in each of the four daily

groups for the cooling period. As shown in Figure 4.12, higher wind speeds (mean monthly values of each six-hour group) were recorded in the afternoon and evening, while the lowest values were predicted during the late morning hours. The smallest wind speed daily fluctuations were predicted during May.

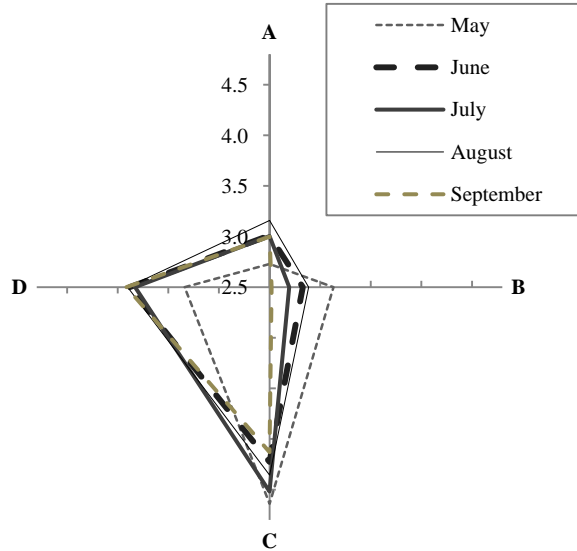


Figure 4.12 Mean wind speeds for the site, per day group during the examined period (m/s)

It was predicted that for 75% of the period, ambient temperatures varied between 24°C and 29°C, with 26°C the most frequent value (hourly DBT values rounded to integer numbers) (Figure 4.13). Highest values of DBT were considered all values above 29°C, with 25% frequency. However, absolute maximum air temperatures of up to 42°C have been recorded in the area during the period between 1955 and 1997, according to the Hellenic national meteorological service (HNMS, 2012). Therefore, DBTs above 29°C would have higher frequency if the data of the climate file were not normalised over a ten-year period. The DBT of 35°C was selected as the highest value despite the low frequency (Figure 4.13). If natural ventilation delivers comfort for DBTs of 35°C, comfort would be delivered for the most of the cooling period.

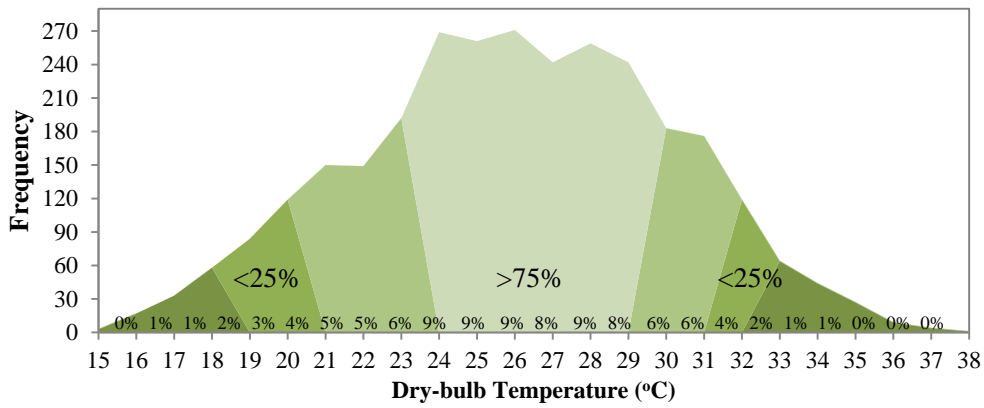


Figure 4.13 Frequency of DBT for the cooling period

An average DBT (mean) of 26°C was predicted using Excel with 15% frequency during the cooling period (Figure 4.14). With regard to the highest daily DBTs during the cooling period, the most frequent value predicted was 29°C (16% frequency). These values vary significantly for the four 6-hour day groups. For the first and second day groups the average DBT was predicted to be 23°C, for the third 27°C and for the fourth 26°C (Figure 4.15). This expresses the significance of evaluating thermal performance in spaces using 6-hour day groups rather than the average daily values.

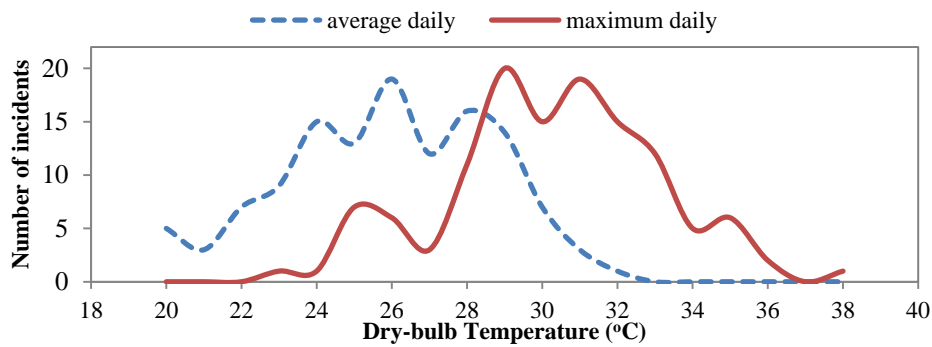


Figure 4.14 Number of daily average and maximum of DBTs

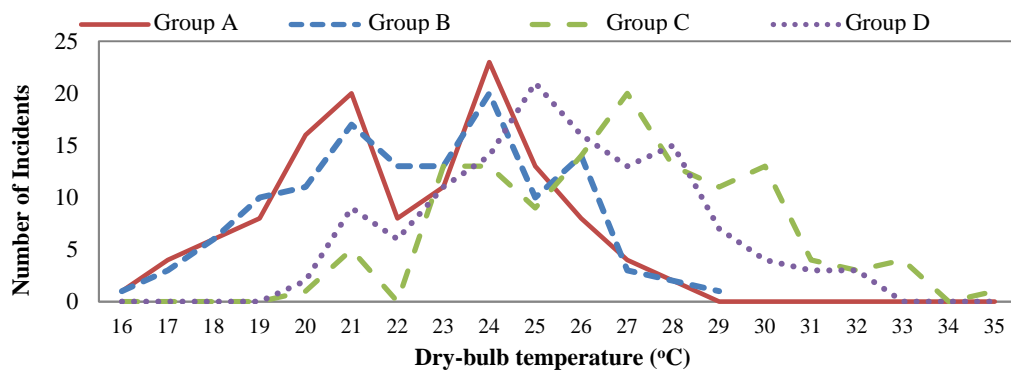


Figure 4.15 Average DBTs values per daily group for the cooling period

4.5. Natural Ventilation Strategies: Design

As described in Chapter 3 (Table 3-1), a number of natural ventilation and cooling strategies were identified for investigation in the literature (Chapter 2.6). These strategies can be implemented in the case study building in relation to the building form, layout and operation. The detailed design characteristics of a wind-catcher, a dynamic façade and the additionally proposed internal openings are presented in the following sections. The zones of interest and connecting points within the case study building are shown in Figure 4.16.

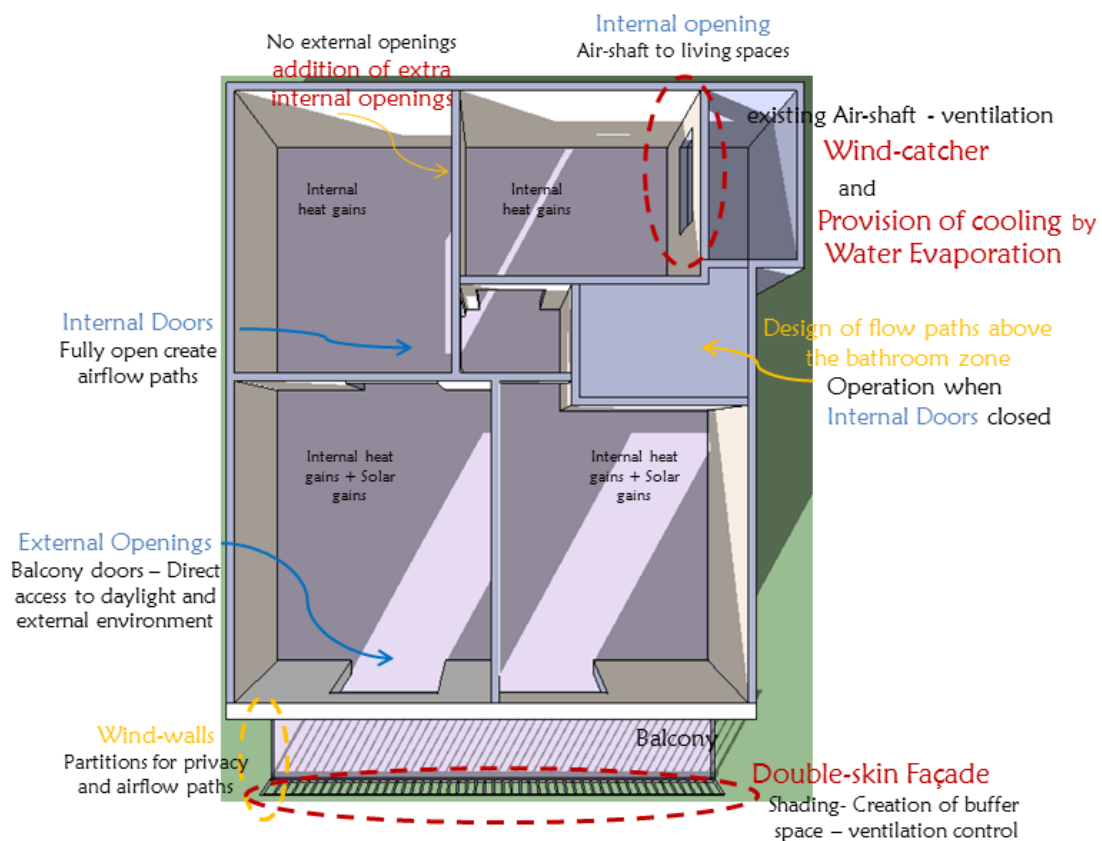


Figure 4.16 Model of the apartment under investigation, showing the zones of interest, connecting points, and the implementation zones of the various natural ventilation systems and strategies

4.5.1. Designing a wind-catcher for the case study building

The integration of four-directional wind-catchers into the core of the case study apartment was investigated. A wind-catcher was designed in the top part of the core light well (2.64m² cross section area), which is connected to the apartment under investigation and to seven more apartments (i.e. 3 above the case study apartment and 4 connected to the other side of the light well). For the total building three identical wind-catchers are proposed.

The wind-catcher design with four openings and four separated channels has been often employed in areas with no prevailing wind, and its ventilation potential has been evaluated by several researchers (Montazeri, 2011). Although the analysis of the climate under investigation predicted two predominant wind direction (north and northeast), as shown in Figure 4.11, a four-direction wind-catcher design that could utilise all available wind directions was favoured (Figure 4.17). It was expected that the surrounding buildings would modify the wind flow-field around the case study building and thus the performance of the wind-catcher under various wind directions should be considered. The proposed wind-catcher has been designed after the typical wind-catcher described by Bahadori (Bahadori, 1985) and with regard to the requirements of this research, as shown in Figure 4.17 and Figure 4.18.

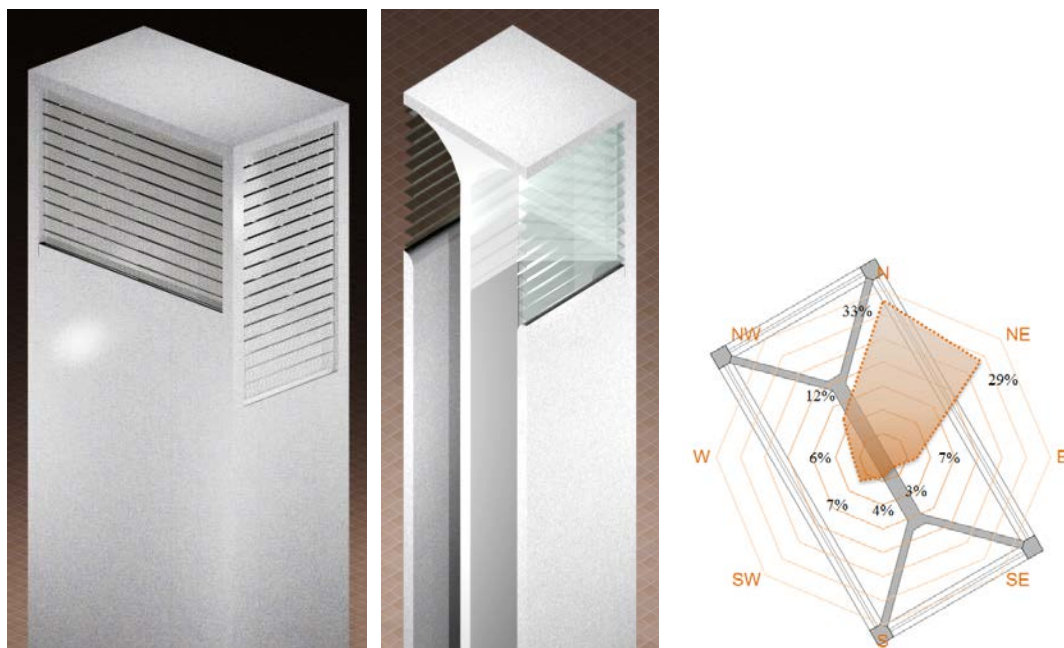


Figure 4.17 Wind-catcher 3-D representations (left) and plan view (right) showing the frequency of wind directions (%), CAD drawing by author

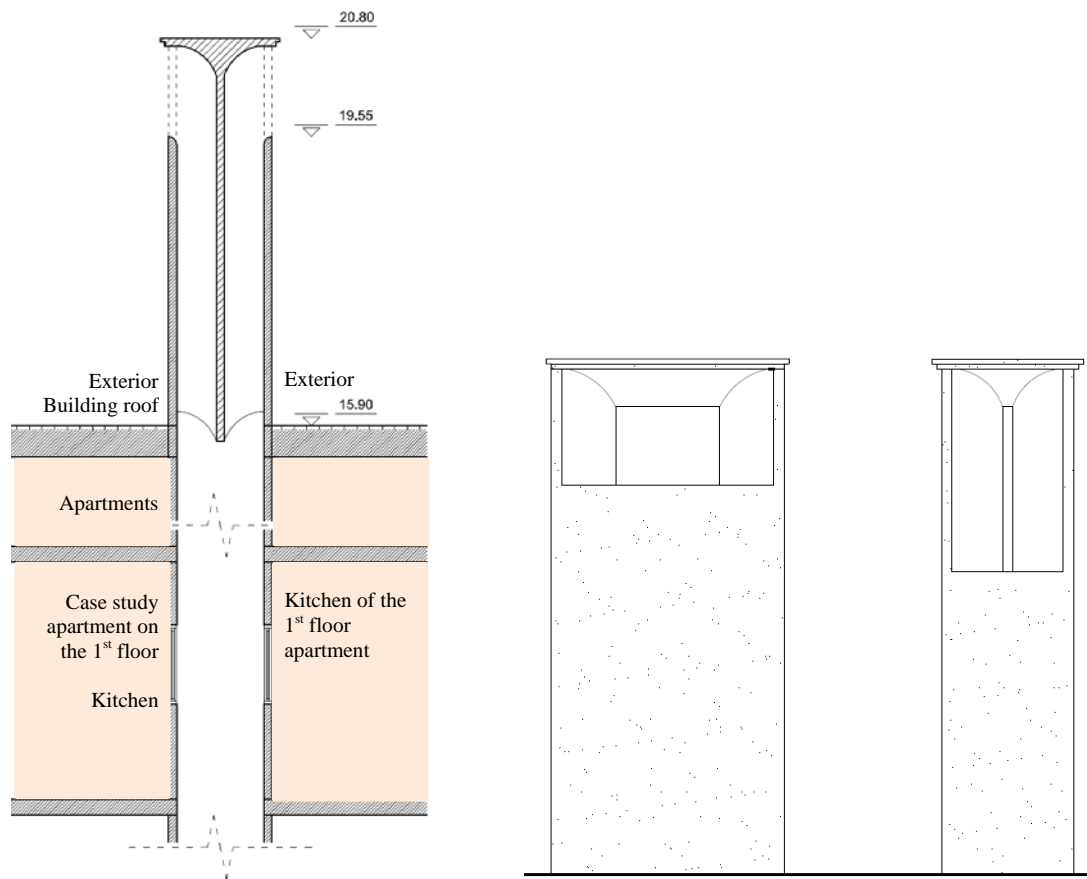


Figure 4.18 Cross-section (left) and elevation (right) of the wind-catcher (CAD drawing by author, nts, after Bahadori, 1985)

The proposed design is added on the top of the existing light well. The size of the wind-catcher openings were defined by the total height of the wind-catcher and the surrounding structures (i.e. the central wind-catcher is attached by two sides to the penthouse). The area of the openings (2.2m^2) was twice the area of the internal connecting opening (kitchen-light well as shown in Figure 4.18). The height of the wind-catcher extends up to 1.5m above the penthouse roof, which is in compliance to the Greek general construction regulation (GOK, 1985). The internal partitions (5m long) extend from the top of the wind-catcher up to the top part of the light well (building roof); the existing design of the light well is not altered by the inclusion of the wind-catcher apart from the removal of the top suspended roof.

The wind-catcher and partitions design was further simplified to accommodate the modelling requirements in CFD and reduce computational time, i.e. reduce the detail in the computational mesh. The final design includes internal partitions on 'X' arrangement, with five metre length and 70mm thickness. The cross-partitions assist

the individual flow entering or escaping each opening and the simultaneous upwards escape of stale air. The final building design with the inclusion of the three wind-catchers is presented in the CAD drawing of the main façade, Figure 4.19.

It was expected that individual automatically controlled dampers located within the lowest part of each channel (created from the cross-partitions) would operate simultaneously with the respective wind-catcher openings, and with regard to the wind direction. The proposed wind-catcher would perform as both inlet of fresh air (for sufficient wind-speeds) and outlet of stale/hot air (for low wind speeds). During buoyancy-driven flows, all dampers would remain open assisting the upwards escape of stale air from the indoor spaces.



Figure 4.19 Southeast elevation of the building under investigation, showing the three wind-catchers in the core spaces (dimensions in metres, nts)

4.5.2. Design characteristics of a dynamic façade (DF)

Most commonly, the term double-skin façade refers to a second layer of glass. The benefits and limitations of them in hot climates were thoroughly addressed in Chapter 2.6. For the purpose of this research, it was decided to introduce a lightweight dynamic façade (DF) of an external horizontal shading system (Figure

4.20). This would assist the natural ventilation of the spaces via openings at the top and lower parts, as in double-skin façades, while the louvres would provide shading and solar gain reductions. This was expected to create a semi-permeable barrier-a buffer space. As with the partitioned by storey, multi-storey louvre type of façades, consisting of pivoting louvres rather than a second layer of glazing, the DF was not expected to be airtight even during the fully closed position of the louvres (Loncour et al., 2004).

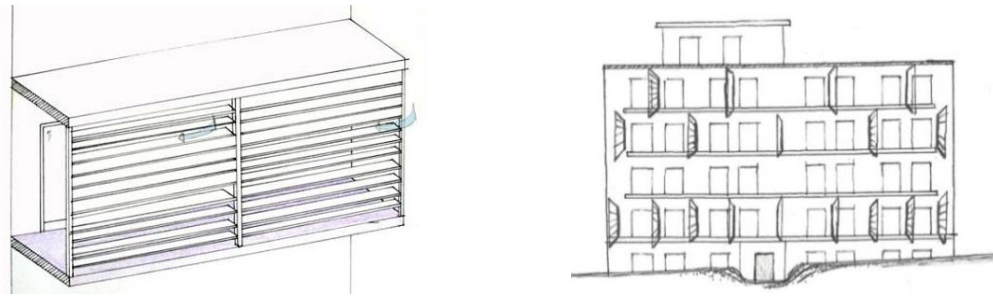


Figure 4.20 Sketch representation of the main façade showing the proposed dynamic façade (left) and the partition walls on the balcony zones (right)

Partition walls perpendicular to the two façades were designed between all apartments, dividing the balconies of each floor in four zones (Figure 4.20). The height of the partition walls was designed equal to the floor to ceiling height and the length to the balcony depth. Each zone encloses the balcony area and two balcony doors of each apartment. These partition walls create isolated zones for each apartment, preventing air circulation between the different ownerships whilst providing privacy. Ideally, these walls would assist provision of daylight in the spaces and thus the proposed material for the partition walls was brick glass.

The louvres were designed according to literature, suggesting on east and west louvres located in the front and parallel to the façades (Palmero-Marrero and Oliveira, 2010). Further, as the main façade of the case study building is oriented southeast, the louvres were designed as recommended for east orientations. The number of louvres was defined by dividing the floor to ceiling height to the width of louvres (i.e. 14 blinds were designed of 21cm width). They were positioned at the edge of the balcony (Figure 4.21). This was in compliance to the Greek general construction regulation defining 40cm the maximum allowed width of façade elements (GOK, 1985).

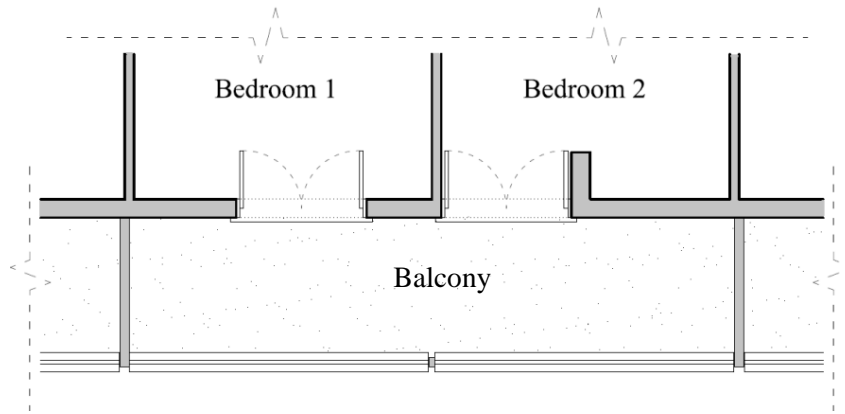


Figure 4.21 Plan view of the apartment's balcony, showing the louvres and partition walls

The design of the shading systems was developed according to an existing manufacturer (Colt, 2006). The proposed louvres material is extruded aluminium alloy, though a wide variety of materials could be proposed, subject to the preferred façade design e.g. glass, wood, and glass with reflective properties or with integrated photovoltaic cells. As presented in the cross-section of Figure 4.22, the carrier system would integrate a central aluminium torsion tube along the length of the louvres assisting their rotational operation. It would be a system of controllable fins that could offer design and operation flexibility (Figure 4.23).

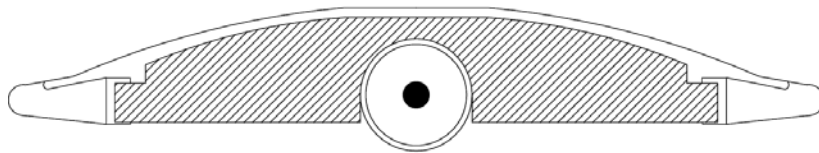


Figure 4.22 Detailed cross-section of the louvres, after: Colt (2006)

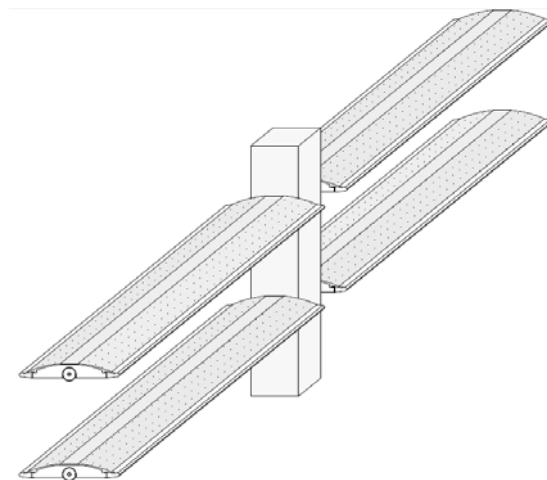


Figure 4.23 Detail 3-dimensional view of the louvres and the carrier system, after: Colt (2006)

Horizontal shading systems and louvres would be adjusted to respond to several climate parameters, glare, direct radiation, obstruction of view, privacy and aesthetics. Evaluating a wide range of control parameters to identify the optimum design was beyond the scope of this research, as the primary intention was to quantify the apartments' thermal performance by utilising a simple design of automated horizontal blinds. According to literature (Chapter 2), automatic control of blinds is recommended on east and west facing façades due to the large amount of sunshine, as they allow controllable shading.

The DF was divided into three parts and designed with three sets of louvres that would provide operation flexibility, uniformity across the building and aesthetic contribution to the existing building façade. It was expected that the louvres would operate in various ways, including fully open, partially, top and bottom, in inclined, horizontal or vertical arrangement etc.

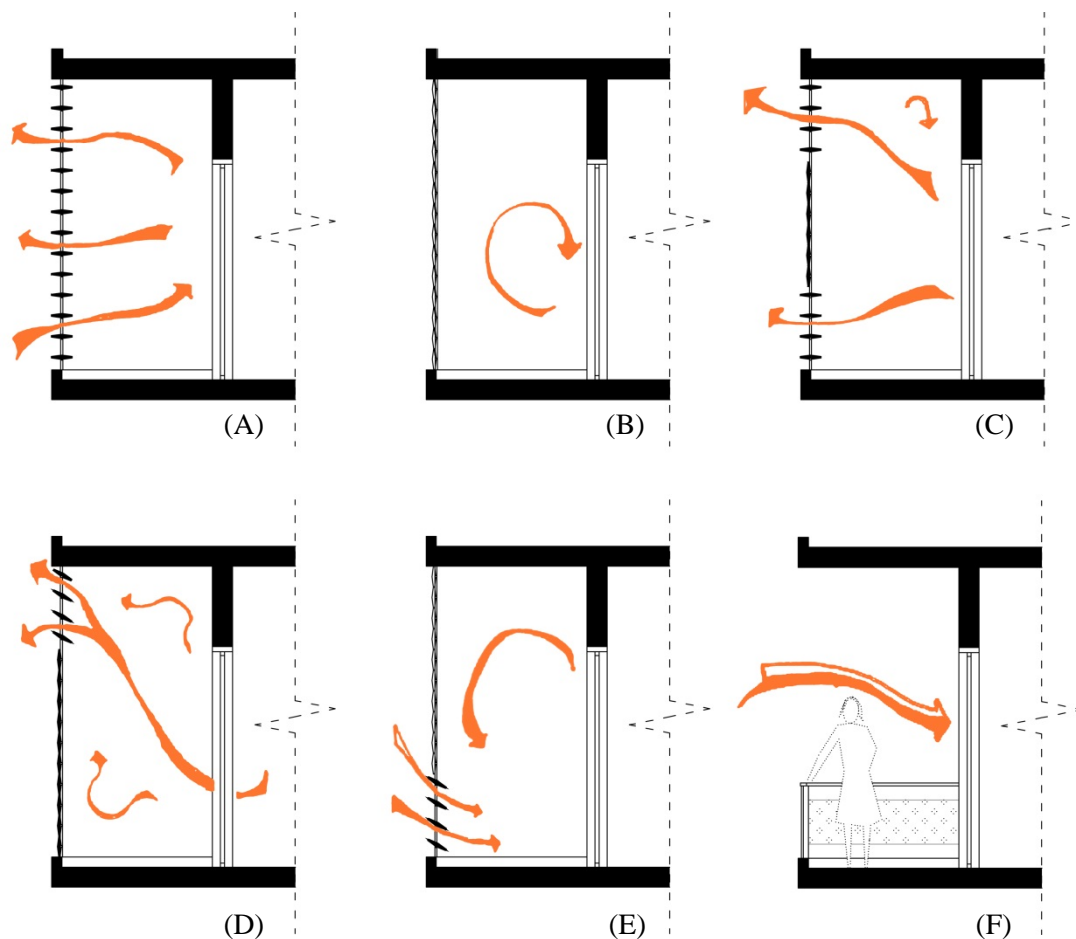


Figure 4.24 Cross-sections of the balcony and the dynamic façade, showing the current (F) operation of the louvres, the proposed (A, B, C) and potential future operations (D, E)

Figure 4.24 illustrates various operation arrangements in reference to the current building design (F). For the purpose of this research, the first three arrangements (A, B and C) were evaluated in Chapter 5 and 6. Further work would involve development of the operation of the louvres to maximise natural daylight whilst controlling solar gains and glare. The controllable louvres could be also linked to a sun-tracking controller. The ‘A’ operation provides angle adjustment for airflow control, solar protection and view, while the ‘B’ operation, privacy and protection from weather. The ‘C’ could be used during the early hours of the day and provide protection from glare, and the ‘E’ during the day to provide adequate shading and ventilation. The ‘D’ could be used during nighttime for privacy, security and extraction of stale air.

The louvres were expected to operate in response to solar gains, individually for each apartment’s requirements. An example operation during solar control is illustrated in Figure 4.25, showing the DF operation when only the middle group of louvres remain closed and when the building is partially shaded by the surroundings (south sun position).



Figure 4.25 A southeast elevation showing the operation of the shading system at each balcony in relation to solar shade.

4.5.3. Supplementary natural ventilation strategies

Further to the proposed natural ventilation strategies, thermal and airflow simulations were performed to evaluate the ventilation efficiency of some additionally suggested strategies. These included the incorporation of wind-catchers at the buildings' façade and creation of internal alternative airflow paths with the inclusion of new internal openings.

4.5.3.1. Façade wind-catchers

Wind-catchers could be introduced in the building design either in the core spaces or at the building's façades such as in the balconies zones, as shown in Figure 4.26. The façade wind-catchers could be designed connected directly to the indoor spaces through the openings, or designed to channel captured ventilation air to the balcony zone. This would then operate as distribution channel for the two front spaces (bedrooms), see Figure 4.27. This strategy would combine the two previously described strategies of wind-catcher and DF. During the incidents of high solar gains, the louvres would remain closed resulting in reduced ventilation rates in the indoor spaces. Therefore, façade wind-catchers could deliver higher ventilation rates in the front spaces (southeast) during the high levels of solar radiation (when the DF louvres would be closed).

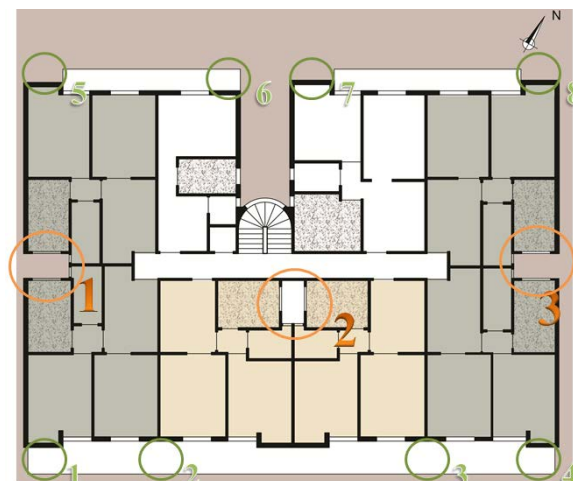


Figure 4.26 Potential areas for wind-catcher inclusion, in the core spaces (light wells) and the balconies

Each wind-catcher would assist the ventilation strategy of one apartment per floor and four apartments across the building height, as shown in Figure 4.28. The

exploratory simulations of this ventilation strategy in Chapter 6, defined a wind-catcher design with $1 \times 1.6\text{m}$ cross section area. For the case study apartment, the wind-catcher position within the balcony and DF are presented in Figure 4.27, indicating expected airflow paths.

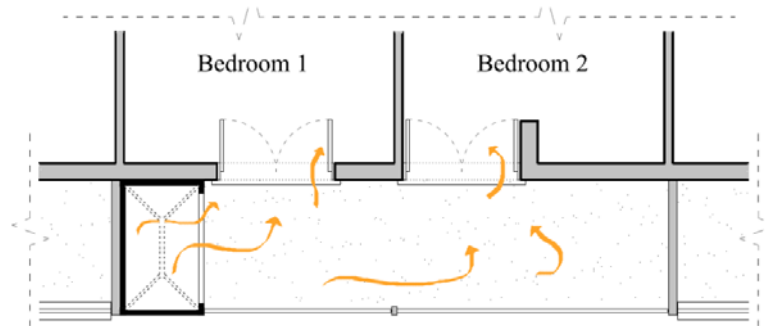


Figure 4.27 Plan view of the apartment's balcony, showing the façade wind-catcher, the closed louvres and the partition walls, nts



Figure 4.28 Southeast elevation of the building under investigation, showing the operation of the shading system on each balcony and the façade wind-catchers, nts

4.5.3.2. Internal openings

The inclusion of supplementary internal openings was required in order to deliver ventilative air when the internal doors would be closed. The contribution of this strategy to the natural ventilation of the spaces was further evaluated and included in Chapters 5 and 6. For the purpose of this, the ancillary space on the top part of the bathroom's false ceiling was used as an air channel. It was connected to the existing

light well and to the hallway with the ancillary space using additional openings (free area 0.30m^2), to enable fresh air into and stale air out of the living spaces. The hallway would now be used as a distribution space. The ventilation air could flow in and out of the two bedroom spaces through the hallway and purpose-provided openings. This strategy utilises the unoccupied space above the bathroom that was also excluded from all ventilation performance simulations. The three openings on the hallway walls, the one connecting to the light well and the specially created partition providing airflow channel in the ancillary space, are shown in Figure 4.29.

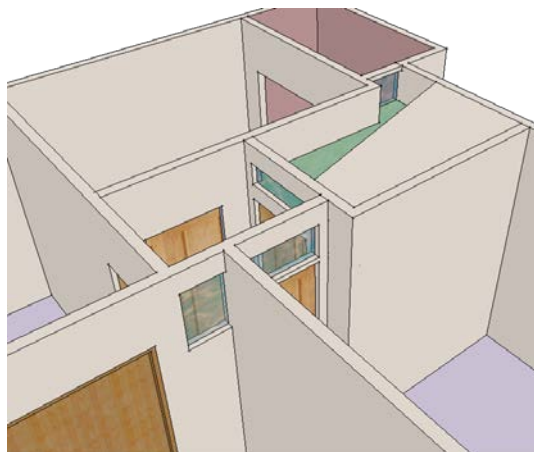


Figure 4.29 Three-dimensional detail representation of the apartment showing the new hallway openings for the ‘internal openings’ ventilation strategy

4.6. Summary

This chapter provided information regarding the design characteristics of the apartment building under investigation and the natural ventilation strategies selected. The presented building design and surrounding buildings (Section 4.3) will be introduced in the two modelling techniques presented in Chapters 5 and 6 in order to evaluate the existing ventilation performance of the apartment studied. The proposed ventilation strategies presented in Section 4.5 will be further designed in the existing building design, and their ventilation performance will be evaluated in Chapters 5 and 6. A suitable climate file was identified for the specific site that will be used in the DTM analysis (Chapter 5). Climate scenarios were generated (Section 4.4) from this file that will feed the ventilation performance analysis using CFD, presented in Chapter 6.

***Chapter 5* : INDOOR ENVIRONMENTAL PERFORMANCE EVALUATION**

5.1. Introduction

Dynamic thermal modelling (DTM) analysis was carried out to evaluate to what extent natural ventilation strategies can improve IAQ and satisfy occupants' comfort. Simulations were performed at the scale of a single apartment using the DTM software, IESVE. Detailed information regarding the building operation (occupants and heat gains) and properties, and the DTM simulations performed, are presented. Section 5.3 includes the parametric study investigating the efficiency of controlled ventilation via different openings operation profiles (Sections 5.3.1 to 5.3.4) and the implementation of natural ventilation systems, i.e. a wind-catcher, a dynamic façade (Sections 5.3.5 to 5.3.8). Details regarding the performance of each strategy evaluated with regard to occupants' thermal comfort and IAQ (Section 5.4) are further discussed, and the quantification of the energy saving potential of the natural ventilation strategies is presented (Section 5.4.1.1). The chapter concludes with the overall ventilation performance evaluation of the building under investigation (Section 5.4.2).

5.2. Parametric Study, Building Operation and Properties: Model Setup

A model of the building was created in IESVE software for the DTM simulations, which included information about the building properties, internal heat gains, occupancy profile, climate data and the building site. The thermal modelling analysis was conducted for the cooling period, between 15th of May and 15th of June (See Chapter 4.4). Although the principal focus of the thermal modelling was the natural ventilation performance of the selected apartment, the overall performance of the building was also obtained.

Following the analysis of the climate data of the site under investigation in Chapter 4.4 (*climate file 2*), the simulation day and the external air properties were divided into four six-hour groups for the cooling period using Excel, with regard to the variations during the day of the air properties and the occupancy levels (described in Section 5.2.1). As shown in Table 5.1, the low DBT and the high wind speeds during the Group A could deliver passive nighttime ventilation. The high values of the DBT and the direct solar radiation of Group C would result in higher indoor air temperatures at the time of the day with the highest occupancy (see Section 5.2.1). These could be controlled by appropriate shading. At all times the low levels of relative humidity (below 54%) and the high wind speed (up to 13m/s) would favour the use of passive ventilation strategies e.g. wind-catchers or evaporative cooling.

Table 5.1 Average, maximum and minimum air properties during the cooling period

		GROUP A 00:00-06:00	GROUP B 06:00-12:00	GROUP C 12:00-18:00	GROUP D 18:00-24:00
DBT (°C)	Average of cooling period	22.6	24.7	29.7	26.9
	Max average	29.0	31.4	36.8	33.9
	Min average	16.0	18.4	22.4	20.5
Wind speed (m/s)	Average of cooling period	3.0	3.0	4.5	3.6
	Max average	11.4	8.8	12.6	12.1
	Min average	0.2	0.3	0.2	0.1
External relative humidity (%)	Average of cooling period	59	52	36	45
	Max average	89	77	54	64
	Min average	43	36	23	32
Direct solar radiation (W/m²)	Average of cooling period	0	441	565	104
	Max average	0	673	925	198
	Min average	0	0	2	0

A parametric study evaluated the potential of optimum natural ventilation strategies (controlled ventilation via openings) and natural ventilation systems (i.e. windcatcher) to improve the ventilation, cooling performance of the case study apartment and provide occupants' comfort. The ventilation strategy of the existing case study apartment was initially evaluated, followed by the investigation of the proposed natural ventilation strategies. Four scenarios of natural ventilation strategies were evaluated; these are presented in the flow diagram of Figure 3.5 of Chapter 3 and in Table 5.2:

- I. **Existing ventilation strategy** of the apartment (base-case): As described in Chapter 4, the apartment under investigation has direct access to daylight through windows (balcony doors) on the southeast façade and is mainly single-side ventilated. A light well connected to the rear spaces (kitchen and bathroom) operates as an air shaft that through the internal connecting openings (Figure 4.5) assists the cross ventilation of the spaces. Stale air escapes from the spaces via the kitchen openings and from the top, horizontal opening of the light well (Figure 4.4), as described in Chapter 4.2.1. All openings operate manually by the occupants according to thermal perception, which is common in naturally ventilated spaces (Papakostas & Sotiropoulos, 1997; Drakou et al., 2011; Fabi et al., 2012; Mavrogianni et al., 2014)(see Chapter 2.5.3).
- II. **Natural ventilation** strategies with daily openings' control: A number of opening profiles were evaluated in order to predict the most efficient daytime, nighttime and day & night ventilation strategy for the selected apartment. The openings would operate automatically and in response to indoor and outdoor environmental conditions. Literature shows that occupants' interact with openings with regard to indoor and outdoor temperatures (Herkel et al., 2008; Yun & Steemers, 2008; Andersen et al., 2009; Fabi et al., 2012), indoor air quality (Drakou et al., 2011) and less frequently with regard to wind speed (Roetzel et al., 2010). Although manual control is a viable option, due to the unpredictability of occupants' behaviour and interaction with the openings, the ventilation performance would improve with automated control of the strategies/ openings, as reported by others for different passive strategies (Ford et al., 2012).

- III. Implementation of **natural ventilation systems**: The ventilation performance of three different systems was evaluated individually and in groups, combined with the previous most efficient natural ventilation strategy (II). A four-sided wind-catcher with cross-partitions was implemented at the top of the existing light well (Chapter 4.5.1). A lightweight dynamic façade of horizontal external louvres was designed on the balconies of the building (Chapter 4.5.2). The performance of new internal openings was explored (Chapter 4.5.3.2).
- IV. **Final ventilation strategy and design**: The strategy with the most significant performance in delivering occupants' thermal comfort and natural ventilation was evaluated.

Table 5.2 List of the natural ventilation strategies and abbreviations

Scenario	Natural ventilation strategy	Abbreviation
I	Existing natural ventilation strategy of the case study building	[base-case]
II	Daytime ventilation	[DV]
II	Nighttime ventilation	[NV]
II	Day & night natural ventilation	[DV & NV]
III	Wind-catcher	[WC]
III	Dynamic façade	[DF]
III	Internal openings arrangement	[InOp]
IV	Wind-catcher and dynamic façade	[DF & WC]

The performance of the aforementioned strategies was evaluated using DTM simulations. The simulation results of the parametric study included hourly, spaced-averaged values for the cooling period of indoor air temperatures (operative) ($^{\circ}\text{C}$), ventilation rates (m^3/s), CO_2 concentration (ppm), air change rates (ach^{-1}) and relative humidity (%). These data were further analysed in Excel spreadsheets (Microsoft, 2010), using calculations, statistical analysis and creation of graphs and tables, as presented in the following sections. Average (mean), minimum, maximum values were predicted, frequencies, distribution and standard deviations, with regard to the parameters examined.

The new ventilation strategies were expected to deliver reductions in the indoor air temperatures, increase in ventilation rates and extension of the percentage hours during which thermal conditions fall within the thermal comfort range, as defined by standards (see comfort temperatures in Chapter 2.5.2). The aim of the DTM

simulations was to evaluate the performance of the ventilation strategies relative to the base-case ventilation strategy of the apartment under investigation. Additionally, a set of environmental conditions, which are acceptable for comfort, were defined according to literature (Chapter 2.5.1) and used for the evaluation of all ventilation performance of the strategies examined. These were included in Table 3.2 of Chapter 3.3.

DTM simulations predicted indoor air temperatures and the operative temperatures, previously known as dry-resultant temperatures (a term also used by IES). These are the weighted average of the indoor air temperature and the mean radiant surface temperatures (CIBSE, 2006). Throughout this chapter, the simulation results of indoor temperature are presented in the form of operative temperatures.

A three-dimensional model of the building in IESVE is presented in Figure 5.1, showing the apartment studied on the first floor, the two façade openings of the apartment in yellow and the horizontal openings of the light well at the top of the building roof shaded red. The layout of the internal spaces of the apartment studied in IESVE is shown in Figure 5.2.

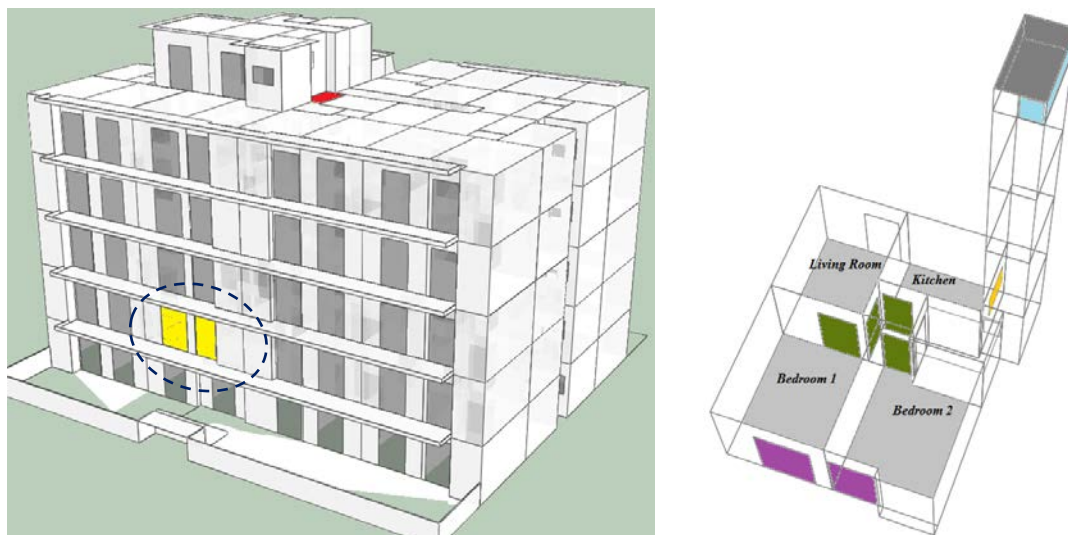


Figure 5.1 (left) A 3D view of the IESVE model of the existing building design, showing as shaded yellow the apartment openings and the horizontal top opening of the light well shaded red

Figure 5.2 (right) Three-dimensional model of the apartment studied in IESVE, showing the location of the internal doors (in green), the internal opening (in yellow), the external openings (in purple), and the openings at the top of the light well (light blue) with the light well cover

The case study building is located in a densely built urban area. It was important to consider the influence of the surrounding buildings to the thermal and ventilation performance of the building and proposed ventilation strategies. The surrounding buildings were introduced in the IESVE model as blocks with defined measured heights and layouts (Figure 5.3), as presented in Chapter 4.3. This would assist the investigation of the influence of shading on the thermal performance of the building.

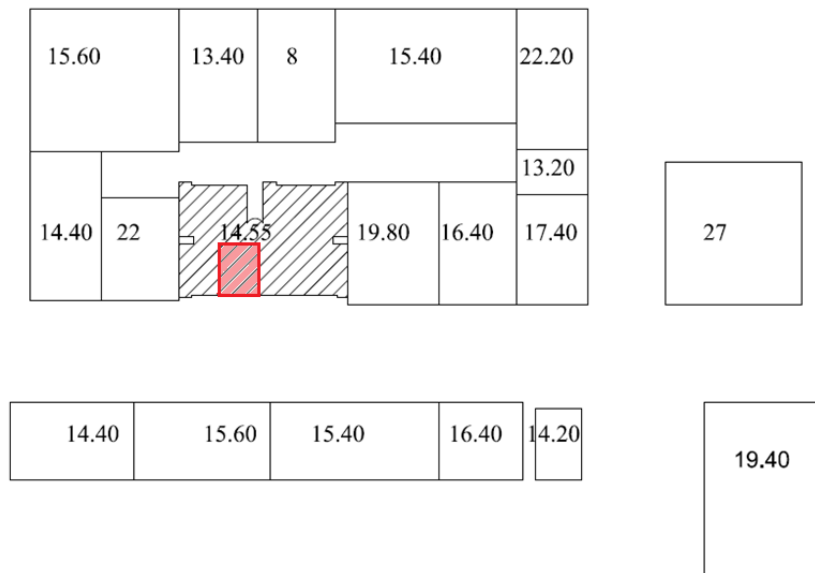


Figure 5.3 Plan layout of the building studied (shaded) and its surroundings in IESVE, indicating the heights of the buildings in metres and the location of the apartment under investigation in the building (shaded red)

A shading analysis was performed to define the hours during which the building was shaded by the neighbouring buildings, thus the hours that additional shading was not required. This was performed within the modelling tool, IESVE. For the four-month period, the building façade was not shaded for 4 ½ hour to 5 ½ hours, from 6am or 7am. The apartment studied had access to direct sunlight between 9am and noon. On the 21st of June, it had access to direct sunlight between 8am and 10:30am (see Figure 5.4). The apartment studied (indicated with a red circle in Figure 5.4) has direct access to sunlight for a shorter period relative to the other building apartments, because it is located on the first floor.

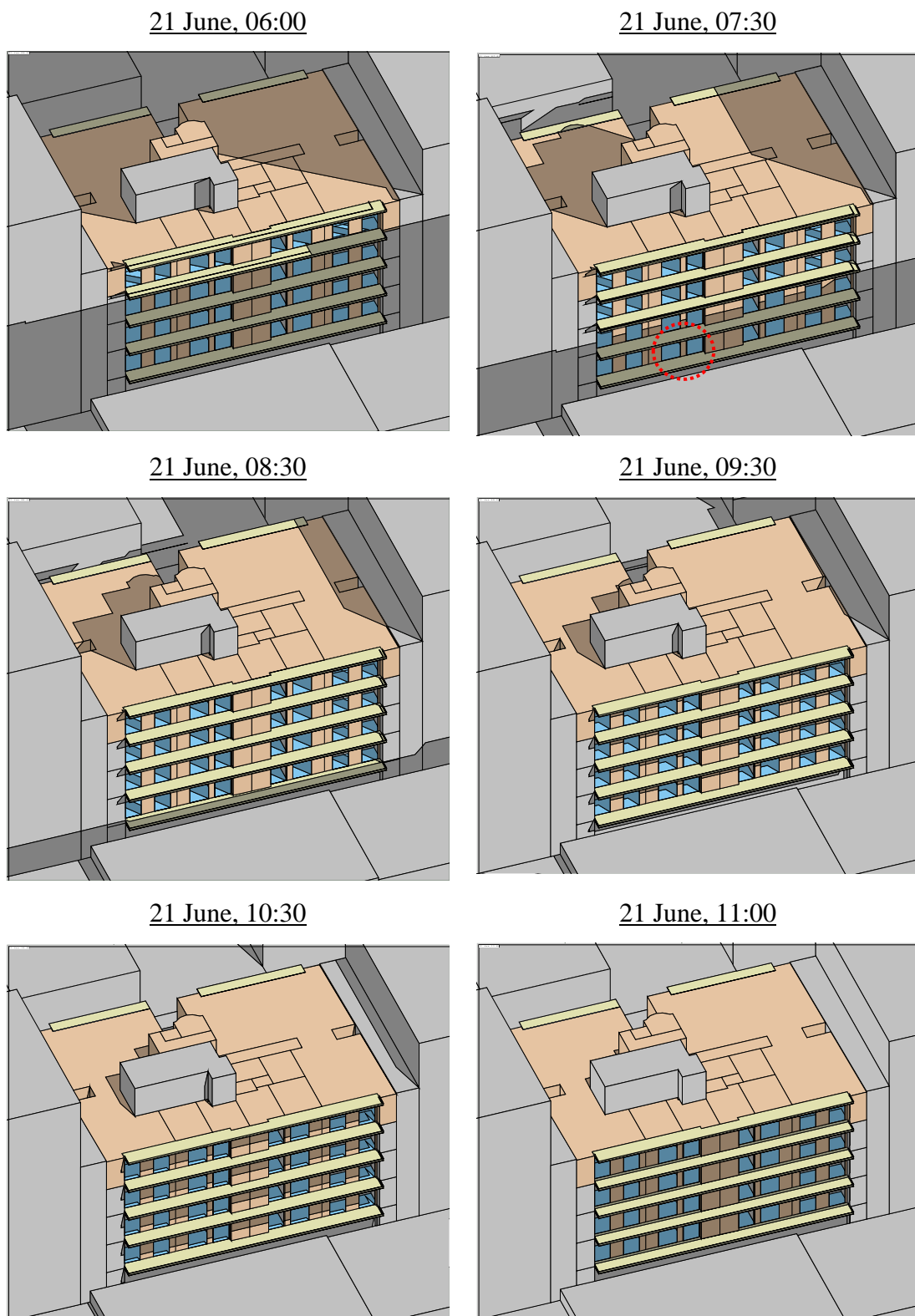


Figure 5.4 Shadows generated at different times during the 21st of June, showing the hours of the day that the main building façade has access to direct sunlight

The construction materials of the buildings elements were corresponded to the default materials included in the software's database, while some had to be approximated. As reported by others, this is a common problem when using thermal modelling software, as the default materials in the software material libraries include those used in the country that the software has been developed (Papadopoulos et al., 2008). Table 5.3, includes information of all construction elements of the building and the passive ventilation systems designed, their thickness and heat transfer coefficients.

Table 5.3 Building element properties

Component of the building	Resulting U-value (W/m²K)	Thickness (mm)	Layers Description
External Wall	2.20	220	Double row of bricks, plastered from both wall faces
Internal Partition	2.40	100	Single row of bricks, plastered from both wall faces
Floors/ceilings	2.06	200	Asphalt Mastic Roofing, cast concrete and plastering
Balcony projection	2.75	200	Asphalt Mastic Roofing, cast concrete and plastering
Ground Floor	3.10	650	Not required for the DTM
Roof	0.95	300	Believed to be insulated after the 1979 and the thermal insulation regulation
External Glazing	4.70		Single Glazing, Wooden Frame 30%, Net curtain (shading coefficient: 0.2)
Internal Glazing	4.13	60	Single Glazing, Wooden Frame 30%
Internal Doors	3.50	50	Oak wood
Components of the natural ventilation systems			
Wing Walls	1.50	80	Glass Brick
DF Openings	2.20		External Shading_ Louvre, U-values based on Passivhaus (Passive House Institute, 2012)
Wind-catcher Walls	0.50		U-values based on KENAK regulations
Wind-catcher Openings	1.20		U-values based on PassivHaus (Passive House Institute, 2012)

5.2.1. Developing an occupancy profile

The Greek national directive of energy efficient buildings TOTEE defines domestic building operation at 18 hours per day (Androutsopoulos et al., 2012). For the purpose of this research, the building was considered occupied at all times according to published work that defined hours of maximum and minimum (never fully unoccupied) occupancy levels during the day (Papakostas and Sotiropoulos, 1997; Mavrogianni et al., 2014). An occupancy profile was created for the typical 24 hours to represent the current operation of the case study building (base-case strategy). This profile was repeated daily during the cooling period, and was kept consistent throughout the different DTM simulations of the natural ventilation strategies.

The case study building is an existing building in the centre of Athens. In order to accurately predict the performance of the apartment studied, survey of the occupants' presence during each day of the cooling period would be required. However, this is a parametric study and if occupancy in the spaces were represented for the specific family of the apartment under investigation, generalisation of the predicted ventilation performance of the strategies to other buildings would not be possible. Therefore, it was decided to represent the building occupancy as percentage of presence (treated as heat sources) and not as predefined number of occupants in the spaces. A profile of the occupants was created in DTM and repeated daily throughout the cooling period.

According to a field survey in 158 Greek domestic buildings by Papakostas and Sotiropoulos (1997), five occupancy groups were defined with different shares of the total number of occupants in the building, as well as a different percentage of presence during the day, as shown in Figure 5.5 and Figure 5.6 respectively. The surveyed sample included 24.6% employed men, 16.4% employed women, 16.8% housewives and elderly members, 30.7% children (aged 5-15), and 11.5% young members.

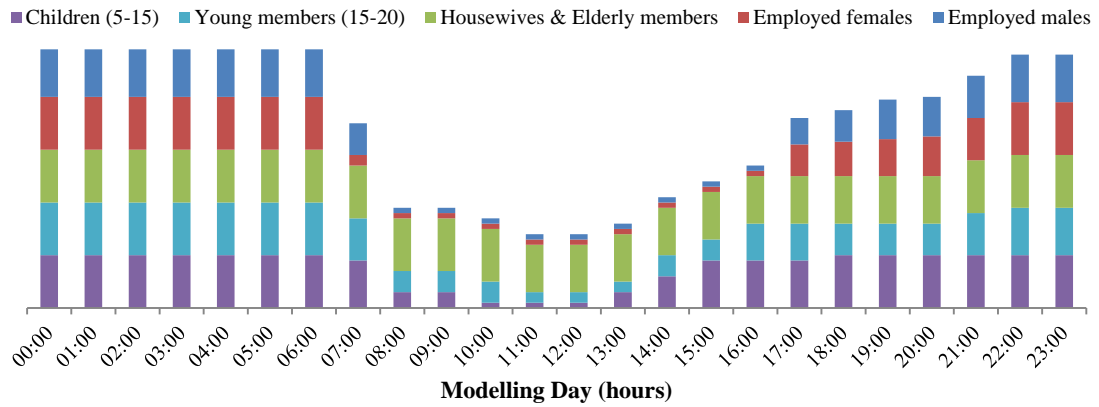


Figure 5.5 Hourly distribution and shares of the different groups of occupants during the typical day, repeated throughout the cooling period, after Papakostas and Sotiropoulos (1997)



Figure 5.6 Overall and individual percentages of occupants' presence during the day, in the apartment under investigation (groups in relation to age, gender and occupation), after Papakostas and Sotiropoulos (1997)

As the survey by Papakostas and Sotiropoulos (1997) was conducted in times of economic growth, the probability of being less representative of the current lifestyle and levels of employment due to the economic condition of the country was considered. The occupancy profile created is a possible projection of the future occupancy levels (after an expected economic growth of the country). Recent work by Mavrogianni et al. (2014) on occupancy patterns in domestic buildings in the United Kingdom reports occupancy patterns similar to those by Papakostas and

Sotiropoulos (1997), thus providing a validation of the occupancy profile created for the purpose of this study.

Although the occupants' presence varies between the apartment spaces relative to both the space and time of the day, the occupancy density was repeated at all living spaces (i.e. kitchen, bedrooms, living room) and occupants were distributed across the apartment spaces. The occupancy profile was designed to vary across the spaces only during the nighttime (between the hours 10pm to 5am) when the two bedrooms would be fully occupied and the other apartment spaces unoccupied.

Theodoridou et al. (2011) surveyed a sample of approximately 900 multi-family households in the second largest city in Greece and predicted that 32.4% of households are occupied by four-member families and 27.3% by families of two. It was further predicted that each household was occupied by 2.8 occupants on average, with density of 33m² per occupant, higher than the value defined by the national directive of energy efficient buildings TOTE (20m² per occupant) (Androutsopoulos et al., 2012). The Greek Census of 2011 similarly defines 2.6 occupants per household (EL.STAT., 2012). Additionally, statistical data for the Municipality of Athens (EL.STAT., 2014) define that 35% of households are occupied by four-member families, 24% by three, and 19% by two. Figure 5.7 demonstrates the correlation of the number of occupants and the number of rooms per household in the county of Athens. As each household of the building under investigation has 3 rooms (living spaces: living room and bedrooms), it is projected that 36% of the households would be occupied by four-member families.

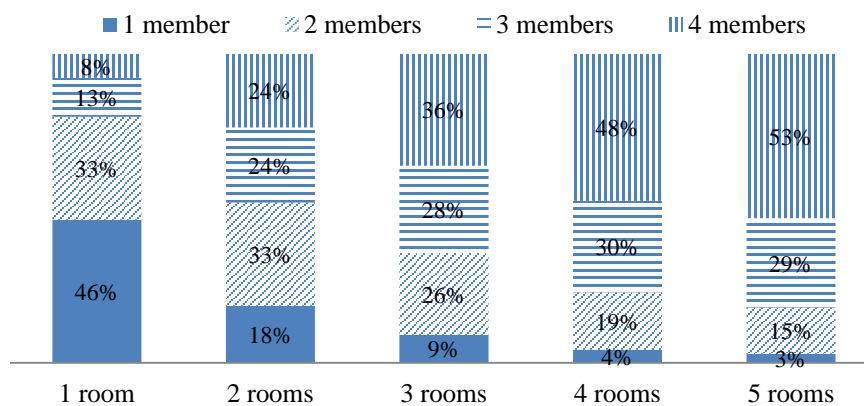


Figure 5.7 Ratio of occupants per property size in the county of Attica, Greece (number of rooms per dwelling) (EL.STAT., 2014).

In order to define the number of occupants per household (80W per occupant), it was decided that two or four occupants in equal shares occupy each of the 40 two-bedroom apartments of the building (120 occupants in total). According to the gross floor area of the building (approximately 1940m²), 16m² was the predicted density of occupants. Although this unit is low, it is in agreement with the relationship between the number of occupants and number of spaces as shown in literature. Further to this, the occupancy profile was created by correlating the occupancy density and the different groups of occupants previously defined (Figure 5.5 and Figure 5.6).

In addition to the internal heat gains due to occupants, a daily profile for the internal heat gains due to lighting and equipment was defined according to published work (Papakostas and Sotiropoulos, 1997; Papadopoulos et al., 2008). The profile was created to comply with the occupancy profile and corresponding activities, such as cooking, cleaning, and use of electronic appliances (Figure 5.8). The units of each energy source and the number of internal heat gains in the living spaces were defined according to the recommended values given by TOTEE (Androutsopoulos et al., 2012) and are summarised in Table 5.4.

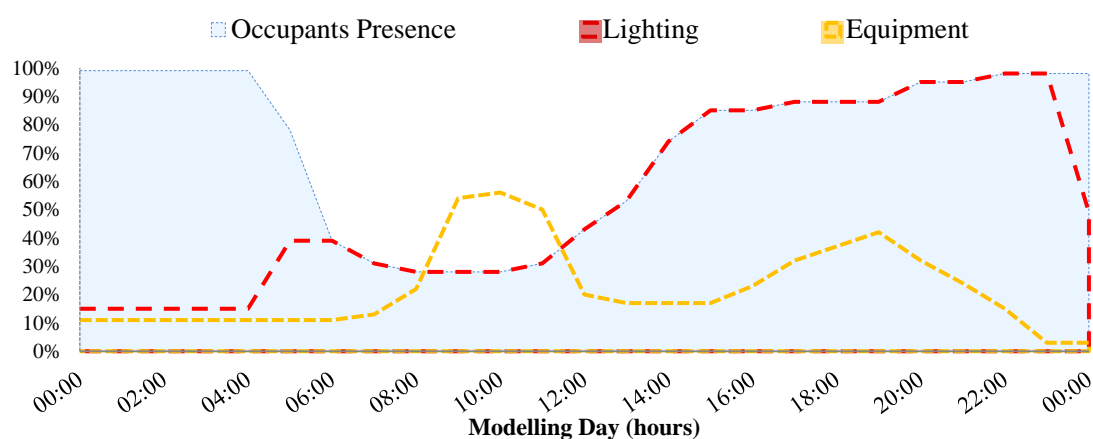


Figure 5.8 Daily profiles of occupancy profile, lighting and equipment operation

Table 5.4 Sensible heat output of the internal heat gains, after Androutsopoulos et al. (2012)

Source	Heat Gains	
Occupants	80W/person	
Lighting	6.4W/m ²	200lm/m ² at a measuring level of 0.80m
Equipment	4W/m ²	average coefficient of operation 0.75
Corridors and Ancillary spaces		
Lighting	6.4W/m ²	200lm/m ² at a measuring level of 0.50m

Furthermore, for the DTM simulations the building was divided into approximately 15 thermal zones, depending on the design of the natural ventilation strategy. The zone distribution, the use of each zone, as well as the floor area of each zone are shown in Table 5.5. The first ten zones are default to all strategies, while additional zones are created for each natural ventilation strategy that required modifications to the DTM building model and design, including the lightweight dynamic façade and the wind-catcher.

Table 5.5 Default thermal zones and additional zones for each natural ventilation strategy

Zone	Use	Area
Zone 1	Living room	10.08m ²
Zone 2	Kitchen	7.44m ²
Zone 3	Hallway	1.80m ²
Zone 4	Bedroom 1	13.695m ²
Zone 5	Bedroom 2	13.115m ²
Zone 6	Bathroom	6.84m ²
Zone 7	Air shaft 1 st floor	2.64m ²
Zone 8	Air shaft 2 st floor	2.64m ²
Zone 9	Air shaft 3 st floor	2.64m ²
Zone 10	Air shaft 4 st floor	2.64m ²
Base-case ventilation strategy		
Zone 11	Air shaft suspended ceiling (h:0.70m)	2.64m ²
Wind-catcher strategy/case		
Zone 12	Wind-catcher channel (SE orientation)	0.66m ²
Zone 13	Wind-catcher channel (NE orientation)	0.66m ²
Zone 14	Wind-catcher channel (NW orientation)	0.66m ²
Zone 15	Wind-catcher channel (SW orientation)	0.66m ²
Dynamic façade strategy/case		
Zone 11	Air shaft suspended ceiling (h:0.70m)	2.64m ²
Zone 16	Balcony	9.9084m ²
Dynamic façade and Wind-catcher strategy		
Zone 12	Wind-catcher channel (SE orientation)	0.66m ²
Zone 13	Wind-catcher channel (NE orientation)	0.66m ²
Zone 14	Wind-catcher channel (NW orientation)	0.66m ²
Zone 15	Wind-catcher channel (SW orientation)	0.66m ²
Zone 16	Balcony	9.9084m ²
Internal openings		
Zone 12	Wind-catcher channel (SE orientation)	0.66m ²
Zone 13	Wind-catcher channel (NE orientation)	0.66m ²
Zone 14	Wind-catcher channel (NW orientation)	0.66m ²
Zone 15	Wind-catcher channel (SW orientation)	0.66m ²
Zone 17	False ceiling – ancillary space	2.21m ²

5.3. Dynamic Thermal Simulations: Analysis and Results

A parametric study was conducted to investigate the performance of control natural ventilation and the implementation of natural ventilation systems, relative to the ventilation strategy of the existing case study apartment. An operation profile was created for all building openings to represent the existing ventilation strategy [base-case] of the apartment (Scenario_I). The performance of controlled ventilation during day and night was then evaluated (Scenario_II), (in sections 5.3.2 to 5.3.4). The performance of the inclusion of a wind-catcher (5.3.5), a second façade (5.3.6) and new internal openings (5.3.7) were further explored (Scenario_III). The most efficient strategy (Scenario_II and III) combining both the wind-catcher and second façade was investigated (5.3.8) (Scenario_IV).

5.3.1. Performance evaluation of the base-case ventilation strategy

(I)

For the performance analysis of the [base-case] ventilation strategy, a window opening profile was created according to published work (see Chapter 2.5.3.) in respect to both occupants' interaction with the openings and the occupancy profile (Papakostas and Sotiropoulos 1997; Drakou et al. 2011). The DTM model of the apartment includes three types of openings: the external openings (two façade balcony doors); the internal (one opening connecting the apartment to the light well); and the internal doors (four openings), as seen in Figure 5.2. The profile was created to represent how the openings would be individually controlled by occupants with regard to comfort and other factors such as housecleaning, cooking activity and occupants' presence (Papakostas and Sotiropoulos, 1997; Fabi et al., 2012; Mavrogianni et al., 2014).

The windows remained closed during nighttime and during the less occupied hours of the day (between 6.30am and 2pm); this openings' profile is presented in detail in Figure 5.9. It was assumed that the sliding shutters were manually operated and were open between 6am to 9pm, as according to literature they operate less frequently to

openings (Raja et al., 2001; Van Den Wymelenberg, 2012). The external openings remained open for 1/2 hour during the morning (provision of fresh air), 1/2 hour at noon (household cleaning time), and then for approximately six hours during the hours of the day with the highest occupancy and until bed-time (the number of open windows increases with the return of occupants, Chapter 2.5.3). No night ventilation was provided. The main door of the apartment was closed throughout the day and the internal doors were continuously open between 6am and 9pm. The internal window connecting the light shaft and the kitchen remained open for two hours before all meal-times (cooking hours), as defined by Papakostas and Sotiropoulos (1997).

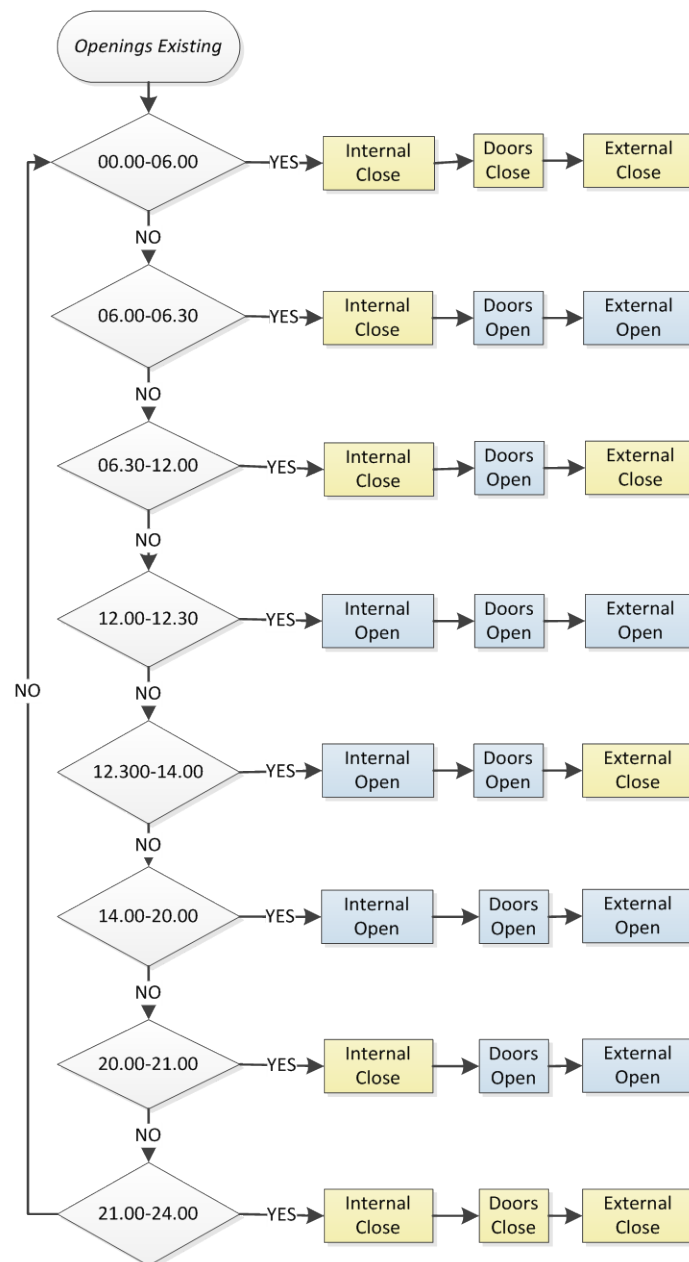


Figure 5.9 Flow diagram of the openings' operation profile for the [base-case] ventilation strategy, DTM simulations

The DTM simulation results, categorised in six-hour daily groups (using Excel), indicate high internal temperatures of up to 60% above the DBT during the [base-case] ventilation, as presented in Table 5.1 and Table 5.6 (average values of the six-hour groups for each month). Comparable values were predicted for the each of the four months of the cooling period, however significantly different for individual groups. During the Group A period, poor indoor air quality (IAQ) was predicted (with regard to Table 3.2) with operative temperatures reaching 35°C (on average 6.7°C above the DBT) and high CO₂ levels with average values up to 2696ppm (Table 5.6), due to high internal gains, the heat radiation from the thermal mass and the closed openings.

The provision of fresh air to all bedrooms during the morning hours (Group B) led to a temperature reduction of almost half of the previous value (Group A). The air temperatures of the Group B remain higher than the DBT (about 4.1°C on average higher, see Table 5.1). During the Group C period, the number of occupants reaches a minimum and as the DBT significantly rises, the internal temperature remain on average 0.5°C lower than the external. During the Group D period, the external openings were closed, while the number of occupants reached a peak, resulting in internal air temperatures above the external (by 2.4°C on average).

Table 5.6 Temperature difference (operative-DBT), for the [base-case] ventilation strategy, and the four groups of the day during the cooling period

Base-case ventilation	Group A 00.00-06.00	Group B 06.00-12.00	Group C 12.00-18.00	Group D 18.00-24.00
May - average	6.7	3.7	-0.8	2.4
June - average	6.7	3.7	-0.5	2.5
July - average	6.5	3.9	-0.5	2.3
August - average	6.6	4.4	-0.3	2.4
September - average	6.9	4.7	-0.2	2.8
Average of cooling period	6.7	4.1	-0.5	2.4
Average of all daily maximum	9.2	7.0	2.7	4.9
Average of all daily minimum	3.6	0.1	-4.3	-0.3

The highest CO₂ levels were calculated during the bed-time, and the highest levels of relative humidity of up to 70% on average (Table 5.7). High values of CO₂ levels (above 1,000ppm) are typical in domestic buildings in Greece with limited ventilation, as reported by others (M Santamouris, Argiroudis, et al., 2007). Insufficient ventilation rates were predicted during Groups A and B lower than the recommended values for adequate ventilation (Table 3.2), while values of up to 21ach⁻¹ for the total apartment during the Group C period.

Table 5.7 Average values of indoor air properties during the cooling period, per daily group, for the [base-case] ventilation strategy

Indoor air properties	Group A 00.00-06.00	Group B 06.00-12.00	Group C 12.00-18.00	Group D 18.00-24.00
CO ₂ concentration (ppm)	1594	609	405	645
Relative humidity (%)	56.3	44.7	37.5	41.4
Volumetric flow rate (m ³ /s)	0	0.05	0.805	0.436
Operative temperature (°C)	29.3	28.7	29.2	29.4
Air change rate (ach ⁻¹)	0.0	1.3	20.9	11.4

In particular, due to the lack of appropriate wall insulation (the building was constructed prior to the first thermal insulation law in Greece), the indoor temperatures closely follow the fluctuation and peaks of the external temperature. The contribution of both shutters and curtains to the solar gains reductions was negligible, due to the building's orientation and location (i.e. densely built urban environment), as described in the shading analysis (Section 5.2.). To ensure that the shutters operated appropriately, an additional DTM simulation was performed for the building without the surrounding buildings in the DTM model, the building as a stand-alone case. This additional study predicted that the shutters provided solar gain reductions in the stand-alone building. This show how important is to evaluate the building within its context, and how much the surrounding buildings can influence the thermal performance of the building studied. All DTM simulations for the purpose of this research were performed with the building and the surroundings.

5.3.2. Performance evaluation of the new natural daytime ventilation strategy (II)

The evaluation of the [base-case] ventilation strategy (Section 5.3.1) suggests insufficient IAQ due to lack of ventilation during the nighttime and the continuous operation of the openings during the evening (Table 5.7). Controlled daytime natural ventilation [DV] could provide indoor air temperature reductions for lower outdoor temperatures, further cooling of the building thermal mass, direct occupants' comfort and assist the preconditioning of the spaces during the less occupied hours.

The [base-case] openings' profile was modified between the hours of 6am and 10pm. Control of openings in response to internal and external thermal environments was introduced (Figure 5.10). The external openings of the two bedrooms would operate

in response to the CO₂ concentration levels (above 1000ppm) and the internal air temperatures (above 22°C), or for internal hourly air temperature exceeding the DBT (for DBT above 18°C) values previously defined in Table 3.2.

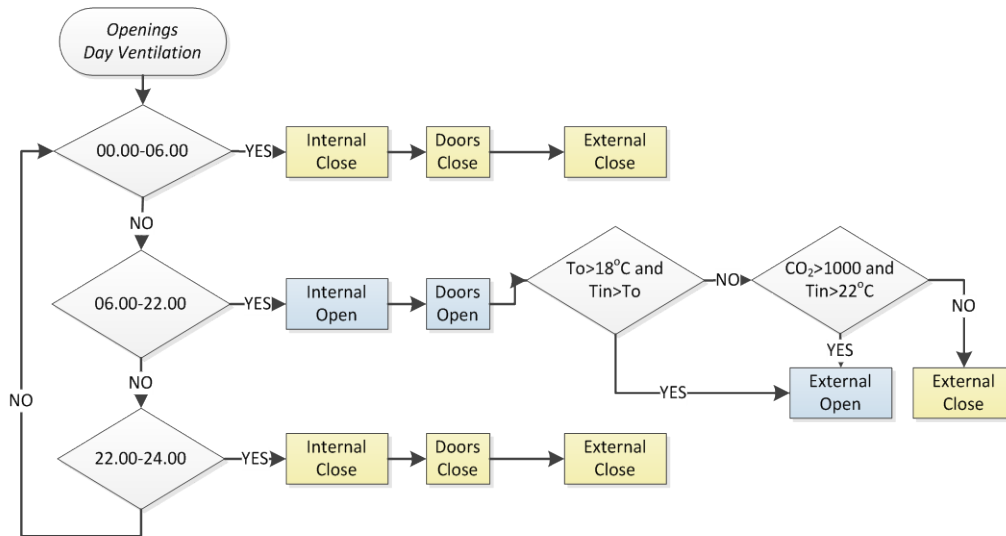


Figure 5.10 Flow diagram of the openings' operational profile used in the [DV] strategy DTM simulations

IAQ was improved during both daytime and nighttime, and primarily between the hours with daytime ventilation (Table 5.9). During the bed-time the internal air temperatures were predicted to be up to 5°C above the DBT. The provision of fresh air during the Group B period contributed to air temperature reductions of up to 2°C on average, being approximately 1.4°C above the DBT during the cooling period. During the Group C, the controlled ventilation strategy in response to the high DBT values (the openings remained open for a short period) and the occupancy levels' increase, resulted in indoor temperatures increase. However, indoor air temperatures were lower than the DBT (by 2.4°C on average for the cooling period) and the respective values of the [base-case] ventilation strategy. Comparable indoor air temperatures were predicted during the Group A and D (Table 5.9), however due to the high values of DBT the temperature difference was lower for the Group D than that of the Group A (Table 5.8).

The provision of morning ventilation (6am) resulted in higher ventilation rates and up to 2°C (average value for the cooling period) indoor air temperature reduction, as shown in Table 5.9. The predicted levels of CO₂ concentration (2596 ppm), indoor air temperatures (28°C) and relative humidity (76%) in the two bedrooms during the Group D were the highest of all six-hour groups. This indicates that night ventilation

would significantly contribute to the performance of the case study apartment (Section 5.3.3).

Table 5.8 Temperature difference (operative-DBT), for the [DV] strategy and the six-hour groups of the day during the cooling period

Daytime Ventilation	Group A	Group B	Group C	Group D
	00.00-06.00	06.00-12.00	12.00-18.00	18.00-24.00
May - average	5.5	1.8	-2.3	1
June - average	5.2	1.2	-2.3	0.9
July - average	4.9	1.2	-2.5	0.5
August - average	4.9	1.4	-2.4	0.6
September - average	5.2	1.6	-2.4	1.1
Average of cooling period	5.1	1.4	-2.4	0.8
Average of all daily maximum	7.7	3.5	1	3.2
Average of all daily minimum	2	-1.6	-6.7	-3

Table 5.9 Average values of indoor air properties of the cooling period per daily group, for the [DV] strategy

Indoor air properties	Group A	Group B	Group C	Group D
	00.00-06.00	06.00-12.00	12.00-18.00	18.00-24.00
CO ₂ concentration (ppm)	1491	402	692	665
Relative humidity (%)	60	50	47	46
Volumetric flow rate (m ³ /s)	0	0.634	0.099	0.305
Operative temperature (°C)	27.7	26.0	27.3	27.7
Air change rate (ach ⁻¹)	0	16.5	2.57	7.94

5.3.3. Performance evaluation of natural nighttime ventilation (II)

The contribution of nighttime ventilation [NV] to the base-case ventilation strategy, during the hours 10pm and 6am, was investigated. The performance of natural ventilation during the time of the day with the highest number of occupants would be significant. Night ventilation would benefit by the lower night ambient temperatures that could provide appropriate temperature difference between internal and external thermal environments, and enhance stack driven flow-rates (see Chapter 2.6.1).

A new profile for the openings was defined for the DTM simulations, shown in Figure 5.11. During the bed-time, the internal openings were fully open and the internal doors open by 20% for privacy, which is typically considered by occupants (Chapter 2.5.3). The external openings operated when the internal air temperature exceeded the ambient and when the ambient was higher than 18°C (this is minimum value for comfort, Table 3.2). Cross ventilation was provided via the external openings, the internal doors and opening, and the light well (kitchen).

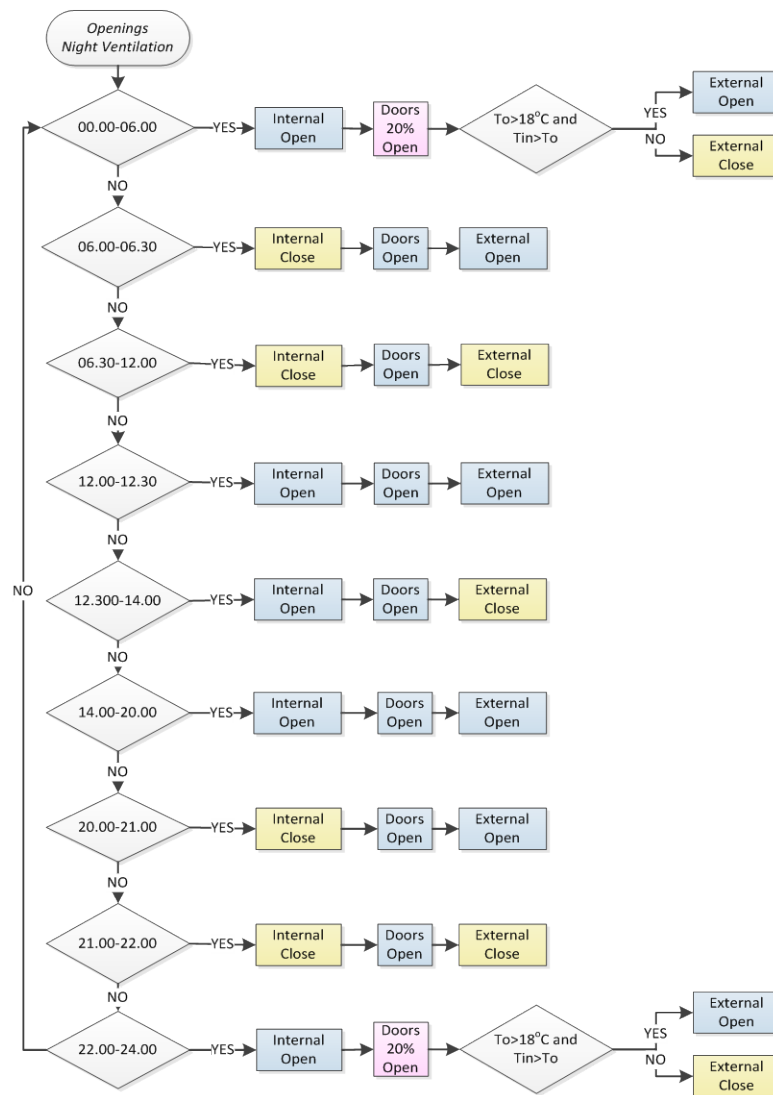


Figure 5.11 Flow diagram of the openings' operational profile used in the [NV] strategy DTM simulations

The night ventilation provided reductions in air temperatures, in CO₂ levels during the bed-time, and contributed to further reduction in air temperatures during the Group B period (Table 5.11). During the bed-time (Group D), the CO₂ levels in the bedrooms (433ppm) were predicted to be lower than the previously described ventilation strategies ([base-case], [DV]). Further, indoor temperatures during the night in the two bedroom were predicted in compliance to standards and below 26°C (25.7°C indoor air temperature and 53% relative humidity levels on average), defined in Table 3.2. Due to the substantial diurnal temperature difference as previously shown in Table 5.1, night ventilation contributed significant air temperature reductions (Table 5.10) throughout the day, with significant reductions during the Group A, relative to the predicted indoor temperatures during the [base-case] strategy (Table 5.6).

Table 5.10 Temperature difference (operative-DBT), for the [NV] strategy and the six-hour groups of the day during the cooling period

Night Ventilation	Group A 00.00-06.00	Group B 06.00-12.00	Group C 12.00-18.00	Group D 18.00-24.00
May – average	4.3	2.0	-1.8	1.3
June – average	3.3	1.3	-2.0	1.0
July – average	3.1	1.5	-2.0	0.9
August – average	3.1	1.9	-1.9	1.0
September - average	3.3	2.1	-1.9	1.3
Average of cooling period	3.3	1.7	-1.9	1.1
Average of all daily maximum	6.1	4.1	0.9	3.0
Average of all daily minimum	0.9	-2.0	-5.6	-1.3

Internal air temperatures were predicted lower to the previous ventilation strategies during the Group C and D, however 28°C on average due to the high ambient temperatures and internal gains. Ventilation rates were predicted high during the Group A, C and D periods. Acceptable levels for IAQ (according to Table 3.2), of CO₂ concentration (below 600 ppm) and relative humidity (approximately 40%) were predicted at all times, as seen in Table 5.11. Ventilation rates (1.1ach⁻¹) were reduced during the Group B, as sufficient ventilation rates were provided during the night (Group A) that contributed to indoor temperature reductions that reduced the need for ventilation during Group B. In addition, during the Group B occupancy levels reduce and thus, comfort was not impaired (see Figure 5.8). The cooling and ventilation performance of the apartment under investigation for the [NV] was improved upon the previous two strategies ([base-case], [DV]).

Table 5.11 Average values of indoor air properties of the cooling period per daily group, for the [NV] strategy

Indoor air properties	Group A 00.00-06.00	Group B 06.00-12.00	Group C 12.00-18.00	Group D 18.00-24.00
CO ₂ concentration (ppm)	416	573	407	433
Relative humidity (%)	51.3	50.5	40.2	42.3
Volumetric flow rate (m ³ /s)	0.74	0.04	0.81	0.67
Operative temperature (°C)	25.9	26.3	27.7	28.0
Air change rate (ach ⁻¹)	19.2	1.1	21.1	17.6

5.3.4. Performance evaluation of natural ‘day & night’ ventilation, (II)

The contribution of the individual [DV] and [NV] strategies to the ventilation performance the apartment for the different hours of the day relative to the [base-case] strategy, express the potential of the combined day and night ventilation. The combined [DV & NV] strategy could provide natural ventilation via openings’ control throughout the day. For the evaluation of the ventilation performance of this strategy with DTM, a profile was created for all openings (Figure 5.12) which combined the previous openings’ profiles of the [DV] and [NV] strategies. During the [DV & NV] strategy, the external openings operated in response to the temperature difference and IAQ, while the internal windows were continuously open.

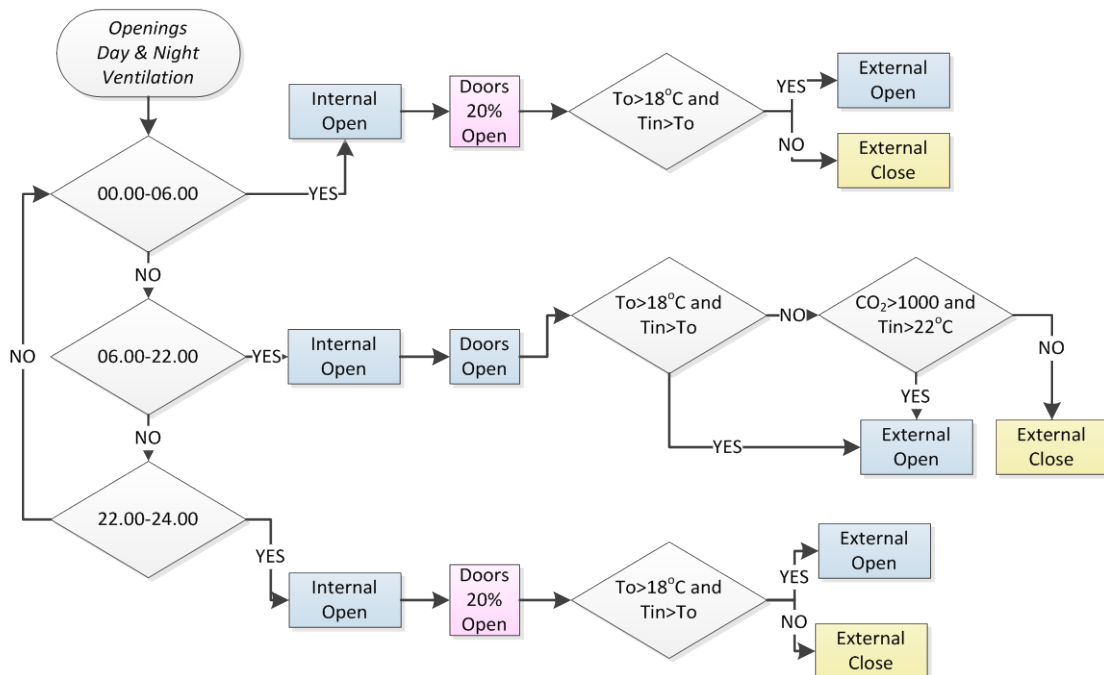


Figure 5.12 Flow diagram of the openings’ operational profile used in the [DV & NV] strategy DTM simulations

The [DV & NV] resulted in significant indoor air temperature reductions, of up to 8°C below the external temperature and during the hours of the day with the highest ambient temperatures (Group C), as shown in Table 5.12. This temperature reduction during the Group C was able with reduction of the ventilation hours, which further resulted in considerably low airflow rates relative to the recommended values for comfort (Table 3.2); however, acceptable levels of CO₂ concentration in the spaces were predicted (Table 5.13).

Table 5.12 Temperature difference (operative-DBT), for the [DV & NV] strategy and the six-hour groups of the day during the cooling period

Day & Night Ventilation	Group A	Group B	Group C	Group D
	00.00-06.00	06.00-12.00	12.00-18.00	18.00-24.00
May – average	3.66	0.94	-3.19	0.12
June – average	2.67	-0.01	-3.52	-0.26
July – average	2.45	0.03	-3.68	-0.55
August – average	2.42	0.32	-3.61	-0.49
September - average	2.61	0.48	-3.59	-0.04
Average of cooling period	2.7	0.3	-3.5	-0.3
Average of all daily maximum	5.4	2.8	-0.2	2.1
Average of all daily minimum	0.4	-2.8	-8.0	-4.0

Table 5.13 Average values of indoor air properties of the cooling period per daily group, [DV & NV] strategy

Indoor air properties	Group A	Group B	Group C	Group D
	00.00-06.00	06.00-12.00	12.00-18.00	18.00-24.00
Room CO ₂ concentration (ppm)	420	414.1	737.0	615.5
Relative humidity (%)	52.7	52.8	51.5	48.6
Volumetric flow rate (m ³ /s)	0.703	0.462	0.056	0.374
Operative temperature (°C)	25.3	24.9	26.1	26.6
Air change rate (ach ⁻¹)	18	12	1	10

The [DV & NV] strategy delivered: CO₂ levels in all spaces lower than 740 ppm on average; relative humidity levels of around 50%; high volume flow rates of up to 703 l/s; and indoor air temperatures on average lower than 27°C (Table 5.13). Acceptable levels of IAQ (Table 3.2) were predicted during the night in the two bedrooms for the cooling period, with up to 437ppm on average levels of CO₂ concentration, operative temperatures of approximately 25.2°C and relative humidity levels of approximately 54%.

5.3.4.1. Overall performance evaluation of the base-case (I) and the new natural ventilation strategies (II)

The three ventilation strategies ([DV], [NV] and [DV & NV]) delivered reduction in indoor air temperatures at all times relative to the previous strategy [base-case]. Adequate ventilation rates were provided during the daytime and particularly during the nighttime. The [DV & NV] strategy resulted in a significant temperature reduction of up to 7°C (4°C on average) from the previous ventilation strategy. Average (mean) daily operative temperatures during the [base-case] strategy exceeded the ambient temperature at all times (Figure 5.13). The combined [DV &

NV] provided lower operative temperatures than the ambient during the 60% of the cooling period, while exceeded the ambient for 1°C on average. The individual [DV] and [NV] ventilation strategies resulted in comparable average daily values of operative temperatures (°C).

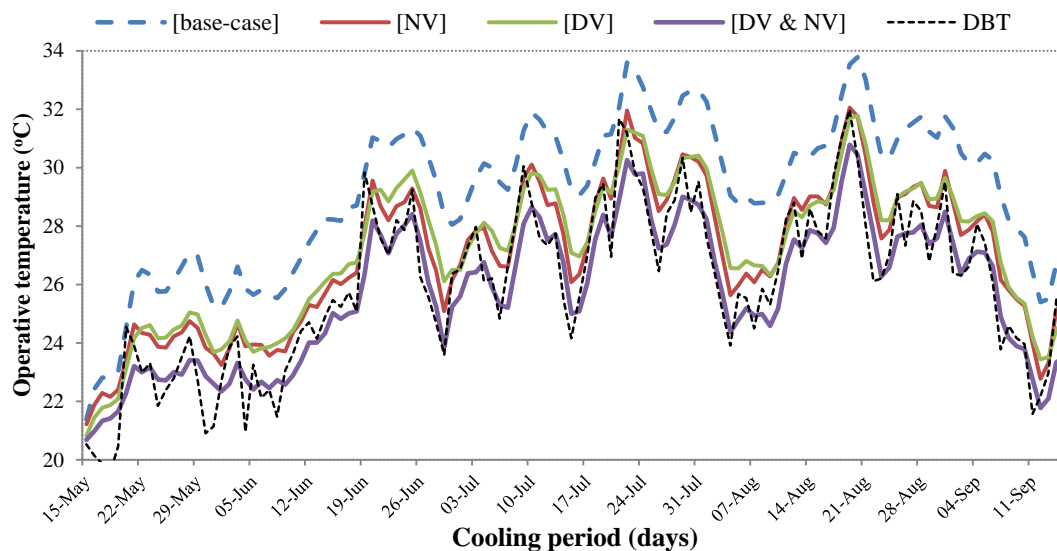


Figure 5.13 Average daily operative temperatures predicted for the four natural ventilation strategies, in the apartment under investigation

The performance of the ventilation strategies varies throughout the day, as shown in Figure 5.14 - Figure 5.17, created using Excel (Microsoft, 2010). During the Group A period, the CO₂ levels for the [NV] and [DV & NV] strategies were predicted to be lower than the maximum acceptable level (1000 ppm). Incidents of higher values were predicted during May, because of the low values of DBT (21°C on average during May) that led to reduction in ventilation hours (the openings were closed for DBTs below 18°C) (Figure 5.14). During the Group B, C, D periods, appropriate CO₂ levels were predicted in the spaces with all four natural ventilation strategies.

During the Group B period, the four strategies delivered high ventilation rates, which resulted in CO₂ levels below 700ppm for all four strategies, varying no more than 200ppm (Figure 5.15). During the Group C period (Figure 5.16), the predicted CO₂ levels in the spaces were the highest for the [DV & NV] strategy, however below 1000 ppm. This was due to the greater openings' control provided during the warmer hours of the day, i.e. the openings were closed when the internal temperatures were lower than the external to avoid overheating. The scattered levels of CO₂ concentration in the occupied spaces during the Group D and the [DV & NV] vary between 400ppm and 900ppm with regard to the openings operation (Figure 5.17).

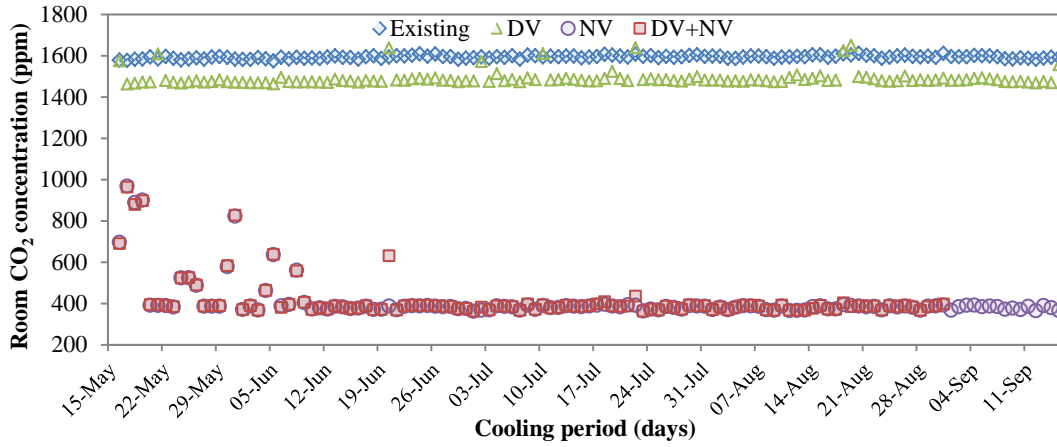


Figure 5.14 Average values of CO₂ concentration during the first six-hour group of the day (midnight-6am) and the four ventilation strategies

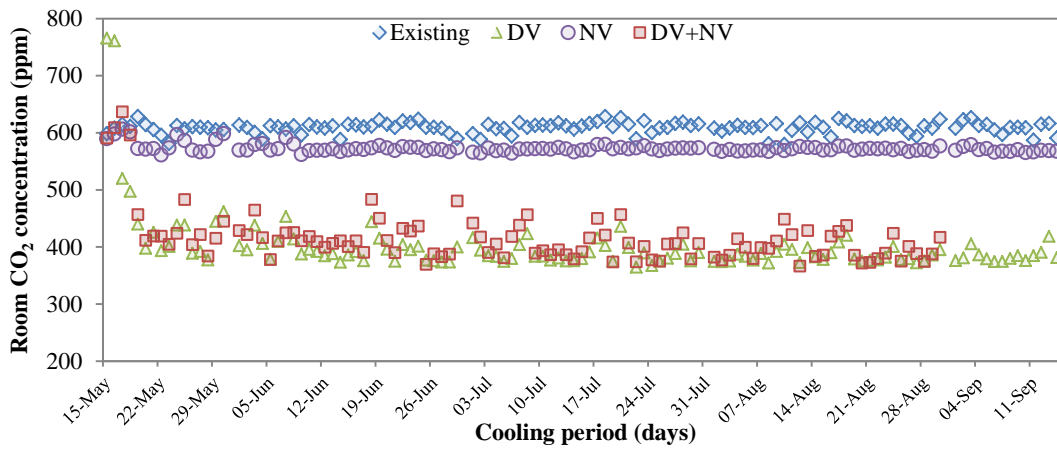


Figure 5.15 Average values of CO₂ concentration during the second six-hour group of the day (6am-12pm) and the four ventilation strategies

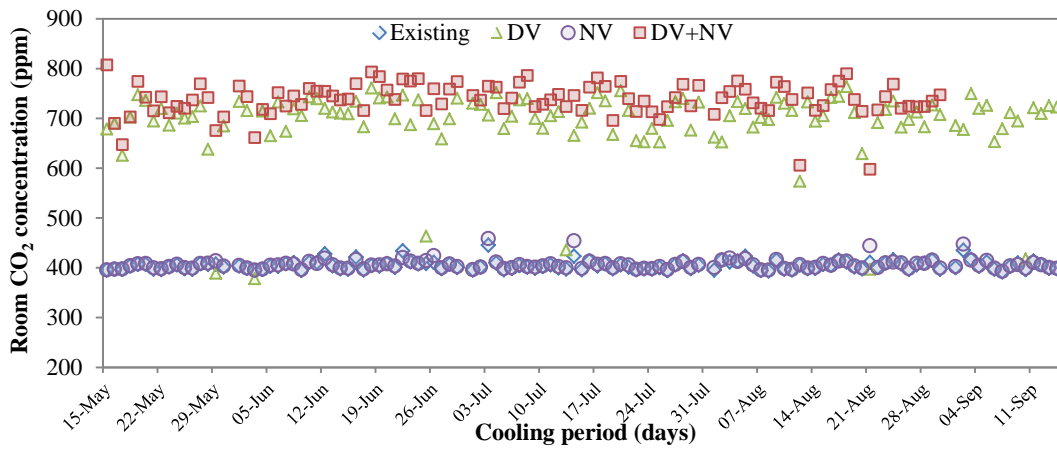


Figure 5.16 Average values of CO₂ concentration during the third six-hour group of the day (12pm-6pm) and the four ventilation strategies

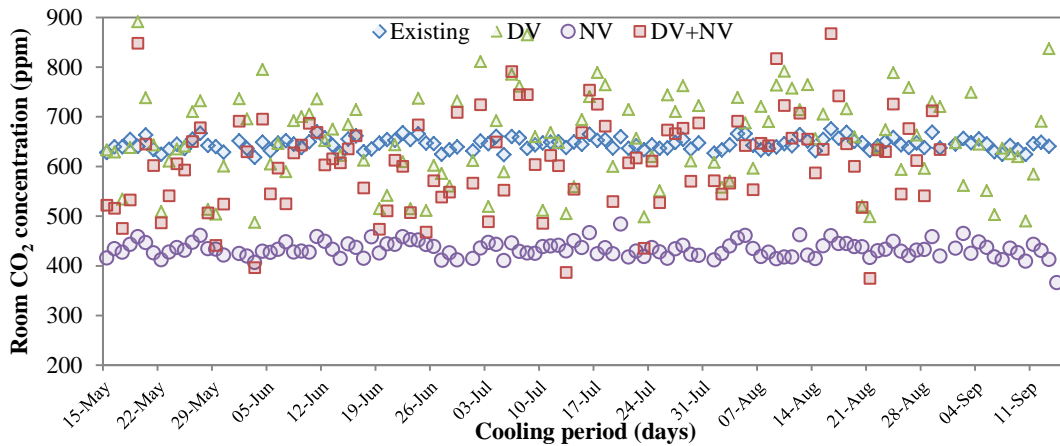


Figure 5.17 Average values of CO₂ concentration during the last six-hour group of the day (6pm-midnight) and the four ventilation strategies

5.3.5. Implementation of a wind-catcher (III)

The integration of a four-directional wind-catcher at the top of the existing light well was investigated. The wind-catcher would operate as an exhaust (low wind speeds) or as a wind-scoop with regard to wind speed. The wind-catcher was designed according to Chapter 4.5.1 and optimised with exploratory DTM simulations. The simulation results were used for the development and the justification of the final design. The properties of the internal partitions (i.e. height, length) were evaluated, as well as the openings' size and their operation strategy. The wind-catcher operated efficiently up to a certain length of the cross-partitions after which, the performance of the system (i.e. ventilation rates) would reduce. It was thus decided to model the internal partitions (5m long) as presented in Chapter 4.5.1, with higher point the top part of the wind-catcher and lower the top part of the existing light well (the light well has no partitions).

The importance of the tower's height was also investigated. Towers with height increased and/or reduced by 0.5m to up to 2m, were evaluated. It was predicted that the taller towers had a positive contribution to the ventilation performance, although insignificant. Further, it was predicted that the bigger openings (twice the size) assisted the increase in ventilation rates; however, this was insignificant for the overall ventilation performance of the strategy. Therefore, the wind-catcher was modelled in the DTM software as presented in Chapter 4.5.1 (Figure 5.18), which was in compliance to the Greek national construction regulations.

Exploratory DTM simulations evaluated the operation of the wind-catcher's top openings. When the leeward and windward openings were simultaneously operating the performance of the system was enhanced, as the one opening assisted the outflow and the other the inflow, respectively. Alternatively, the openings could operate individually in response to the wind direction or they could remain continuously open at all times. The performance of the wind-catcher openings operating in groups of leeward and windward openings was predicted to be the most efficient relative to the other two strategies and able to improve the ventilation performance of the wind-catcher. Accordingly, two openings' profiles were created: one for the northeast and southwest facing openings and one for the southeast and northwest openings. Each group operated for the corresponding wind directions for the values (angle from north) of the wind diagram in Figure 5.19 (the building is oriented 120° east to north).

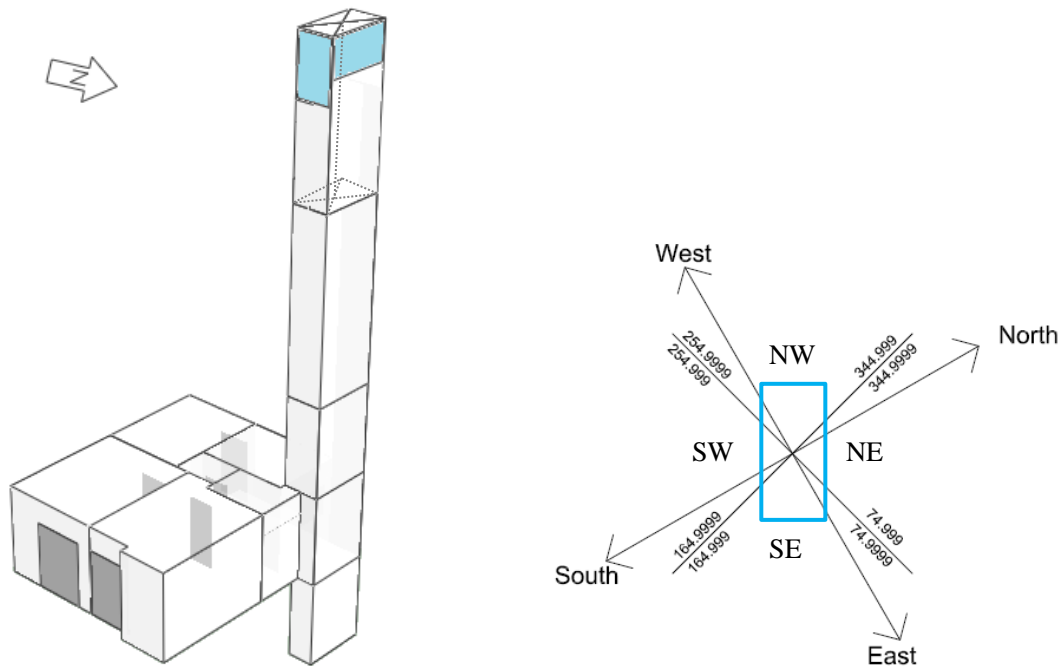


Figure 5.18 A 3D view of the DTS model of the wind-catcher and the apartment studied (left)

Figure 5.19 Wind diagram showing the wind directions (angles) for each of the four wind-catcher openings, nts

At the lower part of the cross partitions, openings were designed (inside the wind-catcher's tower) to represent the operating dampers. These were automatically controlled in response to the corresponding top wind-catcher opening operation (operating simultaneously). When two of wind-catcher openings would operate (leeward and windward), the other two wind-catcher openings and their individual channels would be closed, in order to avoid air-circulation.

The ventilation performance of a wind-catcher was evaluated with the previous [DV & NV] natural ventilation strategy. A new operation strategy (Figure 5.20) was developed for the wind-catcher openings, combined with the [DV & NV] operation strategy (Figure 5.12). Exploratory DTM simulations performed shown that controlled operation of the wind-catcher openings in response to wind direction provided acceptable ventilation rates during specific hours of the day. Between 12pm and 8pm, the wind-catcher openings operated according to the wind direction and during the rest of the day, they were fully open.

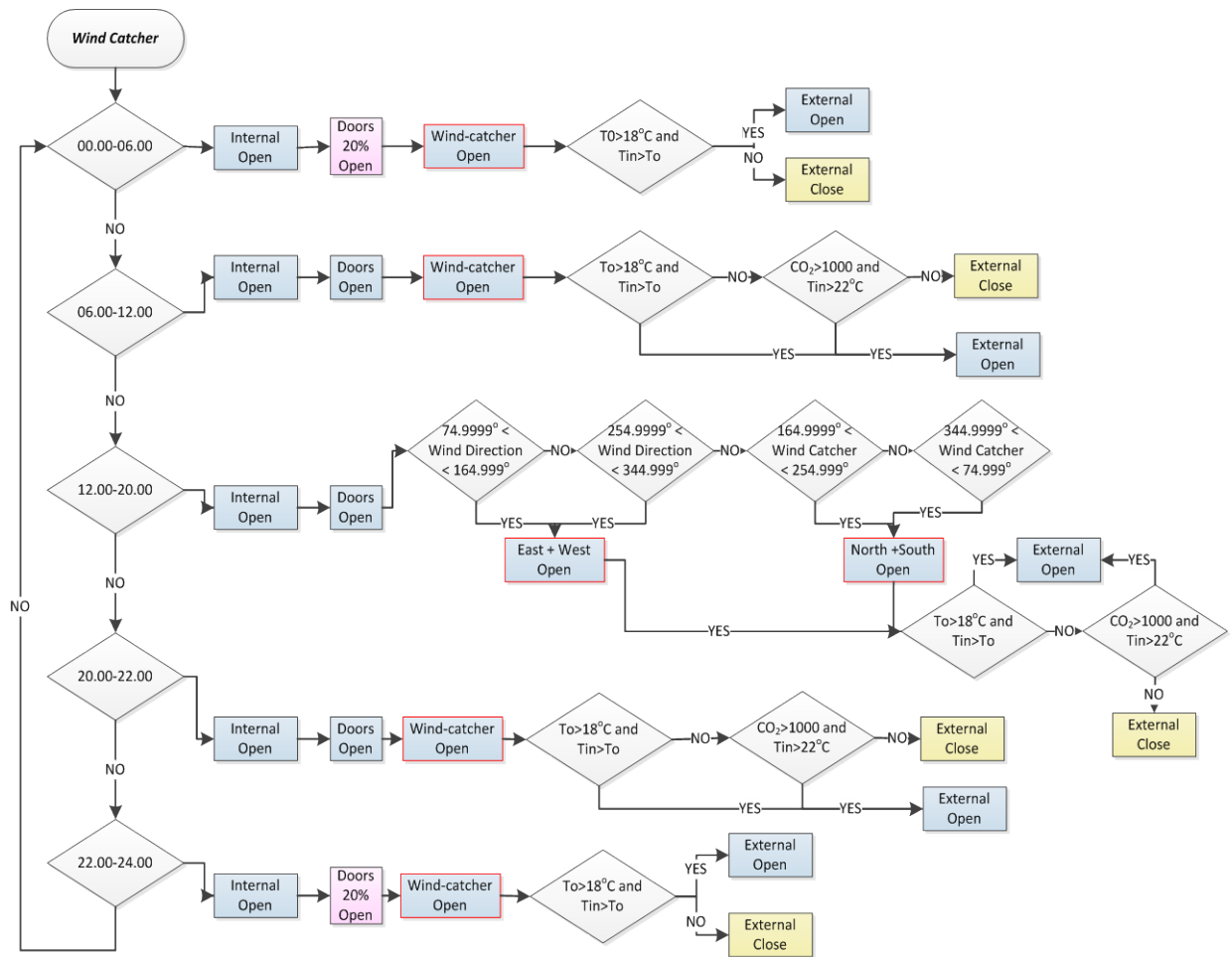


Figure 5.20 Flow diagram of the openings' operational profile used in the [WC] strategy DTM simulations

The [WC] strategy was expected to contribute to indoor air temperature reductions relative to the previously described [DV & NV] strategy, due to the potential of the strategy to capture air at higher speeds from the top of the building, as described in the literature (Calautit et al., 2012). Despite this, comparable values of operative temperatures were predicted for both strategies ([DV & NV] and [WC]), as shown in Figure 5.21. This is because the DTM software calculates the effect of wind on the

building surfaces using default and approximated values of pressure coefficients, which are not representative of the real scale and the conditions on the site under investigation.

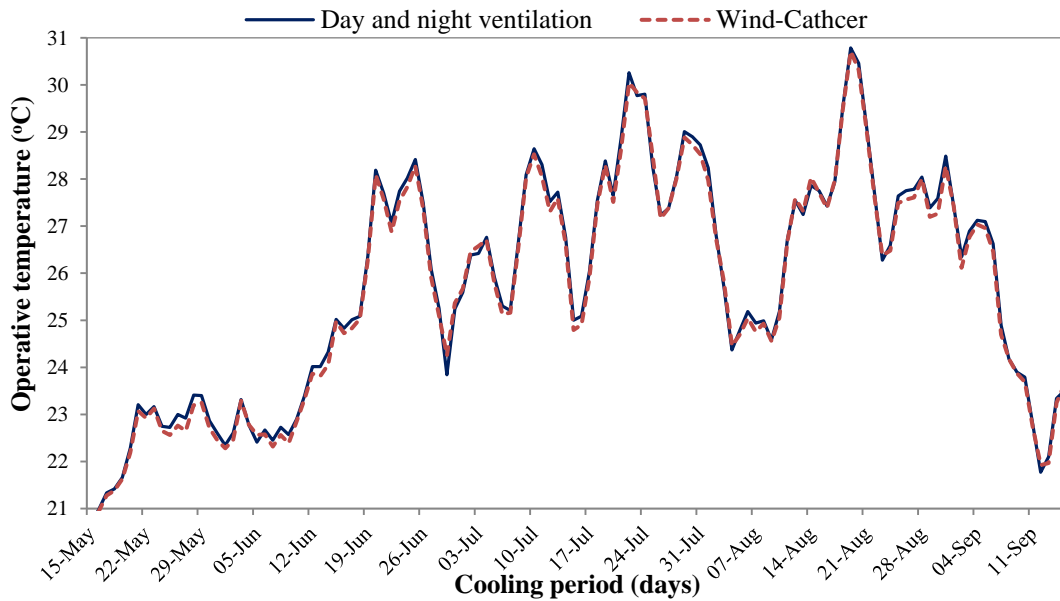


Figure 5.21 Comparison of the average daily indoor air temperatures predicted at the [DV & NV] and the [WC] strategies

Table 5.14 Temperature difference (operative-DBT), for the [WC] strategy and the six-hour groups of the day during the cooling period

Wind-catcher	Group A 00.00-06.00	Group B 06.00-12.00	Group C 12.00-18.00	Group D 18.00-24.00
May – average	3.6	0.8	-3.3	0.0
June – average	2.6	-0.1	-3.6	-0.3
July – average	2.4	-0.1	-3.8	-0.6
August – average	2.4	0.2	-3.7	-0.6
September - average	2.6	0.4	-3.7	-0.1
Average of cooling period	2.6	0.2	-3.7	-0.4
Average of all daily maximum	5.2	2.7	-0.4	2.1
Average of all daily minimum	0.5	-2.9	-8.1	-4.1

The [WC] provided indoor temperature reductions during the Group B period, relative to the [DV & NV] strategy; however, higher operative temperatures were predicted during the Group C and D (Table 5.14). During the Group A and D periods, the air temperature in the bedrooms varied on average between 25.1°C (May) to 26.7°C (August) which is appropriate for comfort (Table 3.22). Low levels of average CO₂ concentration (approximately 436ppm) and relative humidity (54%) were predicted in the two bedrooms during bed-time to be, providing acceptable IAQ. Despite the overall reductions in ventilation rates, the wind-catcher contributed to a CO₂ levels reduction during Groups C and D, as shown in Table 5.13 and Table 5.15.

Table 5.15 Average values of indoor air properties of the cooling period per day group, for the [WC] ventilation strategy

Indoor air properties	Group A 00.00-06.00	Group B 06.00-12.00	Group C 12.00-18.00	Group D 18.00-24.00
Room CO ₂ concentration (ppm)	420.9	417.7	767.8	648.5
Relative humidity (%)	53	53	52	49
Volume flow in (m ³ /s)	0.653	0.418	0.055	0.327
Operative temperature (°C)	25.2	24.8	26.0	26.6
Air change rate (ach ⁻¹)	17	11	1.4	8.5

5.3.6. Implementation of a dynamic façade (III)

The lightweight dynamic façade consists of three groups of horizontal louvres, as described in Chapter 4.5.2. One of the limitations of the DTM software was that it was not possible to model operating in response to environmental parameters, custom-designed louvres. As a result, the model of the DF design in IESVE was simplified and modelled as a second layer of three external glazings, as shown in Figure 5.22. Each of the three glazings incorporated blinds operating individually, the shape and size of which was defined by the software, while the reflectance properties by the user. Partition walls were created between the individual apartments, as wing walls made of brick-glasses. The partition walls provided privacy between the different apartments at each floor, natural daylight and prevented the air circulation between the individual properties.

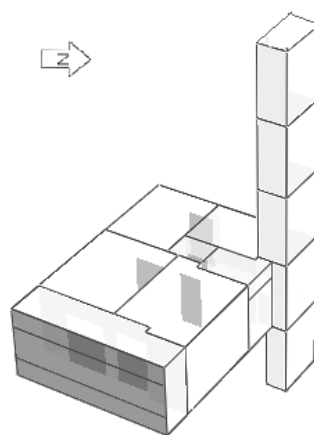


Figure 5.22 A 3D-model of the apartment, the dynamic façade and the air shaft, in IESVE

The three groups of the DF openings (consisting of louvres) were designed in DTM to operate vertically in response to the levels of direct solar radiation and time of the day. The building's openings operated according to the [DV & NV] profile. The top

and low sets of louvres operated for the same environmental parameters (Figure 5.23) and they were open during levels of horizontal solar radiation below 550 W/m^2 (30% of the hours with direct radiation). The middle groups of louvres operated individually and they were open for solar radiation below 200 W/m^2 (45% of the hours with direct radiation). The value of 200 W/m^2 was the average value of solar radiation for the cooling period (of the average monthly values) at horizontal plane for the area of Athens, provided by KENAK (Argiriou et al., 2010).

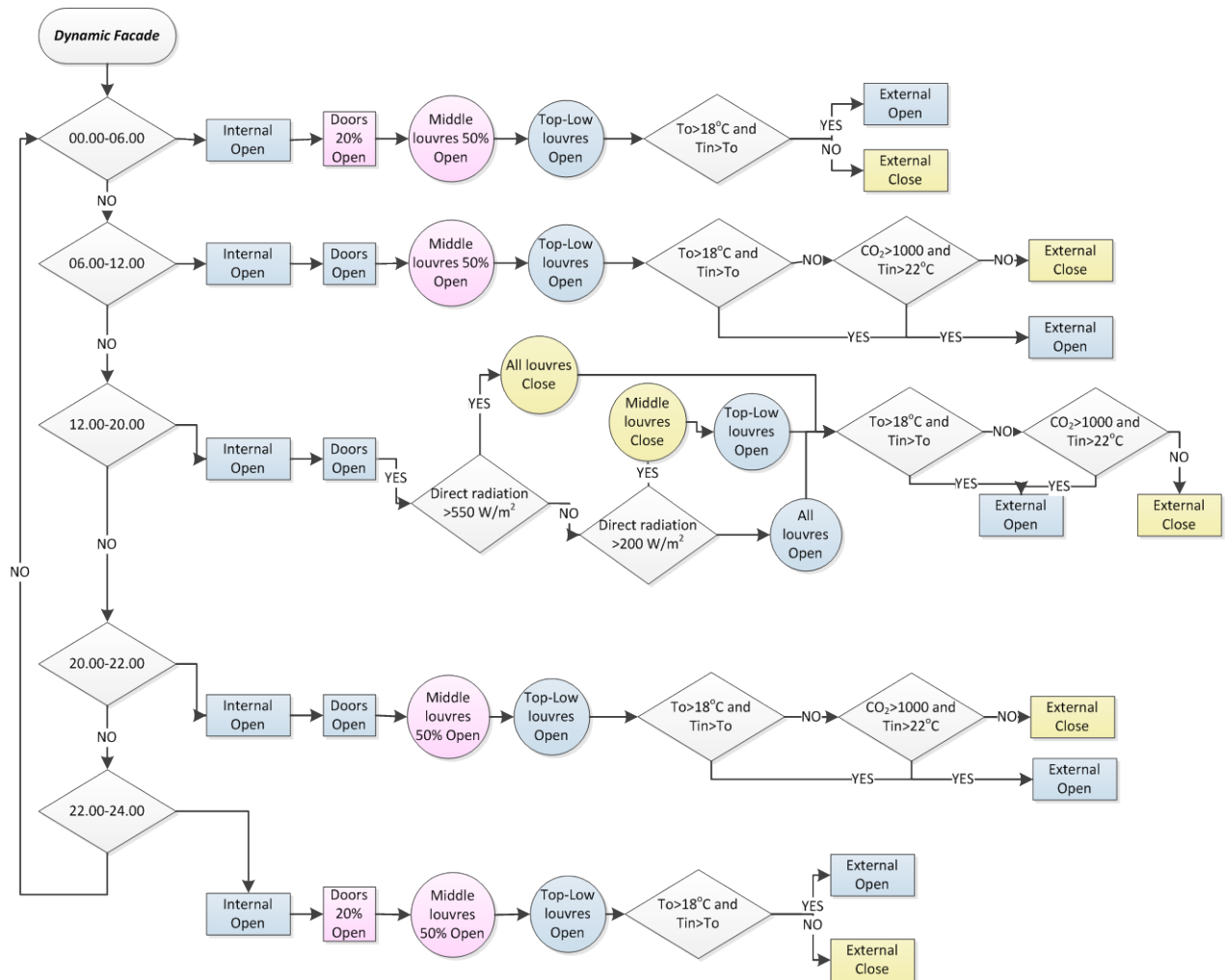


Figure 5.23 Flow diagram of the openings' operational profile used in the [DF] strategy DTM simulations

The dynamic façade was modelled in DTM with louvres integrated in three openable glazings (described above); these operated simultaneously to the two bedrooms' external openings using the [DV & NV] openings' profile. However, between the hours 12pm-8pm the three horizontal glazings operated with regard to the direct radiation, i.e. they were closed when the louvres were closed. The high thermal performance of the glazing (Uvalue of $2.2 \text{ W/m}^2\text{k}$ in Table 5.3) provided a layer of

insulation when all three glazings were closed, as the current building openings are single-glazed.

During bed-time, the apartment was cross-ventilated through: the internal openings (fully open); the partially opened bedroom doors; the external openings (operating in response to air temperature) and the top and low DF sets of louvres. The middle louvres were partially open to provide privacy. During the afternoon and evening (12pm-8pm) and the incidents of high direct radiation, all blinds were closed. This, created a shaded buffer space between the internal and external environments able to deliver reductions in air temperatures and consequently in the building’s cooling load.

Using DTM, it was predicted that during the cooling period the middle louvres were fully closed for approximately 783 hours (78.9% of the time) and the low and top for 534 hours (54% of the cooling period). The partially open louvres during nighttime, contributed in internal air temperature increase relative to the previous wind-catcher strategy, although by a small magnitude, as shown in Table 5.14 and Table 5.16. Between noon and midnight, the operation of the louvres provided further temperature reductions of 0.2°C on average, relative to [WC] and [DV & NV] strategies.

Table 5.16 Temperature difference (operative-DBT), for the [DF] strategy and the six-hour groups of the day during the cooling period

Dynamic façade	Group A 00.00-06.00	Group B 06.00-12.00	Group C 12.00-18.00	Group D 18.00-24.00
May – average	3.7	1.0	-3.5	-0.1
June – average	2.7	0.0	-3.9	-0.6
July – average	2.4	0.0	-4.0	-0.9
August – average	2.5	0.4	-3.9	-0.8
September - average	2.7	0.6	-3.8	-0.2
Average of cooling period	2.7	0.3	-3.8	-0.6
Average of all daily maximum	5.4	2.9	-0.4	2.1
Average of all daily minimum	0.3	-3.0	-8.5	-4.6

Acceptable levels of CO₂ concentration and relative humidity were predicted at all times (Table 5.17), as defined in Table 3.2. On average, indoor air temperature were predicted within the comfort limits defined by standards. During bed-time, the indoor air temperature in the two bedrooms was predicted to be approximately 25.3°C (which in accordance with CIBSE, 2006) and the levels of CO₂ concentration approximately 457ppm, on average for the cooling period.

Table 5.17 Average values of indoor air properties of the cooling period per daily group, for the [DF] ventilation strategy

Indoor air properties	Group A 00.00-06.00	Group B 06.00-12.00	Group C 12.00-18.00	Group D 18.00-24.00
Room CO ₂ concentration (ppm)	441.1	426.3	741.9	671.9
Relative humidity (%)	52.7	52.8	52.3	50.0
Volumetric flow rate (m ³ /s)	0.552	0.353	0.055	0.259
Operative temperature (°C)	25.3	24.9	25.8	26.3
Air change rate (ach ⁻¹)	14.4	9.2	1.4	6.7

5.3.7. Evaluation of new internal openings (III)

The ancillary space located above the false ceiling of the bathroom is a typical element of the multi-storey apartment buildings in Greece. This unoccupied space was connected to the existing light well using an additional opening (with free area 0.3m²) and to the hallway of the apartment under investigation via an opening with twice the area of the first. The ventilation air could flow in and out of the living spaces through the hallway and the purpose-provided openings, designed above the party walls of the hallway. The hallway was used as a distribution space. These openings would operate when all internal doors were closed. This would assist the indirect cross ventilation of the apartment. The DTM model of the apartment under investigation with the new internal openings [InOp] was designed according to Chapter 4.5.3.2.

For the ventilation performance of this strategy using DTM, the external windows operated according to the [DV & NV] strategy, the internal doors were closed during the nighttime (10pm to 6am) and the new internal openings were open (Figure 5.24). The contribution of the [InOp] to the ventilation performance of the apartment under investigation was evaluated with and without the inclusion of a wind-catcher design. Simulation results predicted higher ventilation rates for the strategy with the wind-

catcher model. Thus, only the simulation results from the [InOp] with the wind-catcher, were presented.

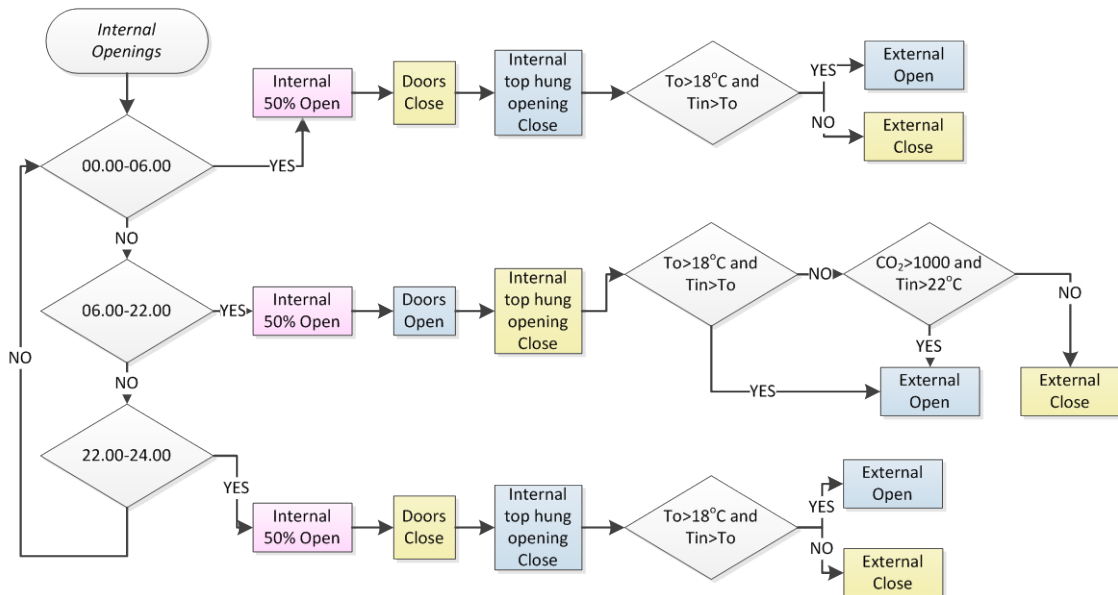


Figure 5.24 Flow diagram of the openings' operational profile used in the [InOp] ventilation strategy DTM simulations

During the nighttime, air entering through the bedroom openings (combined flow in and out through these openings) would pass through the new connecting openings to the hallway (the internal doors were closed). Then through the purpose-provided openings on the top of the suspended bathroom ceiling through the air shaft, finally escaping from the top wind-catcher openings (continuously open during night), as shown in Figure 5.25.

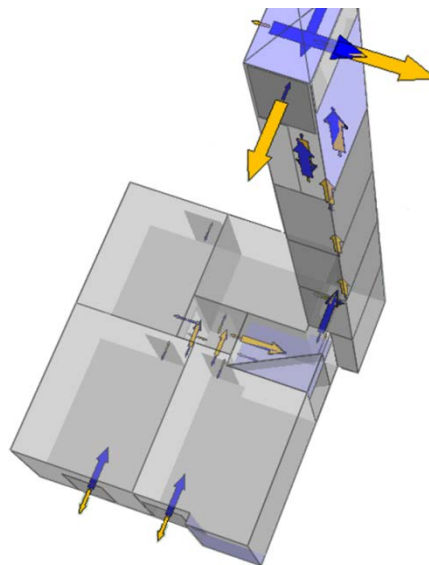


Figure 5.25 The DTM three-dimensional model of the apartment and wind-catcher, showing the operation of the [InOp]

The purpose of this ventilation strategy was to deliver adequate ventilation rates and ensure privacy within the apartment spaces (the internal bedroom doors were fully closed). This strategy was evaluated only during the nighttime; however, it could be further considered for different times of the day and for privacy.

Simulation results predicted increased indoor air temperatures (Table 5.18) relative to the previous ventilation strategies evaluated, and particularly the [WC] ventilation strategy (Section 5.3.5 and Table 5.14). Highest levels of CO₂ concentration were predicted during the day, reaching up to 770 ppm (Table 5.19), and lower during the Group A. In the two bedrooms, the air temperature during Group A was predicted to be lower than the average of all the apartment spaces and 25.2°C on average (54.2% relative humidity and CO₂ of 468).

This strategy had a comparable performance to the previous strategies and was able to provide comfort relative to the [base-case] strategy (Table 5.7 and Table 5.19). However, due to the smaller cross-section area of the hallway openings relative to the area of the internal doors the strategy had negligible contribution to the natural ventilation of the apartment under investigation. Further work would be required to optimise the performance of this strategy.

Table 5.18 Temperature difference (operative-DBT), for the [InOp] strategy and the six-hour groups of the day during the cooling period

Internal openings	Group A 00.00-06.00	Group B 06.00-12.00	Group C 12.00-18.00	Group D 18.00-24.00
May – average	3.96	1.03	-3.11	0.22
June – average	3.06	0.08	-3.42	-0.13
July – average	2.82	0.12	-3.57	-0.45
August – average	2.81	0.39	-3.51	-0.38
September - average	2.98	0.49	-3.52	0.06
Average of cooling period	3.0	0.3	-3.4	-0.2
Average of all daily maximum	5.6	2.9	-0.1	2.2
Average of all daily minimum	0.6	-2.6	-7.8	-3.9

Table 5.19 Average values of indoor air properties of the cooling period per daily group, [InOp] strategy

Indoor air properties	Group A 00.00-06.00	Group B 06.00-12.00	Group C 12.00-18.00	Group D 18.00-24.00
Room CO ₂ concentration (ppm)	442.4	417.7	766.7	660.2
Relative humidity (%)	51.3	52.7	51.7	48.8
Volume flow in (m ³ /s)	0.018	0.014	0.001	0.009
Operative temperature (°C)	25.6	25.0	26.2	26.7
Air change rate (ach ⁻¹)	13	11	1	7

5.3.8. Combined ventilation performance of a wind-catcher and a dynamic façade (IV)

With regard to the predicted ventilation performance of the [WC] and [DF] strategies, it was expected that the combined operation would increase further the ventilation rates and provide reductions in indoor air temperatures by appropriate control of solar gains. The ventilation performance of the [DF & WC] was explored (Figure 5.26) and the ventilation performance of the strategy was evaluated in DTM using a combined strategy for the openings' operation, presented in Figure 5.27.

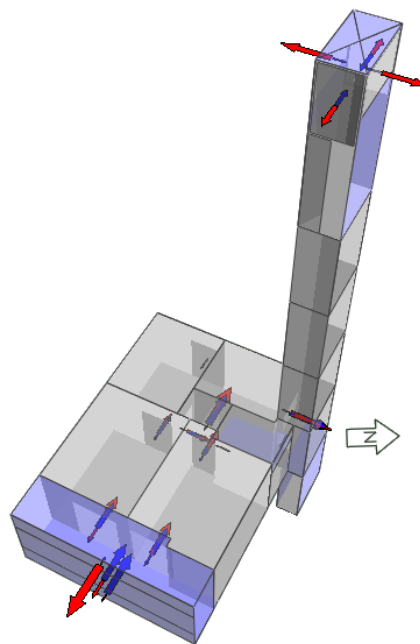


Figure 5.26 Three-dimensional model of the apartment, showing the operating dynamic façade and the wind-catcher in IESVE

Comparable results were predicted relative to the two individual strategies; see Table 5.14, Table 5.16 and Table 5.20, for the [WC], [DF] and [DF & WC] respectively. However, the combined [DF & WC] delivered further temperature reductions in the spaces relative to the [DV & NV] strategy during Group D period of up to 0.4°C on average. This was due to the shading performance of the second façade and the provision of ventilation air at higher rates through the wind-catcher. The combined [DF & WC] contributed to enhancement of the ventilation rates during the nighttime by 25% (average value for the cooling period). Acceptable average indoor temperatures were predicted for occupants' comfort, as defined in Table 3.2.

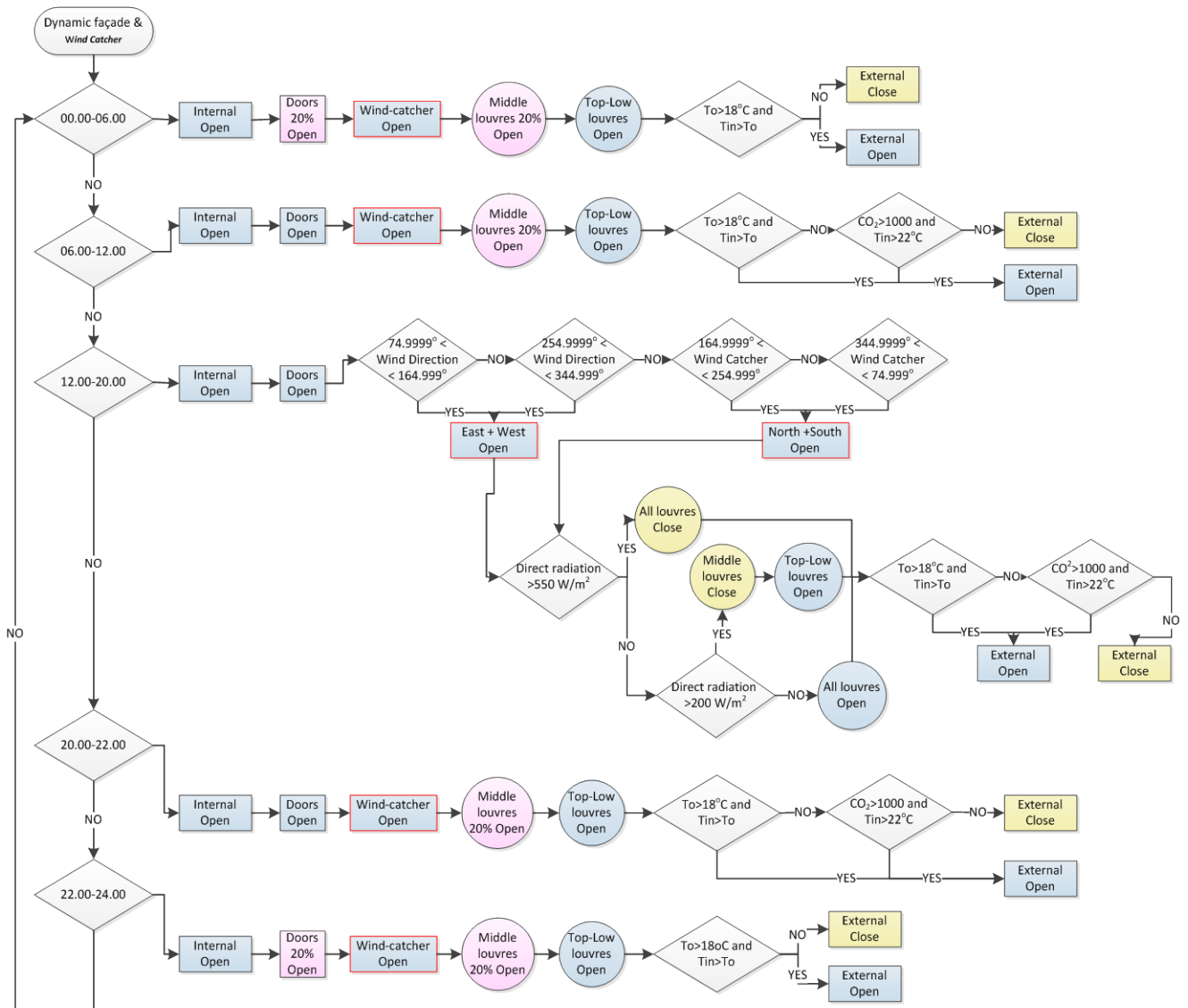


Figure 5.27 Flow diagram of the openings' operational profile used in the [DF & WC] ventilation strategy DTM simulations

During the cooling period, acceptable levels of CO₂ (below 770 ppm) and relative humidity (around 53%) were predicted, as shown in Table 5.21. The average temperature of the two bedrooms during the Group A was predicted on average 25°C and the CO₂ concentration approximately 448ppm; these are considered acceptable for occupants' comfort (Table 3.2). Although ventilation rates were improved during the Group C from the [DV & NC] strategy, higher air change rates would be required to deliver direct natural cooling. The combined operation of a wind-catcher and a dynamic façade resulted in lower indoor air temperatures at all times, relative to all previous ventilation strategies. The control of the openings operation with day and night ventilation [DV & NV] had a significant contribution to this.

Table 5.20 Temperature difference (operative-DBT), for the [DF & WC] strategy and the six-hour groups of the day during the cooling period

DF & WC	Group A 00.00-06.00	Group B 06.00-12.00	Group C 12.00-18.00	Group D 18.00-24.00
May – average	3.59	0.81	-3.62	-0.25
June – average	2.65	-0.14	-3.96	-0.63
July – average	2.43	-0.08	-4.09	-0.94
August – average	2.48	0.30	-3.94	-0.81
September - average	2.74	0.55	-3.79	-0.19
Average of cooling period	2.7	0.2	-3.9	-0.7
Average of all daily maximum	5.4	2.7	-0.4	2.1
Average of all daily minimum	0.3	-3.0	-8.5	-4.6

Table 5.21 Average values of indoor air properties of the cooling period per daily group, for the [DF & WC] strategy

Indoor air properties	Group A 00.00-06.00	Group B 06.00-12.00	Group C 12.00-18.00	Group D 18.00-24.00
Room CO ₂ concentration (ppm)	429.9	417.4	767.2	685.4
Relative humidity (%)	52.6	52.9	53.0	50.4
Volume flow in (m ³ /s)	0.554	0.407	0.050	0.245
Operative temperature (°C)	25.3	24.9	25.7	26.3
Air change rate (ach ⁻¹)	14.4	10.6	1.3	6.4

5.4. DTM Results: IAQ Assessment and Performance Evaluation of the Different Ventilation Strategies

Reductions in indoor air temperatures and increase in ventilation rates were predicted for the new strategies, relative to the [base-case] ventilation strategy of the apartment under investigation. Indoor air temperatures varied insignificantly between the strategies [DV & NV] (the most efficient strategy from the openings' operation strategies II), [WC], [DF], [DF & WC], and the [InOp]. Predicted average daily operative temperatures of each of the five strategies for an example 7-day period are presented in Figure 5.28. The [DF & WC] ventilation strategy delivered up to 0.5°C lower operative temperatures throughout the day, relative to the other interventions. During this period, all strategies reduced the indoor temperatures by up to 4°C relative to the base-case strategy.

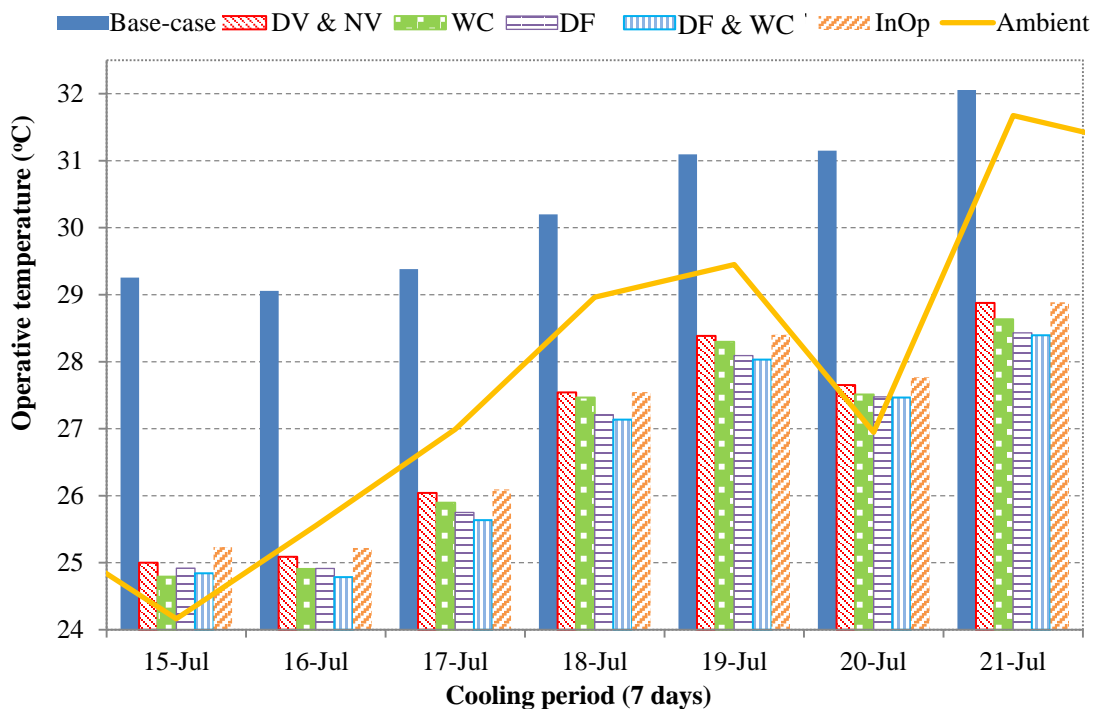


Figure 5.28 Daily average operative temperatures for five natural ventilation strategies during an example 7-day period

Average indoor temperatures of the six-hour groups during an example 7-day period, of the two most efficient strategies and the [base-case] strategy, are presented in Figure 5.29. The internal temperatures followed the fluctuations of the external due

to the lack of adequate thermal mass and wall insulation, however to a lesser extent for the [base-case] strategy. Indoor air temperatures significantly exceeded the external of the [base-case] strategy. The [DF & WC] strategy led to a further temperature reduction to the previous [DV & NV] natural ventilation, although to a small degree (on average 0.2°C throughout the cooling period). These two strategies were able to maintain indoor air temperatures lower than the ambient (up to 8°C) during the late hours of the day that the number of occupants increases.

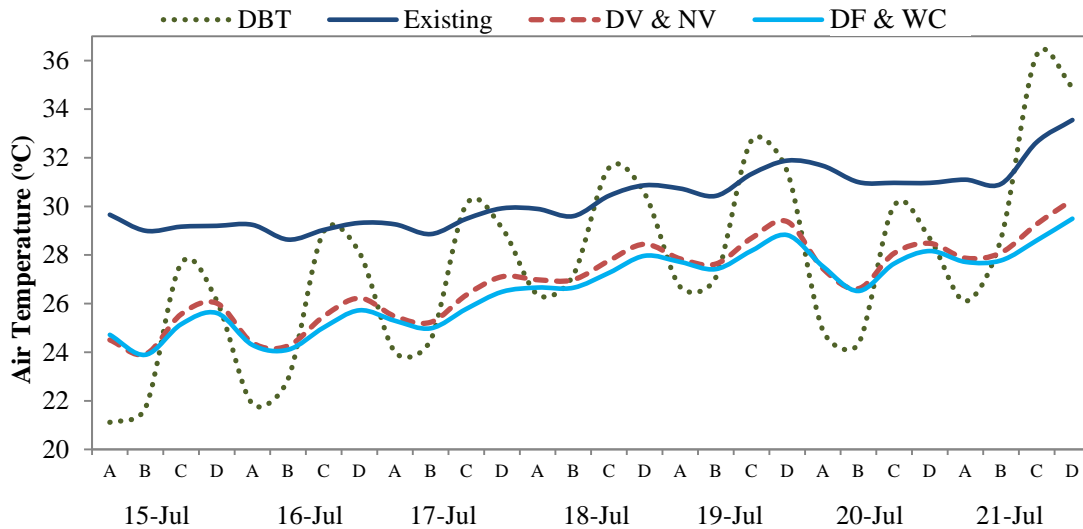


Figure 5.29 Average per 6-hour group predicted operative temperatures of three natural ventilation strategies and DBTs during an example 7-day period

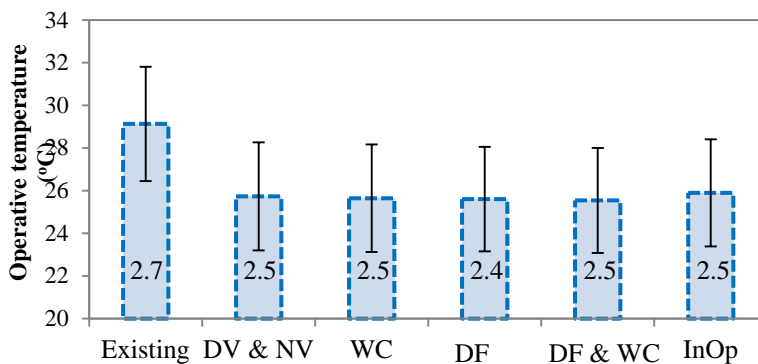


Figure 5.30 Predicted average values of hourly operative temperatures (°C) for the cooling period, and their standard deviation, for six natural ventilation strategies

An average temperature difference between the strategies of 3.6°C was predicted, as presented in Figure 5.30. The proposed strategies were predicted with smaller standard deviation than the [base-case] ventilation, as shown in Figure 5.29 and Figure 5.30. However, comparable values of standard deviation were predicted for all six natural ventilation strategies, as previously described.

It was important to predict the number of hours during the cooling period that the internal operative temperatures were below the ambient temperature, as this would ensure comfort during high summer temperatures, see Table 5.22. The highest percentage was predicted during the [DF & WC], which shows that it was the most efficient strategy in delivering occupants' comfort. Although this figure appears small, it should be noted that for a significant time during the cooling period, ambient temperatures were predicted below the acceptable for indoor comfort (i.e. 10% below 20°C).

The proposed ventilation strategies reduced the levels of CO₂ concentration below 1000ppm, and below 500ppm during 55% of the cooling time on average (Table 5.22), providing appreciable IAQ (Table 3.2). The predicted CO₂ emissions during the [base-case] strategy are comparable to values predicted by others in existing dwellings in Athens (up to 1800ppm maximum concentrations, according to M Santamouris, Argiroudis, et al., 2007).

Table 5.22 Percentage of hours during the cooling period that the operative temperatures were lower than the DBT, and of CO₂ concentration in the spaces within three ranges

	Base-case	Day	Night	DV & NV	WC	DF & WC	InOp
T _{in} < DBT	19%	39%	36%	49%	49%	51%	48%
0-500	34%	34%	72%	56%	55%	53%	55%
500-1,000	37%	40%	27%	43%	44%	45%	44%
Above 1,000	29%	26%	1%	1%	1%	2%	1%

Predicted average air change rates (ach⁻¹) for the period of a week, for the four daily groups, are presented in Figure 5.31. All strategies delivered air change rates above the minimum acceptable values for comfort, according to literature (Chapter 2.5.1 and Table 3.2) (1ach⁻¹), except for the [base-case] during the Group A. A large standard deviation was predicted for the results from the [base-case] (Figure 5.32). Small standard deviations were predicted for the ACH values of the [WC], [DF], and [DF & WC], showing that they were clustered closely around the respective predicted mean. The combined [DF & WC] strategy delivered adequate air change rates (9ach⁻¹ on average) with small standard deviation. In particular, the new ventilation strategies delivered appropriate ventilation rates and reduced the hours during the cooling period with 1ach⁻¹ (27% of the cooling period [DF & WC]) and the hours with values exceeding the 20ach⁻¹. During the 65% of the cooling period, the [DF & WC] contributed to air change rates between one to 20ach⁻¹, as shown in

Figure 5.33. These are expected values in domestic urban buildings in Greece according to published work by (Geros et al., 1999; Niachou et al., 2005)

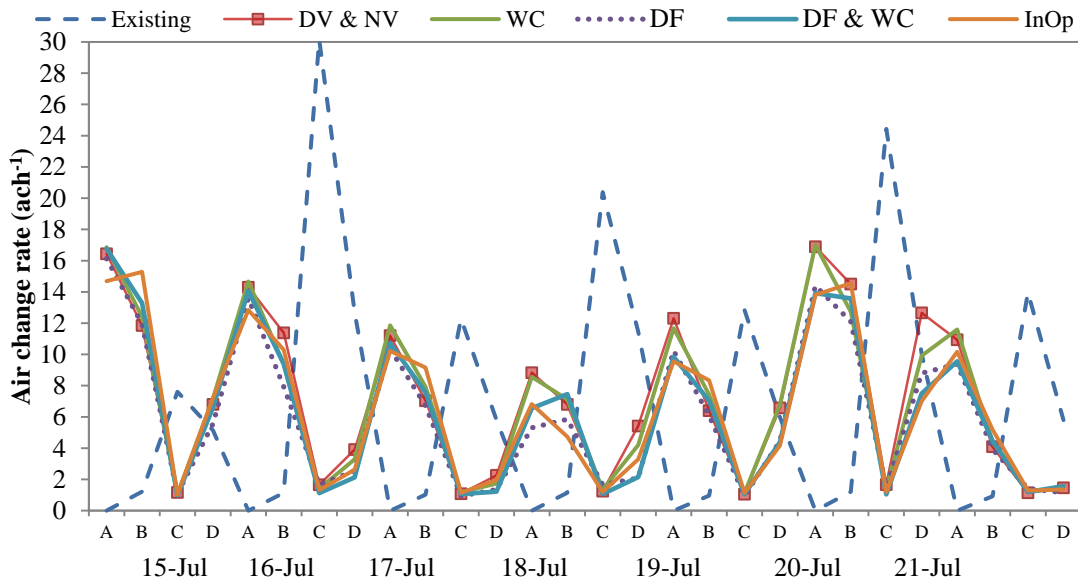


Figure 5.31 Predicted average, air change rate (ach⁻¹) during each of the four daily groups, during an example 7-day period

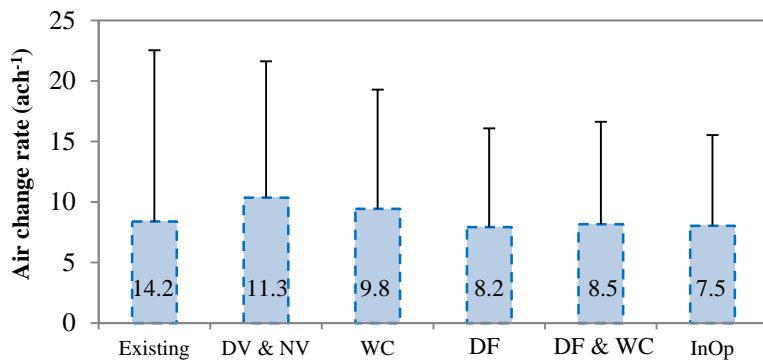


Figure 5.32 Predicted average hourly air change rate (ach⁻¹) of the apartment under investigation for the cooling period, and their standard deviation, for six ventilation strategies

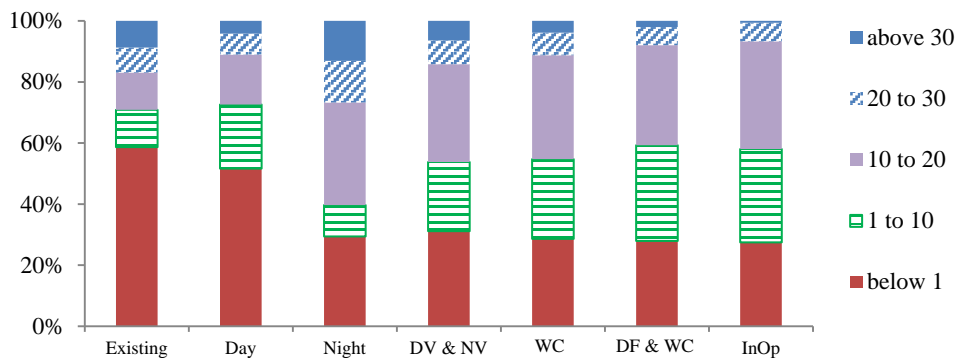


Figure 5.33 Predicted air change rate distribution (5) at five ranges (in ach⁻¹) during the cooling period, for seven natural ventilation strategies

5.4.1. Evaluation of occupants' thermal comfort

CIBSE Guide A defines overheating criteria for the indoor air temperatures that exceed the 26°C (bedrooms) and 28°C (other rooms) for minimum 1% of the occupied hours (CIBSE, 2006). The hours that the predicted operative temperature was above 26, 28 and 30°C (the standard was developed for cold climates, higher temperatures will need to be considered for hot climates) were defined for the four daily groups, as presented in Table 5.23.

Table 5.23 Percentage of hours above the temperature thresholds for overheating, during all natural ventilation strategies evaluated, per daily group

	Strategy	Group A	Group B	Group C	Group D
% of hours above 26°C	Base-case	85.2	81.2	85.9	87.1
	DV	72.4	54.3	69.5	72.3
	NV	50.9	54.6	73.3	76.1
	DV & NV	45.2	40.1	53.5	60.3
	WC	44.8	38.6	52.2	59.4
	DF	45.8	41.3	51.1	54.8
	DF & WC	45.3	39.8	50.2	54.3
	InOp	50.0	42.7	52.4	62.9
% of hours above 28°C	Base-case	71.0	64.0	69.5	70.8
	DV	51.2	24.9	46.4	51.3
	NV	24.1	32.1	50.4	52.7
	DV & NV	11.8	9.4	26.7	35.9
	WC	11.4	7.1	24.2	34.7
	DF	11.4	7.1	18.7	32.7
	DF & WC	11.3	6.7	18	30.4
	InOp	15.3	7.3	27.4	37.9
% of hours above 30°C	Base-case	48.5	40.6	46.1	48.3
	DV	19.5	3.1	11	18.4
	NV	4.3	5.2	19.1	23.3
	DV & NV	1.6	0.7	3.9	7
	WC	1.6	0.5	3.6	5.9
	DF	1.2	0.5	2.7	4.4
	DF & WC	1.2	0.4	2.6	4.4
	InOp	2.4	0.8	4.0	6.5

All ventilation strategies evaluated failed to meet the overheating criteria defined by CIBSE Guide A. The lowest percentages of hours above these thresholds were predicted during the Group B, having though the lowest number of occupants. The combined [DF & WC] strategy resulted in the least overheating hours (47% of the cooling period above 26°C, and 17% above 28°C) relative to the other six ventilation strategies, although higher than the acceptable percentage of hours for comfort. Up to

50% of the cooling period, indoor temperatures exceed the 30°C. This is in accordance with measurements in free-running domestic buildings in Athens by Sakka et al. (2010), predicting mean indoor temperatures during summer of 30°C for up to 70% of the period. The proposed ventilation strategies successfully reduced the number of hours above 30°C, thus providing comfort.

These thresholds have been originally defined for the dimensioning of mechanical building systems (cooling and ventilation). Occupants' thermal comfort expectations differ between conditioned and free-running buildings: occupants' are able to adapt to higher indoor temperatures (see Chapter 2.5). Therefore, these should be treated as a general guide of the evaluation of natural ventilation in free-running buildings. In order to ensure efficient performance evaluation in naturally ventilated buildings, occupants' response to discomfort, their interaction with openings and their adaptation levels, should be considered.

In order to consider occupants' adaptation, the simulation results were plotted against the acceptable levels of the internal air temperatures for comfort, defined by adaptive control algorithms (ACAs). Two ACAs were used to assess the performance of the various ventilation strategies, previously described in Chapter 2.5.2. Within the SCATs project¹ an ACA was developed specifically for the climate of Greece (McCartney and Nicol, 2002) expressed by the *Equation 2-3* (Figure 5.34).

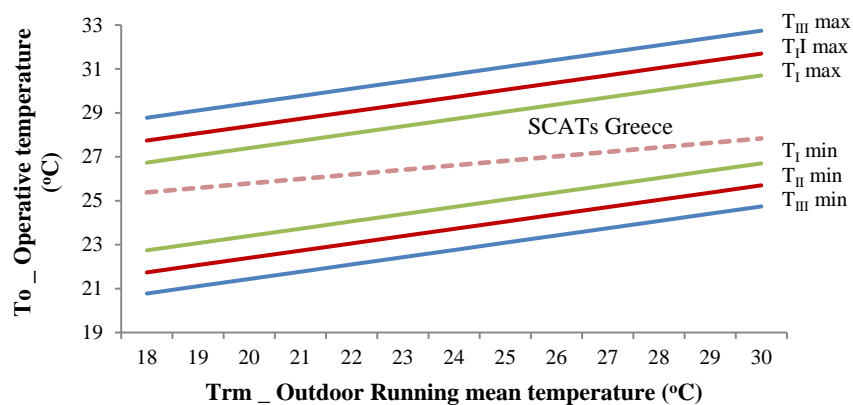


Figure 5.34 Comfort temperature ranges defined by EN15251 and the ACA by the SCATs project

The second ACA was provided by the British standard EN15251 (BS EN15251 CEN, 2007), which has also derived by the SCATs project and is considered more

¹ The EU Project Smart Controls and Thermal Comfort with measurements made in 26 European office buildings in different countries (Nicol and Humphreys, 2010)

applicable to Europe. This ACA is regarded an improvement to the ASHRAE standard 55-2004 (Nicol and Humphreys, 2010) and is expressed by the *Equation 2-2*. These limits apply for T_{rm} below 30°C, while indoor operative temperatures above 25°C could be balanced with increased ventilation rates. This equation could be modified to define the acceptable upper and lower limits for three categories of buildings, see Figure 5.34. For this research, only the first (high level of expectations) and the third bands (moderate expectations, existing buildings) of acceptable limits were used representing the ultimate and expected comfort temperatures, respectively.

Average daily simulation results from all natural ventilation strategies were predicted within the acceptable levels of the third band of the BSEN15251. Highest operative temperatures were predicted at the existing ventilation strategy [base-case], which exceeded the upper limit of the first band ($T_{I \max}$) for almost 50% of the time and for 10% the upper limit of the third band ($T_{III \max}$) (Figure 5.35). Enhancement of the IAQ with regard to temperature reductions between the [base-case] and the [DV & NV] was evident. Up to 52% of the predicted daily operative temperatures for the [DV & NV] lie within the narrowest band of minimum and maximum (T_I) acceptable comfort temperatures.

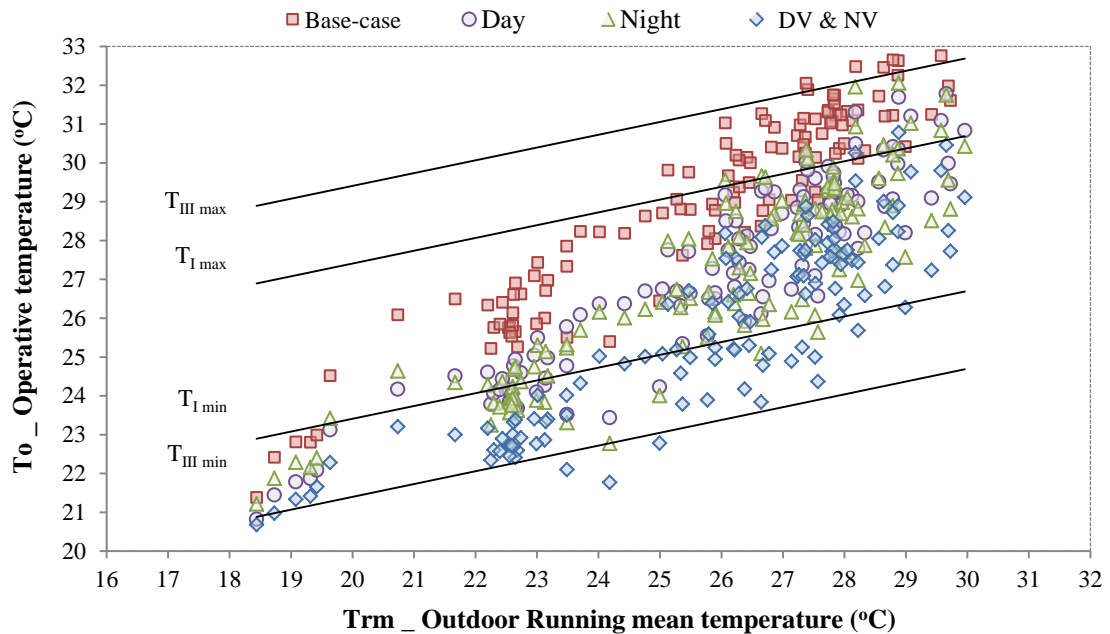


Figure 5.35 Relationship between outdoor running mean and operative temperatures for the four openings operation strategies

Following Table 5.23 presenting the percentage of hours above thresholds, Figure 5.36 illustrates the relationship between the outdoor running mean temperatures and

the predicted operative temperatures during [DV & NV] for six-hour daily groups. Operative temperatures were predicted within the third comfort band (T_{III}), varying between 77% (Group B) to 98% (Groups C and D). The least hours within the first comfort band (T_I) were predicted for the Group B and the most for the Group D. However, all operative temperatures were below the top limit of the first band ($T_{I\max}$), which was exceeded for only 5% during the Group D. For up to 56% of the time (Group B), operative temperatures were below the lower limit of the first band ($T_{III\min}$). Therefore, the most hours within the first comfort band were predicted during the Group C and D periods, 61% and 68% respectively. During the Group A and B the lowest operative temperatures were predicted. These were below $T_{III\min}$ during up to 23% of the time (day divided in four six-hour groups). However, temperatures were above 20°C. By dividing the day into four six-hour groups of similar occupancy patterns and outdoor air properties, it was possible to identify the hours of the day that occupants' comfort could not be achieved by utilising entirely natural ventilation strategies.

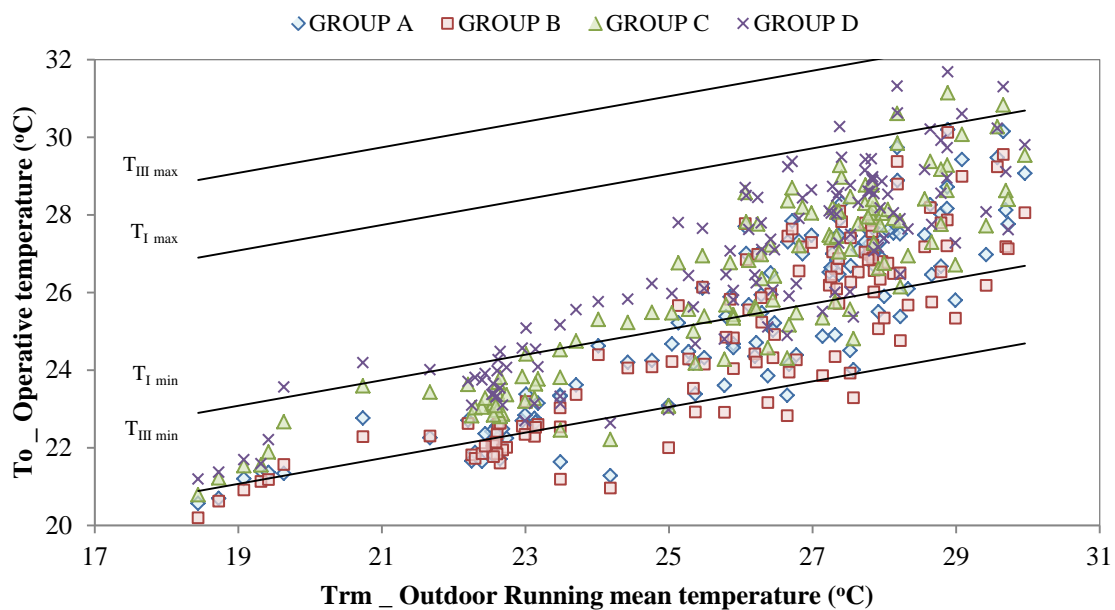


Figure 5.36 Relationship between outdoor running mean and average operative temperatures for the [DV & NV] ventilation strategy, showing the maximum and minimum acceptable levels according to BSEN15251

Furthermore, the relationship between the outdoor running mean temperatures and predicted operative temperatures for the [DF & WC] strategy was evaluated for the four daily groups, as in Figure 5.36 for [DV & NV]. As the two strategies provided comparable operative temperatures, they were thus not presented in this section.

During the Group C and D, the hours within the comfort limits of the first group (T_I), were less for the [DF & WC] relative to the [DV & NV], by 6%. This was because the number of operative temperatures during the six-hour groups below T_{Imin} , increased by 8% (51%, 56%, 44%, and 34% for the Groups A, B, C and D respectively). Comfort temperatures above the T_{Imax} were also reduced by 3%. Therefore, although comparable results were predicted during [DV & NV] and [DF & WC], the latter provided lower operative temperatures during all six-hour groups varying between 20 and 31°C (20 and 32°C for [DV & NV]).

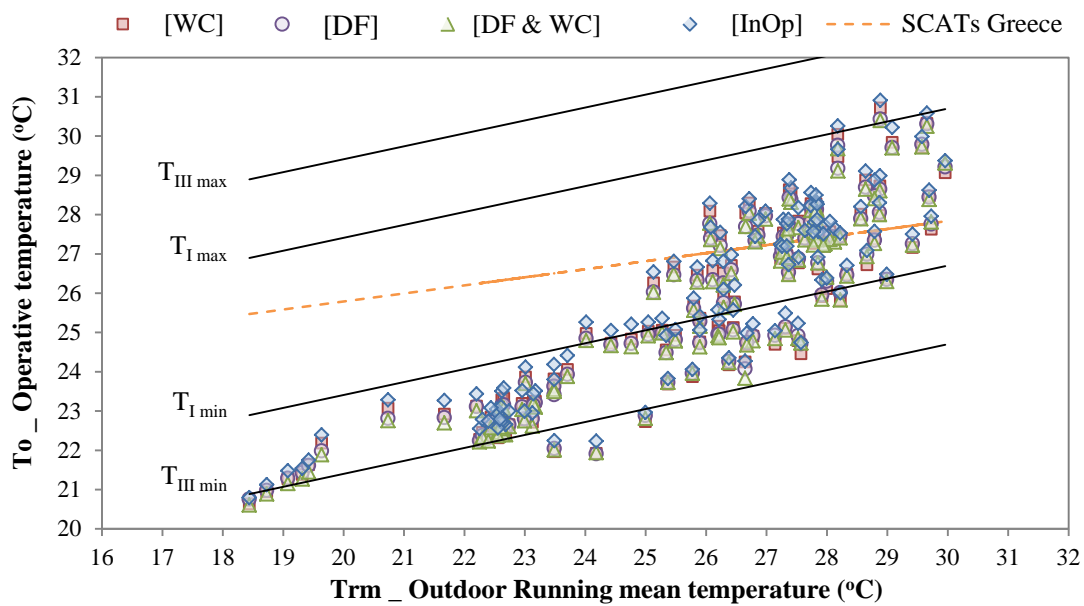


Figure 5.37 Relationship between outdoor running mean and average operative temperatures for four natural ventilation strategies, showing the maximum and minimum acceptable levels according to BSEN15251

Average daily values of operative temperatures predicted for four natural ventilation strategies ([WC], [DF], [DF & WC], and [InOp]) were plotted against the outdoor running mean temperatures (Figure 5.37). All strategies delivered operative temperatures within the acceptable comfort limits for high outdoor temperatures. During the lower values of T_{rm} , temperatures were below the comfort zone of the first band (T_I). Insignificant temperature difference was predicted between the simulation results from the four strategies. For all strategies, on average 52% of the cooling period, operative temperatures were within the T_I upper and lower limits. These exceed the $T_{I\ max}$ for only 1% of the cooling period: the strategies contributed even further in delivering low indoor temperatures than expected. During up to 48% of the cooling period, operative temperatures were below the $T_{I\ min}$ for the [DF & WC]

strategy; however, these were above the minimum temperatures for comfort as shown in Table 3.2 and below the 22°C for only 6% of the time. These were predicted lower than the expected indoor temperatures in domestic buildings in Athens, typically characterised by 30°C mean for 70% of the time (Sakka et al., 2010)

Although operative temperatures failed to meet the acceptable limits for overheating (Table 5.23), they were predicted within the acceptable comfort limits for high level of expectations (up to 70% for the six-hour groups) and for moderate expectations (up to 98%) as defined by adaptive control algorithms; occupants' comfort was achieved. For the purpose of this analysis, predicted average daily and six-hour average operative temperatures were used. Therefore, during each day these values would vary considerably. For operative temperatures during natural ventilation predicted outside the comfort limits for prolonged periods, alternative strategies could be employed such as provision of mechanical cooling by A/C units.

5.4.2. Quantification of the potential energy savings

The energy saving potential of natural ventilation and cooling systems relative to the operation of entirely mechanical cooling systems was quantified. Supplementary DTM simulations were performed during hybrid natural ventilation and mechanical cooling operation of the apartment under investigation. The A/C system was evaluated with the natural ventilation [base-case] strategy, as this represents the existing building operation within the existing building design.

For the hybrid ventilation and cooling strategy [hybrid], the mechanical cooling system was active during the hours of the highest occupancy (10pm-6am and 12pm-7pm). The building was in free-running mode for rest, seven hours during the day. The optimum indoor air temperature of operation was 26°C, as recommended by the National Greek standards (see Chapter 2.5.1). The mechanical system selected for the purpose of this study was an energy efficient mini-split system (Energy Efficiency Class A++) that supplied chilled air to the bedrooms (2 units) (nominal EER 3.85W/W and COP 4.38W/W).

The hybrid strategy provided indoor air temperatures with small fluctuations throughout the cooling period (Figure 5.38). Simulation predicted that during the cooling period the indoor air temperature exceeded the threshold of 26°C by 72% and the threshold of 28°C by 0%. These are particularly low values relative to the rest of the ventilation strategies. Comfort with regard to cooling was achieved according to CIBSE (2006) and Table 3.2. However, further natural ventilation would be required to achieve indoor environmental quality, as CO₂ in the spaces were predicted up to 1,300ppm. This was as expected in existing buildings with low ventilation rates, reported by M Santamouris, Argiroudis, et al. (2007).

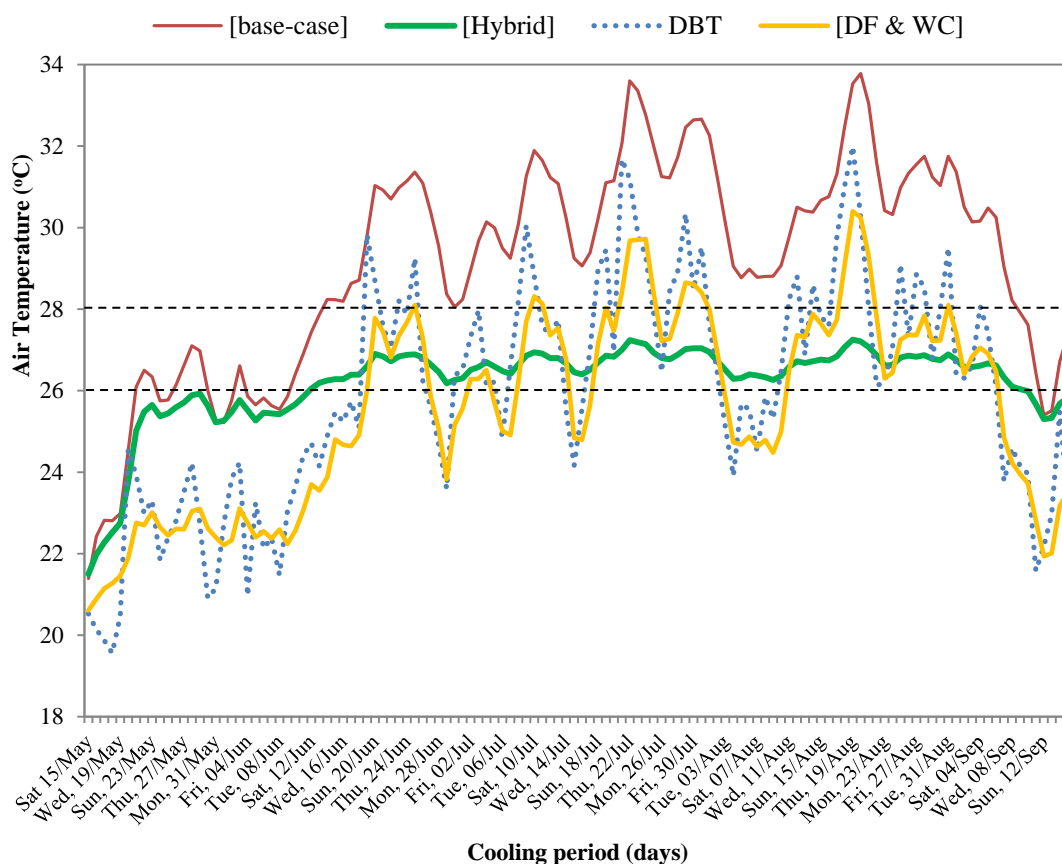


Figure 5.38 Predicted daily operative temperatures for mechanical and natural ventilation strategies during the cooling period

The mechanical system operated for 1,859 hours (40%) throughout the cooling period and the total energy consumption was predicted up to 1135.3kW. This figure indicates that by utilising the proposed natural ventilation strategies (this figure was predicted for the [base-case]), and with occupants' adaptation to higher indoor air temperatures, significant energy savings could be achieved. As shown in Figure 5.38, the [hybrid] strategy delivered higher operative temperatures for 60% of the cooling

period than those predicted during [DF & WC] (described in Section 5.3.8). This was because the [hybrid] system represents the ventilation ([base-case]) and cooling strategy that occupants are currently utilising in the existing building. The [DF & WC] strategy provided lower indoor air temperatures by exploiting the lower ambient temperatures and the high wind speeds. However, during the [DF & WC] strategy, indoor air temperatures exceeded the 26°C and 28°C thresholds for 47% and 16% of the cooling period respectively. If mechanical cooling were provided during only the hours that indoor temperatures exceeded the 28°C with the [DF & WC] strategy, then comfort and substantial energy savings could be achieved: the A/C would operate for the one third of the hours it operated during the [hybrid] strategy. This is in accordance to published work by others reporting that free-running buildings consume 50% less energy than the air-conditioned buildings (O'Sullivan & Kolokotroni, 2014).

The A/C system selected for the purpose of this research was a very energy efficient system, which was not representative of the vast majority of systems currently installed and operated in domestic buildings in Greece, especially considering fuel poverty and the cost of systems' replacement. The energy consumption (kW) could significantly increase if a less energy efficient A/C unit was in operation. Therefore, this value can only be indicative of the performance of the system. The actual performance would depend on external parameters such as the systems' installation, maintenance, exposure of the unit to direct solar gains, local microclimate and urban heat island (up to 25% COP reduction was predicted in Athens due to UHI (Santamouris et al., 2001)), as described in Chapter 2.3.

5.4.3. Ventilation performance evaluation of the apartment studied and the adjacent spaces

The case study apartment was connected to a light well that was also connected by openings to the three apartments located above the apartment under investigation and the four at the other side of the light well. The DTM simulations performed for the purpose of this research investigated the ventilation performance of the case study apartment and natural ventilation strategies, when only the selected apartment was connected to the light well (the connecting openings of the other apartments were closed). This provided information of the maximum ventilation performance of the light well and the wind-catcher, in benefit of the apartment under investigation (exclusive operation). Additional DTM simulations were performed to investigate how the surrounding apartments influence the ventilation performance of the selected apartment (1/8th potential).

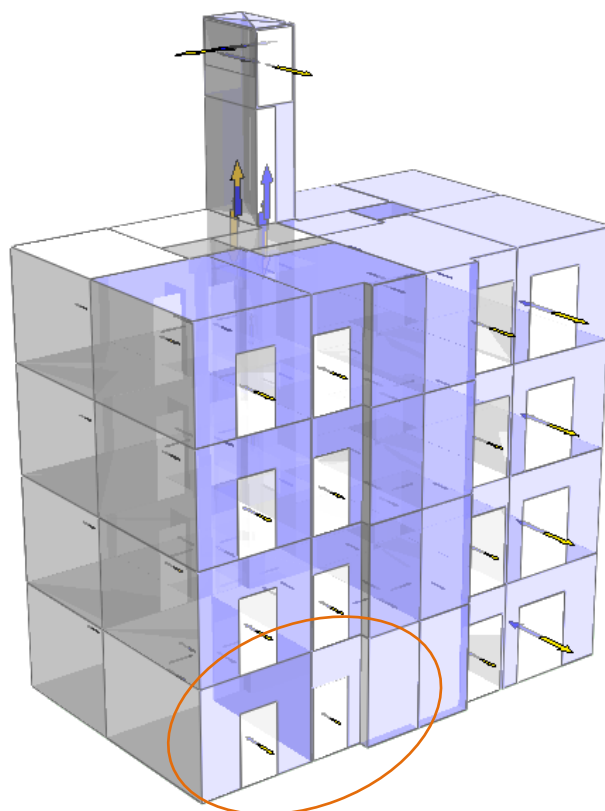


Figure 5.39 Three-dimensional model of the building connected to the central wind-catcher, in IESVE, showing the apartment under investigation and the five apartments attached to the air shaft

Simulations were performed for the wind-catcher strategy [WC] as a representative strategy. All the surrounding apartments were considered to have the same openings' operation profiles, internal heat gains and occupancy profiles, to the case study apartment. The DTM model of the eight apartments evaluated is presented in Figure 5.39. Different flow rates were predicted at each opening operating according to the same openings' profile (Figure 5.20) and in response to parameters of the internal and external thermal environments.

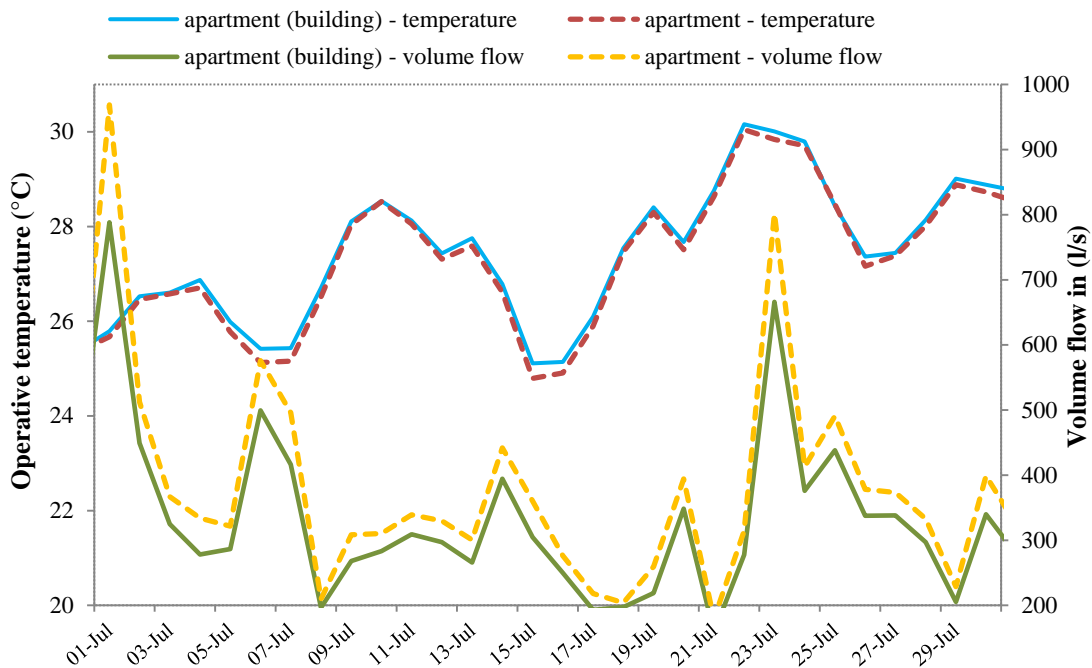


Figure 5.40 Average daily values of operative temperatures ($^{\circ}\text{C}$) and volume flow rates (l/s) predicted in the apartment studied, with (building) or without the surrounding apartments, for the period of a month

The ventilation performance of the $1/8^{\text{th}}$ operation of the [WC] strategy was evaluated and compared to the performance of the apartment modelled during the full usage of the light well (described in Chapter 5.3.5). Comparable values of operative temperatures and volume flow rates were predicted for both modelling techniques, as presented in Figure 5.40.

Lower volume flow rates were predicted for the apartment ($1/8^{\text{th}}$) modelled with the surroundings (less than 40l/s for the cooling period) relative to the building as a stand-alone case. Reduced values of relative humidity (0.3% less on average), higher CO_2 levels (about 13ppm on average), and higher indoor air temperatures of up to 0.2°C (1% on average increase during the cooling period) were calculated.

Despite the overall decrease of the ventilation rates and the air temperature increase, comfort temperatures in the case study apartment for the [WC] during the 1/8th light well were predicted within the T_I and T_{III} comfort limits. This was predicted for longer periods (55% and 98% respectively) relative to values predicted during the full use of the light well, presented in Section 5.3.5 (52% and 96% respectively). Operative temperatures exceeded the upper comfort limit $T_{I\max}$ for no more than 1% of the cooling period. Therefore, the insignificant difference between in the predicted values from the two modelling techniques (the apartment with exclusive use of the air shaft or for 1/8th use) justifies the method selected for the purpose of this work.

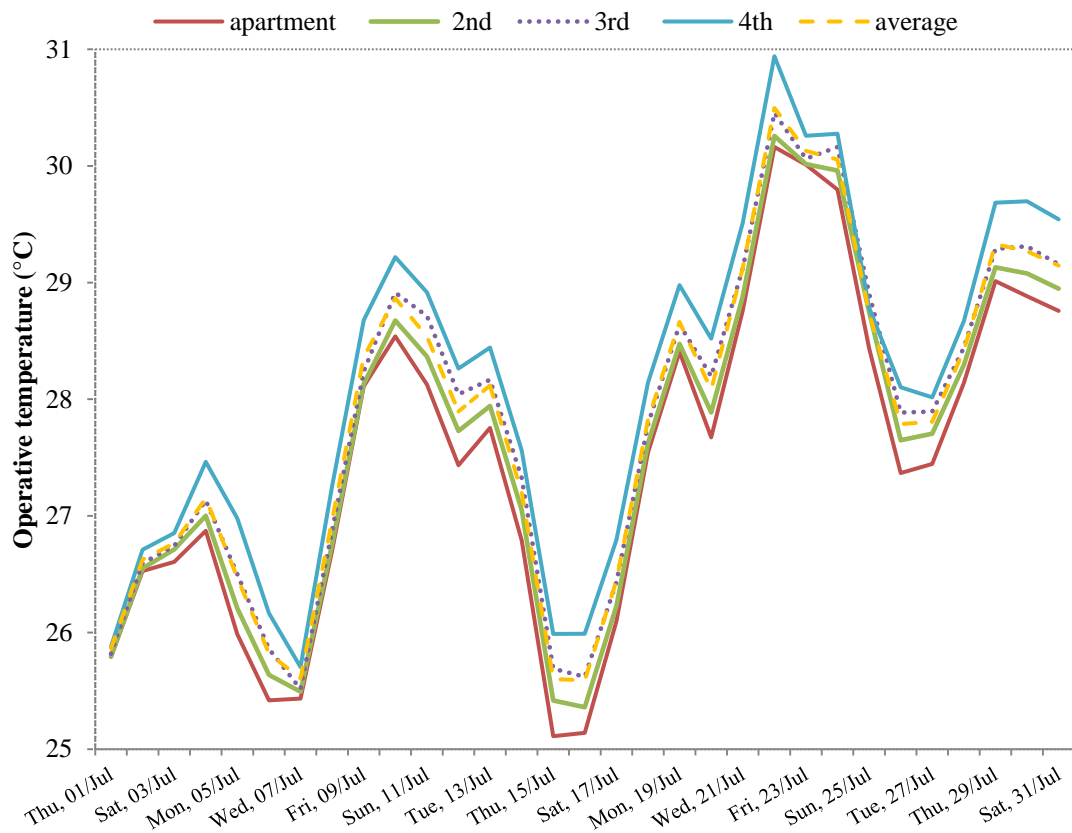


Figure 5.41 Predicted operative temperatures for the apartment studied, the three apartments above, and the average of the eight apartments connected to the wind-catcher for a period of a month

Furthermore, the study of the surrounding apartments provided information regarding the overall ventilation performance of the building and the [WC] strategy. The simulations predicted total average daily temperatures of the eight apartments up to 0.5°C above the average daily temperatures of the case study apartment. Higher indoor air temperatures were predicted to the apartments located above the case study. Predicted indoor air temperatures gradually increased from the case study

apartment (1st floor) towards the top of the building (4th floor). This temperature difference was predicted up to 1°C of the daily average values (Figure 5.41). This was due to the longer number of hours with direct solar radiation at the top floors, the reduced length of the wind-catcher shaft, the influence of thermal mass and particularly the insufficient roof insulation.

5.4.4. Modelling wind-driven flows: Limitations

Some limitations of modelling wind-driven natural ventilation in DTM software were identified. The pressure due to wind at the openings is a complex function of wind speed, direction and geometry. The IESVE software considers the influence of surrounding structures (e.g. surrounding buildings, wind-walls) at the CFD mode, however not during the DTM simulations. Because of this, the software provides the user with the option to modify the properties of the openings according to their exposure level and height (e.g. exposed to semi-exposed) in order to consider the influence of obstacles. These values have been approximated, and are not specific to the building design and climate; this is thus a limitation of this method. The driving pressures due to wind used by the software, are estimated values of pressure coefficients predicted within wind tunnel experiments on simple building models, which are considered applicable to a range of surface types (exposure types) and wind directions (angles).

Accordingly, for the wind-driven ventilation performance evaluation of the ventilation strategies, approximated pressure values were used by the DTM software. Thus, the properties of the building design, surroundings and the site, were not taken into account. As a result, the evaluation of different properties of the wind-catcher openings predicted comparable ventilation rates between the different scenarios (e.g. openings simultaneously open according to wind direction or operating in pairs, openings dimensions, and wind-catcher height). The [WC] ventilation strategy was anticipated to provide high ventilation rates in the occupied spaces, however it delivered comparable results to the [DV & NV] strategy (that utilised only an air shaft of a shaded, horizontal opening). This is not representative of the usual performance of a wind-catcher as seen in the literature (see Chapter 2.6.1.2.) and in full-scale projects.

5.5. Discussion

Using DTM simulations it was possible to evaluate the ventilation performance of the apartment studied and the various natural ventilation strategies. It was predicted that optimization of the openings' operation in response to environmental conditions could provide significant increase in ventilation rates and a reduction in air temperatures. The combined day and night ventilation provided comfort ventilation relative to the [base-case], the [DV] and [NV] ventilation strategies (see Section 5.3.4). The inclusion of a wind-catcher was expected to yield a greater enhancement to the natural ventilation of the spaces than the results suggest, relative to the previous [DV & NV] strategy and with regard to literature. Despite the potential of the [DF] in reducing the solar gains in the occupied spaces and providing temperature reduction particularly during the evening, it has also contributed in considerable reductions in ventilation rates. The introduction of the new 'internal openings' resulted in an increase in indoor air temperatures and reductions in ventilation rates.

This chapter presented the ventilation and cooling performance of the strategies over the cooling period, showing performance in response to environmental and time parameters. This is important for the evaluation of the overall ventilation performance of the strategies over a period. Despite the significant performance of the DTM to evaluate natural ventilation with openings control, simulation results show limitations of the modelling technique to appropriately evaluate wind-driven natural ventilation. This was because of the use of approximated driving pressures across the building openings (e.g. wind-catcher openings, façade openings). Accordingly, advance investigation of the different natural ventilation strategies was required using steady state CFD simulations, described in detail in the following chapter. This would provide detailed information about the natural ventilation performance of the different strategies and apartment studied for both buoyancy and wind driven flows, predicted specifically for the case study building within its surroundings.

***Chapter 6* : AIRFLOW MODELLING ANALYSIS AND VENTILATION PERFORMANCE RESULTS**

6.1. Introduction

This chapter describes the computational fluid dynamics (CFD) simulations carried out to evaluate the ventilation performance of the retrofit options of the apartment building under investigation, described in Chapters 3 and 4. De-coupled airflow modelling was employed to predict the airflow patterns around the case study building at the neighbourhood scale, along with the prediction of the internal airflow patterns and IAQ (e.g. air temperature, ventilation rates) at the scale of a single apartment. Cross ventilation strategies, implementation of wind-catchers, a lightweight dynamic façade and introduction of cooling by water evaporation have been investigated to enhance the natural ventilation of the building and improve performance of the original single-sided ventilation strategy. Optimization of individual natural ventilation system designs was outside the scope of this research. Detailed information regarding the simulation model and characteristic are presented. Simulation results of the most representative climate conditions for the site are then presented for all natural ventilation strategies. The chapter concludes with the ventilation performance evaluation of all the natural ventilation strategies and climate scenarios explored, and the limitations of each strategy.

6.2. Description of the Individual Natural Ventilation Strategies and CFD Models

Following the ventilation performance evaluation using DTM simulations of the natural ventilation strategies under investigation (Chapter 5), steady state CFD simulations were performed to evaluate detailed wind and buoyancy-driven ventilation in the spaces. It was important to understand how neighbouring buildings modify the prevailing winds and the natural ventilation behaviour of the apartment under investigation (study of the external flow field). The sensitivity of the ventilation rates due to wind direction and speed were then evaluated at the scale of a single apartment (base-case). The ventilation and cooling performance of the natural ventilation strategies was evaluated for specific climate scenarios and buoyancy and/or wind driven flows.

The performance of the strategies was established under both buoyancy and wind-driven forces subject to different climate scenarios and by maintaining the same internal heat gains and construction properties at all strategies. The ventilation performance of the case study building was evaluated during 14 climate conditions/scenarios defined at the climate data analysis for the cooling period (15th May until 15th September, defined by the Greek regulations (Androutsopoulos et al., 2012)) described in detail in Chapter 4.4 and presented in Figure 4.9. The climate analysis predicted the average DBT, 26°C (DBTs between 25-27 °C for 26% of the cooling period), and the highest DBT, 35°C (DBTs above 30°C for the 21% of the period). The average wind speed, 3.6m/s (up to 40% wind speeds between 2.5-4.5m/s), and the highest, 7m/s (15% of the period, 85 percentile), were also predicted. Three predominant wind directions were also defined (north for 33%, east for 7% and northwest 12%). The low wind scenario (wind speeds of 0-2m/s for 23% of the period), i.e. buoyancy-driven flows, was also explored. If the proposed strategies deliver natural ventilation for these climate scenarios, comfort will be provided for the vast of the cooling period (more than 50% of the period).

The natural ventilation and cooling efficiency of the different ventilation strategies was evaluated relative to the existing natural single-sided strategy of the apartment under investigation. The proposed ventilation strategies were expected to deliver

increased ventilation rates in the spaces and reductions in the indoor air temperatures relative to the base-case ventilation strategies and up to or lower than the DBT, with regard to the fully open building openings and the lack of thermal mass. The influence of the openings operation was not considered. The building openings (internal/external) were fully open at all strategies in order to evaluate their maximum ventilation potential.

Further to this, acceptable values of indoor air speed, ventilation rates, air changes per hour and indoor temperatures were defined according to literature (Chapter 2.5.1). A set of environmental conditions that are acceptable was defined and used as metrics for the evaluation of all ventilation strategies examined, included in Table 3.2 of Chapter 3.3. CIBSE Guide A recommends indoor air temperatures up to 28°C in the living spaces and 26°C in the bedrooms (CIBSE, 2006). However, it is important to consider occupants' adaptation. As shown in Figure 5.34, for 26°C DBT, acceptable operative temperatures would vary between 23°C and 31°C in order to satisfy occupants' comfort expectations in existing building designs. Despite the minimum acceptable values recommended by standards (described in Chapter 2.5.1), measurements in existing free running buildings in Greece (Geros et al., 1999) predicted high ACH per hour (up to 80ACH). It was anticipated that the proposed natural ventilation strategies would deliver indoor air speeds above the minimum values for comfort (0.2m/s, see Chapter 2.5.1) that could provide passive cooling by natural ventilation.

The natural cooling and ventilation potential of the following ventilation strategies was explored using the CFD software PHOENICS (CHAM Ltd., 2013), (a list of the strategies and their abbreviations are included in Table 6.1):

- I. **Single-sided double opening ventilation:** Evaluation of the existing ventilation strategy of the apartment, utilising the two façade ventilation openings (balcony doors) and the internal doors (open at all times). The internal window connecting the kitchen to the existing light well was closed at all times.
- II. **Cross ventilation:** The ventilation potential of cross ventilation via the façade openings, the internal doors, the internal connecting openings and the light well, was investigated.

- III. **Wind-catcher:** A four-sided wind-catcher with cross-partitions was implemented at the top part of the existing light well. It would be able to harness the wind from all directions, channel it into the occupied zones and exhaust it via the two façade openings (wind-scoop, downward airflow). However, under insufficient wind speeds, the wind-catcher would assist the extraction of stale air from the spaces (upward airflow movement) via the four individual channels and fully open openings.
- IV. Cooling by **water evaporation:** The concept of a passive downdraught evaporative cooling tower was investigated using water evaporation techniques in the core of the wind-catcher shaft and below the cross partitions. The performance of this strategy was investigated during the operation of the wind-catcher as a wind-scoop.
- V. **Lightweight dynamic façade:** A semi-outdoor environment was formed with the addition of a lightweight second façade comprising with three sets of partially open horizontal openings, extending the indoor spaces to the edge of the balconies. Following the improved performance of this ventilation strategy when combined with the wind-catcher predicted with DTM (presented in Chapter 5.3.8), this combined strategy was also evaluated using CFD.
- VI. Cooling by **water evaporation:** The performance of the previously described cooling by water evaporation strategy (IV) was also investigated with the lightweight façade and the wind-catcher strategies (V).

Table 6.1 List of the natural ventilation strategies and their abbreviations

Scenario	Natural ventilation strategy	Abbreviation
I	Single-sided ventilation	[SS]
II	Cross ventilation	[CV]
III	Wind-catcher	[WC]
V	Dynamic façade	[DF]
V	Dynamic façade and Wind-catcher	[DF & WC]
IV	Passive downdraught evaporative cooling with wind-catcher	[PDEC-WC]
VI	Passive downdraught evaporative cooling with wind-catcher & dynamic façade	[PDEC-DF]
	Internal openings	[InOp]
	Façade wind-catcher	[fWC]

The adjacent building spaces to the case study apartment were excluded from the building model during the internal flow investigation. All the strategies described were modelled with the fully and exclusive use of the air shaft, which was connected to the rear spaces with an internal opening (the other adjacent building apartments would not utilise the air shaft). The wind-catcher design proposed (Chapter 4.5.1) was considered suitable to accommodate the ventilation needs of the apartment under investigation. Further utilisation of the wind-catcher by the adjacent building apartments requires design refinement of the wind-catcher in order to deliver optimum ventilation performance for all apartments, which was beyond the scope of this research.

For the investigation of the wind driven ventilation in buildings, Jiru and Bitsuamlak (2010) discretise two modelling techniques, the whole domain and the domain-decoupling approach, providing simulation results in good agreement. For the purpose of the research reported here, the domain de-coupling approach was employed. This is favoured because it is less time consuming (Graça et al., 2002), requiring optimum mesh refinement (Norton et al., 2007), and allows changes to the interior without affecting the exterior, offering modelling design flexibility (Jiru and Bitsuamlak, 2010). This modelling technique was utilised only for the study of the airflow patterns due to wind-induced ventilation and not due to buoyancy-driven flows. This reduces the computational power required to simultaneously model both internal and external thermal environments. Hence, the building and its surroundings were first simulated to obtain the external airflow distribution and pressure values at the location of the openings. These were subsequently included as input values on the building's openings for the study of the internal flow.

The flow diagram of Figure 6.1 illustrates the step by step process of the de-coupled airflow modelling simulations (inputs and outputs) performed for each of the ventilation strategies employed. It also presents the climate scenarios (i.e. DBT, wind speed and wind direction) for which the simulations were performed. Throughout this research, the term wind-driven ventilation is used to describe the combined forces due to wind and buoyancy. The number of simulations for the different strategies performed for both internal and external flow fields, for all natural ventilation strategies and climate scenarios, are included in Table A.5 and A.6 of Appendix A.4.

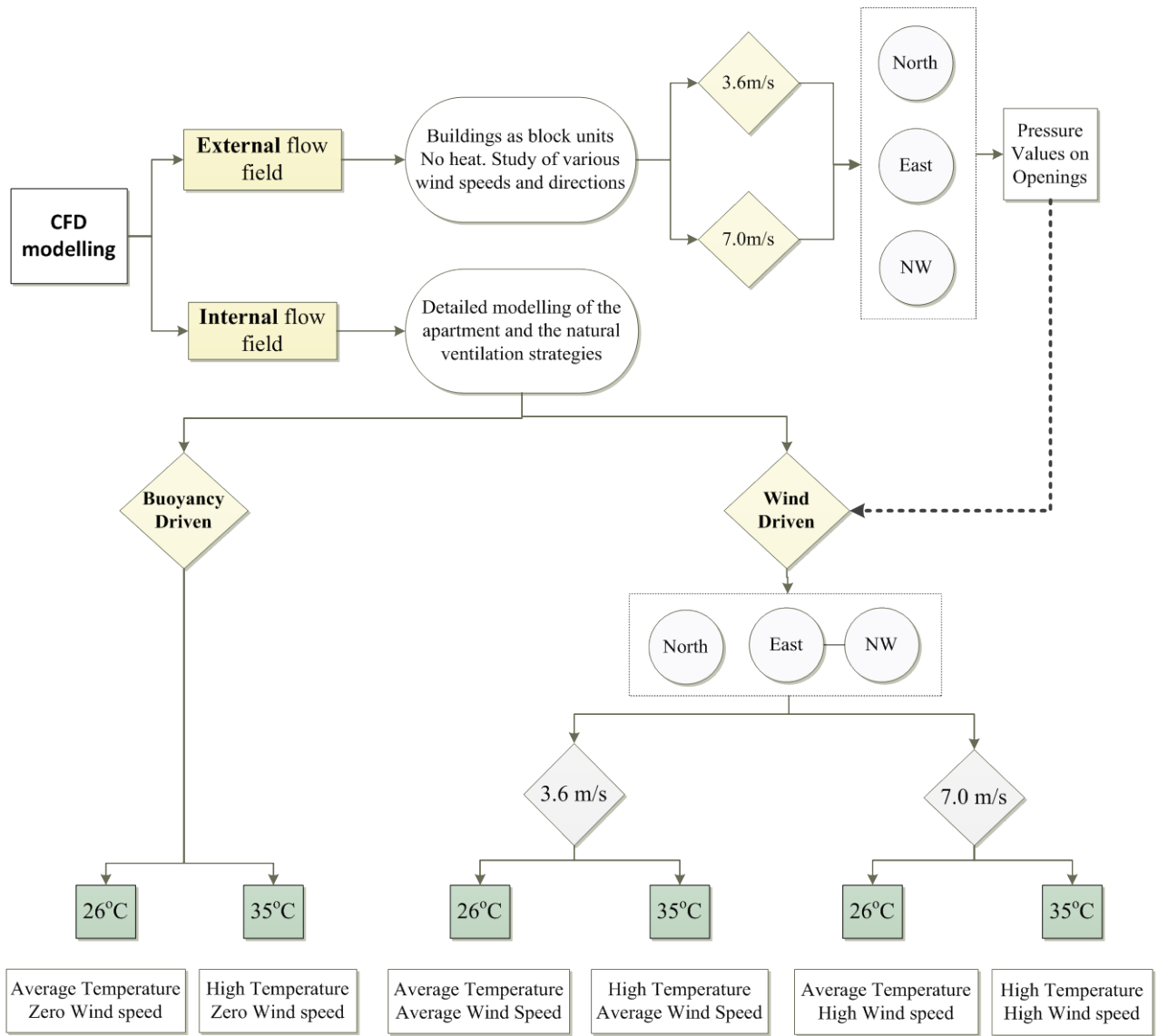


Figure 6.1 Graphical representation of the de-coupled internal/external airflow modelling flow diagram showing inputs and outputs, repeated for all natural ventilation strategies examined

6.3. Study of the External Flow: Model Setup

De-coupled CFD external flow simulations predicted wind pressures at location of the building's openings, which were used for the prediction of the performance of the wind-induced ventilation strategies. The building under investigation and the neighbouring buildings were simulated as individual blocks with all openings 'closed'. The design was simplified to reduce computational time and therefore shading systems, balconies and trees were excluded from the simulation process. The terrain heights were initially included in the CFD model although after preliminary simulations it was predicted that their influence on the flow field was insignificant, and mostly up to the height of the ground floor level. The terrain heights were excluded from the CFD simulations. The heights of all buildings were increased proportionally to represent the natural differences in height due to the terrain, as described in detail in Chapter 4.3. The domain size, location of the building and computational mesh properties were developed according to existing published work (Chapter 2.6.3)

For the evaluation of the external flow field at first, the case study building was simulated as a stand-alone building according to Visagavel and Srinivasan (2009) and Yik and Lun (2010). However it was considered important to evaluate the performance of the ventilation strategies and the building within its context: the simulation results of the stand-alone simulations were considered insufficient and unrealistic (see Section 6.3.1). Different domain sizes were evaluated, according to literature (Chapter 2.6.3). After exploratory simulations and by considering the recommendations by the software developer, it was decided to model the computational domain proportional to the outline of all buildings. This provided appreciable simulation results at an acceptable computational time, while enabling efficient investigation of various wind directions. The selected building was modelled centred in nine urban blocks and the computational domain faces on x and y were designed 300m offset to the building and the surroundings' outline (more than 8 times the height of the tallest building). The dimensions of the computational domain (Figure 6.2) were equal to 900m×750m×136.8m and the nine blocks occupied a central area of 40677m² (the domain height was 4 times the height of the tallest building). These were found to be sufficient to model the exterior airflow.

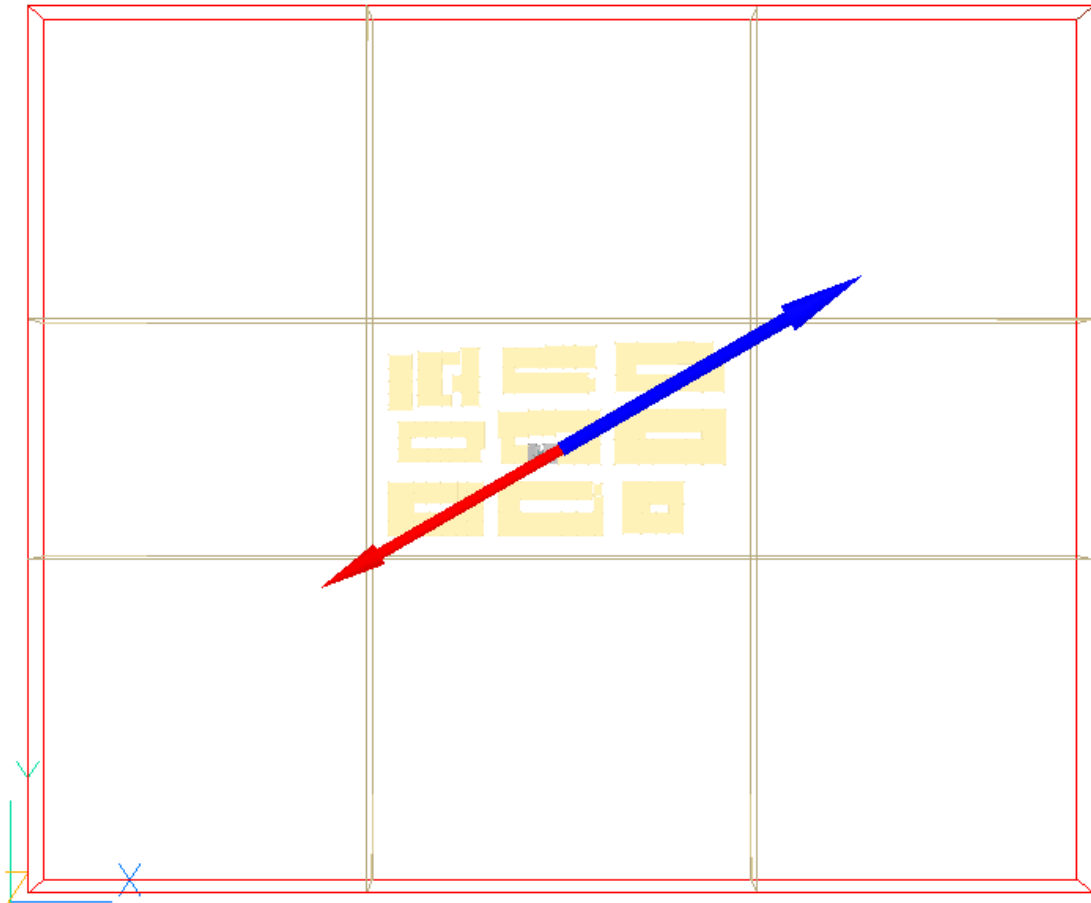


Figure 6.2 Plan view of the building (centred in grey) and its surroundings' at the neighbourhood scale, with blue and red arrows pointing at north and the wind direction, respectively. Invisible objects that do not affect the airflow calculations assist the refinement of the computational mesh and divide the domain into 9 zones

Wind was modelled using a simulation option in PHOENICS known as the 'wind object' that occupied the entire domain. The wind object creates inflow boundaries at the domain edges with a logarithmic profile on the upwind faces and fixed pressure boundaries on the downwind faces, sky and ground plane (Ludwig and Mortimore, 2011). Atmospheric pressure was set at all faces of the wind object, while "the mass flow through the pressure boundaries is a linear function of pressure difference" (Ludwig and Mortimore, 2011). A series of simulations with different ground plane effective roughness heights predicted that this had negligible influence in the occupied zones. The increase in roughness height resulted in computational time increase. The ground plane was modelled with an effective roughness height of 0.75m because it provided accurate and less computationally demanding results.

The turbulence was modelled with the modified k-epsilon model of Chen and Kim (CHAM Ltd., 2008) which reduces the dissipative nature of the standard k-epsilon

model of Launder and Spalding (Launder and Spalding, 1974), whilst the energy equation was not calculated. The probe used to monitor convergence was located at 7.7m height above the ground level, among the buildings and at varying locations in relation to wind direction. The solution was considered converged when the spot values (of the pressure and the three components of velocity) at a defined monitoring point in the domain, remained unchanged and when the logarithms of the sums of the absolute residual of each variable (errors) in the finite-volume equation were reduced to an acceptable magnitude and below 1E-03.

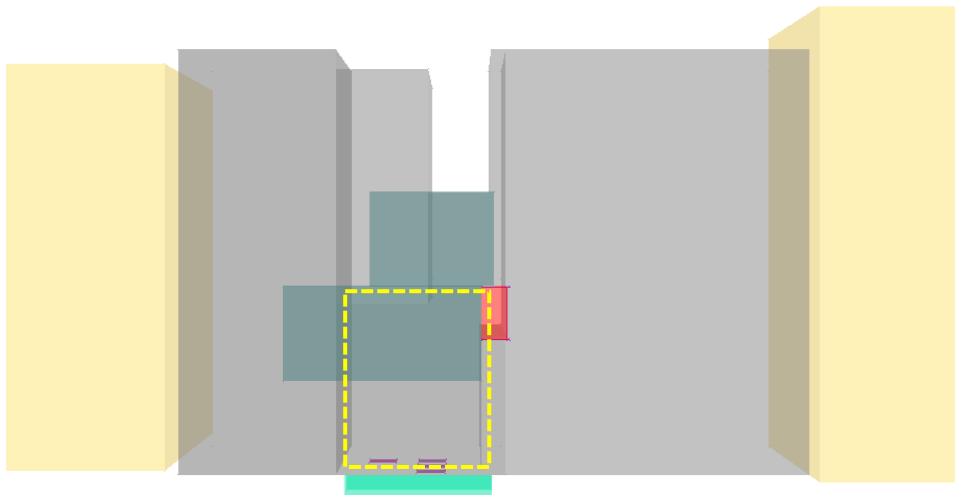


Figure 6.3 Plan view of the three-dimensional model of the building in PHOENICS, showing the air shaft highlighted in red, the position of the apartment with dash line, the position of the balconies (in light blue) and the penthouse (in dark blue)

A plan view of the building model in CFD is presented in Figure 6.3. The external flow field was modelled for three ventilation scenarios. Pressure values predicted at some models could be used at the study of the internal flow field of different ventilation strategies with the same building design, the three models are:

- **Base-case ventilation** strategy of the building under investigation using the existing design of the light well. The simulation results assisted the study of the internal flow field of single-sided and cross ventilation strategies ([SS], [CV]).
- The addition of the **wind-catcher** model to the previous design was investigated, providing pressure values for the study of the wind-catcher and ‘water evaporation’ strategies ([WC], [PDEC-WC]).
- The addition of the **dynamic façade** provided input values for the dynamic façade and water evaporation strategies ([DF & WC], [PDEC-DF]).

The proposed three models were evaluated for three wind directions (north, east, northwest), the selection criteria of which are presented in Section 6.5, and two wind speeds (3.6m/s and 7m/s), as illustrated in Figure 6.1. A total number of 38 external flow CFD simulations were performed for the purpose of this research. All simulations reached convergence after approximately 8,000 iterations within 50 to 130 hours, with regard to the building model, orientation and the resources available at the time of the simulation. Simulations were performed both in serial and parallel options of the software, the limitations and potential of each are further discussed in Appendix A.4.1.

6.3.1. Mesh independency study

In order to ensure a solution independent of the mesh resolution, six different computational meshes (Cartesian) were created, included in Table 6.2, with dense areas at zones of complex or rapidly changing flow. The CFD model of the ‘wind-catcher’ scenario [WC] was selected for the mesh investigation due to the complex geometry of the wind-catcher requiring very fine mesh elements.

Table 6.2 Computational meshes evaluated for the study of the external flow showing the number of cells at the wind catcher zone, the number of cells of each domain axis and the total number of cells

Type	Wind Catcher (xy)	Domain (x,y,z)	Number of cells
Mesh 1	5×10	186×161×76	2,275,896
Mesh 2	4×7	194×170×80	2,638,400
Mesh 3	5×9	205×182×79	2,947,490
Mesh 4	6×11	215×189×86	3,494,610
Mesh 5	7×12	221×198×94	4,113,252
Mesh 6	8×13	227×199×98	4,426,954

The first five meshes converged to an acceptable level (see convergence plot for Mesh 5 in Figure 6.4), however, convergence was more difficult to achieve for the sixth mesh. Meshes 4 and 5 provided the most comparable results (Figure 6.5); mesh five was chosen because it provided sufficient design flexibility to include further natural ventilation strategies. Convergence could only be achieved by specifying under-relaxation factors of 0.1 on the three velocity components, which by slowing-down the solved-for variables avert the divergence of the built-in iterative solution process-the convergence rate was noticeably reduced.

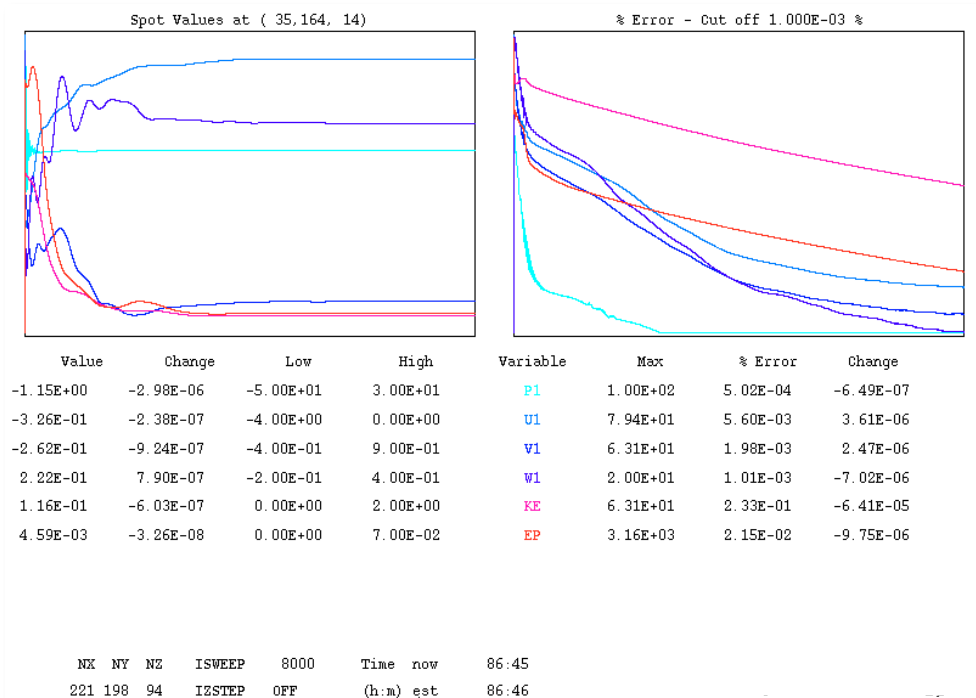


Figure 6.4 Convergence monitoring plot showing the reduction in error and the variable values at a user-specified monitor location in the grid ([DF & WC], northeast, Mesh 5)

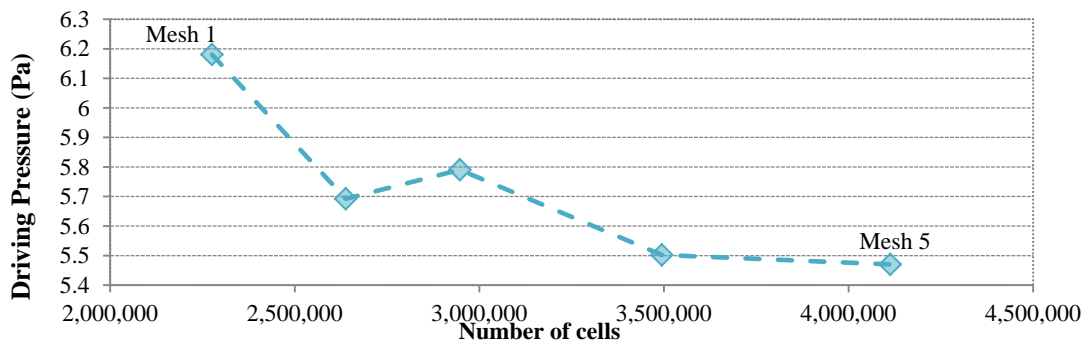


Figure 6.5 Driving pressures (Pa) predicted by simulations with different number of cells, study of the external flow field.

A plan view and a front view of the building studied with the surrounding buildings and computational domain are presented in Figure 6.6 (xy axis 7m height above the ground level) and Figure 6.7 (x,z axis) respectively. The coarser mesh areas were located towards the corners of the domain and the denser in the centre, where the building of interest was located (i.e. centred among the buildings). Finer mesh was generated at the location of the light wells (or the wind-catcher with regard to the ventilation strategy).

Grid control objects with no effect on the calculations ('null' object in PHOENICS) were created at a short distance from the corners of the buildings in x, z and y, z

areas (Figure 6.2). These provide higher levels of grid control, enabling a fine mesh to be created over the buildings and the more rapid expansion of the grid further away of the building zone (i.e. coarse).

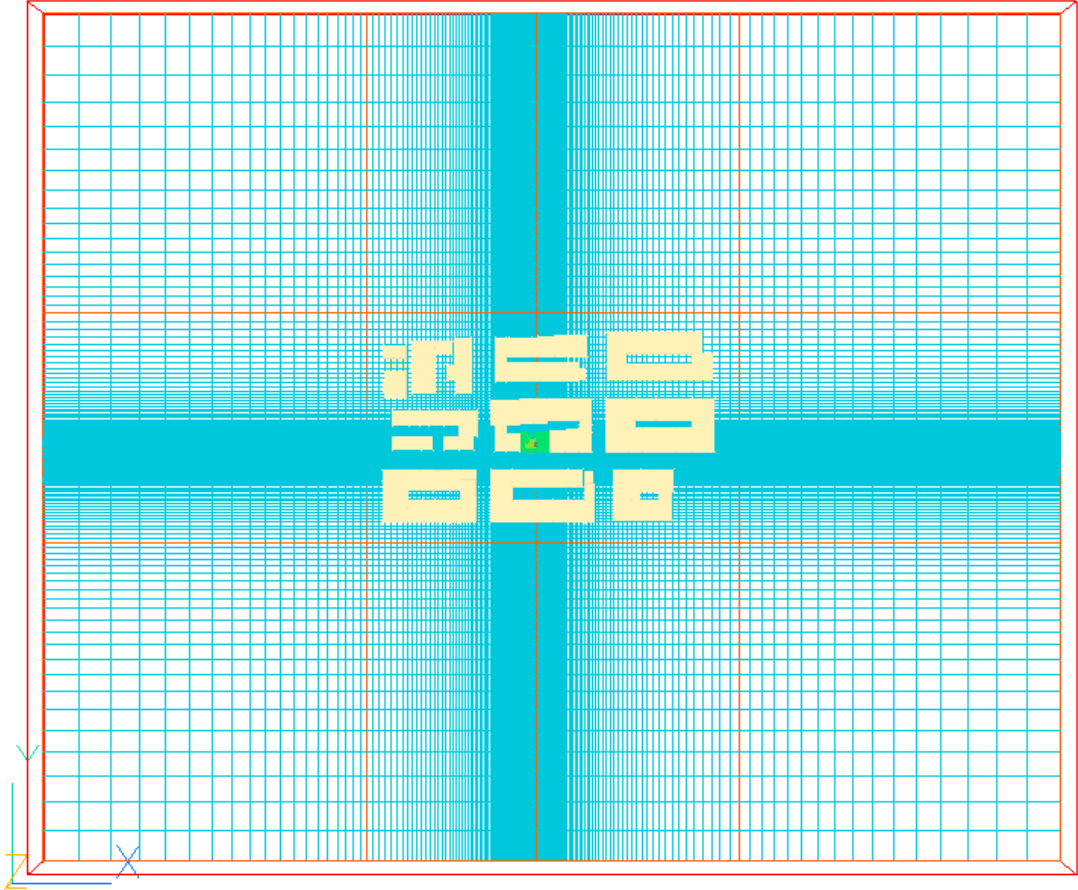


Figure 6.6 Representation of the building studied, surroundings, computational mesh and domain size in plan xy view for the study of the external flow.

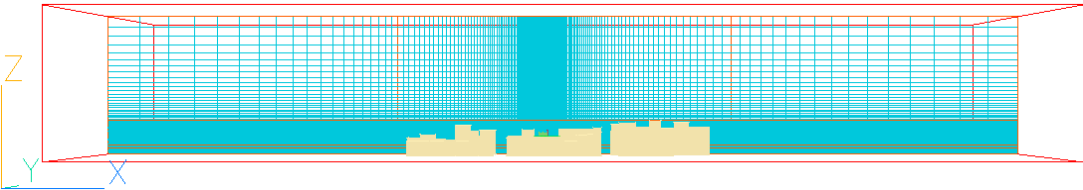


Figure 6.7 Representation of the buildings, computational mesh and domain in x,z view.

6.3.2. Study of the contribution of the surrounding buildings in the modelling process

The significance of simulating the building within its surroundings was recognised early in the modelling process. The existing building was located in a densely urban populated area and the ventilation efficiency would be defined by the neighbouring buildings (Cheung and Liu, 2011). To further justify this, exploratory external flow CFD simulations of the building with and without (i.e. stand-alone) the surrounding buildings were performed. The two cases were modelled having the same domain and boundary condition. The building was simulated with the wind-catcher ventilation strategy. Driving pressures were predicted for the openings of the building and the wind-catcher, with and without the surroundings, for north wind velocity of 7m/s, included in Table 6.3.

The predicted pressure values at the openings of the stand-alone case could potentially generate a driving pressure of up to 60% greater than that of the building with its surroundings, for the environmental properties evaluated. These could result in higher ventilation rates of up to 30% in the occupied spaces, and up to 50% higher average values of velocity through internal doors. The modelling techniques predicted significantly different flow fields around the case study building, as shown in Figure 6.8 and Figure 6.9.

Table 6.3 Average pressure values (Pa) at the openings, and driving pressures for north wind direction of 7m/s, predicted by the external flow simulation of the building under investigation with and without the surrounding buildings

	Building with surroundings	Stand-alone case
Bed 1	-10.884	-22.556
Bed 2	-10.901	-22.851
WC A	-22.765	-78.033
WC B	15.986	20.626
WC C	0.616	2.137
WC D	-25.317	-61.101
<i>Difference</i>	26.870	43.182

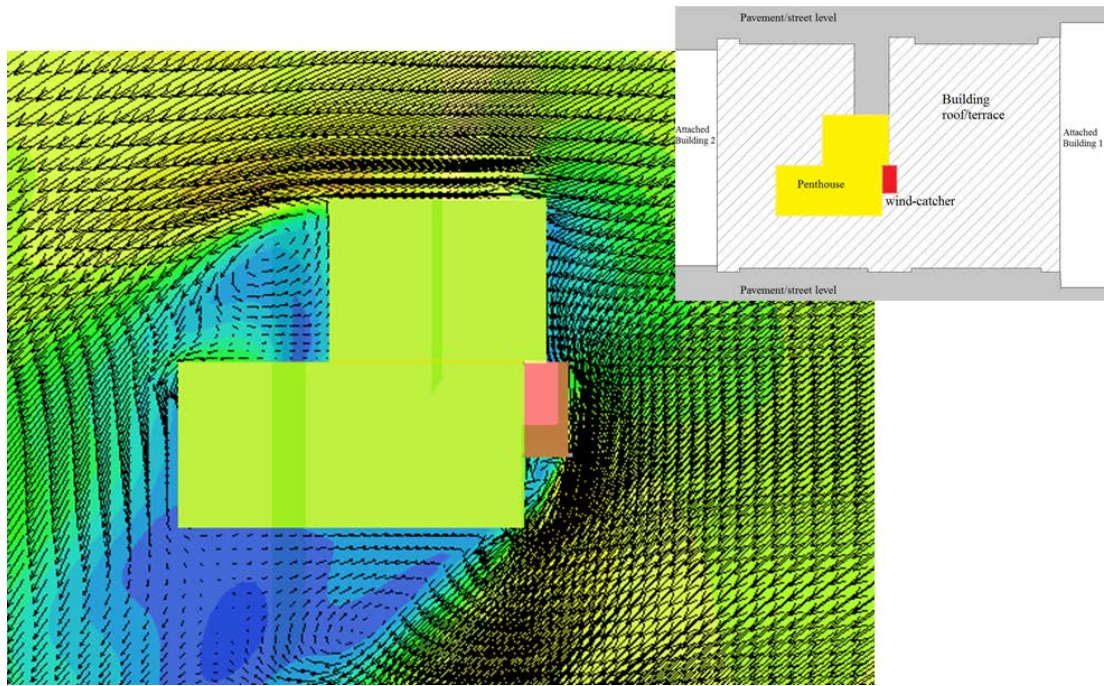


Figure 6.8 Plan view of the flow field around the wind-catcher and the penthouse, showing contour lines of the pressure distribution and vectors of the wind direction at 20m above the ground (north wind of 7m/s) (stand-alone building).

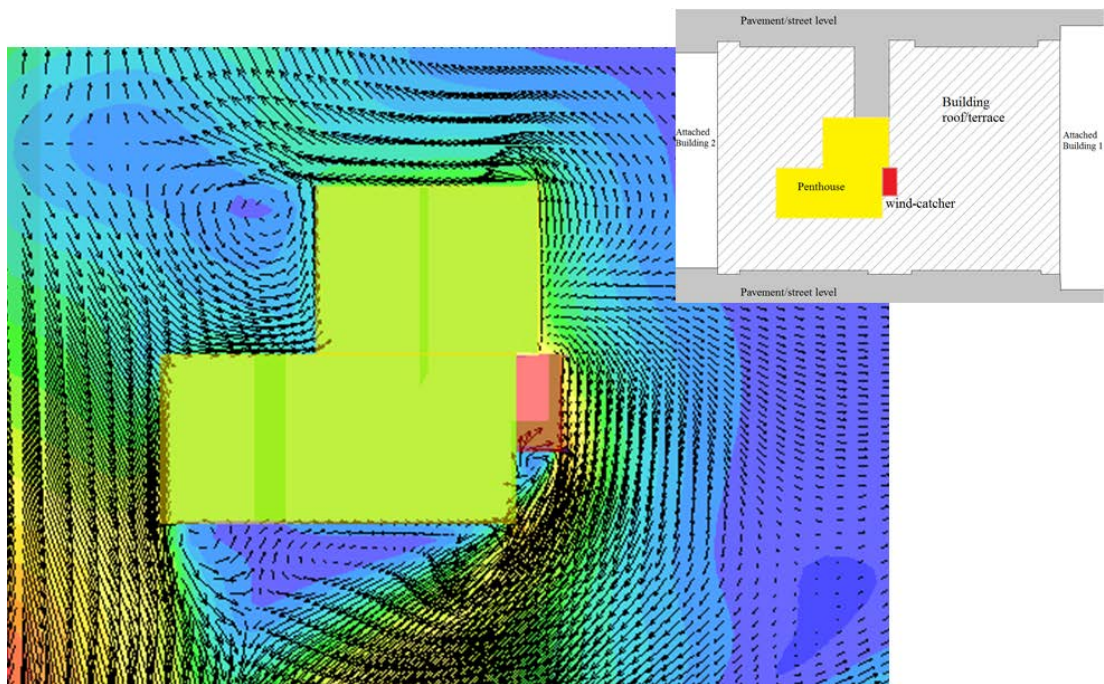


Figure 6.9 Plan view of the flow field, showing contour lines of the pressure distribution and vectors of the wind speed around the wind-catcher and the penthouse at 20m height level above the ground (north wind of 7m/s), study of the building with its' surroundings.

6.3.3. Prediction of pressure values at the building's openings

Primary objective of the external flow simulations was to provide average pressure values at the position of each opening, for each ventilation strategy that would then be used as input for the study of the internal flow. Two-dimensional user-defined objects were created at the size and location of the openings of each strategy. Inform² coding was written to predict the average pressure values over each surface including: the two openings on the main façade; the horizontal opening on the top of the existing light well; the four openings of the wind-catcher; and three openings on the dynamic façade (Figure 6.10).

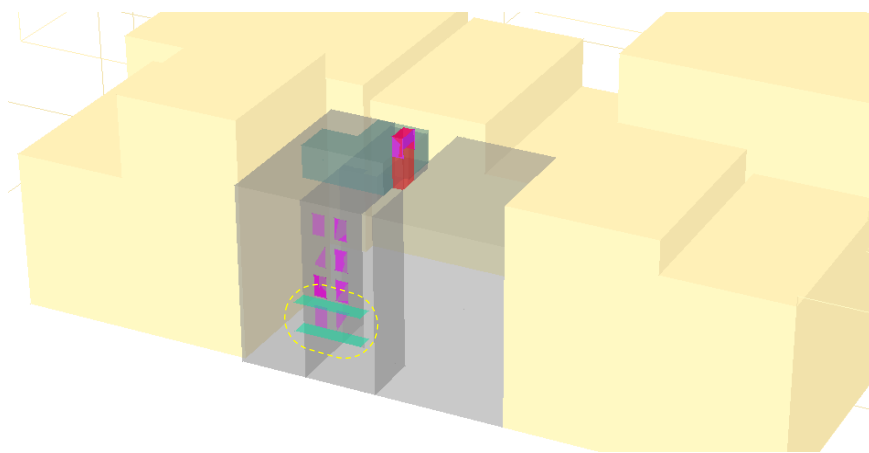


Figure 6.10 View of the three-dimensional model of the building in PHOENICS, the air shaft highlighted in red, the penthouse in blue and the apartment examined with dashed line

For the base-case ventilation strategy (used at the [SS] and [CV] strategies), three values of average pressure were predicted for each orientation (two at the location of the bedroom openings and one at the horizontal top opening of the air shaft). For the wind-catcher case ([WC] and [PDEC-WC]) six values were predicted (two at the location of the bedroom openings and four at the vertical openings of the top part of the wind-catcher), and for the dynamic façade case ([DF & WC] and [PDEC-DF]) seven values (three for the [DF & WC] openings and 4 at the openings of the wind-catcher). For all simulations, the pressure values at the openings of all apartments above the case study apartment were additionally calculated (apartments on the second, third and fourth floors). Further information regarding the additional code is included in Appendix A.1.1, with a detailed table of the predicted pressure values across the apartment openings from all simulations performed.

² The supplement to the PHOENICS Input Language (PIL), facilitating the input of problem-defining data

6.4. Study of the Internal Flow: Model Setup

The case study apartment and proposed strategies were modelled without the attached building apartments in order to reduce computational time and resources. The computational domain boundaries were reduced to the size of the model, i.e. the outline of the indoor spaces and the adjacent air shaft. Detailed modelling methods of the six natural ventilation strategies explored are presented in the following subsections, including: the number of openings, the number of cells and the number of iterations required for convergence. As described in Section 6.2, six natural ventilation strategies were investigated, for these four building design were created (i.e. the water evaporation strategies do not influence the building geometry). The four models are presented in Figure 6.11. Table 6.4 includes the number of computational cells of each strategy.

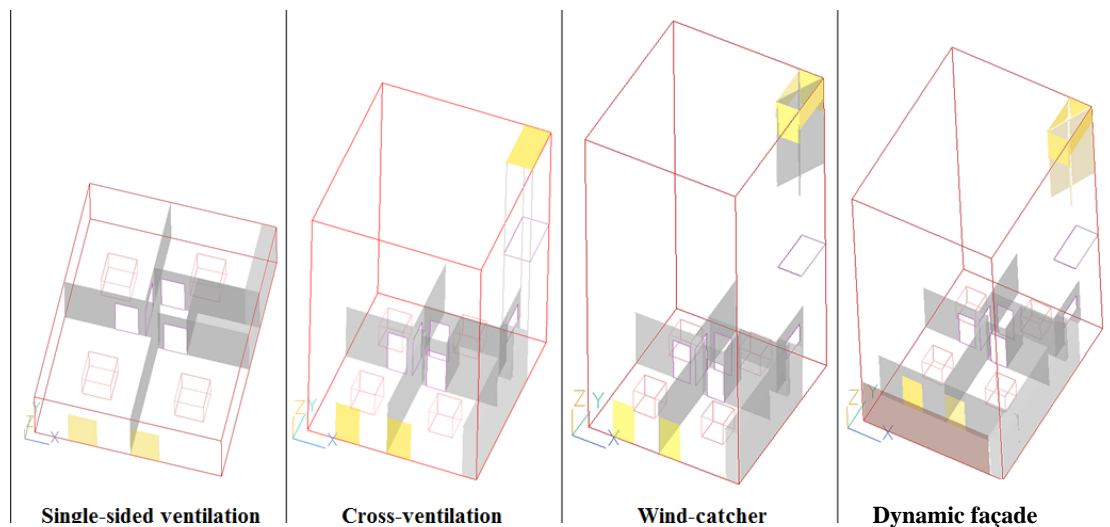


Figure 6.11 Three-dimensional models of the apartment in CFD for the four ventilation strategies, study of the internal flow field

Table 6.4 Computational domains and mesh for the internal flow investigation

Strategy	Domain Size (m)	No. cells on (x,y,z)
Single-Sided Ventilation	$6.45 \times 7.70 \times 3$	61, 69, 20
Cross ventilation	$7.05 \times 7.70 \times 12.80$	61, 69, 38
Wind-Catcher	$7.05 \times 7.70 \times 17$	61, 69, 51
Dynamic façade	$7.05 \times 9.30 \times 17$	61, 83, 51

Heat gains due to occupants, lighting, equipment and solar gains were modelled as a volumetric heat source, centred at each of the four main spaces studied (Table 6.5).

These values were predicted using DTM simulations, presented in Chapter 5, during incidents of average DBT and wind speeds. The values of internal gains remained unchanged for all CFD simulations to provide comparable steady state results of internal air characteristics. All further surfaces have been modelled as impermeable no-slip adiabatic surfaces.

Table 6.5 Heat gains of each of the four occupied building spaces, explained

Space	Area (m ²)	Convective Heat Individual sources	Convective Heat Total of spaces
Bedroom 1	13.70	1 occupant seated (51.1W)	164 Watts
		1 computer (53W)	
		Lighting (4.32W per m ²)	
Bedroom 2	12.13	1 occupant seated (51.1W)	157 Watts
		1 computer (53W)	
		Lighting (4.32W per m ²)	
Kitchen	7.40	1 occupant seated (51.1W)	83.1 Watts
		Lighting (4.32W per m ²)	
Living Room	9.94	1 occupant light work (46.5W)	120.6 Watts
		Equipment (31.2W)	
		Lighting (4.32W per m ²)	
Typical heat gains, values according to Tables 6.3, 6.6, 6.7, 6.8, 6.12 (CIBSE, 2006)			

The energy equation was solved for temperature. Buoyancy was modelled using the Boussinesq approximation expressing that the variations of density in the inertia terms of the governing equations are retained during buoyancy (Cook, 1998). Turbulence was modelled using the k-epsilon model of Launder-Spalding (1974). At each opening, the following condition was imposed on pressure:

$$\Delta p_{loss} = -\frac{1}{2} f \rho U_n^2 \quad (6-1)$$

where, f is the loss coefficient, ρ is the air density (kg/m³) and U_n is the velocity component normal to the opening boundary (m/s).

Accordingly, for the study of the buoyancy-driven flow the velocity components normal to each external opening were 'deduced' at run-time from the mass flow rate divided by the in-cell density and the cell area (Ludwig and Mortimore, 2011) with air pressure at the opening equal to the ambient ($p=0$) and loss coefficient equal to 2.69 (Cook et al., 2011). For the study of the wind-driven flow the velocity

components normal to each opening were also ‘deduced’ at openings serving as inlets based on their pressure values (the highest pressure value) and IN-CELL³ at openings serving as outlets (lower pressure values).

The flow rate through internal openings such as doors was calculated with additional inform coding added in the existing CFD code. Details of the additional CFD code created for the purpose of this research work, as well as the predicted values at each internal opening are included in Appendix A.2.1. For all different strategies, calculations were also made at set points, one at each of the five spaces examined, predicting air temperatures, velocities and humidity levels (Figure 6.12).

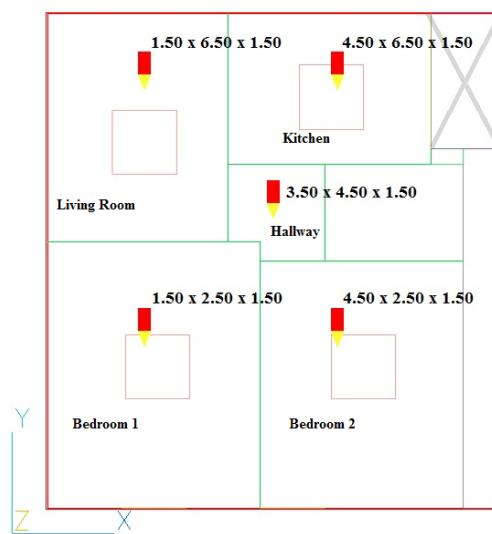


Figure 6.12 Plan view of the apartment's layout, the five measuring points (red arrow) and their coordinates from x,y,z zero point

The solution was considered converged when the spot values (of pressure, temperature and three components of velocity) at a defined monitoring point in the domain remained unchanged and when the logarithms of the sums of the absolute residual of each variable (errors) in the finite-volume equation were reduced to an acceptable magnitude. Also, when good source balance of less than 1% for each heat source or sink was accomplished of the heat input (when the enthalpy residual fell to a value below 1% (Cook et al., 2003)). All simulations converged after 4,000 to 10,000 iterations within three to nine hours. Up to 22 hours were required for the study of water evaporation and higher numbers of iterations were required for the buoyancy-driven flows.

³ In-Cell expresses the continuous update of the inflow values during the simulation, to match the currently predicted value of each cell

6.4.1. Single-Sided natural ventilation

For the buoyancy and wind-driven single-sided ventilation performance of the apartment under investigation, the apartment was modelled in PHOENICS without the attached light well and its additional height, in order to reduce the computational time (the connecting opening would remain closed), see Figure 6.11. The domain size was $6.45 \times 7.70 \times 3\text{m}$, the Cartesian computational mesh comprised of 84,180 cells and the orifice equation (Equation 6-1) was used. Average values of airflow through internal openings were calculated at four internal doors (Door1-4 shown in Figure 6.13). For the study of the wind-driven ventilation, pressure values were included at the properties of the two bedroom openings. The solution was considered converged after approximately 6,000 iterations and about two hours at a serial run. For the study of the buoyancy-driven flow, the two façade openings of the bedrooms operated as both inlets and outlets. The solution was considered converged after approximately 10,000 iteration and about three hours on a serial run.

6.4.2. Cross ventilation

For cross ventilation [CV] performance of the apartment under investigation, the apartment was modelled in PHOENICS with the attached light well (the internal opening was open), see Figure 6.13. The computational domain of the cross ventilation strategy was increased in height, relative to the study of the single-sided ventilation, to incorporate the total height of the light well ($7.05 \times 7.7 \times 12.8\text{m}$), and was divided into 159,942 computational cells. Airflow and mass flow rates through internal openings were predicted at six internal doors (door and door 1- 5).

For the study of the wind-driven [CV] strategy, of pressure values were included in the two bedroom openings and the horizontal opening at the top of the light well. The solution was considered converged after 3,000 to 5,000 iteration and about three hours at a serial run, with regard to the driving pressures. For the study of the buoyancy-driven flow, the solution was considered converged after approximately 8,000 iteration and about six hours on a serial run.

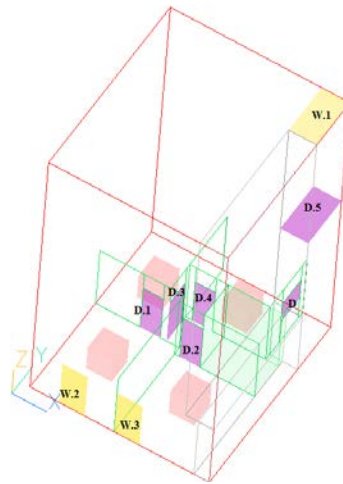


Figure 6.13 Three-dimensional building model of the ‘cross ventilation’ strategy, showing the areas of flow calculations (internal openings ‘D’) and the external openings (‘W’)

6.4.3. Natural ventilation with a wind-catcher

For the ventilation performance evaluation of the building with the inclusion of the wind-catcher [WC], the domain size on the z-axis was increased by 4.20m height ($7.05 \times 7.7 \times 17\text{m}$) relative to the [CV] strategy. The four openings on the top of the wind-catcher have an area of 2.2m^2 on both the long and short sides. The internal partitions were designed on ‘X’ arrangement of five metre length (described in Chapter 4); there were not any partitions inside the existing light well. Due to the fine elements of the wind-catcher (thin internal partitions and narrow openings), the Cartesian mesh was refined at the wind-catcher zone relative to the [CV] strategy, creating finer properties to avoid double-cutting of cells⁴, see Figure 6.14 and Figure 6.15. The total number of cells for the [WC] was 294,372; the wind-catcher had the highest number of cells at xy-axis (825 out of 5772) as shown in Figure 6.16.

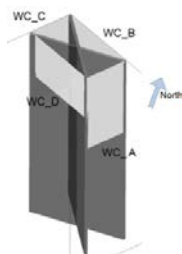


Figure 6.14 Proposed design of the four-directional wind-catcher in PHOENICS

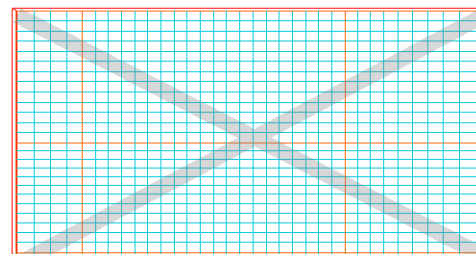


Figure 6.15 Detailed plan view of the final partitions arrangement and mesh properties.

⁴ Double cutting occurs when the bounding surface of an object cuts a cell more than once. In such cases the solver does not recognise the object, replacing it by the domain material (air).

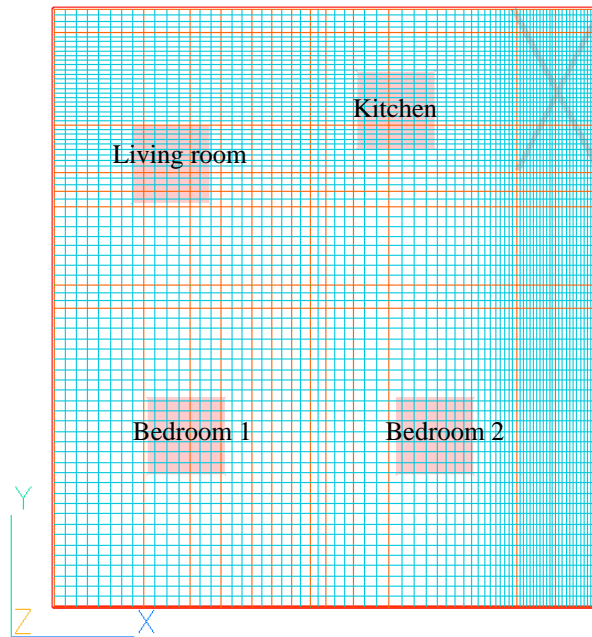


Figure 6.16 Plan view of the apartment studied and [WC] ventilation strategy, showing the computational mesh (coarse and fine zones) for the evaluation of buoyancy-driven flow

During exploratory simulations of wind-driven flows, it was noticed that due to all four openings of the wind-catcher being continuously open, the fresh air recirculated within the wind-catcher shaft and escaped from the top leeward openings. Only a small percentage of the fresh air continued downwards the shaft and towards the occupied zones. It was thus decided when evaluating wind driven flows to maintain only one of the four wind-catcher openings open, the one that could create the highest driving pressure with respect to the pressure values at the two bedroom openings. However, for the study of the buoyancy-driven flow all four openings were simultaneously open.

For the evaluation of the wind-driven simulations, the mesh was refined again around the wind-catcher to reduce computational time. The cross partitions were redesigned as solid wedges (see Figure 6.17), allowing one channel out of the four to be open during each simulation according to the predominant wind direction. This was a modelling simplification of the automatic dumpers described in Chapter 4.5.1.

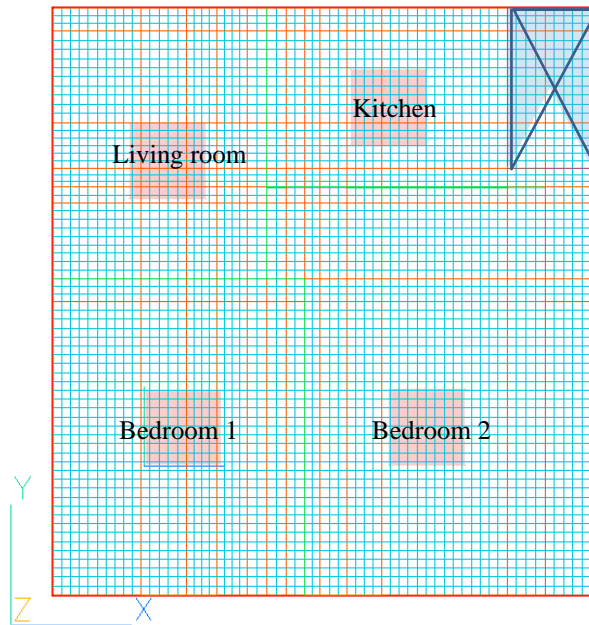


Figure 6.17 Plan view of the apartment studied and [WC] ventilation strategy, showing the computational mesh (coarse and fine zones) for the evaluation of wind-driven flow.

In order to be certain that the solution was independent of the mesh resolution, seven different meshes were investigated as shown in Table 6.6 for the wind induced ventilation of the wind-catcher strategy, with a 15% increase in cells from the previous mesh size in each direction, being evenly distributed on the 'x' and 'y' axis. All seven meshes converged to an acceptable level and provided comparable results, although convergence was more difficult to achieve for mesh 6 and mesh 7. Mesh 2 was chosen because it provided the most appropriate convergence, with regard the residual error reduction within the least computational time, as shown in Figure 6.18.

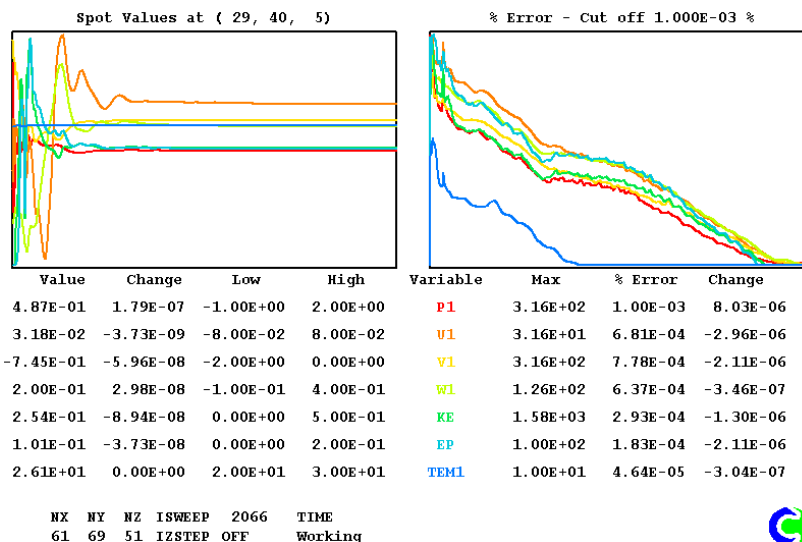


Figure 6.18 Convergence monitoring plot showing the residual for each solved variable and the variable values at a user-specified monitor location in the grid ([WC], north wind, Mesh 2)

Table 6.6 Computational meshes and their properties, for the study of the internal flow of the [WC] ventilation strategy and the evaluation of wind-driven flow

Type	Domain (x,y,z)	Number of cells
Mesh 1	52×59×43	131,924
Mesh 2	61×69×51	214,659
Mesh 3	70×79×59	282,030
Mesh 4	79×90×66	469,260
Mesh 5	88×100×74	651,200
Mesh 6	98×110×82	883,960
Mesh 7	107×121×89	1,152,283

Comparable indoor air temperatures at horizontal plane at all spaces were predicted for all seven meshes investigated, with variations below 0.05°C (Figure 6.19). Figure 6.20 presents calculated indoor air velocities at regular positions across a defined measuring line (1.5m height above the apartment floor level) and through three spaces. The predicted values vary considerably with the increase in distance from the façade (up to 0.4°C difference).

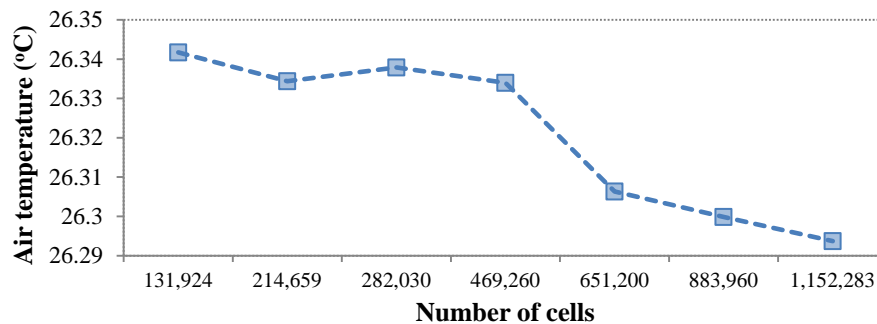


Figure 6.19 Indoor air temperatures at horizontal plane across all spaces (1.5m above the apartment floor) and number of cells for the study of the [WC] ventilation strategy

For both wind and buoyancy-driven strategies, the air and mass flow rates through internal openings were calculated at six internal doors (Figure 6.13). The solution was considered converged after 4,000 to 10,000 iterations, completed within four to nine hours on a serial run. For the study of the buoyancy-driven flow, the solution was considered converged after approximately 10,000 iterations on serial run (around nine hours).

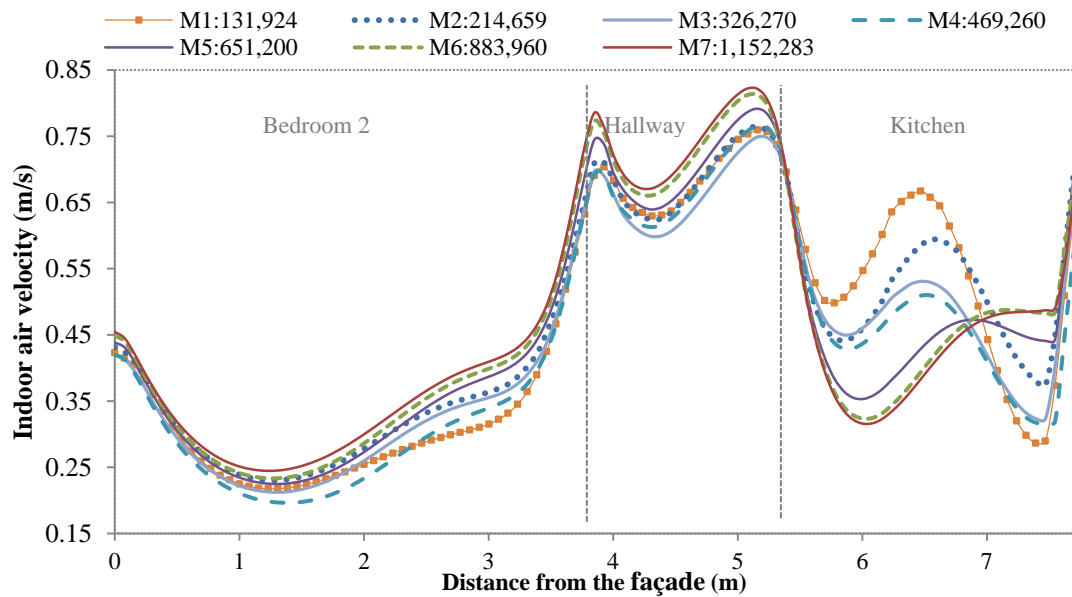


Figure 6.20 Predicted indoor air velocities (m/s) at 100 points along a line (from (3.65, 0, 1.5) to (3.65, 9.3, 1.5)) for 7 different computational meshes

6.4.4. Dynamic louvered façade

The second lightweight façade [DF & WC] was modelled in CFD as a second layer of openings fully open, representing the external horizontal shading devices located at the edge of the apartment’s balcony. The boundary conditions were redefined to include three continuous, vertically arranged rows of openings. The domain was increased on ‘y’ axis to the previous strategies (7.05×9.30×17m). The three rows of openings have 6.35m length and heights of: 0.8m (DF1); 1.40m (DF2); and 0.80m (DF3) respectively. Figure 6.21 shows the position of the internal and external openings of the [DF & WC] model and the areas of flow predictions.

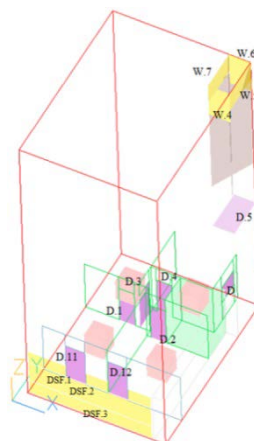


Figure 6.21 Three-dimensional building model of the [DF & WC] strategy, showing the areas of flow predictions (internal openings ‘D’), the DF openings and external openings (D11-12)

Table 6.7 Computational meshes and their properties, for the internal flow investigation of the [DF & WC] ventilation strategy, for the evaluation of wind-driven flow.

Type	Domain (x,y,z)	Total No. cells
Mesh 1	36×50×36	64,800
Mesh 2	44×60×43	113,520
Mesh 3	52×71×46	169,832
Mesh 4	61×83×51	258,213
Mesh 5	60×82×59	290,280

Exploratory simulations were performed using the computational mesh used for the [WC] strategy, however convergence was difficult to achieve. An additional mesh independency study was performed for the [DF & WC] strategy. Five different meshes were assessed as shown in Table 6.7. All meshes converged to an acceptable level and provided comparable results, as shown in the convergence plots of Figure 6.22 for north wind direction and Mesh 4. Mesh 1 required less computational time relative to Mesh 5. Mesh 4 was selected for the evaluation of the dynamic façade strategy. However, convergence was difficult to achieve for a number of individual models with Mesh 4, as shown in Figure 6.23 for northwest wind speed (Mesh 4). Mesh 2 was used at these specific models (around 1/3 of the simulations).

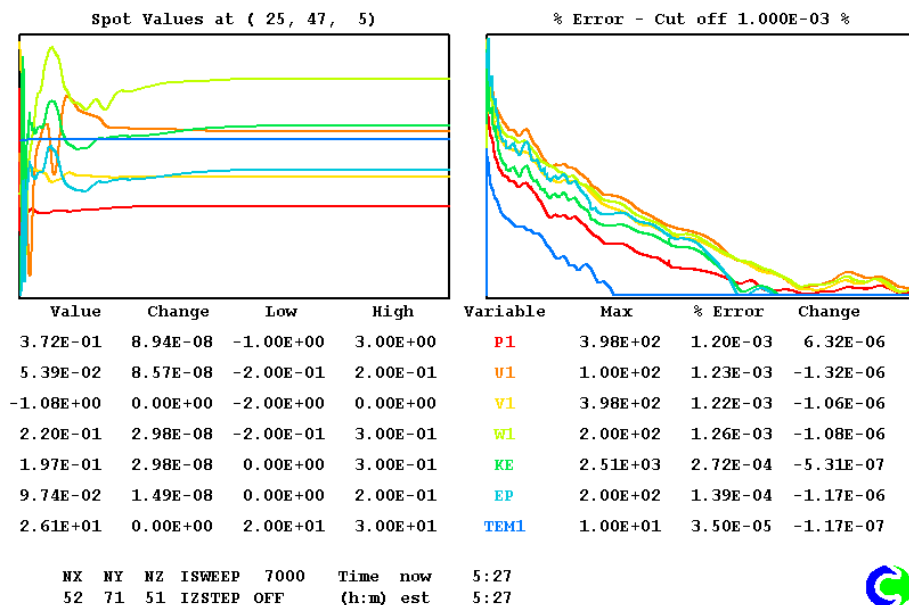


Figure 6.22 Convergence monitoring plot showing the residual for each solved variable and the variable values at a user-specified monitor location in the grid ([DF&WC], north, Mesh 4)

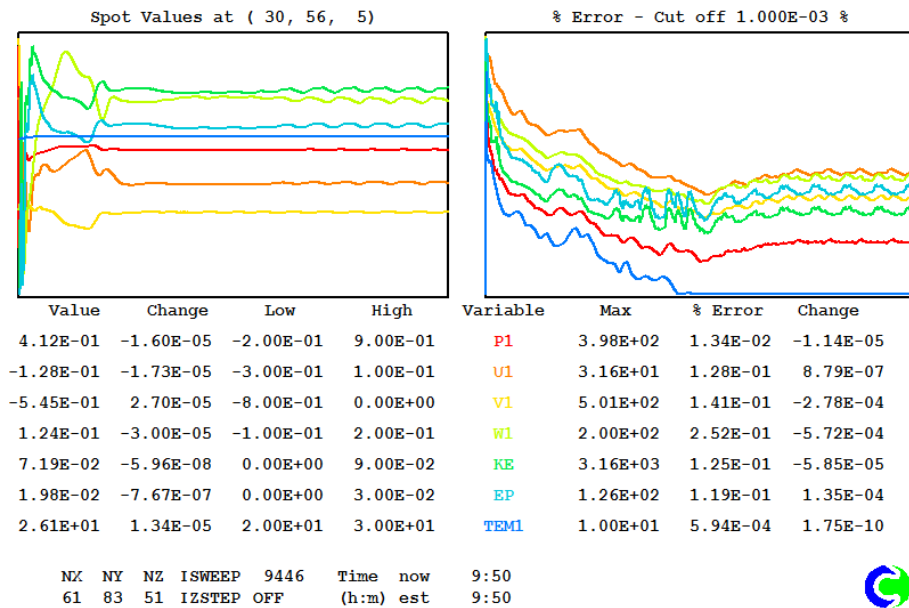


Figure 6.23 Convergence monitoring plot showing the residual for each solved variable and the variable values at a monitor location in the grid ([DF&WC], northwest, Mesh 4)

Predicted average indoor air temperatures, measured at a horizontal plane across all spaces show comparable results between the five meshes, with variations predicted to be lower than 0.06°C (Figure 6.24). Further, Figure 6.25 presents calculated indoor air velocities along a defined measuring line (1.5m height above the floor level) through the balcony, internal doors and the indoor spaces, predicted in close agreement.

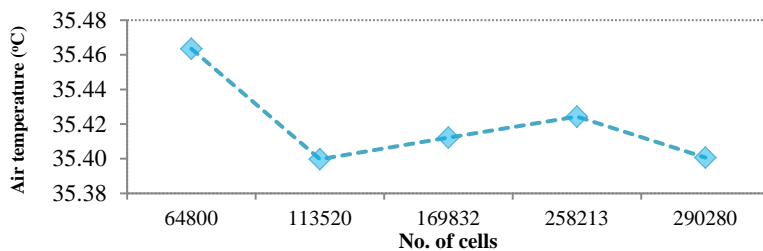


Figure 6.24 Indoor air temperatures (°C) at horizontal plane across all spaces (1.5m above the apartment floor) and number of cells, for the study of the [DF & WC] strategy

For the wind-induced ventilation, the solution was considered converged within 6,000 to 8,000 iterations (about 5 to 10 hours) at a serial run, with regard to the climate scenario. Exploratory simulations predicted higher ventilation rates when the dynamic façade was modelled with the top opening open and the other two closed at all times. For the buoyancy-driven flow investigation, the solution was considered converged after about 10,000 iterations after nine hours at a serial run.

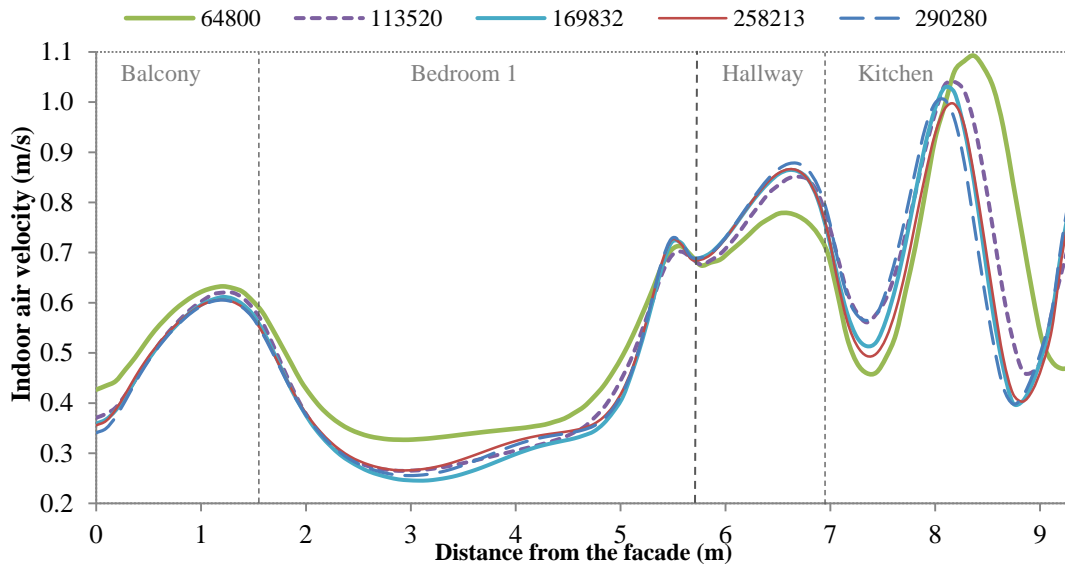


Figure 6.25 Predicted air velocities (m/s) at 100 points along a line at 1.5m height (from (3.65, 0, 1.5) to (3.65, 9.3, 1.5)) for 5 different meshes of the [DF & WC]

6.4.5. Passive draught evaporative cooling (PDEC)

The passive draught evaporative cooling tower (PDEC) consists of an arrangement of micronisers, spraying mist water in the air passing through the wind-catchers tower. The PDEC was modelled as a negative heat source with moisture content, a ‘box’ of air in the domain (1.1×2.1×9m and at 3m height above the ground level) positioned in the air shaft, which represent the mist of water sprayed and uniformly evaporated. As air enters from the top of the wind catcher openings, it moves downwards and before entering the occupied spaces, passes through the negative heat source that reduces its temperature and increases its moisture content to a degree with respect to the predefined volume of water sprayed.

Table 6.8 Average temperatures (°C) of the water supply network in Athens, Argiriou et al.(2010)

Jan	Feb	March	Apr	May	Jun	Jul	Aug	Sep	Oct	Nov	Dec
11.3	10.9	11.8	14.3	17.7	21.6	24.7	25.7	24.2	21.1	16.9	13.5

The cooling rate due to water evaporation (the negative heat source in Watts) was calculated by multiplying the equivalent of the water mass flow rate (kg/s) to the water latent heat of vaporisation (J/kg). As the temperature of the water modifies the water density, it was important to consider the seasonal water temperature fluctuations. The selected water temperature was 22.78°C, as the average water

temperature of the cooling season (May-September) of the water supply network in Athens (Argiriou et al., 2010), see Table 6.8. The system was evaluated for water consumption between 6 and 14 litres per hour (l/h). As reported by Ford et al (2012), 8l/h was the predicted peak consumption in relevant studies. Table 6.9 illustrates the process and values required for the prediction of the cooling rate due to evaporation, used as negative heat sources.

In addition, the negative heat flux of uniform water evaporation incorporated a source of water vapour in order to model the evaporation effect on the moisture content of the indoor air. The models presumed that the droplets entering the air in the spaces were in the form of saturated liquid. The influence of the evaporated water overall to continuity and mean density were considered insignificant under the current conditions and thus ignored. It was decided to disregard the enthalpy of the evaporating water to avoid complication of the process and potential miscalculation of the cooling, as it was recommended by the software developers. The strategy of cooling by water evaporation was implemented in both cases of the wind-catcher [PDEC-WC] and the wind-catcher and the double skin façade [PDEC-DF]. The cooling efficiency of the water evaporation system was evaluated only during wind incidents. The number of iterations within the solver was increased for the water variable from the default 30, to 50, and the model solving the relative humidity of the air was also activated. For the [PDEC-WC] the solution was considered converged after a number of 5,000 to 10,000 iterations achieved in 7 to 22 hours at a serial run, depending on the strategy. For the [PDEC-DF] strategy the solution was considered converged in about 6,000-10,000 iterations (5 to 17 hours in a serial run).

Table 6.9 Heat reduction of incoming air due to water evaporation for water at 22.78°C

Sprayed Water	Volume of Water		Density at 23°C	Mass	Latent heat of vaporisation	Cooling rate due to water evaporation	
	Litres/h	Litres/s	m ³ /s	kg/m ³	kg/s	J/kg	J/s = Watts
4	0.001111	1.11E-06		997.5	0.001108	2,260,000	2504.833
6	0.001667	1.67E-06		997.5	0.001663	2,260,000	3757.25
8	0.002222	2.22E-06		997.5	0.002217	2,260,000	5009.667
10	0.002778	2.78E-06		997.5	0.002771	2,260,000	6262.083
12	0.003333	3.33E-06		997.5	0.003325	2,260,000	7514.5
14	0.003889	3.89E-06		997.5	0.003879	2,260,000	8766.917

6.5. Ventilation Performance Simulation Results: External Flow

This section presents simulation results of the decoupled external flow field simulations on a neighbourhood scale and the pressure distribution at the openings of the building under investigation, for different climate scenarios and ventilation strategies. The predicted values of average pressures at the location of each opening of the three building models (described in 6.3) are included in Appendix A.1.1.

Extremal flow CFD simulations were performed for the five most frequent wind directions of the site (i.e. north, northeast, east, southwest, and northwest) as defined by climate analysis presented in Chapter 4.4. This was required in order to predict the most favourable wind direction for the natural ventilation of the specific building, site and strategies investigated. Driving pressures at the openings (inlet-outlet) evaluated for two wind speeds are presented in Figure 6.26 and Figure 6.27. Absolute values are used for simplification and for an indication of the expected ventilation rates. North and east wind directions are the most favourable for wind-driven natural ventilation. Due to the building design and height of the wind-catcher, the driving pressures of the [WC] and [DF & WC] show small variations. With regard to the ventilation strategy, the driving pressures at all wind directions were predicted having up to 3:1 ratio for wind speed of 3.6m/s, and more than 5:1 for wind speed of 7m/s, with values varying between zero and 30.1Pa.

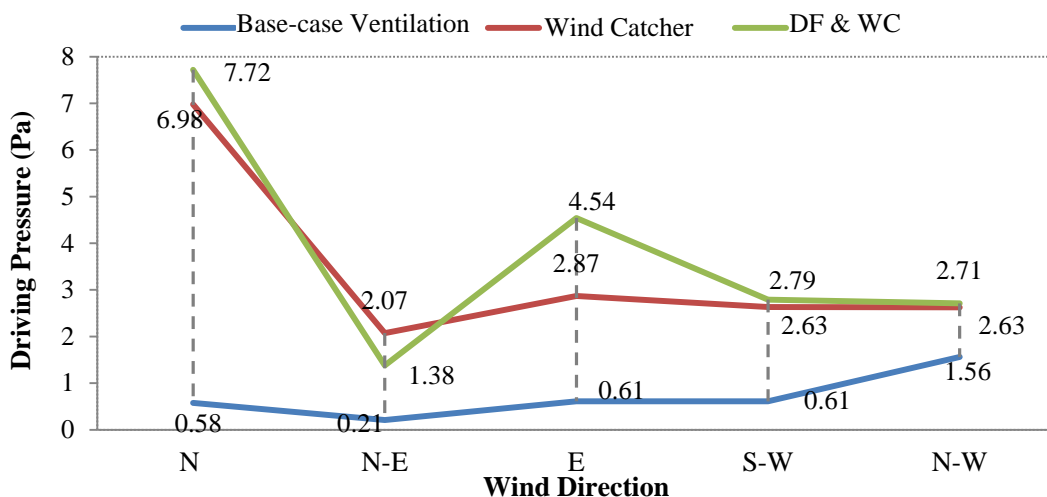


Figure 6.26 Driving pressures for 3.6m/s wind speed, 5 wind directions and 3 models

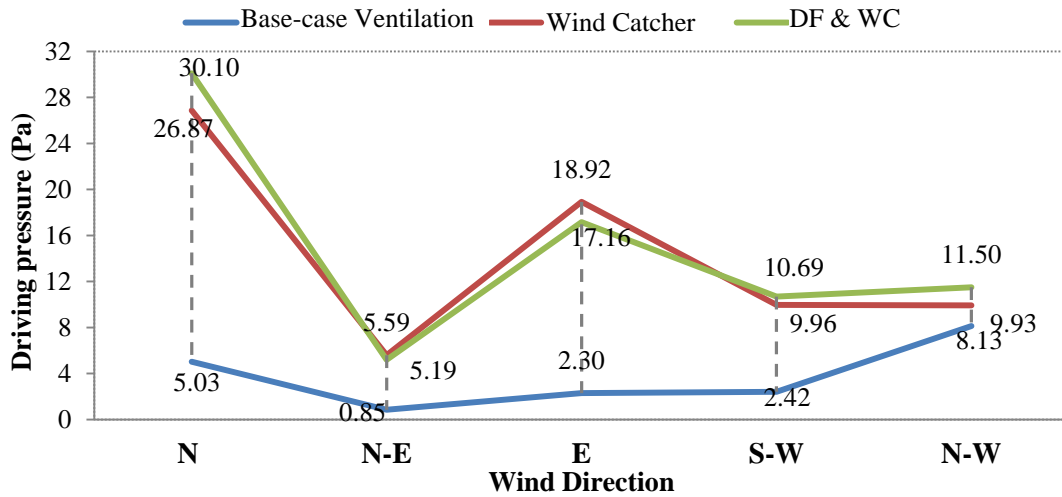


Figure 6.27 Driving pressure for 7m/s wind speed, 5 wind directions and 3 models

The inclusion of the wind-catcher to the previous existing building design (base-case strategy) contributed to a significant increase in driving pressures, although with respect to the individual wind directions and wind speeds evaluated. The introduction of the wind-catcher could deliver up to 10 times higher ventilation rates relative to the base-case ventilation strategy, as shown in Figure 6.28. The inclusion of a wind-catcher is expected to provide significant increase in ventilation rates.

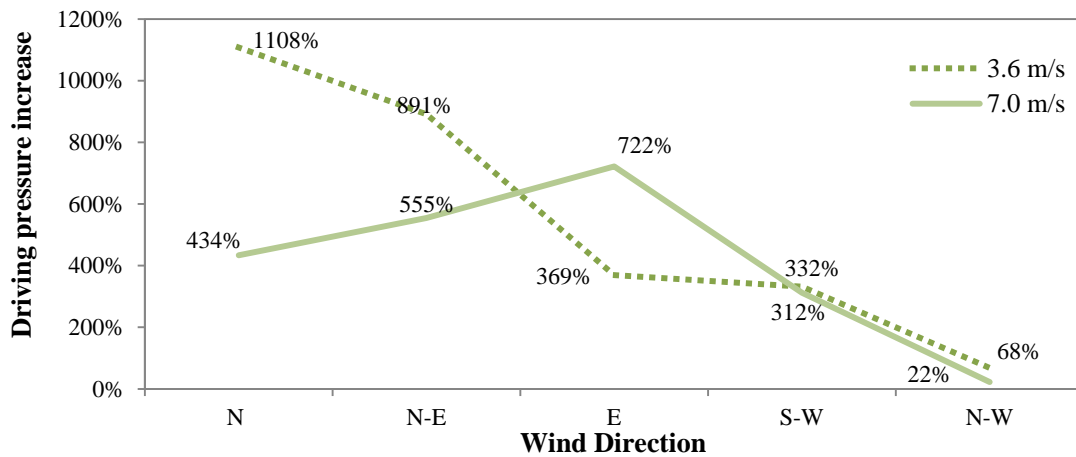


Figure 6.28 Driving pressure increase (%) with regard to the addition of the wind-catcher [WC] to the base-case strategy (existing building design)

Three wind directions (north, east, northwest) were selected to be evaluated with regard to: the driving pressures of each wind direction (Figure 6.26 and Figure 6.27); the percentage of driving pressure increase with the inclusion of the wind-catcher (Figure 6.28); and the number of incidents of each wind direction (Chapter 4.4).

The inclusion of the wind-catcher would be mostly favoured for north wind direction followed by northeast, east, southwest and northwest. However, for northeast wind directions the predicted driving pressures are the lowest of all strategies (see Figure 6.26 and Figure 6.27). In addition, the wind direction incidents of the site (Chapter 4.4) were predicted higher for north wind speeds (around 33%), followed by the northeast (29%), northwest (12%), and southeast and then east (both 7%). Despite the high frequency of northeast winds, they were not evaluated because they delivered the lower driving pressures.

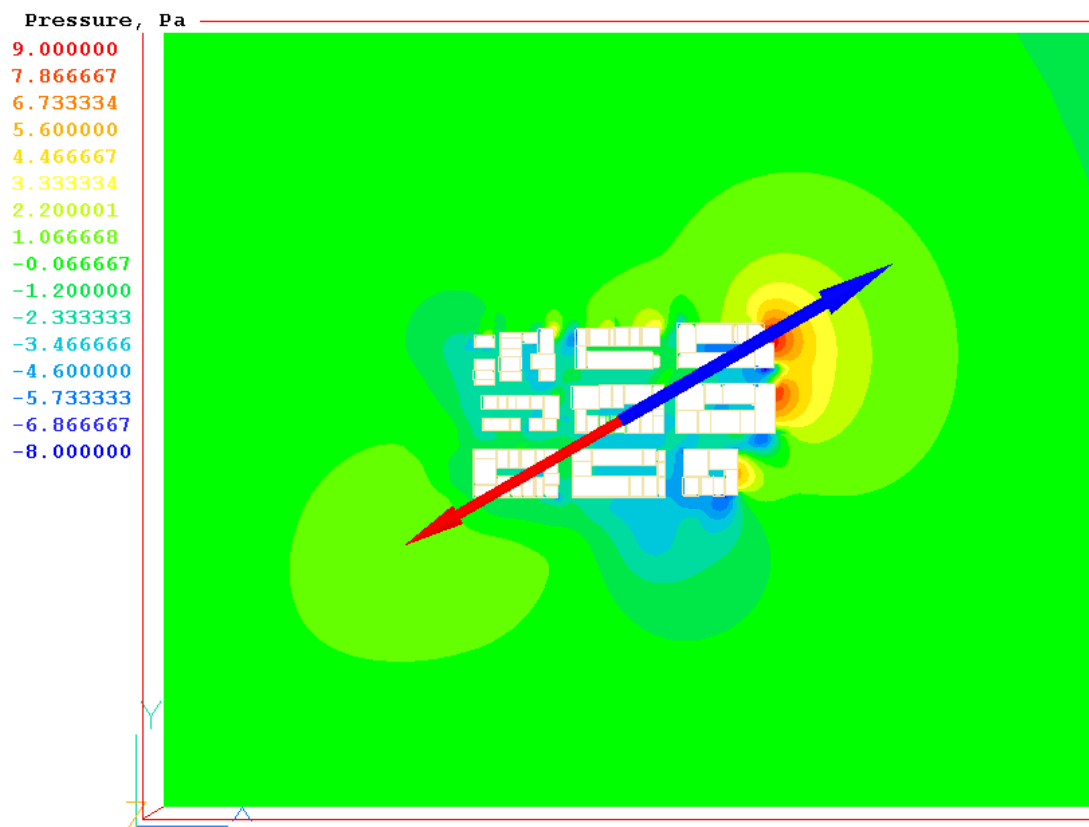


Figure 6.29 Pressure contours on xy plane at 7.50m height above the ground, showing the 9 urban blocks, areas of low (leeward buildings) and high pressure (windward buildings). The blue arrow points at north and the red indicates the wind direction for 3.6m/s wind speed.

The predominant wind direction of the site was north, with the highest number of incidents during the cooling season (as described in Chapter 4.4). Results from simulations during north wind direction were presented in this section. Pressure contours on horizontal plane for 3.6m/s north wind are presented in Figure 6.29. Areas of low pressure were identified at the leeward faces and between the urban building blocks, while high values of pressure were predicted at the windward faces of the first row of buildings at north.

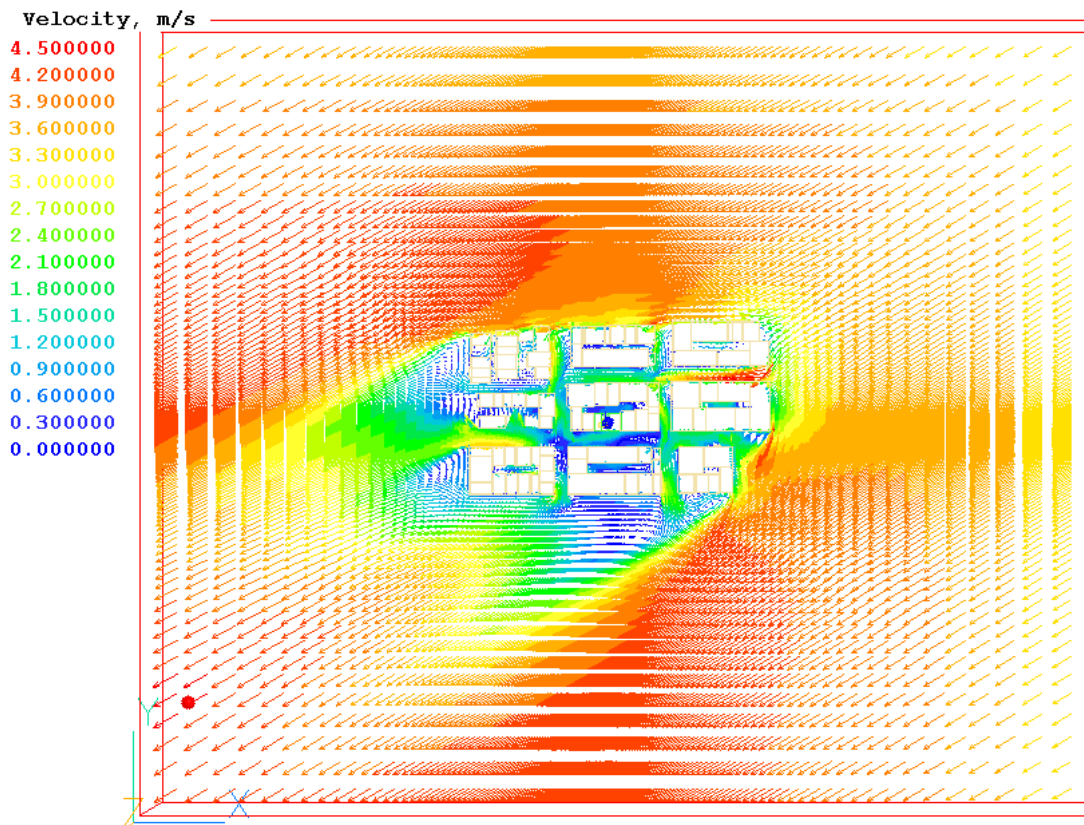


Figure 6.30 Velocity vectors (*xy* plane) at the neighbourhood scale. The blue dot at the centre of the buildings arrangement shows the location of the lowest wind speed value, and the red, the maximum of the domain, at 7.5m height above the ground level

The laminar airflow produces accelerated flow near the boundaries of the first building blocks, resulting in complex flow patterns of high and low airflow speeds at the street-level (urban canyons). Accelerated airflow above the highest rooftops was noticed, creating eddies on the top of the lower rooftops, a phenomenon clearly observed at the case study building’s rooftop (Figure 6.32). The lowest wind speeds were predicted at the central open space of each urban block, and the higher at the downstream and close to the domain boundaries. Very low wind speeds were observed around the central urban block and the case study building (between zero and 1.5m/s), as expected in densely populated urban environments (Niachou et al., 2008). The flow distribution along urban passages was investigated for the three dominant wind directions and one wind speed (3.6m/s), presented in Appendix A.1.2. All these express the significance of evaluating the case study building with the surroundings.

Additionally, the wind-flow distribution at three horizontal sections along the building height was observed for a single strategy (Figure 6.31 below the level of the

top floor, Figure 6.32 above the top floor, and Figure 6.33 above the penthouse roof). The pressure distribution along the height of the wind-catcher predicted to be up to three times higher at the top parts of the wind-catcher to the lower.

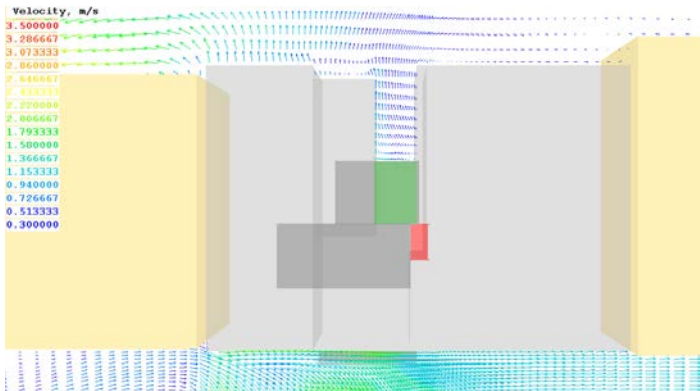


Figure 6.31 Velocity vectors on xy plane at 18m height (North wind direction and 3.6m/s wind speed) predicting wind speeds of up to 2m/s in the apartments' façade windows

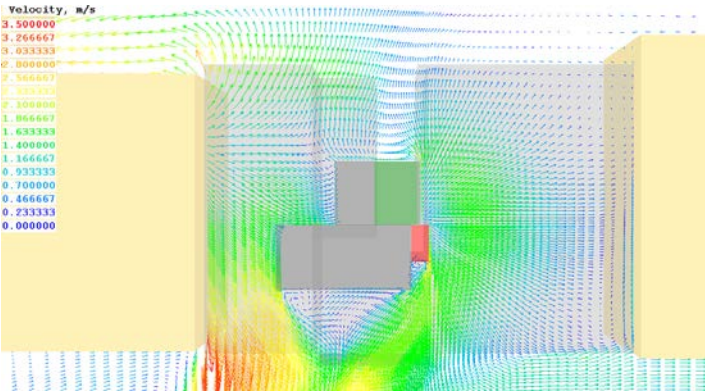


Figure 6.32 As previous at 19m height, showing wind distribution around the wind-catchers shaft and the attached penthouse, as well as recirculation areas at the leeward sides

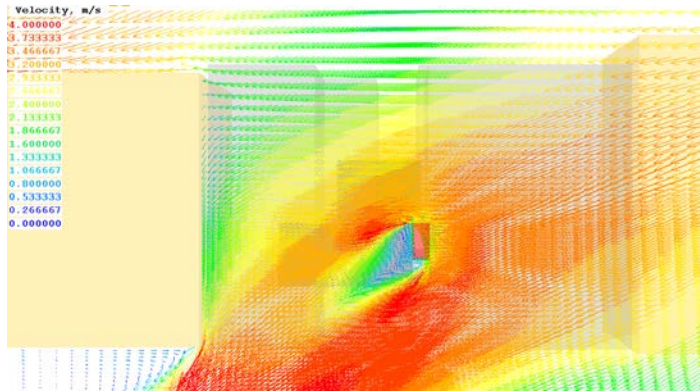


Figure 6.33 As previous, at 23m height showing wind speeds of up to 4m/s at the wind-catchers windward surfaces

The pressure distribution along the height of the main building façade was explored. Average values of wind pressure were predicted at the openings of three apartments located above the apartment under investigation. Figure 6.34 and Figure 6.35 present the average pressure values: of the façade openings at all four floors (levels 1, 2, 3 and 4); of the wind-catcher top openings (level 5) (wind-catcher model); and respectively of the horizontal opening of the air shaft (base-case ventilation). The pressure difference across the façade openings and the wind-catcher openings indicate the driving pressure for each floor. The non-linear increase of pressure values from level 1 to level 4 indicates flow eddies created because of the horizontal obstacles (balconies) and the surrounding structures. At level 5 (the top of the wind-catcher), positive pressure values were predicted demonstrating inflow at the top. Up to 1Pa difference was predicted between the upper and lower apartments' driving pressures.

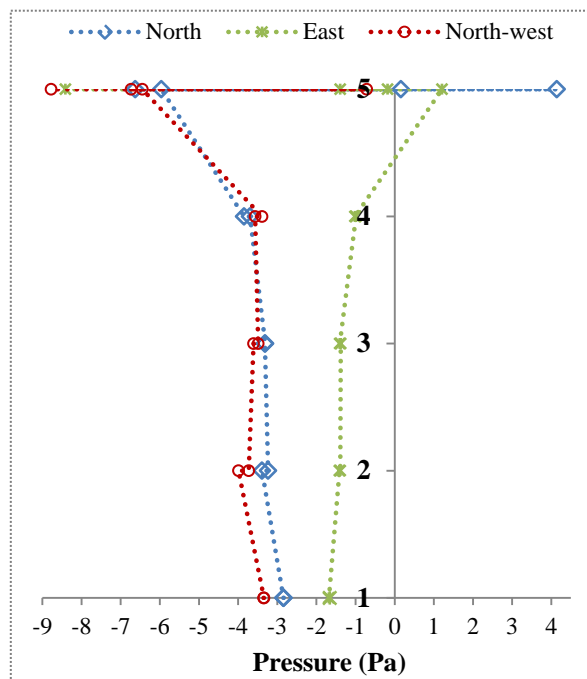


Figure 6.34 Pressure distribution across all openings (low to high) for 3.6m/s north wind direction, at the wind-catcher model

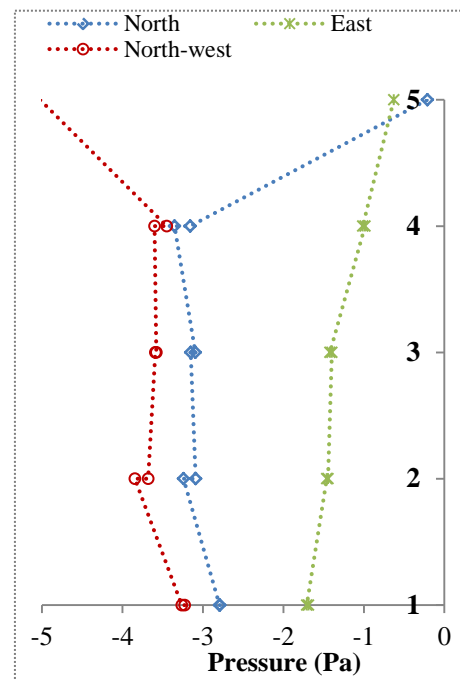


Figure 6.35 Pressure distribution at the building openings (low to high) for 3.6m/s north wind direction, base-case ventilation

The pressure values predicted in the building openings, during the climate scenarios used for the evaluation of the internal flow field included in the following section, are presented in Table 6.10.

Table 6.10 Predicted average pressure values at the openings of each natural ventilation strategy and CFD model (for WC openings see Figure 6.14)

Wind Speed	3.60 m/s			7.00 m/s		
Wind Direction	North	East	NW	North	East	NW
Strategy	Base-case ventilation					
Bed 1	-2.83	-1.67	-3.16	-10.59	-6.30	-11.89
Bed 2	-2.82	-1.71	-3.18	-10.68	-6.42	-11.88
Shaft top	-2.25	-1.10	-4.72	-5.64	-4.12	-20.01
<i>Driving pressure</i>	0.58	0.58	-1.53	4.95	2.18	-8.13
Strategy	Wind-Catcher					
Bed 1	-2.84	-1.66	-3.35	-10.88	-7.52	-12.7
Bed 2	-2.84	-1.68	-3.34	-10.9	-7.83	-12.66
WC A	-5.96	1.21	-6.45	-22.77	11.41	-24.45
WC B	4.14	-1.39	-6.73	15.99	-4.85	-25.57
WC C	0.16	-0.18	-0.71	0.62	-0.77	-2.72
WC D	-6.63	-8.41	-8.78	-25.32	-37.76	-33.39
<i>Driving pressure</i>	6.98	2.87	2.63	26.87	18.92	9.93
Strategy	Dynamic façade & wind-catcher					
Av.DF_2 nd floor	-3.47	-3.91	-3.68	-13.7	-14.43	-15.09
Av.DF_3 rd floor	-3.65	-3.65	-3.66	-14.37	-13.27	-14.89
Av.DF_4 th floor	-4.11	-2.6	-3.41	-16.28	-9.63	-13.6
Bed 1	-3.41	-3.61	-3.63	-13.4	-13.3	-14.99
Bed 2	-3.34	-3.67	-3.47	-13.22	-13.49	-14.3
WC A	-5.83	0.88	-7.61	-22.27	3.69	-26.76
WC B	4.41	-1.3	-6.61	17.04	-5.15	-26.74
WC C	0.16	-0.15	-0.76	0.62	-0.68	-2.79
WC D	-6.27	-8.16	-9.29	-23.99	-31.47	-35.13
<i>Driving pressure</i>	7.72	4.54	2.71	30.14	17.16	11.55

6.6. Ventilation Performance Simulation Results for a Climate Scenario: Internal Flow Field

CFD simulation results from the ventilation performance investigation of buoyancy- and wind-driven flows are presented in this section. Comparable airflow rates (see Figure 7.19) and values of temperature difference (internal-external) were predicted at the simulations performed for the average (26°C) and highest (35°C) DBTs. A decision was therefore made to present only the simulation results from the average DBT (26°C) in this section (results for 35°C DBT are included in Appendix A.2.2).

6.6.1. Evaluation of buoyancy-driven flows: North winds

The single-sided ventilation strategy [SS] resulted in insufficient ventilation rates (average velocities below 0.03 m/s) relative to the recommended values presented in Table 3.2 (Chapter 3.3.4). This was expected, as the effective depth of single-sided ventilation is only twice the floor to ceiling height (CIBSE, 2005). The average indoor air temperatures were predicted up to 2°C above the DBTs, as seen in Figure 6.36. The cross ventilation [CV] strategy (Figure 6.37) increased the ventilation rates (0.1 m/s) to an acceptable level (Table 3.2). It further improved the airflow distribution at the rear space connected to the shaft and led to reductions in air temperatures by up to 1°C relative to [SS].

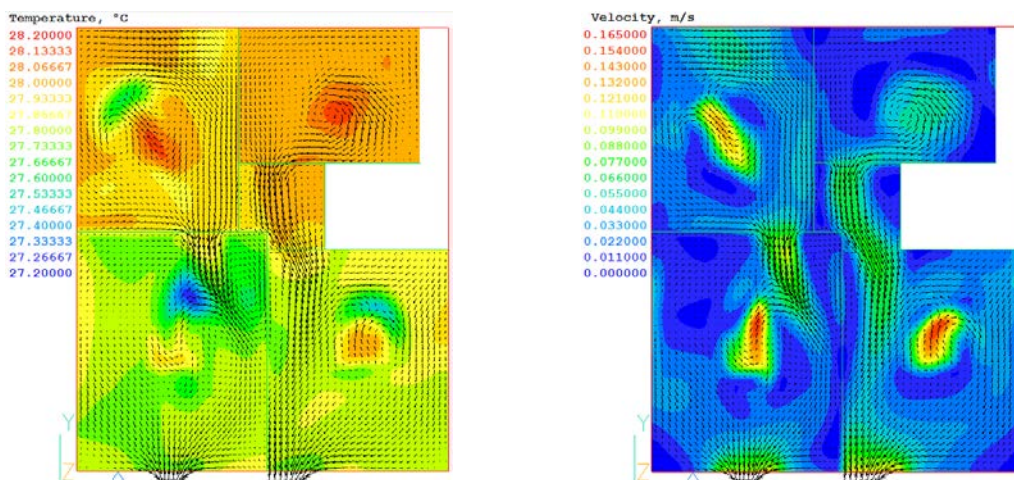


Figure 6.36 Temperature (left figure) and velocity contours and vectors (right figure) on *xy* plane, during buoyancy-driven ventilation of the [SS] strategy (for 26°C DBT)

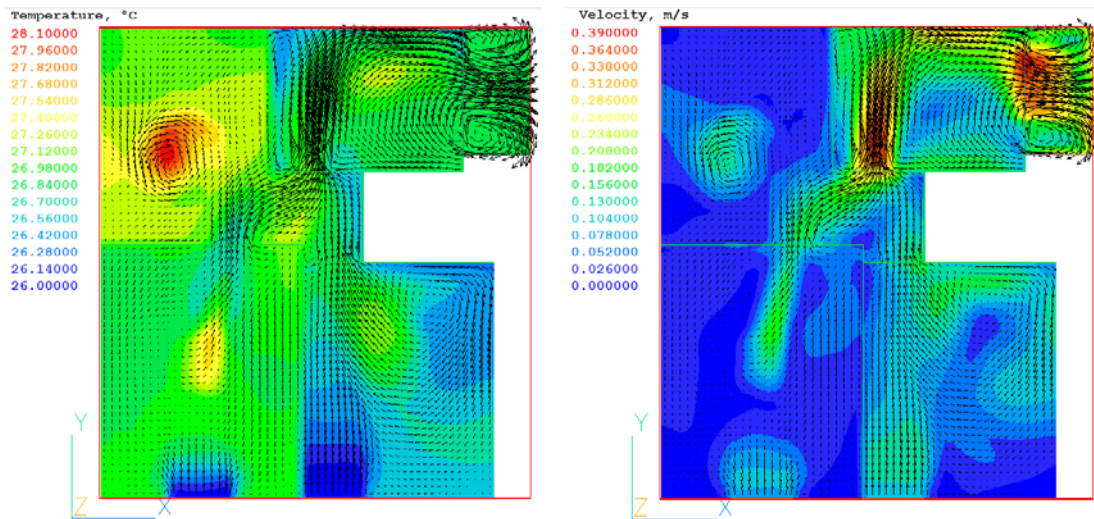


Figure 6.37 Temperature (left figure) and velocity contours (right figure) on xy plane, during buoyancy-driven ventilation of the [CV] strategy (for 26°C DBT)

The wind-catcher strategy [WC] predicted comparable airflow patterns to the [CV], showing lower indoor temperatures and improved ventilation rates (0.6 kg/s mass flow rate). Figure 6.38, shows the outflow of stale air from the four vertical wind-catcher top openings. The airflow in the spaces and the age of the time required for the stale air to escapes from the wind-catcher are shown in Figure 6.39.

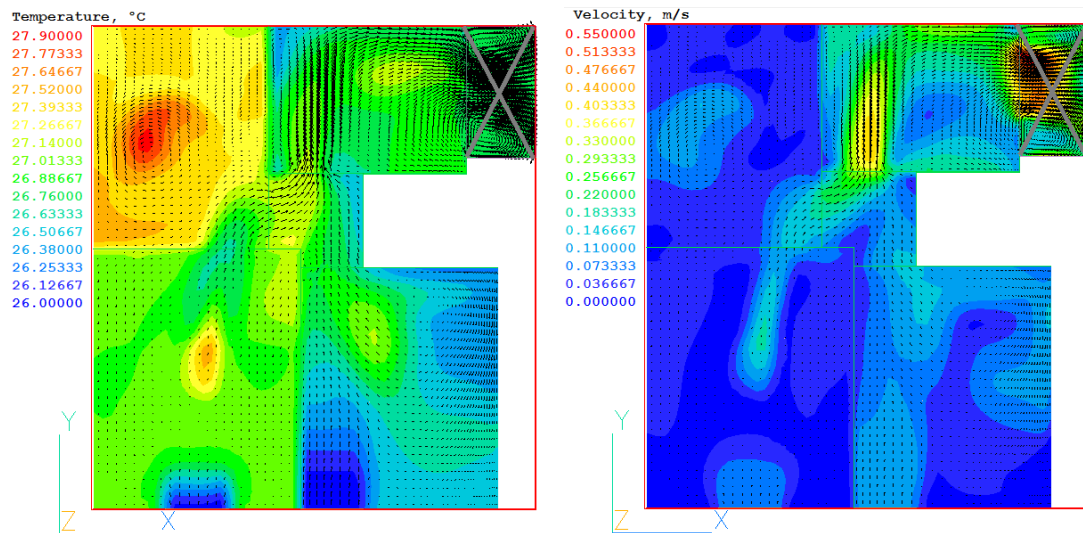


Figure 6.38 Temperature (left figure) and velocity contours and vectors (right figure) on plan view, during buoyancy-driven ventilation of the [WC] strategy (for 26°C DBT) (at 1.50m height above the apartment floor level)

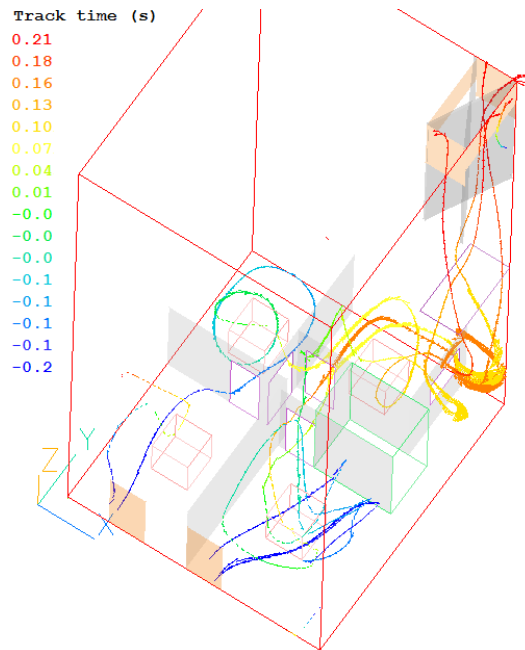


Figure 6.39 Streamlines of the airflow movement in the spaces, showing the starting (blue) and ending point (red) of the flow ([WC], buoyancy-driven flow, 26°C)

Likewise, the buoyancy-driven ventilation of the dynamic façade [DF & WC] strategy provided comparable airflow distributions relative to the [WC] strategy (Figure 6.40). The large area of the double skin façade openings contributed to recirculation of fresh air at the balcony zone, from the lower openings toward the higher openings, and reduction in the ventilation potential of the apartment studied.

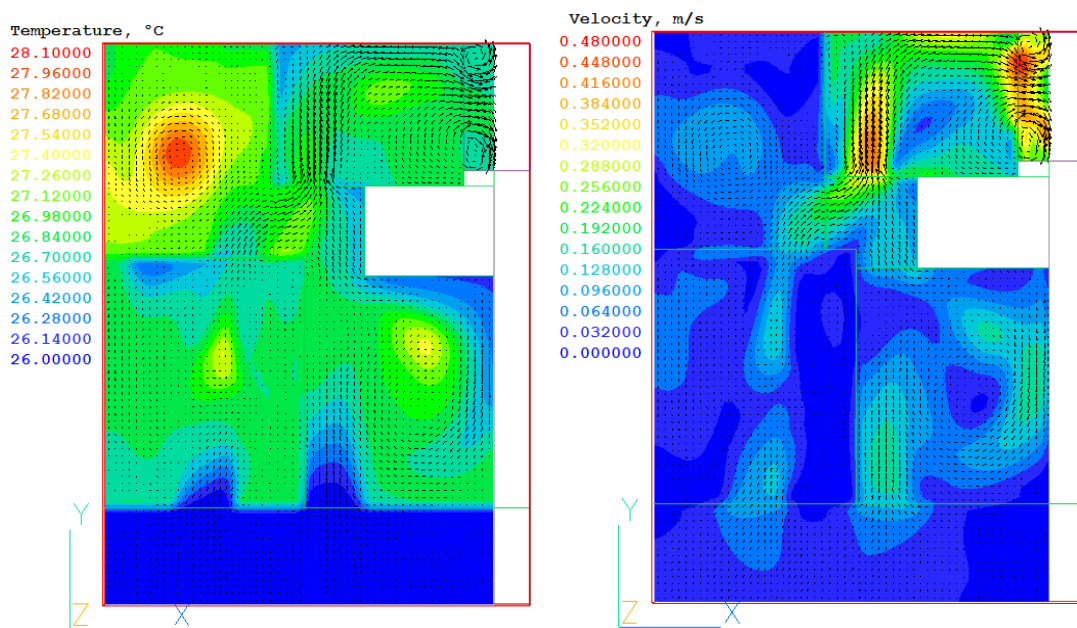


Figure 6.40 Temperature (left figure) and velocity contours and vectors (right figure) on plan view, during buoyancy-driven ventilation of the [DF & WC] strategy (for 26°C DBT)

The contribution of the three ventilation strategies, [CV], [WC], [DF & WC], to the previous single-sided ventilation [SS] was evident under buoyancy forces. Highest values of air temperatures were predicted in the living room (no direct access to fresh air), of up to 1°C above the average (Figure 6.41). Lower temperatures were predicted on average for the [WC] strategy, and then at the [DF & WC]. Higher velocities were calculated in the two bedrooms: on average the [CV] and [WC] strategies delivered the highest values (Figure 6.42). Average values of ventilation rates predicted at the two bedroom internal doors during buoyancy-driven flow were equal to 0.01, 0.23, 0.25 and 0.26m³/h for the strategies [SS], [CV], [WC] and [DF & WC] respectively. These values are considered insufficient for occupants' comfort as described in Table 3.2.

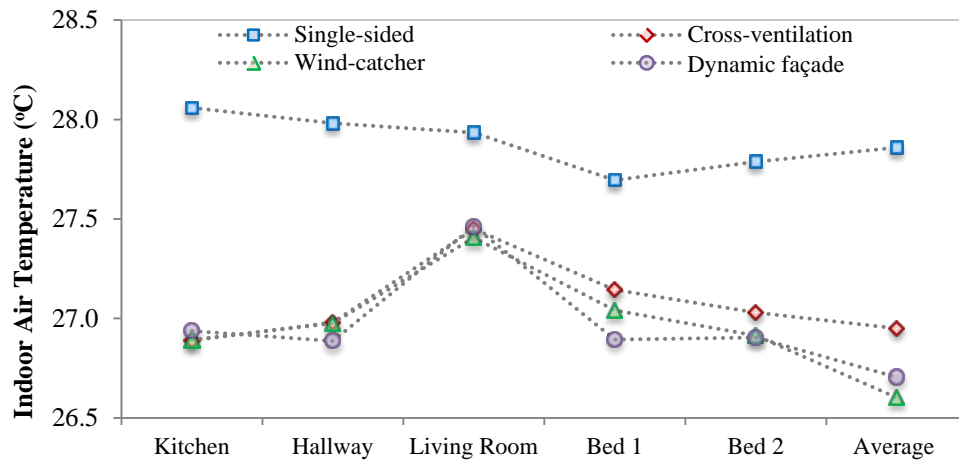


Figure 6.41 Indoor air temperatures (°C) for each of the four strategies during buoyancy-driven flow, calculated at set points of each room, at 1.50m height above the apartment floor

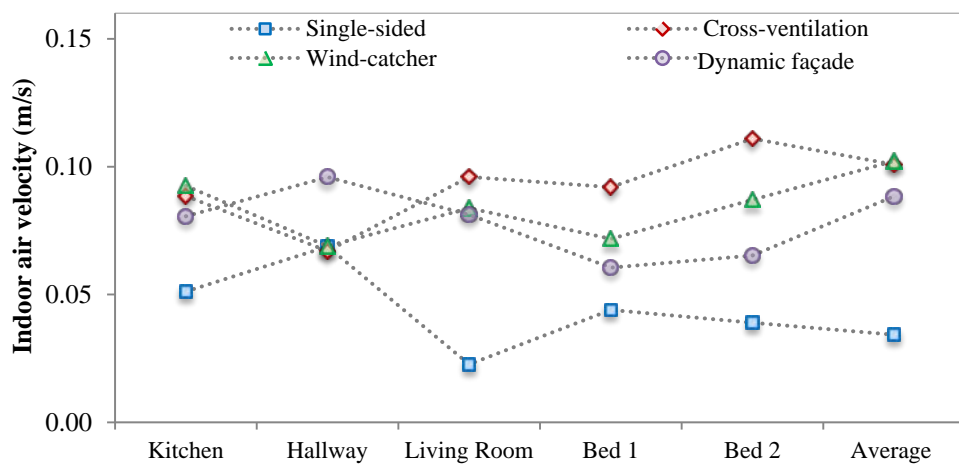


Figure 6.42 Indoor air velocity (m/s) for each of the four strategies during buoyancy-driven flow, calculated at set points of each room, at 1.50m height above the apartment floor

6.6.2. Evaluation of wind-driven flows: North winds

The contribution of wind to the previous buoyancy-driven flows was explored. It is not possible to present detailed results from all simulations performed for different climate scenarios within the present section. Northern wind was the most predominant wind direction from the climate data within the cooling period and thus, results from north wind at 7m/s and 26°C DBT are presented. Presentation of results from a single climate scenario still allows the relative performance of the different passive cooling strategies to be demonstrated and quantified.

6.6.2.1. Assessment of individual wind-driven ventilation strategies

The wind-driven [SS] strategy provided indoor air velocities (see Figure 6.43, left) of less than 0.2 m/s (lower than the acceptable mean, see Table 3.2.) and average indoor air temperatures of up to 2°C higher to the DBT. The introduction of wind to the previous buoyancy-driven flow was expected to deliver higher reductions in air temperature (see Figure 6.36). The airflow movement in the spaces is presented with the use of streamlines in Figure 6.44, showing the time required for the airflow movement (from the blue to the red points). Blue streamlines in the kitchen area indicate the flow with respect to the temperature difference due to internal heat gains.

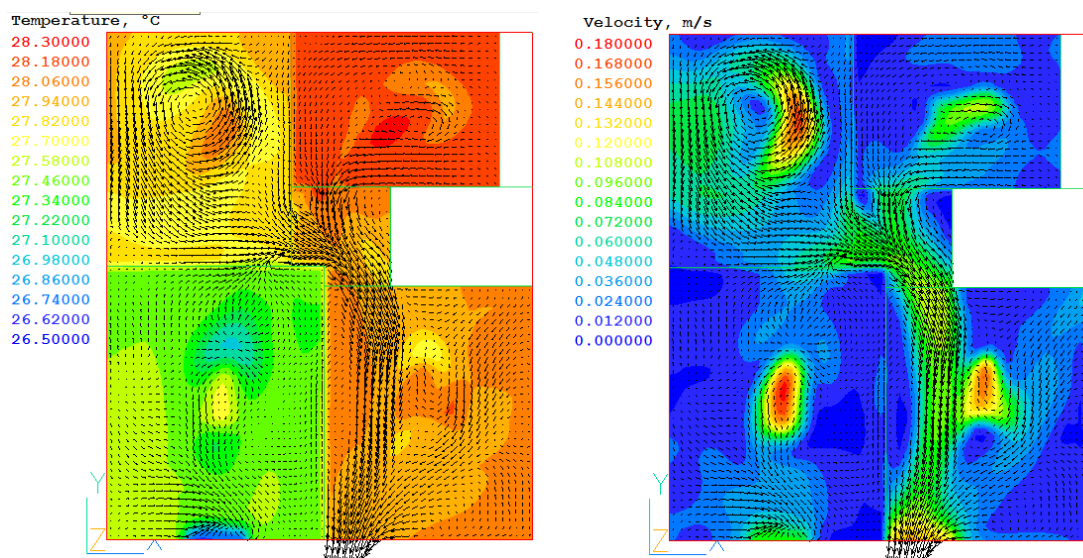


Figure 6.43 Temperature (left) and velocity (right) contours and vectors on xy plane during the wind-driven ventilation of the [SS] strategy (north, 7 m/s at 26°C)

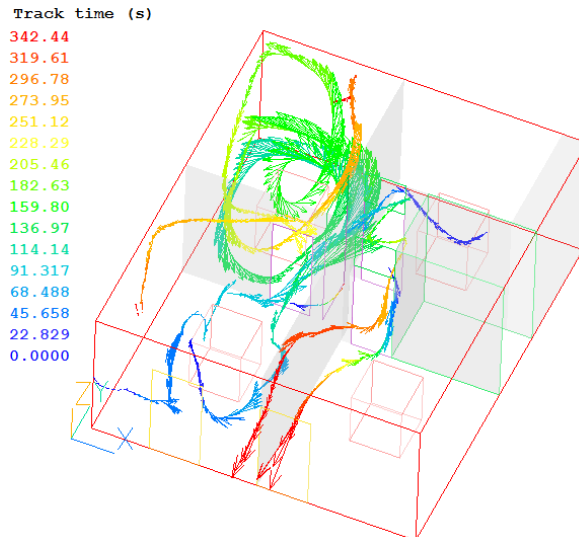


Figure 6.44 Streamlines of the airflow movement in the spaces, showing the starting and final point of the flow ([SS] ventilation, 7m/s north wind, 26°C).

The wind-driven [CV] strategy delivered higher ventilation rates and average velocities of approximately 0.6m/s in the bedrooms, 1.5m/s in the kitchen area and less than 0.20m/s in the living room (see Figure 6.45). These values would be appropriate for occupants' comfort (Table 3.2). It also resulted in reductions in indoor temperatures relative to the buoyancy-driven flow (1°C), as well as relative to the [SS] strategy (by 2°C). Similarly, Figure 6.46 shows streamlines in the three-dimensional space, indicating inflow from the horizontal top shaft opening and outflow at locations of the two bedroom openings.

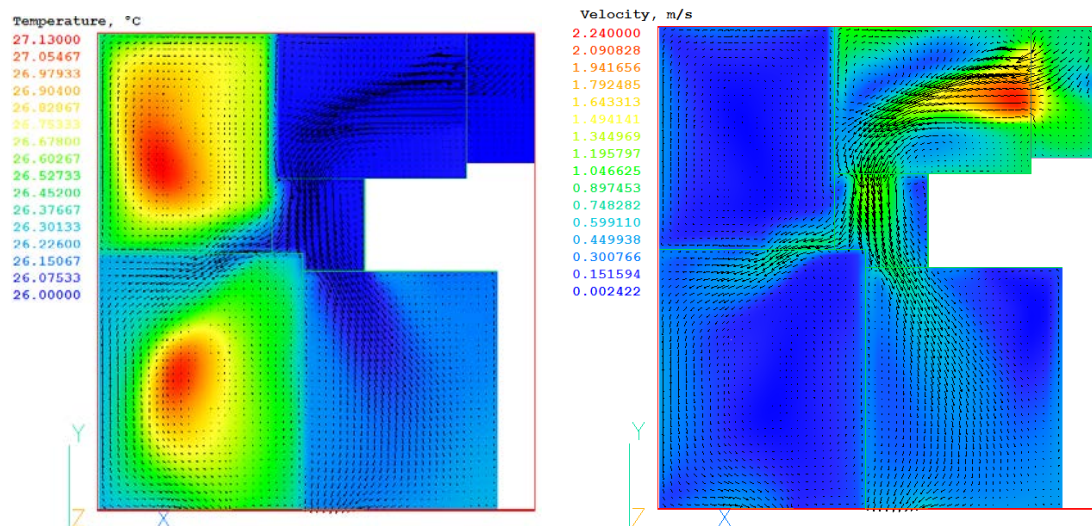


Figure 6.45 Temperature (left) and velocity (right) contours and vectors on xy plane during the wind-driven ventilation of the [CV] strategy (north, 7 m/s at 26°C)

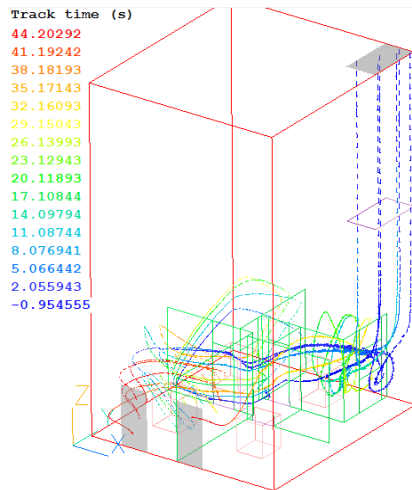


Figure 6.46 Streamlines of the airflow movement in the spaces, showing the initial and final points of the flow ([CV], 7m/s north wind, 26°C).

The [WC] resulted in improved ventilation rates relative to the previous strategies and in air temperature reductions of almost 0.5°C (Figure 6.47). Internal temperatures closely followed the external. The maximum air temperature was equal to 26.7°C (living room) and about 1°C lower than the buoyancy-driven strategy. The highest velocity of indoor air (3m/s in the kitchen) was up to six times higher relative to that of the buoyancy-driven flow (Figure 6.38). This is in accordance with published work by others, reporting higher ventilation rates (up to 76%) for wind than buoyancy driven wind towers in buildings (Calautit et al., 2012). Airflow paths were comparable to the [CV] strategy (Figure 6.48).

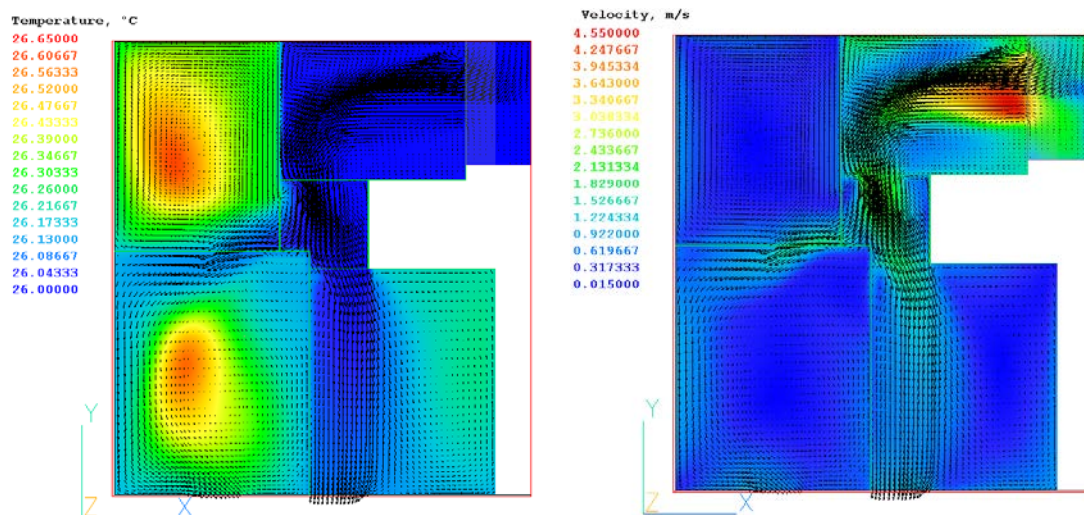


Figure 6.47 Temperature (left) and velocity (right) contours and vectors on xy plane during the wind-driven ventilation of the [WC] model (north, 7m/s at 26°C)

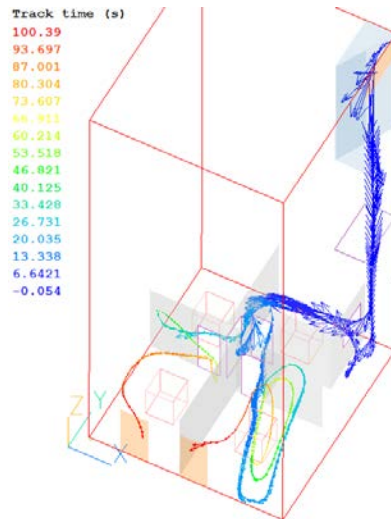


Figure 6.48 Streamlines of the airflow movement in the spaces, showing the starting and final points of the flow ([WC], 7m/s north wind, 26°C).

The wind-driven ventilation of the [WC] strategy delivered reductions in air temperatures, relative to the [SS] and [CV] strategies. However, the cooling potential of this strategy was further enhanced by utilising the passive cooling of water evaporation techniques. The cooling performance of the [WC] strategy with the passive draught evaporative cooling, [PDEC-WC], was investigated. Results indicate further reductions in air temperatures by at least 1.5°C in all occupied spaces, with lower values predicted in the kitchen area and the second bedroom. An increase was also observed of the air velocity principally in the kitchen area, for water consumption of eight litres per hour (Figure 6.49).

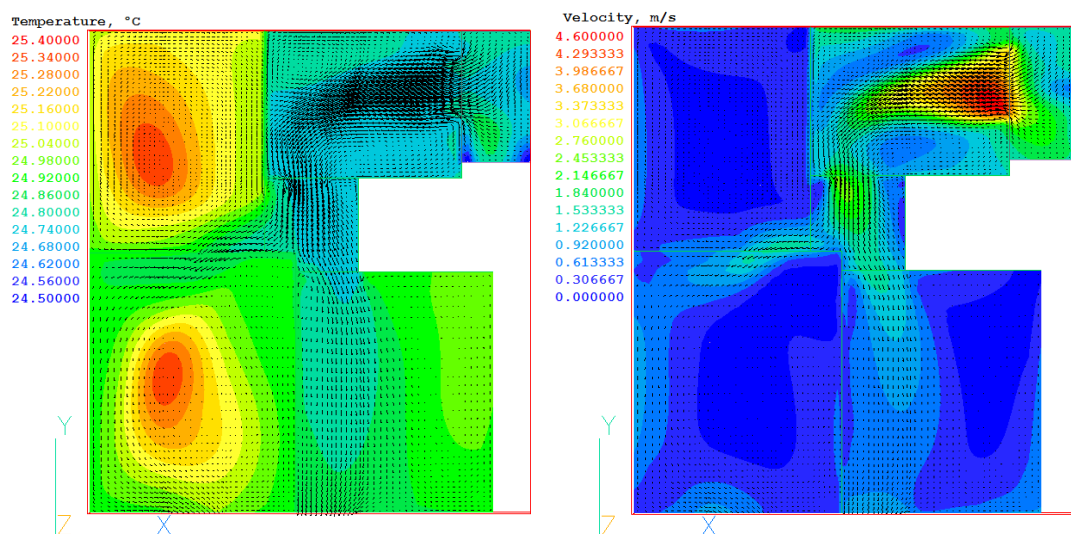


Figure 6.49 Temperature (left) and velocity (right) contours and vectors on xy plane during wind-driven ventilation of the [PDEC-WC] of 8L/h (North, 7m/s at 26°C)

The wind-driven ventilation of the dynamic façade [DF & WC] delivered reductions in air temperatures by up to 2°C below the values predicted during the buoyancy-driven flow of the strategy (Figure 6.40). Despite this, it contributed to comparable results with the [WC]. The [DF & WC] strategy delivered appropriate ventilation rates for comfort by up to 2m/s in the bedrooms, 4m/s in the kitchen and 1m/s in the living room (see Figure 6.50). Similarly, Figure 6.51 shows the inflow from the wind-catcher openings and outflow from the [DF & WC] openings.

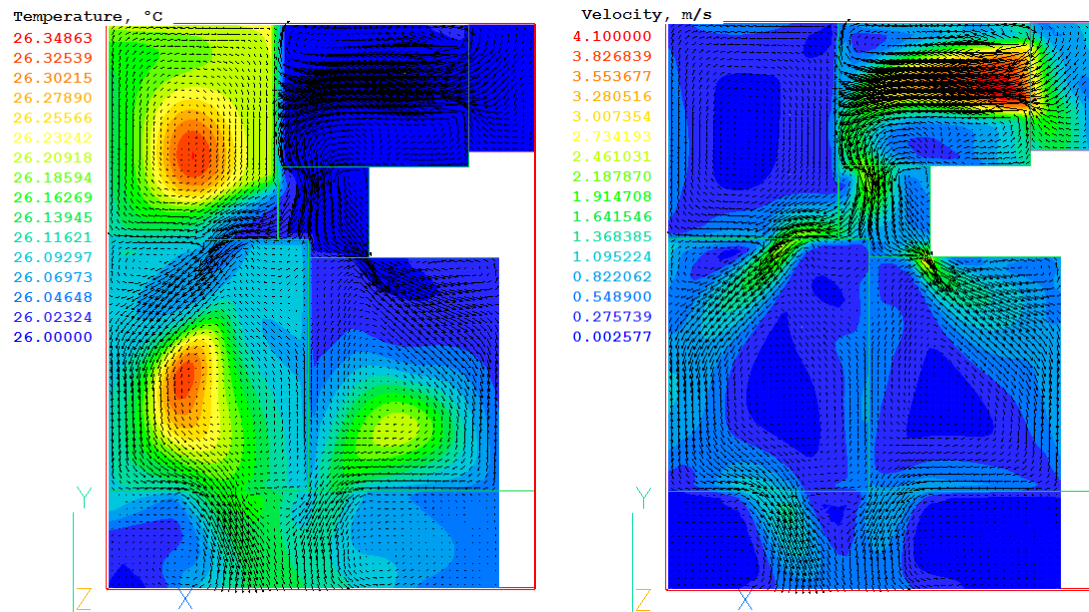


Figure 6.50 Temperature (left) and velocity (right) contours and vectors on xy plane during the wind-driven ventilation of the [DF & WC] (north, 7m/s at 26°C)

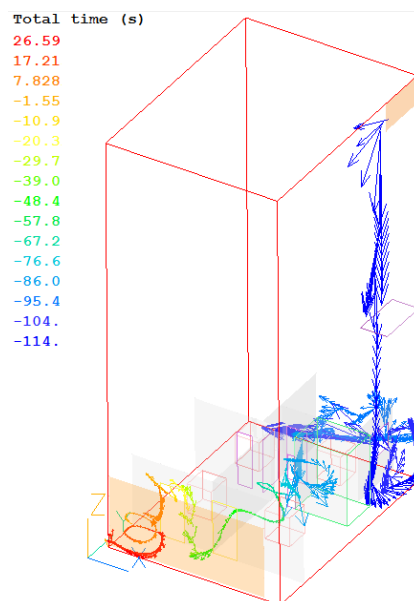


Figure 6.51 Streamlines of the airflow movement in the spaces, showing the initial and final points of the flow ([DF & WC], 7m/s north wind, 26°C)

Simulation results from the [PDEC-DF] during water consumption of 8 L/h, predicted lower air temperatures by up to 1°C and enhanced ventilation rates in all spaces. Average temperatures of 25°C were predicted in the two bedrooms, as shown in Figure 6.53.

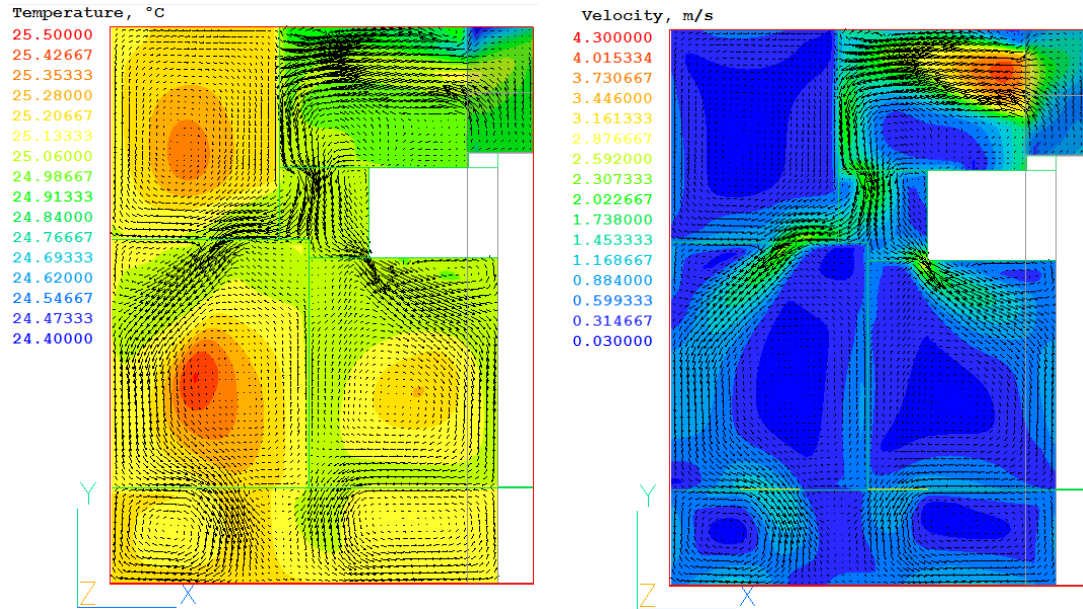


Figure 6.52 Temperature (left) and velocity (right) contours and vectors on xy plane during the wind-driven ventilation of the [PDEC-DF] (north, 7m/s at 26°C)

It should be acknowledged that shading provided by the dynamic façade was not taken into account during the CFD simulations. The steady state simulation results could represent conditions predicted during the hours of the day without solar gains. As predicted with the DTM simulations, the DF louvres could deliver further temperature reductions during the hours of the day with high solar incidents. Thus, the ventilation performance of this strategy could be further improved.

6.6.2.2. Overall performance evaluation of the simulation results: North wind direction

The contribution of wind to the previous buoyancy-driven flows was evident, and in response to the acting surface pressures on the external openings. For the average wind speed of the site under study (3.6m/s) and north wind direction, the wind-driven [SS] ventilation provided indoor air velocities of less than 0.1 m/s and average indoor air temperature approximately 2°C above the DBT, as shown in Figure 6.53 and Figure 6.54 (north wind direction). Average indoor air velocities across all occupied spaces for the [SS] and [CV] strategies were predicted insufficient to offset high indoor air temperatures and provide direct comfort (Table 3.2). The wind-driven [CV] strategy significantly contributed to a reduction in air temperatures, although to a less extent than the increase in ventilation rates.

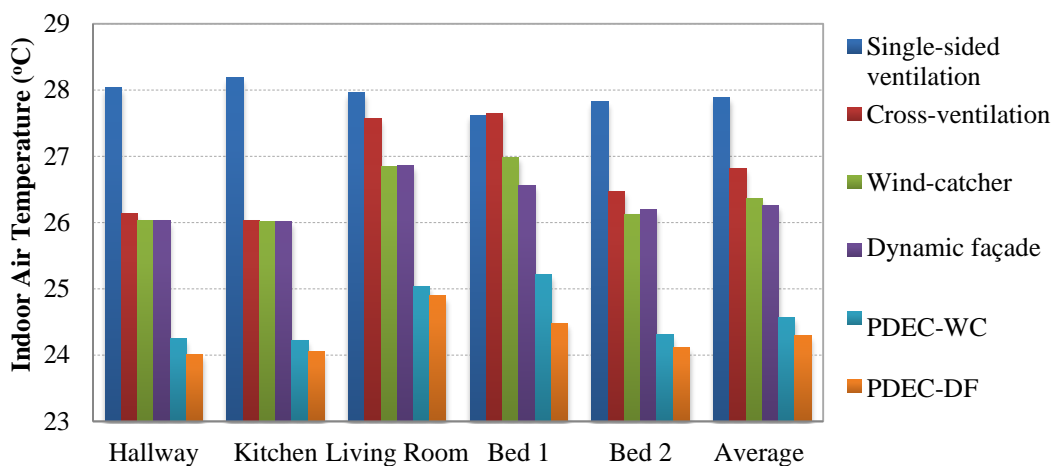


Figure 6.53 Indoor air temperatures predicted at 5 points in the spaces (at xy points, 1.50m on z) and the average of the six strategies (north wind direction, 3.6m/s and 26°C DBT)

Similarly, the inclusion of the wind-catcher delivered higher ventilation rates relative to the previous strategies and reductions in air temperatures by up to 0.5°C. Despite the almost twice higher driving pressures relative to the previous [CV] strategy, the ventilation rates did not increase accordingly, because of the substantial length of wind-catcher's shaft. However, the performance of the [WC] under wind-driven flows was significant relative to the buoyancy driven and in accordance with published work by others (Calautit et al., 2012). The cooling effect of the [WC] and [DF & WC] strategies was further enhanced by the introduction of water evaporation; these strategies delivered lower indoor air temperatures for comfort (see Table 3.2).

and Androutsopoulos et al., 2012). More than 2°C temperature reductions were predicted with comparable ventilation rates to those of the strategies without the water evaporation. The [PDEC-DF] delivered lower air temperatures than the [PDEC-WC] strategy.

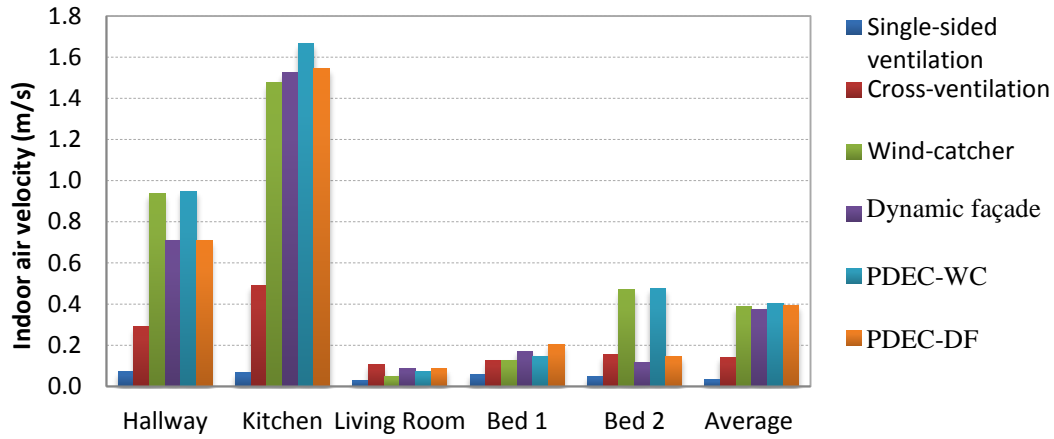


Figure 6.54 Indoor air velocity predicted at 5 points in the spaces (at xy points, 1.50m on z) and the average of the six ventilation strategies (north wind direction, 3.6m/s and 26°C DBT)

A wind speed increase from 3.6m/s to 7m/s, resulted in ventilation rates enhancement, and up to twice-higher indoor air velocities (Figure 6.55 and 6.56). Simulation results from the water evaporation strategies (water consumption of 8 L/h), predicted increase in air temperatures in response to the wind speed increase, and by up to 1°C in all occupied spaces. In addition to this, the increase of the moisture content of the incoming air, due to the water sprayed and evaporated at the PDEC, delivered indoor air relative humidity levels above the external by up to 7% (value predicted during 6L/hour water consumption).

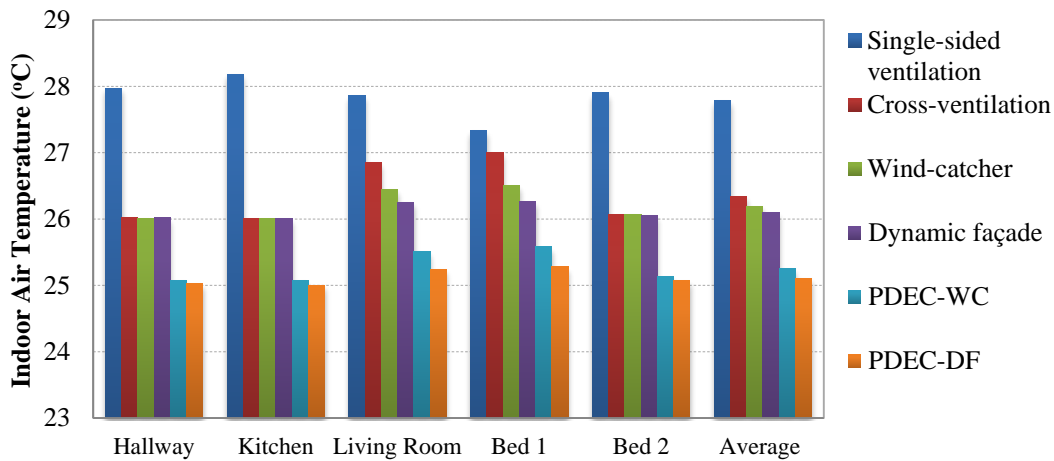


Figure 6.55 Indoor air temperatures (°C) of the six natural ventilation strategies (north wind of 7m/s at 26°C DBT) at 5 points in the spaces and the average of the apartment

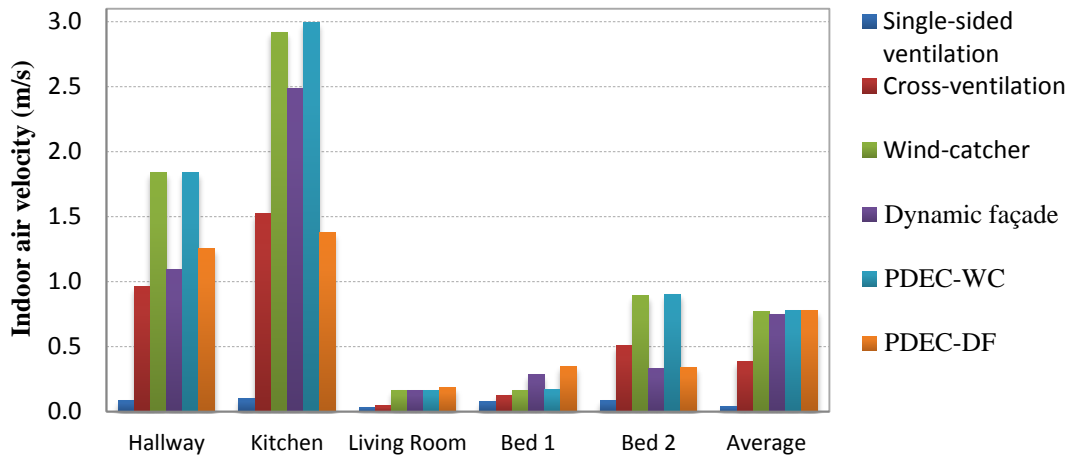


Figure 6.56 Indoor air velocity (m/s) at five spaces and the apartment's average (north wind direction, 7 m/s and 26°C DBT)

Average values of indoor air velocities calculated in the internal openings (described in Figure 6.13) are presented in Figure 6.57. The wind-driven [SS] ventilation strategy was excluded as it delivered the lowest and insufficient for IAQ indoor air velocities (up to 0.01m/s). Results indicate indoor air velocities up to ten times higher in the kitchen area than the two bedrooms, and up to four times above the average of all spaces. The lowest values of indoor air movement of all spaces were predicted in the living room (on average below 0.3 m/s) during all ventilation scenarios (air temperatures of up to 0.5°C above the average). The velocity of the airflow is higher in the kitchen than in the air shaft (measured at a cross section of the air shaft at 7m height of the apartment floor) due to the internal heat gains.

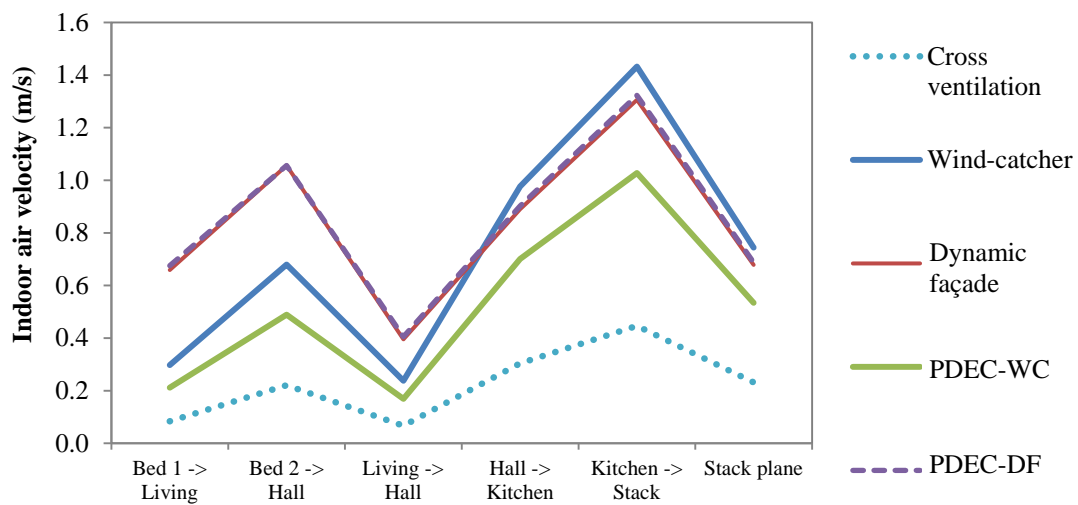


Figure 6.57 Average air velocities (m/s) predicted at the internal openings during the wind-driven ventilation of 5 strategies (North wind, 3.6m/s and 26°C DBT)

6.7. Discussion: Ventilation Performance Evaluation of the Apartment During all Climate Scenarios

Results from all CFD simulations performed according to Figure 6.1 (for all climate conditions evaluated), expressed the potential for wind-driven ventilation to improve upon the buoyancy-driven ventilation. Wind-driven ventilation provided up to 3% reductions in indoor air temperatures relative to the buoyancy-driven flow and for all natural ventilation strategies evaluated. Wind driven ventilation further increased the ventilation rates in the spaces, delivering up to 750% enhancement of the indoor air velocities (able to improve occupants' thermal comfort, Table 3.2).

Predicted mass flow rates in the openings of each strategy are summarised in Table 6.11, showing the contribution of the wind driven flows relative to the buoyancy-driven ventilation (% of increase). Wind flows contributed to increase in mass flow rates for the [DF & WC] and the [WC] strategies. The ventilation performance of the [WC] was particularly improved with the contribution of wind relative to the previous buoyancy driven ventilation (increase between 52% and 574%). This was predicted similar to experimental and CFD results by Calautit et al. (2012) predicting increase in ventilation rates during wind driven flows by up to 76% relative to buoyancy flows.

Table 6.11 Mass flow rates (kg/s) on the inlets of each ventilation strategy and percentage of increase due to the contribution of wind than the buoyancy-driven ventilation for each strategy respectively

	Buoyancy	North		East		Northwest	
		3.6m/s	7m/s	3.6m/s	7m/s	3.6m/s	7m/s
Single-sided Ventilation	0.01	0.02	0.16	0.06	0.27	0.09	0.15
		100%	1500%	500%	2649%	800%	1400%
Cross ventilation	0.54	0.64	1.93	0.63	1.29	1.11	2.53
		19%	260%	19%	141%	108%	372%
Wind-catcher	0.6	2.04	4.01	1.05	2.75	0.91	1.71
		241%	574%	75%	358%	52%	185%
Dynamic façade & WC	0.61	1.86	3.75	1.36	2.78	1.18	2.3
		205%	514%	123%	356%	93%	277%

Indoor air quality in the spaces was enhanced with the implementation of the new natural ventilation strategies, relative to the previous condition of the [SS] ventilation strategy. Cross ventilation significantly improved the ventilation rates, resulting in an

increase of up to 14 times relative to the single-sided ventilation (Figure 6.58). Up to three times higher ventilation rates have been predicted by others in Greek domestic buildings during cross ventilation relative to single-sided ventilation (Niachou et al., 2005).

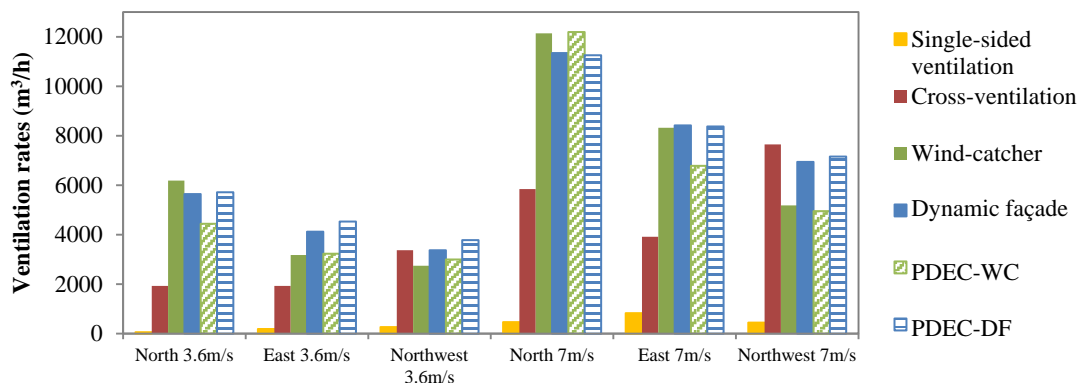


Figure 6.58 Predicted ventilation rates of each natural ventilation scenario for different wind speeds and directions (m^3/hr)

The inclusion of a wind-catcher assisted the ventilation performance under north and east wind incidents, resulting in increased mass flow rates by two to three times (Figure 6.58). It was anticipated to yield a greater enhancement of the natural ventilation of the spaces than the results suggest, for the lower wind speeds. However, the performance of the wind-catcher was found comparable to that predicted by others: Calautit et al. (2012) evaluated the performance of a roof-mounted wind-catcher that delivered $3,830m^3/h$ for $4m/s$ wind speed while the proposed wind-catcher in the case study building delivered $3,000$ to $6,000m^3/h$ for $3.6m/s$ wind (see Figure 6.58). These values vary with regard to wind directions, the different building and wind-catcher designs, the internal heat gains, the number of openings and the operable areas.

In overall, the introduction of the dynamic façade enhanced the natural ventilation of the previous strategies, delivering higher volume flow rates by up to 40% at the inlets. However, this improved performance was dependent on the climate scenario, showing less improvement than the [WC] strategy in some cases.

Except for the [CV] and [SS] strategies, north wind direction appears to be the most favourable for wind-driven ventilation (Figure 6.58). The contribution of higher air wind speeds (from $3.6m/s$ to $7m/s$) led to increase in ventilation rates by 4.6 times for the [SS], 2.4 times for the [CV], and by 2.1 times for the [WC], [DF & WC], [PDEC-

WC], [PDEC-DF]. The ventilation performance of the strategies varies with regard to wind speed and direction. Particularly for the [WC] strategy, the ventilation rates vary significantly with regard to wind-directions evaluated. This was also predicted by others evaluating the performance of wind-catchers (Montazeri et al., 2010; Calautit et al., 2012)

The difference between the delivered indoor air temperatures was insignificant between the various wind directions (Figure 6.59). Indoor temperature reductions relative to the buoyancy-driven flows of up to 0.5°C and 1°C were predicted for the wind-driven ventilations of 3.6m/s and 7m/s respectively. The cooling performance of the PDEC strategy reduces with the wind speed increase. For most wind directions, the [DF & WC] strategy delivered the lowest air temperatures relative to the other ventilation strategies (except for the PDEC) and below the outdoor temperature.

Further reductions in indoor temperatures would be expected with continuous operation over a short period of the PDEC strategies, as the values of Figure 6.59 were predicted using steady state simulations. Ford et al. (2012) evaluated the cooling potential of a PDEC in a residential buildings and predicted indoor temperatures lower than the ambient by 14°C when the PDEC was operating for 6.5hours (15-minute intervals) and by 1.5°C for 2-hours of operation (intermediate performance). This provides confidence in the predicted performance of the proposed PDEC in the apartment studied.

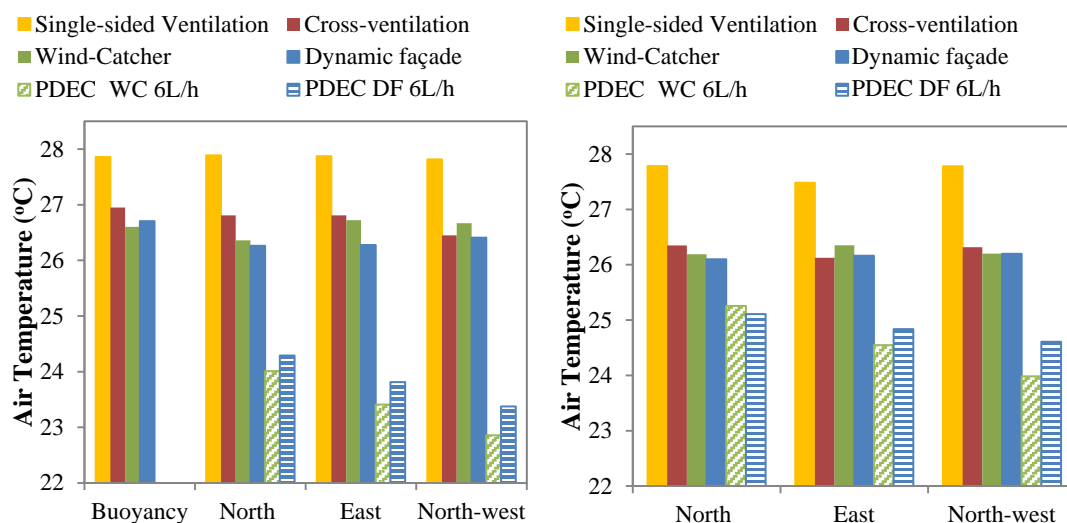


Figure 6.59 Average values of indoor air temperature (°C) at a horizontal plane at 1.5m height for 3.6m/s (left) and 7m/s (right) wind incidents (26°C DBT)

Indoor air velocities calculated at the location of the two bedrooms' internal doors for the [DF & WC] strategy were predicted higher (up to 100% higher) than the other natural ventilation strategies (Figure 6.60), with values up to 1.7m/s. These values were high according to requirements of national standards (of up to 0.2m/s), as shown in Chapter 2.5.1. However, according to BS EN15251 (2007), high ventilation rates are required to offset the increased temperature and thus deliver occupants' comfort. Values up to 1.5m/s could extend the operative temperatures in the spaces by up to 4 degrees (see Table 3.2). Also, the potential of the wind-catcher in delivering high indoor air velocities was according to published work by others: indoor velocities of up to 0.55m/s for wind-speed of 4m/s were predicted for a wind-catcher application using CFD by Calautit et al. (2012).

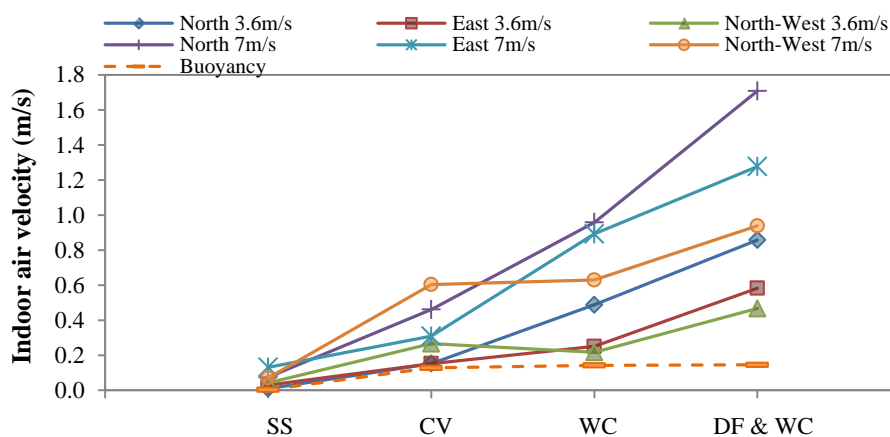


Figure 6.60 Average indoor air velocities (m/s) predicted in the two internal bedroom doors

Absolute air velocities in the bedroom openings were predicted to be 50% more than the average values of all apartment spaces, as shown in Figure 6.60 and Figure 6.61. This shows the indoor air velocities predicted at the internal bedrooms doors are not indicative of the actual airflow distribution in the spaces. Therefore, occupants would be subject to higher velocities at specific zones of each space, according to the position of the inlet and outlet openings.

Comparable values of average indoor air velocities across all spaces were predicted for the [WC] and [DF & WC] strategies (Figure 6.61). These values were significantly higher to the [CV] and [SS], apart for the north-west wind directions. The strategies of water evaporation delivered comparable ventilation rates to the corresponding [WC], [DF & WC] strategies. The ventilation performance of the [WC] was comparable to the performance of wind-catchers as predicted by others: for 4m/s wind internal velocities varied between 0.34 and 0.55m/s (Calautit et al., 2012).

Buoyancy-driven flows delivered higher indoor air velocities at the [WC] and [DF & WC] strategies relative to the wind-driven ventilation of the [SS] strategy. This is significant as occupants' comfort could be provided by direct cooling during windless periods, which are up to 14% of the cooling period (wind speeds below 1m/s for the climate data of the site examined, Chapter 4.4).

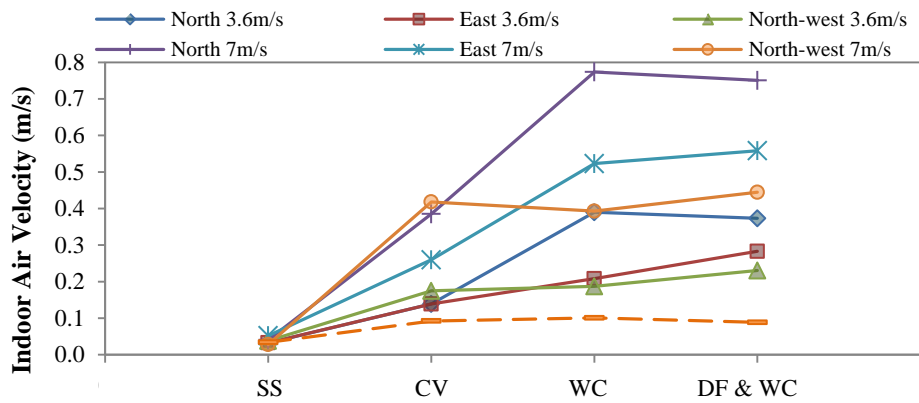


Figure 6.61 Average indoor air speeds (m/s) across all spaces calculated at a horizontal plane at 1.5m height above the apartment floor, across all apartment spaces (26°C)

High air change rates were expected with the inclusion of the improved ventilation strategies and with regard to the existing building design; the apartment was modelled in CFD with fully open openings, adiabatic surfaces and without considering the contribution of the thermal mass. Higher values were predicted in the kitchen of the apartment under investigation, directly connected to the air shaft and wind-catcher, and lower in the two bedrooms.

Predicted air change rates vary in response to wind directions by 9, 4, 4, and 3 times (higher to lower) for the [SS], [CV], [WC], and [DF & WC] strategies respectively (Figure 6.62). Predicted air change rates in the apartment under investigation for the strategies [PDEC-WC] and [PDEC-DF] varied by 1% and 3% to the values predicted during [WC] and [DF & WC] respectively. The values predicted for [WC] and [DF & WC] have a wide range as for the respective values predicted using DTM, presented in Figure 5.33. Both [SS] and [CV] strategies provided air change rates according to published work by others, providing validation of the designs and modelling techniques used. Measurements in existing apartments in Athens shown up to 6ach^{-1} during single sided ventilation via dual openings and up to 12ach^{-1} during cross ventilation for as low as 0.5m/s wind speeds (Niachou et al., 2005); these values are comparable to the predicted air change rates for the apartment under investigation, presented in Figure 6.62.

Although the air change rates were predicted higher than the acceptable values defined by national standards (Table 3.2), high values are expected in free running buildings as predicted with measurements in Greek buildings (up to 80ach⁻¹) by Geros et al. (1999). The predicted values are representative of steady state conditions and it would be thus expected to vary throughout the cooling period, especially with appropriate openings' control as described in Chapter 5. Likewise, the relationship between the actually replaced volumes of air is a function of the airflow uniformity in the spaces. As previously described, the air velocity is non-uniform across the individual spaces (see Figure 6.60 and Figure 6.61). Utilising these high values of air change rates during the nighttime (night ventilation) could reduce the need for cooling in the morning hours and postpone the peak indoor temperatures in the occupied spaces (see Chapter 2.5.1 (Geros et al., 1999)).

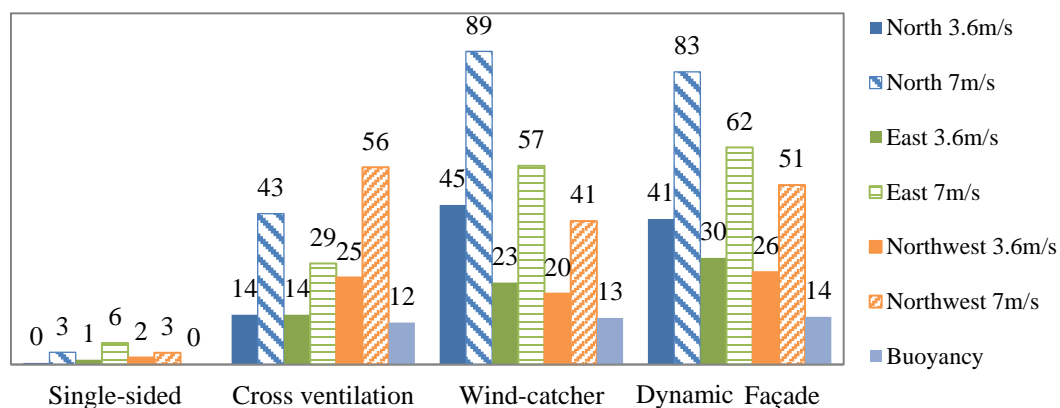


Figure 6.62 Predicted air change rates (ach-1) at the building under investigation for all natural ventilation strategies (26°C DBT)

The apartment under investigation was modelled without the adjacent apartments of the building (i.e. as a stand-alone case) and thus utilising in full the operation of the wind-catcher. As the air shaft was also connected to seven more apartments (three above the case study and four connected to the opposite side of the air shaft, see Chapter 4), the apartment under investigation would utilise the 1/8 of the air shaft's and the wind-catcher ventilation potential/ability. However, it was not expected that the 1/8 of the ventilation rates would be correspondingly delivered. The ventilation performance of the apartment under investigation utilising the 1/8th (8 adjacent apartments) and the 1/4th (4 adjacent apartments above the case study apartment) of the air shaft's ventilation potential were also investigated and presented in Section 6.9.1.

6.7.1. Description of the most efficient strategy

Results from all CFD simulations performed demonstrate the potential for wind-driven ventilation to improve upon the buoyancy-driven ventilation, assisting reductions in indoor temperature of up to 0.5°C and 1°C relative to the buoyancy-driven flows, for 3.6m/s and 7m/s wind speed respectively. It was predicted that:

- The wind-driven [SS] ventilation delivered the highest indoor temperatures (up to 2°C above the DBT) under all climate scenarios.
- Wind-driven [CV] contributed to temperature reduction in the occupied spaces of up to 5% relative to the [SS] ventilation, for average DBT of 26°C (4% for 35°C DBT). It also resulted in an increase in the ventilation rates of up to 14 times relative to [SS] ventilation.
- The [WC] strategy contributed to air change rates increase of 76% on and up to 0.5°C reductions in indoor temperature, relative to the [CV] strategy.
- The [DF & WC] enhanced the natural ventilation performance of the previous strategies by delivering higher ventilation rates of up to 40% in the inlets relative to the [WC] strategy and further reductions in air temperatures of up to 0.5°C. However, this improved performance was dependent on the climate scenario. The [DF & WC] was considered the most efficient solution.
- The [PDEC] strategies delivered reductions in indoor temperature up to 18%, 14%, and 14% relative to the [SS], the [CV], and the [WC] strategies respectively. The natural cooling performance of the [PDEC] reduced with respect to the ventilation rates increase.

Although the PDEC strategy was predicted to deliver the largest temperature reduction, due to potentially excessive water consumption (up to 8litres per hour), the combined operation of a wind-catcher and a lightweight dynamic façade [DF & WC] was considered the most efficient solution for the Mediterranean sub-climate and building type studied. This strategy led to significant increase in ventilation rates, contributed to reductions in indoor air temperatures, and provided occupants' comfort, relative to all natural ventilation strategies investigated.

6.8. Characteristics of Individual Ventilation Strategies

6.8.1. Passive downdraught evaporative cooling system

The relationship between the water consumption and the ventilation performance (i.e. indoor air temperature, air velocity and relative humidity) of the PDEC strategies was investigated. Five volumes of water consumption (i.e. 4, 6, 8, 10, and 12 L/h) were examined for the two natural ventilation strategies ([WC] and [DF & WC]) examined, for 7m/s north wind and 26°C DBT.

Average values of indoor air temperature, velocity and relative humidity predicted on a horizontal plane across the apartment spaces (1.5m height above apartment floor) for the [PDEC-DF] (five volumes of water) and the [DF & WC] (zero water consumption) strategies, are presented in Figure 6.63. The steady rate of temperature reductions predicted indicates up to 2°C reduction during 12 L/hour consumption. At all cases, this linear increase of relative humidity was predicted below 11%, for incoming air of 50% relative humidity. The water consumption increase resulted in negligible increase in indoor velocities.

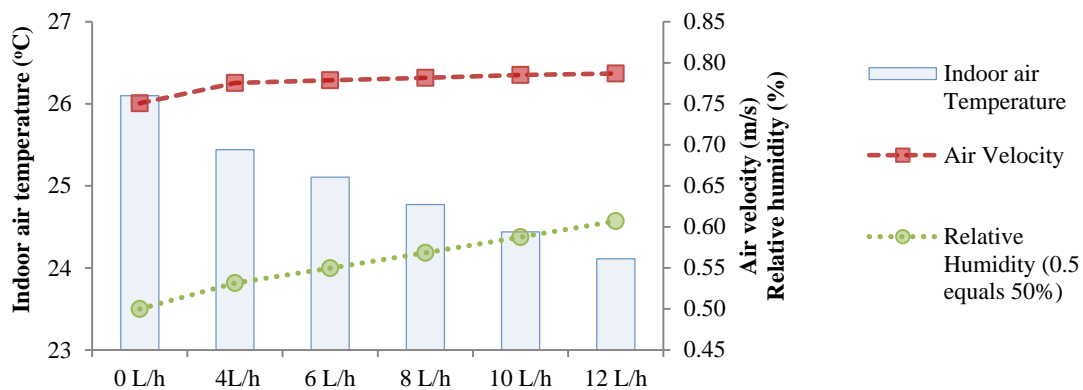


Figure 6.63 Predicted indoor values of air velocity, temperature and relative humidity predicted at a horizontal plane for different water consumptions for [PDEC-DF] (26°C and 7m/s north)

Indoor air temperature and the relative humidity difference, normalised as a percentage of the respective values without water evaporation (strategies [WC] and [DF & WC]) predicted for the [PDEC-WC] (three volumes of water) and the [PDEC-DF] (5 volumes of water), as presented in Figure 6.64. It was noticed that, twice more water consumption resulted in: up to 100% air temperature reductions; 25% to

30% air velocity increase (4 to 8 L/h and 6 to 12 L/h, respectively); and 115% relative humidity increase. Although the increase in water consumption delivered reductions in air temperatures, it has similarly contributed to increase in the moisture content. Thus, the capacity of the strategy shows a reduction after a certain amount of water consumption. However, the relative humidity increase of 21% above the 50% of the external air (12 L/hour), was considered within the acceptable limits for occupants' thermal comfort (below 70% RH, see Chapter 3.3, Table 3.2).

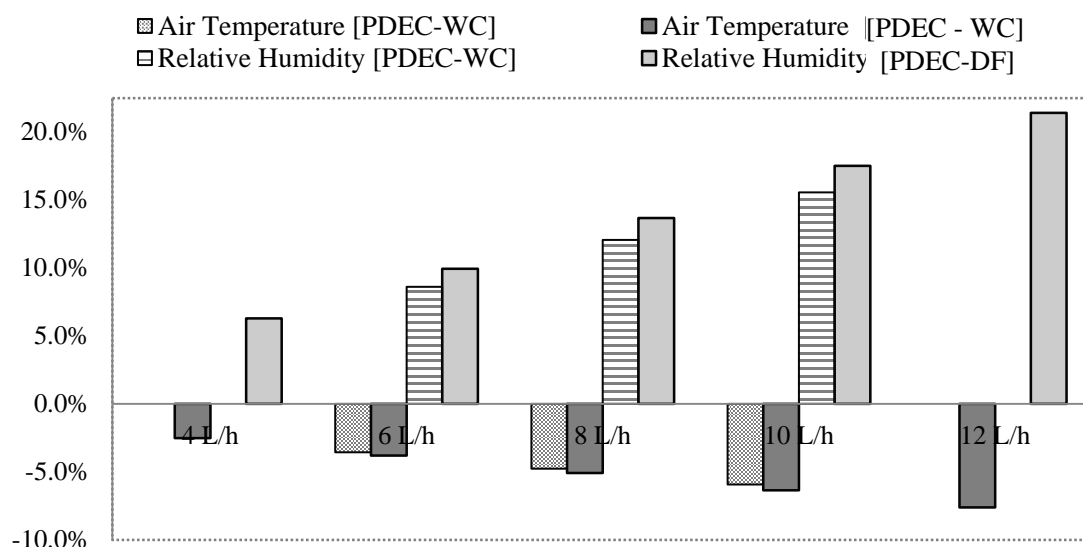


Figure 6.64 Temperature and relative humidity change for the [PDEC-WC] and [PDEC-DF], normalised as a percentage of the values predicted for the [WC] and [DF & WC] strategies respectively (averaged temperature and velocity values, at 1.50m level above the floor level, 7m/s north wind, 26°C DBT)

6.8.2. Lightweight dynamic façade

The ventilation performance of the lightweight [DF] was evaluated as a second layer of three continuous, vertically arranged, rows of openings (6.35m length and heights of 0.80m, 1.40m and 0.80m respectively). These represented a layer of external horizontal operable louvres, in order to reduce the computational time and power requirements, as previously described in Section 6.4. Fine mesh elements would be required at the louvres' zone relative to the other building zones.

Supplementary CFD simulations were performed for the wind-driven [DF & WC] strategy in order to evaluate different operation patterns of the louvres. Characteristics of the louvres' design and dimensions are included in Chapter 4. The new mesh properties varied between 2.30E-04 cell sizes to 10.7. Simulation results

(plotted indoor air velocity contour and vectors) for a single climate scenario and three operations of the louvres are presented in Figure 6.65, Figure 6.66 and Figure 6.67, showing the fully open operation, the top part only, and the lower and the top parts, respectively.

Convergence was difficult to achieve due to the refined mesh. Up to 15,000 iterations and four times more computational time were required relative to the refined modelling of the [DF & WC] (Section 6.6.2.2). Although a large number of different climate scenarios were investigated, as convergence was particularly difficult to achieve for the strategies evaluated, results from only three cases were included in this section. The results offer visualisation of the flow paths of the different louvres operation. The operation of the ‘top’ or ‘top & lower’ group of louvres resulted in increased ventilation rates, almost twice, relative to the fully open operation of the louvres, as shown in Figure 6.65, Figure 6.66 and Figure 6.67.

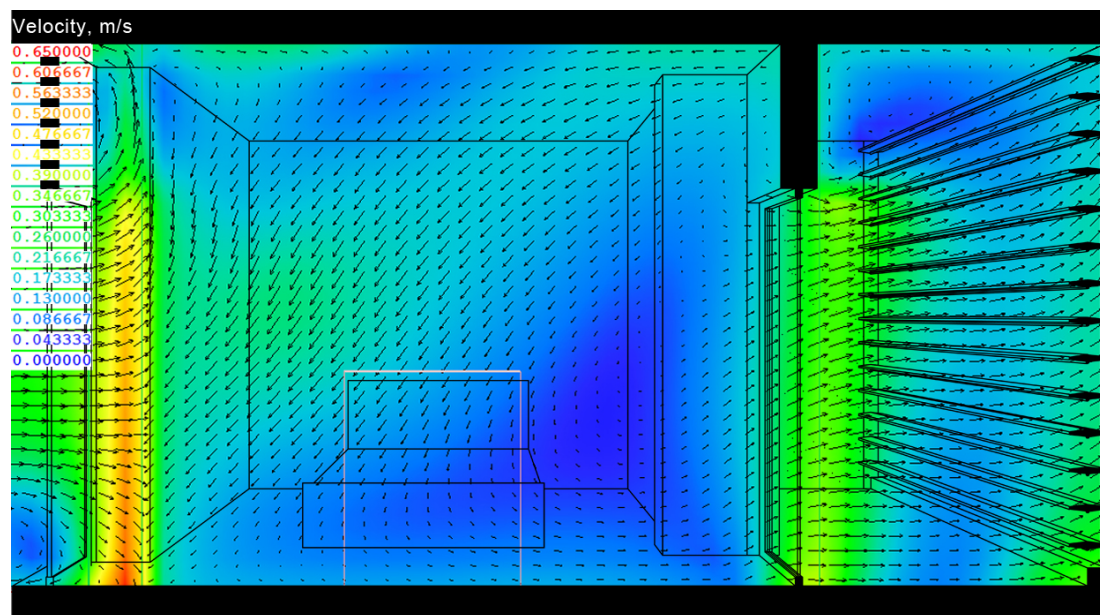


Figure 6.65 Velocity contours and vectors at y,z cross section of the second bedroom, balcony and DF. All louvres fully open (3.6 m/s east wind at 26°C)

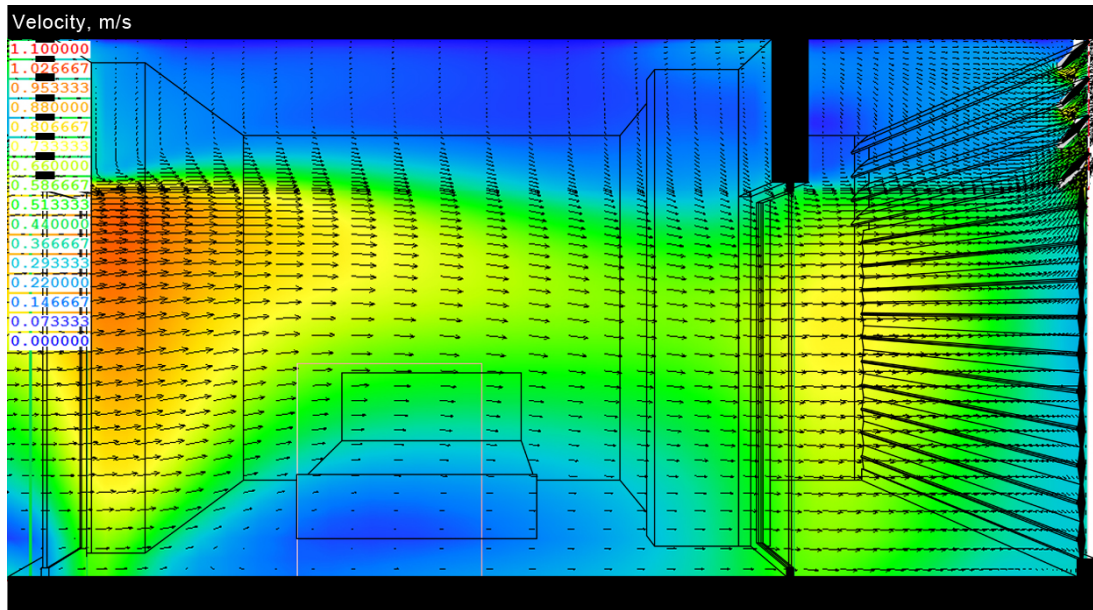


Figure 6.66 Velocity contours and vectors at y,z cross section of the second bedroom, balcony and dynamic façade. Only the top louvres open (3.6 m/s east wind at 26°C)

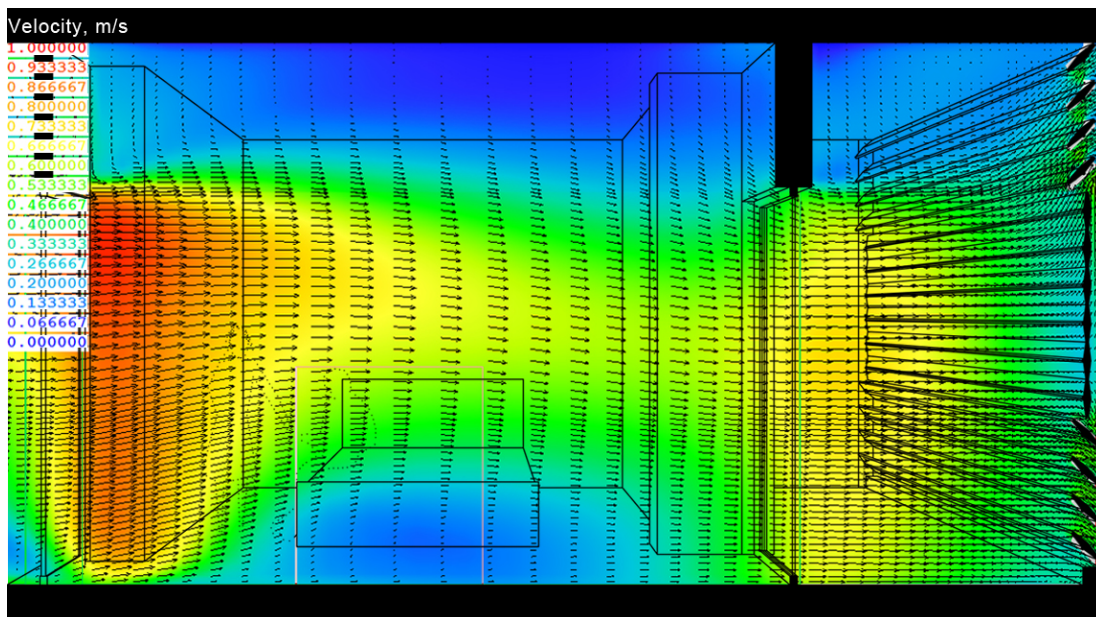


Figure 6.67 Velocity contours and vectors at y,z cross section of the second bedroom, balcony and dynamic façade. The top and bottom louvres open (3.6 m/s east wind, 26°C)

Comparable results were predicted during the ‘up & lower’ and ‘up’ strategies. Predicted indoor air temperatures and air velocities at regular positions along a defined line (at 1.5m height above the apartment floor) from the façade to the rear spaces and through the two bedroom doors, during the three louvres positions, are presented in Figure 6.68 and Figure 6.69. The predicted indoor air temperatures of the ‘fully open’ DF vary significantly across the measuring line (up to 1.5°C

temperature difference in the first bedroom) and relative to the other two DF operations. Similarly, indoor air velocities varied at the ‘fully open’ DF relative to the other two operations, by up to 0.4m/s in the second bedroom.

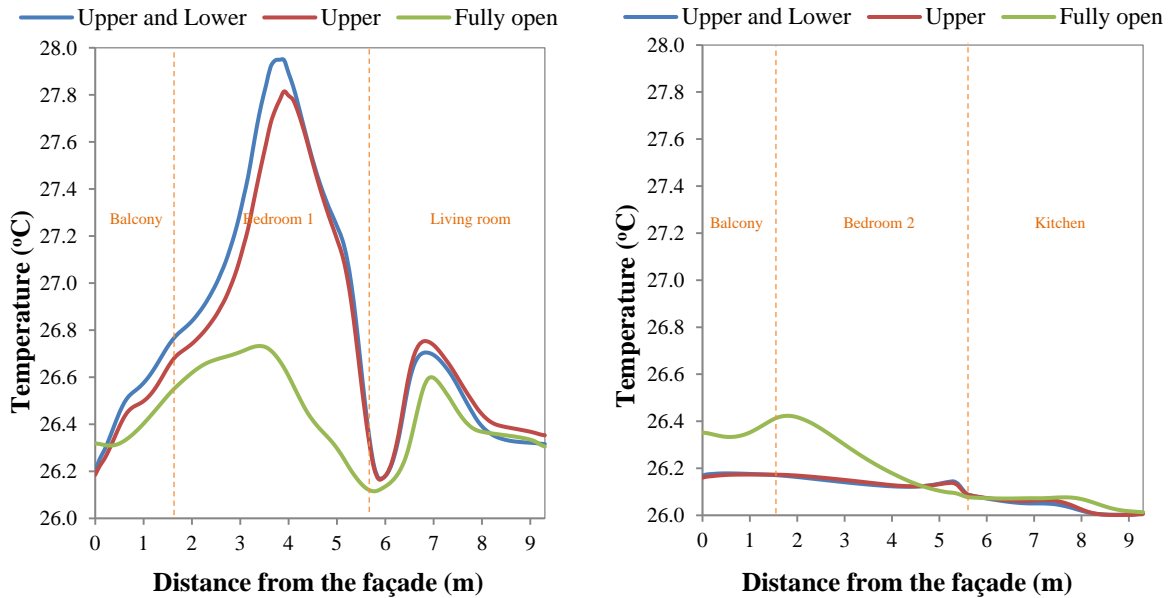


Figure 6.68 Predicted temperatures ($^{\circ}\text{C}$) at 100 points along two lines at 1.5m height (from (1.2,0,1.5) to (1.2,9.3,1.5) and from (3.6,0,1.5) to (3.6,9.3,1.5) respectively) from the façade to the rear spaces, for 3 louvres positions

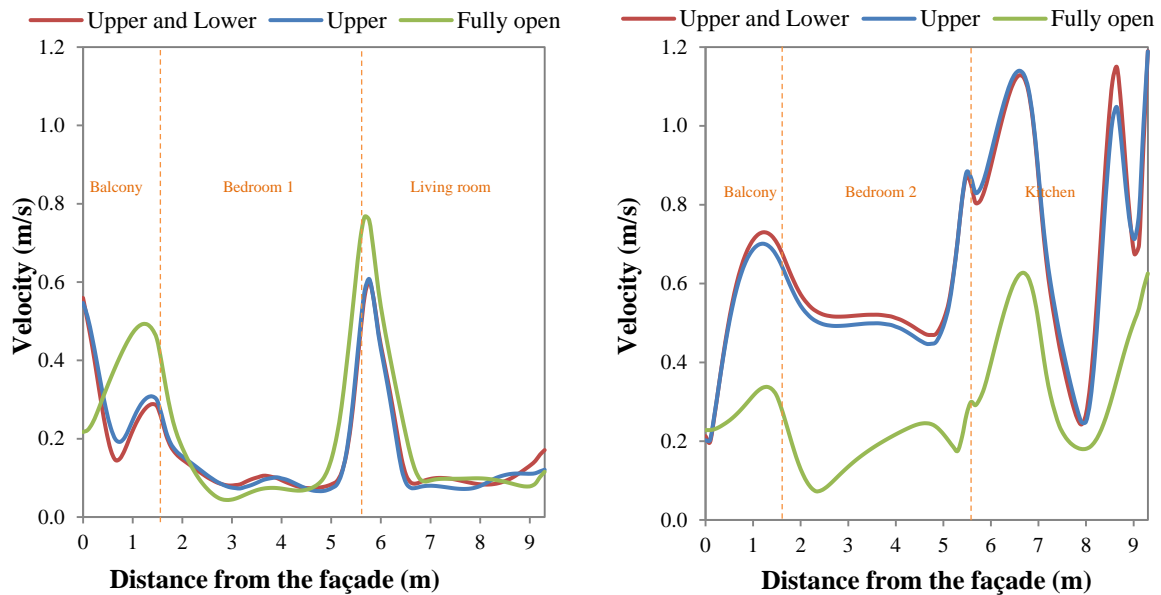


Figure 6.69 Predicted velocity (m/s) at 100 points along a line at 1.5m height (from (1.2,0,1.5) to (1.2,9.3,1.5) and from (3.6,0,1.5) to (3.6,9.3,1.5) respectively), for 3 louvres positions

6.9. Ventilation Performance Study of Additional Designs and Justification of the CFD Modelling Methods Used

This section presents CFD simulations performed to explore the ventilation performance of the total building and the apartment under investigation. Description of the additional simulations performed is presented in Appendix A.4. Although optimization of the openings design and position was beyond the scope of this research, CFD simulations were performed to evaluate the ventilation efficiency of additional strategies. These included the incorporation of wind-catchers at the building's main façade and the creation of internal alternative airflow paths utilising new openings.

6.9.1. Ventilation performance study of the total building

The case study apartment was connected to an air shaft shared by eight apartments. Three apartments were located above the apartment under investigation and four connected to the other side of the air shaft. As previously described, the CFD simulations investigated the ventilation performance of the strategies when only the apartment under investigation was connected to the light well. Further CFD simulations explored how the adjacent apartments influence the ventilation performance of the case study apartment.

Initially, the ventilation performance of the natural ventilation strategies under investigation was evaluated during the minimum operation of the air shaft, i.e. when all the connected apartments also utilise the air shaft and wind-catcher. Thus, the 1/8th of the air shaft potential was utilised by the apartment under investigation. Supplementary simulations were performed for the [CV], [WC] and [DF & WC] strategies with reduced size (1/8th of the opening size as modelled in Sections 6.4) of the top air shaft opening (i.e. horizontal top openings for [CV] strategy) and correspondingly of the wind-catcher's openings (i.e. four top openings for [WC] and [DF & WC]).

Air change rates were predicted lower than those predicted during the full utilisation of the air shaft. Average air change rates of the two bedrooms were predicted to be

61% lower on average. These were reduced in all apartment spaces (Figure 6.70) by 3.2, 2.2, and 2.4 times respectively for the [CV], [WC], and [DF & WC] relative to the full operation of the air shaft (Figure 6.62). Despite being lower, these values were considered sufficiently high (i.e. 29ach^{-1} average of the two bedrooms, and 19ach^{-1} of the apartment under investigation) and appreciable in delivering occupants' comfort, as shown in Table 3.2. Comparable values were predicted on average for the buoyancy and wind-driven ventilation of 3.6m/s wind speed, for each ventilation strategy. Higher ACH were predicted for the [WC] strategy and up to 4 times higher to those of [CV] strategy (Figure 6.70). Air change rates of the water evaporation strategies [PDEC-WC] and [PDEC-DF] during the $1/8^{\text{th}}$ operation were not presented in this section as they varied by 10% and 7% to the values of the [WC] and [DF & WC] respectively.

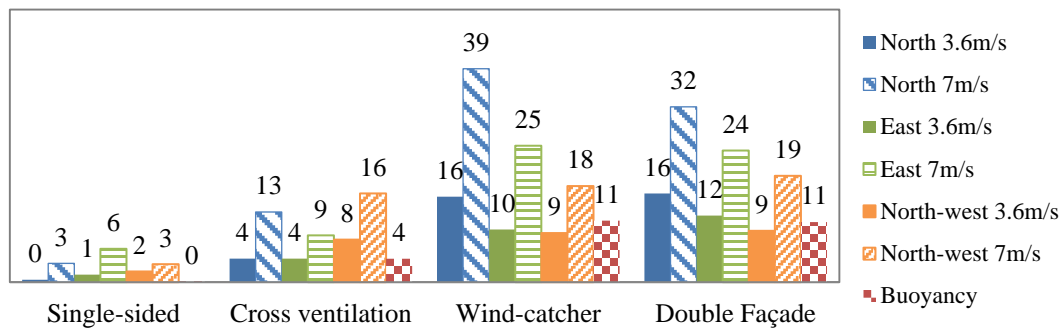


Figure 6.70 Predicted air change rates (ach^{-1}) of the apartment spaces for the natural ventilation strategies (26°C DBT) during the part operation of the air shaft ($1/8^{\text{th}}$)

Indoor air velocities predicted at the two bedroom openings during the $1/8^{\text{th}}$ air shaft utilisation, were lower by up to 60% than the values predicted during utilisation of the air shaft by full, as shown in Figure 6.60 and Figure 6.71. The wind-driven [WC] strategy during 3.6m/s wind speed, delivered indoor air velocities comparable to the values predicted for all climate scenarios of the wind-driven [CV] strategy. Indoor air velocities were predicted between 0.1m/s and 0.2m/s ; these were less than during the fully utilisation of the air shaft and insufficient for IAQ (Table 3.2). Appropriate indoor air velocities for provision of natural cooling were delivered for specific climate scenarios of the [WC] and [DF & WC] strategies.

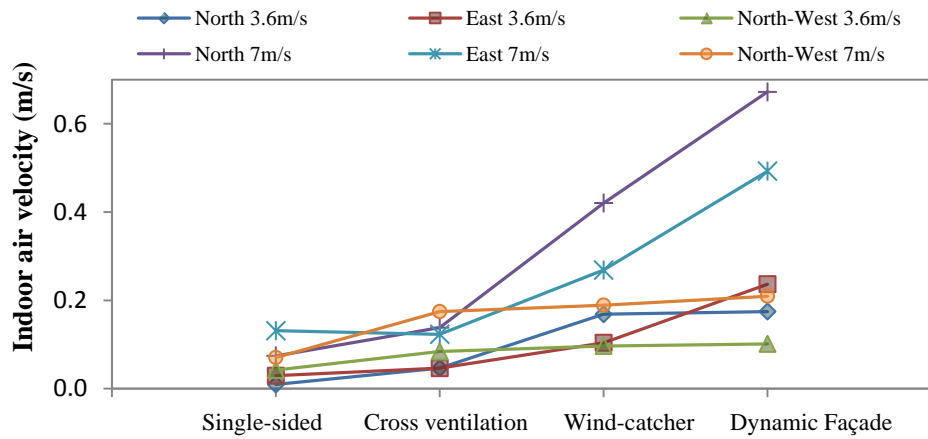


Figure 6.71 Average values of indoor air velocity in the two bedrooms (average of the two internal doors), during the part operation of the air shaft (1/8th)

Furthermore, the reduction in ventilation rates during the 1/8th operation resulted in indoor air temperatures increase by 0.4°C on average for all strategies, and 0.6°C, 0.4°C and 0.4°C for all climate scenarios of the [CV], [WC], [DF & WC] respectively. This 2% on average temperature increase varied in response to wind speed. Wind speed of 7m/s resulted in 1% temperature increase for the 1/8th operation. On the contrary, reductions in ventilation rates (for the 1/8th) improved the PDEC operation. This provided a further reduction in indoor air temperatures by 4% (0.9°C) and 10% (2.4°C) on average for the [PDEC-WC] and [PDEC-DF] respectively relative to the predicted air temperatures during the full operation of the air shaft (Figure 6.72). A temperature reduction of up to 3.6°C was predicted in the case study apartment spaces, reaching temperatures as low as 19.8°C (east wind of 3.6m/s [PDEC-DF]). For both strategies, the higher driving pressures delivered less reduction in air temperatures (above 15ΔP less than 2°C reduction to the values of the full operation). Therefore, although the ventilation performance of the [CV], [WC], [DF & WC] was significantly higher during the full utilisation of the shaft by the case study apartment (i.e. higher ventilation rates and lower indoor air temperatures), the cooling potential of the water evaporation strategies [PDEC-WC], [PDEC-DF] was optimum during the minimum ventilation potential of the air shaft (1/8th).

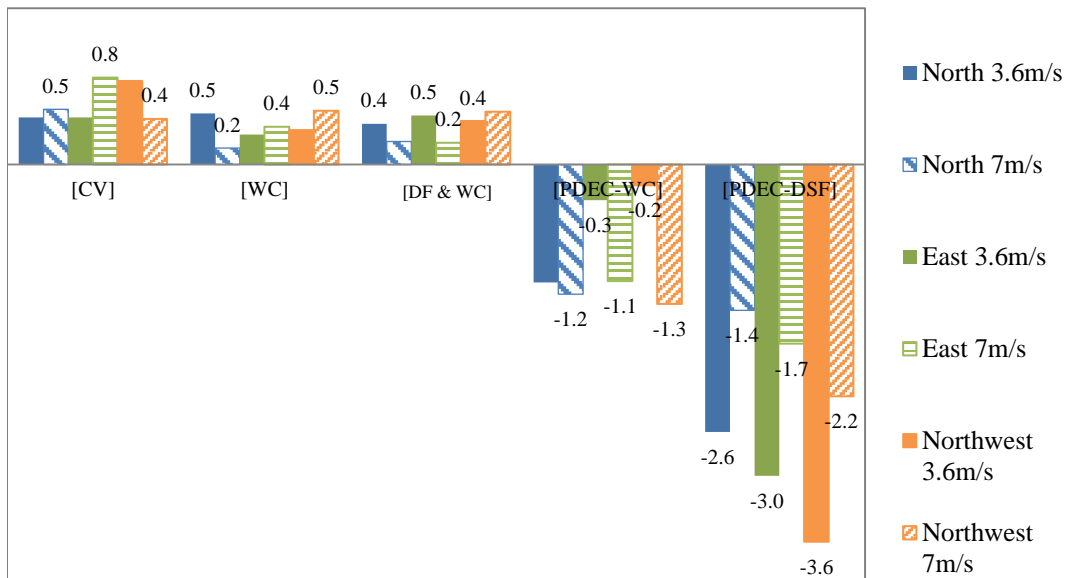


Figure 6.72 Temperature difference ($^{\circ}\text{C}$) during the $1/8^{\text{th}}$ shaft operation relative to the previous full operation of the shaft

Furthermore, the average ventilation potential of the air shaft for the apartment under investigation was explored during the utilisation of the air shaft by three apartments located at the upper floors above the apartment under investigation (4 out of 8 apartments connected to the air shaft, $1/4^{\text{th}}$ ventilation potential). The four apartments were appropriately designed within the CFD model and simulated. Due to the computational power required to model simultaneously four storeys, the study was conducted for only six ventilation scenarios of the wind-catcher strategy, as shown in Table 6.12. The purpose of modelling the four apartments (including the case study) was twofold. Firstly, comparison of the simulation results of this strategy with those of the ventilation performance evaluation of the apartment as a stand-alone case (without the adjacent apartments described in Section 6.7), could identify the potential magnitude of error of the two modelling processes. Secondly, evaluating the ventilation performance of the strategies on the upper floor apartments would give insights of their overall ventilation performance.

All four apartments were simulated with the same internal heat gains, number of occupants and usage. Each CFD model was created according to the building drawings of Chapter 4. The layout and plan view of the selected apartment was repeated to all four floors. All openings had the same size and position on xy axis to the examined apartment. For each strategy, the CFD model was created according to Section 6.4 respectively. External flow CFD simulations (Section 6.3) predicted

pressure values at the surface of each opening of the four apartments in addition to those in the openings of the apartment studied (see Appendix A.1.1). These were included in the openings of all apartments in order to evaluate wind-driven ventilation. All simulations reached convergence after 10,000 iterations on average.

Table 6.12 Description of the strategies evaluated and climate scenarios and results from the performance evaluation of the case study apartment when modelled with the adjacent apartments (percentage difference relative to stand-alone)

Natural cooling strategy	Air temperature	Wind direction	Wind speed	Temperature percentage difference	Velocity percentage difference
Wind-catcher	26°C	North	7m/s	0.4%	-13.9%
Wind-catcher	26°C	North	3.6m/s	1.0%	-27.7%
Wind-catcher	35°C	North	3.6m/s	0.7%	-27.6%
Wind-catcher	26°C	Buoyancy		1.9%	-31.4%
Wind-catcher	35°C	Buoyancy		0.6%	-30.2%
PDEC-WC 10L/h	26°C	North	7m/s	-1.4%	-67.0%

Higher indoor air temperatures were predicted at the lower floors relative to the top apartments (Figure 6.73). Higher values of indoor air velocity, up to 3m/s, were predicted at the top apartments and very low at the case study apartment (first floor).

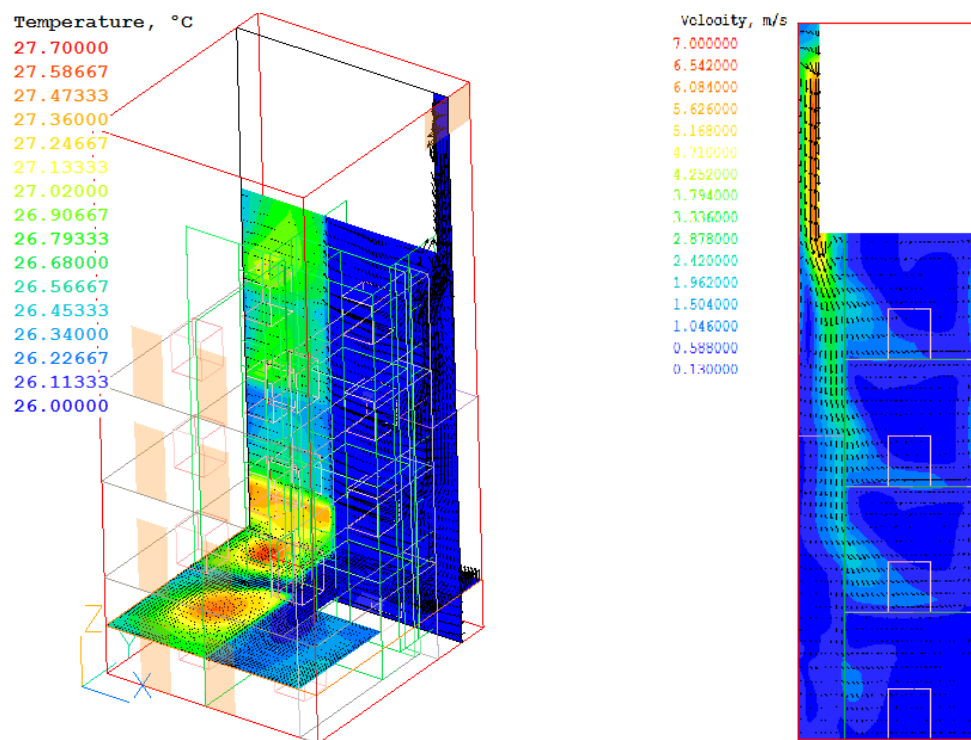


Figure 6.73 Air temperature contours and vectors on xyz view (left) and of velocity on xz plane (right) during wind-driven ventilation of the [WC] strategy (north, 7m/s at 26°C) showing the flow field in the four building floors and apartments

The difference between the two modelling techniques, with regard to the apartment's ventilation performance was established. This difference was smaller for wind-driven flows than for buoyancy-driven. The 1/4th operation predicted higher indoor air temperatures in the case study apartment by approximately 0.7% and lower air velocities by 23% (see Figure 6.74 and Figure 6.47). For the buoyancy-driven flows, higher indoor air temperatures by 1.2% and lower air velocities by approximately 31% were predicted (see Figure 6.75 and Figure 6.38). On the contrary, lower indoor air temperatures by 1.4% were predicted for the PDEC strategies. The average error - the indoor air temperature difference between the two modelling methods - was predicted to be 1% that was considered insignificant. However, the averaged difference of the indoor air velocities between the two modelling processes was 33%. This substantial difference needs to be valued when reviewing simulation results from the stand-alone case.

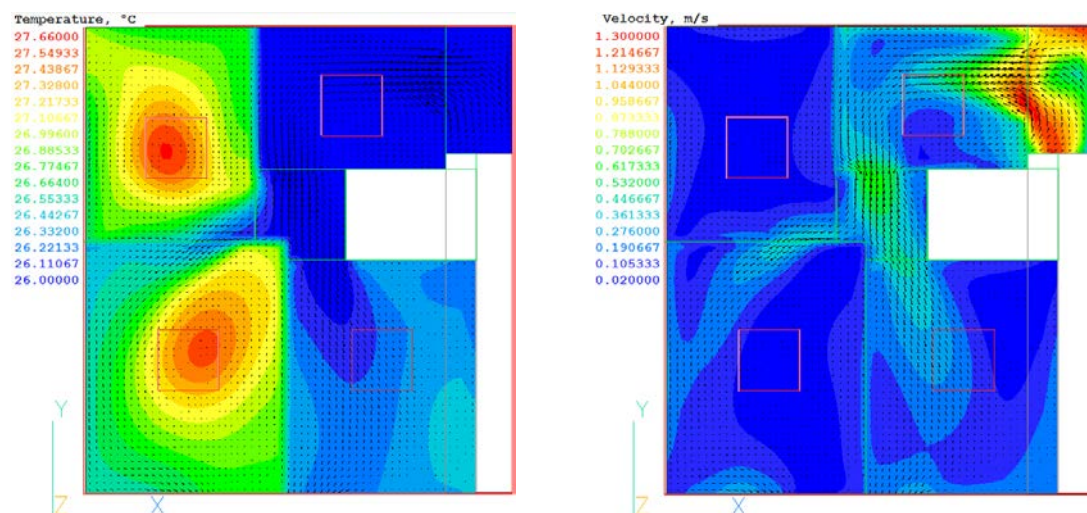


Figure 6.74 Temperature (left) and velocity (right) contours and vectors on xy plane, during wind-driven [WC] strategy (north, 7m/s at 26°C) of the apartment modelled with the top 3 floors

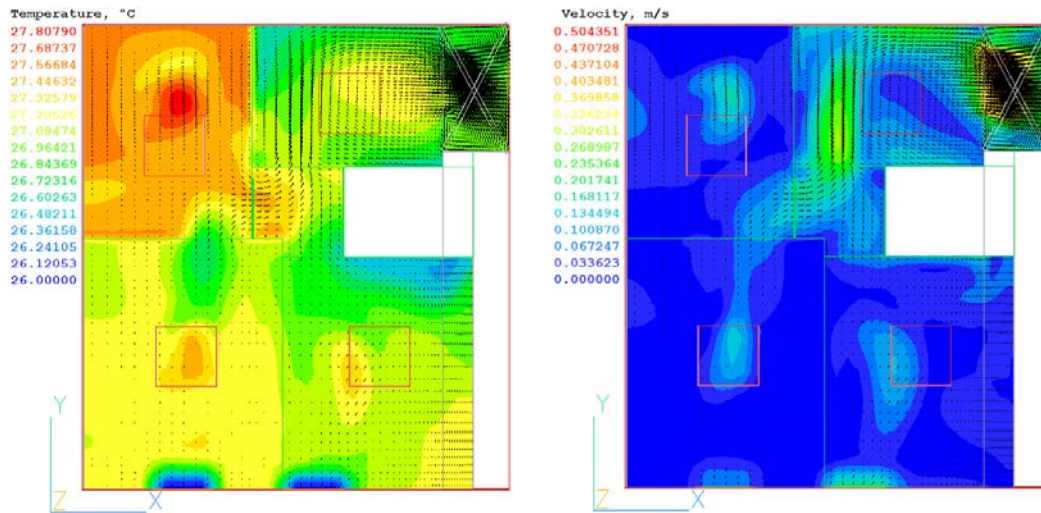


Figure 6.75 Temperature (left) and velocity (right) contours and vectors on xy plane, of the buoyancy-driven wind-catcher strategy (26°C) of the apartment modelled with the top 3 floors

Further, the ventilation potential across all four floors, was evaluated. As presented in Figure 6.76, for each ventilation strategy the predicted ventilation rates at the location of the two bedroom openings varied significantly with the increase of the building height. During buoyancy-driven flows, the ventilation rates reduced in response to the increase in the building height at a constant rate and by approximately 56%. Smaller fluctuations were predicted between the first and second floors. During the wind driven [PDEC-WC] strategies, ventilation rates reduced towards the upper floors.

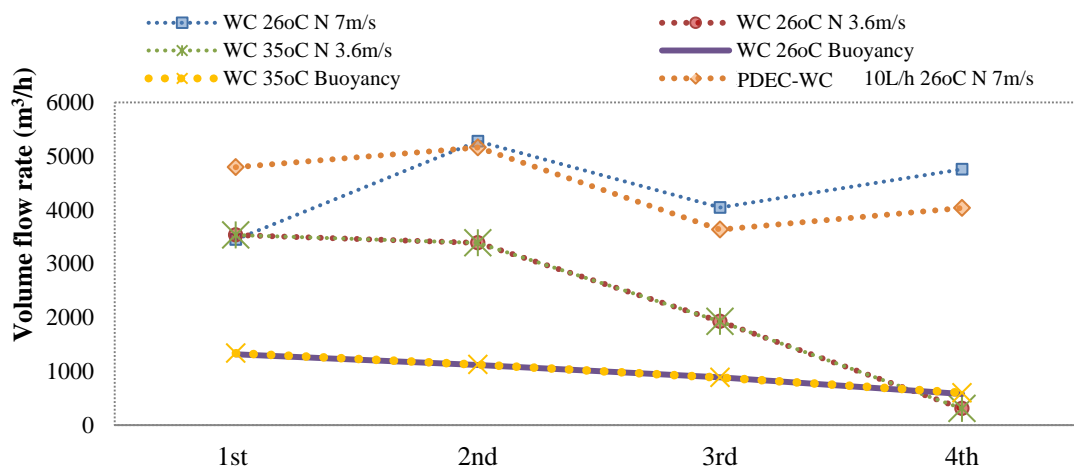


Figure 6.76 Volume flow rates (m^3/h) predicted in the bedroom openings of each apartment studied, at the four floors, for six ventilation strategies

Further to this, indoor average values of air temperatures and velocities were predicted at a horizontal plane (at 1.5m distance above each apartment's floor,) (Table 6.13). Indoor air temperatures varied between 0.3°C to 2°C across the four apartments, with the least difference predicted during buoyancy and wind driven flows of 7m/s wind speed. The cooling performance of the PDEC reduced towards the upper floors due to the reduced length of the water evaporation zone. A possible solution to this would be to create two zones of water evaporation within the same shaft, by installing two spraying systems. One would assist the upper two apartments (larger volume of water) and one at a lower level the lower apartments. This strategy was evaluated with exploratory simulations, although convergence was difficult to achieve; further work would be required to optimise this.

Furthermore, air velocities at a horizontal plane varied between 0.01m/s to 0.6m/s across the four apartments. Lowest values were predicted during buoyancy-driven flows and highest for the PDEC system. The PDEC strategy delivered greater cooling at the lower apartments although provided higher ventilation rates in the upper apartments. Redesign and relocation of the openings (currently fully open, same cross section areas at all spaces), particularly of the upper floor apartments, would potentially optimise the performance of the ventilation strategies evaluated and deliver occupants' comfort expectations.

Table 6.13 Predicted indoor average air temperatures and velocities at a horizontal plane (1.5m height above each apartment floor) for the natural ventilation strategies studied at the four apartments

Apartment		1 st	2 nd	3 rd	4 th	Max-min difference
WC 26°C North 7m/s	°C	26.5	26.3	26.4	26.4	0.27
	m/s	0.22	0.33	0.31	0.39	0.17
WC 26°C North 3.6m/s	°C	26.6	26.5	26.8	27.9	1.45
	m/s	0.20	0.23	0.18	0.14	0.09
WC 35°C North 3.6m/s	°C	35.6	35.5	35.8	36.9	1.45
	m/s	0.20	0.23	0.18	0.14	0.09
WC 26°C Buoyancy	°C	27.1	27.1	27.2	27.4	0.3
	m/s	0.07	0.07	0.07	0.06	0.01
WC 35°C Buoyancy	°C	36.1	36.1	36.2	36.4	0.3
	m/s	0.07	0.07	0.07	0.06	0.01
PDEC-WC 10L/h 26°C North 7m/s	°C	24.3	25.0	25.8	26.2	2.0
	m/s	0.26	0.35	0.32	0.86	0.60

6.9.2. Additional ventilation strategies: Façade wind-catchers

As previously described, the ventilation performance of the apartment with the [DF & WC] strategy was evaluated for the fully open louvres. However, during the incidents of high solar gains, the group of louvres would remain closed, reducing the ventilation potential of the apartment studied. Additional CFD simulations were performed to investigate how the inclusion of additional wind-catchers on the building's façade could enhance the ventilation rates in the front spaces during the high levels of solar radiation (closed louvres operation). The exploratory simulation of this ventilation strategy included the design of a wind-catcher of 1×1.6m cross section area, as described in Chapter 4. This was implemented in the [DF & WC] ventilation strategy. During this strategy [fWC], the apartment would be benefited by the ventilation potential of the simultaneous operation of two wind-catchers, delivering different ventilation patterns.

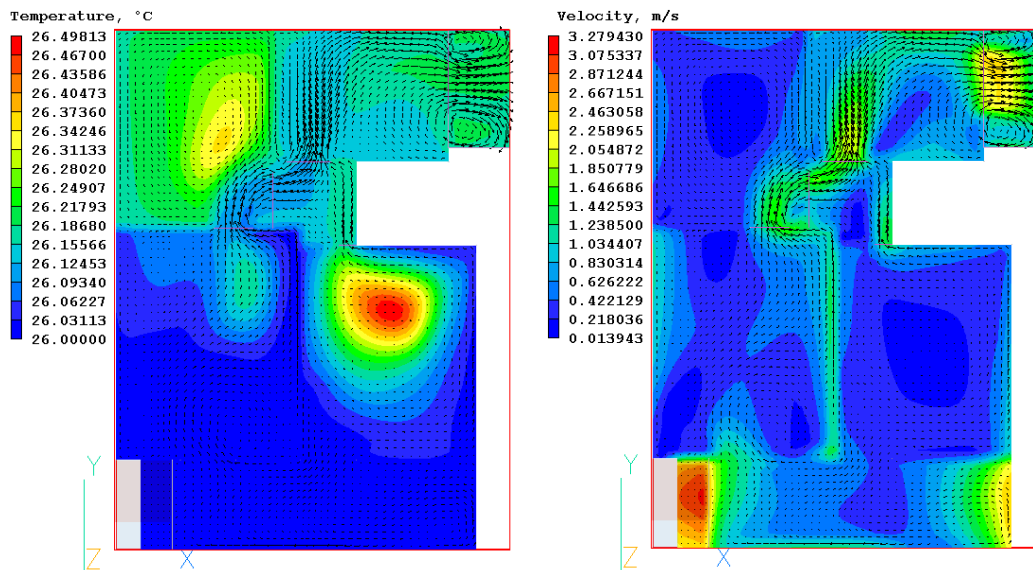


Figure 6.77 Temperature (left) and velocity (right) contours and vectors on xy plane of the selected apartment for the [fWC] strategy (wind-driven flow, north, 7 m/s at 26°C)

This section includes results from one example simulation performed for the wind-driven [fWC] ventilation strategy for north wind speed, of 7 m/s at 26°C DBT. The [fWC] operated as inlet, delivering fresh air to the spaces. Stale air was escaping from the wind-catcher located in the core spaces. During this strategy, captured ventilate air at the top openings of the façade wind-catcher was channelled from the

lower wind-catcher opening into the first and then the second bedrooms (balcony doors). This significantly improved the fresh air distribution in the front spaces, as seen in Figure 6.77. Furthermore, the increased ventilation rates led to reductions in air temperature in the living room, relative to the [DF & WC] strategy (Figure 6.50). The flow path direction and age of the ventilating air are presented in Figure 6.78.

The design of this natural ventilation strategy [fWC] could be improved by the addition of operating partitions located at the balcony zone, able to redirect the airflow to the second bedroom, or with further implementation of the PDEC strategy at one of the two wind-catchers. The potential IAQ benefits of this strategy are upon the fact that would provide ventilation air captured at higher speeds above the building level, in the spaces during the hours of the day with direct solar gains and high DBTs.

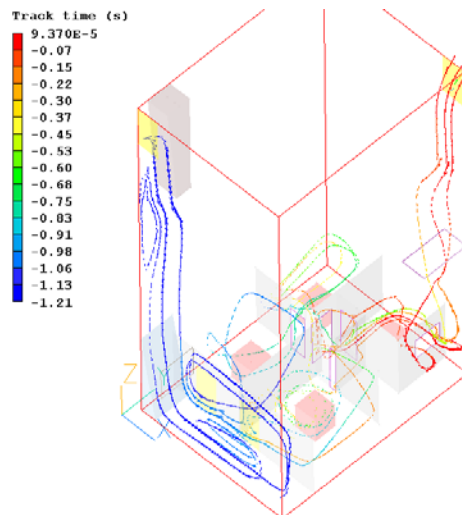


Figure 6.78 Streamlines of the airflow movement in the spaces, showing the inflow and the outflow from the spaces ([fWC], 7m/s north wind, 26°C)

6.9.3. Additional ventilation strategies: Internal openings configuration

Simulation results predicted non-uniform airflow distribution across the occupied spaces for all natural ventilation strategies evaluated. This was due to the layout of the spaces (i.e. internal partitions), the openings' design and position. For example, the living room has no external openings and only two internal openings arranged closely to each other. The significant influence of the spaces layout on the flow and the natural ventilation of the spaces was also reported by Geros et al. (1999) evaluating night ventilation in Greek buildings. The idea of new internal openings that could provide a uniform fresh air distribution was explored. Alternative openings could be implemented at the internal walls of the apartment, e.g. a connecting opening between the living room and the kitchen that could improve the distribution of fresh air to the rear.

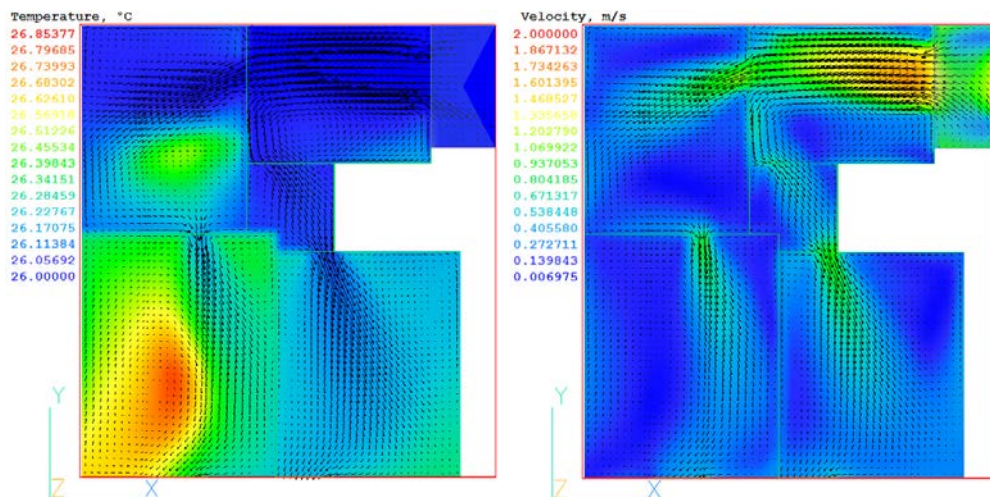


Figure 6.79 Temperature (left) and velocity (right) contours and vectors on xy plane of the selected apartment. New openings configuration for the wind-driven [WC] (north, 7 m/s at 26°C)

Supplementary CFD simulations were performed to investigate the ventilation performance of this strategy for a single climate scenario. The new openings were implemented at the wind-catcher ventilation strategy (North wind, 7m/s wind speed, and 26°C DBT). The internal doors of the two bedrooms were partially open (about 30%). Results indicate indoor air temperature reductions in the living room by more than 0.5°C, and improved airflow distribution, as shown in Figure 6.79, relative to the simulation results from the building design without the new internal opening

presented in Figure 6.47. This strategy delivered increase in indoor air velocities in the living room by up to 1m/s, particularly in the core of the space.

Furthermore, as described in Chapter 4, new internal openings could be designed to connect the occupied spaces to the shaft via the ancillary space on the top of the false ceiling of the bathroom (1.1m height). The thermal performance of this strategy was also evaluated with DTM simulations, presented in Chapter 5.3.7. This ventilation strategy would be suitable when the internal doors would be closed (e.g. bed-time, privacy) in order to assist cross ventilation.

New internal openings were designed at the [WC] ventilation strategy: two small openings on the top or side of the bedroom doors; two openings on the ancillary space above the bathroom (one on the hallway wall and one connecting the space with the air shaft); and partitions above the false ceiling to redirect and channel the flow (see Chapter 4). CFD simulations were performed; the computational mesh was refined at the false ceiling zone to assist the new partition walls and openings. Simulations were performed for a single climate scenario (26°C and 7m/s north wind).

Contour and vectors of Figure 6.80 (at 1.5m height above the apartment floor) indicate low indoor air temperatures in the bedrooms exceeding by maximum 1°C the DBT. Higher by up to 2.5°C air temperatures were predicted in the living spaces relative to the DBT. High ventilation rates were predicted in the ancillary space (Figure 6.81) of more than 6m/s velocity, calculated at 2.5m above the apartment floor. This strategy delivered insufficient IAQ (i.e. air temperature and ventilation rates) in the two living spaces. However, this could be an alternative strategy for cross ventilation when all internal doors would be closed. Further design investigations under various climate conditions, would be required for the design and operation optimization of these two strategies described. This was beyond the scope of this research.

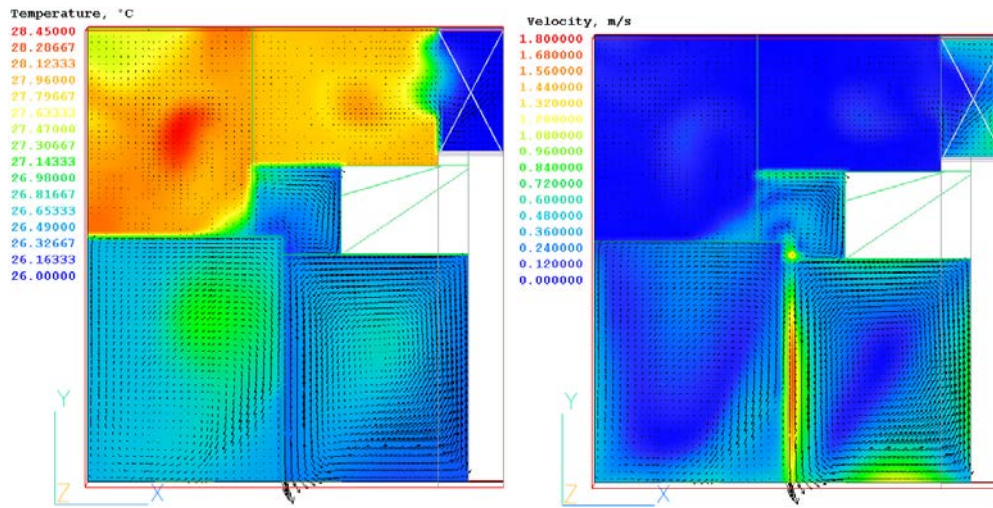


Figure 6.80 Temperature (left) and velocity (right) contours and vectors on xy plane (at 1.5m height) of the apartment studied during wind-driven ventilation of the ‘internal openings’ strategy (north, 7 m/s , 26°C)

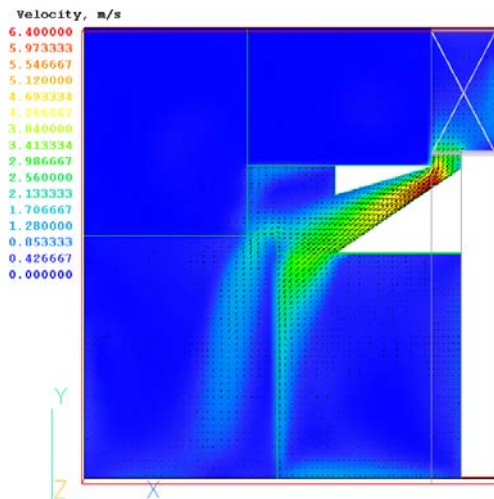


Figure 6.81 Velocity contours and vectors on xy plane (at 2.5m height) of the apartment at the ‘internal openings’ configuration (north, 7 m/s, 26°C)

6.9.4. Performing steady state CFD simulations: Justification

Accompanying study by Lin (2014) within the context of this research project, evaluated the differences between the time-dependent and steady state CFD simulations when modelling natural ventilation. A number of transient CFD simulations in PHOENICS were performed, for the case study apartment and the cross ventilation strategy [CV]. The boundary and environmental conditions (e.g. external air temperature, wind speed, indoor wall surface temperature, and heat gains) were modified as a one-step-change function, in order to study the response time of the buoyancy and/or wind-driven airflow regimes. Time-dependent simulation results with a time step of 5 to 30 minutes performed at real-time of up to 24 hours, were plotted against steady state simulation results. The simulations were performed using the building geometry and computational domain characteristics described in Section 6.4.

The response time of the indoor air properties to the changing outdoor conditions was predicted as low as one minute for wind-driven flows, depending on: the type of boundary conditions varied; the fluctuation range; and the distribution of heat sources in the spaces. Indoor air temperature experiences the slowest response time, reaching up to 30 minutes, compared to the air velocity and pressure. Despite this, air velocity and pressure responded faster to the variation of the wind speed (e.g. less than 2 minutes), rather than for variations of the DBT (9-17 minutes until 99% change).

Additionally, the time-dependent simulations performed for two levels of change of outdoor air temperature and wind speed, predicted values of indoor air properties in agreement to the values predicted during individual steady state simulations for these conditions. Strong correlation between the steady state and time-dependent results was observed of less than 0.1% error and 1%, with regard to variations of outdoor air temperature and wind speed respectively. All these, justify the use of the steady state modelling when evaluating natural ventilation in buildings.

6.10. Discussion

This chapter reported the ventilation performance evaluation of the natural ventilation strategies implemented in the case study building, using CFD modelling techniques. The performance of natural ventilation strategies was evaluated with regard to their potential: to deliver lower indoor air temperatures (i.e. equal to the DBT or lower); to enhance the ventilation rates (i.e. higher to the [SS]); and to deliver comfort ventilation.

The addition of a wind-catcher [WC] to the building design, significantly improved the IAQ upon the other ventilation strategies. The inclusion of the dynamic façade [DF & WC] has been the most efficient strategy with regard to the ventilation rates improvement, while the introduction of the PDEC system appears to be the most efficient strategy in indoor air temperature reductions. It was further explored how alterations to the building design (e.g. new internal openings) and different openings' operation modes (e.g. partially open external openings) could further enhance the performance of the examined natural ventilation strategies and provide uniform temperature reduction in the spaces. However, optimization of these designs was outside the scope of this research.

The performance of the CFD simulations was significant in predicting driving pressures due to wind at the building openings, with regard to the building geometry and the surrounding buildings. This assisted the efficient evaluation of the wind driven strategies in the case study building within its context, which the DTM simulations could not provide. Although the CFD simulation results predicted ventilation performance under steady state conditions, they are representative of real world behaviours and are considered realistic. However, these would vary throughout the ventilation period with regard to: the occupants, the building characteristics (thermal mass) and environmental conditions, as shown by the DTM results.

***Chapter 7* : FURTHER ANALYSIS AND DESIGN IMPLICATIONS**

7.1. Introduction

This chapter investigates the relationship between steady state CFD and time-dependent DTM simulation results. Broad patterns in ventilation performance were extrapolated with regard to the operation and performance of the natural ventilation strategies and apartment building investigated. Statistical methods were employed to provide further visual representation of the results. The results from the parametric sensitivity analysis included in this chapter contributed to the overall output of this research, summarised in an example low-energy refurbishment design guide. The example guide includes recommendations for potential natural ventilation refurbishment studies in existing apartment buildings in the Mediterranean Region.

7.2. Establishing Relationships between Driving Pressure, Wind Speed and Ventilation Rates

Following the CFD modelling work described in Chapter 6, the relationship between pressure difference across the openings and the wind speed was established in order to evaluate and validate the model outputs. The study of the external flow (Chapter 6.5) provided driving pressures for a number of wind scenarios evaluated, and for the three building models and ventilation strategies (simple-ventilation, wind-catcher and dynamic façade), described in Chapter 6.3. The three ventilation strategies were evaluated for an additional number of wind speeds in CFD, in order to provide further driving pressures. This would subsequently generate multiple points for the relationships investigation between different variables. The setup description and results from these simulations were not previously presented in Chapter 6 as the climate scenarios performed for, were out of the scope of the performance evaluation of the ventilation strategies. These are included in Table A.4 of Appendix A.3. The

additional and existing simulation results defined the relationship between wind speed and driving pressure for one wind direction. This relationship was further projected at the wind directions of each strategy with only two data points.

For the building models of [CV], [WC] and [DF & CV] natural ventilation strategies, the relationship between driving pressures and wind speeds is presented in Figure 7.1, Figure 7.2 and Figure 7.3 respectively. The relationship established in all cases, $\Delta P \propto U^2$ agrees with Bernoulli's equation:

$$\Delta P = 1/2 \cdot C_p \cdot \rho \cdot U^2 \quad (7-1)$$

where C_p is the wind pressure coefficient, ρ is the air density, U the velocity through the openings (m/s) and therefore provides confidence in the CFD model of the external flow and the results predicted.

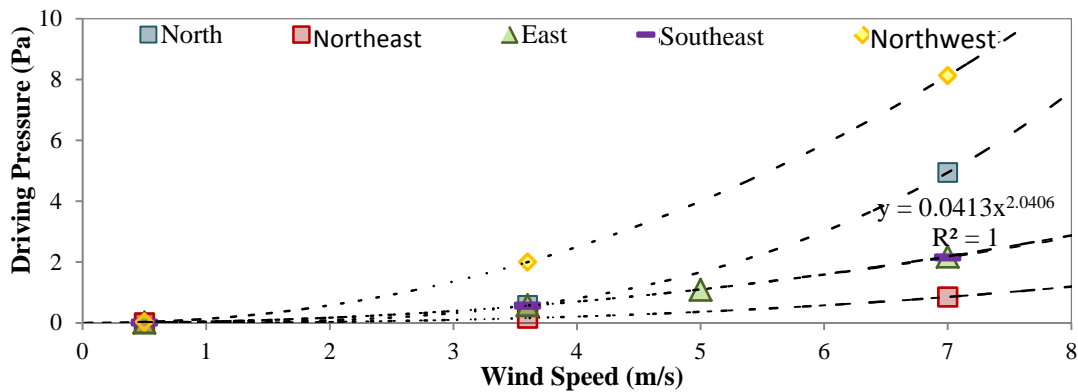


Figure 7.1 Relation of wind speed and pressure difference across the openings for the [CV] strategy

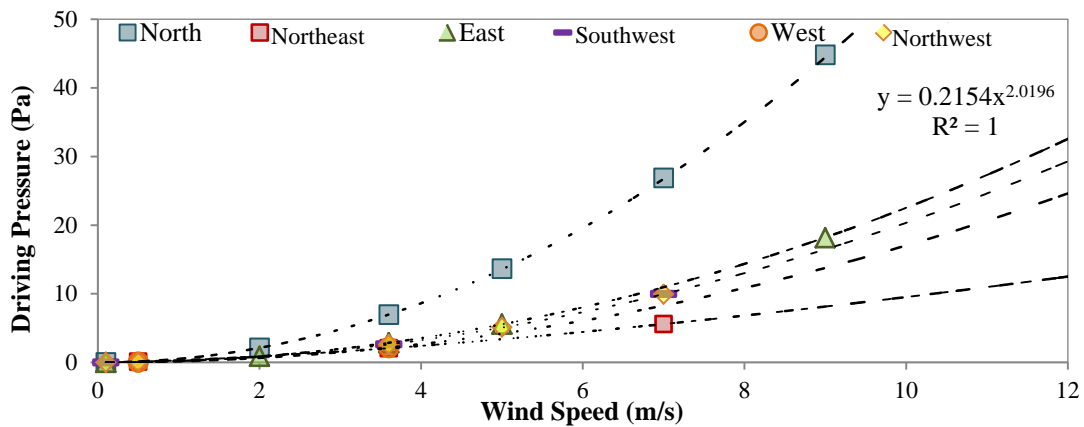


Figure 7.2 Relation of wind speed and pressure difference across the openings for the [WC] strategy

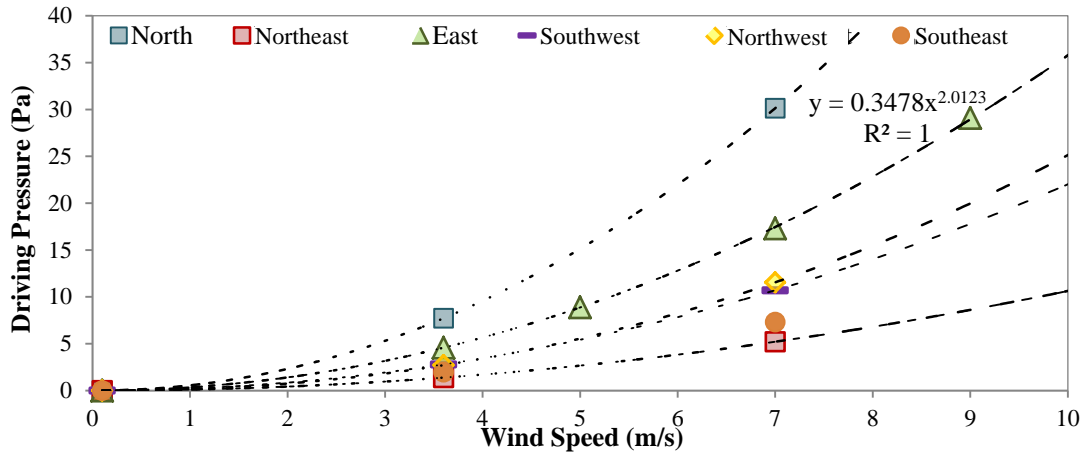


Figure 7.3 Relation of wind speed and pressure difference across the openings for the [DF & WC] strategy

As described in Chapter 6, the predicted driving pressures of the external flow were used as inputs for the study of the ventilation performance of the internal building spaces, and thus assisted the prediction of the ventilation rates and defined the $Q-\Delta P$ relationship. Figures 7.4-7.8 express the relationship between pressure difference across the openings and volumetric flow rates for five natural ventilation strategies ([CV], [WC], [DF & WC], [PDEC-WC] and [PDEC-DF]). Similar power regression equations were defined, with high R^2 values (close to 1) suggesting that the regression model appropriately explains the variation between the two variables.

As described in CIBSE Guide B (CIBSE, 2005), when the airflow rate due to wind is higher to the airflow rate due to only temperature difference, then the total airflow rate due to temperature difference and wind is equal to the airflow rate due to wind alone. The relationship between airflow rates is defined by the equation 2.11 in CIBSE B, showing $Q_w \propto \Delta C_p^{0.5}$ where Q_w is the airflow rate due to wind alone (m^3/s) and ΔC_p is the difference in pressure coefficient between inlet and outlet. The relationship defined by CIBSE Guide B justifies the relationship predicted by all five natural ventilation strategies and therefore evaluates the CFD model of the internal flow study presented in Chapter 6.4.

The Figures 7.1-7.3 and the Figures 7.4-7.8 could be used by designers to predict the driving pressures and the ventilation rates in the spaces, using the wind speeds of the climate under investigation. These could assist the implementation of the selected natural ventilation strategies in similar buildings and microclimates. The following section explores the direct relationship between ventilation rates and wind speed.

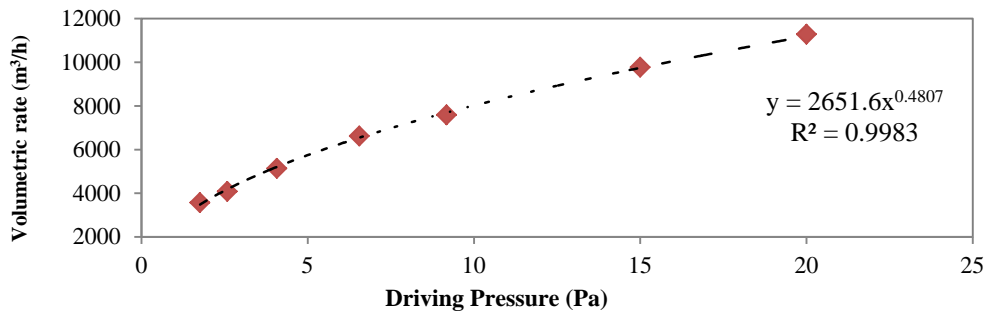


Figure 7.4 Relation of driving pressure at the openings and ventilation rates, [CV] strategy

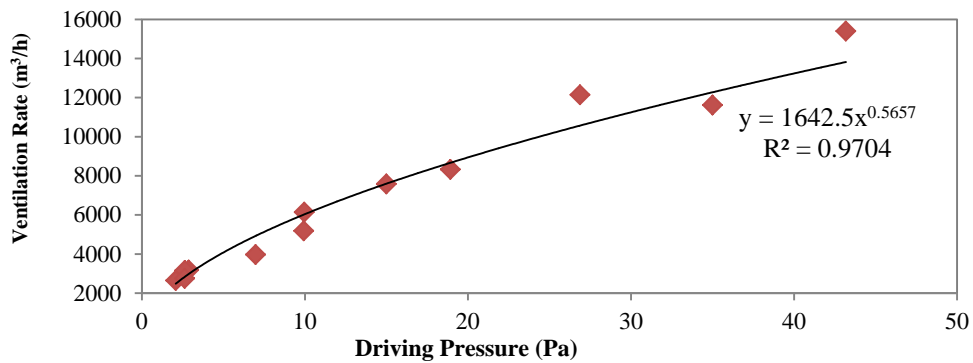


Figure 7.5 Relation of driving pressure in the openings and ventilation rates, [WC] strategy

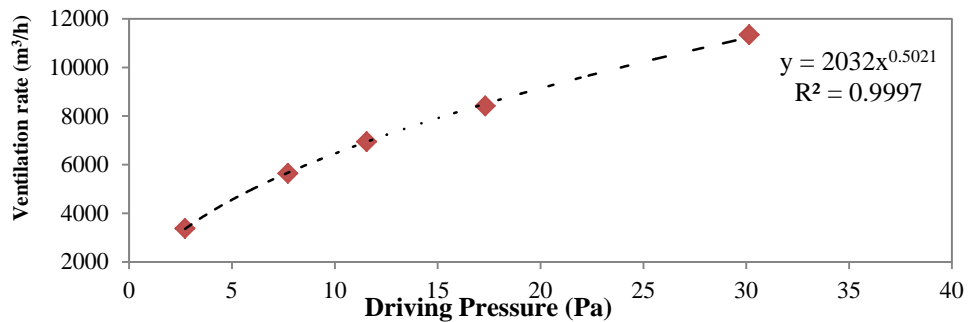


Figure 7.6 Relation of driving pressure at the openings and ventilation rates, [DF & WC] strategy

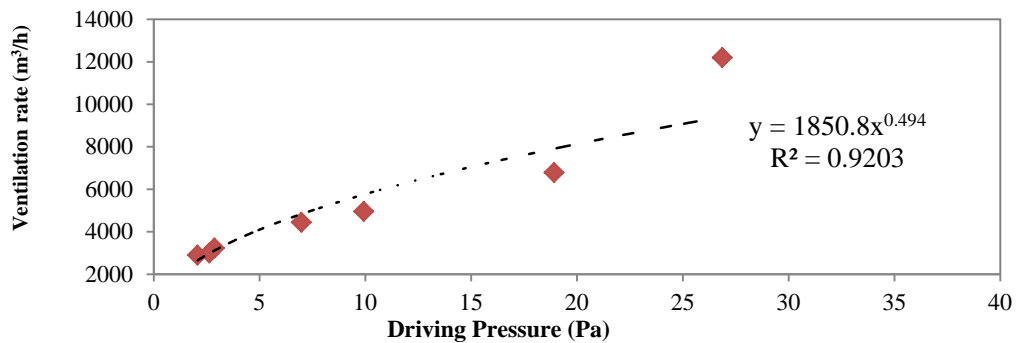


Figure 7.7 Relation of driving pressure at the openings and ventilation rates, [PDEC-WC] strategy

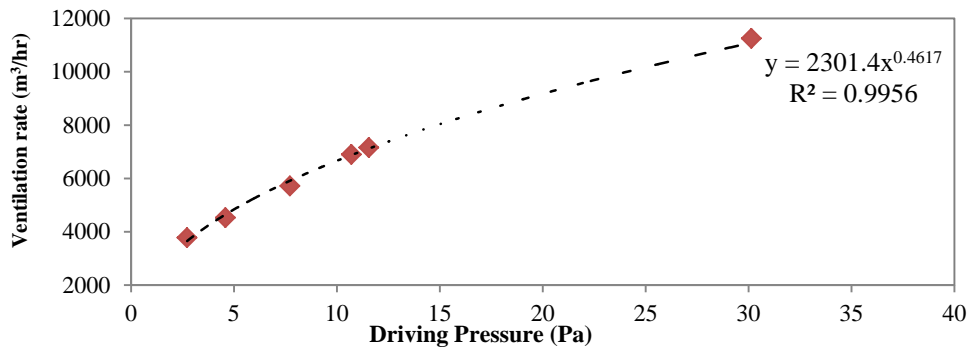


Figure 7.8 Relation of driving pressure at the openings and ventilation rates, [PDEC-DF] strategy

7.3. Defining Relationships between Ventilation Rates and Wind Speeds for the Climate Studied

The two relationships predicted between the driving pressure and wind speed, and the ventilation rates and driving pressure, for each ventilation strategy, were employed to establish the relationship between wind speed and ventilation rates. Ventilation rates were analysed as functions of the wind speed, wind direction and temperature difference (internal and external). The corrected values of wind speed included at the climate file of the site, were plotted in tables for each wind direction, and graphs of the ventilation rates and wind speeds were plotted. The same process was repeated for each natural ventilation strategy.

Wind direction			
Wind speed-U (m/s)	Driving pressure (Pa)	Ventilation flow rates (m³/hr)	Internal-external temperature difference (%)
Measured values - Climate file	$\Delta P \propto U^2$	$Q \propto \Delta P^{0.5}$	$\Delta T \propto Q$

Meteorological climate files contain wind data collected in meteorological stations in open country sites, at the height of 10m. It is recommended by CIBSE Guide A (CIBSE, 2006) to proceed to corrections of the wind speed by specifying the terrain conditions and the building heights. An approximate correction is given by the Equation 4.5 in CIBSE Guide A (CIBSE, 2006):

$$v_z = v_m \cdot k \cdot z^a \quad (7-2)$$

where v_z is the wind speed at the building height (m/s), v_m is the wind speed measured at 10m height (m/s), z is the building height (m), k and a are constants dependent on the terrain. For the k and a constants, the values of 0.35 and 0.25 were used respectively are recommended by CIBSE Guide A for urban areas (Table 7.2).

Ventilation rates increased approximately linearly with wind speed for each wind direction, as expected, see Figures 7.9-7.13. However, some Q-U relationships show non-linearity (e.g. for North wind direction of the cross ventilation strategy, shown in Figure 7.9 and for northeast in Figure 7.12). This is hypothesised to be a result of: extrapolating beyond the range of wind speed values for which the original P-Q relationship was defined; assuming a Q-U relationship through two data points in certain cases; and/or complex external airflow-surrounding building interaction and natural ventilation system's design. Table 7.1 includes the range of values within which relationships were defined for five natural ventilation strategies.

Table 7.1 Interpolation within different ranges of volumetric flow rates for each strategy

Strategy	Range of values (m ³ /hr)	Figure presented
Cross ventilation	1622 - 11287	Figure 7.9
Wind-catcher	1762 - 16564	Figure 7.10
Dynamic façade	1829 - 11343	Figure 7.11
PDEC-WC	2899 - 12194	Figure 7.12
PDEC-DF	3782 - 11252	Figure 7.13

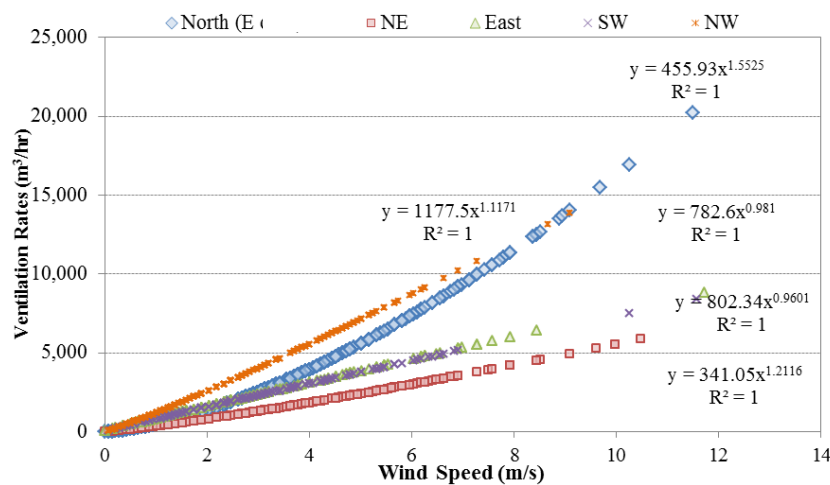


Figure 7.9 Ventilation rates as a function of wind speeds of the [CV] strategy

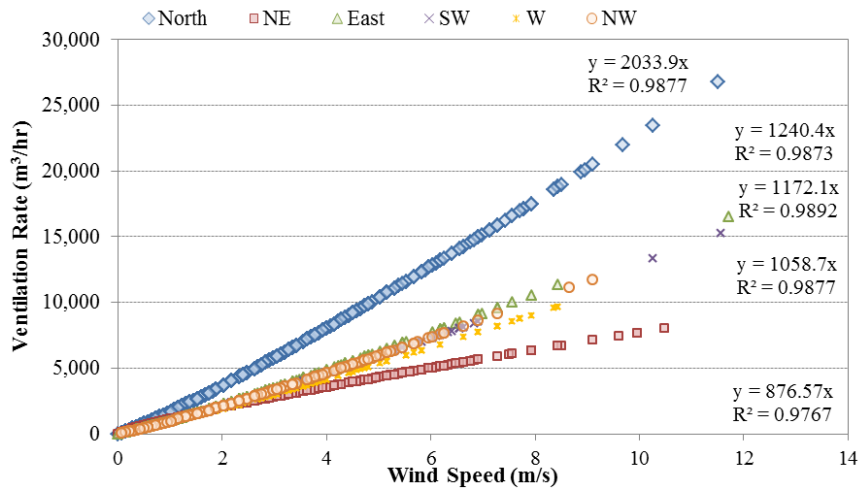


Figure 7.10 Ventilation rates as a function of wind speeds of the [WC] strategy for various wind directions

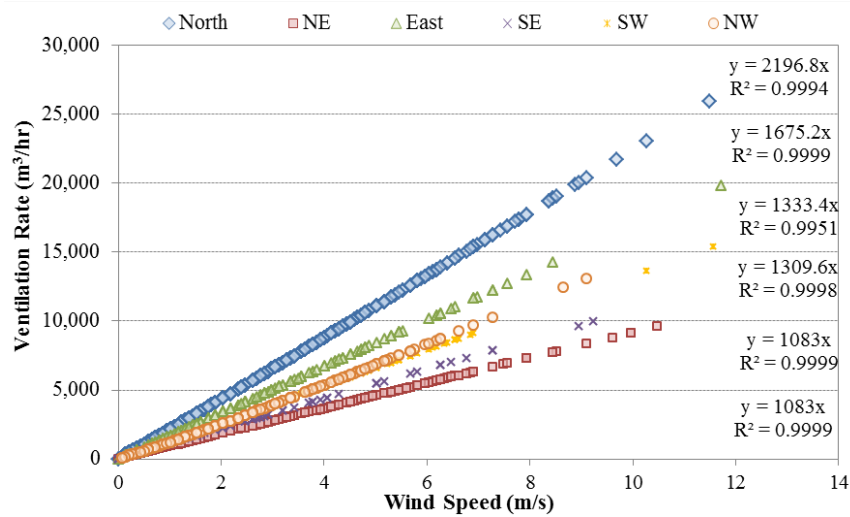


Figure 7.11 Ventilation rates as a function of wind speeds of the [DF & WC] strategy

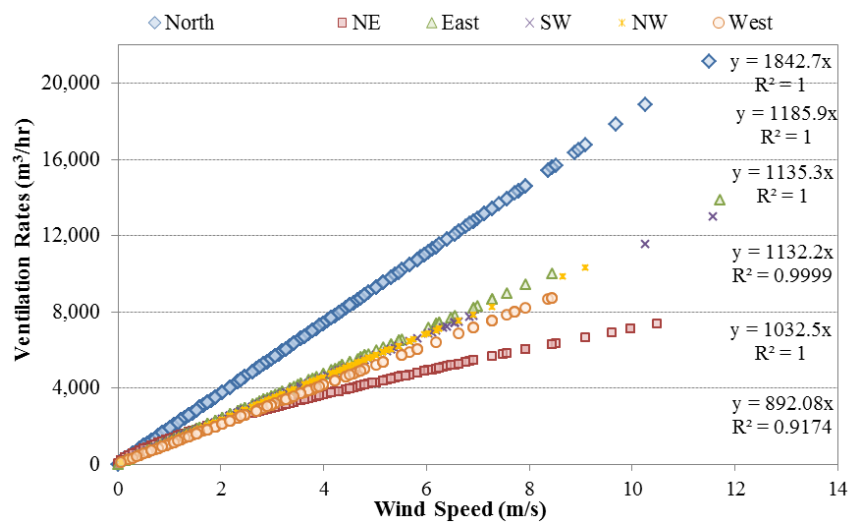


Figure 7.12 Ventilation rates as a function of wind speeds of the [PDEC-WC] strategy

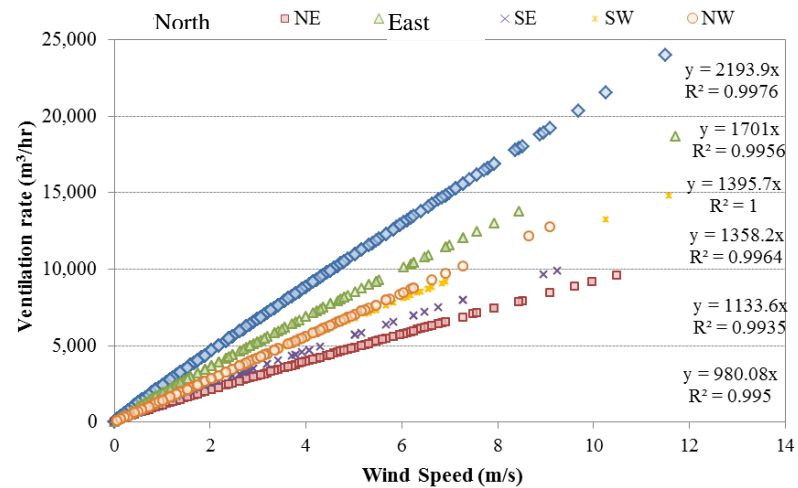


Figure 7.13 Ventilation rates as a function of wind speeds of the [PDEC-DF] strategy

7.4. Defining Relationships between Indoor Air Temperatures and Wind Speeds

Average indoor air temperatures of the apartment studied at 1.5m height were used to establish the relationship between indoor air temperature and ventilation rates. The temperature change due to the ventilation rates varies for different DBT values, although the relationship remains the same for all natural ventilation strategies examined, as shown in Figures 7.14-7.18. The relationships were defined for specific range of values (Table 7.1). Indoor air temperatures are dependent on the ventilation rates. For the [CV], [WC], [DF & WC] strategies, the increase of the ventilation rates intensifies the temperature reduction in the spaces. After a certain value, equilibrium is reached between the indoor and outdoor temperatures. However, for the [PDEC] strategies, the increase in ventilation rates reduces the systems' cooling performance (Figure 7.17 and 7.18); this strategy performs better for lower wind speeds.

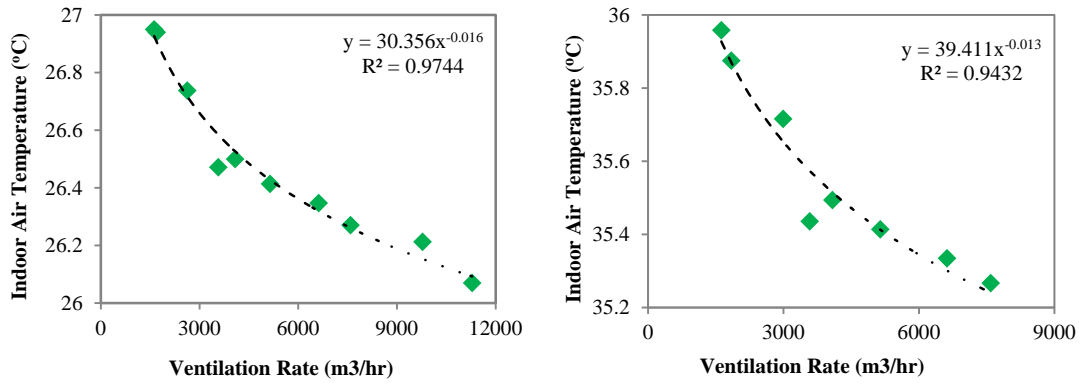


Figure 7.14 Indoor air temperature and ventilation rates relationship for the [CV] strategy for DBT 26°C (left) and 35°C (right)

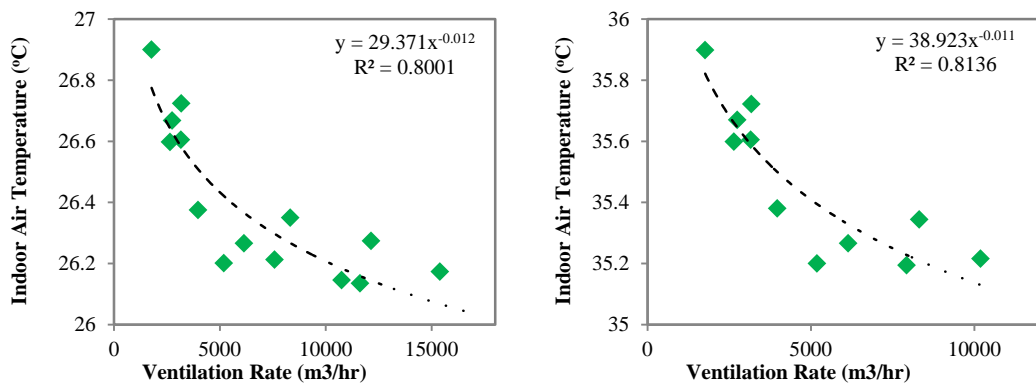


Figure 7.15 Indoor air temperature and ventilation rates relationship for the [WC] strategy for DBT 26°C (left) and 35°C (right)

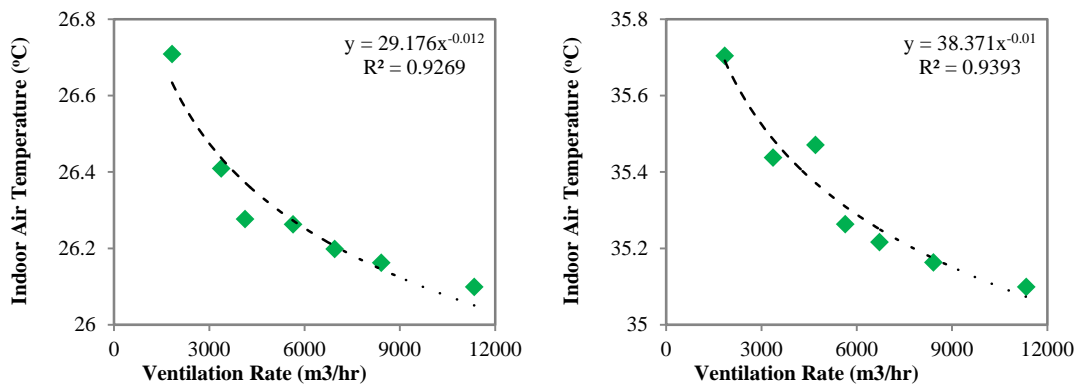


Figure 7.16 Indoor air temperature and ventilation rates relationship for the [DF & WC] strategy for DBT 26°C (left) and 35°C (right)

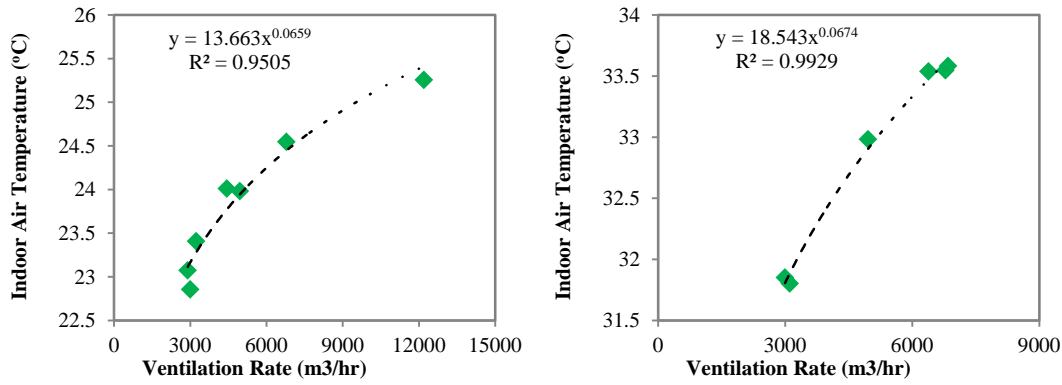


Figure 7.17 Indoor air temperature and ventilation rates relationship, [PDEC-WC] strategy for DBT 26°C (left) and 35°C (right)

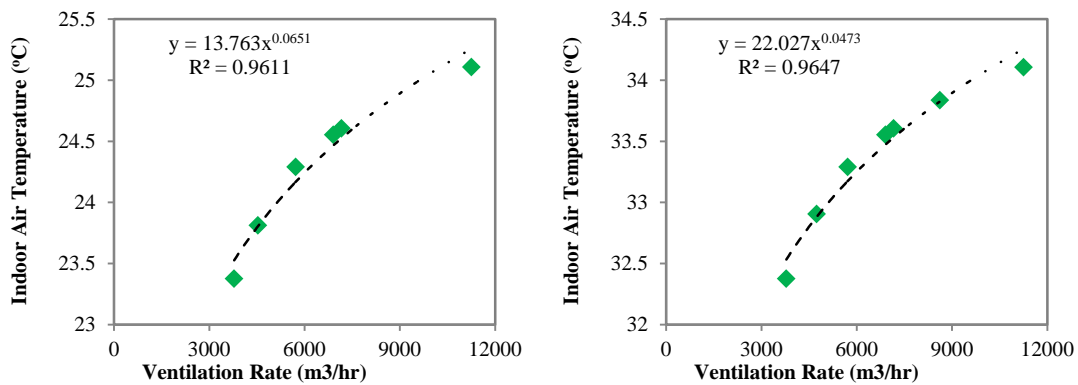


Figure 7.18 Indoor air temperature and ventilation rates relationship, [PDEC-DF] strategy for DBT 26°C (left) and 35°C (right)

The predicted relationships between the temperature difference (internal-external, ΔT) and the ventilation rates for the [CV], [WC] and [DF & WC] strategies and the two DBTs examined (26°C and 35°C) were evaluated. During low ventilation rates, up to the 1000m³/hr, the temperature difference for both the external temperatures was predicted comparable. Beyond this value the cases with higher external temperature (35°C) began to generate greater temperature differences by small magnitudes of up to 0.23°C (at [CV] strategy for 10,000m³/hr ventilation rates), as shown in Figure 7.19. This shows that although the higher external temperatures would potentially impair occupants comfort, the performance of the strategies would improve although to a small degree.

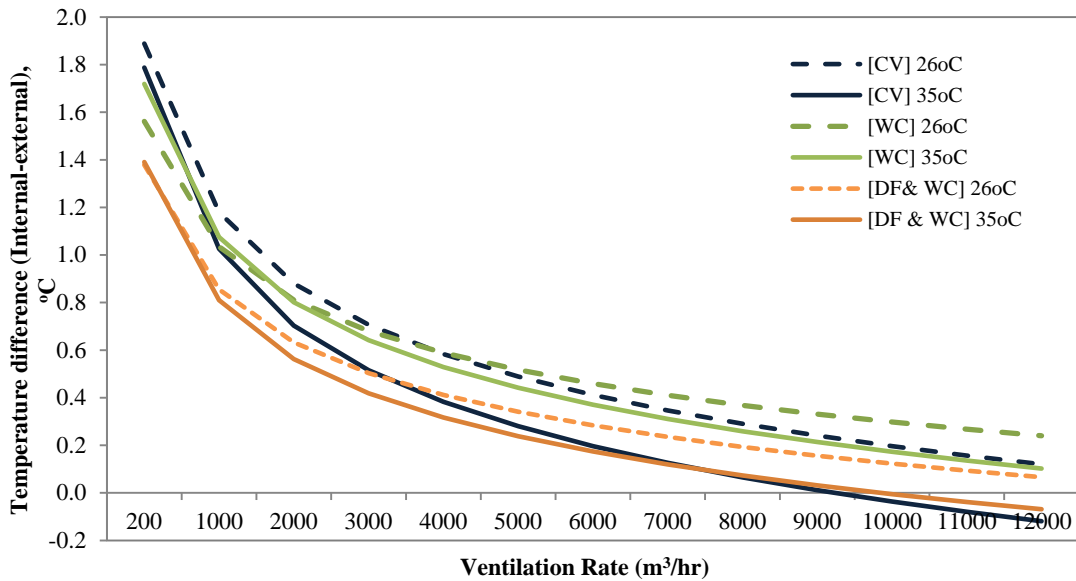


Figure 7.19 Relationship between temperature difference (internal-external, ΔT) and ventilation rates for three natural ventilation strategies (for 26°C and 35°C external temperatures)

7.4.1. Projecting the relationship between wind speed and temperature difference

Following the relationship established in Figure 7.19 between ventilation rates and resulted temperature change due to the natural ventilation strategies, the relationship between wind speed and temperature change was evaluated Figure 7.20. For each natural ventilation strategy, the predicted indoor air temperatures for the various wind directions were averaged in order to provide a single relationship between these variables, as shown in Appendix B for 26°C DBT. It was predicted that the cooling performance of all natural ventilation strategies examined would vary for the two DBTs examined (26°C and 35°C) during the lowest wind speeds (on average below for wind speeds below 2m/s). However, the cooling performance of the [PDEC-WC] significantly varies for the two DBTs, showing better performance for the higher DBTs. Overall, indoor air temperature change was more sensitive to the wind speed change than the external temperature change, thus prediction of ventilation performance could be possible with regard to wind direction.

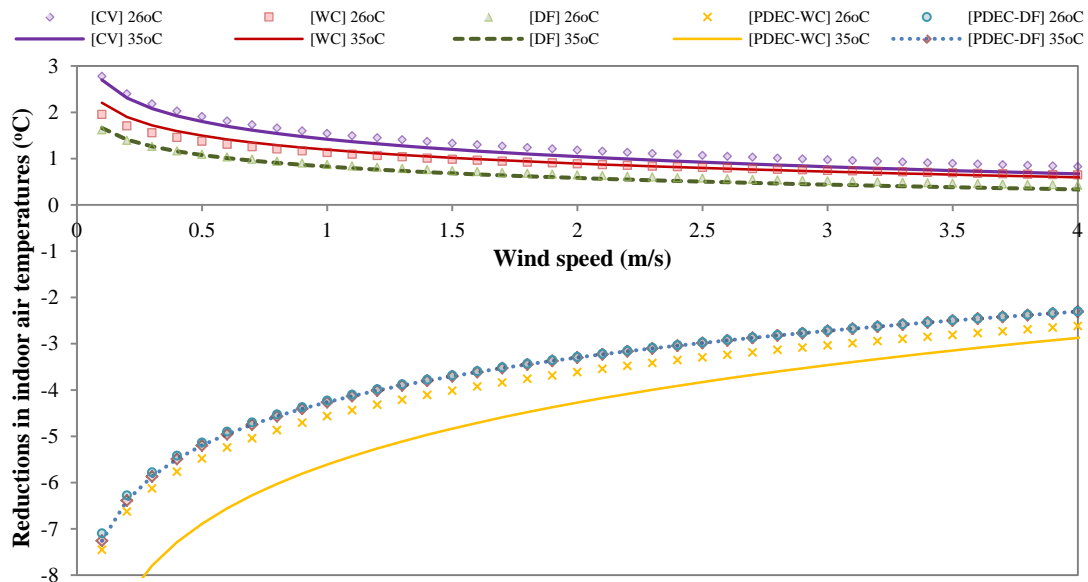


Figure 7.20 Predicted indoor air temperature with regard to the wind speed and each ventilation strategy examined, for 26°C and 35°C DBTs and wind speeds below 4m/s

The relationships established in Figure 7.20 between resulted indoor temperature change and wind speed were averaged for the two DBTs and each ventilation strategy (Figure 7.21). Although the relationship defined between the temperatures and wind speed (for 26°C DBT) is not otherwise established, it is an indication of the performance of the evaluated strategies under specific air temperatures (Figure 7.21).

Empirical relationships were developed from simulation results that could be used to predict ventilation performance behaviours under conditions that have not been examined using simulations. Higher wind speeds enhance the cooling performance of the [CV], [WC], and [DF] strategies. After a certain value of wind speed (different for each strategy), equilibrium is reached between the internal-external thermal environments. On the contrary, the cooling performance of the PDEC strategies reduces with the wind speed increase. The performance of the strategies varies during the lower wind speeds:

- For buoyancy driven flows (considered for wind speeds below 0.5m/s) the combined [DF & WC] strategy provides up to 1°C lower indoor air temperatures than the [CV] and the [PDEC-DF] up to 8°C
- For average wind speeds (3.6m/s), the combined [DF & WC] strategy provides up to 0.4°C lower indoor air temperatures than the [CV] and the [PDEC-DF] up to 3.7°C.

- For higher wind speeds (8m/s), the [CV], [WC] and [DF & WC] strategies provide the same amount of natural cooling (0.2°C difference) and the [PDEC-DF] up to 1.9°C lower indoor air temperatures than the [CV].

The difference between the external and internal temperatures was predicted with steady state CFD simulations. The simulations were performed for the maximum ventilation potential of the case study apartment (openings fully open) and without taking into consideration the building's thermal mass. Due to the internal heat gains, higher indoor air temperatures than the external were predicted for the strategies without evaporative cooling. Under real world conditions, the thermal mass would regulate the indoor air temperatures, as predicted using DTM results described in Chapter 5, and therefore the strategies would provide further cooling. However, the relative difference between the performances of the difference strategies would remain the same.

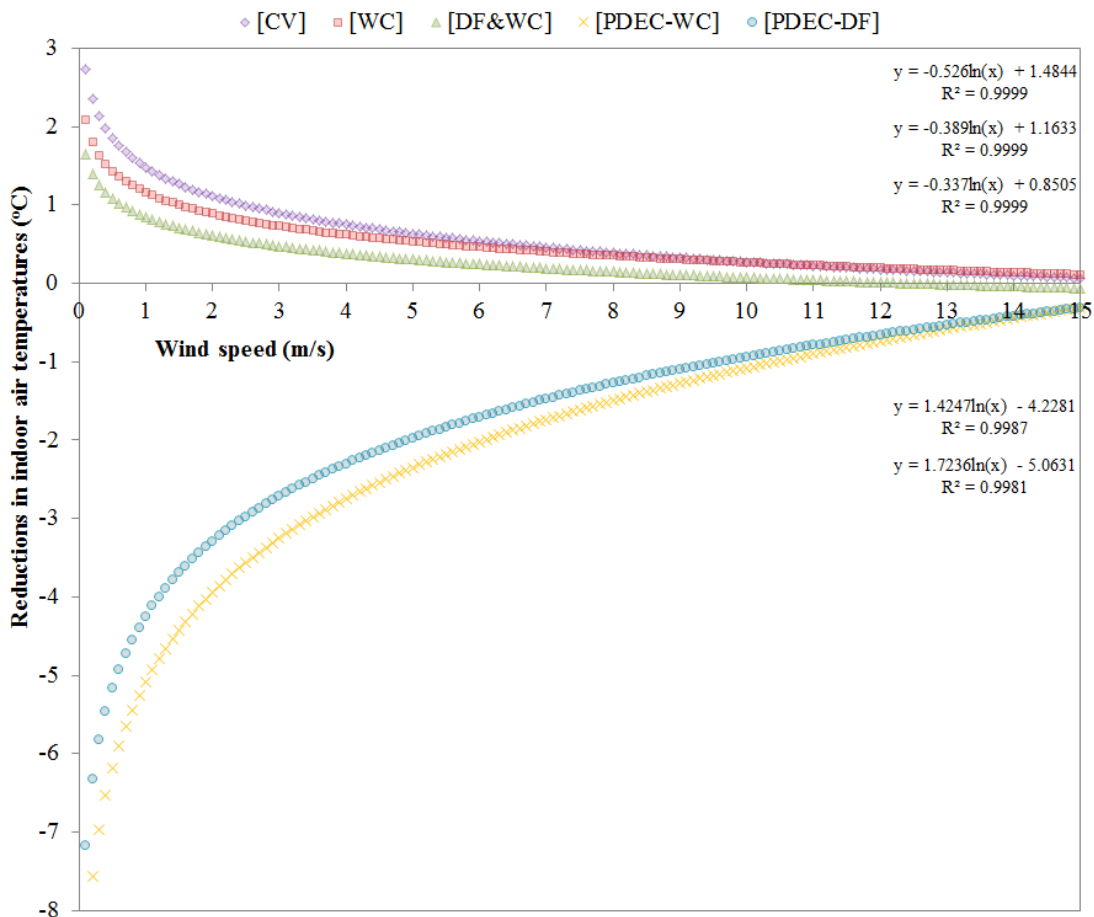


Figure 7.21 Predicted indoor air temperature with regard to the wind speed and each ventilation strategy examined, averaged values for 26°C and 35°C DBTs

7.5. Comparative analysis: DTM-CFD simulation results

The previously established relationships between ventilation rates, wind speeds, and internal air temperatures of the steady state CFD simulation results, were further explored under the influence of time-dependent variables. These included: the occupancy profile; the internal gains; the solar gains; the openings' operation in response to different variables; and the thermal mass. The DTM hourly simulation results during a four-month period were presented in Chapter 5. A parametric sensitivity analysis was performed to explore how the ventilation performance of the different strategies varies in response to a number of variables.

The wind speed values were corrected according to Equation 7-2 recommended by CIBSE Guide A (CIBSE, 2006). Different k and a constants were used than previously for the wind correction of the CFD results (Section 7.3). For the DTM results, k and a constants were selected according to the IESVE manual (values from ASHRAE Handbook of Fundamentals, 2001) in order to be in agreement with the model setup of the simulations (IESVE, n.d.), see Table 7.2.

The building is located in an 'urban' area (according to CIBSE Guide A values), although due to lack of respective values for the k and a CIBSE Guide A within the IES, the category 'suburbs' was selected. Therefore, for building height of 18m, the correction equation is predicted to be equal to:

$$v_z = v_m \cdot 0.4319 \cdot 18^{0.22}$$

The relationships established between the CFD results of wind speed and ventilation rates were further explored for the DTM simulation results (included in Chapter 5), presented in the following sections: [base-case] strategy (7.5.1); [DV & NV] ventilation (7.5.2); [WC] (7.5.3); and [DF & WC] (7.5.4).

Table 7.2 Terrain coefficients for wind speed corrections

CIBSE Guide A			IES data		
Terrain	k	a	Terrain	K	a
Open, flat country	0.68	0.17	Country	0.7244	0.14
Country with scattered wind breaks	0.52	0.2	Suburbs	0.4319	0.22
Urban	0.35	0.25			
City	0.21	0.33	City	0.2097	0.33

7.5.1. Evaluation of natural ventilation strategies: Base-case strategy

The relationship between wind speed and volumetric flow rates was evaluated for the DTM results of the [base-case] ventilation strategy of the apartment studied, presented in detail in Chapter 5.3.1. The hourly simulation results from the resulting ventilation rates during the cooling period were plotted against the corrected wind speed of the meteorological data. As Figure 7.22 shows, different trends were observed without providing a clear relationship between the wind speed and the ventilation rates, due to the large number of data and the different time-dependent parameters and building characteristics.

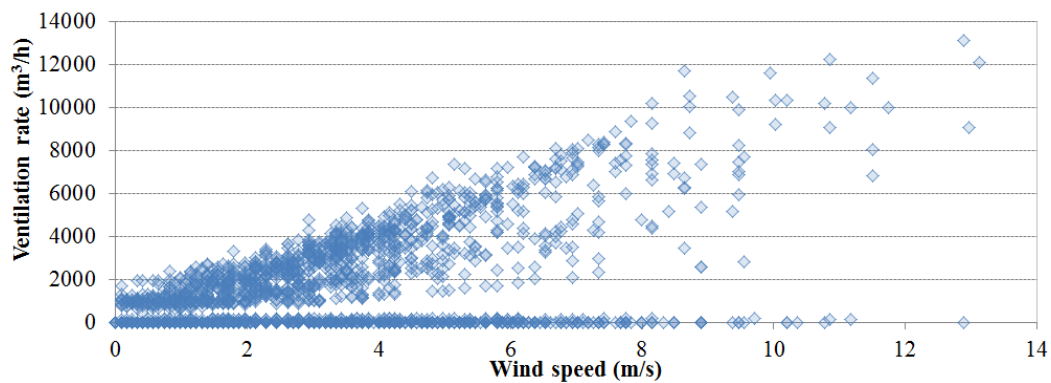


Figure 7.22 Wind speed and ventilation rates relationship, for the cooling period, DTM results from the [base-case] ventilation strategy

The openings operated independently of environmental parameters, and in three openings states (open, partially open and closed) according to the time of the day. The distribution of ventilation rates during the day shows higher ventilation rates during the afternoon and early evening due to the prolonged operation of the openings (Figure 7.23).

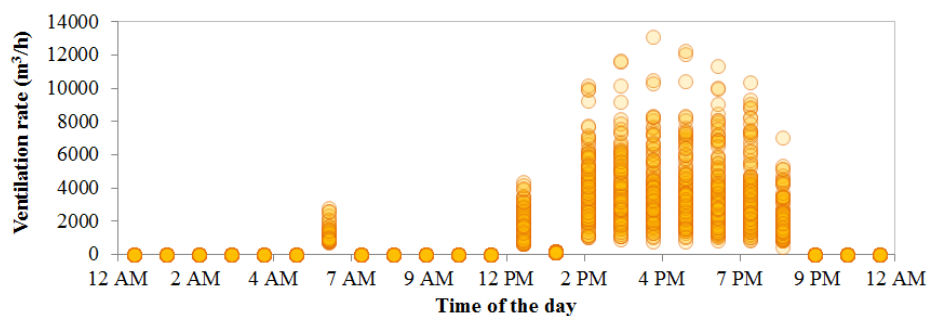


Figure 7.23 Daily distribution of ventilation rates for the cooling period, [base-case] strategy

By excluding the observations with zero ventilation rates (58% of the cooling period), two main trends were observed, shown in Figure 7.24:

1. No correlation was found between the ventilation rates and the wind speed when the openings were partially open, showing no change in the ventilation rates with the increase of wind speed and a zero slope. These observations correspond to the 4% of the cooling period (124 hours).
2. A modest positive association between these variables was found, with a relatively zero slope for wind speeds below 1m/s, but with overall good fit of the regression line. This shows dependency between wind speed and ventilation rates increments. This was expected considering that the openings were fully open for specific hours during the day. Similar relationships were predicted for the CFD results, presented in Section 7.3 and in Figures 7.9 and 7.10. Therefore, environmental parameters, such as the air temperature and wind direction, could be responsible for the sub-populations with different variabilities. Discretisation of the different wind directions could possibly provide a number of populations with homogeneity of variance. The simulation data were predicted during the full operation of the openings corresponding to the 38% of the cooling period (1116 hours), of which 9% were predicted for wind speeds below 1m/s.

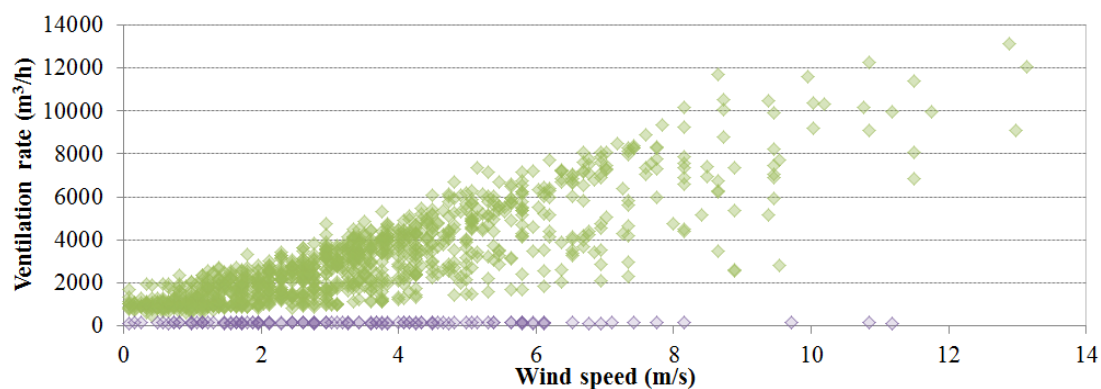


Figure 7.24 Relationship between wind speed and ventilation rates, with elimination of the zero flow rates due to closed openings, DTM results from the [base-case] strategy

7.5.2. Evaluation of natural ventilation strategies: Day and night ventilation strategy

The relationship between wind speed and ventilation rates was further explored for the DTM simulation results from the [DV & NV] strategy (presented in Chapter 5.3.4). Similarly to the [base-case] strategy (Section 7.5.1), different trends were observed without a clear relationship between the wind speed and the ventilation rates for this strategy (Figure 7.25).

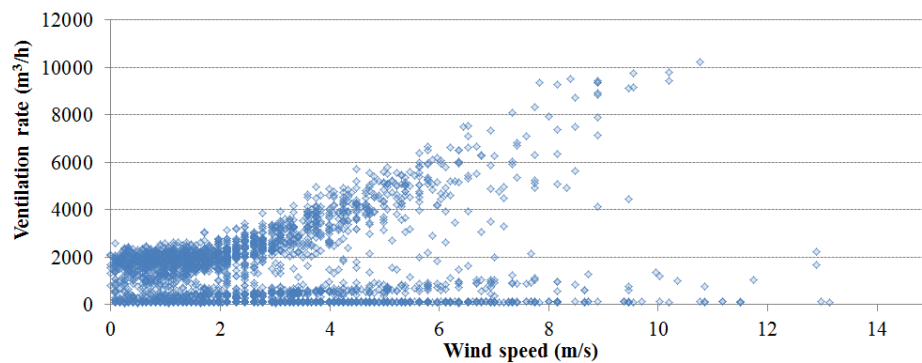


Figure 7.25 Wind speed and ventilation rates relationships through the apartment's openings, for the cooling period, DTM results from the [DV & NV] strategy.

The ventilation rates were found lowest during the day between the hours 12pm to 7pm (Figure 7.26). However, the wind speed varies insignificantly throughout the day as shown in Figure 7.27. The ventilation rates were dependent on the occupancy profile (low occupancy levels reduced the ventilation requirements) and the operation of the openings (the openings were closed for indoor air temperatures exceeding the DBT). In particular, the peak DBTs between 1pm-8pm and the low occupancy density in the afternoon (Figure 7.28) reduced the need for ventilation as shown by the ventilation rates.

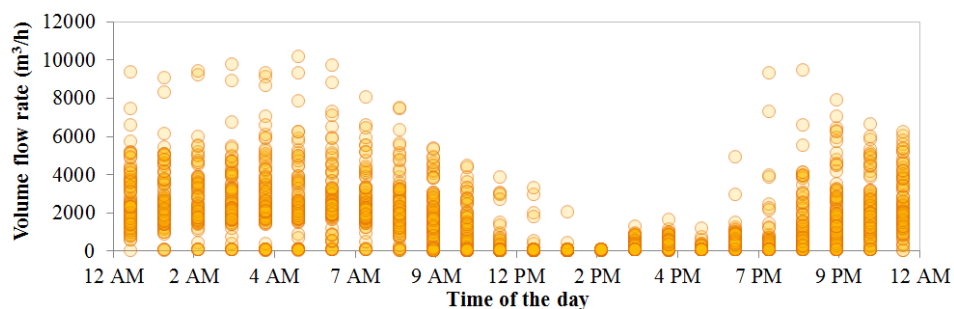


Figure 7.26 Daily distributions of ventilation rates, for the cooling period, [DV & NV] strategy

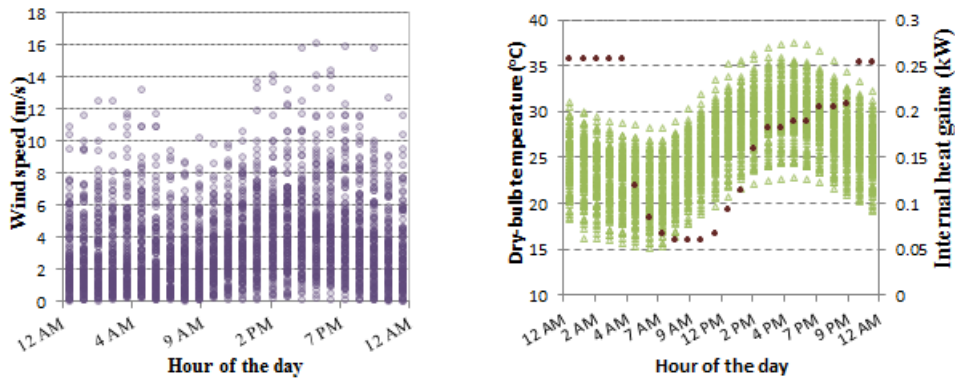


Figure 7.27 Wind speed distribution during the day (corrected weather file values)
 Figure 7.28 Internal heat gains due to occupants, lighting and equipment throughout the day presented with red dots and DBTs of the climate file for the cooling period

For the cooling period, the ventilation hours were defined. These are the hours that the openings are fully open. The simulation results were discretised in order to investigate a comparable sample of data to the CFD results (as the openings were fully open for all CFD simulations). Three relationship trends were observed as shown in Figure 7.29:

1. A change in the gradient was observed for wind speeds above 2.5m/s. For the first group of data, the small increase in ventilation rates with the increase in wind speeds was considered negligible: no correlation between these variables was identified. This population corresponds to the 56% of the ventilation hours and the 36% of the cooling period.
2. The second group includes wind speeds above 2.5m/s and ventilation rates above 1000m³/h. A modest positive association between the variables with overall good fit of the regression line, showing dependence between wind speed increase and ventilation rates increase was predicted. These values correspond to the 31% of the ventilation hours (full operation of the openings) and the 20% of the cooling period. Ventilation rates increase is independent of the wind speed for low values of wind speed.
3. Lastly, the third population group shows a negligible increase in ventilation rates in response to the wind speed increase; no correlation was found. This population corresponds to the 13% of the ventilation hours and the 8% of the cooling period.

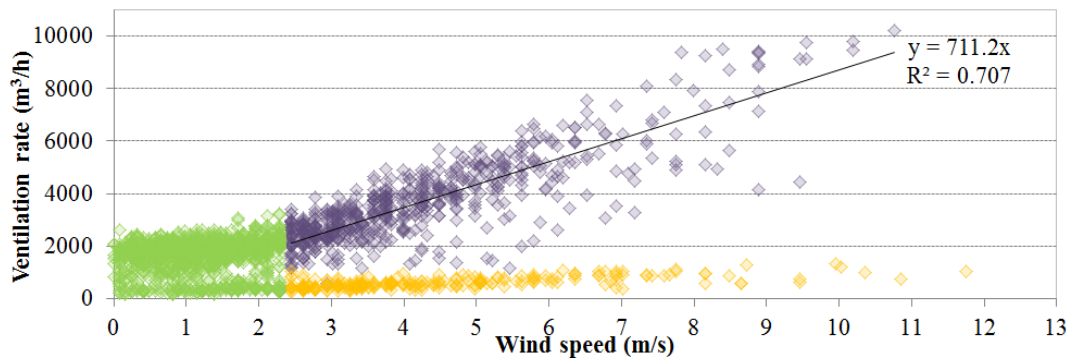


Figure 7.29 Relationships established between wind speed and ventilation rates for the cooling period, with elimination of the zero flow rates due to closed openings, for [DV & NV] strategy

The positive correlation established for the wind speed and the ventilation rates of the CFD results (see Figure 7.9) was established for the corresponding DTM values during the [base-case] and [DV & NV] strategies (for fully open openings). For the [base-case] strategy, the relationship was considered applicable to the 83% of the ventilation hours (35% of the entire cooling period). For the [DV & NV] the relationship defined by the CFD results would fit the 31% of the ventilation hours (20% of the cooling period), as shown by the DTM simulation results. However, for the [DV & NV], natural ventilation occurs during the 65% of the cooling period relative to the 42% of the [base-case]. The operation of the openings in response to varying conditions contributed to a weak relationship between the wind speeds and ventilation rates.

Using both Figure 7.24 and Figure 7.29, it is possible to predict the ventilation rates in the spaces for set values of wind speed, and thus predict the ventilation performance of the strategies if implemented in similar buildings and microclimates.

7.5.3. Evaluation of natural ventilation strategies: Wind-catcher strategy

As in previous Sections 7.5.1-2, due to the openings' operation, different trends were observed without a strong relationship between the variables of wind speed and the ventilation rates (Figure 7.30) for the [WC] ventilation strategy. Three trends were identified: 20% of the ventilation rates increased in relation to the wind speed increase (572 out of 2975); 34% of the ventilation rates (between 500 and 3000 m³/h) shown no correlation to the wind speed; and 46% remained below 500m³/h showing

again no correlation to the wind speed. The distribution of flow rates during the day vary significantly in relation to time, showing a dependency to the DBT and the occupancy profile.

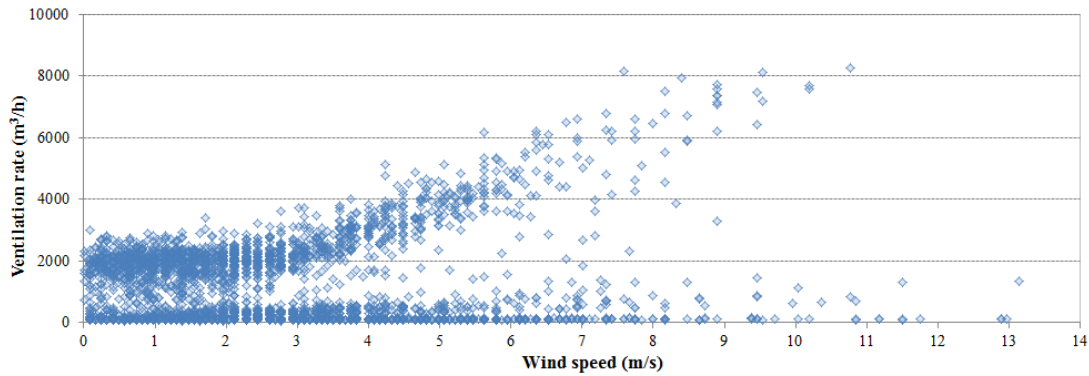


Figure 7.30 Wind speed and total ventilation rate relationship during the cooling period. DTM results from the [WC] strategy investigated

Additionally, the computational day was divided into two groups with regard to the openings operation: the hours of the day that all wind-catcher openings were continuously open (hours 8pm to 8am); and those that they operated in pairs and in response to the wind direction (hours 8am to 8pm), presented in Chapter 5.3.5. Lower ventilation rates were predicted at the latter, as shown in Figure 7.31.

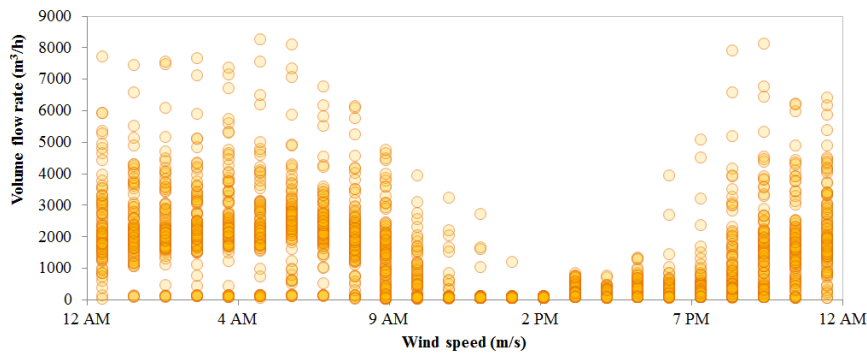


Figure 7.31 Daily distributions of ventilation rates for the cooling period, [WC] strategy

Further, three population groups were identified for the cooling period. The first population group includes observations for wind speeds above 3m/s and ventilation rates above 1000m³/h, occupying the 24% of the ventilation hours (16% of the cooling period). A strong correlation of the wind speed and ventilation rates was predicted, however no relation between ventilation rates and temperature difference (internal – external temperatures) (Figure 7.32). This shows that for higher values of wind speed, the ventilation is mainly wind driven.

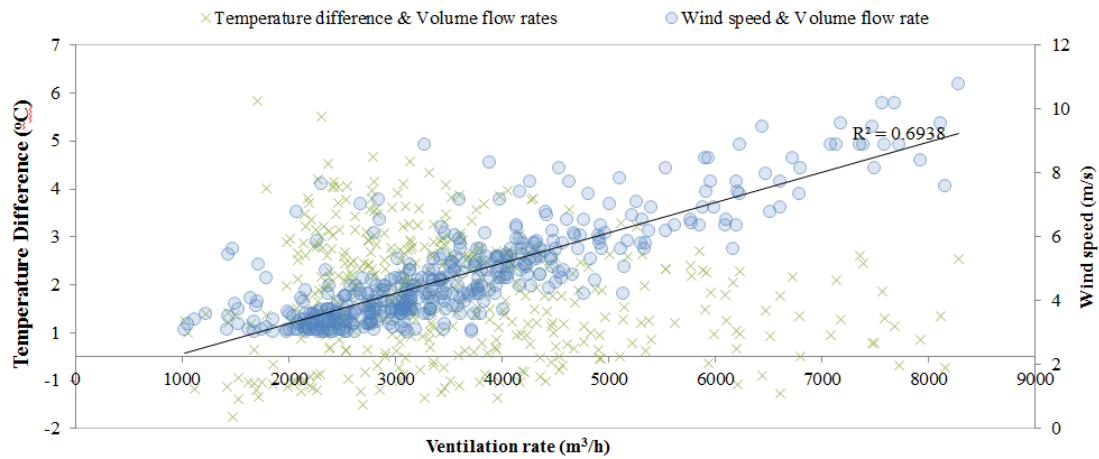


Figure 7.32 First population group above 3m/s wind speeds and 1,000m³/h ventilation rates, showing correlation only between wind speed and ventilation rates

The second population group accounts for the 53% of the ventilation hours (36% of the cooling period) and includes observations of wind speed below 3m/s and ventilation rates above 500m³/h. No correlation was predicted between wind speed and ventilation rates. The ventilation rates increased with respect to the temperature change (internal-external) increase (Figure 7.33). Low wind speeds, below 3m/s, were unable to provide further increase to the ventilation rates than the resulted rates due to buoyancy forces.

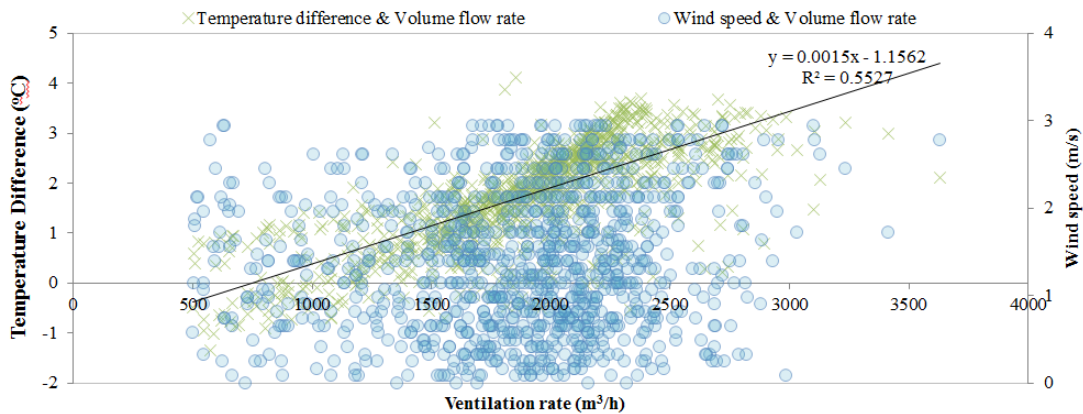


Figure 7.33 Second population group, below 3m/s wind speed and above 500m³/h ventilation rates, showing correlation only between temperature difference (Tin-Text) and ventilation rates

The third population occupies the 23% of the ventilation hours (15% of the cooling period), includes ventilation rates below 500 m³/h, and below 1000m³/h for wind speeds above 3m/s (Figure 7.34). A moderate linear relationship was predicted between the wind speed and ventilation rates, and no correlation between the temperatures and ventilation rates. The DBT increase resulted in reduction of the

ventilation hours and thus lower ventilation rates. The third population is characterised by the highest DBTs relative to the other two populations (67% of the total cooling season). This confirms the assumption that ventilation rates were more sensitive to environmental parameters rather than to the wind-catcher openings operation, due to the openings operation.

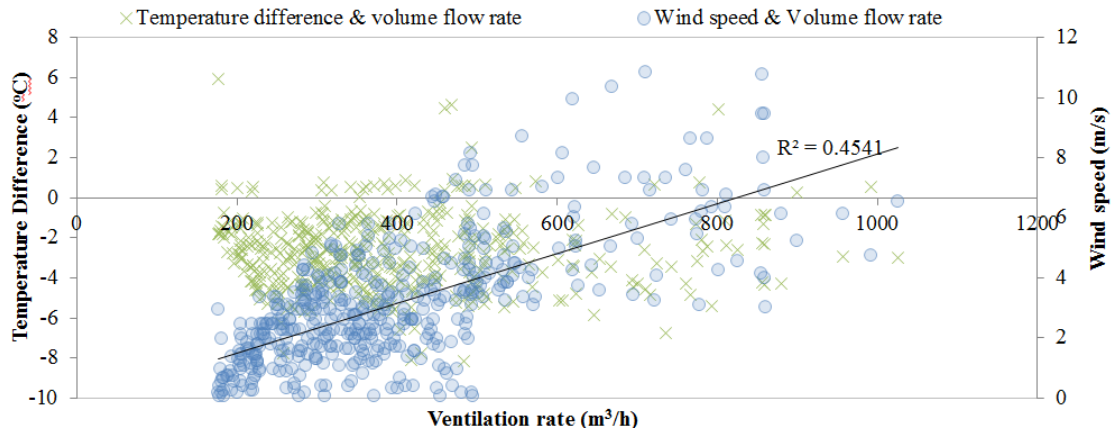


Figure 7.34 Third population group of ventilation rates below $1,000\text{m}^3/\text{h}$

7.5.4. Evaluation of natural ventilation strategies: Dynamic façade and wind-catcher strategy

Results from the [DF & WC] strategy show relationship between wind speed and ventilation rates for wind speeds above 3m/s (16% of the values). Up to 37% of the values show no-correlation for wind speeds below 3m/s and ventilation rates above $500\text{m}^3/\text{h}$. Up to 45% are ventilation rates below $500\text{m}^3/\text{h}$. The distribution of the ventilation rates throughout the day (Figure 7.35) was comparable to that during the [WC] strategy (Figure 7.31).

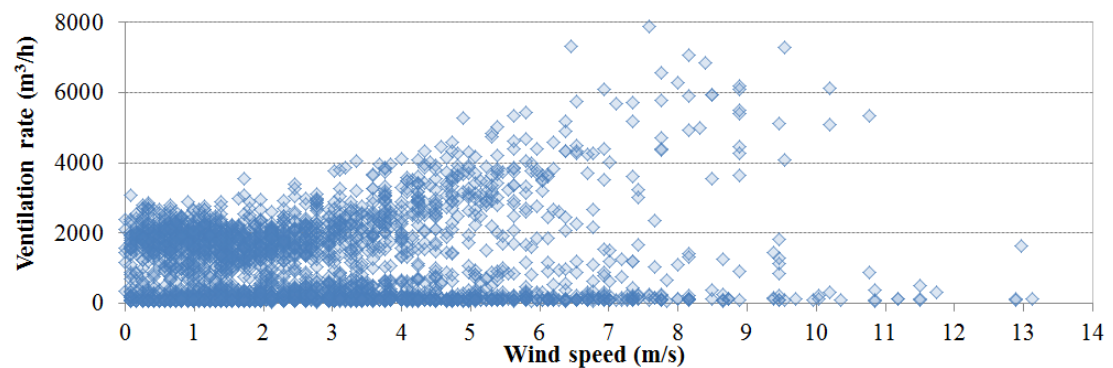


Figure 7.35 Wind speed and ventilation rates relationship, for the cooling period [DF & WC]

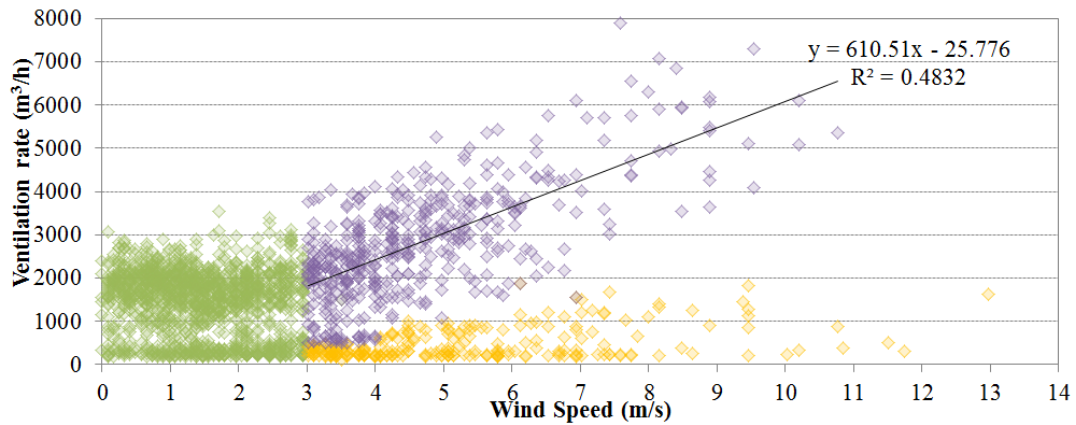


Figure 7.36 Relationship defined between wind speed and ventilation rates for the cooling period, DTM results from the [DF & WC] strategy.

Similarly, a small sample of the ventilation rates predicted was correlated to the wind speed, corresponding to 23% of the ventilation hours (15% of the entire cooling period) (Figure 7.36). For the rest of the ventilation hours, the ventilation rates were correlated to the indoor-outdoor temperature difference. Due to the lower internal to external air temperature, the ventilation rates were significantly low (below $100\text{m}^3/\text{h}$) as openings for indoor temperatures exceeding the external. The increase in indoor temperatures above the DBTs resulted in ventilation rates increase, up to approximately $2,500\text{m}^3/\text{h}$. Ventilation rates exceeding this value delivered natural cooling in the spaces as shown by the lower temperature difference. The relationship established for ventilation rates approximately above $2,000\text{m}^3/\text{h}$ was comparable to that defined by the CFD values shown in Figure 7.21. Thus, the relationship established within the CFD observations would fit less the 21% of the cooling period as expressed by the DTM relationships (Figure 7.37), as further discretisation would be required.

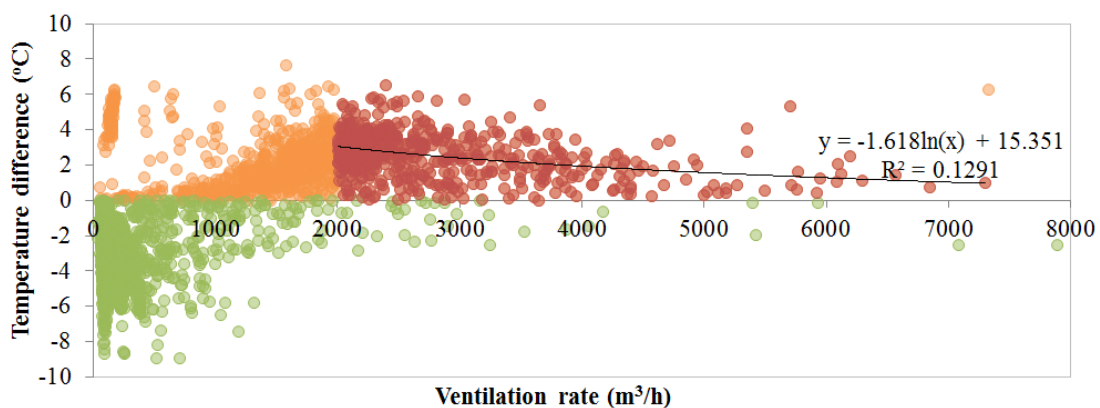


Figure 7.37 Ventilation rates and temperature difference ($T_{in} - T_{ext}$) relationships, during the cooling period and for the [DF & WC] strategy

7.6. Overview of the comparative analysis between the DTM-CFD simulation results

The parametric sensitivity analysis performed, identified the variables with the greatest impact to the indoor environment, even though it is only an approximation of the real world situation. It was important to develop empirical relationships for both CFD and DTM simulation results that could be used to predict broad patterns in ventilation performance under conditions that have not been examined using simulations (e.g. the ventilation rates could be predicted for any driving pressure at the different natural ventilation strategies, according to the Figure 7.4 to Figure 7.8). The relationships established (Sections 7.3, 7.4 and 7.5) could be used by designers and practitioners aiming to assess the expected performance of the ventilation strategies if implemented in similar buildings and climates, with regard to their performance in the case study building. This information could be used to extrapolate patterns of ventilation performance to facilitate the design of various natural ventilation strategies in new or existing buildings, by showing potential in the case study.

Designers could use these relationships to predict internal air characteristics with regard to climate characteristics, for similar buildings and microclimates. For example, using the relationships established between wind-speeds and ventilation rates (Section 7.3) it is possible to identify the resulted ventilation rates for every wind speed and direction. The designers could use the wind speed of each site (from meteorological data) for a defined period in order to predict the expected indoor temperatures, as shown in Figure 2.21 for external temperatures approximately at the range of 25-35°C.

It should be noted that for the relationships between climate and indoor air temperatures identified within the CFD results, the relative difference between the performances of the strategies should be considered and not the actual value of temperature. This is with regard to the modelling methods used, such as the fully open openings and the lack of thermal mass, presented in Chapter 6.

The relationships established for the DTM results show how the openings operation can modify the relationships established using steady state CFD. These relationships

can be used to evaluate the performance of the strategies over a period of time and with regard to a number of environmental parameters.

Clearly, the DTM and CFD simulation results should not be directly compared due to the different calculation methods involved and their input data (e.g. predefined by the software pressure coefficients in DTM). The relationship between indoor air temperatures and ventilation rates defined for the CFD results was further established for the DTM simulation results for ventilation rates above a certain value, although for a short period (for the [DF & WC] for 20% of the cooling period). These percentages could be further increased by, for example appropriate evaluation of the ventilation rates in DTM utilising predicted driving pressures for the specific building and site.

7.7. Low-Energy refurbishment design guide: Strategy

This research provided detailed information regarding the natural ventilation and cooling performance of passive strategies designed for an existing typical apartment building in Greece. The output of this research formed as a low-energy refurbishment design guide could assist designers, professionals, developers and householders in dealing with energy refurbishments of domestic buildings for future and current climates. The design guide would aim to promote sustainable development of the existing building stock, energy efficiency in buildings and encourage adaptation to climate change within good design practice of natural ventilation strategies, able to deliver occupants' thermal comfort expectations.

The widespread need for energy refurbishment of the existing building stock is reflected to the recently declared commitment of the EU countries to 80-95% reduction relative to the 1990 baseline in EU carbon emissions by the year 2050 (European Commission, 2011). Designing for future climates should not be a strategy only for new builds. Reductions in carbon emissions, managing the use of resources, and adapting to climate change largely involves the existing domestic building stock.

The large existing building stock of the typical multi-family buildings of the Mediterranean countries represents a substantial opportunity for energy refurbishment plans. The domestic sector corresponds to the 79% of the existing building stock in Greece, and accounts for the highest energy consumption in Europe. The 2011 census results shown that in Greece there are up to 4 million multi-storey buildings, of which, 50% were constructed in times of no energy regulations (prior to 1980) (EL.STAT., 2012). Greek occupants and householders' needs are closely linked, as 73% of the occupants own the property they live in thus, showing personal interest in energy and cost reduction measures. The energy required for cooling indicates a substantial opportunity for energy savings. The efficient performance of natural ventilation strategies could replace the need for conventional mechanical cooling during the cooling period or parts of it (hybrid ventilation).

The low-energy refurbishment design guide for apartments in the Mediterranean region, would recognise the lack of know-how within developers and householders,

and provide a link between knowledge and application for both minor and major energy refurbishments within individual and multiple buildings. The use of this guide would be complementary to the energy efficiency standards and regulations provided by respective authorities.

The cooling performance evaluation of natural ventilation strategies at the case study building provided an appreciable platform of recommended solutions. Due to the diversity of the building stock with regard to the architectural, planning and energy characteristics, as described in literature, it should be emphasized that the application of natural ventilation systems is subjective, and dependent on the specific building, climate and use. The content of the guide would not be a generalised answer on ways to design natural ventilation strategies, as each building has to be regarded at its individual context. It should be thus treated as warehouse of possibilities providing design influences with regard to the specific needs and design considerations of each building. Relevant guidance should be considered, and sources of further information should be identified in addition to the existing portfolio of this work.

A first proposal of the content and layout of the low-energy refurbishment design guide is included in the following section. This is an example of the design guide that would be further developed after the completion of the research reported here. The guide was presented in the way it was anticipated it would be used and circulated. As a short version of the potential final design guide, it illustrates: brief details of the use; purpose and need for the guide; a short introduction of available natural ventilation strategies; the example building under investigation; and the performance evaluation of the two principal natural ventilation strategies with the most significant performance (with regard to IAQ). List of references is provided at the end of the design guide.

7.8. Low-Energy Refurbishment Design Guide for apartments in the Mediterranean: Natural Ventilation

Contents

1. Purpose of the guide
2. Background - Defining the Need
3. Natural ventilation and cooling strategies
4. Building design - potential and considerations
5. Implementation of strategies
6. Performance evaluation

1. Purpose of the guide

Existing knowledge codified into typologies, in the form of typical solutions, assists designers in developing design solutions [1]. The guide as a handbook will assist professionals, architects, developers and householders in dealing with energy refurbishments for future and current climates. Particular goal will be to deliver occupants' thermal comfort, energy reduction and increase the value (e.g. life span and energy efficiency rating) of existing properties.

The guide illustrates the potential (i.e. indoor air quality improvement) of the inclusion of natural ventilation and cooling strategies in existing buildings in hot climates. It provides required information regarding the systems characteristics, design, implementation and performance within an example building.

This design guide recognises the lack of know-how within developers and householders, and provides a link between knowledge and application for both minor and major energy refurbishments within individual or multiple buildings. When proceeding to introduce energy reduction measures in buildings, use of this guide is complementary to the energy efficiency standards and regulations

provided by respective authorities. The content of the guide should not be treated as a generalised answer on ways to design, as each building has to be regarded at its individual context.

The guide focuses on the application of passive strategies that provide free energy from the environment in the building, and deliver occupants' thermal comfort during the cooling period, with the aim to eliminate the dependency on delivered energy (fossil fuel and renewables) formed within active designs, see Figure 7.38.

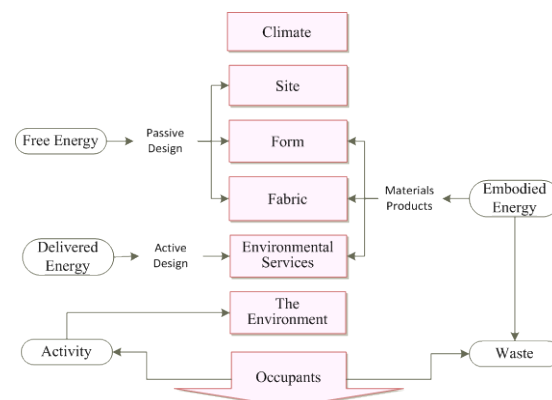


Figure 7.38 Thermal designs for thermal comfort (after [2])

2. Background - Defining the Need

Authorities have now recognised an urgent need to reduce energy consumption within sustainable development, due to: the emergence of climate change, energy shortage, population increase, IAQ health related problems, global recession and fuel poverty.

Designing for future climates should not be a strategy only for new builds. Reduction in carbon emissions, managing the use of resources, and adapting to climate change largely

involves the existing domestic building stock. A green design should satisfy occupants' comfort, health (i.e. IAQ) and take into account the environmental impact of the building (i.e. energy, waste) [3].

International and national regulations provide set point values and/or a range of comfort conditions which occupants feel comfortable at. This information is primarily appropriate for system sizing and thermal comfort evaluation. Thermal comfort is described as the "state of mind which expresses satisfaction with the thermal environment" [4]. Occupants proceed to adaptive adjustments either consciously or unconsciously [4], while this adaptation may refer to psychological, physiological, and acclimatization parameters [5]; [6]; [7].

In hot climates, it is possible that occupants' thermal comfort expectations can be met through natural ventilation strategies [8]. Natural ventilation systems could be implemented in existing apartment buildings in hot climates, to provide an efficient alternative to conventional mechanical cooling during the cooling period.

Greece is a country classified with a typical Mediterranean warm, dry climate, having the lowest levels of relative humidity and the highest wind speeds in the Mediterranean [9], and is therefore a location considered suitable for inclusion of natural ventilation strategies. The large existing energy consuming domestic building stock (Greek building stock has the highest energy consumption in Europe [10]), with representative building example the multi-family buildings in the Mediterranean countries, represent a substantial opportunity for energy refurbishments.

3. Natural ventilation and cooling strategies

Ventilation is important for: IAQ (i.e. removal of stale air, odours and harmful chemicals); provision of natural cooling (reductions in excess heat) during or prior the occupied periods; removal of heat and pollution at localised sources; and prevention of condensation within the building fabric [11].

Natural cooling techniques concern the disposal of excess heat to environmental sinks (e.g. ambient air, sky, ground and water) from spaces with higher air temperatures. Their efficiency depends on the availability of sinks, the thermal coupling and the air temperature [12]. Key practices of heat dissipation techniques are the: radiant cooling (sky); soil cooling (ground); natural ventilation (air); and direct/ indirect evaporative cooling (water) [13]; [8].

Natural ventilation is the air exchange between indoor spaces and the environment through openings [14]. It is one of the most common applications of natural cooling that employs both the natural forces of pressure difference induced by wind, and the temperature gradients between interior and exterior [8]; [15]; [16]; [17]. The efficiency of natural ventilation systems depends on the building design and characteristics (such as orientation, openings size, location, building shape, form), site properties (surrounding buildings, microclimate) and occupants' behaviour (interaction with the building envelope and openings) [15].

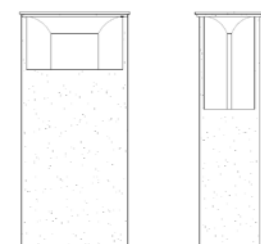


Figure 7.39
Wind-catcher
elevations. CAD
drawings by
author after [18]

Wind-catchers, (Figure 7.39) are examples of the vernacular architecture which utilise the pressure differences on the building surfaces and maximise the driving pressure for ventilation (i.e. the pressure difference between inlet and outlet) [19]. Wind-catchers capture wind at high levels and channel it down in the occupied spaces [17] and, depending on the design, can operate as both inlet and exhaust, under both wind and/or buoyancy-driven pressures [20]. Their performance is strongly influenced by the tower's shape, height, position on the building structure, size and the number of openings.

Single-sided ventilation of apartment buildings, commonly found in urban areas, could be improved by exploitation of façade relief elements (e.g. opening configurations, wing walls, balconies, overhangs, shadings) [21]; [22]. Dynamic façades (DF), consist of multiple layer skins [23] usually a pair of glass skins [24]; [25] and sun-shading systems (commonly Venetian blinds) located in the cavity [26]. The exterior skin layer could be replaced by a layer of shading systems that provides a semi-enclosed environment, shading and natural ventilation of the spaces.

Comfort ventilation is considered suitable for warm, humid regions, with small diurnal range ($<10^{\circ}\text{C}$) and when the indoor air speed is within 1.5-2.0m/s and the external air temperature should not exceed 28-32 $^{\circ}\text{C}$ [13].

Designing natural ventilation strategies for specific building designs and climates is a multi-dimensional and interactive problem that incorporates factors of physics (e.g. ventilation, solar gains), psycho-physics (e.g. thermal comfort) and psychology (e.g. privacy) [27]. With regard to the individual characteristics of each building (i.e. design, microclimate, use

and operation), prior to an energy refurbishment briefing, it is necessary to undertake energy audit of the building. Information regarding the potential for energy refurbishments will be attained and the suitability of natural ventilation and cooling strategies will be explored.

4. Building design - potential and considerations

An existing five storey apartment building in Greece was used as an example to demonstrate application of the approach. The building was constructed in the early 1970s for domestic use (eight apartments per floor), and is located in an urban zone within the centre-north of Athens (Figure 7.40), with a typical Mediterranean climate. It is considered one of the most typical urban Greek domestic buildings due to its design, year of construction, materials used, operation and its location (there are over 4 million multi-storey buildings in Greece [28]).



Figure 7.40 Street view of the apartment building studied

A residential unit was selected, centred on the first floor (53m²), oriented south-east with room height of 2.7m (Figure 7.41). The two bedrooms are located at the front (south-east) having one patio window each, while the living room, kitchen and bathroom are located on the rear with no direct access to light. The two windows of the kitchen and bathroom

provide indirect access to daylight, being connected to one of the three light wells within the building, and assist the extraction of stale air from the core spaces. The apartment is naturally ventilated via primarily single-sided ventilation.



Figure 7.41 Plan view of the building floor, showing with different colours the 8 apartments and the apartment under study

The microclimate of each site (i.e. wind, sunlight and air quality) is defined by urban forms, spaces, and urban densities [3]. When evaluating airflow, lighting and energy performance of buildings it is important to ensure that adequate surveys of the site are conducted, over a radius defined by the site itself, to attain information about the building form, the characteristics of the surrounding buildings, and the street layout.



Figure 7.42 Plan view of the urban building blocks with their heights in metres and front view of the building studied

A survey conducted of the case study building and its surroundings provided

information regarding the site topography and surrounding structures. The information was conveyed in the form of a ‘map’ of the main building, surrounding buildings forms (e.g. dimensions and location), street layout, and ground morphology (Figure 7.42).

Climate characteristics (i.e. wind speed and direction, air temperature, solar radiation, and relative humidity) are important for the thermal design of buildings and the natural ventilation strategies. During the cooling period, the rounded to integer values hourly dry-bulb temperatures (DBT) of the site studied, predicted that for 75% of the period the temperature varies between 24°C and 29°C, while 26°C is the most frequent DBT (Figure 7.43).

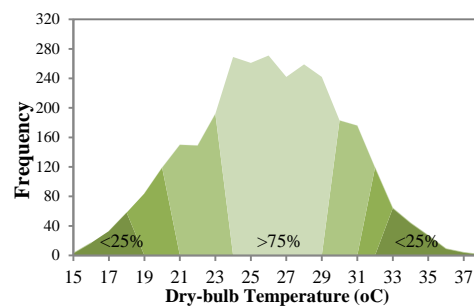


Figure 7.43 Frequency of DBTs for the cooling period

The operation of the building is dependent on the occupancy profile, use of systems, equipment and lighting. The daily operational profile of the apartment studied is presented in Figure 7.44.

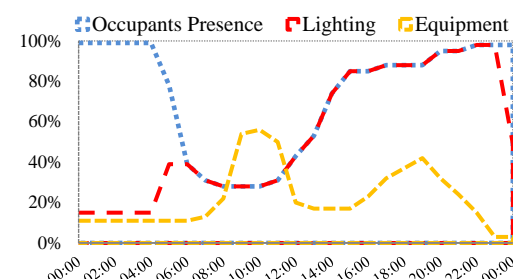


Figure 7.44 Daily profiles of occupants, lighting and equipment operation

Potential areas for the implementation of natural ventilation strategies were identified for the apartment studied as

well as the flow passages (connecting areas between the spaces), as illustrated at Figure 7.45. The refurbishment project could involve:

- Investigation of various openings' operation patterns, positions and dimensions in relation to climate, as well as occupants' behaviour and adaptation level.
- Optimization of indoor airflow paths: unoccupied spaces could be used to create new flow paths, eliminating the use of spaces with higher internal gains (i.e. kitchen), such as the ancillary space above the false-ceiling in the bathroom.
- Four-directional wind-catchers: A vernacular cooling system engaged with different ventilation strategies e.g. day and/or night, could provide direct access to fresh air at the core building spaces.
- Façade relief techniques: A lightweight double-skin (external layer of horizontal shading systems) and wing walls could provide new flow paths and protection from direct solar gains.
- Passive downdraught evaporative cooling within the wind-catcher tower: Further passive cooling could be provided with the inclusion of a water evaporation system, spraying fine droplets of water.

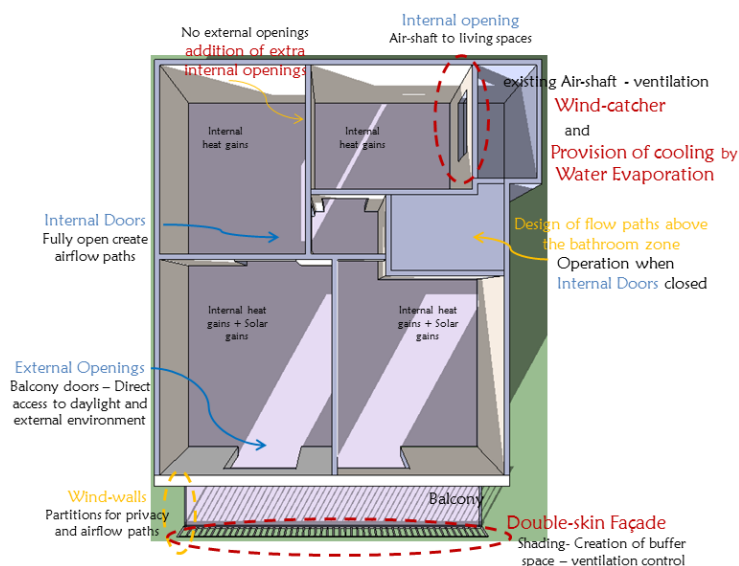


Figure 7.45 Schematic 3D presentation of the spaces, connecting openings and points of interest

5. Implementation of strategies

The ventilation and cooling performance of two natural ventilation strategies, implemented in the building under investigation, were evaluated in relation to the building form, layout and operation.

There are a variety of performance prediction and evaluation techniques that architects and designers can use during the design process to achieve efficient thermal design. Computer based modelling techniques such as

computational fluid dynamics (CFD) provide estimation of airflow patterns in and around spaces that by calculating velocities, temperatures and pressures at numerous locations throughout spaces recreate the entire flow field.

5.1. Four-directional wind-catcher

Wind-catchers could be introduced at the building form either within the core spaces or at the buildings' façades within the balcony zones. Three identical four-directional wind-

catchers implemented in the top part of the existing light wells, would assist the ventilation of two apartments each on every building floor, for the entire building. The operation of wind-catchers within the core spaces was considered significant due to the lack of access to the external environment Figure 7.46.

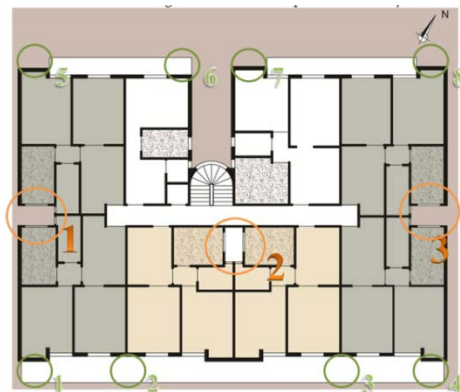


Figure 7.46 Location on of potential areas for wind-catcher inclusion, within the core spaces (light wells) and the balconies

The wind-catcher design with four openings and four separate channels has been often employed in areas with no prevailing wind, and its' ventilation efficiency has been evaluated by several researchers [29]. The proposed wind-catcher arrangement elevations are shown in Figure 7.47.



Figure 7.47 South-east elevation of the building under investigation, showing the three wind-catchers at the core spaces

Important parameters for the ventilation performance of the wind-

catcher are the wind-incidents on the wind-catcher openings and the pressure difference between the ventilation inlets and outlets. For the example building the prevailing wind direction is north (Figure 7.48).

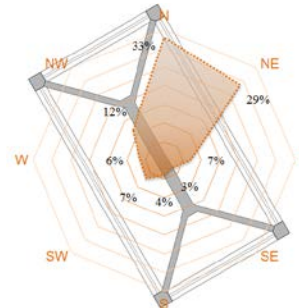


Figure 7.48 Frequency of wind directions (%) on the wind-catcher openings

Sizing the wind-catchers was driven by the existing building design and form, with the aim to deliver the least disruption to occupants and alteration to the architectural characteristics of the building design.

Wind-catcher (internal)		
Dimensions	2.3×1.3m	1.5m above the penthouse roof
Openings	2.1×1.15m & 1.15×2m	2 times the area of the kitchen openings/inlet (1.2 × 1m)
External wind-catchers		
Dimensions	1.6×1m	1m above the penthouse roof
Openings	1.5×1.15m & 0.8×2m	Outlet:

The implementation of a wind-catcher in the top part of the existing light wells was evaluated. The previous single-sided ventilation was greatly improved upon with the introduction of the wind-catcher, which resulted in reductions in indoor temperatures by up to 2°C.

The ventilation rates in the spaces vary considerably in response to wind direction and wind speed. The implementation of the strategy assisted natural ventilation under north and east wind incidents, resulting in ventilation rates increase by two to three times. North wind direction delivers the highest ventilation rates (north-east the lowest), whereas during

5m/s wind incidents it delivers up to 10,000 m³/hr (Figure 7.49). The predicted ventilation rates are independent of outdoor air temperature, subject to internal conditions (heat gains, building and envelope operation) and a combination result of the wind speed and direction. They are applicable only to the apartment and building under investigation.

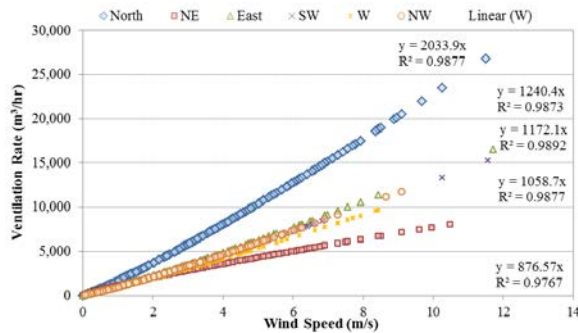


Figure 7.49 Relation of ventilation rates and wind speeds of the wind-catcher strategy for various wind directions

5.1. Dynamic façades

Lightweight dynamic façades (DF) are façade relief techniques that could be designed combining wing walls and an external layer of horizontal shading systems (control-lable fins that offer design and operation flexibility). Designed on the edge of the balconies, DFs re-establish the use of the balconies into buffer spaces (Figure 7.50).

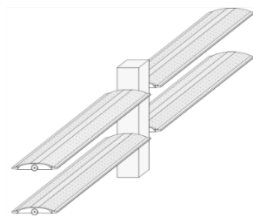


Figure 7.50 Detail three-dimensional view of the louvres, and carrier system (after: [30])



Figure 7.51 South-east elevation of the building studied, showing the operation of the shading system in response to solar shade.

The horizontal louvres (Figure 7.51) would be designed adjustable to offer daylight control and flexibility, reduce glare and heat gains during the daylight hours. Most importantly they assist the ventilation strategy by providing a variety of airflow paths, relative to the location, urban site and orientation.

The louvres material selected for the building under investigation was extruded aluminium alloy, although a wide variety of materials could be suggested subject to the preferred façade design (e.g. glass, wood, and glass with integrated photovoltaic cells).

The carrier system integrates a central aluminium torsion tube along the length of the louvres assisting a rotational operation. Partition walls perpendicular to the two façades are designed between all apartments.

Sizing the louvres was dictated by the existing floor to ceiling height, and by dividing the height of the opening into the width of louvres.

Second layer Façade	Louvres No: 14	0.21m × 0.04m (3.20 length)
	0.10m in from the balcony edge.	Centre support 100mm × 60mm

The dynamic façade was divided into three independent sets of louvres that could provide operation flexibility and aesthetic contribution at the existing

building façade. It would operate in response to climate and occupants' thermal comfort, as: fully open; partially; top and bottom; in inclined; horizontal or vertical arrangement etc., as shown in Figure 7.52. In addition, operating according to the time of the day would provide protection against solar gains (e.g. by only having the bottom louvre group open), privacy (e.g. by only having the top louvre group open), further to natural ventilation.

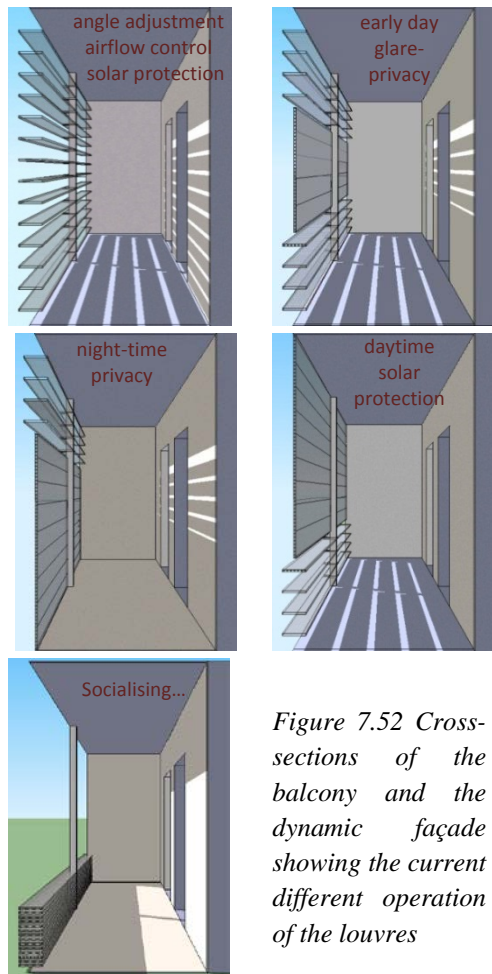


Figure 7.52 Cross-sections of the balcony and the dynamic façade showing the current different operation of the louvres

The introduction of the second façade skin to the building design improved the ventilation rates within the apartment, and the overall ventilation performance of the wind-catcher. CFD simulation results demonstrated that the ventilation performance varies considerably in response to wind direction and wind speed. North wind direction delivers the highest ventilation rates: at 5m/s wind incident delivers up to 12,000 m³/hr. With

regard to indoor air temperature reduction, this strategy delivered an additional 0.2-0.5°C reduction (additionally to the reductions by the wind-catcher) on average at maximum, depending on the wind-characteristics.

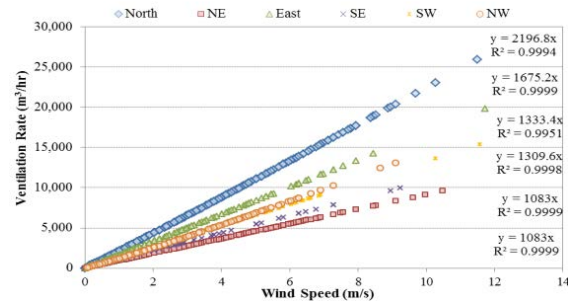


Figure 7.53 Relation of ventilation rates and wind speeds of the DF strategy

According to simulation results included in Figure 7.53, regardless of the outdoor air temperature, and under the same internal conditions (e.g. heat gains and envelope operation) ventilation rates can be predicted with regard to different wind speeds and direction.

6. Performance evaluation and design considerations

Indoor air quality in the spaces was enhanced with the implementation of the new natural ventilation strategies, when compared to the previous condition of the 'single-sided' ventilation strategy of the apartment under investigation.



Figure 7.54 South-east elevation of the building studied, showing the operation of the shading system in response to solar radiation, and the wind-catchers

Wind-catchers can be designed on the top of existing light wells, typical elements of traditional multi-storey apartment buildings, as on the example building, or at the building façades, as shown on Figure 7.54 and Figure 7.55. The inclusion of wind-catchers at the building façades would require planning permissions and possibly result in minor occupants' disruption. This is on the contrary to the implementation of wind-catchers at the top of the existing light wells. Utilising the unoccupied spaces of the light wells, the wind-catcher could be installed and operated in a short period of time.

The implementation of a wind-catcher in the top part of the existing light wells was evaluated. Simulation results from the case study apartment showed that this strategy was able to enhance the fresh air distribution at the core spaces of the apartment, previously being single-sided

ventilated (or being inadequately cross ventilated through the light well), and provided reductions in indoor temperatures, removal of stale air and contaminants, and provision of fresh air at higher speed. Despite the densely populated environment, the wind-catcher enhances the ventilation potential of the apartment studied, as it captures fresh air from all directions and of higher speeds.

The wind-catcher top openings operate according to: the wind direction (one wind-catcher opening operating at a time); the need for ventilation (indoor air temperatures, ventilation rates, and CO₂ concentration); outdoor air properties (outdoor temperatures, wind speed); and occupants' preference (need for night-ventilation, ventilation during unoccupied hours, during bed-time etc.).



Figure 7.55 Plan view (left) and updated plan view (right) of the apartment studied showing the wind-catcher, the façade wind-catcher and optimization the dynamic façade

A lightweight dynamic façade of horizontal louvres, located at the edge of the balcony could transform the balcony zone into a semi-outdoor, buffer space of air circulation. The three groups of louvres provide multiple operational controls with respect to: solar radiation; glare; privacy; time of day; outdoor air properties (air temperature, wind speed); and need for ventilation.

The specific design is recommended for balconies facing east or west. The traditionally used in domestic buildings in Greece canvas shading devices, could be replaced by these automatic operation louvres of versatile use. The three groups of louvres could be arranged in different ways and tilted individually, to provide optimum control.

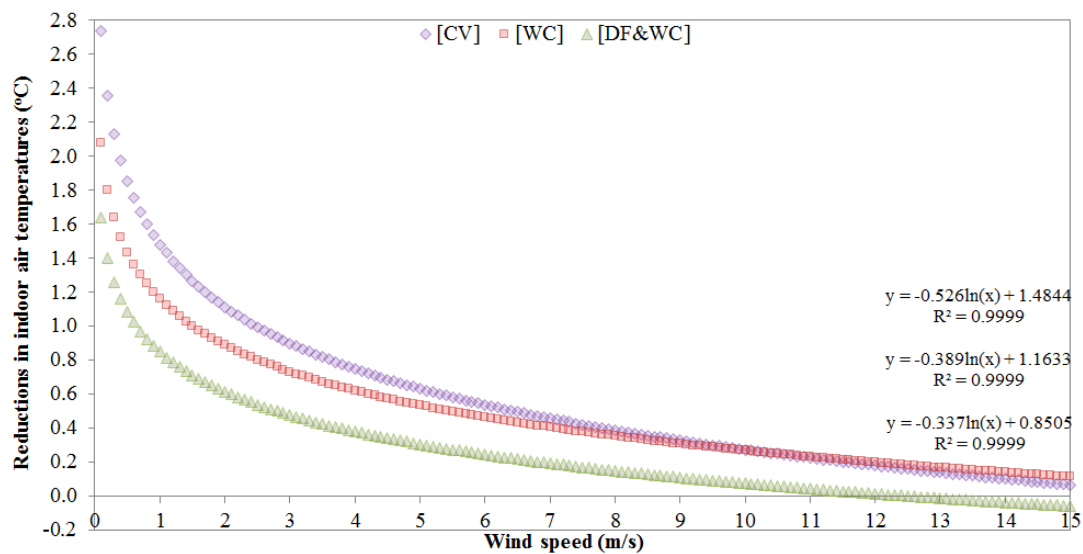


Figure 7.56 Predicted indoor air temperature with regard to the wind speed and each ventilation strategy examined, averaged values for 26°C and 35°C DBTs

Simulation results from the inclusion of this strategy to the example apartment shown that the dynamic façade enhanced the natural ventilation relative to the previous strategies, delivering ventilation rates on the inlets up to 40% greater. However, this improved performance was dependent on the climate scenario, showing less improvement than the wind-catcher strategy in some cases.

It was predicted that the addition of the wind-catcher noticeably improved the IAQ. The implementation of the dynamic façade has been the most efficient strategy with respect to ventilation rates increase.

Figure 7.56 show the relationship defined between the air temperature difference (internal-external) and wind

speed. This expresses the performance of the evaluated strategies under specific air temperature with regard to wind speed. The relationship defined between these variables is an approximation following the simulation results. The performance of the wind-catcher and dynamic façade was established relative to the previous cross ventilation strategy of the apartment under investigation. The cooling potential of the dynamic façade is greater relative to that of the wind-catcher for higher wind speeds.

References

- [1] Emmitt, S. (2012) *Architectural Technology*. second. West Sussex, UK, John Wiley & Sons, Ltd.
- [2] Littlefield, D. ed. (2008) *Metric Handbook. Planning and Design Data*. Third. Ooxford UK, Burlington USA, Elsevier Ltd.
- [3] THERMIE (1999) *A Green Vitruvius - Principles and Practice of Sustainable Architectural Design*. London, UK, James & James(Science Publishers) Ltd.
- [4] ASHRAE (2009) *2009 ASHRAE Handbook Fundamentals*. SI Edition. Atlanta, American Society of Heating, Refrigerating and Air-Conditioning Engineers, Inc.
- [5] Brager, G. & Dear, R. de (2000) A standard for natural ventilation. *ASHRAE journal*, (October).
- [6] Peeters, L., Dear, R. De, Hensen, J. & D'haeseleer, W. (2009) Thermal comfort in residential buildings: Comfort values and scales for building energy simulation. *Applied Energy*, 86 (5), pp.772–780.
- [7] Wang, Z., Zhang, L., Zhao, J. & He, Y. (2010) Thermal comfort for naturally ventilated residential buildings in Harbin. *Energy and Buildings*, 42 (12), pp.2406–2415.
- [8] Santamouris, M. & Asimakopoulos, D. (1996) *Passive cooling of buildings*. London, UK, James & James Ltd.
- [9] Psomas, T., Holzer, P. & Santamouris, M. (2014) A Naturally Ventilated Efficient Residential Building under the Impact of Climate Change. *International Journal of Ventilation*, 13 (2), pp.169–178.
- [10] Asimakopoulos, D.A., Santamouris, M., Farrou, I., Laskari, M., Saliari, M., Zanis, G., Giannakidis, G., Tigas, K., Kapsomenakis, J., Douvis, C., Zerefos, S.C., Antonakaki, T. & Giannakopoulos, C. (2012) Modelling the energy demand projection of the building sector in Greece in the 21st century. *Energy and Buildings*, 49, pp.488–498.
- [11] CIBSE (2005) *CIBSE Guide B. Heating, ventilating, air conditioning and refrigeration*. London, UK.
- [12] Santamouris M. (2006) *Natural Techniques to Improve Indoor and Outdoor Comfort During the Warm Period – A Review*. In: *Comfort and Energy Use in Buildings - Getting them Right*. Cumberland Lodge, Windsor, UK, London: Network for Comfort and Energy Use in Buildings.
- [13] Givoni, B. (1994) *Passive and Low Energy Cooling of Buildings*. USA, Van Nostrand Reinhold.
- [14] Papakonstantinou, K., Kiranoudis, C. & Markatos, N. (2000) Numerical simulation of air flow field in single-sided ventilated buildings. *Energy and Buildings*, 33 (1), pp.41–48.
- [15] Jiru, T.E. & Bitsuamlak, G.T. (2010) Application of CFD in Modelling Wind-Induced Natural Ventilation of Buildings - A Review. *International Journal of Ventilation*, 9 (2), pp.131–147.
- [16] Prajongsan, P. & Sharples, S. (2012) Enhancing natural ventilation, thermal comfort and energy savings in high-rise residential buildings in Bangkok through the use of ventilation shafts. *Building and Environment*, 50, pp.104–113.
- [17] Dehghan, A.A., Esfeh, M.K. & Manshadi, M.D. (2013) Natural ventilation characteristics of one sided wind catchers, experimental and analytical evaluation. *Energy and Buildings*, 61, pp.366–377.
- [18] Bahadori, M.N. (1985) An improved design of wind towers for natural ventilation and passive cooling. *Solar Energy*, 35 (2), pp.119–129.
- [19] Hughes, B.R., Calautit, J.K. & Ghani, S.A. (2012) The development of commercial wind towers for natural ventilation: A review. *Applied Energy*, 92, pp.606–627.

- [20] Calautit, J.K., Hughes, B.R. & Ghani, S.A. (2012) A numerical investigation into the feasibility of integrating green building technologies into row houses in the Middle East. *Architectural Science Review*, (September 2013), pp.1–18.
- [21] Mohamed, M.F., Prasad, D., King, S. & Hirota, K. (2009) The Impact of Balconies on Wind Induced Ventilation of Single-sided Naturally Ventilated Multi-storey Apartment. In: PLEA2009 - 26th Conference on Passive and Low Energy Architecture. Quebec City, Canada, PLEA2009, pp.22–24.
- [22] Mohamed, M., Behnia, M., King, S. & Prasad, D. (2011) The Potential of Natural Ventilation in Single-Sided Ventilated Apartment to Improve Indoor Thermal Comfort and Air Quality. In: ASME ed. ASME 2011 5th International Conference on Energy Sustainability ES2011. Washington, DC, USA, pp.1–8.
- [23] Zhou, J. & Chen, Y. (2010) A review on applying ventilated double-skin facade to buildings in hot-summer and cold-winter zone in China. *Renewable and Sustainable Energy Reviews*, 14 (4), pp.1321–1328.
- [24] Koinakis, C.J. & Sakellaris, J.K. (2007) Office building facades and energy performance in urban environment in Greece. In: 2nd PALENC Conference and 28th AIVC Conference on Building Low Energy Cooling and Advanced Ventilation Technologies in the 21st Century. Crete island, Greece, PALENC 2007, pp.541–546.
- [25] Pappas, A. & Zhai, Z. (2008) Numerical investigation on thermal performance and correlations of double skin façade with buoyancy-driven airflow. *Energy and Buildings*, 40 (4), pp.466–475.
- [26] Hanby, V.I., Cook, M.J., Infield, D., Ji, Y., Loveday, D.L., Mei, L. & Holmes, M.J. (2008) Nodal network and CFD simulation of airflow and heat transfer in double skin facades with blinds. *Building Service Engineering Research and Technology*, 29 (1), pp.45–59.
- [27] Lawson, B. (1997) *How designers think: the design process demystified*. third. Oxford, UK, Architectural Press, A division of Reed Education and Professional Publishing.
- [28] ELSTAT (2012) PRESS RELEASE. Announcement of the results from the 2011 Population Census for the Resident Population. Piraeus, Greece.
- [29] Montazeri, H. (2011) Experimental and numerical study on natural ventilation performance of various multi-opening wind catchers. *Building and Environment*, 46 (2), pp.370–378.
- [30] Colt (2006) Shadometal - catalogue [Internet]. Available from: <<http://pdf.archiexpo.com/pdf/colt/colt-shadometal/52229-48866.html>> [Accessed 15 May 2014].

7.9. Discussion

The relationship between external and internal air properties was investigated for the simulation results from both DTM and CFD, using statistical methods. The relationships predicted for the CFD results between wind speed, driving pressure, and ventilation rates, provided confidence in the modelling techniques involved. This chapter provided a further analysis of the performance of the ventilation strategies.

The purpose of this analysis was to convey the simulation results in a form that could be used by designers and practitioners interested in implementing natural ventilation strategies in similar buildings. It was expected that the predicted ventilation and cooling performance of the individual strategies within the case study building would contribute to the design process of new builds or refurbishment projects. Designers would be able to compare the performance of different strategies with regard to climate characteristics of the site under investigation, as presented in the analysis of this Chapter (e.g. Figure 7.21). The patterns in ventilation performance explored are expected to aid the design of the various natural ventilation strategies.

Accordingly, an example of a low-energy refurbishment design guide was proposed, providing information regarding the inclusion of natural ventilation strategies in existing buildings in the Mediterranean. The design guide summarised findings and observations of the performance evaluation of two natural ventilation strategies (wind-catcher and dynamic facade) designed in the case study building as an example of good practice. Development of the design guide could have a significant impact, as it would contribute to a large number of refurbishments for natural ventilation. The following chapter will summarise the conclusions of this research as presented in the Chapters 5, 6 and 7.

***Chapter 8* : CONCLUSIONS AND FUTURE WORK**

8.1. Summary of the Research Carried Out

A study of the literature provided information regarding the design and energy performance characteristics of the existing building stock in Greece. The typical Mediterranean climate and the occupants' comfort expectations were reviewed. Suitable natural ventilation strategies were identified in the literature and selected for the purpose of this research. The selection criteria included: climate applicability (hot, dry conditions with high local winds); design flexibility; ease of implementation and with minimum disruption to the occupants (systems designed primarily at the building envelope); ease of use (i.e. controlled operation of openings); and performance potential (with regard to reductions in mechanical cooling loads and to the IAQ improvements). The literature review was supported by elite interviews, which explored the opinion of professionals in Greece and highlighted the potential for natural ventilation refurbishment of the most typical domestic building type in Greece: the multi-storey apartment buildings. The literature review and the interviews were conducted to address objective one (in Chapter 1.3) and they were presented in Chapters 1 and 2.

A multi-storey apartment building in Athens was selected for the purpose of this work, representative of over 4 million buildings in Greece according to the output of the elite interviews and the literature review. The identified strategies for natural ventilation in apartment buildings were re-designed to meet the design and performance criteria of the study and the most common domestic building in Greece. Evaluation of the ventilation performance of these strategies in the case study apartment achieved the aim of this research project: to explore the potential for natural ventilation refurbishments of existing domestic buildings in order to provide summer comfort. Overall and specific strategy-focused conclusions drawn for each of the objectives are included in the following sections.

8.1.1. Methods of performance evaluation

As reported by others, the efficiency of natural ventilation depends on the building design and properties, the site characteristics (i.e. surroundings and microclimate) and the occupants' behaviour (i.e. presence and interaction with systems). Accordingly, it was decided to use two different modelling techniques for the performance evaluation of the various natural ventilation strategies in the case study building, with regard to the benefits and limitations of each technique. The DTM software was selected in order to deliver whole-building thermal modelling analysis at 1-hour intervals for the cooling period, considering the microclimate, the building design and the occupants. Although DTM provided spaced-averaged values of indoor air properties, these were time-dependent providing performance characteristics for the cooling period. This evaluated the thermal performance and estimated the cooling energy saving potential of the natural ventilation strategies, addressing the second objective of this research

Using steady-state CFD simulations, the detailed characteristics of natural flows due to wind and/or temperature difference were evaluated by considering the site characteristics and the building design. CFD results delivered detailed airflow rates through the building openings, indoor temperatures in all spaces, and predicted IAQ in response to the building geometry and climate. The CFD simulations were performed to address the third objective of this research.

Using the DTM it was possible to evaluate the performance of controlled day and night ventilation, and using CFD it was possible to evaluate the ventilation performance of a wind-catcher and water evaporation techniques. Despite the significant performance of the DTM to evaluate natural ventilation with openings control, simulation results show limitations of the modelling technique to appropriately evaluate wind-driven natural ventilation. This was because of the use of approximated driving pressures at the building openings. Using CFD it was possible to overcome the limitation of DTM and evaluate the ventilation performance of the building within its context (i.e. surrounding buildings). However, CFD was not able to predict the influence of the openings operation on the ventilation performance of the strategies and apartment building. The fully open building openings, the lack of thermal mass and the internal heat gains resulted in indoor air temperatures exceeding the ambient temperatures. However, for a number of climate scenarios and

by maintaining a fixed number of parameters (internal gains, adiabatic walls and percentage of openings operation) it was possible to ensure performance evaluation of the different natural ventilation strategies with regard to the base-case ventilation strategy.

The ventilation performance results predicted using the two modelling techniques should be reviewed in conjunction to each other in order to understand the more realistically modelled performance of the strategies.

8.2. Principal Findings

Findings of this research addressing Objectives 2, 3 and 4 suggest that all the proposed natural ventilation strategies evaluated delivered occupant comfort (natural cooling and adequate ventilation rates) and improved the IAQ. This was according to criteria defined by energy regulations, published work by others and with regard to the performance of the existing ventilation strategy (single-sided, typical method of ventilation in urban apartment buildings). The principal findings of this research project are included in the following list:

1. Using DTM it was predicted that the combined day and night ventilation strategy [DV & NV] performed the best. Using CFD it was possible to overcome the limitation of DTM and predict average pressures at the location of the openings, considering the location of the building and its surroundings (both external and internal flow simulations), leading to more accurate results. This predicted the significant ventilation performance of the wind-catcher [WC] relative to the simple single or cross-ventilation strategy [CV].
2. Results from all CFD simulations performed demonstrated the potential for wind-driven ventilation to improve upon the buoyancy-driven ventilation, assisting reductions in indoor temperatures of up to 0.5°C and 1°C relative to the buoyancy-driven flows, for 3.6m/s and 7m/s wind speeds respectively. However, indoor comfort was also provided during windless hours for specific strategies (buoyancy driven). This is significant as occupants' comfort could be provided by direct cooling during windless periods, which are up to 14% of the cooling period (wind speeds below 1m/s for the climate data of the site examined). In

addition, the downdraft evaporative cooling performed best at low ventilation rates, providing significant temperature reductions.

3. Wind speed and direction significantly influenced the performance of the strategies, particularly the wind-catcher strategy as also reported by others (Calautit, Hughes, & Ghani, 2012; Montazeri, Montazeri, Azizian, & Mostafavi, 2010). Higher wind speeds (from 3.6m/s to 7m/s) increased the ventilation rates by 4.6 times for the [SS] and by 2.1 times for the [DF & WC] strategy, they were thus more beneficial to the [SS] ventilation.
4. Evaluation of the ventilation performance of the strategies under different ambient temperatures (26°C and 35°C) predicted comparable results of internal-external temperature difference. However, when ventilation rates were beyond the value of 1000m³/h, the cases with higher external temperature begun to generate greater temperature differences by small magnitudes of up to 0.24°C. This shows that the cooling performance of the strategies increases with increase ambient temperatures, which is important considering the concerns over reported heat waves.
5. All strategies delivered air change rates above the minimum acceptable values for comfort according to standards, except for the base-case strategy. High values of air change rates with regard to the minimum acceptable for comfort were predicted in the apartment for the improved ventilation strategies and particularly for the combined wind-catcher and dynamic façade strategy (44ach⁻¹ on average) using CFD. These values represent steady state conditions that would vary throughout the ventilation period. This was confirmed by the DTM analysis predicting a wide range of air change rates during the cooling period (from 1ach⁻¹ up to 57ach⁻¹). High values are expected in free running buildings as predicted with measurements in Greek buildings by Geros et al. (1999). If these values are delivered during the night, they could provide cooling during the morning hours, and an additional delay of the peak temperatures, as predicted for the performance evaluation of nighttime ventilation using DTM. In addition, the high air velocities offset the increased temperature and provide direct occupants' comfort. Therefore, the contribution of the ventilation strategies in delivering natural cooling was substantial.

6. Evaluation of the lowest ventilation potential ($1/8^{\text{th}}$ performance-shared by the adjacent apartments) of the air shaft for the apartment studied, predicted an average of 66% lower air change rates, although also predicted higher than the minimum values for IAQ (18ach^{-1} on average for the [DF & WC]). These enhanced the cooling potential of the water evaporation strategies, providing further temperature reductions by up to 3.6°C . Comfort could be achieved even during the lowest ventilation potential of the strategies.
7. Provision of mechanical cooling (A/C split units) in the current building design and [base-case] ventilation strategy could result in energy consumption of 1135kW during the cooling period, for energy efficient systems. During this sufficient cooling was provided although CO_2 concentrations were predicted insufficient for IAQ. This figure is high and therefore if only natural ventilation strategies are used and if occupants' adaptation to higher indoor air temperatures is considered, significant energy savings could be achieved. During the [DF & WC] strategy, indoor air temperatures exceeded the 28°C threshold for 16% of the cooling period. With regard to the significant ventilation and cooling performance of the [DF & WC] it is proposed that mechanical cooling would be provided during only the hours that indoor temperatures exceeded the 28°C . This would achieve comfort and substantial energy savings as the A/C would operate for a maximum of one third of the hours it would operate if it were implemented in the existing building design and ventilation strategy. This is in accordance to published work by others reporting that free-running buildings consume 50% less energy than the air-conditioned buildings (O'Sullivan & Kolokotroni, 2014).
8. Although the PDEC strategy was predicted to deliver the largest temperature reduction, due to potentially excessive water consumption (up to 8litres per hour), the combined operation of a wind-catcher and a lightweight dynamic façade [DF & WC] was considered the most efficient solution for the Mediterranean sub-climate and building type studied. This strategy led to significant increase in ventilation rates, contributed to reductions in indoor air temperatures, and provided occupants' comfort, relative to all natural ventilation strategies investigated. The combined wind catcher and dynamic façade strategy performed the best and would be recommended, supplemented with evaporative cooling for windless hours, and mechanical cooling only when these strategies do not provide sufficient performance.

This research recognises that natural ventilation strategies could be effectively introduced in apartment buildings in Greece, and be an alternative to conventional mechanical cooling and ventilation systems during the cooling period.

8.2.1. Predicted performance: natural ventilation and cooling strategies

The overall performance of the individual ventilation strategies, existing and new, evaluated within this research project are presented as follows:

➤ *Existing ventilation strategy [base-case]:*

The existing ventilation strategy of the apartment under study [base-case] resulted in high levels of CO₂ concentration exceeding the maximum for comfort (1,000ppm), particularly during the nighttime. These values are commonly expected in domestic buildings in Greece with limited ventilation (Santamouris et al., 2007). Due to the lack of appropriate wall insulation (the building was constructed prior to the first thermal insulation law in Greece) and the un-controlled ventilation (openings operating specific hours per day with regards to occupants) the indoor temperatures closely follow the fluctuation and peaks of the external temperature. As predicted during the evaluation of an A/C system operation, very low ventilation rates were provided, and thus even if mechanical cooling was provided occupants' comfort would not be achieved.

➤ *Individual day ventilation [DV] and night ventilation [NV]:*

Comfort was provided throughout the day with adequate controlled natural day-only ventilation [DV]. Night-ventilation [NV] provided significant indoor temperature reduction during the morning hours (on average 2.5°C) and reduction of the peak temperatures. During the nighttime, the CO₂ levels in the bedrooms (433ppm) were predicted to be lower than the previously described ventilation strategies ([base-case], [DV]) and acceptable for IAQ. The contribution of the individual [DV] and [NV] strategies to the ventilation performance the apartment for the different hours of the day relative to the [base-case] strategy, demonstrate the potential of the combined day and night ventilation.

➤ *Combined day and night ventilation [DV & NV]:*

The combined day and night ventilation strategy [DV & NV] resulted in up to 7°C indoor air temperature reductions relative to the base-case strategy, particularly during the hours of the day with the highest ambient temperatures. Operative temperatures were predicted within the comfort range defined by EN15251 (BS EN15251 CEN, 2007), exceeding the top limit of the narrowest comfort range ($T_{I \max}$) for only 5% of the cooling period. This strategy marginally reduced the hours during the cooling period for which the CO₂ levels exceeded the upper acceptable limit for comfort (i.e. 1000ppm) relative to the base-case ventilation strategy (29% above 1000ppm), to as little as 1%. This is significant considering the reported concerns in the literature over high values of CO₂ emissions in domestic buildings, and particularly in mechanically ventilated spaces (Santamouris et al., 2007). Automatic control of the openings in response to environmental parameters and the occupants delivered occupants' comfort and adequate ventilation rates.

➤ *Internal openings [InOp]:*

This strategy was able to deliver sufficient ventilation rates, ensure privacy within the apartment spaces (the internal bedroom doors were fully closed) and to provide comfort relative to the [base-case] strategy. However, due to the smaller cross-section area of the hallway openings relative to the area of the internal doors the strategy had negligible contribution to the natural ventilation of the apartment under investigation. All natural ventilation strategies explored performed better when all internal doors were fully open. Further work would be required to optimise the performance of this strategy.

➤ *Single-sided ventilation [SS]:*

The performance of this [SS] strategy was considered insufficient for IAQ during windless hours, predicting ventilation rates as low as zero (buoyancy-driven), and insufficient to deliver comfort. Comfort could be achieved for more than 14% of the cooling period. Even under wind-driven forces, the [SS] ventilation delivered high indoor temperatures (up to 2°C above the DBT) under all climate scenarios examined.

➤ *Cross-ventilation [CV]:*

Wind-driven [CV] contributed to temperature reduction in the occupied spaces of up to 5% relative to the [SS] ventilation, for average DBT of 26°C. It also resulted in an

increase in the ventilation rates of up to 14 times relative to [SS] ventilation. Both [SS] and [CV] strategies resulted in air change rates comparable to those predicted by others in existing apartments in Athens (Niachou et al., 2005), providing evaluation of the designs and modelling techniques used.

➤ *Wind-catcher [WC]:*

The ventilation performance of the inclusion of a wind-catcher in the building design was evaluated using both DTM and CFD tools. DTM results indicate comparable performance of the wind-catcher strategy to the previous simple day and night ventilation strategy. This was due to the limitations of the DTM software in modelling wind driven flows, using approximated pressure coefficients. Using CFD it was possible to predict the significant performance of the wind-catcher; this was compared with published work by others (Calautit et al., 2012). Particularly, the inclusion of a wind-catcher [WC] assisted the increase in air change rates of 8% during buoyancy driven flow and up to 76% during wind driven flow, relative to the simple natural cross ventilation [CV] strategy under steady state conditions. The performance of the [WC] under wind-driven flows was significant relative to the buoyancy driven and in accordance with published work (Calautit et al., 2012).

➤ *Combined wind-catcher and dynamic façade [DF & WC]:*

In overall, the introduction of the dynamic façade enhanced the natural ventilation of the previous strategies, delivering higher volume flow rates by up to 40% at the inlets. However, this improved performance was dependent on the wind scenario (direction and speed), showing less improvement than the [WC] strategy in some cases.

The [DF & WC] strategy delivered sufficient air change rates (9ach^{-1} on average) with small standard deviation (i.e. 8.5 relative to the 14.2 of the [base-case]). The new ventilation strategies reduced the hours during the cooling period for which the air change rates were as low as 1ach^{-1} (27%) and the hours above 20ach^{-1} , which for a prolonged period could result in impaired air quality and discomfort. Air velocities at the internal doors (bedrooms) of up to 1.7m/s were predicted, being substantially higher relative to the other natural ventilation strategies and the minimum recommended values for comfort. Direct comfort cooling with natural ventilation was provided.

This strategy provided further temperature reductions and reduced the daily temperature fluctuations relative to the rest of the ventilation strategies. For high outdoor air temperatures, exceeding 30°C, up to 8°C lower internal air temperatures were predicted. This offered reduction of the highest temperatures achieving operative temperatures in the spaces, exceeding the top limit of the narrowest comfort range for 1% of the cooling season (BS EN15251 CEN, 2007). Sufficient natural cooling was provided for 65% of the cooling period; lower than the minimum for comfortable indoor temperatures were predicted and above the minimum (18°C) for outdoor temperature for ventilation during winter (BS EN15251 CEN, 2007). Comfort was achieved.

➤ *Passive downdraught evaporative cooling [PDEC]:*

The introduction of passive cooling by water evaporation in both ventilation strategies of [WC] and [DF & WC] resulted in an average reduction in the ventilation rates of 7%, and in significant temperature reductions of 3°C. The natural cooling performance of the [PDEC] reduced with increasing ventilation rates. Further reductions in indoor temperatures would be expected with continuous operation over a short period of the PDEC strategies, which could be evaluated using time-dependent methods. Work by Ford et al. (2012) provides confidence in the predicted performance of the proposed PDEC strategy in the apartment studied.

8.2.2. Research output

A parametric sensitivity analysis performed identified the variables with the greatest impact to the indoor environment, even though it is only an approximation of the real world situation. It was important to develop empirical relationships for both CFD and DTM simulation results that could be used to predict broad patterns in ventilation performance under conditions that have not been examined using simulations.

The relationships established would be used by designers and practitioners aiming to assess the expected performance of the ventilation strategies if implemented in similar buildings and climates, with regard to their performance in the case study building. This information could be used to extrapolate patterns of ventilation performance to facilitate the design of various natural ventilation strategies in new or existing buildings, by seeing how they perform in the case study. In addition, these

findings could be used as valuable feedback to improve the individual operation scenarios of the ventilation systems (i.e. openings) in order to provide optimum control and occupants' comfort. Designers could use these relationships to predict internal air characteristics with regard to climate characteristics, for similar buildings and microclimates.

The established performance of the natural ventilation strategies assists the development of a prototype scenario for similar building and microclimates; this addresses the last objective of this research project. Concerns over increasing fuel poverty and energy consumption in the domestic building stock highlight the significant impact that implementation of such effective natural ventilation strategies could have. The output of this work was used to produce a low-energy refurbishment design guide, with the aim of assisting designers, professionals, developers and householders in dealing with the implementation of natural ventilation strategies in domestic buildings for future and current climates. A first proposal of the content and layout of the low-energy refurbishment design guide for apartments in the Mediterranean was presented. This is an example of the guide with recommendations for the inclusion of wind-catchers and dynamic façades in buildings. This would be further developed after the completion of the research reported here. Development of the design guide will offer a way to disseminate the output of this work to practitioners in a concise and user-friendly way in order: to promote sustainable development of the existing building stock; deliver energy reduction in buildings; and encourage adaptation to climate change within good design practice of natural ventilation strategies.

8.3. Contribution to knowledge

This research has focused on the performance evaluation of combined natural ventilation strategies, within an existing apartment building using quantitative techniques. By predicting the ventilation and natural cooling performance efficiency of the natural ventilation strategies implemented in an apartment building, valuable guidance for future refurbishment projects could be identified.

The building under investigation is representative of over 4 million buildings in Greece (70% of the total domestic building stock in Greece), therefore, if natural ventilation delivers occupants' thermal comfort expectations, there is a potential to implement this on a large scale in order to proceed to a significant energy consumption reduction. This is important because it will reduce costs and also contribute significantly to the battle against climate change. Therefore, this research has demonstrated a way to ensure resilience of the existing building stock, deliver sustainable development, and provide solutions to a country under economic recession.

The natural ventilation strategies evaluated have been shown to have potential in reducing mechanical cooling in the apartment building studied. This research was important to identify which strategies can be more efficient if implemented in an apartment building in a densely populated area of Athens. The natural ventilation strategies and apartment studied were evaluated using computational tools for the building within its 'physical' context with regard to the operation, microclimate and characteristics of the urban environment. This provided a representative picture of the performance of the strategies. Certain strategies have been shown to have significant performance (combined wind-catcher and dynamic façade) relative to the others.

The implementation of modified conventional natural ventilation strategies, which were combined and evaluated within the context of the case study building and climate, provided new insights into their potential performance in practice.

8.4. Limitations of this Research

This research focused on a representative apartment building with a real-life context. Exploring the properties of a single phenomenon or instance under specific conditions helped generalisations in a larger set of cases. Even though the study focused on a single apartment, often, working with specific examples provides better understanding of the whole. The simulations were based on several assumptions or parameters (heat gains, openings operation, thermal mass, obstacles etc.) that were kept consistent for each of the cooling strategies examined. Therefore, the relative performance between the natural ventilation strategies that were determined from this modelling campaign is representative of real behaviour trends. This section summarises the limitations of this research and the decisions and assumptions made in response to these.

8.4.1. Occupancy and Building Design

The daily occupancy levels of the single apartment under investigation for the purpose of the DTM simulations were predicted according to published work on domestic buildings in Greece. The assumptions made included distribution of occupants in the spaces throughout the day; during the nighttime, only two spaces were exclusively occupied. The occupancy density was treated as heat sources and not as an actual number of occupants in the spaces. The occupancy profile was the average of different behaviours as defined by literature. Further, the profiles of the internal heat gains (e.g. equipment and lighting) were created to comply with the occupancy profile and corresponding activities. This was important for provision of comparative daily results. People may behave differently and therefore modelling their behaviour can only give an indication of use and performance.

Detailed weekly and monthly profiles of individual spaces could potentially provide realistic values of internal heat gains. However, such profile could only be designed according to the occupancy and operation of the specific household; generalisation of the simulation results in similar buildings would be difficult. Further research would

explore ways to attain specific occupancy patterns via real life measurements for DTM studies.

Alterations to the building design and envelope, such as redesigning of the existing internal and external openings of the building under investigation, were beyond the scope of this research. The openings' size and position on the walls were kept consistent for all simulations. It was important to implement strategies that would not result in occupants' disruption. Future work could focus on optimisation of the openings' position and operable area to potentially improve the performance of the ventilation strategies.

8.4.2. CFD modelling

Due to the computational time required to evaluate the airflow around the case study building in CFD, simplifications were required in the CFD model with regard to the form, design of the building, and its surroundings. The surrounding buildings were simplified and their layout was modified to 'fit' in a perpendicular mesh. Variables such as the number of penthouses of the surrounding buildings, the street obstacles (e.g. trees, parked cars, litterbins, light posts), the external shadings and the balconies of the surroundings, were all excluded from the computational models. These variables would result in a significant increase of the number of computational cells in zones that detailed evaluation of the airflow was not required (i.e. at various domain locations and distances from the building under investigation). These would result in a substantial increase in the computational power required. Further, the area was modelled on a horizontal terrain and the building heights were increased to account for varying terrain heights. This was decided with regard to early stage simulations performed, which experienced convergence difficulties (i.e. an inclined object representing the natural ground increase required high number of cells close to the domain edges).

Investigation of the relationship between the building's thermal mass and the ventilation performance of the natural ventilation strategies investigated was evaluated using the DTM. However, this was beyond the scope of the CFD modelling work. The internal heat gains (e.g. occupants, lighting, equipment and solar gains) were modelled in all CFD simulations as volumetric heat sources centred

in each occupied space in order to provide comparable steady state results of internal air properties. Distribution of the heat sources in the spaces according to real behaviour following predicted or measured data is ideally to result in different airflow distributions to those predicted. However, as occupants may behave differently to what was modelled, heat gains can only be represented in the spaces with a certain probability.

Furthermore, the ventilation performance of the building under investigation and passive strategies was evaluated for a number of climate scenarios (18 in total) of combinations of DBTs, wind speeds and wind directions. Although this number was appropriate for the evaluation of the performance of the natural ventilation strategies, it was considered relatively small to draw conclusions on the relationship trends between wind speed, ventilation rates and indoor air temperatures. Thus, a number of additional simulations were performed using more climate scenarios. Ideally, an extensive number of climate scenarios would be explored to gain further understanding of these relationships. This would include the exploitation of various wind speeds and outdoor air temperatures, and other variables, such as the moisture content and solar gains. Further research could explore the influence of a range of low wind speeds to the indoor air quality (below approximately 2m/s) with additional CFD simulations.

8.5. Recommendations for Further Work

In order to improve the validity of the numerical model, it is recommended that field measurements taken from the case study building should be implemented in the model to improve the accuracy of its representation of the building. The presented and evaluated strategies would be thoroughly designed and then installed in the building under investigation, along with monitoring equipment. Performance of the ventilation strategies and the case study building would then be monitored over a full year to capture the behaviour during all seasons. Occupants' behaviour and interaction with the ventilation strategies will be also monitored and supported by interviews. This will also provide information regarding the in detail implementation, running cost and the amount of disruption to occupants. The simulation results would be validated with the measurements obtained from the building, while further

simulations would be performed in order to model different scenarios. Qualitative research exploring the occupants' satisfaction, comfort, disruption etc. would be performed, within purpose-designed questioners addressing thermal comfort satisfaction.

Results from this research could assist the development of optimum designs that could be further investigated using numerical modelling in a number of existing buildings (same building type and different microclimates). This would assist the prediction of comprehensive natural ventilation and cooling performance values, and promote further low energy refurbishment projects.

To achieve extensive application of natural ventilation strategies in the large domestic building stock, there is a need to proceed to further research in developing low-cost versions of these natural ventilation strategies, in order to be widely available to occupants that currently suffer from fuel poverty. These would be developed according to experimental results using modelling techniques and measurements in the case study building, and by evaluating the overall performance of each strategy, i.e. the relation between cost and efficiency. This would create affordable and more appealing energy refurbishment systems that would potentially eliminate their need for mechanical techniques to deliver appreciable IAQ.

All future work performed will be further incorporated in the low-energy refurbishment design guide for natural ventilation, proposed and developed within this research. As this research was initiated by contacting industry to develop the need, a way to ensure impact will be by making the low-energy refurbishment design guide available to practitioners and designers. The opinion of the designers and developers in Greece will be obtained through an iterative process where they are able to provide feedback on the practicality and efficiency of the energy refurbishment guide. This will ensure the efficient development of the guide and its value to the industry.

REFERENCES

Akbari, H., Davis, S., Dorsano, S., Huang, J. & Winnett, S. (1992) *Cooling our communities: A guidebook on tree planting and light-colored surfacing*. Lawrence Berkeley Lab., CA (United States); Environmental Protection Agency, Washington, DC (United States). Climate Change Div. Available from: <http://www.osti.gov/energycitations/product.biblio.jsp?osti_id=5032229> [Accessed 14 December 2011].

Allocca, C., Chen, Q. & Glicksman, L.R. (2003) Design analysis of single-sided natural ventilation. *Energy and Buildings*, 35 (8), pp.785–795. Available from: <<http://linkinghub.elsevier.com/retrieve/pii/S0378778802002396>> [Accessed 17 July 2014].

Andersen, R.V., Toftum, J., Andersen, K.K. & Olesen, B.W. (2009) Survey of occupant behaviour and control of indoor environment in Danish dwellings. *Energy and Buildings*, 41 (1), pp.11–16. Available from: <<http://linkinghub.elsevier.com/retrieve/pii/S0378778808001655>> [Accessed 12 November 2012].

Androutsopoulos, A., Aravantinos, D., Gaglia, A., Giannakidis, C., Gidaki, C., Dimoudis, A., Droutsas, K., Efthimiadis, A., Zacharias, P., Iliadis, C., Theodosiou, T., Kalliakoudi, K., Katsimihas, S., Kteniadakis, M., Ladopoulos, C., Lampropoulou, L., Laskos, K., Malahias, C., Mantas, D., Maris, A., Maris, T., Balaras, K., Polychronia, E., Sagia, G., Sofronis, H., Tsagkrasoulis, A., Tsikaloudaki, K. & Chasapis, D. (2012) *T.O.T.E.E. 20701-1/2010 Detailed national requirements of parameters for calculating the energy performance of buildings and issuing the energy performance certificate [in Greek]*. 2nd ed. Athens, Greece, TEE, Technical Chamber of Greece. Ministry of Environment, Energy and Climate Change-YPEKA-Special Secretariat for Environmental Inspectorate and Energy. Special Ministry of Energy Inspectorate.

Argiriou, A., Gaglia, A., Daskalaki, E., Zaharias, P., Katsanos, D., Kontogiannidis, S., Ladopoulos, G. & Ladopoulos, I. (2010) *T.O.T.E.E. 20701-3/2010 Climate data of Greek Cities [In Greek], Technical Directive by the Technical Chamber of Greece*. Athens. Available from: <<http://www.helapco.gr/ims/file/installers/totee-klimatika.pdf>>.

ASHRAE (2009) *2009 ASHRAE Handbook Fundamentals*. SI Edition. Atlanta, American Society of Heating, Refrigerating and Air-Conditioning Engineers, Inc. Available from: <<http://www.ncbi.nlm.nih.gov/pubmed/22081950>>.

ASHRAE (2013) *ANSI/ASHRAE Standard 62.1-2013. Ventilation for Acceptable Indoor Air Quality*. Atlanta.

Asimakopoulos, D.A., Santamouris, M., Farrou, I., Laskari, M., Saliari, M., Zanis, G., Giannakidis, G., Tigas, K., Kapsomenakis, J., Douvis, C., Zerefos, S.C., Antonakaki, T. & Giannakopoulos, C. (2012) Modelling the energy demand projection of the building sector in Greece in the 21st century. *Energy and Buildings*, 49, pp.488–498. Available from: <<http://linkinghub.elsevier.com/retrieve/pii/S0378778812001351>> [Accessed 30 March 2012].

Asquith, L. & Vellinga, M. (2006) *Vernacular architecture in the twenty-first century: theory, education and practice*. 1st ed. Abingdon, Oxon, Taylor and Francis. Available from: <http://books.google.com/books?hl=en&lr=&id=rZqkTvJoHQMC&oi=fnd&pg=PP1&dq=Vernacular+architecture+in+the+twenty-first+century:+theory,+education+and+practice&ots=RyxTB9T2Dg&sig=BRY7htzME6IY_UXB3cUfDJe0hIM> [Accessed 25 January 2012].

Assimakopoulos, V.D., Stathopoulou, O.I., Halios, C. & Helmis, C.G. (2008) Numerical Investigation of Indoor Environmental Conditions in an Office. *Journal of Ventilation*, 6 (4), pp.315–326.

Attia, S., Beltrán, L., Herde, A. De & Hensen, J. (2009) ‘Architect Friendly’: A Comparison of Ten Different Building Performance Simulation Tools. In: *Building Simulation 2009*. Glasgow, Scotland, Eleventh International IBPSA Conference, pp.204–211. Available from: <http://orbi.ulg.ac.be/bitstream/2268/167578/1/BS09_0204_211.pdf> [Accessed 29 October 2014].

Ayad, S.S. (1999) Computational study of natural ventilation. *Journal of Wind Engineering and Industrial Aerodynamics*, 82 (1-3), pp.49–68. Available from: <<http://linkinghub.elsevier.com/retrieve/pii/S0167610598002104>>.

Bahadori, M.N. (1985) An improved design of wind towers for natural ventilation and passive cooling. *Solar Energy*, 35 (2), pp.119–129. Available from: <<http://linkinghub.elsevier.com/retrieve/pii/0038092X85900027>>.

Baharvand, M., Bin Ahmad, M.H., Safikhani, T. & Chung, L.P. (2014) Double Skin Facade and Opening Configurations Effect on Indoor Air Distribution. *Journal of Engineering and Applied Sciences*, 9 (4), pp.69–77.

Balaras, K. (2001) *Guide on energy saving in dwellings [In Greek]*. Athens, National Observatory of Athens. Ministry of Environment and Public Works. Available from: <http://www.minenv.gr/4/47/00_4701/odigos_katoikion.pdf>.

Baldinelli, G. (2009) Double skin façades for warm climate regions: Analysis of a solution with an integrated movable shading system. *Building and Environment*, 44 (6), pp.1107–1118. Available from: <<http://linkinghub.elsevier.com/retrieve/pii/S0360132308001935>> [Accessed 16 September 2013].

Batty, W.J., Al-Hinai, H. & Probert, S.D. (1991) Natural-cooling techniques for residential buildings in hot climates. *Applied Energy*, 39 (4), pp.301–337. Available from: <[http://dx.doi.org/10.1016/0306-2619\(91\)90002-F](http://dx.doi.org/10.1016/0306-2619(91)90002-F)> [Accessed 13 June 2012].

Becker, R. & Paciuk, M. (2009) Thermal comfort in residential buildings – Failure to predict by Standard model. *Building and Environment*, 44 (5), pp.948–960. Available from: <<http://linkinghub.elsevier.com/retrieve/pii/S0360132308001601>> [Accessed 5 September 2012].

Belarbi, R., Ghiaus, C. & Allard, F. (2006) Modeling of water spray evaporation: Application to passive cooling of buildings. *Solar Energy*, 80 (12), pp.1540–1552. Available from: <<http://linkinghub.elsevier.com/retrieve/pii/S0038092X06000351>> [Accessed 29 January 2014].

Berry, J.M. (2002) Validity and Reliability Issues in Elite Interviewing. *Political Science and Politics*, 35 (4), pp.679–682. Available from: <http://keats.kcl.ac.uk/pluginfile.php/1196836/mod_resource/content/1/eliteInterviewing.pdf> [Accessed 29 July 2015].

Brager, G. & Dear, R. de (2000) A standard for natural ventilation. *ASHRAE journal American Society of Heating, Refrigerating and Air-Conditioning Engineers, Inc.*, (October). Available from: <http://www.cbe.berkeley.edu/research/pdf_files/brager2000_ashrae-ventilation.pdf> [Accessed 21 December 2012].

BS EN15251 CEN (2007) *Indoor environmental input parameters for design and assessment of energy performance of buildings addressing indoor air quality, thermal environment, lighting and acoustics*. London, UK, British Standards Institute (BSI).

Butera, F.M. (1994) Energy and buildings in Mediterranean countries: Present and future. *Renewable Energy*, 5 (5-8), pp.942–949. Available from: <<http://www.sciencedirect.com/science/article/B6V4S-4903FF2-FC/2/a0595de189c0fd6eecba9029db0479c5>>.

Calautit, J.K., Hughes, B.R. & Ghani, S.A. (2012) A numerical investigation into the feasibility of integrating green building technologies into row houses in the Middle East. *Architectural Science Review*, (September 2013), pp.1–18. Available from: <<http://www.tandfonline.com/doi/abs/10.1080/00038628.2012.686433>>.

Canas, I. (2004) Recovery of Spanish vernacular construction as a model of bioclimatic architecture. *Building and Environment*, 39 (12), pp.1477–1495. Available from: <<http://linkinghub.elsevier.com/retrieve/pii/S0360132304001295>> [Accessed 17 August 2011].

Cândido, C., Dear, R. de, Lamberts, R. & Bittencourt, L. (2008) Natural ventilation and thermal comfort: air movement acceptability inside naturally ventilated buildings in Brazilian hot humid zone. In: *Air Conditioning and the Low Carbon Cooling Challenge, Cumberland Lodge, Windsor, UK, 27-29 July 2008*. London: Network for Comfort and Energy Use in Buildings.

Cândido, C., Lamberts, R., de Dear, R., Bittencourt, L. & de Vecchi, R. (2011) Towards a Brazilian standard for naturally ventilated buildings: guidelines for thermal and air movement acceptability. *Building Research & Information*, 39 (2), pp.145–153. Available from:

<<http://www.tandfonline.com/doi/abs/10.1080/09613218.2011.557858>> [Accessed 13 January 2015].

Cardinale, N., Micucci, M. & Ruggiero, F. (2003) Analysis of energy saving using natural ventilation in a traditional Italian building. *Energy and buildings*, 35 (2), pp.153–159. Available from: <<http://www.sciencedirect.com/science/article/pii/S0378778802000245>> [Accessed 23 November 2011].

Carter, T. & Cromley, E.C. (2005) *Invitation To Vernacular Architecture: A Guide To The Study Of Ordinary Buildings And Landscapes*. Knoxville, Univ. of Tennessee Press. Available from: <<http://books.google.com/books?id=JdAI73YVMEoC&pgis=1>> [Accessed 9 July 2012].

CHAM Ltd. (2008) *Phoenics Encyclopaedia* [Internet]. Available from: <http://www.cham.co.uk/phoenics/d_polis/d_enc/encindex.htm>.

CHAM Ltd. (2013) PHOENICS software, version 2012 (64bit Intel), Project Licence, UK–Headquarters Concentration, Heat and Momentum Limited, Wimbledon Village, London.

Chen, Q. & Srebric, J. (2002) A procedure for verification, validation, and reporting of indoor environment CFD analyses. *HVAC&R Research*, 8 (2), pp.201–216. Available from: <<http://www.tandfonline.com/doi/full/10.1080/10789669.2002.10391437>> [Accessed 27 April 2013].

Cheung, J.O.P. & Liu, C.-H. (2011) CFD simulations of natural ventilation behaviour in high-rise buildings in regular and staggered arrangements at various spacings. *Energy and Buildings*, 43 (5), pp.1149–1158.

CIBSE (2006) *CIBSE Guide A. Environmental design*. London, UK.

CIBSE (2005) *CIBSE Guide B. Heating, ventilating, air conditioning and refrigeration*. London, UK.

ClimateConsultant (2014) Climate Consultant, software, version 5.5 (build 5), free licence, Department of Architecture and Urban Design University of California, Los Angeles.

Colt (2006) Shadometal - catalogue [Internet]. Available from: <<http://pdf.archiexpo.com/pdf/colt/colt-shadometal/52229-48866.html>> [Accessed 15 May 2014].

Cook, M., Ji, Y. & Hunt, G. (2003) CFD modelling of natural ventilation: combined wind and buoyancy forces. *International Journal of Ventilation*, 1 (3), pp.169–180. Available from: <<http://usir.salford.ac.uk/15841/>>.

Cook, M., Yang, T. & Cropper, P. (2011) Thermal comfort in naturally ventilated classrooms: Application of coupled simulation models. In: *Proceedings of Building Simulation 2011: 12th Conference of International Building Performance Simulation*

Association, Sydney, 14-16 November. Sydney, IBPSA International Building Performance Simulation Association, pp.2257–2262. Available from: <http://www.ibpsa.org/proceedings/BS2011/P_1714.pdf>.

Cook, M.J. (1998) An Evaluation of Computational Fluid Dynamics for Modelling Buoyancy- Driven Displacement Ventilation. PhD Thesis, De Montford, Leicester.

Creswell, J.W. (2009) *Research Design. Qualitative, Quantitative, and Mixed Methods Approaches*. 3rd ed. USA, SAGE Publications, Inc.

Dagnew, A.K., Bitsuamalk, G.T. & Merrick, R. (2009) Computational evaluation of wind pressures on tall buildings. In: *11th Americas Conference on Wind Engineering*. San Juan, Puerto Rico, pp.1–17.

Dascalaki, E., Santamouris, M., Argiriou, A., Helmis, C., Asimakopoulos, D., Papadopoulos, K. & Soilemes, A. (1995) Predicting single sided natural ventilation rates in buildings. *Solar Energy*, 55 (5), pp.327–341. Available from: <<http://www.sciencedirect.com/science/article/pii/0038092X9500057X>> [Accessed 11 April 2013].

Dascalaki, E., Santamouris, M. & Asimakopoulos, D.N. (1999) On the use of deterministic and intelligent techniques to predict the air velocity distribution on external openings in single-sided natural ventilation configurations. *Solar Energy*, 66 (3), pp.223–243. Available from: <<http://linkinghub.elsevier.com/retrieve/pii/S0038092X99000213>>.

Dascalaki, E.G., Drousta, K., Gaglia, A.G., Kontoyiannidis, S. & Balaras, C.A. (2010) Data collection and analysis of the building stock and its energy performance - An example for Hellenic buildings. *Energy and Buildings*, 42 (8), pp.1231–1237. Available from: <<http://linkinghub.elsevier.com/retrieve/pii/S0378778810000459>> [Accessed 11 March 2013].

De Dear, R.J. & Brager, G.S. (2002) Thermal comfort in naturally ventilated buildings: revisions to ASHRAE Standard 55. *Energy and Buildings*, 34 (6), pp.549–561. Available from: <<http://linkinghub.elsevier.com/retrieve/pii/S0378778802000051>>.

DECC Explaining Climate Change [Internet]. Available from: <<http://www.decc.gov.uk/en/content/cms/tackling/explaining/explaining.aspx>> [Accessed 15 March 2012].

Dehghan, A.A., Esfeh, M.K. & Manshadi, M.D. (2013) Natural ventilation characteristics of one sided wind catchers, experimental and analytical evaluation. *Energy and Buildings*, 61, pp.366–377. Available from: <<http://linkinghub.elsevier.com/retrieve/pii/S0378778813001424>> [Accessed 11 March 2013].

Dimitroulopoulou, C. (2012) Ventilation in European dwellings: A review. *Building and Environment*, 47, pp.109–125. Available from: <<http://linkinghub.elsevier.com/retrieve/pii/S0360132311002241>> [Accessed 24 July 2012].

Douglas, J.F., Gasiorek, J.M., Swaffield, J.A. & Lynne, B.J. (2005) *Fluid Mechanics*. Fifth. Essex, England, Pearson Education Limited.

Drakou, A., Tsangrassoulis, A. & Roetzel, A. (2011) Occupant interaction with the interior environment in Greek dwellings during summer. In: *Plea 2011 - 27th Conference on Passive and Low Energy Architecture, Volume 1 of (2)*. Louvain-la-Neuve, Belgium, Presses universitaires de Louvain, pp.475–480. Available from: <<http://books.google.com/books?hl=en&lr=&id=KKZMp2kotAEC&pgis=1>> [Accessed 22 November 2012].

Drymiotis, A. (2014) The refugee house of Alexandras Avenue [in greek]. *H Kathimerini*. Available from: <www.kathimerini.gr/759372/opinion/epikairothta/politikh/ta-prosfygika-ths-lewforoy-ale3andras>.

Durrani, F., Cook, M.J. & McGuirk, J.J. (2012) Modelling Buoyant Thermal Plumes in Naturally Ventilated Buildings. In: *BSO12. First Building Simulation and Optimization Conference*. Loughborough, UK, IBPSA-England, pp.117–123. Available from: <<http://www.ibpsa-England.org/resources/files/bs0-2012/2B1.pdf>>.

Durrani, F., Cook, M.J., Mcguirk, J.J. & Kaye, N.B. (2013) Large Eddy Simulation of buoyancy-Driven natural ventilation – Twin-plume flow. *International Journal of Ventilation*, 11 (4), pp.353–366. Available from: <<http://ijoint.org/doi/abs/10.5555/2044-4044-11.4.353>>.

EL.STAT. (2012) *Press release: Announcement of the results of the 2011 Population Census for the Resident Population*. Piraeus, Greece.

EL.STAT. (2014) Statistical Database [Internet]. Available from: <www.statistics.gr>.

Emmitt, S. (2012) *Architectural Technology*. second. West Sussex, UK, John Wiley & Sons, Ltd.

Emmitt, S. & Ruikar, K. (2013) *Collaborative Design Management*. 1st ed. Abingdon, Oxon, Routledge.

Encinas Pino, F. & de Herde, A. (2011) Definition of occupant behaviour patterns with respect to ventilation for apartments from the real estate market in Santiago de Chile. *Sustainable Cities and Society*, 1 (1), pp.38–44. Available from: <<http://linkinghub.elsevier.com/retrieve/pii/S2210670710000065>> [Accessed 12 November 2012].

Erell, E. (2007) Evaporative Cooling. In: M. Santamouris ed. *Advances in Passive Cooling*. UK, USA, Earthscan, pp.228–261.

European Commission (2011) *Communication from the commission to the European parliament, the council, the European economic and social committee and the committee of the regions. A roadmap for moving to a competitive low carbon economy in 2050*. Brussels. Available from: <<http://eur-lex.europa.eu/legal-content/EN/NOT/?uri=CELEX:52011DC0112>> [Accessed 21 July 2015].

Eurostat (2011a) *Consumption of energy: tables and figures*. European Commission Directorate-General for Energy and Transport (DG TREN). Available from: <http://epp.eurostat.ec.europa.eu/statistics_explained/index.php/Consumption_of_energy#>.

Eurostat (2008) *Energy Statistics for Greece. Table 2.6.10*. European Commission Directorate-General for Energy and Transport (DG TREN). Available from: <http://ec.europa.eu/dgs/energy_transport/figures/pocketbook/doc/2007/2007_energy_en.pdf>.

Eurostat (2011b) Map of the total greenhouse gas emissions (in CO₂ equivalent) indexed to Kyoto base year [Internet]. Available from: <<http://epp.eurostat.ec.europa.eu/tgm/refreshMapView.do?tab=map&plugin=1&init=1&toolbox=types&pcode=tsdcc100&language=en>> [Accessed 10 February 2012].

F.E.K. (2003) *Greek Government Gazette (Φ.Ε.Κ.) [In Greek]. No of issue 58*. Athens, Greece.

Fabi, V., Andersen, R.V., Corgnati, S. & Olesen, B.W. (2012) Occupants' window opening behaviour: A literature review of factors influencing occupant behaviour and models. *Building and Environment*, 58, pp.188–198. Available from: <<http://linkinghub.elsevier.com/retrieve/pii/S0360132312001977>> [Accessed 2 November 2012].

FAO (1999) Koeppen Climate Classification map [Internet]. Available from: <<http://www.fao.org/sd/EIdirect/climate/EIsp0002.htm>> [Accessed 12 July 2012].

Fathy, H. (1986) *Natural Energy and Vernacular Architecture. Principles and Examples with reference to Hot Arid Climates*. W. Shearer & A. A. Sultan eds. Chicago, USA, University of Chicago Press. Available from: <http://www.osti.gov/energycitations/product.biblio.jsp?osti_id=6094230> [Accessed 12 December 2011].

Fellows, R. & Liu, A. (2008) *Research Methods for Construction*. third. West Sussex, UK, Blackwell Publishing Ltd.

Ford, B., Wilson, R., Gillott, M., Ibraheem, O., Salmeron, J. & Sanchez, F.J. (2012) Passive downdraught evaporative cooling: performance in a prototype house. *Building Research & Information*, 40 (3), pp.290–304. Available from: <<http://www.tandfonline.com/doi/abs/10.1080/09613218.2012.669908>> [Accessed 22 November 2013].

Foruzanmehr, A. & Vellinga, M. (2011) Vernacular architecture: questions of comfort and practicability. *Building Research & Information*, 39 (3), pp.274–285. Available from: <<http://www.tandfonline.com/doi/abs/10.1080/09613218.2011.562368>> [Accessed 23 November 2011].

Gaglia, A. (2010) KENAK & The new technical instructions of TEE [In Greek]. In: *Hellenic Chapter ASHRAE: Event on Targets for energy upgrades and building designs*. Athens, Greece. Available from: <<http://www.ashrae.gr/Gaglia.pdf>>.

Geros, V., Santamouris, M., Karatasou, S., Tsangrassoulis, A. & Papanikolaou, N. (2005) On the cooling potential of night ventilation techniques in the urban environment. *Energy and Buildings*, 37 (3), pp.243–257. Available from: <<http://www.sciencedirect.com/science/article/pii/S0378778804001963>> [Accessed 30 April 2015].

Geros, V., Santamouris, M., Tsangrassoulis, A. & Guarracino, G. (1999) Experimental evaluation of night ventilation phenomena. *Energy and Buildings*, 29 (2), pp.141–154. Available from: <<http://linkinghub.elsevier.com/retrieve/pii/S0378778898000565>>.

Ghadiri, M.H., Ibrahim, N.L.N. & Mohamed, M.F. (2013) Performance evaluation of four-sided square wind catchers with different geometries by numerical method. *Engineering Journal*, 7 (4), pp.9–17.

GhaffarianHoseini, A., Berardi, U., GhaffarianHoseini, A. & Makaremi, N. (2012) Intelligent facades in low-energy buildings. *British Journal of Environment & Climate Change*, 2 (4), pp.437–464. Available from: <http://works.bepress.com/cgi/viewcontent.cgi?params=/context/amirhosein_ghaffarianhoseini/article/1031/type/native/&path_info=>>.

Gialamas, I. (2011) Climate Classification of Greece in Köppen-Geiger [In Greek] [Internet]. Available from: <<http://www.meteoclub.gr/themata/egkyklopaideia/2618-klimatiki-katataksi-elladas>>.

Gildemeister, H. (2004) What is a mediterranean climate? [Internet]. Available from: <<http://www.mediterraneangardensociety.org/climate.html>> [Accessed 15 December 2011].

Givoni, B. (1998) *Climate considerations in building and urban design*. J. Degenhardt ed. USA, Van Nostrand Reinhold. Available from: <http://books.google.co.uk/books/about/Climate_considerations_in_building_and_u.html?id=MGkArZ_berAC&redir_esc=y>.

Givoni, B. (2011) Indoor temperature reduction by passive cooling systems. *Solar Energy*, 85 (8), pp.1692–1726. Available from: <<http://linkinghub.elsevier.com/retrieve/pii/S0038092X09002357>> [Accessed 11 August 2012].

Givoni, B. (1994) *Passive and Low Energy Cooling of Buildings*. USA, Van Nostrand Reinhold. Available from: <<http://books.google.com/books?id=rJsVoRw1geoC&pgis=1>> [Accessed 22 February 2012].

Givoni, B. (1997) Performance of the ‘shower’ cooling tower in different climates. *Renewable energy*, 10 (213), pp.173–178. Available from: <<http://www.sciencedirect.com/science/article/pii/0960148196000596>> [Accessed 30 October 2014].

GOK (1985) *General Construction Regulation of Greece Article 11 and 16 [Γενικός οικοδομικός κανονισμός]*. available at portal.tee.gr. Available from: <<http://portal.tee.gr/>>.

Gong, N., Tham, K.W., Melikov, A.K., Wyon, D.P., Sekhar, S.C. & Cheong, K.W. (2006) The Acceptable Air Velocity Range for Local Air Movement in The Tropics. *HVAC&R Research*, 12 (4), pp.1065–1076.

Google Maps (2013) Galatsi, Greece [Internet]. Available from: <<https://maps.google.co.uk/>> [Accessed 6 May 2013].

Graça, G.C. da, Chen, Q., Glicksman, L.R. & Norford, L.K. (2002) Simulation of wind-driven ventilative cooling systems for an apartment building in Beijing and Shanghai. *Energy and Buildings*, 34 (1), pp.1–11. Available from: <<http://www.sciencedirect.com/science/article/pii/S0378778801000834>>.

Gratia, E. & De Herde, A. (2004) Natural ventilation in a double-skin facade. *Energy and Buildings*, 36 (2), pp.137–146. Available from: <<http://linkinghub.elsevier.com/retrieve/pii/S0378778803001336>> [Accessed 16 September 2013].

Greenfield, T. (1996) *Research Methods. Guidance for postgraduates*. London and New York, Arnold and John Wiley & Sons Inc.

Grix, J. (2004) *The Foundations of Research*. Hampshire, UK, Palgrave MacMillan.

Guy Palmer (2002) UK - Fuel poverty [Internet]. Available from: <<http://www.poverty.org.uk/80/index.shtml>> [Accessed 1 May 2012].

Hammad, F. & Abu-Hijleh, B. (2010) The energy savings potential of using dynamic external louvers in an office building. *Energy and Buildings*, 42, pp.1888–1895.

Hamza, N. (2008) Double versus single skin facades in hot arid areas. *Energy and Buildings*, 40, pp.240–248.

Hamza, N., Cook, M. & Cropper, P. (2011) Non-uniform double skin facades in temperate climates. In: *Building Simulation 2011: 12th Conference of International Building Performance Simulation Association*. Sydney, 14-16 November, IBPSA, pp.2401–2406.

Hanby, V.I., Cook, M.J., Infield, D.G., Ji, Y., Loveday, D.L.L., Mei, L. & Holmes, M.J. (2008) Nodal network and CFD simulation of airflow and heat transfer in double skin facades with blinds. *Building Service Engineering Research and Technology*, 29 (1), pp.45–59. Available from: <<http://bse.sagepub.com/cgi/doi/10.1177/01436244080290010401>> [Accessed 30 April 2013].

Hashemi, N., Fayaz, R. & Sarshar, M. (2010) Thermal behaviour of a ventilated double skin facade in hot arid climate. *Energy and Buildings*, 42 (10), pp.1823–1832. Available from: <<http://linkinghub.elsevier.com/retrieve/pii/S0378778810001817>> [Accessed 12 July 2013].

Hassid, S., Santamouris, M., Papanikolaou, N., Linardi, A., Georgakis, C. & Assimakopoulos, D.N. (2000) The effect of the Athens heat island on air conditioning load. *Energy and Buildings*, 32 (2), pp.131–141. Available from: <<http://linkinghub.elsevier.com/retrieve/pii/S0378778899000456>>.

Herkel, S., Knapp, U. & Pfafferott, J. (2008) Towards a model of user behaviour regarding the manual control of windows in office buildings. *Building and Environment*, 43 (4), pp.588–600. Available from: <<http://linkinghub.elsevier.com/retrieve/pii/S036013230600326X>> [Accessed 11 November 2012].

HNMS (2012) Climatology. Hellenic National Meteorological Service [In Greek] [Internet]. Available from: <http://emy.gr/hnms/english/climatology/climatology_html> [Accessed 26 August 2012].

HNMS The climate of Greece [Internet]. Available from: <http://www.hnms.gr/hnms/english/climatology/climatology_html?> [Accessed 15 December 2011].

Hughes, B.R., Calautit, J.K. & Ghani, S.A. (2012) The development of commercial wind towers for natural ventilation: A review. *Applied Energy*, 92, pp.606–627. Available from: <<http://linkinghub.elsevier.com/retrieve/pii/S0306261911007720>> [Accessed 30 August 2013].

Iatridis, M. & Karamani, F. (2009) *Energy Efficiency Policies and Measures in Greece. Monitoring of Energy Efficiency in EU 27, Norway and Croatia (ODYSSEE-MURE)*. Pikermi, Athens. Available from: <http://www.odyssee-indicators.org/publications/PDF/greece_nr.pdf> [Accessed 26 February 2012].

Ibraheem, O. & Ford, B. (2012) The feasibility of passive draught evaporative cooling for high-rise office buildings in Cairo. *Architectural Science Review*, 55 (4), pp.307–319. Available from: <<http://www.tandfonline.com/doi/abs/10.1080/00038628.2012.722071>> [Accessed 20 December 2013].

IEA (2011) Electricity in Greece in 2009 [Internet]. Available from: <http://www.iea.org/stats/electricitydata.asp?COUNTRY_CODE=GR> [Accessed 11 February 2012].

IEA (2006) Energy Policies of IEA Countries, Greece 2006. *International Energy Agency*. Available from: <<http://www.iea.org/textbase/nppdf/free/2006/greece2006.pdf>>.

IESVE *MacroFlo Calculation Methods. Virtual Environment 6.0*. Available from: <<http://www.iesve.com/downloads/help/Thermal/Reference/MacroFloCalculationMethods.pdf>>.

IESVE (2012) Virtual Environment, software, version 6.4.0.11, student licence.

IPCC (2007) Climate Change 2007: Synthesis Report. Contribution of Working Groups I, II and III to the Fourth Assessment Report of the Intergovernmental Panel on Climate Change. , p.104.

Iravani, H., Etessam, I., Masoud, M. & Mofidi, S.M. (2009) The role of wind and natural ventilation in the vernacular architecture of Zavareh. *International Journal of Ventilation*, 8 (2), pp.175–186. Available from:

<<http://ijoint.org/doi/abs/10.5555/ijov.2009.8.2.175>> [Accessed 20 November 2014].

Ji, Y., Cook, M.J., Hanby, V., Infield, D., Loveday, D.L. & Mei, L. (2008) CFD modelling of naturally ventilated double-skin facades with Venetian blinds. *Journal of Building Performance Simulation*, 1 (3), pp.185–196.

Jiru, T.E. & Bitsuamlak, G.T. (2010) Application of CFD in modelling wind-induced natural ventilation of buildings - A review. *International Journal of Ventilation*, 9 (2), pp.131–147. Available from: <<http://ijoint.org/doi/abs/10.5555/ijov.2010.9.2.131>> [Accessed 20 March 2013].

John Gerring (2007) *Case Study Research: Principles and Practices*. First. New York, USA, Cambridge University Press.

Kalogirou, C. & Sagia, A. (2010) Examination of the vernacular architecture bioclimatic attributes in Metsovo area- potential of contemporary constructing technologies adjustment [In Greek]. In: *6th Interdisciplinary Interuniversity Conference. The Integrated Development of Mountainous Regions*. Metsovo, Greece, National Technical University of Athens. Available from: <[http://www.ntua.gr/MIRC/6th_conference/presentations/1_main_sessions/2nd_session/KALOGIROU C - SAGIA A.pdf](http://www.ntua.gr/MIRC/6th_conference/presentations/1_main_sessions/2nd_session/KALOGIROU_C - SAGIA_A.pdf)> [Accessed 7 June 2012].

Kang, D. & Strand, R.K. (2013) Modeling of simultaneous heat and mass transfer within passive down-draft evaporative cooling (PDEC) towers with spray in FLUENT. *Energy and Buildings*, 62, pp.196–209. Available from: <<http://linkinghub.elsevier.com/retrieve/pii/S0378778813001278>> [Accessed 29 January 2014].

Khedari, J., Yamtraipat, N., Pratintong, N. & Hirunlabh, J. (2000) Thailand ventilation comfort chart. *Energy and Buildings*, 32, pp.245–249.

Kim, T.J. & Park, J.S. (2010) Natural ventilation with traditional Korean opening in contemporary house. *Building and Environment*, 45 (1), pp.51–57. Available from: <<http://linkinghub.elsevier.com/retrieve/pii/S0360132309001334>> [Accessed 15 July 2011].

Kimura, K. (1994) Vernacular technologies applied to modern architecture. *Renewable energy*, 5 (5-8), pp.900–907. Available from: <<http://www.sciencedirect.com/science/article/pii/0960148194901104>> [Accessed 23 November 2011].

King, N. & Horrocks, C. (2010) *Interviews in qualitative research*. Los Angeles, SAGE Publications Ltd. Available from: <<http://books.google.co.uk/books?vid=ISBN9781412912570>>.

Koch-Nielsen, H. (2002) *Stay Cool. A Design Guide for the Built Environment in Hot Climates*. T. C. Press ed. London, UK, James & James(Science Publishers) Ltd.

Koinakis, C.J. (2005) Combined thermal and natural ventilation modeling for long-term energy assessment: validation with experimental measurements. *Energy and Buildings*, 37 (4), pp.311–323. Available from:

<<http://linkinghub.elsevier.com/retrieve/pii/S0378778804002129>> [Accessed 29 April 2013].

Koinakis, C.J. & Sakellaris, J.K. (2007) Office building facades and energy performance in urban environment in Greece. In: *2nd PALENC Conference and 28th AIVC Conference on Building Low Energy Cooling and Advanced Ventilation Technologies in the 21st Century*. Crete island, Greece, PALENC 2007, pp.541–546.

Kolokotroni, M., Zhang, Y. & Watkins, R. (2007) The London heat island and building cooling design. *Solar Energy*, 81 (1), pp.102–110. Available from: <<http://linkinghub.elsevier.com/retrieve/pii/S0038092X06001757>> [Accessed 18 September 2011].

Kolokotsa, D., Psomas, A. & Karapidakis, E. (2009) Urban heat island in southern Europe: The case study of Hania, Crete. *Solar Energy*, 83 (10), pp.1871–1883. Available from: <<http://linkinghub.elsevier.com/retrieve/pii/S0038092X0900156X>> [Accessed 23 July 2011].

Koukousianos, S. (2011) Meteorological Station of Galatsi [Internet]. Available from: <<http://galatsi.meteoclub.gr>> [Accessed 11 January 2013].

Lai, A.C.K., Mui, K.W., Wong, L.T. & Law, L.Y. (2009) An evaluation model for indoor environmental quality (IEQ) acceptance in residential buildings. *Energy and Buildings*, 41 (9), pp.930–936. Available from: <<http://linkinghub.elsevier.com/retrieve/pii/S0378778809000723>> [Accessed 4 March 2013].

Launder, B.E. & Spalding, D.B. (1974) The numerical computation of turbulent flows. *Computer Methods in Applied Mechanics and Engineering*, 3 (2), pp.269–289.

Lawson, B. (1997) *How designers think: the design process demystified*. third. Oxford, UK, Architectural Press, A division of Reed Education and Professional Publishing.

Leedy, P.D. & Ormrod, J.E. (2001) *Practical Research. Planning and Design*. 7th ed. New Jersey, USA, Merrill Prentice Hall.

Li, L. & Mak, C.M. (2007) The assessment of the performance of a windcatcher system using computational fluid dynamics. *Building and Environment*, 42 (3), pp.1135–1141. Available from: <<http://linkinghub.elsevier.com/retrieve/pii/S0360132305005160>> [Accessed 2 September 2013].

Lin, C.L. (2014) Time-dependent CFD Modelling in Hot Climates-Application to an apartment building in the Mediterranean. (Unpublished MSc dissertation). School of Civil and Building Engineering, Loughborough University, UK.

Lionello, P., Malanotte-Rizzoli, P., Boscolo, R., Alpert, P., Artale, V., Li, L., Luterbacher, J., May, W., Trigo, R., Tsimplis, M. & others (2006) The Mediterranean climate: an overview of the main characteristics and issues. *Developments in Earth and Environmental Sciences*, 4, pp.1–26. Available from:

<<http://www.sciencedirect.com/science/article/pii/S1571919706800030>> [Accessed 18 February 2012].

Littlefield, D. ed. (2008) *Metric Handbook. Planning and Design Data*. Third. Oxford UK, Burlington USA, Elsevier Ltd.

Loncour, X., Deneyer, A., Blasco, M., Flamant, G. & Wouters, P. (2004) *Ventilated Double Facades, Classification & illustration of facade concepts*. Belgian Building Research Institute, Department of Building Physics, Indoor Climate & Building Services.

Ludwig, J.C. & Mortimore, S. (2011) *PHOENICS - VR reference guide TR 326*. CHAM/TR326 ed. J C Ludwig ed. Wimbledon Village, London, CHAM. Available from: <http://www.cham.co.uk/phoenics/d_polis/d_docs/tr326/tr326top.htm>.

Luo, Z., Zhao, J., Gao, J. & He, L. (2007) Estimating natural-ventilation potential considering both thermal comfort and IAQ issues. *Building and Environment*, 42 (6), pp.2289–2298. Available from: <<http://linkinghub.elsevier.com/retrieve/pii/S0360132306001193>> [Accessed 26 July 2012].

Mak, C.M., Cheng, C. & Niu, J.L. (2005) The application of computational fluid dynamics to the assessment of green features in buildings: Part 1: Wing walls. *Architectural Science Review*, 48 (2), pp.121–134. Available from: <<http://www.tandfonline.com/doi/abs/10.3763/asre.2005.4816>> [Accessed 16 September 2013].

Mak, C.M., Niu, J.L., Lee, C.T. & Chan, K.F. (2007) A numerical simulation of wing walls using computational fluid dynamics. *Energy and Buildings*, 39 (9), pp.995–1002. Available from: <<http://linkinghub.elsevier.com/retrieve/pii/S0378778806002751>> [Accessed 24 April 2013].

Matzarakis, A.P. & Katsoulis, V.D. (2005) Sunshine duration hours over the Greek region. *Theoretical and Applied Climatology*, 83 (1-4), pp.107–120. Available from: <<http://www.springerlink.com/index/10.1007/s00704-005-0158-8>> [Accessed 15 December 2011].

Mavrogianni, A., Davies, M., Taylor, J., Chalabi, Z., Biddulph, P., Oikonomou, E., Das, P. & Jones, B. (2014) The impact of occupancy patterns, occupant-controlled ventilation and shading on indoor overheating risk in domestic environments. *Building and Environment*, 78, pp.183–198. Available from: <<http://linkinghub.elsevier.com/retrieve/pii/S0360132314001048>> [Accessed 23 May 2014].

Mavrogianni, A. & Mumovic, D. (2010) On the Use of Windcatchers in Schools: Climate Change, Occupancy Patterns, and Adaptation Strategies. *Indoor and Built Environment*, 19 (3), pp.340–354. Available from: <<http://ibe.sagepub.com/cgi/doi/10.1177/1420326X09341507>> [Accessed 22 November 2011].

McCartney, K.J. & Fergus Nicol, J. (2002) Developing an adaptive control algorithm for Europe. *Energy and Buildings*, 34 (6), pp.623–635. Available from: <<http://linkinghub.elsevier.com/retrieve/pii/S0378778802000130>>.

Met Office (2012) Climate change [Internet]. Available from: <<http://www.metoffice.gov.uk/climate-change>> [Accessed 15 March 2012].

Meteonorm 7 (2012) Software, version 7 Meteotest ed.

Microsoft (2010) Excel.

Mihalakakou, G., Santamouris, M., Papanikolaou, N., Cartalis, C. & Tsangrassoulis, a. (2004) Simulation of the Urban Heat Island Phenomenon in Mediterranean Climates. *Pure and Applied Geophysics*, 161 (2), pp.429–451. Available from: <<http://www.springerlink.com/openurl.asp?genre=article&id=doi:10.1007/s00024-003-2447-4>> [Accessed 23 November 2011].

Ministry for the Environment (2009) *Climate Change. Projections of GHG emissions – Policies and Measures for reducing GHG emissions*. Athens, Greece. Available from: <http://cdr.eionet.europa.eu/gr/eu/ghgmm/envsg1jqtq/20090515_Resubmission_of_GHG_Projections_and_PAMS_May_2009.pdf> [Accessed 31 July 2015].

Ministry of Development. Energy & Natural Resources Sector Θερμομόνωση [thermal insulation] [Internet]. Available from: <http://www.cres.gr/energy-saving/enimerosi_thermomonomosi.htm> [Accessed 26 February 2012].

Moghaddam, E.H., Amindeldar, S. & Besharatizadeh, a. (2011) New Approach to Natural Ventilation in Public Buildings Inspired by Iranian’s Traditional Windcatcher. *Procedia Engineering*, 21, pp.42–52. Available from: <<http://linkinghub.elsevier.com/retrieve/pii/S1877705811048193>> [Accessed 1 October 2012].

Mohamed, M., Behnia, M., King, S. & Prasad, D. (2011) The potential of natural ventilation in single-sided ventilated apartment to improve indoor thermal comfort and air quality. In: ASME ed. *ASME 2011 5th International Conference on Energy Sustainability ES2011*. Washington, DC, USA, pp.1–8. Available from: <[http://itme000.louisiana.edu/assign/Solar Thermal Project/Literature/ASME ES 2011/ES2011-54129.pdf](http://itme000.louisiana.edu/assign/Solar%20Thermal%20Project/Literature/ASME%20ES2011/ES2011-54129.pdf)> [Accessed 26 April 2013].

Mohamed, M.F., King, S., Behnia, M., Prasad, D. & Ling, J. (2010) Wind-driven natural ventilation study for multi-storey residential building using CFD. In: *ANZAScA 2010, 44th Annual Conference of the Architectural Science Association*.

Mohamed, M.F., Prasad, D., King, S. & Hirota, K. (2009) The impact of balconies on wind induced ventilation of single-sided naturally ventilated multi-storey apartment. In: *PLEA2009 - 26th Conference on Passive and Low Energy Architecture*. Quebec City, Canada, PLEA2009, pp.22–24.

Montazeri, H., Blocken, B., Janssen, W.D. & Hooff, T. van (2013) CFD evaluation of new second-skin facade concept for wind comfort on building balconies: Case study for the Park Tower in Antwerp. *Building and Environment*, 68, pp.179–192.

Available from:
<<http://www.sciencedirect.com/science/article/pii/S0360132313001959>> [Accessed 30 October 2014].

Montazeri, H., Montazeri, F., Azizian, R. & Mostafavi, S. (2010) Two-sided wind catcher performance evaluation using experimental, numerical and analytical modeling. *Renewable Energy*, 35 (7), pp.1424–1435. Available from: <<http://linkinghub.elsevier.com/retrieve/pii/S0960148109005394>> [Accessed 8 August 2013].

Morris, Z.S. (2009) The Profession. The truth about Interviewing Elites. *Politics, Political Studies Association*, 29 (3), pp.209–217.

Moujalled, B., Cantin, R. & Guarracino, G. (2008) Comparison of thermal comfort algorithms in naturally ventilated office buildings. *Energy and Buildings*, 40 (12), pp.2215–2223. Available from: <<http://linkinghub.elsevier.com/retrieve/pii/S0378778808001473>> [Accessed 4 March 2013].

Mpalafoutis, X. (2004) *General Climatology [In Greek]*. Thessaloniki, Greece, Aristotle University of Thessaloniki. Department of Meteorology and Climatology. Available from: <<http://www.geo.auth.gr/courses/gmc/gmc431e/th/Climatology.pdf>>.

Narumi, D., Shigematsu, K. & Shimoda, Y. (2009) Effect of the Evaporative Cooling Techniques by Spraying Mist Water on Reducing Urban Heat Flux and Saving Energy in Apartment House. In: *2nd International Conference on Countermeasures to Urban Heat Islands*. Berkeley, California, SICCUHI. Available from: <<http://heatiland2009.lbl.gov/docs/221000-narumi-doc.pdf>> [Accessed 13 June 2012].

Nastos, P.T. & Zerefos, C.S. (2009) Spatial and temporal variability of consecutive dry and wet days in Greece. *Atmospheric Research*, 94 (4), pp.616–628. Available from: <<http://linkinghub.elsevier.com/retrieve/pii/S016980950900088X>> [Accessed 3 August 2011].

Niachou, K., Hassid, S., Santamouris, M. & Livada, I. (2005) Comparative monitoring of natural, hybrid and mechanical ventilation systems in urban canyons. *Energy and Buildings*, 37, pp.503–513.

Niachou, K., Hassid, S., Santamouris, M. & Livada, I. (2008) Experimental performance investigation of natural, mechanical and hybrid ventilation in urban environment. *Building and Environment*, 43 (8), pp.1373–1382.

Nicol, F. (2004) Adaptive thermal comfort standards in the hot–humid tropics. *Energy and Buildings*, 36 (7), pp.628–637. Available from: <<http://linkinghub.elsevier.com/retrieve/pii/S0378778804000155>> [Accessed 12 July 2014].

Nicol, F. & Humphreys, M. (2002) Adaptive thermal comfort and sustainable thermal standards for buildings. *Energy and Buildings*, 34 (6), pp.563–572. Available from: <<http://linkinghub.elsevier.com/retrieve/pii/S0378778802000063>>.

- Nicol, F. & Humphreys, M. (2010) Derivation of the adaptive equations for thermal comfort in free-running buildings in European standard EN15251. *Building and Environment*, 45 (1), pp.11–17. Available from: <<http://linkinghub.elsevier.com/retrieve/pii/S036013230800303X>>.
- Niu, J.L., Tang, Y.M. & Mak, C.M. (2005) The application of computational fluid dynamics to the assessment of green features in buildings: Part 2: Communal sky Gardens. *Architectural Science Review*, 48 (4), pp.337–344. Available from: <<http://www.tandfonline.com/doi/abs/10.3763/asre.2005.4841>> [Accessed 16 September 2013].
- Norton, T., Sun, D.-W., Grant, J., Fallon, R. & Dodd, V. (2007) Applications of computational fluid dynamics (CFD) in the modelling and design of ventilation systems in the agricultural industry: a review. *Bioresource technology*, 98, pp.2386–2414. Available from: <<http://www.ncbi.nlm.nih.gov/pubmed/17207996>> [Accessed 8 March 2013].
- O’Sullivan, P.D. & Kolokotroni, M. (2014) Time-averaged single sided ventilation rates and thermal environment in cooling mode for a low energy retrofit envelope. *International Journal of Ventilation*, 13 (2), pp.153–168.
- Oesterle, E. (2001) *Double-skin facades. integrated planning: building physics, construction, aerophysics, air-conditioning, economic viability*. Munich ; London ; New York, Prestel.
- Oh, M.H., Lee, K.H. & Yoon, H.J. (2013) Automated slat angle control of venetian blind considering energy and visual comfort. In: *13th Conference of International Building Performance Simulation Association*. Chambéry, France, BS2013, pp.930–934.
- Oikonomou, A. (2008) Bioclimatic elements and design principles of the traditional architecture in northern Greece. In: *25th Conference on Passive and Low Energy Architecture*. Dublin, PLEA 2008. Available from: <http://architecture.ucd.ie/Paul/PLEA2008/content/papers/poster/PLEA_FinalPaper_ref_269.pdf>.
- Oikonomou, A. & Bougiatioti, F. (2011) Architectural structure and environmental performance of the traditional buildings in Florina, NW Greece. *Building and Environment*, 46 (3), pp.669–689. Available from: <<http://linkinghub.elsevier.com/retrieve/pii/S0360132310002829>> [Accessed 10 October 2011].
- Oke, T.R. (1978) *Boundary layer climates*. 1st ed. Methuen & Co Ltd, London, Psychology Press. Available from: <<http://books.google.co.uk/books?vid=ISBN0416705200>> [Accessed 14 December 2011].
- Palmero-Marrero, A.I. & Oliveira, A.C. (2010) Effect of louver shading devices on building energy requirements. *Applied Energy*, 87 (6), pp.2040–2049.
- Papadopoulos, A.M., Oxizidis, S. & Papathanasiou, L. (2008) Developing a new library of materials and structural elements for the simulative evaluation of buildings’

energy performance. *Building and Environment*, 43 (5), pp.710–719. Available from: <<http://linkinghub.elsevier.com/retrieve/pii/S0360132307000613>> [Accessed 12 November 2012].

Papakonstantinou, K., Kiranoudis, C. & Markatos, N. (2000) Numerical simulation of air flow field in single-sided ventilated buildings. *Energy and Buildings*, 33 (1), pp.41–48. Available from: <<http://www.sciencedirect.com/science/article/pii/S0378778800000633>> [Accessed 11 April 2013].

Papakostas, K.T. & Sotiropoulos, B.A. (1997) Occupational and energy behaviour patterns in Greek residences. *Energy and Buildings*, 26 (2), pp.207–213. Available from: <<http://linkinghub.elsevier.com/retrieve/pii/S0378778897000029>>.

Papamanolis, N. (2006) Characteristics of the environmental and energy behaviour of contemporary urban buildings in Greece. *Architectural Science Review*, 49 (2), pp.120–126. Available from: <<http://www.tandfonline.com/doi/abs/10.3763/asre.2006.4916>> [Accessed 3 October 2012].

Papamanolis, N. (2000) Natural ventilation as a design factor in buildings in Greece. *Architectural Science Review*, 43 (4), pp.175–182. Available from: <<http://dx.doi.org/10.1080/00038628.2000.9696905>>.

Papamanolis, N. (2015a) The first indications of the effects of the new legislation concerning the energy performance of buildings on renewable energy applications in buildings in Greece. *International Journal of Sustainable Built Environment*, (June). Available from: <<http://linkinghub.elsevier.com/retrieve/pii/S221260901500028X>>.

Papamanolis, N. (2015b) The main characteristics of the urban climate and the air quality in Greek cities. *Urban Climate*, 12, pp.49–64. Available from: <<http://www.sciencedirect.com/science/article/pii/S221209551400087X>> [Accessed 31 July 2015].

Papamanolis, N. (2005) The main constructional characteristics of contemporary urban residential buildings in Greece. *Building and Environment*, 40 (3), pp.391–398. Available from: <<http://linkinghub.elsevier.com/retrieve/pii/S036013230400191X>> [Accessed 17 August 2011].

Pappas, A. & Zhai, Z. (2008) Numerical investigation on thermal performance and correlations of double skin façade with buoyancy-driven airflow. *Energy and Buildings*, 40 (4), pp.466–475. Available from: <<http://linkinghub.elsevier.com/retrieve/pii/S0378778807001181>> [Accessed 30 April 2013].

Passive House Institute (2012) Passive House requirements [Internet]. Available from: <<http://passiv.de/en>> [Accessed 10 May 2012].

Pavlou, K., Vasilakopoulou, K. & Santamouris, M. (2007) The impact of several construction elements on the thermal performance of solar chimneys. *International Journal of Ventilation*, 8 (3), pp.277–285.

- Peel, M.C., Finlayson, B.L. & McMahon, T.A. (2007) Updated world map of the Köppen-Geiger climate classification. *Hydrology and Earth System Sciences Discussions*, 4 (2), pp.1633–1644. Available from: <<http://www.mendeley.com/research/updated-world-map-of-the-kppengeiger-climate-classification/>> [Accessed 2 February 2012].
- Peeters, L., Dear, R. De, Hensen, J. & D’haeseleer, W. (2009) Thermal comfort in residential buildings: Comfort values and scales for building energy simulation. *Applied Energy*, 86 (5), pp.772–780. Available from: <<http://linkinghub.elsevier.com/retrieve/pii/S0306261908001785>> [Accessed 18 July 2012].
- Peppes, A.A., Santamouris, M. & Asimakopoulos, D.N. (2002) Experimental and numerical study of buoyancy-driven stairwell flow in a three storey building. *Building and Environment*, 37, pp.497–506.
- Prajongsan, P. & Sharples, S. (2012) Enhancing natural ventilation, thermal comfort and energy savings in high-rise residential buildings in Bangkok through the use of ventilation shafts. *Building and Environment*, 50, pp.104–113. Available from: <<http://linkinghub.elsevier.com/retrieve/pii/S0360132311003696>> [Accessed 26 July 2012].
- Psomas, T., Holzer, P. & Santamouris, M. (2014) A naturally ventilated efficient residential building under the impact of climate change. *International Journal of Ventilation*, 13 (2), pp.169–178. Available from: <<http://www.ijoint.org/doi/abs/10.5555/2044-4044-13.2.169>> [Accessed 19 November 2014].
- Raja, I.A., Nicol, J.F., McCartney, K.J. & Humphreys, M.A. (2001) Thermal comfort: use of controls in naturally ventilated buildings. *Energy and Buildings*, 33 (3), pp.235–244. Available from: <<http://linkinghub.elsevier.com/retrieve/pii/S0378778800000876>>.
- Refalo, M. (2014) Promoting Energy Saving Measures in Low Income Housing [Internet]. Available from: <<http://www.energeia-med.eu/index.php/component/k2/item/14-promoting-energy-saving-measures-in-low-income-housing>> [Accessed 1 October 2014].
- Rizk, A. a. & Henze, G.P. (2010) Improved airflow around multiple rows of buildings in hot arid climates. *Energy and Buildings*, 42 (10), pp.1711–1718. Available from: <<http://linkinghub.elsevier.com/retrieve/pii/S0378778810001672>> [Accessed 16 September 2013].
- Roetzel, A., Tsangrassoulis, A., Dietrich, U. & Busching, S. (2010) A review of occupant control on natural ventilation. *Renewable and Sustainable Energy Reviews*, 14, pp.1001–1013.
- Roetzel, A., Tsangrassoulis, A., Drakou, A. & De Siqueira, G. (2011) Comparison of the EN 15251 and Ashrae Standard 55 adaptive thermal comfort models in the context of a Mediterranean climate. In: *Plea 2011 - 27th Conference on Passive and Low Energy Architecture*. Louvain-la-Neuve, Belgium, Organizing Committee of PLEA’2011, pp.583–588.

Roubien, D. (2014) Construction techniques in nineteenth century Greece and their impact on today's restoration projects. *Journal of Architectural Conservation*, 20 (2), pp.91–107.

Safer, N., Woloszyn, M. & Roux, J.J. (2005) Three-dimensional simulation with a CFD tool of the airflow phenomena in single floor double-skin facade equipped with a venetian blind. *Solar Energy*, 79 (2), pp.193–203. Available from: <<http://linkinghub.elsevier.com/retrieve/pii/S0038092X04002920>> [Accessed 25 July 2013].

Sakka, A., Wagner, A. & Santamouris, M. (2010) Thermal comfort and occupant satisfaction in residential buildings – Results of field study in residential buildings in Athens during the summer period. In: *Adapting to Change: New Thinking on Comfort*. Network for Comfort and Energy Use in Buildings, Windsor, UK, NCEUB. Available from: <<http://nceub.commoncense.info/uploads/51-01-01-Sakka.pdf>> [Accessed 14 January 2013].

Salmeron, J.M., Sánchez, F.J., Sánchez, J., Álvarez, S., Molina, J.L. & Salmeron, R. (2012) Climatic applicability of draught cooling in Europe. *Architectural Science Review*, 55 (4), pp.259–272. Available from: <<http://www.tandfonline.com/doi/abs/10.1080/00038628.2012.723393>> [Accessed 21 August 2014].

Santamouris M. (2006) Natural Techniques to Improve Indoor and Outdoor Comfort During the Warm Period – A Review. In: *Comfort and Energy Use in Buildings - Getting them Right*. Cumberland Lodge, Windsor, UK, London: Network for Comfort and Energy Use in Buildings. Available from: <<http://nceub.commoncense.info/uploads/Santamouris.pdf>> [Accessed 9 June 2012].

Santamouris, M., Argiroudis, K., Georgiou, M., Livada, I., Doukas, P., Assimakopoulos, M., Sfakianaki, A., Pavlou, K., Geros, V. & Papaglastra, M. (2007) Indoor air quality in fifty residences in Athens. *International Journal of Ventilation*, 5 (4), pp.367–80.

Santamouris, M. & Assimakopoulos, D. (1996) *Passive cooling of buildings*. London, UK, James & James Ltd. Available from: <http://books.google.com/books?hl=en&lr=&id=tLHsJ0-vEkYC&oi=fnd&pg=PR9&dq=Passive+Cooling+of+Buildings&ots=MW_BZmsyJj&sig=tHDVHYbAZKrBs9JByifJyGgQLSY> [Accessed 30 April 2012].

Santamouris, M., Kapsis, K., Korres, D., Livada, I., Pavlou, C. & Assimakopoulos, M. (2007) On the relation between the energy and social characteristics of the residential sector. *Energy and Buildings*, 39 (8), pp.893–905. Available from: <<http://linkinghub.elsevier.com/retrieve/pii/S0378778806002519>> [Accessed 2 August 2011].

Santamouris, M., Papanikolaou, N. & Livada, I. (2001) On the impact of urban climate on the energy consumption of buildings. *Solar Energy*, 70 (3), pp.201–216. Available from: <<http://linkinghub.elsevier.com/retrieve/pii/S0038092X00000955>> [Accessed 5 December 2011].

Santamouris, M., Paraponiaris, K. & Mihalakakou, G. (2007) Estimating the ecological footprint of the heat island effect over Athens, Greece. *Climatic Change*, 80 (3-4), pp.265–276. Available from: <<http://www.springerlink.com/index/10.1007/s10584-006-9128-0>> [Accessed 18 July 2011].

Santamouris, M., Pavlou, K., Synnefa, A., Niachou, K. & Kolokotsa, D. (2007) Recent progress on passive cooling techniques. Advanced technological developments to improve survivability levels in low-income households. *Energy and Buildings*, 39 (7), pp.859–866. Available from: <<http://linkinghub.elsevier.com/retrieve/pii/S0378778807000564>> [Accessed 8 August 2011].

Santamouris, M., Sfakianaki, A. & Pavlou, K. (2010) On the efficiency of night ventilation techniques applied to residential buildings. *Energy and Buildings*, 42 (8), pp.1309–1313. Available from: <<http://linkinghub.elsevier.com/retrieve/pii/S0378778810000666>> [Accessed 9 June 2012].

Santamouris, M. & Sfakianaki, K. (2009) The energy impact of the EN 15251 comfort categories The energy impact of the EN 15251 comfort categories. *EIE/07/190/SI2.467619 COMMONCENSE Comfort monitoring for CEN standard EN15251 linked to EPBD*, (May).

SATE (2012) B/2011 The Greek Construction Sector [In Greek] [Internet]. Available from: <http://www.sate.gr/nea/Press/FINAL_6-2011.pdf> [Accessed 22 June 2012].

Serghides, D.K. (2010) The Wisdom of Mediterranean Traditional Architecture Versus Contemporary Architecture- The Energy Challenge. *Open Construction and Building Technology Journal*, 4, pp.29–38. Available from: <<http://www.benthamscience.com/open/tobctj/articles/V004/29TOBCTJ.pdf>> [Accessed 30 January 2012].

Sinou, M. (2006) From the traditional to the contemporary Cycladic sustainable house. *Management of Environmental Quality: An International Journal*, 17 (5), pp.555–569. Available from: <<http://www.emeraldinsight.com/10.1108/14777830610684521>> [Accessed 23 November 2011].

Stasinopoulos, T.N. (2006) The Four Elements of Santorini Architecture. Lessons in Vernacular Sustainability. In: *23rd International Conference on Passive and Low Energy Architecture*. Geneva, Switzerland, Plea2006. Available from: <<http://www.delaxo.net/plea06/paper783sec.pdf>> [Accessed 15 June 2012].

Stavrakakis, G.M., Zervas, P.L., Sarimveis, H. & Markatos, N.C. (2010) Development of a computational tool to quantify architectural-design effects on thermal comfort in naturally ventilated rural houses. *Building and Environment*, 45 (1), pp.65–80. Available from: <<http://linkinghub.elsevier.com/retrieve/pii/S0360132309001218>> [Accessed 5 September 2012].

Suleiman, S. & Himmo, B. (2012) Direct comfort ventilation. Wisdom of the past and technology of the future (wind-catcher). *Sustainable Cities and Society*, 5, pp.8–15. Available from: <<http://linkinghub.elsevier.com/retrieve/pii/S2210670712000583>>.

Sundell, J., Levin, H., Nazaroff, W.W., Cain, W.S., Fisk, W.J., Grimsrud, D.T., Gyntelberg, F., Li, Y., Persily, A.K., Pickering, A.C., Samet, J.M., Spengler, J.D., Taylor, S.T. & Weschler, C.J. (2011) Commemorating 20 years of Indoor Air. Ventilation rates and health: multidisciplinary review of the scientific literature. *Indoor Air*, 21 (3), pp.191–204.

Tassiopoulou, T., Grindley, P.C. & Probert, S.D. (1996) Thermal behaviour of an eighteenth-century Athenian dwelling. *Applied Energy*, 53 (4), pp.383–398. Available from: <<http://linkinghub.elsevier.com/retrieve/pii/0306261995000682>>.

The World Bank (2012) CO2 emissions (metric tons per capita) | Data | Map [Internet]. Available from: <data.worldbank.org> [Accessed 11 February 2012].

Theodoridou, I., Papadopoulos, A.M. & Hegger, M. (2012) A feasibility evaluation tool for sustainable cities – A case study for Greece. *Energy Policy*, 44, pp.207–216. Available from: <<http://linkinghub.elsevier.com/retrieve/pii/S0301421512000687>> [Accessed 3 October 2012].

Theodoridou, I., Papadopoulos, A.M. & Hegger, M. (2011) A typological classification of the Greek residential building stock. *Energy and Buildings*, 43 (10), pp.2779–2787. Available from: <<http://linkinghub.elsevier.com/retrieve/pii/S0378778811002854>> [Accessed 25 August 2011].

Theodoridou, I., Papadopoulos, A.M. & Hegger, M. (2011) Statistical analysis of the Greek residential building stock. *Energy and Buildings*, 43 (9), pp.2422–2428. Available from: <<http://www.sciencedirect.com/science/article/pii/S0378778811002489>>.

THERMIE (1999) *A Green Vitruvius - Principles and Practice of Sustainable Architectural Design*. London, UK, James & James(Science Publishers) Ltd.

Tominaga, Y. & Stathopoulos, T. (2007) CFD analysis of flow and concentration fields around a building with a roof stack. In: *6th International Conference on Indoor Air Quality, Ventilation & Energy Conservation in Buildings IAQVE 2007*. Sendai, Japan. Available from: <http://www.inive.org/members_area/medias/pdf/Inive/IAQVEC2007/Tominaga.pdf?origin=publication_detail> [Accessed 19 November 2014].

Torres, M., Alavedra, P. & Guzmán, A. (2007) Double skin facades-Cavity and Exterior openings Dimensions for Saving energy on Mediterranean climate. In: *Building Simulation 2007*. Beijing, China, IBPSA International Building Performance Simulation Association, pp.198–205. Available from: <http://www.ibpsa.org/proceedings/BS2007/p407_final.pdf> [Accessed 11 December 2014].

- Tsangrassoulis, A., Santamouris, M. & Asimakopoulos, D.. (1997) On the air flow and radiation transfer through partly covered external building openings. *Solar Energy*, 61 (6), pp.355–367. Available from: <<http://www.sciencedirect.com/science/article/pii/S0038092X9700073X>>.
- Tsinonis, A., Koutsogiannakis, I., Santamouris, M. & Tselepidaki, I. (1993) Statistical analysis of summer comfort conditions in Athens, Greece. *Energy and Buildings*, 19 (4), pp.285–290. Available from: <<http://linkinghub.elsevier.com/retrieve/pii/037877889390013K>>.
- UNFCCC (2013) *Kyoto Protocol to the United Nations Framework Convention on Climate Change (Informal consolidated version of the Kyoto Protocol, incorporating the Doha Amendment version)*. Doha, Qatar. Available from: <http://unfccc.int/files/kyoto_protocol/application/pdf/kp_consolidated_text.pdf>.
- Viklund, A. (2010) Elevation Finder [Internet]. Available from: <www.freemaptools.com/elevation-finder> [Accessed 22 July 2013].
- Visagavel, K. & Srinivasan, P.S.S. (2009) Analysis of single side ventilated and cross ventilated rooms by varying the width of the window opening using CFD. *Solar Energy*, 83 (1), pp.2–5. Available from: <<http://linkinghub.elsevier.com/retrieve/pii/S0038092X08001515>> [Accessed 26 July 2012].
- Vissilia, A.M. (2009) Evaluation of a sustainable Greek vernacular settlement and its landscape: Architectural typology and building physics. *Building and Environment*, 44 (6), pp.1095–1106. Available from: <<http://linkinghub.elsevier.com/retrieve/pii/S0360132308001297>> [Accessed 22 August 2011].
- Wang, L. & Wong, N.H. (2008) Coupled simulations for naturally ventilated residential buildings. *Automation in Construction*, 17 (4), pp.386–398. Available from: <<http://linkinghub.elsevier.com/retrieve/pii/S092658050700091X>> [Accessed 20 July 2012].
- Wang, Z., Zhang, L., Zhao, J. & He, Y. (2010) Thermal comfort for naturally ventilated residential buildings in Harbin. *Energy and Buildings*, 42 (12), pp.2406–2415. Available from: <<http://linkinghub.elsevier.com/retrieve/pii/S0378778810002859>> [Accessed 17 September 2012].
- Wei, S., Buswell, R. & Loveday, D. (2013) Factors affecting ‘end-of-day’ window position in a non-air-conditioned office building. *Energy and Buildings*, 62, pp.87–96. Available from: <<http://dx.doi.org/10.1016/j.enbuild.2013.02.060>>.
- Wong, N.H. & Huang, B. (2004) Comparative study of the indoor air quality of naturally ventilated and air-conditioned bedrooms of residential buildings in Singapore. *Building and Environment*, 39 (9), pp.1115–1123.
- Van Den Wymelenberg, K. (2012) Patterns of occupant interaction with window blinds: A literature review. *Energy and Buildings*, 51, pp.165–176. Available from:

<<http://linkinghub.elsevier.com/retrieve/pii/S0378778812002630>> [Accessed 8 November 2012].

Yik, F.W.H. & Lun, Y.F. (2010) Energy saving by utilizing natural ventilation in public housing in Hong Kong. *Indoor and Built Environment*, 19 (1), pp.73–87. Available from: <<http://ibe.sagepub.com/cgi/doi/10.1177/1420326X09358021>> [Accessed 20 November 2012].

Yun, G.Y. & Steemers, K. (2011) Behavioural, physical and socio-economic factors in household cooling energy consumption. *Applied Energy*, 88 (6), pp.2191–2200. Available from: <<http://linkinghub.elsevier.com/retrieve/pii/S0306261911000134>> [Accessed 25 March 2014].

Yun, G.Y. & Steemers, K. (2008) Time-dependent occupant behaviour models of window control in summer. *Building and Environment*, 43 (9), pp.1471–1482. Available from: <<http://linkinghub.elsevier.com/retrieve/pii/S036013230700159X>> [Accessed 12 November 2012].

Zhang, Y. & Barrett, P. (2012) Factors influencing the occupants' window opening behaviour in a naturally ventilated office building. *Building and Environment*, 50, pp.125–134. Available from: <<http://linkinghub.elsevier.com/retrieve/pii/S0360132311003672>> [Accessed 12 November 2012].

Zhou, J. & Chen, Y. (2010) A review on applying ventilated double-skin facade to buildings in hot-summer and cold-winter zone in China. *Renewable and Sustainable Energy Reviews*, 14 (4), pp.1321–1328. Available from: <<http://linkinghub.elsevier.com/retrieve/pii/S1364032109002792>> [Accessed 11 April 2013].

APPENDICES

Appendix A. Airflow modelling using CFD simulations

A.1. Study of the external flow field

As described in Chapter 4.3, information collected during a survey conducted by the author of the case study and surrounding buildings, was used during both the DTM and CFD simulations performed. Figure A.1 shows a plan view of the area from Google Maps, with added information of the buildings layout and height in metres. An online tool generating elevation maps was employed to provide information regarding the height differences of the site, showing significant variations between the urban blocks (Viklund, 2010). Measuring points were the midpoints of the different blocks, while all elevation values were modified (height in metres above sea level) to a zero point defined manually (in relation to the case study building) indicated with a cross in Figure A.2. Geometrical ‘corrections’ were applied as explained in Chapter 4.3, to simplify the computational modelling of the site. The layout of each building was further simplified to a rectangular shape, as shown in Figure A.3.

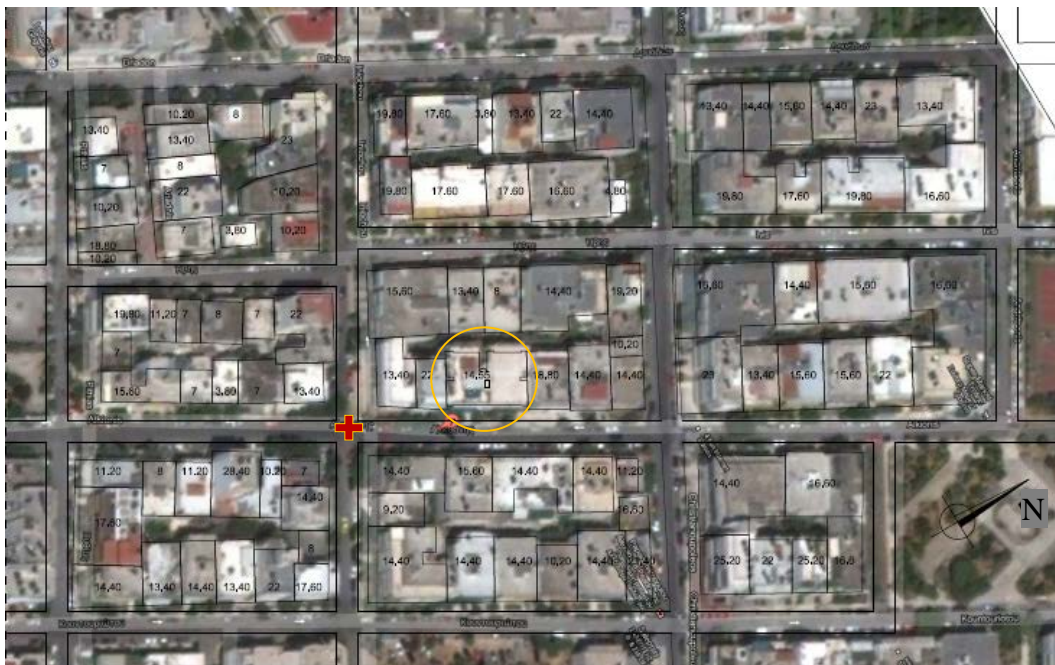


Figure A. 1 Defining the plan layout of the surrounding, after Google Maps (2013), showing the layout of each building, the building height, location of the building under investigation and a measuring point of the terrain heights

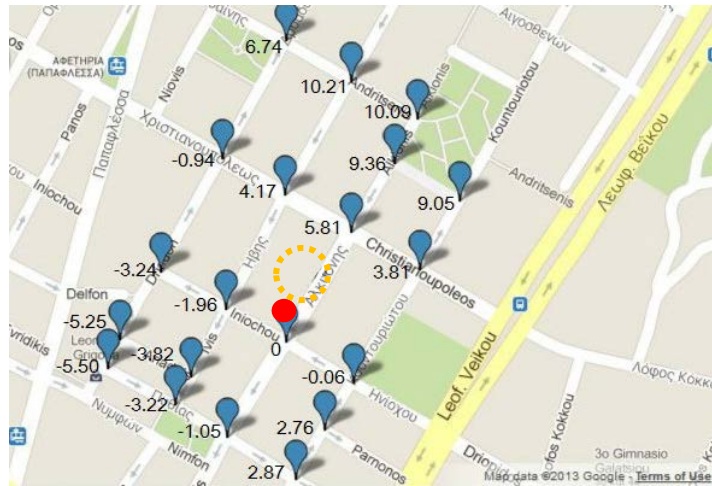


Figure A. 2 Map showing ground elevation measurements on every crossroad, modified with zero level the 'red' point on the map (Viklund, 2010)

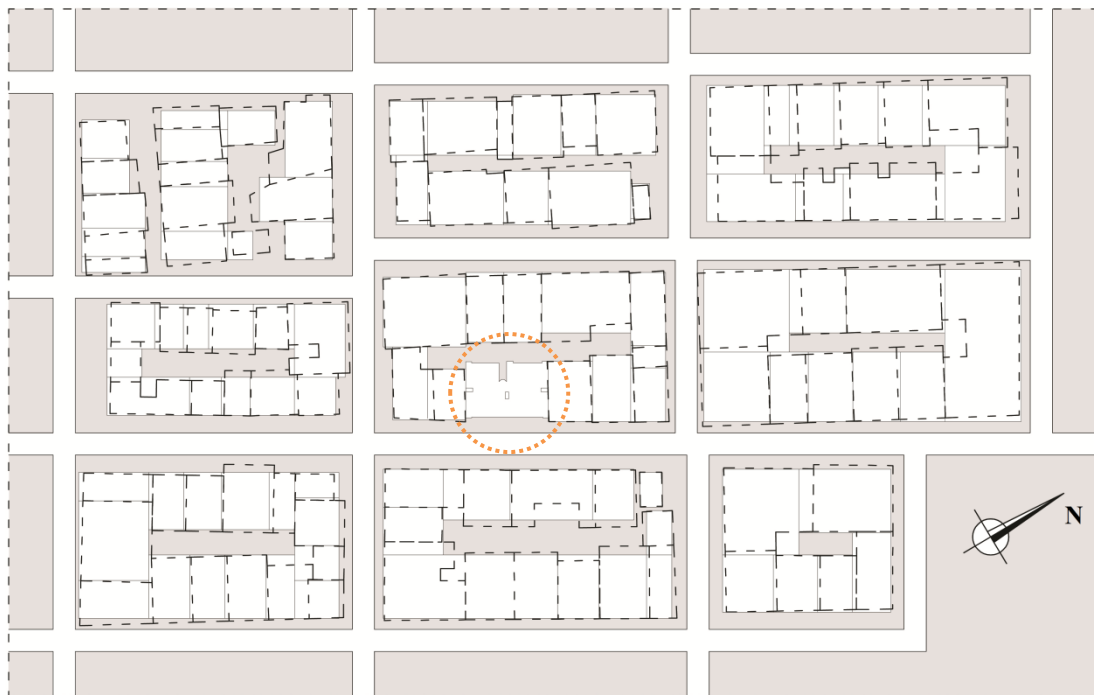


Figure A. 3 Refinement stage of the urban building blocks, showing with dashed line the layout of the existing buildings and with solid the new layout, CAD drawing by author, nts

The main road at the front of the building was used as a guide, with the lowest and highest end points of this line considered to be the maximum and minimum levels of the site. These values were interpolated with the annotated in the building drawings percentage of grade of the road (provided by the local authorities). A new map was created including the gradually increasing simplified contour lines from southwest towards northeast. All these information was combined into Figure 4.8 (Chapter 4.3).

These simplifications reduced significantly the number of computational cells and computational time required during the study of the external flow field in CFD (see Chapter 6.3). A 3D model of the developed layout of the buildings and the terrain heights are presented in Figure A.4. Convergence was difficult to achieve in preliminary CFD simulations, and thus further simplifications of the site layout were required. The angled terrain was potentially excluded and replaced by an increase in be buildings' height equal to the terrain heights.

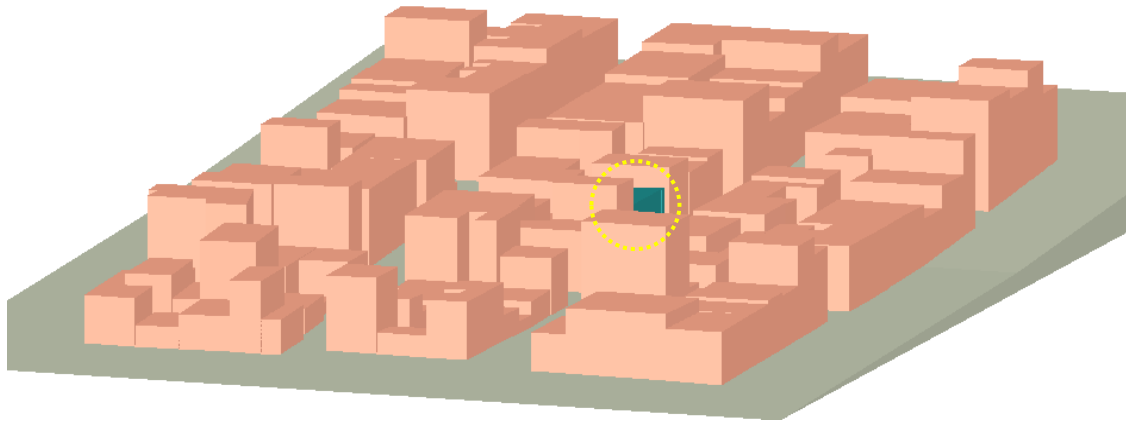


Figure A. 4 Three dimensional representation of the site in CAD software

A.1.1. Additional codes and driving pressures

An additional code was created to predict the average wind pressure incident at the buildings' openings, for the external flow de-coupled CFD simulations. Two-dimensional object (a 'user-defined'⁵ object in PHOENICS) was created to represent the position of the openings on the building façades. The additional coding to the existing CFD code accompanying each two-dimensional object is presented in Figure A.5, with an example for an x-facing window. Within the three-dimensional mesh, for x-facing windows 'aeast' was required, for y-facing windows 'anorth' and 'ahigh' for z-facing windows. The group number ("19") has no significance, apart from custom.

```
save19begin
(make atot is 0.)
(make aptot is 0.)
(store1 of atot at WINDOW is sum(aeast))
(store1 of aptot at WINDOW is sum(aeast*p1))
(print of av-pressure is aptot/atot)
save19end
```

Figure A. 5 Additional coding for the prediction of average pressures at the openings in PHOENICS

The predicted average pressure values (Pa) with the additional coding at the building openings during the external flow field CFD simulations, as well the driving pressures (highest and lowest), are presented in Table A.1.

⁵ A user-defined object is 2D or 3D, for setting user-defined sources that define the location of the PATCH commands, together with their COVALs (PATCH/COVAL) (CHAM Ltd., 2008).

Table A. 1 Average pressure values (Pa) at the openings and driving pressure for four ventilation strategies.

Case	Natural Ventilation									
Wind Speed	3.60 m/s					7.00 m/s				
Wind Direction	North	NE	East	SW	NW	North	NE	East	SW	NW
Bed 1	-2.83	-1.74	-1.67	-1.60	-3.16	-10.59	-6.63	-6.30	-5.83	-11.89
Bed 2	-2.82	-1.79	-1.71	-1.56	-3.18	-10.68	-6.82	-6.42	-5.57	-11.88
Bed 1_2 nd floor	-3.19	-1.75	-1.44	-1.73	-3.74	-12.45	-6.66	-5.42	-6.33	-12.95
Bed 2_2 nd floor	-3.07	-1.80	-1.43	-1.59	-3.59	-11.81	-6.85	-5.35	-5.76	-12.73
Bed 1_3 rd floor	-3.12	-1.74	-1.46	-1.57	-3.52	-11.75	-6.61	-5.46	-5.71	-12.25
Bed 2_3 rd floor	-3.06	-1.78	-1.48	-1.48	-3.52	-11.51	-6.79	-5.53	-5.29	-12.35
Bed 1_4 th floor	-3.29	-1.71	-1.05	-1.55	-3.52	-11.65	-6.49	-3.92	-5.64	-12.01
Bed 2_4 th floor	-3.09	-1.76	-1.07	-1.40	-3.45	-11.34	-6.72	-3.96	-5.17	-11.81
Shaft top	-2.25	-1.95	-1.10	-0.99	-4.72	-5.64	-7.48	-4.12	-3.41	-20.01
<i>Difference</i>	<i>0.58</i>	<i>-0.16</i>	<i>0.58</i>	<i>0.57</i>	<i>-1.53</i>	<i>4.95</i>	<i>-0.85</i>	<i>2.18</i>	<i>2.15</i>	<i>-8.13</i>
Case	Wind-Catcher									
Wind Speed	3.60 m/s					7.00 m/s				
Wind Direction	North	NE	East	SW	NW	North	NE	East	SW	NW
Bed 1	-2.84	-1.48	-1.66	-1.53	-3.35	-10.88	-5.88	-7.52	-5.81	-12.70
Bed 2	-2.84	-1.51	-1.68	-1.46	-3.34	-10.90	-5.97	-7.83	-5.54	-12.66
Bed 1_2 nd floor	-3.39	-1.51	-1.41	-1.65	-3.99	-12.87	-5.92	-5.41	-6.27	-15.13
Bed 2_2 nd floor	-3.24	-1.55	-1.39	-1.51	-3.73	-12.32	-6.07	-4.83	-5.72	-14.14
Bed 1_3 rd floor	-3.32	-1.47	-1.38	-1.49	-3.60	-12.66	-5.83	-6.69	-5.64	-13.65
Bed 2_3 rd floor	-3.31	-1.51	-1.40	-1.40	-3.49	-12.61	-5.95	-6.55	-5.26	-13.21
Bed 1_4 th floor	-3.70	-1.44	-0.99	-1.45	-3.57	-14.22	-5.76	-3.82	-5.50	-13.49
Bed 2_4 th floor	-3.85	-1.48	-1.01	-1.31	-3.29	-14.57	-5.94	-3.40	-4.99	-12.43
WC A	-5.96	-1.96	1.21	-2.66	-6.45	-22.77	-6.93	11.41	-10.09	-24.45
WC B	4.14	0.60	-1.39	-2.36	-6.73	15.99	-3.41	-4.85	-8.96	-25.57
WC C	0.16	-0.05	-0.18	-0.09	-0.71	0.62	-0.28	-0.77	-0.36	-2.72
WC D	-6.63	-2.99	-8.41	1.17	-8.78	-25.32	-10.51	-37.76	4.42	-33.39
<i>Difference</i>	<i>6.98</i>	<i>2.07</i>	<i>2.87</i>	<i>2.63</i>	<i>2.63</i>	<i>26.87</i>	<i>5.60</i>	<i>18.92</i>	<i>9.96</i>	<i>9.93</i>
Case	Wind-Catcher & DF									
Wind Speed	3.60 m/s					7.00 m/s				
Wind Direction	North	NE	East	SW	NW	North	NE	East	SW	NW
Av.DF	-3.32	-1.45	-3.70	-1.90	-3.48	-13.10	-5.44	-13.62	-7.18	-14.34
Av.DF_2 nd fl	-3.47	-1.52	-3.91	-1.87	-3.68	-13.70	-5.73	-14.43	-7.04	-15.09
Av.DF_3 rd fl	-3.65	-1.60	-3.65	-1.80	-3.66	-14.37	-6.02	-13.27	-6.76	-14.89
Av.DF_4 th fl	-4.11	-1.67	-2.60	-1.62	-3.41	-16.28	-6.28	-9.63	-6.05	-13.60
Bed 1	-3.41	-1.45	-3.61	-2.06	-3.63	-13.40	-5.44	-13.30	-7.77	-14.99
Bed 2	-3.34	-1.44	-3.67	-1.92	-3.47	-13.22	-5.41	-13.49	-7.25	-14.30
WC A	-5.83	-1.85	0.88	-2.60	-7.61	-22.27	-6.99	3.69	-10.19	-26.76
WC B	4.41	-0.32	-1.30	-2.58	-6.61	17.04	-1.16	-5.15	-10.15	-26.74
WC C	0.16	-0.06	-0.15	-0.13	-0.76	0.62	-0.23	-0.68	-0.51	-2.79
WC D	-6.27	-2.85	-8.16	0.89	-9.29	-23.99	-10.77	-31.47	3.53	-35.13

<i>Difference</i>	7.72	1.38	4.54	2.79	2.71	30.10	5.19	17.16	10.69	11.50
Case	Façade Wind-Catchers									
Wind Speed	3.60 m/s					7.00 m/s				
Wind Direction	North		East	SW		North		East	SW	NW
Av.DF	-2.59		-3.43	-1.58		-11.95		-13.25		
WC A	-4.99		0.86	-2.80		-20.04		3.54		
WC B	2.75		-1.77	-2.57		14.04		-5.86		
WC C	0.09		-0.17	-0.10		0.42		-0.61		
WC D	-5.33		-8.36	0.93		-21.13		-31.50		
WC A _tower	-6.46		0.73	-2.08		-28.55		3.18		
WC B _tower	2.72		-0.05	-2.09		11.32		0.64		
WC C _tower	-1.00		-4.63	-2.05		-3.33		-17.74		
WC D _tower	-4.60		-4.64	-0.29		-21.28		-17.50		

A.1.2. Study of the flow along urban passages

The flow distribution along urban passages was investigated for the three dominant wind directions and one wind speed (3.6m/s). Velocity and pressure values were predicted along a line as shown in Figure A.6, between the urban blocks extending up to the domain boundaries (900m), at 7.5m height above the domain level.

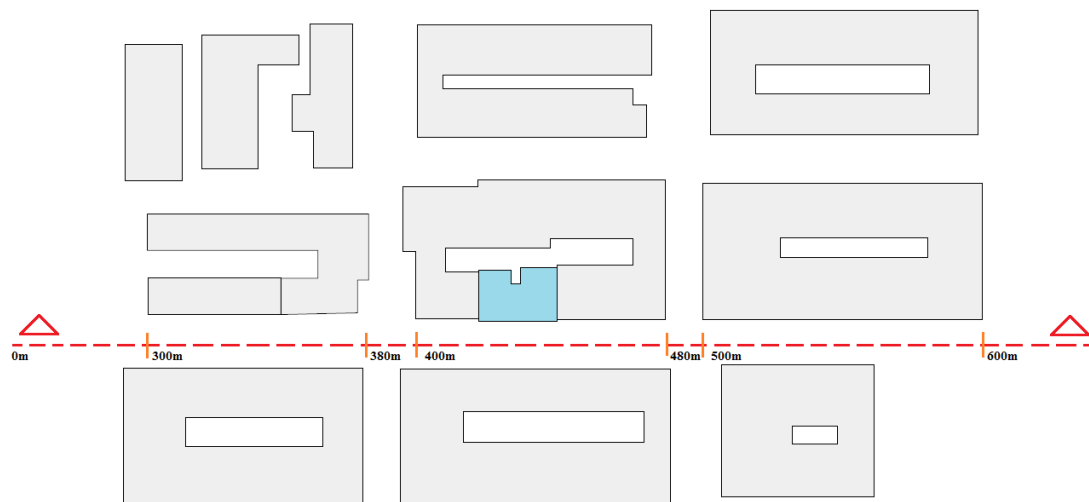


Figure A. 6 Site view of the building under investigation, the surroundings and the measuring line

During the three wind directions investigated, it was predicted that the wind speed reduces at the passages between the urban blocks, and increases at the centre point between two passages (Figure A.7). The wind pressure reduces in front of the case

study building and along the measuring line (Figure A.8). With a potential implementation of a wind-catcher, the low values of wind pressure at the façade openings of the building under investigation, and the potentially higher at the wind-catcher level (higher above the buildings) would increase the ventilation performance of the apartment under investigation.

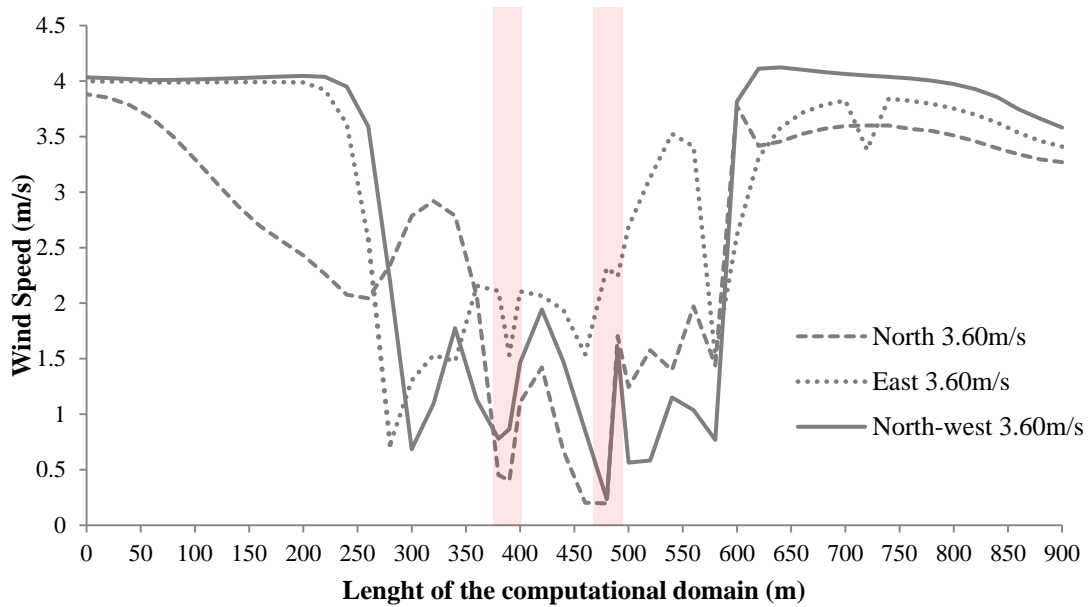


Figure A. 7 Prediction of wind velocities, at measured points every 20m at 1.5m height above the ground plane, along a line throughout the domain, 3 wind directions, 3.6m/s wind speed.

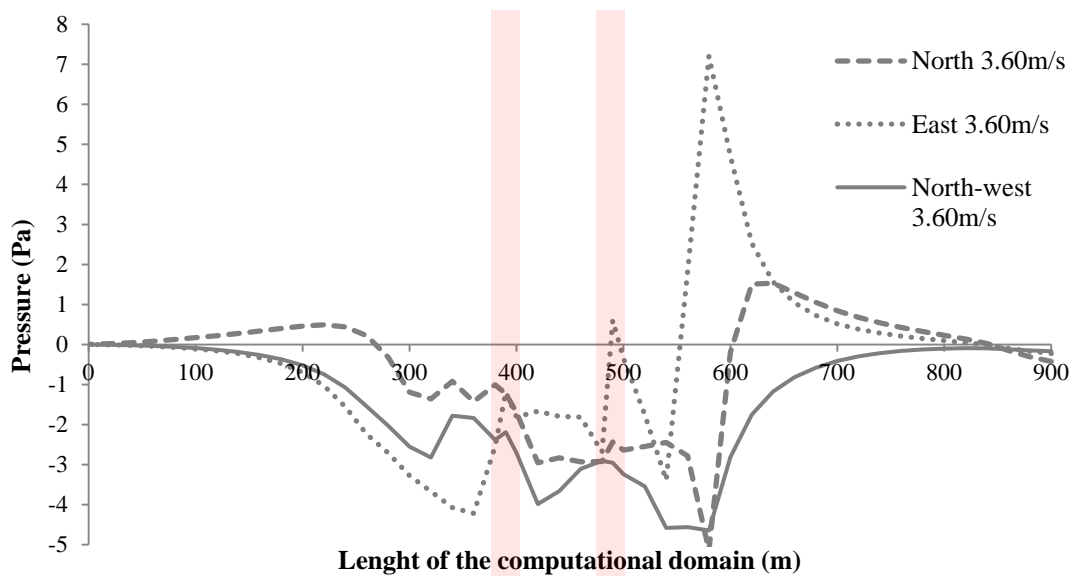


Figure A. 8 Prediction of pressure distribution, at measured points every 20m at 1.5m height above the ground plane, along a line throughout the domain, 3 directions, 3.6m/s wind speed.

A.2. Study of the internal flow field

A.2.1. Prediction of airflow at internal passages

During the study with CFD of the internal flow field, two-dimensional user-defined objects were designed at each internal opening incorporating developed code for the explicit purpose of this research (Figure A.9). The additional coding at each object with no effect to the computation or to the airflow distribution in the spaces, predicted the average velocity, volume flow rate and mass flow rate, at each internal opening, door or passage. Each internal opening was names as 'DOOR', with an additional number representing each measuring object. With regard to the domain axis each two-dimensional object was facing to, the velocity component would vary, and the script as well (i.e. for x-facing DOOR 'u1' and 'aeast', y-facing DOOR 'v1' and 'anorth', and z-facing DOOR 'w1' and 'ahigh'). The predicted values for the CFD simulations performed for the investigation of the internal flow field are included in Tables A.2 and A.3.

```
save13begin
(make areat is 0.)
(make volfl is 0.)
(make masfl is 0.)
(store1 of areat at DOOR is sum(aeast))
(store1 of volfl at DOOR is sum(aeast*u1))
(store1 of masfl at DOOR is sum(aeast*u1*den1))
(print of av-vel is volfl/areat)
(print of volflow is volfl)
(print of massflow is masfl)
save13end
```

Figure A. 9 Additional coding for the prediction of airflow through measuring 2D-objects at the computational domain

Table A. 2 Calculated values of average velocity, volume flow rate and mass flow rate in the internal openings of each ventilation strategy and climate scenario evaluated.

Single-Sided Ventilation Strategy				DBT: 26°C Wind speed: 3.6m/s			
		Buoyancy	North		East		North-west
Iterations		10000	6000		6000		6000
Door Bed1 - LR	Av-Vel 1	0.003	0.010		0.030		0.042
	VolFlow 1	0.006	0.017		0.052		0.075
	MassFlow 1	0.007	0.020		0.062		0.089
Door Bed2 - LR	Av-Vel 2	-0.003	-0.010		-0.030		-0.042
	VolFlow 2	-0.006	-0.017		-0.052		-0.075
	MassFlow 2	-0.007	-0.020		-0.062		-0.089
Door LR - Hallway	Av-Vel 3	0.003	0.008		0.024		0.034
	VolFlow 3	0.006	0.017		0.052		0.075
	MassFlow 3	0.007	0.020		0.062		0.089
Door Hallway - Kitchen	Av-Vel 4	0.000	0.000		0.000		0.000
	VolFlow 4	0.000	0.000		0.000		0.000
	MassFlow 4	0.000	0.000		0.000		0.000
Cross ventilation Strategy				DBT: 26°C Wind speed: 3.6m/s			
		Buoyancy	North	North-East	East		North-west
Iterations		10000	4500	10000	10000		12000
Win Kitchen - Stack	Av-Vel	0.375	-0.446	0.394	-0.446		0.781
	VolFlow	0.451	-0.536	0.473	-0.536		0.937
	MassFlow	0.536	-0.637	0.562	-0.637		1.114
Door Bed1 - LR	Av-Vel 1	0.110	-0.084	0.135	-0.084		0.250
	VolFlow 1	0.193	-0.147	0.237	-0.147		0.440
	MassFlow 1	0.230	-0.175	0.282	-0.175		0.523
Door Bed2 - LR	Av-Vel 2	0.146	-0.221	0.134	-0.221		0.283
	VolFlow 2	0.257	-0.389	0.236	-0.389		0.497
	MassFlow 2	0.306	-0.462	0.280	-0.462		0.591
Door LR - Hallway	Av-Vel 3	0.088	-0.067	0.108	-0.067		0.200
	VolFlow 3	0.193	-0.147	0.237	-0.147		0.440
	MassFlow 3	0.230	-0.175	0.282	-0.175		0.523
Door H - Kitchen	Av-Vel 4	0.256	-0.304	0.269	-0.304		0.532
	VolFlow 4	0.451	-0.536	0.473	-0.536		0.937
	MassFlow 4	0.536	-0.637	0.562	-0.637		1.114
Stack Horizontal	Av-Vel 5	0.195	-0.232	0.205	-0.232		0.406
	VolFlow 5	0.451	-0.536	0.473	-0.536		0.937
	MassFlow 5	0.536	-0.637	0.562	-0.637		1.114
Wind-Catcher Ventilation Strategy				DBT: 26°C Wind speed: 3.6m/s			
		Buoyancy	North	North-East	East	South-West	North-west
Iterations		9706	5300	4000	12000	9355	10000
Win Kitchen - Stack	Av-Vel	0.417	-1.43	-0.612	-0.735	-0.731	-0.636
	VolFlow	0.500	-1.72	-0.735	-0.882	-0.877	-0.763
	MassFlow	0.595	-2.04	-0.874	-1.049	-1.043	-0.907
Door	Av-Vel 1	0.124	-0.30	-0.200	-0.130	-0.201	-0.180

Bed1 - LR	VolFlow 1	0.218	-0.52	-0.353	-0.228	-0.354	-0.316
	MassFlow 1	0.259	-0.62	-0.419	-0.271	-0.421	-0.376
Door Bed2 - LR	Av-Vel 2	0.161	-0.68	-0.434	-0.372	-0.297	-0.254
	VolFlow 2	0.283	-1.20	-0.382	-0.654	-0.523	-0.447
Door LR - Hallway	MassFlow 2	0.336	-1.42	-0.454	-0.778	-0.622	-0.532
	Av-Vel 3	0.099	-0.24	-0.160	-0.104	-0.161	-0.144
Door H - Kitchen	VolFlow 3	0.218	-0.52	-0.353	-0.228	-0.354	-0.316
	MassFlow 3	0.259	-0.62	-0.419	-0.271	-0.421	-0.376
Stack Horizontal	Av-Vel 4	0.284	-0.98	-0.418	-0.501	-0.498	-0.434
	VolFlow 4	0.500	-1.72	-0.735	-0.882	-0.877	-0.763
Stack Horizontal	MassFlow 4	0.595	-2.04	-0.874	-1.049	-1.043	-0.907
	Av-Vel 5	0.217	-0.74	-0.318	-0.382	-0.380	-0.330
Stack Horizontal	VolFlow 5	0.500	-1.72	-0.735	-0.882	-0.877	-0.763
	MassFlow 5	0.595	-2.04	-0.874	-1.049	-1.043	-0.907
Dynamic façade Ventilation Strategy				DBT: 26°C Wind speed: 3.6m/s			
	Wind Direction	Buoyancy	North		East		North-west
Iterations		10000	7000		7000		7800
Win Ki - Stack	Av-Vel	0.4271	-1.3058		-0.9561		-0.829
	VolFlow	0.5125	-1.5670		-1.1475		-0.994
	MassFlow	0.6094	-1.8632		-1.3644		-1.182
Door Bed1 - LR	Av-Vel 1	0.1277	-0.6590		-0.4299		-0.344
	VolFlow 1	0.2247	-0.8699		-0.6622		-0.605
	MassFlow 1	0.2672	-1.0343		-0.7873		-0.719
Door Bed2 - LR	Av-Vel 2	0.1635	-1.0563		-0.7352		-0.590
	VolFlow 2	0.2878	-0.6972		-0.4853		-0.390
	MassFlow 2	0.3422	-0.8289		-0.5770		-0.463
Door LR Hallway	Av-Vel 3	0.1021	-0.3953		-0.3010		-0.275
	VolFlow 3	0.2247	-0.8699		-0.6622		-0.605
	MassFlow 3	0.2672	-1.0343		-0.7873		-0.719
Door H - Kitchen	Av-Vel 4	0.2912	-0.8903		-0.6519		-0.565
	VolFlow 4	0.5125	-1.5670		-1.1475		-0.994
	MassFlow 4	0.6094	-1.8632		-1.3643		-1.182
Stack Horizontal	Av-Vel 5	0.2219	-0.6784		-0.4968		-0.430
	VolFlow 5	0.5125	-1.5670		-1.1475		-0.994
	MassFlow 5	0.6094	-1.8632		-1.3644		-1.182
Bed 1-balcony	Av-Vel 11	0.1021	-0.3954		-0.3010		-0.275
	VolFlow 11	0.2247	-0.8699		-0.6622		-0.605
	MassFlow11	0.2672	-1.0343		-0.7873		-0.719
Bed 2-balcony	Av-Vel 12	0.1308	-0.3169		-0.2206		-0.177
	VolFlow 12	0.2878	-0.6972		-0.4853		-0.390
	MassFlow12	0.3422	-0.8289		-0.5770		-0.463
PDEC and Wind-Catcher				DBT: 26°C Wind speed: 3.6m/s			
	Wind Direction	North	North	North-East	East		North-west
WATER		8L/s	6 L/h	6 L/h	6 L/h		6 L/h
Iterations		6283	5900	3400	7000		4000
Win Kitchen - Stack	Av-Vel	-1.315	-1.028	-0.671	-0.749		-0.694
	VolFlow	-1.579	-1.234	-0.805	-0.899		-0.832
	MassFlow	-1.877	-1.467	-0.958	-1.069		-0.990
Door Bed1 -	Av-Vel 1	-0.280	-0.212	-0.152	-0.153		-0.240
	VolFlow 1	-0.493	-0.372	-0.268	-0.268		-0.422

LR	MassFlow 1	-0.586	-0.443	-0.319	-0.319		-0.502
Door Bed2 - LR	Av-Vel 2	-0.617	-0.489	-0.305	-0.358		-0.414
	VolFlow 2	-1.086	-0.861	-0.537	-0.631		-0.410
Door LR - Hallway	MassFlow 2	-1.291	-1.024	-0.638	-0.750		-0.488
	Av-Vel 3	-0.224	-0.169	-0.122	-0.122		-0.192
	VolFlow 3	-0.493	-0.372	-0.268	-0.268		-0.422
Door H - Kitchen	MassFlow 3	-0.586	-0.443	-0.319	-0.319		-0.502
	Av-Vel 4	-0.897	-0.701	-0.458	-0.511		-0.473
	VolFlow 4	-1.579	-1.234	-0.805	-0.899		-0.832
Stack Horizontal	MassFlow 4	-1.877	-1.467	-0.957	-1.069		-0.990
	Av-Vel 5	-0.684	-0.534	-0.349	-0.389		-0.360
	VolFlow 5	-1.579	-1.234	-0.805	-0.899		-0.832
	MassFlow 5	-1.877	-1.467	-0.958	-1.069		-0.990
PDEC and Dynamic façade				DBT: 26°C Wind speed: 3.6m/s			
	Wind Direction		North		East	South-West	
WATER			6 L/h		6 L/h	6 L/h	
Iterations			12000		10000	10000	
Win Ki - Stack	Av-Vel		-1.323		-1.049	-0.875	
	VolFlow		-1.588		-1.259	-1.051	
	MassFlow		-1.888		-1.497	-1.249	
Door Bed1 - LR	Av-Vel 1		-0.675		-0.531	-0.439	
	VolFlow 1		-0.891		-0.701	-0.579	
	MassFlow 1		-1.059		-0.833	-0.688	
Door Bed2 - LR	Av-Vel 2		-1.056		-0.846	-0.715	
	VolFlow 2		-0.697		-0.558	-0.472	
	MassFlow 2		-0.829		-0.664	-0.561	
Door LR Hallway	Av-Vel 3		-0.405		-0.318	-0.263	
	VolFlow 3		-0.891		-0.701	-0.579	
	MassFlow 3		-1.059		-0.833	-0.688	
Door H - Kitchen	Av-Vel 4		-0.902		-0.715	-0.597	
	VolFlow 4		-1.588		-1.259	-1.051	
	MassFlow 4		-1.888		-1.497	-1.249	
Stack Horizontal	Av-Vel 5		-0.687		-0.545	-0.455	
	VolFlow 5		-1.588		-1.259	-1.051	
	MassFlow 5		-1.888		-1.497	-1.249	
Bed 1-balcony	Av-Vel 11		-0.405		-0.318	-0.263	
	VolFlow 11		-0.891		-0.701	-0.579	
	MassFlow11		-1.059		-0.833	-0.688	
Bed 2-balcony	Av-Vel 12		-0.317		-0.254	-0.214	
	VolFlow 12		-0.697		-0.559	-0.472	
	MassFlow12		-0.829		-0.664	-0.561	

Table A. 3 Calculated values of average velocity, volume flow and mass flow rates in the internal openings of each ventilation strategy for 26°C DBT and 7m/s wind speed.

Single-Sided Ventilation Strategy				DBT: 26°C Wind speed: 7m/s			
		North	East			North-west	
Iterations		6000	6000			6000	
Door Bed1 - LR	Av-Vel 1	0.074	0.245			0.071	
	VolFlow 1	0.131	0.430			0.124	

	MassFlow 1	0.155	0.512		0.148
Door Bed2 - LR	Av-Vel 2	-0.074	-0.245		-0.071
	VolFlow 2	-0.131	-0.430		-0.124
	MassFlow 2	-0.155	-0.512		-0.148
Door LR - Hallway	Av-Vel 3	0.059	0.196		0.057
	VolFlow 3	0.131	0.431		0.124
	MassFlow 3	0.155	0.512		0.148
Door H - Kitchen	Av-Vel 4	0.000	0.000		0.000
	VolFlow 4	0.000	0.000		0.000
	MassFlow 4	0.000	0.000		0.000
Cross ventilation Strategy				DBT: 26°C Wind speed: 7m/s	
		North	East		North-west
Iterations		3899	11760		3882
Win Ki - Stack	Av-Vel	-1.353	-0.907		1.770
	VolFlow	-1.623	-1.088		2.124
	MassFlow	-1.930	-1.293		2.526
Door Bed1 - LR	Av-Vel 1	-0.307	-0.182		0.537
	VolFlow 1	-0.541	-0.320		0.945
	MassFlow 1	-0.643	-0.380		1.124
Door Bed2 - LR	Av-Vel 2	-0.615	-0.437		0.670
	VolFlow 2	-1.083	-0.768		1.179
	MassFlow 2	-1.287	-0.913		1.402
Door LR - Hallway	Av-Vel 3	-0.246	-0.145		0.430
	VolFlow 3	-0.541	-0.320		0.945
	MassFlow 3	-0.643	-0.380		1.124
Door H - Kitchen	Av-Vel 4	-0.922	-0.618		1.207
	VolFlow 4	-1.623	-1.088		2.124
	MassFlow 4	-1.930	-1.293		2.526
Stack Horizontal	Av-Vel 5	-0.703	-0.471		0.920
	VolFlow 5	-1.623	-1.088		2.124
	MassFlow 5	-1.930	-1.293		2.526
Wind-Catcher Ventilation Strategy				DBT: 26°C Wind speed: 7m/s	
		North	East	South-West	North-west
Iterations		4650	2455	3500	2965
Win Ki - Stack	Av-Vel	-2.81	-1.783	-1.421	-1.287
	VolFlow	-3.37	-2.140	-1.705	-1.545
	MassFlow	-4.01	-2.545	-2.027	-1.837
Door Bed1 - LR	Av-Vel 1	-0.59	-0.646	-0.368	-0.496
	VolFlow 1	-1.03	-1.138	-0.648	-0.873
	MassFlow 1	-1.23	-1.353	-0.770	-1.038
Door Bed2 - LR	Av-Vel 2	-1.33	-1.139	-0.601	-0.763
	VolFlow 2	-2.34	-1.003	-1.057	-0.672
	MassFlow 2	-2.78	-1.192	-1.257	-0.799
Door LR - Hallway	Av-Vel 3	-0.47	-0.517	-0.294	-0.397
	VolFlow 3	-1.03	-1.138	-0.648	-0.873
	MassFlow 3	-1.23	-1.352	-0.770	-1.038
Door H - Kitchen	Av-Vel 4	-1.92	-1.216	-0.969	-0.878
	VolFlow 4	-3.37	-2.140	-1.705	-1.545
	MassFlow 4	-4.01	-2.545	-2.027	-1.837
Stack	Av-Vel 5	-1.46	-0.926	-0.738	-0.669

Horizontal	VolFlow 5	-3.37	-2.140	-1.705	-1.545
	MassFlow 5	-4.01	-2.545	-2.027	-1.837
Dynamic façade Ventilation Strategy				DBT: 26°C Wind speed: 7m/s	
		North	East		North-west
Iterations		2900	5000		10000
Win Ki - Stack	Av-Vel	-2.6249	-1.9484		-1.610
	VolFlow	-3.1505	-2.3381		-1.932
	MassFlow	-3.7459	-2.7800		-2.297
Door Bed1 - LR	Av-Vel 1	-1.3569	-0.9891		-0.630
	VolFlow 1	-1.7913	-1.3056		-1.109
	MassFlow 1	-2.1299	-1.5523		-1.319
Door Bed2 - LR	Av-Vel 2	-2.0590	-1.5645		-1.247
	VolFlow 2	-1.3591	-1.0325		-0.823
	MassFlow 2	-1.6160	-1.2277		-0.978
Door LR - Hallway	Av-Vel 3	-0.8142	-0.5934		-0.504
	VolFlow 3	-1.7914	-1.3056		-1.109
	MassFlow 3	-2.1299	-1.5523		-1.319
Door H - Kitchen	Av-Vel 4	-1.7899	-1.3285		-1.098
	VolFlow 4	-3.1505	-2.3381		-1.932
	MassFlow 4	-3.7459	-2.7800		-2.297
Stack Horizontal	Av-Vel 5	-1.3638	-1.0122		-0.836
	VolFlow 5	-3.1505	-2.3381		-1.932
	MassFlow 5	-3.7459	-2.7800		-2.297
Bed 1- balcony	Av-Vel 11	-0.8142	-0.5934		-0.504
	VolFlow 11	-1.7914	-1.3056		-1.109
	MassFlow 11	-2.1299	-1.5523		-1.319
Bed 2- balcony	Av-Vel 12	-0.6177	-0.4693		-0.374
	VolFlow 12	-1.3591	-1.0325		-0.823
	MassFlow 12	-1.6160	-1.2277		-0.978
PDEC and Wind-Catcher				DBT: 26°C Wind speed: 7m/s	
		North	East		North-west
WATER		6 L/h	6 L/h		6 L/h
Iterations		10000	6000		6000
Win Ki - Stack	Av-Vel	-2.821	-1.570		-1.146
	VolFlow	-3.387	-1.884		-1.376
	MassFlow	-4.027	-2.240		-1.636
Door Bed1 - LR	Av-Vel 1	-0.605	-0.528		-0.407
	VolFlow 1	-1.066	-0.929		-0.717
	MassFlow 1	-1.267	-1.105		-0.853
Door Bed2 - LR	Av-Vel 2	-1.319	-1.085		-0.748
	VolFlow 2	-2.322	-0.955		-0.659
	MassFlow 2	-2.760	-1.135		-0.783
Door LR - Hallway	Av-Vel 3	-0.484	-0.422		-0.326
	VolFlow 3	-1.066	-0.929		-0.717
	MassFlow 3	-1.267	-1.105		-0.853
Door H - Kitchen	Av-Vel 4	-1.924	-1.070		-0.782
	VolFlow 4	-3.387	-1.884		-1.376
	MassFlow 4	-4.027	-2.240		-1.636
Stack Horizontal	Av-Vel 5	-1.466	-0.816		-0.596
	VolFlow 5	-3.387	-1.884		-1.376
	MassFlow 5	-4.027	-2.240		-1.636
		North	East	North	East

WATER		8 L/h	8 L/h	10L/s	10L/s
Iterations		10000	2350	10000	8000
Win Ki - Stack	Av-Vel	-2.820	-1.584	-2.824	-1.635
	VolFlow	-3.386	-1.901	-3.390	-1.963
	MassFlow	-4.025	-2.261	-4.031	-2.334
Door Bed1 - LR	Av-Vel 1	-0.624	-0.540	-0.627	-0.573
	VolFlow 1	-1.098	-0.951	-1.104	-1.009
	MassFlow 1	-1.306	-1.131	-1.312	-1.200
Door Bed2 - LR	Av-Vel 2	-1.300	-1.080	-1.299	-1.084
	VolFlow 2	-2.287	-0.950	-2.286	-0.954
	MassFlow 2	-2.720	-1.130	-2.719	-1.134
Door LR - Hallway	Av-Vel 3	-0.499	-0.432	-0.501	-0.459
	VolFlow 3	-1.098	-0.951	-1.104	-1.009
	MassFlow 3	-1.306	-1.131	-1.312	-1.200
Door H - Kitchen	Av-Vel 4	-1.923	-1.080	-1.926	-1.115
	VolFlow 4	-3.386	-1.901	-3.390	-1.963
	MassFlow 4	-4.025	-2.261	-4.031	-2.334
Stack Horizontal	Av-Vel 5	-1.466	-0.823	-1.468	-0.850
	VolFlow 5	-3.386	-1.901	-3.390	-1.963
	MassFlow 5	-4.025	-2.260	-4.031	-2.334
PDEC and Dynamic façade			DBT: 26°C Wind speed: 7m/s		
		North	East	South-West	North-west
WATER		6 L/h	6 L/h		6 L/h
Iterations		10000	3500	10000	10000
Win Ki - Stack	Av-Vel	-2.604	-1.939	-1.60	-1.66
	VolFlow	-3.125	-2.327	-1.92	-1.99
	MassFlow	-3.716	-2.767	-2.28	-2.36
Door Bed1 - LR	Av-Vel 1	-1.280	-0.981	-0.79	-0.81
	VolFlow 1	-1.690	-1.295	-1.04	-1.07
	MassFlow 1	-2.009	-1.540	-1.23	-1.28
Door Bed2 - LR	Av-Vel 2	-2.175	-1.563	-1.33	-1.38
	VolFlow 2	-1.435	-1.032	-0.88	-0.91
	MassFlow 2	-1.707	-1.227	-1.05	-1.09
Door LR - Hallway	Av-Vel 3	-0.768	-0.589	-0.47	-0.49
	VolFlow 3	-1.690	-1.295	-1.04	-1.07
	MassFlow 3	-2.009	-1.540	-1.23	-1.28
Door H - Kitchen	Av-Vel 4	-1.776	-1.322	-1.09	-1.13
	VolFlow 4	-3.125	-2.327	-1.92	-1.99
	MassFlow 4	-3.716	-2.767	-2.28	-2.36
Stack Horizontal	Av-Vel 5	-1.353	-1.007	-0.83	-0.86
	VolFlow 5	-3.125	-2.327	-1.92	-1.99
	MassFlow 5	-3.716	-2.767	-2.28	-2.36
Bed 1- balcony	Av-Vel 11	-0.768	-0.589	-0.47	-0.49
	VolFlow 11	-1.690	-1.295	-1.04	-1.07
	MassFlow11	-2.009	-1.540	-1.23	-1.28
Bed 2- balcony	Av-Vel 12	-0.652	-0.469	-0.40	-0.42
	VolFlow 12	-1.435	-1.032	-0.88	-0.91
	MassFlow12	-1.707	-1.227	-1.05	-1.09
		North	North	North	
WATER		8 L/h	10 L/h	12 L/h	
Iterations		10000	10000	10000	
Win Ki - Stack	Av-Vel	-2.610	-2.613	-2.622	
	VolFlow	-3.133	-3.137	-3.147	

	MassFlow	-3.725	-3.729	-3.742
Door Bed1 - LR	Av-Vel 1	-1.284	-1.286	-1.290
	VolFlow 1	-1.694	-1.698	-1.703
	MassFlow 1	-2.015	-2.019	-2.024
Door Bed2 - LR	Av-Vel 2	-2.179	-2.180	-2.189
	VolFlow 2	-1.438	-1.439	-1.445
	MassFlow 2	-1.710	-1.711	-1.718
Door LR - Hallway	Av-Vel 3	-0.770	-0.772	-0.774
	VolFlow 3	-1.694	-1.698	-1.703
	MassFlow 3	-2.015	-2.019	-2.024
Door H – Kitchen	Av-Vel 4	-1.780	-1.782	-1.788
	VolFlow 4	-3.133	-3.137	-3.147
	MassFlow 4	-3.725	-3.729	-3.742
Stack Horizontal	Av-Vel 5	-1.356	-1.358	-1.363
	VolFlow 5	-3.133	-3.137	-3.147
	MassFlow 5	-3.725	-3.729	-3.742

A.2.2. Study of the internal flow for DBT 35°C.

The simulation results from the evaluation of the ventilation performance of the apartment under investigation for 35°C DBT were considered comparable to the results from the 26°C DBT (i.e. similar resulted ventilation rates in the spaces and temperature difference between the internal and external environments) and were thus not included in Chapter 6. Predicted indoor air temperatures and velocities from the different ventilation strategies for north wind direction and 35°C DBT are presented in Figures A.10 to A.13. Predicted average values of indoor temperature and air velocity at a horizontal plane at 1.5m height above the apartment floor, for 35°C DBT for all natural ventilation strategies and wind directions, are included in Figures A.14 and A.15.

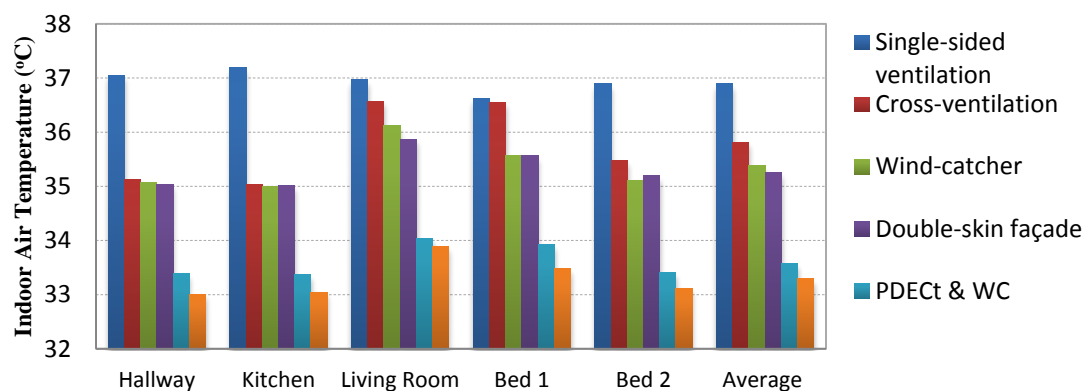


Figure A. 10 Indoor air temperatures (at xy points at 1.50m height above the apartment floor level) of the six natural ventilation strategies, north wind direction of 3.6m/s and 35°C DBT.

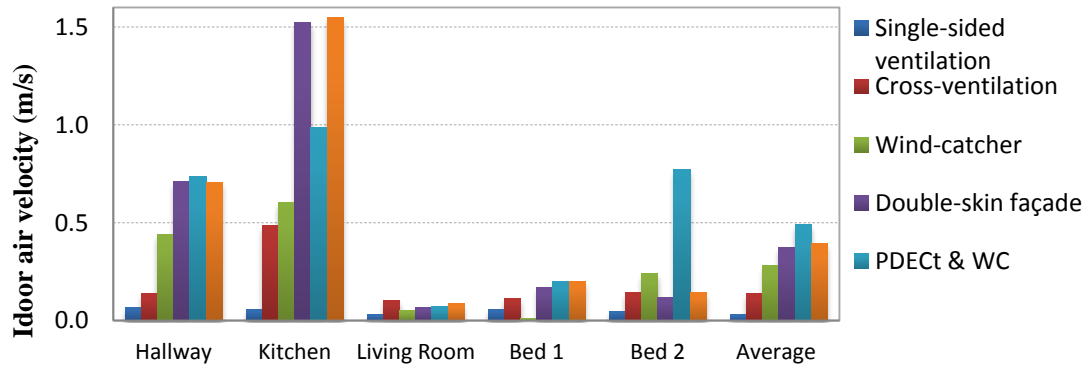


Figure A. 11 Indoor air velocity (at xy points at 1.50m height above the apartment floor level) of the six natural ventilation strategies at five spaces, north wind direction, 3.6m/s and 35°C DBT.

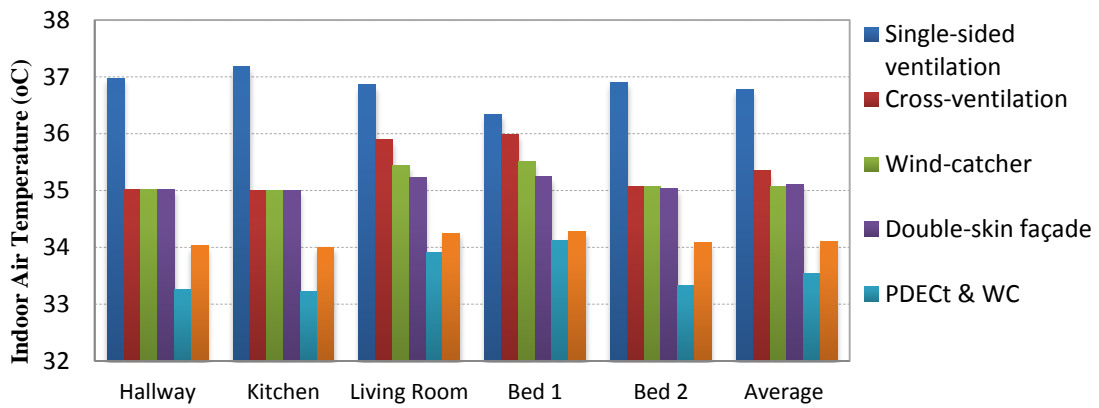


Figure A. 12 Indoor air temperatures (at xy points at 1.50m height above the apartment floor level) of the six natural ventilation strategies, north wind direction of 7m/s and 35°C DBT.

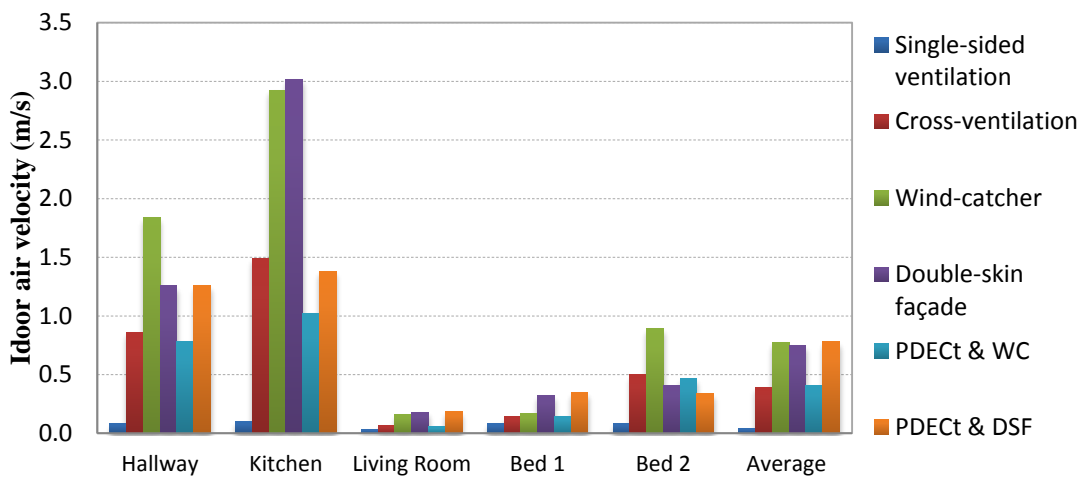


Figure A. 13 Indoor air velocity (at xy points at 1.50m height above the apartment floor level) of the six natural ventilation strategies at five spaces, north wind direction of 7m/s and 35°C DBT.

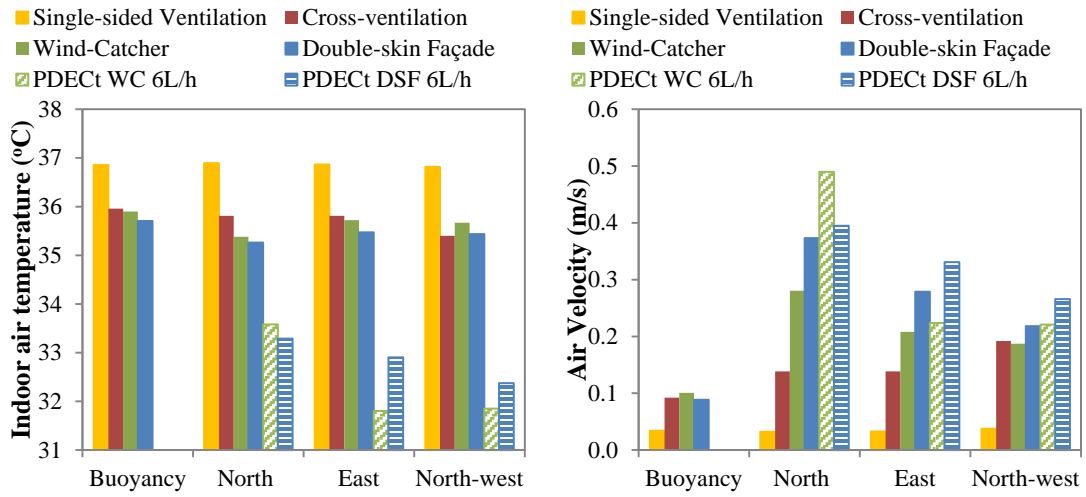


Figure A. 14 Average measured values of indoor temperature and velocity at horizontal plane (at 1.5m above the floor) for 35°C and 3.6m/s wind speed

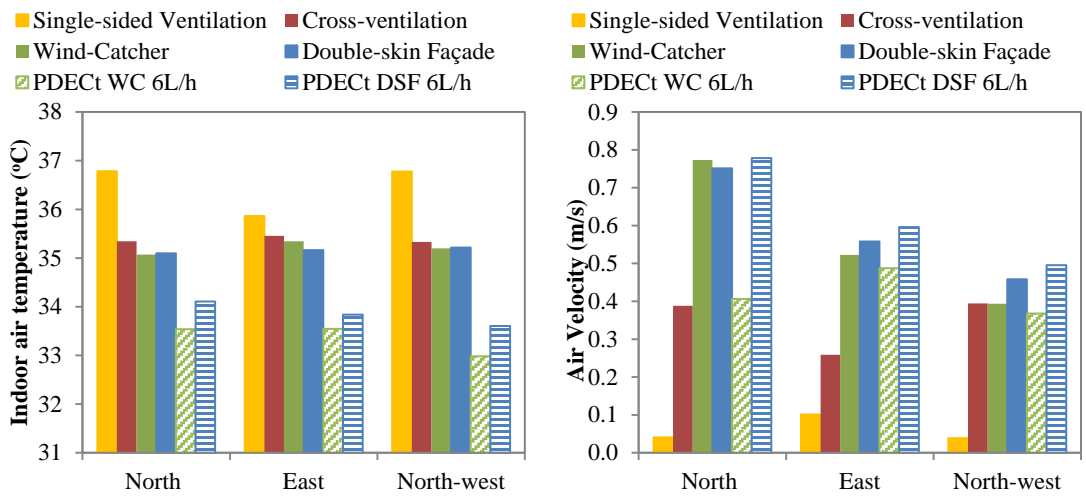


Figure A. 15 Average measured values of indoor temperature and velocity at horizontal plane for 35°C and 7m/s wind speed

A.3. Predicted average pressure values on openings

Table A. 4 Pressure difference at the openings for every wind speed and direction, predicted by the external flow CFD simulations

Wind Direction	North		North-east		East		South-east		South		South-west		West		North-west	
	Wind Speed	ΔP	Wind Speed	ΔP	Wind Speed	ΔP	Wind Speed	ΔP	Wind Speed	ΔP	Wind Speed	ΔP	Wind Speed	ΔP	Wind Speed	ΔP
	m/s	Pa	m/s	Pa	m/s	Pa	m/s	Pa	m/s	Pa	m/s	Pa	m/s	Pa	m/s	Pa
Base-case ventilation model					0.5	0.01										
	3.6	0.58	3.6	0.16	3.6	0.58	--	--	--	--	3.6	0.57	--	--	3.6	1.53
					5	1.09										
	7	4.95	7	0.85	7	2.18					7	2.15			7	8.13
Wind-catcher model	2	2.12			2	0.87										
	3.6	6.98	3.6	2.07	3.6	2.87					3.6	2.63	3.6	2.16	3.6	2.63
	5	13.66			5	5.57									0.5	0.05
	7	26.87	7	5.59	7	18.92	--	--	--	--	7	9.96			7	9.93
	9	44.80			9	18.17									5	5.12
	11	65.75														
Dynamic façade and Wind-catcher model	3.6	7.72	3.6	1.380	3.6	4.6	3.6	1.98			3.6	2.79			3.6	2.71
					5	8.9										
	7.0	30.14	7	5.21	7	17.3	7	7.31	--	-	7	10.7	--	--	7	11.55
				9	29.1											

A.4. Simulations performed

Table A. 5 Study of the External Flow field; simulations performed for each ventilation strategy for different wind direction and wind speeds (m/s)

Ventilation Strategy	North	Northeast	East	Southeast	Southwest	West	Northwest
Base-case Ventilation			0.5				
	3.6	3.6	3.6		3.6		3.6
			5				
	7	7	7		7		7
Wind-catcher	2		2				
	3.6	3.6	3.6		3.6	3.6	3.6
	5		5				0.5
	7	7	7		7		7
	9		9				5
	11						
Dynamic façade	3.6	3.6	3.6	3.6	3.6		3.6
			5				
	7	7	7	7	7		7
			9				
Façade wind-catchers	3.6		3.6		3.6		
	7		7				

Table A. 6 Simulations of the ventilation performance of the natural ventilation strategies investigated for different climate scenarios; Internal Flow. With '×' are marked the simulations included in the analysis of Chapter 6 and with '■' the simulations performed for the additional studied

Ventilation Strategy	Wind Speed	Buoyancy		North		Northeast		East		Southwest		Northwest	
		26°C	35°C	26°C	35°C	26°C	35°C	26°C	35°C	26°C	35°C	26°C	35°C
DB Temperature	--	×	×										
[SS]	--	×	×										
	3.6m/s			×	×			×	×			×	×
	7m/s			×	×			×	×			×	×
[CV]	--	×	×										
	3.6m/s			×	×	■		×	×			×	×
	7m/s			×	×			×	×			×	×
[CV] 1/8th	--	■											
	3.6m/s			■				■				■	
	7m/s			■				■				■	

[WC]	--	×	×												
	3.6m/s			×	×	■	■	×	×	■	■	×	×		
	7m/s			×	×			×	×	■	■	×	×		
[WC] 1/8th	--	■													
	3.6m/s			■				■				■			
	7m/s			■				■				■			
[DF&WC]	--	×	×												
	3.6m/s			×	×			×	×			×	×		
	7m/s			×	×			×	×			×	×		
[DF&WC] 1/8th	--	■													
	3.6m/s			■				■				■			
	7m/s			■				■				■			
[PDEC-WC]															
6L/h	3.6m/s			×	×	■		×	×			×	×		
	7m/s			×	×			×	×			×	×		
8L/h	3.6m/s			×											
	7m/s			×	×			×							
10L/h	7m/s			×				×							
[PDEC-WC] 1/8th															
6L/h	3.6m/s			■				■				■			
	7m/s			■				■				■			
[PDEC-DF]															
6L/h	3.6m/s			×	×			×	×			×	×		
	7m/s			×	×			×	×	■	■	×	×		
8L/h	7m/s			×	×										
10L/h	7m/s			■											
12L/h	7m/s			■											
4L/h	7m/s			■											
[PDEC-DF] 1/8th															
6L/h	3.6m/s			■				■				■			
	7m/s			■				■				■			
Detached case		7m/s		■											
Four Apartments 1/4th		--	■	■											
[WC]	3.6m/s			■	■										
	7m/s			■											
[PDEC-WC] 10L/h	7m/s			■											
[InOp]	3.6m/s			■				■				■			
	7m/s			■											
[F-WC]	3.6m/s			■											
	7m/s			■											
[DF] Louvres operations	3.6m/s							■ 3							

A.4.1. Limitations and advantages of CFD computer simulations in serial and parallel operations

For the detailed study of the natural ventilation of the building under investigation, CFD simulations were performed in serial (windows version of PHOENICS) and in parallel runs (Linux version), with regard to the requirements of each natural ventilation strategy evaluated for this research.

For the conduction of parallel computing, Loughborough university IT services provided access to the high performance computing service (HPC) which comprises of the hydra cluster, running the Red Hat Linux operating system (Bull Linux AS5), of 1956 64-bit Intel Xeon processors. The simulations of the external flow study were performed utilising in 12 to 24 processors (one or two compute nodes) each having two of six-core Intel Westmere Xeon X5650 CPUs and 24GB of memory (connected by an Infiniband network).

Despite the vast potential of the parallel simulations with regard to time reduction (in Linux PHOENICS VR parallel system), the simulations are submitted to a batch queue and then performed when scheduled by the system. Therefore, each job has to be initially created and built using a windows computer, then saved, copied on the HPC, submitted using a job submitting script, and finally executed in parallel. With the completion of the simulation, the results were manually transferred to a windows computer to be accessed, visualised and saved. One of the concerns was that the user could not visualise or access the progress of the simulation during the run, via the convergence monitor plot. Therefore, an additional script was developed to assist the job submission. This created a fake display, used a variable to help PHOENICS trace it, and then automatically deleted the fake display from the system, providing a final convergence plot saved as an image file.

In the case of parallel computation, different solver is utilised than to serial, and additional changes at the pre-processor stage of the models were required to ensure efficient simulations. It was recommended by the software developers to solve all computed variables within a whole-field manner. Possible convergence problems of the whole-field solution of the turbulence variables KE and EP could be potentially

reduced by lowering the linear relaxation factor on KE and EP, and the number of solver iterations on the pressure correction equation momentum equations.

Further, it was noticed that the study of the external flow field was the most computationally demanding with regard to the time and power required: all external flow simulations were performed in parallel simulations. That reduced the computational time of each simulation by up to 4 times relative to performing the simulations in serial. Using parallel computing, up to five simulations on average could be performed simultaneously as more than one node was available per user. That resulted in a considerable computational time reduction required for the total number of external flow simulations. It was predicted that on average they would require up to 200 days of continuous computational time if performed on the windows serial version.

On the other hand, preliminary simulations shown that convergence was difficult to achieve for some strategies of the internal flow field evaluation, which required modification of the under-relaxation factors used during the simulations. As the solution in Linux parallel could not be assessed and visualised during the run, the vast majority of the internal flow simulation were thus performed in windows serial version. These internal flow simulations were performed on a Windows 7 desktop computer with two Intel Xeon E5520 processors of 2.27GHz (2 processors) and 64Gb RAM.

Appendix B. Extrapolation of patterns in ventilation performance: CFD simulation results

Following the relationships defined between the indoor air temperatures and ventilation rates (Figures 7.20-7.21), and between ventilation rates and wind speeds for each strategy and wind direction evaluated (Figure 7.9-7.13) in Chapter 7, the relationship between wind speed and indoor temperature was explored (Figures A.16 to A.20). These relationships were averaged and contributed to the prediction of the relationships between temperature difference and wind speed, presented in Chapter 7.4.1.

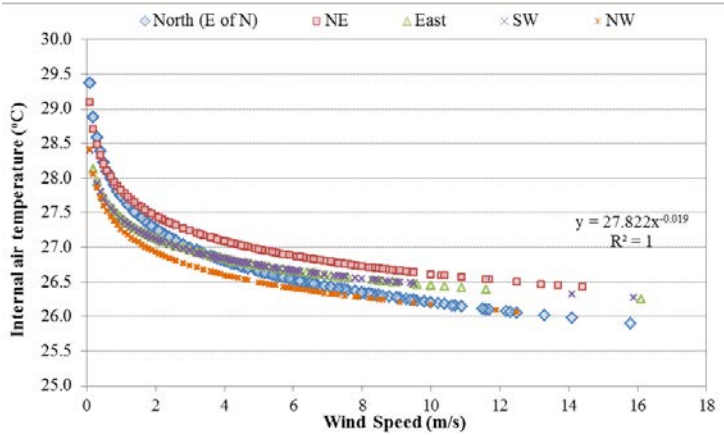


Figure A. 16 Indoor temperature and wind speed relationships for the [CV] strategy, for DBT 26°C and different wind directions

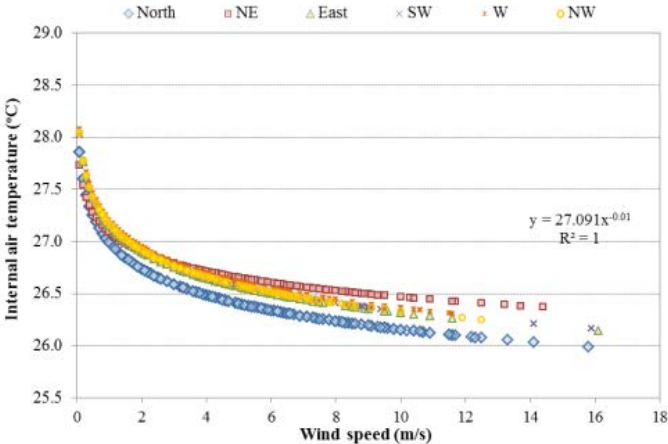


Figure A. 17 Indoor temperature and wind speed relationships for the [WC] strategy, for DBT 26°C and various wind directions.

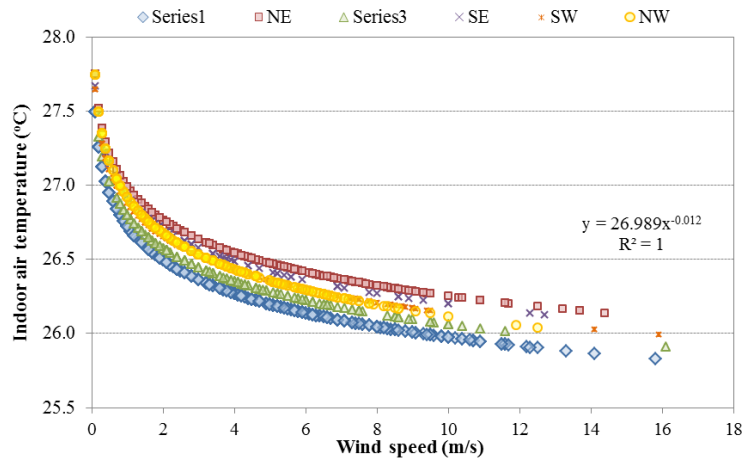


Figure A. 18 Indoor temperature and wind speed relationships for the [DF & WC] strategy, for DBT 26°C and various wind directions

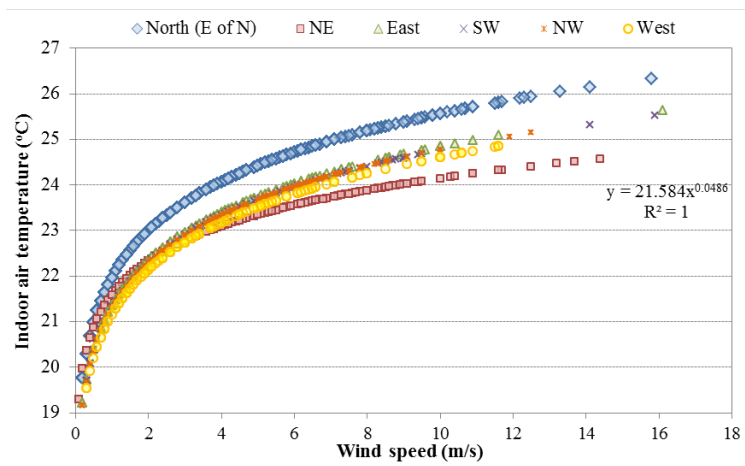


Figure A. 19 Indoor temperature and wind speed relationships for the [PDEC-WC] strategy, for DBT 26°C and various wind directions

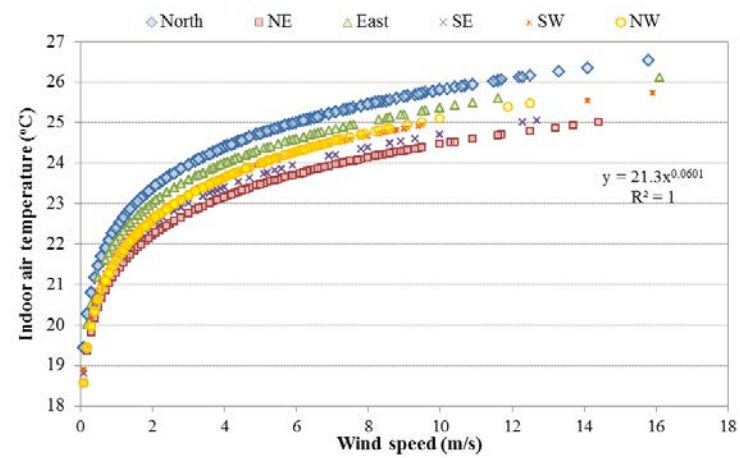


Figure A. 20 Indoor temperature and wind speed relationships for the [PDEC-DF] strategy, for DBT 26°C and various wind directions